DANIELA FIETZ

Rezeptor- und Transporterexpression für freie und konjugierte Steroidhormone bei normaler und gestörter Spermatogenese

HABILITATIONSSCHRIFT
zur Erlangung der Lehrbefähigung für die Fächer Anatomie, Histologie und Embryologie im Fachbereich Veterinärmedizin der Justus-Liebig-Universität Gießen

édition scientifique
VVB LAUFERSWEILER VERLAG

1. Auflage 2018

1st Edition 2018

édition linguistique
VVB LAUFERSWEILER VERLAG

STAUFENBERGRING 15, D-35396 GIESSEN
Tel: 0641-5599888 Fax: 0641-5599890
email: redaktion@doktorverlag.de

www.doktorverlag.de

Justus-Liebig-Universität Gießen

Fachbereich Veterinärmedizin

Institut für Veterinär-Anatomie, -Histologie und -Embryologie

Rezeptor- und Transporterexpression für freie und konjugierte Steroidhormone bei normaler und gestörter Spermatogenese

HABILITATIONSSCHRIFT

zur Erlangung der Lehrbefähigung für die
Fächer Anatomie, Histologie und Embryologie
im Fachbereich Veterinärmedizin
der Justus-Liebig-Universität Gießen

vorgelegt von

Dr. med. vet. Daniela Fietz

Gießen 2018

Für meine Familie

Inhaltsverzeichnis

1. Abkürzungsverzeichnis

17-OH-PREGS 17-Hydroxy-Pregnenolonsulfat, **A4** Androstenedion, **ABC** *ATP binding cassette*, z.B. ABCB1, ABCC1-8, **AIS** Androgeninsensitivitätssysdrom, **AMH** Anti-Müller-Hormon, **AR** Androgenrezepor, **ASBT** *apical sodium-dependent bile transporter,* **AZF** Azoospermie-Faktor, z.B. AZFc, **BHS** Blut-Hodenschranke, **cAMP** cyclisches Adenosinmonophosphat, **CBAVD** *congenital bilateral aplasia of vasa deferentia,* **CRPC** *castration resistant prostata carcinoma,* **CS** Cholesterolsulfat, **CYP, P_{450}** Cytochrom P_{450}, z.B. CYP11A1, CYP17A1, CYP19A1, CYP21A1, P_{450}scc, P_{450}aro, **DHEA** Dehydroepiandrosteron, **DHEAS** Dehydroepiandrosteronsulfat, **DHT** Dihydrotestos-teron, **DOC** Desoxycorticosteron, **EGF** *Epidermal growth factor,* **elSd** elongierte Spermatiden, **ESR1** Estrogenrezeptor 1, auch ERalpha oder Erα, **ESR2** Estrogenrezeptor 2, auch ERbeta oder ERβ, **FSH** Follikelstimulierendes Hormon, **GnRH** *Gonadotropin releasing hormone,* **GPCR** *G protein coupled receptor*, z.B. GPRC6A, **HSD** Hydroxysteroiddehydrogenase, z.B. 3β-HSD, 17β-HSD1, 17β-HSD3, **IHC** Immunohistochemie, **ISH** *in situ*-Hybridisierung, **ISZ** immature Sertolizellen, **LACP** *Laser-assisted cell picking,* **LC** Leydigzellen, **LDL** *low-density lipoprotein,* **LH** Luteinisierendes Hormon, **Ligamentum/Lig.** Bandstruktur, **Lp** Lamina propria (Tubuluswand), **lSz** leptotäne Spermatozyten, **MA** Maturationsarrest, **MDR1** *multidrug resistance protein 1,* **mPRα** membranständiger Progesteronrezeptor, **MRPs** *multidrug resistance-related proteins,* **Musculus/M.** Muskel, **NOA** nicht-obstruktive Azoospermie, **NTCP** *Na^+-taurocholate cotransporting peptide,* **OA** obstruktive Azoospermie, **OATPs** *organic anion transporting polypeptides*, gehören zur SLCO-Superfamilie (O = OATP), **OSCP1** *organic solute carrier protein 1,* **PGCs** *primordial germ cells*/Urkeimzellen, **P-gp** P-Glycoprotein, **PREG** Pregnenolon, **PREGS** Pregnenolonsulfat, **Processus/Proc.** Fortsatz, **PTC** peritubuläre Myoidzellen, **qRT-PCR** quantitative RT-PCR, **rSd** runde Spermatiden, **RT-PCR** Reverse-Transkription Polymerasekettenreaktion, **SC** Sertolizellen, **SCO** Sertoli cell only Syndrom, **SDA** Spermatidenarrest, **Sg** Spermatogonien, **SGA** Spermatogonienarrest, **SLC** *Solute carrier*-Superfamilie, z.B. SLC10A1, SLC10A2, SLC10A6, **SO_3^-** Sulfitrest, **SOAT** *sodium-dependent organic anion transporter,* **SRY** *Sex determining region on Y chromosome,* **StAR** *Steroidogenic Acute Regulatory Protein,* **STS** Steroidsulfatase, **SULT** Sulfotransferase, z.B. SULT2A1, **Sz** Spermatozyten, **SZA** Spermatozytenarrest, **TAF** Transaktivierungsfunktion, z.B. AF-1, AF-2, AF-5, **TS** Testosteronsulfat, **TubS** Tubulusschatten, **UGT** Uridindiphosphoglucuronisyltransferase, z.B. UGT1, UGT2, **WB** Western Blot, **WHO** *World Health Organisation,* **ZIP9** membranständiger Androgenrezeptor aus der Zinkfinger-Superfamilie

2. Abbildungsverzeichnis

3. Auflistung der Publikationen als Teil der Habilitationsschrift

Die nachfolgend aufgelisteten Publikationen sind nicht chronologisch, sondern nach Arbeitsthemen geordnet.

Arbeiten zur Expression und Funktion klassischer Steroidhormonrezeptoren

1. K.A. Hose, K. Häffner, **D. Fietz**, J. Gromoll, T. Eckert, S. Kliesch, H. Siebert, M. Bergmann. A novel sequence variation in the transactivation regulating domain of the human androgen receptor. Fertil Steril 2009 92:390.e9-390.e11. **Impact factor 2009: 3,97**
2. **D. Fietz**, J. Geyer, S. Kliesch, J. Gromoll, M. Bergmann. Evaluation of CAG repeat length of Androgen Receptor expressing cells in human testes showing different pictures of spermatogenic impairment. Histochem Cell Biol 2011 136:689-697. **Impact factor 2011: 2,59**
3. **D. Fietz***, C. Ratzenböck*, O. Raabe, K. Hartmann, S. Kliesch, W. Weidner, J. Klug, M. Bergmann. Expression pattern of estrogen receptors α and β and G-protein-coupled estrogen receptor 1 in the human testis. Histochem Cell Biol 2014 142(4):421-432. **Impact factor 2014: 2,93**
4. **D. Fietz***, M. Markmann*, D. Lang, L. Konrad, S. Kliesch, T. Chakraborty, H. Hossain*, M. Bergmann. Transfection of Sertoli cells with Androgen Receptor alters gene expression without androgen stimulation. BMC Mol Biol 2015 Dec 29;16(1):23. doi: 10.1186/s12867-015-0051-7. **Impact factor 2015: 2,19**

Arbeiten zur Expression und Funktion von Transportern für konjugierte Steroidhormone im Hoden

5. **D. Fietz***, K. Bakhaus*, B. Wapelhorst, G. Grosser, S. Günther, J. Alber, B. Döring, S. Kliesch, W. Weidner, C.E. Galuska, M.F. Hartmann, S.A. Wudy, M. Bergmann, J. Geyer. Membrane transporters for sulfated steroids in the human testis - Cellular localization, expression pattern and functional analysis. PLoS One 2013 8(5): e62638. **Impact factor 2013: 3,53**
6. G. Grosser, **D. Fietz**, S. Günther, K. Bakhaus, H. Schweigmann, B. Ugele, R. Brehm, E. Petzinger, M. Bergmann, J. Geyer. Cloning and functional characterization of the mouse sodium-dependent organic anion transporter Soat (Slc10a6). J Ster Biochem Mol Biol 2013 138C:90-99. **Impact factor 2013: 4,01**
7. K. Hartmann, J. Bennien, B. Wapelhorst, K. Bakhaus, V. Schumacher, S. Kliesch, W. Weidner, M. Bergmann, J. Geyer, **D. Fietz**. Current insights into the sulfatase pathway in human testis

and cultured Sertoli cells. Histochem Cell Biol 2016 Dec;146(6):737-748. **Impact factor 2015/2016: 2,78**

8. J. Geyer, K. Bakhaus, R. Bernhardt, C. Blaschka, Y. Dezhkam, **D. Fietz**, G. Grosser, K. Hartmann, M.F. Hartmann, J. Neunzig, D. Papadopoulos, A. Sánchez-Guijo, G. Scheiner-Bobis, G. Schuler, M. Shihan, C. Wrenzycki, S.A. Wudy, M. Bergmann. The role of sulfated steroid hormones in reproductive processes. J Steroid Biochem Mol Biol 2016 Jul 15; pii: S0960-0760(16)30201-1. **Impact factor 2016: 3,63 REVIEW**
9. K. Bakhaus*, J. Bennien*, **D. Fietz**, A. Sánchez-Guijo, M. Hartmann, R. Serafini, C.C. Love, A. Golovko, S.A. Wudy, M. Bergmann, J. Geyer. Sodium-dependent organic anion transporter (Slc10a6-/-) knockout mice show normal spermatogenesis and reproduction, but elevated serum levels for cholesterol sulfate. J Steroid Biochem Mol Biol 2017 Jul 22. pii: S0960-0760(17)30184-X. doi: 10.1016/j.jsbmb.2017.07.019 **Impact factor 2015/2016: 3,98**
10. K. Bakhaus, **D. Fietz**, S. Kliesch, W. Weidner, M. Bergmann, J. Geyer. The polymorphism L204F affects transport and membrane expression of the sodium-dependent organic anion transporter SOAT (SLC10A6). J Steroid Biochem Mol Biol 2017 Sep 23. pii: S0960-0760(17)30265-0. doi: 10.1016/j.jsbmb.2017.09.017 **Impact factor 2015/2016: 3,98**
11. **D. Fietz**. Transporter for sulfated steroid hormones in the testis - expression pattern, biological significance and implications for fertility in men and rodents. J Steroid Biochem Mol Biol 2017 Oct 7. pii: S0960-0760(17)30270-4. doi: 10.1016/j.jsbmb.2017.10.001 **Impact factor 2015/2016: 3,98 REVIEW**

* gleichwertige Erstautoren

Zu Beginn meiner wissenschaftlichen Arbeit im Institut für Veterinär-Anatomie, -Histologie und -Embryologie arbeitete ich am Thema des klassischen Androgenzeptors im Hoden (Publikation #1 und #2), die Teil meiner Dissertationsschrift sind. So konnte ich Kontakte zum Institut für Veterinär-Pharmakologie und -Toxikologie (Prof. Dr. Ernst Petzinger und Prof. Dr. Joachim Geyer), sowie zu den andrologischen Kliniken des Universitätsklinikums Gießen-Marburg (UKGM, Prof. Dr. Wolfgang Weidner) und des Universitätsklinikums Münster (Prof. Dr. Sabine Kliesch) aufbauen. Das Nachfolgeprojekt von Dr. Dennis Lang (Promotion 2017) wurde von mir mit betreut und von mir zusammen mit dem Institut für Mikrobiologie der JLU Gießen (PD Dr. Hamid Hossain) zur Publikation gebracht (Publikation #4). Neben dem Androgenrezeptor arbeitete ich auch auf dem Gebiet der klassischen (ERS1, ERS2) und nicht-klassischen Estrogenrezeptoren (GPER) zusammen mit Dr. Jörg Klug (Institut für Humananatomie, JLU Gießen, Publikation #3). Die Publikation #3 führte zu einer

Einladung des Springerverlags für eine Veröffentlichung in *Methods Mol Biol* (Fietz et al. 2016), die allerdings nicht Teil der Habilitationsschrift ist.

Durch die Betreuung von Dr. Britta Wapelhorst (Promotion 2014) stieg ich in der ersten Förderperiode der DFG-Forschergruppe FOR1369 „Sulfated Steroids in Reproduction“ in die Untersuchung der sulfatierten Steroidhormone und ihrer spezifischen Transportsysteme mit ein. Die Ergebnisse der Arbeit von Dr. Wapelhorst wurden von mir in Zusammenarbeit mit dem Institut für Veterinär-Pharmakologie und Toxikologie veröffentlicht (Publikation #5). Parallel arbeitete ich mit Dr. Katharina Bakhaus (Promotion 2014) und Dr. Gary Grosser an der Maus (Publikation #6). In der zweiten Förderperiode der FOR 1369 konnte ich mit einem eigenen Teilprojekt (TP2 – „Membrane transporters for sulfated steroid hormones in the testis and their role for spermatogenesis and fertility“ (DFG FI 1927/1-2)) weiter an den sulfatierten Steroiden, ihren Transportern im Hoden und ihrer Bedeutung für die Spermatogenese und Fertilität des Mannes arbeiten. Aus dieser Zeit sind die Publikationen #7-11 entstanden.

Die Arbeiten für alle Publikationen fanden überwiegend im Institut für Veterinär-Anatomie, -Histologie und -Embryologie statt. Die Microarray-Versuche (Publikation #4) wurden im Institut für Humanmikrobiologie der JLU durchgeführt, die Transportversuche für die Publikationen #5-10 im Institut für Veterinär-Pharmakologie und -Toxikologie. Die Slc10a6 KO Maus wurde von Prof. Dr. Joachim Geyer sowie Dr. Katharina Bakhaus generiert und im Tierstall des Biomedizinischen Forschungszentrums (BFS) der JLU Gießen gehalten. Die histologische Phänotypisierung der Maus fand im Institut für Veterinäranatomie statt.

4. Einleitung I: Anatomie und Histologie des Hodens, Grundprinzipien der Spermatogenese

4.1. Anatomie des Hodens

Der Hoden ist sowohl endokrine Drüse als auch Keimdrüse, da hier Sexualhormone (Androgene und Estrogene) produziert werden und die Spermien heranreifen. Die Hoden liegen bei allen Säugetieren mit einzelnen Ausnahmen wie zum Beispiel bei Elefanten, Robben und Walen umgeben von den Hodenhüllen außerhalb des Körpers. Die Keimzellreifung ist stark temperaturabhängig. Innerhalb des Skrotums ist die Temperatur um 1-2°C niedriger als im Körper.

4.1.1. Hodenhüllen

Zu den Hodenhüllen gehören das *Scrotum* und der *Proc. vaginalis*. Das *Scrotum* wird durch *Septum scroti* und *Raphe scroti* in zwei mehr oder minder gleichgroße Höhlen unterteilt, in denen jeweils ein Scheidenfortsatz, *Proc. vaginalis*, liegt.

Das *Scrotum* gehört zu den sekundären Geschlechtsorganen und entsteht unter dem Einfluss der fetalen Androgene beim Menschen etwa in der achten Woche nach der Befruchtung, indem sich die labioskrotalen Falten zum Skrotum schließen (Übersicht bei Wartenberg et al. 1993). Es besteht aus mehreren Schichten; ganz außen befindet sich die schwach behaarte, äußere Haut mit Schweiß- und Talgdrüsen, darunter eine modifizierte Unterhaut (*Tunica dartos*) und als innerste Schicht liegt eine Abspaltung der äußeren Rumpffaszie (*Fascia spermatica externa*) dem *Proc. vaginalis* direkt auf. Die *Tunica dartos* enthält viele glatte Muskelfasern, da die Haut zu Zwecken der Thermoregulation gerunzelt werden kann.

An die Schichten des Skrotums schließen sich die beiden Schichten des *Proc. vaginalis* an. Der Scheidenhautfortsatz entsteht in etwa in der 13 Woche der Schwangerschaft als Ausbuchtung der inneren Rumpffaszie (hier: *Fascia spermatica interna)* und des parietalen Peritoneums (hier: paritales Blatt der *Tunica vaginalis*). Diese Ausstülpung bewegt sich durch den Leistenkanal (*Canalis inguinalis*), der von den Aponeurosen des inneren und äußeren schiefen Bauchmuskels (*M. obliquus internus et externus abdominis*) gebildet wird, in das Skrotum hinein. In den *Proc. vaginalis* senkt sich der vom viszeralen Blatt der *Tunica vaginalis* überzogene Hoden beim Hodenabstieg (s. 4.1.3.). Ein Gekröse, *Mesorchium* und *Mesepididymidis*, verbindet beide Schichten der *Tunica vaginalis* (Übersicht bei Gray et al. 1918; Singh 2014). Zwischen der *Fascia spermatica externa et interna* liegt der *M. cremaster*, eine Abspaltung des *M. obliquus internus abdominis*. Er wird als Heber des *Proc.*

vaginalis bezeichnet, da er diesen mitsamt seines Inhalts in Richtung Bauchwand bewegen kann. Innerhalb des *Proc. vaginalis* liegen Hoden, Nebenhoden, Samenstrang mit Gefäßen, Nerven sowie der Samenleiter.

Anders als beim Tier im Allgemeinen verschließt sich beim Menschen der flaschenhalsähnliche Anfangsteil des *Proc. vagnialis* um die Geburt herum, so dass beim Menschen keine offene Verbindung zwischen Bauchhöhle, Leistenkanal sowie Skrotum mehr besteht. Ein mangelnder Schluss des *Proc. vaginalis* ist die Hauptursache für Leistenbrüche mit Vorfall von Darmschlingen in das *Scrotum* bei Kindern und Jugendlichen. Außerdem kann ein mangelnder Verschluss zu Hydrozelen (Ansammlung von Bauchhöhlenflüssigkeit im *Proc. vaginalis*), Samenstranghydatiden sowie Leistenbrüchen im Erwachsenenleben führen (Übersicht bei Hutson et al. 1997). Im Gegensatz dazu bleibt bei den Tieren im Allgemeinen die offene Verbindung über den Leistenkanal physiologisch ein Leben lang bestehen, so dass der *M. cremaster* den *Proc.vaginalis* samt seines Inhalts anheben bzw. sogar in die Bauchhöhle hineinziehen kann. Dieses Phänomen kann vor allem bei Nagern und Kaninchen beobachtet werden.

4.1.2. Bänder des Hodens

Während der Entwicklung sind das kraniale und das kaudale Keimdrüsenband ausgebildet. Während sich das kraniale Keimdrüsenband zurückbildet, leitet das kaudale Keimdrüsenband den sich entwickelnden Hodens durch den Leistenkanal und bleibt mit dessen kaudalen Pol verbunden (s. 4.1.3.). Beim Menschen bildet sich nach dem erfolgten Hodenabstieg der vordere Teil des kaudalen Keimdrüsenbandes (*Gubernaculum testis*) zurück, der hintere Anteil wird zu den Bändern des Skrotums, *Ligamenta scroti*, die den Hoden und Nebenhoden mit dem Grund des *Proc. vaginalis* verbinden. Dieses Band ist bei den meisten Männern sichtbar (Shafik 1977). Das kaudale Keimdrüsenband bzw. seine Überreste beim Mann sind normalerweise sehr kurz und fest (Übersicht bei Migaleddu et al. 2012). Verlängerte bzw. zu lockere Bänder in diesem Bereich können eine Prädisposition für eine Hodentorsion sein, ein urologischer Notfall, der vor allem bei Kindern und jungen Männern auftritt (Shimizu et al. 2016). Hodentorsionen führen zu einer Ischämie des betroffenen Hodens, was akut zu starken Schmerzen und subchronisch zu Spermatogenesestörungen und im schlimmsten Fall zum Verlust eines oder beider Hoden führen kann (erworbene Anorchie) (Übersicht bei Nieschlag et al. 2010).

Bei unseren Haussäugetieren können zwei Anteile aus dem kaudalen Keimdrüsenband differenziert werden. Diese sind das *Ligamentum testis proprium* vom kaudalen Pol des Hodens zum

Nebenhodenschwanz und das *Ligamentum caudae epididymidis* vom Nebenhodenschwanz zum Grund des *Proc. vaginalis* (siehe Übersicht bei Gasse 2004).

4.1.3. Hodenabstieg (Descensus testis)

Der Hodenabstieg ist für die Hodenfunktion essentiell, da die Spermatogenese nur bei einer Temperatur von 1-2 °C unter der Körpertemperatur korrekt ablaufen kann und zudem die Mutationsrate in der Keimbahn minimiert werden kann (Übersicht bei Mamoulakis et al. 2015). Fieberhafte Allgemeinerkrankungen und hochfieberhafte Virusinfektionen können zu einer vorübergehenden Schädigung der Keimzellentwicklung führen, die allerdings meist reversibel ist (Übersicht bei Sartorius and Handelsman 2010).

Die embryonale Hodenanlage entsteht kaudal der Nieren und wandert durch das Längenwachstum des Körpers sowie geführt durch das *Gubernaculum testis* von dieser Position an der lateralen Bauchwand entlang zum inneren Leistenring (*Anulus inguinalis profundus*), der vom *M. obliquus internus abdominis* und dem *Ligamentum inguinale* gebildet wird. Durch den inneren Leistenring tritt der Hoden dann in den Leistenspalt (*Canalis inguinalis*) ein und durch den äußeren Leistenring (*Anulus inguinalis superficialis*) hindurch in den *Proc. vaginalis* (Übersicht bei Gasse 2004; Singh 2014). Der Hodenabstieg umfasst zwei aufeinanderfolgende Phasen. Die erste Phase des Abstiegs ist androgen-unabhängig. Die Hoden gelangen durch die Verkürzung des kaudalen Keimdrüsenbandes vom Kaudalrand der Nieren vor den Inguinalspalt. In der zweiten Phase wächst dann das kaudale Keimdrüsenband durch den Inguinalkanal in das Skrotum hinein und zieht den Hoden mit sich. Dieser Vorgang ist androgen-abhängig und wird durch einen erhöhten intraabdominellen Druck noch begünstigt. Ein weiterer Faktor, der den Abstieg in das Skrotum beeinflusst, ist der Insulin-like Faktor 3 (INSL3), der von den Leydigzellen produziert wird. Alle Faktoren führen dazu, dass bis ca. 12 Wochen nach der Geburt bei 97% der Jungen die Hoden den Boden des Skrotums erreichen (Übersicht bei Weinbauer et al. 2010; Mamoulakis et al. 2015). Während bei Schwein und Pferd der Hodenabstieg um die Geburt herum stattfindet, ist er bei Rindern schon nach der Hälfte der Trächtigkeit abgeschlossen (Übersicht bei Amann und Veeramachaneni 2007). Bei Nagern und Kaninchen dagegen ist der Abstieg erst 3-14 Tage nach der Geburt vollendet.

Störungen des Hodenabstiegs, z.B. durch eine insuffiziente Androgen- und/oder INSL3-Produktion der Leydigzellen sowie Rezeptordefekte, führen zu Krytporchismus (Übersicht bei Amann und Veeramachaneni 2007). Dieser wird in eine abdominelle und eine inguinale Form eingeteilt. Während bei einem abdominellen Kryptorchismus der Hoden vollständig in der Bauchhöhle verbleibt, ist er bei einem inguinalen Kryptorchismus vor den inneren Leistenring bzw. in den *Canalis inguinalis*

eingetreten. Beim Menschen liegt die Prävalenz für einen ein- bzw. beidseitigen Kryptorchismus zwischen 0,5% (Erwachsene) und 2,2% (Kinder und Jugendliche). Auch in anderen Spezies liegt die Prävalenz für Kryptorchismus bei < 5% mit einer eventuellen Häufung beim Schwein. Die Frequenz des Kryptorchismus beim Schwein liegt bei 0,2 - 2,0% und die Ursache ist häufig ein erblicher Defekt der Gubernakulumfunktion. Neben einem mangelhaften Abstieg eines oder beider Hoden ist bei diesen Ebern in der Regel auch kein *Proc. vaginalis* ausgebildet (Übersicht bei Bickhardt et al. 2004). Meistens handelt es sich um einen unilateralen Kryptorchismus. Die Lage variiert allerdings zwischen den Spezies: während beim Menschen meistens ein inguinaler oder retraktiler Kryptorchismus vorliegt (Übersicht bei Nieschlag et al. 2010), findet man den/die Hoden beim Hengst meistens in der Bauchhöhle (Übersicht bei Amann und Veeramachaneni 2007). Beim Menschen handelt es sich in 85% der Fälle um einen idiopathischen Kryptorchismus, in nur 15% der Fälle können Ursachen wie endokrine Störungen oder anatomische Anomalien benannt werden. Neben gentischen Faktoren wird auch die Exposition mit sog. *endocrine disruptors,* Umweltfaktoren mit androgener oder estrogener Wirkung (Übersicht bei Amann und Veeramachaneni 2007) als mögliche Ursache für den Kryptorchismus diskutiert. Alle Formen des Kryptorchismus prädisponieren für die Entstehung von Neoplasien, da die erhöhte Umgebungstemperatur Mutationen in den Keimzellen und somit deren Entartung begünstigen kann. Des Weiteren schädigt die erhöhte Temperatur die Entwicklung der Keimzellen, so dass es zu leichten bis schweren Störungen der Spermatogenese kommen kann. Menschen bzw. Tiere mit beidseitigem Kryptorchismus sind meist infertil, während bei einem einseitigen Kryptorchismus in dem abgestiegenen Hoden eine normale Spermatogenese möglich ist (Übersicht bei Nieschlag et al. 2010).

4.2. Histologie des Hodens

4.2.1. *Tunica albuginea* und *Septulae testis*

Die *Tunica albuginea* ist eine derbe, aus straffem kollagenen Bindegewebe bestehende Organkapsel, die sowohl den Hoden als auch den Nebenhoden umgibt. Sie hält das Hodenparenchym unter stetem Druck, was beim Anschneiden der *Tunica albuginea* zu einem Herausquellen des Hodenparenchyms führt. Direkt unter der *Tunica albuginea* befindet sich die gefäßreiche *Tunica vasculosa*, die Gefäße in das Innere des Organs führt. Des Weiteren spalten sich von der *Tunica albuginea* bindegewebige Septen ab (*Septula testis*), die das Hodenparenchym in Läppchen (*Lobuli testis*) unterteilen und in der Mitte (Wiederkäuer, Schwein) bzw. dem Rand des Hodens (Mensch, Pferd) das bindegewebige *Mediastinum testis* bilden (Übersicht bei Gasse 2004; Singh 2011) (Abb. 1).

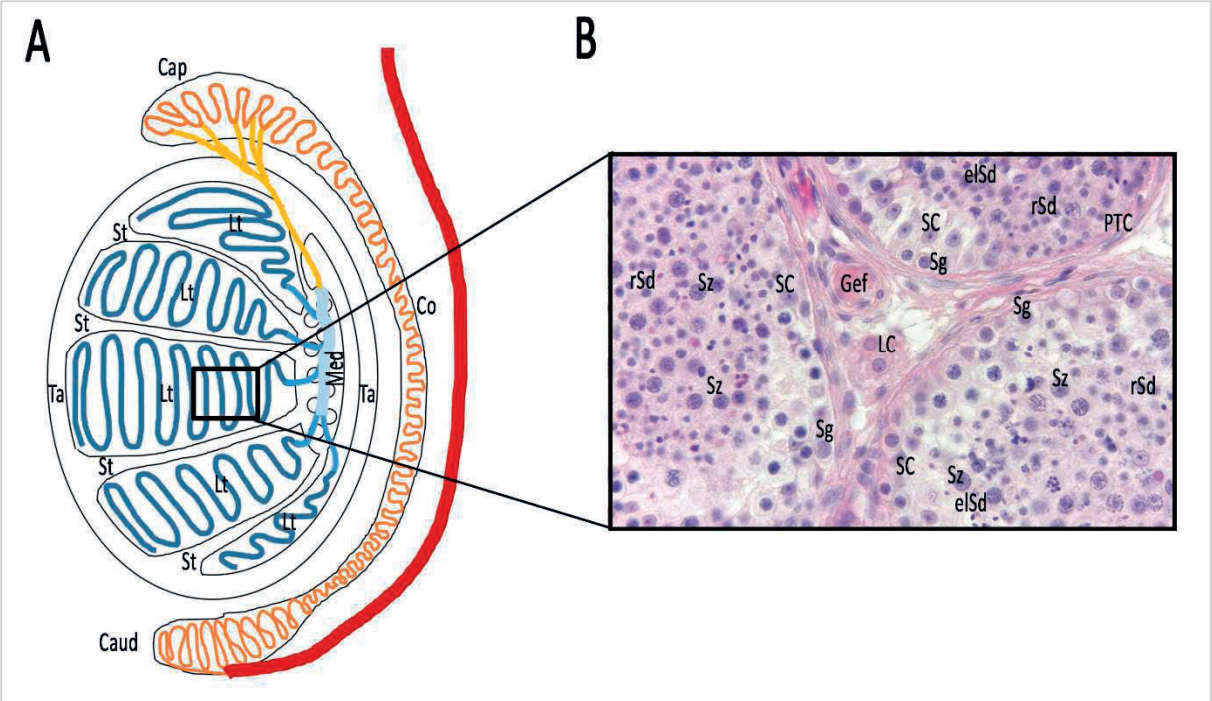

Abb. 1 Hodenanatomie und -histologie

A Schematische Darstellung des Hodens und des Nebenhodens: Ta *Tunica albuginea*, St *Septula testes*, Med *Mediastinum* mit *Rete testis* (hellblau), Lt *Lobuli testes* mit *Tubuli seminiferi contorti* (dunkelblau) und *Tubuli seminiferi recti* (mittelblau), *Ductuli efferentes testis* (gelb), Cap *Caput epididymidis*, Co *Corpus epididymidis*, Caud *Cauda epididymidis,* jeweils mit *Ductus epididymidis* (orange), *Ductus deferens* (rot)

B Der Ausschnitt zeigt Tubuli seminiferi contorti mit dem umgebendem interstitiellen Bindegewebe: PTC *peritubuläre Myoidzellen*, LC *Leydigzellen*, Gef *Gefäße*, SC *Sertolizellen*, Sg *Spermatogonien*, Sz *Spermatozyten*, rSd *runde Spermatiden*, elSd *elongierte Spermatiden*; primäre Vergrößerung x 40, Färbung: Hämatoxylin und Eosin

4.2.2. *Tubuli seminiferi contorti* mit Keimepithel

In den *Lobuli testis* liegen die gewundenen Samenkanälchen, *Tubuli seminiferi contorti*, in denen das Keimepithel liegt. Von außen sind sie von der sog. Tubuluswand (*Lamina propria*) umgeben. Diese besteht aus kollagenen Fasern und vier bis fünf Schichten von peritubulären Myoidzellen. An die nachfolgende Basalmembran schließt sich das Keimepithel an.

Die peritubulären Myoidzellen sind modifizierte, kontraktile Fibrozyten, die die peristaltische Bewegung der *Tubuli seminiferi contorti* erzeugen und so den Spermientransport unterstützen (Übersicht bei Albrecht 2009). Des Weiteren sezernieren die peritubulären Myoidzellen Strukturproteine wie z.B. Kollagen unterschiedlicher Typen, Laminin und Fibronectin sowie Faktoren, die die Spermatogenese beeinflussen können. Eine Verdickung der *Lamina propria* kann häufig bei Störungen der Spermatogenese beobachtet werden (Sato et al. 2008). Bei einer testikulären Prä-Kanzerose (*germ cell neoplasia in situ*, Berney et al. 2016) kann dagegen eine Auflösung der Tubuluswand beobachtet werden, die zu einer Ausbreitung der Tumorzellen im Interstitium führt

(Donner et al. 2004). Dies steht im Gegensatz zu der bis dahin geltenden Hypothese, dass die entarteten Keimzellen aktiv aus dem Tubulus auswandern können.

Das Keimepithel besteht aus somatischen Sertolizellen und aus den verschiedenen Keimzellstadien und -assoziationen (s. 4.3.) (Abb. 2).

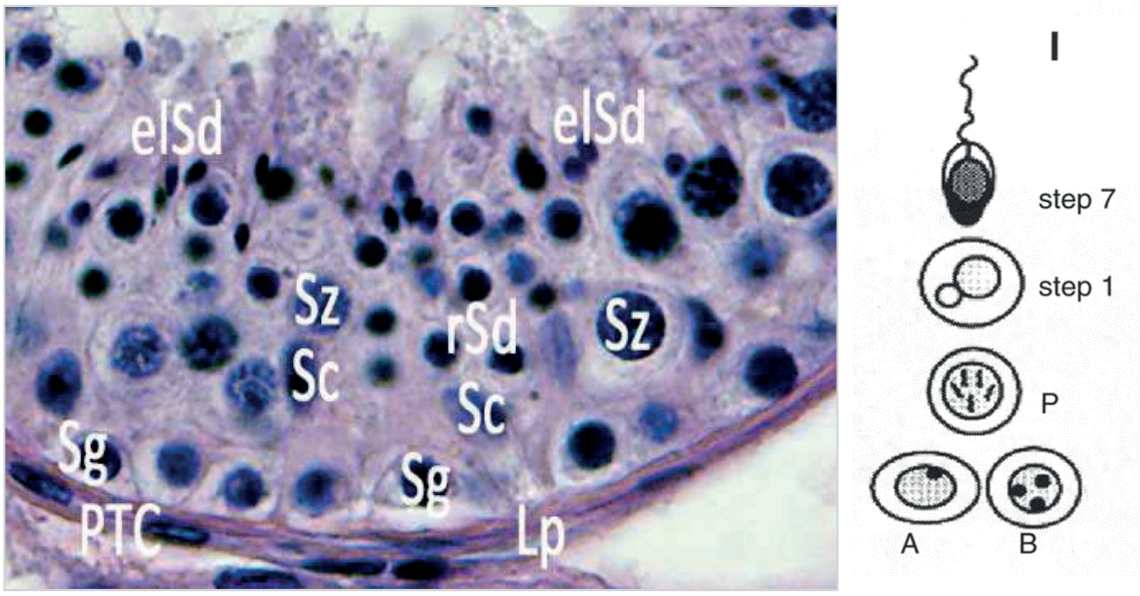

Abb. 2 Keimepithel

Sertolizellen (SC) umfassen mit ihrem Zytoplasma verschiedene Keimzellstadien, z.B. A und B Spermatogonien (Sg), pachytäne Spermatozyten (Sz), runde Step 1 und elongierte Step 7 Spermatiden (rSd und elSd). Das Keimepithel baut auf der Basalmembran und der *Lamina propria* (Lp) auf, in die peritubuläre Myoidzellen (PTC) eingelagert sind. Primäre Vergrößerung x40, Färbung Hämatoxylin und Eosin. **Rechts** Schematische Darstellung des Spermatogenesestadiums (hier: Stadium I)

Die Sertolizellen werden auch als „Ammenzellen“ bezeichnet, da sie mit ihrem weit auslaufenden Zytoplasma die verschiedenen Keimzellstadien umgeben und somit Ernährungs- und Stützfunktion haben (Sertoli 1865, Übersicht bei Griswold 1998) (Abb. 3A). Sie differenzieren sich aus dem Zölomepithel und sind die ersten Zellen in der fetalen Gonade. Sie initiieren die Bildung der Keimtubuli, ermöglichen die Besiedlung des fetalen Hodens durch die primordialen Keimzellen (Gonozyten) und führen zur Differenzierung fetaler Leydigzellen (Übersicht bei Sharpe et al. 2003; Cupp und Skinner 2005). Die Sertolizellreifung wird als essentieller Schritt zur Initiierung und Erhaltung der Spermatogenese gesehen. Diese Reifungsvorgänge sind sowohl morphologisch als auch molekularbiologisch definiert: Während unreife Sertolizellen einen runden, dunklen Zellkern haben (Abb. 3B, unteres Bild), zeigen reife Sertolizellen einen eher dreieckigen Zellkern mit deutlichen Kernkörperchen (Abb. 3B, oberes Bild), eine vergrößerte Zelloberfläche und ein erhöhtes Kernvolumen (Bruning et al. 1993).

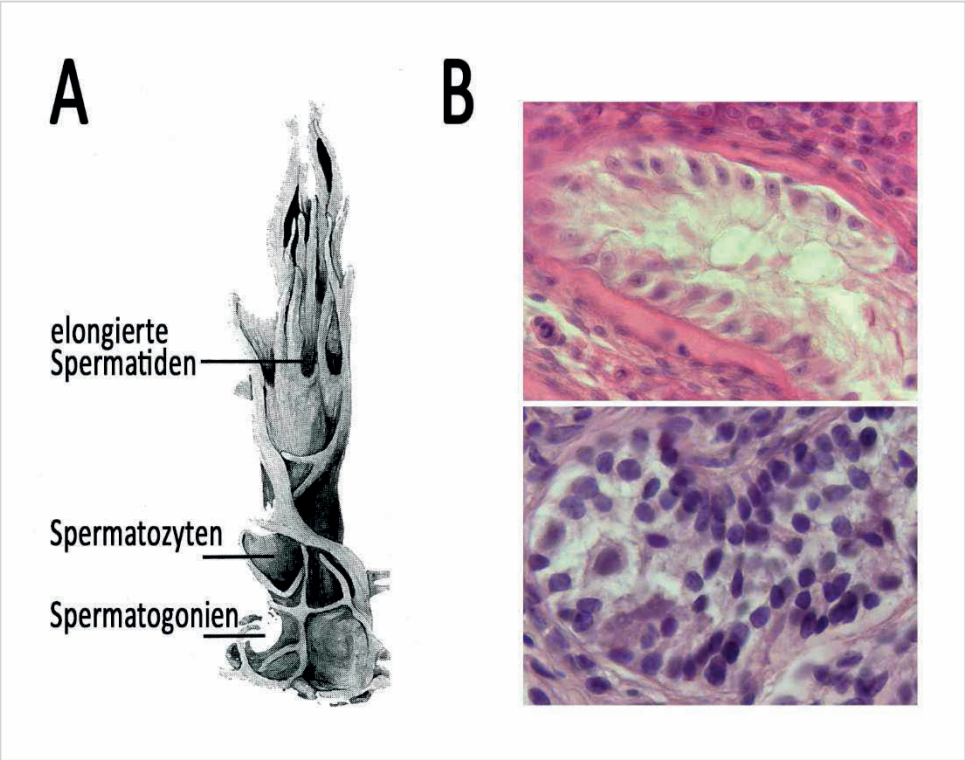

Abb. 3 Sertolizellmorphologie

A Schematische Darstellung der Sertolizellmorphologie bei normaler Spermatogenese (modifiziert von Hess und França 2005). In den zytoplasmatischen „Taschen" liegen die verschiedenen Keimzellstadien wie hier angedeutet.

B Vergleich zwischen den reifen Sertolizellen eines Patienten mit sekundärem Keimzellverlust (Sertoli cell only Syndrom, oberes Bild) und den unreifen Sertolizellen eines juvenilen Patienten (Vorstellung wegen testikulärer Feminisierung, unteres Bild). Während die reifen Sertolizellkerne eher eckig sind und einen deutlichen Nukleolus aufweisen, sind die Zellkerne unreifer Sertolizellen rund bis oval und einheitlich dunkler gefärbt. Primäre Vergrößerung oberes Bild x 20, unteres Bild x 40; Färbung Hämatoxylin und Eosin.

Einer der wichtigsten Reifungsprozesse der Sertolizellen ist die Bildung der Blut-Hoden-Schranke (BHS). Diese wurde erstmals 1970 bei der Ratte beschrieben (Dym and Fawcett 1970) und bildet sich, sobald die ersten pachytänen Spermatozyten (s. 4.3.1.) im Keimepithel detektiert werden können (Bergmann und Dierichs 1983). Beim Menschen wurde die BHS erstmals 1989 beschrieben (Bergmann et al. 1989). Die BHS besteht aus interzellulären Kontaktzonen (*Zonulae occludentes* oder *Tight junctions*), Aktinfilamenten und Spezialisierungen der Sertolizellmembran, die auch als ektoplasmatische Spezialisierungen bezeichnet werden (Abb. 4). Während sich Spermatogonien und präleptotäne Spermatozyten (s. 4.3.1.) noch im basalen Kompartiment des Keimepithels befinden, sind spätere Keimzellstadien mit ihren neu gebildeten Oberflächenmarker im adluminalen Kompartiment vor dem Immunsystem (Aufbau des testikulären Immunprivilegs) und anderen endo- und exogenen Stoffen geschützt. Nur Stoffe mit einem sehr geringen Molekulargewicht können noch

frei zwischen den Sertolizellen hindurch zu den Keimzellen oberhalb der BHS diffundieren, alle anderen Stoffe müssen erst die Sertolizellen passieren. Durch die Bildung der BHS sind die Sertolizellen auch in der Lage, die intratubuläre Flüssigkeit zu sezernieren, was schlussendlich zur Bildung des Tubuluslumens führt, ein weiteres Reifezeichen im adulten Hoden. Im Bereich des *Rete testis* (s. 4.2.4.) ist die BHS nicht mehr durchgehend dicht. Aus diesem Grund nehmen die meisten Entzündungsvorgänge mit Immunzellinfiltration hier ihren Anfang (Johnson 1970; Naito and Itoh 2008).

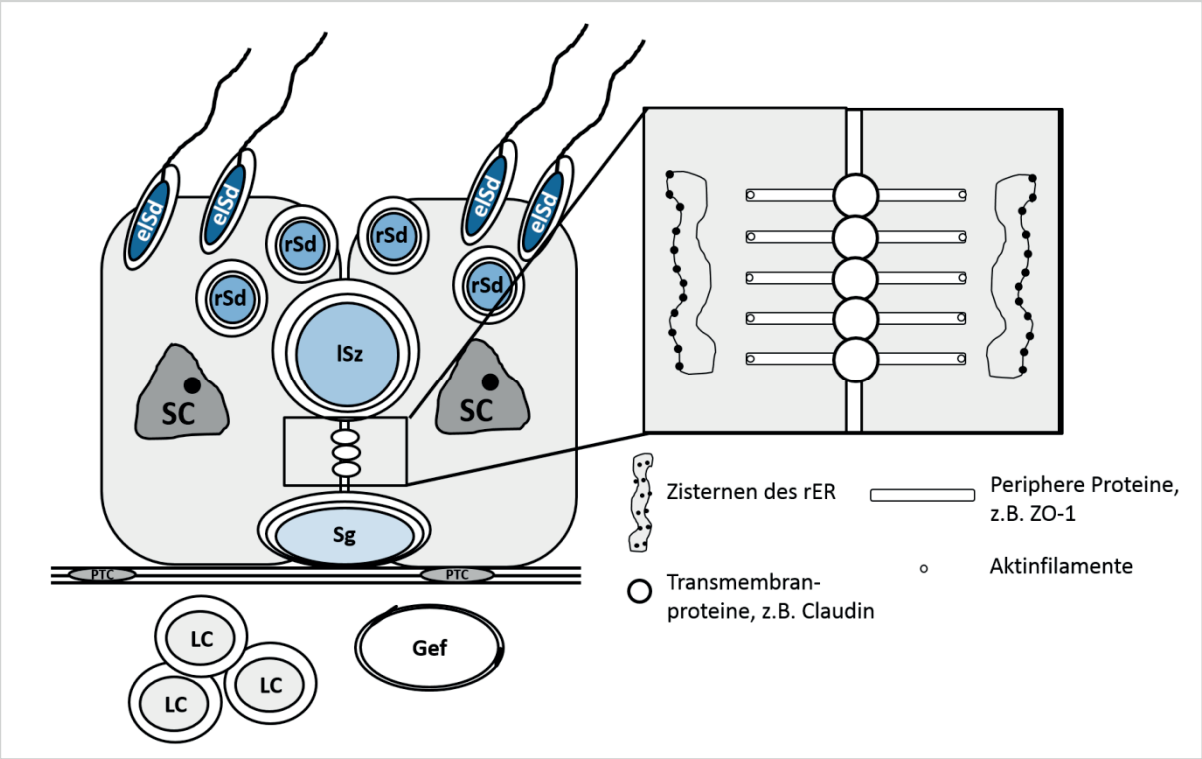

Abb. 4 Schematische Darstellung der Blut-Hoden-Schranke

Die *tight junctions* zwischen zwei benachbarten Sertolizellen unterteilen das Keimepithel in ein basales und ein adluminales Kompartiment. Während sich im basalen Kompartiment Spermatogonien (Sg) und präleptotäne Spermatozyten befinden, halten sich die weiteren Keimzellstadien ab den leptotänen Spermatozyten (lSz), d.h. runde und elongierte Spermatiden (rSd, elSd) im adluminalen Kompartiment des Keimepithels auf. Die *tight junctions* bestehen aus transmembranären Proteinen (z.B. Claudin beim Menschen, Claudin und Occludin bei Nagern), peripheren Proteinen (z.B. Zona occludens-Proteine 1 und 2) und ektoplasmatischen Spezialisierungen. Aktinfilamente verbinden die *tight junctions* mit dem Zytoskelett der Sertolizelle und Zisternen des rauen endoplasmatischen Retikulums sind in der Nähe der *tight junctions* lokalisiert. Beide Sertolizellmembranen verschmelzen in diesem Bereich so eng miteinander, dass kein interzellulärer Spalt mehr sichtbar ist.

Molekularbiologische Reifungsvorgänge umfassen die Umstellung des „fetalen“ auf das „adulte“ Expressionsprofil. Fetale Sertolizellen exprimieren als wichtigsten Marker das Anti-Müller-Hormon (AMH), das zu einer Regression der Müllerschen Gänge führt. Im Gegensatz dazu exprimieren reife

Sertolizellen u.a. den Androgenrezeptor und Inhibin B (Übersicht bei Sharpe et al. 2003; Walker 2009). Sertolizellen werden durch das hypophysäre Follikelstimulierende Hormon (FSH) stimuliert und vermitteln die Hormonwirkung auf die Keimzellen.

Etwa 35-40% der Zellen im Keimepithel sind Sertolizellen, das sind in einem adulten Hoden mit normaler Spermatogenese ca. 800-1200 x 10^6 Sertolizellen. Eine Sertolizelle steht im engen Kontakt zu etwa zehn Keimzellen bzw. 1,5 Spermien (Zhengwei et al. 1998). Im Gegensatz dazu ist beim Makaken eine Sertolizelle mit ca. 22 Keimzellen und 2,7 Spermien assoziiert (Zhengwei et al. 1997). Die Effizienz der Spermatogenese und damit der Spermienproduktion ist eng mit der Zahl der Sertolizellen verknüpft. Von Sharpe et al. (2003) wurde deshalb postuliert, dass eine verringerte Spermatogeneseeffizienz mit einer abnehmenden Sertolizellzahl im Alter assoziiert sei. Die elongierten Spermatiden werden aktiv von den Sertolizellen in das Tubuluslumen entlassen. An diesem Vorgang, dem sog. *sperm release*, ist die Modifikation von apikalen ektoplasmatischen Spezialisierungen essentiell (Übersicht bei Berruti und Paiardi 2014).

Lange Zeit galten reife Sertolizellen als postmitotische, endgültig differenzierte Zellen. Neuere Studien dagegen beschreiben durchaus die Fähigkeit zur Proliferation und DNA-Reparatur (Brehm et al. 2006; Ahmed et al. 2009; Tarulli et al. 2012). Brehm et al. (2006) beschrieben die Proliferationsaktivität von Sertolizellen bei Patienten mit sog. immaturen Sertolizellen.

Bei Störungen der Spermatogenese (s. 3.4.) kommt es sowohl zu morphologischen als auch molekularbiologischen Veränderungen in der Sertolizelle bzw. ihrer Biologie. Deswegen können die Sertolizellen als Marker für Spermatogenesestörungen verwendet werden. Morphologische Veränderungen umfassen v.a. die Kernmorphologie. Während eine Sertolizelle bei normaler Spermatogenese ein mittleres Kernvolumen von 410 μm^3 und eine mittlere Zelloberfläche von 430 μm^2 zeigt, sind beide Werte bei einer bunten Atrophie der Spermatogenese (Sigg 1979) (s. 4.4.) deutlich kleiner (Bruning et al. 1993). Bei primärem oder auch sekundärem Keimzellverlust kann eine Differenzierung der Sertolizellen entweder ausbleiben oder die Sertolizelle kann de-differenzieren. Beides wird durch die Expression fetaler Marker wie AMH oder Zytokeratin 18 deutlich, wie sie bei gestörter Sertolizellfunktion bzw. in Kontakt mit testikulärer Prä-Kanzerose (GCNIS) vorkommt (Bergmann und Kliesch 1994; Kliesch et al. 1998).

4.2.3. Interstitium

Im lockeren Bindegewebe des Hodeninterstitiums, dem Bereich zwischen den *Tubuli seminiferi contorti*, liegen Leydigzellen, Blut- und Lymphgefäße, Zellen des Immunsystems sowie einzelne Nervenfasern. Das Interstitium macht beim Menschen ähnlich wie bie Bulle und Schafbock etwa 12-

15% des Hodenvolumens aus. Im Gegensatz dazu findet man bei Eber und Hengst mit ca. 40% deutlich mehr interstitielles Gewebe (Übersicht bei Dyce et al. 2002; Weinbauer et al. 2010). Bei Nagern und beim Hund dagegen ist das interstitielle Bindegewebe eher spärlich und besteht aus kleineren Leydigzellgruppen, die sich um die Blutgefäße sammeln (Übersicht bei Setchell und Breed 2006).

Die Leydigzellen sind die häufigsten Zellen im Interstitium und liegen dort entweder einzeln oder auch in kleineren Gruppen vor. Sie wurden 1850 von Franz von Leydig beschrieben und sind in die testikuläre *de novo* Steroidhormonsynthese eingebunden. Man unterscheidet zwischen Stamm-, Vorläufer-, fetalen und adulten Leydigzellen nach morphologischen und funktionellen Gesichtspunkten (Übersicht bei Svechnikov et al. 2010). Der Ursprung der Leydigzellen ist immer noch nicht endgültig geklärt, denn fetale Leydigzellen lassen sich von verschiedenen embryonalen Geweben, u.a. dem Zölomepithel, dem Mesenchym der Genitalfalte und wandernden Mesonephroszellen, aber auch von Zellen der fetalen Nebenniere ableiten (Hatano et al. 1996, Übersicht bei Wen et al. 2016). Im humanen Fetus können die ersten fetalen Leydigzellen bereits in der 7. bis 8. Schwangerschaftswoche detektiert werden und stellen hier die einzige Quelle für Androgene dar. Diese sog. „Mini-Pubertät“ ist unabhängig von der Ausschüttung des luteinisierenden Hormons (LH) und ermöglicht die Virilisierung des Fetus (Übersicht bei Davidoff et al. 2009; Svechnikov et al. 2010). Fetale Leydigzellen produzieren allerdings kein Testosteron, sondern Androstenedion, da ihnen das Enzym 17β-Hydroxysteroiddehydrogenase (17β-HSD, s. 5.1.1.) fehlt. Im fetalen Hoden wird Testosteron durch die Sertolizellen gebildet, die das Enzym exprimieren. Erst in den adulten Leydigzellen wird hauptsächlich Testosteron produziert. Anders als bisher gedacht, bleibt ein nicht unbedeutender Anteil der fetalen Leydigezellen auch im adulten Hoden erhalten (Übersicht bei Wen et al. 2016).

Adulte Leydigzellen zeichnen sich durch eine große Menge an glattem endoplasmatischen Retikulum, Lipidtröpfchen und Mitochondrien vom Tubulus-Typ aus. Neben Androgenen und Estrogenen produzieren Leydigzellen das Hormon Insulin-like Faktor 3 (INSL3), das bei der Verkürzung des kaudalen Keimdrüsenbandes und somit dem Hodenabstieg eine entscheidende Rolle spielt (s. 4.1.3.). Seine Expression wird als Reifungsmarker für die Leydigzellen und den Anfang der Pubertät gewertet (Ferlin et al. 2006).

Andere Zelltypen im Interstitium sind Fibroblasten bzw. -zyten, die das lockere Bindegewebe des Interstitiums aufbauen und somit die freien Zellen, wie Makrophagen, Mastzellen und einzelne Lymphozyten im Interstitium halten. Die Fibroblastenaktivität kann durch verschiedene Faktoren, die

u.a. auch von den Mastzellen sezerniert werden, beeinflusst werden. In Hodenbiopsien infertiler Männer wird häufig eine Fibrose bzw. eine Verdickung der *Lamina propria* deutlich, was für eine Überaktivierung der Fibroblasten spricht.

Die im Hodeninterstitium vorhandenen Immunzellen bauen dort (zusammen mit der BHS der Sertolizellen, s. 4.2.2.) das sog. Immunprivileg auf. Die Urkeimzellen erreichen schon in der siebten Gestationswoche die Urkeimanlage und vermehren sich mitotisch bis zur 16 - 18 Gestationswoche. Die weitere Entwicklung der spermatogonialen Stammzellen erfolgt dann aber erst mit Erreichen der Pubertät (Goto et al. 1999). Dabei entstehen neue Oberflächenmarker und auch intrazelluläre Proteine. Da das Immunsystem zu diesem Zeitpunkt ausgereift ist, würden die Zellen nun als „körperfremd“ erkannt und angegriffen werden. Dieses Immunprivileg kann auch durch Allo- und Xenotransplantationen gezeigt werden, wenn z.B. Inselzellen des Pankreas in den Hoden von nicht-immunsupprimierten Beagle-Hunden oder Affen transplantiert werden (Gores et al. 2003; Isaac et al. 2005, Übersicht bei Fijak et al. 2011). Das immunsuppressive Milieu des Hodens wird durch verschiedene Zytokine, die von Makrophagen, Mastzellen, Monozyten, dendritischen Zellen und auch B- und T-Lymphozyten sezerniert werden, aufrecht erhalten. Diese Zytokine nehmen aber nicht nur Einfluss auf die Immunzellen, sondern auch auf die Leydig-, Keim- und Sertolizellen, Fibroblasten sowie peritubuläre Myoidzellen (Übersicht bei Schuppe and Meinhardt 2005; Albrecht 2009; Windschüttl et al. 2014).

Im gesunden menschlichen Hoden kommen Makrophagen, Mast- und vereinzelte T-Zellen vor, während B- Zellen und dendritische Zellen nicht vorhanden sind. B-Zellen und dentritische Zellen können in Patienten mit GCNIS detektiert werden, sie entwickeln sich dort unter Einfluss eines pro-inflammatorischen Zytokinmilieus (Klein et al. 2016). Entzündungen des Hodens (Orchitiden) werden in akute und chronische Entzündungen unterschieden. Isolierte Orchitiden sind relativ selten, meistens sind auch Prostata und Nebenhoden betroffen. Akute Hodenentzündungen sind ebenfalls selten und entstehen meist bei viralen Infektionskrankheiten, wie z.B. Mumps (Übersicht bei Nieschlag et al. 2010). Chronische Hodenentzündungen und Autoimmunerkrankungen dagegen sind häufiger, können aber lange unentdeckt bleiben und dann auch zu Störungen der Spermatogenese führen (Übersicht bei Schuppe und Meinhardt 2005; Schuppe et al. 2008).

4.2.4. *Rete testis* und *Ductuli efferentes testis*, Transport im Nebenhoden

Die *Tubuli seminiferi contorti* werden zum Mediastinum hin zu den geraden *Tubuli seminiferi recti*. In diesen findet dann keine Spermatogenese mehr statt und sie sind mit einem modifizierten Keimepithel ausgekleidet, das nur noch vereinzelte Sertolizellen enthält. In den *Tubuli seminiferi recti*

werden die reifen Spermien zum *Rete testis* transportiert, welches in das Mediastinum eingebettet ist. Das *Rete testis* besteht aus einem einschichtigen, isoprismatischem Epithel ohne Keim- oder Sertolizellen (Übersicht bei Zhang 1999). Wie in 4.2.2. beschrieben, besteht hier auch keine vollständige Blut-Hoden-Schranke mehr, so dass im Bereich des *Rete testis* die meisten inflammatorischen Vorgänge ihren Anfang nehmen und deswegen hier auch immer antigen-präsentierende Makrophagen vorliegen. Vom *Rete testis* werden die Spermien über die *Ductuli efferentes testis* in den Nebenhodenkopf verbracht. Die 10-12 *Ductuli efferentes testis* münden in den *Ductus epididymidis*, den Nebenhodengang, ein. Während die *Ductuli efferentes testis* mit einem mehrreihigen Epithel mit Kinozilien ausgestattet sind, ist der *Ductus epididymidis* von einem mehrreihigen Epithel mit Stereozilien ausgekleidet. Durch die Peristaltik der glatten Muskulatur um den Nebenhodengang herum sowie durch die passive Beweglichkeit der Stereozilien werden die Spermien im Nebenhoden transportiert. Eingeteilt wird der Nebenhodengang in einen Kopf-, Körper- und Schwanzbereich (*Caput, corpus et cauda epididymidis*). Während der Passage findet die weitere Reifung der Spermien statt, die dort auch ihre Bewegungsfähigkeit erlangen. Im Nebenhodenschwanz werden die ausgereiften Spermien gespeichert. Die stetig dicker werdende *Lamina muscularis* um den Nebenhodengang erreicht im Nebenhodenschwanz ihre maximale Ausprägung und geht dort fließend in die kräftige *Lamina muscularis* des Samenleiters (*Ductus deferens*) über (Übersicht bei Gray et al. 1918; Singh 2011).

4.3. Spermatogenese

4.3.1. Keimzellentwicklung

Die Spermatogenese besteht aus zwei getrennten Vorgängen: der Spermatozytogenese (Entwicklung von diploiden Spermatogonien zu haploiden runden Spermatiden) und der Spermiogenese (Reifung der runden Spermatiden zu elongierten Spermatiden, die dann aus dem Keimepithel abgegeben werden). Sobald die elongierten Spermatiden das Keimepithel verlassen haben, werden sie als Spermien oder Spermatozoen bezeichnet und reifen im Nebenhoden zu motilen Spermien heran.

Die Urkeimzellen (*primordial germ cells*, PGCs) oder auch Gonozyten differenzieren sich schon sehr früh aus dem kaudalen Epiblast der Keimscheibe und werden während des ersten Monats nach der Befruchtung in die Dottersackwand ausgelagert (Tu et al. 2007, Übersicht bei Felici 2016). Etwa im Laufe der fünften Woche bildet sich durch die Vermehrung der Zölomepithelzellen und des lokalen Mesenchyms der Gonadenleiste die geschlechtlich noch undifferenzierte Gonadenanlage. In diese fetale Gonadenanlage wandern die PGCs nun über die Wand des Intestinaltraktes und das dorsale Mesenterium ein. Diese Wanderung wird durch drei Faktoren ermöglicht: die amöboide Eigenbewegung der PGCs, die Abfaltung des Embryos und chemotaktische Faktoren. Schon während

der Wanderung finden mitotische Teilungen statt. Nach Erreichen der fetalen Keimdrüse wird das Zölomepithel mehrschichtig, verliert kurze Zeit darauf seine Basalmembran und umgibt zusammen mit Zellen des Mesonephros die PGCs mit sog. Gonadensträngen. Bis zur 6. Woche nach Befruchtung kann nicht zwischen männlicher und weiblicher Keimanlage unterschieden werden. In der 7. Woche beginnt dann die Differenzierung in die männliche Gonade durch die Expression des Y-Chromosom-spezifischen Gens SRY (*Sex determining region on Y chromosome*), das als Transkriptionsfaktor für die Aktivierung weiterer hodenspezifischer Gene verantwortlich ist. Die Sertolizellen bilden daraufhin interzelluläre Verbindungen aus und umgeben die PGCs strangartig. Aus diesen Gonadensträngen bilden sich dann über die Hodenstränge die *Tubuli seminiferi contorti et recti*. Innerhalb dieser Hodenkanälchen teilen sich die PGCs nun mitotisch und besiedeln so den fetalen Hoden (Übersicht bei Wartenberg et al. 1993).

Die PGCs, die sich zu diesem Entwicklungszeitpunkt noch im Zentrum der Tubuli befinden, differenzieren sich schon vor der Geburt zu Stamm-Spermatogonien, die auch als A-Spermatogonien bezeichnet werden und der Basalmembran aufsitzen. Hier unterscheidet man morphologisch weiter zwischen den sog. A_{dark}- und A_{pale}-Spermatogonien (Clermont 1963). Während die A_{dark} ein dunkleres Chromatin mit einem hellen Halo aufweisen, zeigen die A_{pale}-Spermatogonien einen deutlich helleren und homogeneren Zellkern. Beide Typ A-Spermatogonien stellen den Stammzellpool im Hoden dar. Die erste Vermehrungsphase der Spermatogonien wird vor der Geburt beendet und die Spermatogenese ruht bis zum Eintritt der Pubertät. Mit Eintritt in der Pubertät findet eine asymmetrische mitotische Teilung statt. Aus einer A_{pale}-Spermatogonie wird dann eine A_{pale}-Spermatogonie, die als Stammzelle erhalten bleibt, und eine B-Spermatogonie, die dann in die Meiose eingeht (Übersicht bei Ehmcke und Schlatt 2006). B- Spermatogonien zeigen eine höhere Proliferationsaktivität als A-Spermatogonien (Steger et al. 1998). Während die A-Spermatogonien breitflächig der Basalmembran aufsitzen, lösen sich die B-Spermatogonien von der Basalmembran. Das Chromatin der B-Spermatogonien ist deutlich inhomogener als das der A_{pale}-Spermatogonien. Schon in dieser frühen Phase der Spermatogenese sind die B-Spermatogonien durch Zytoplasmabrücken miteinander verbunden. Diese bleiben bis zu den elongierten Spermatiden beim Menschen (Übersicht bei Holstein und Roosen-Runge 1981) bzw. bis kurz vor den *sperm release* bei der Ratte bestehen (Weber und Russell 1987, Übersicht bei Greenbaum et al. 2011). Die Keimzellen entwickeln sich dadurch in Kohorten. Der erste Schritt in der Meiose I ist die Verdopplung des Chromatins. Aus der diploiden B-Spermatogonie mit einfachem Chromatid (2n 2C) entsteht durch Verdopplung des Chromatids die diploide Spermatozyte I. Ordnung (2n 4C), die sich nun vollständig von der Basalmembran gelöst hat und durch ihre charakteristische Chromatinstruktur in die verschiedenen Stadien der Prophase I eingeteilt werden kann (prä-leptotän, leptotän, zygotän, pachytän und die Diakinese). Während der Prophase I kommt es zu einer Rekombination der

homologen Chromosomen und somit zu einem Austausch von Erbgut („*crossing over*"). Hierfür muss sich der sogenannte synaptonemale Komplex bilden, mit dem die beiden homologen Chromosomen zusammengehalten werden (Übersicht bei Fraune et al. 2012). Im weiteren Verlauf der Prophase I kann es dann zur Induktion von Doppelstrangbrüchen, einem Austausch von Genmaterial und nachfolgend zur Reparatur der Doppelstrangbrüche kommen. Aus diesem Grund ist die Prophase I mit ca. 24 Tagen sehr lang. In der ersten meiotischen Reife- oder auch Reduktionsteilung werden die homologen Chromosomen getrennt und es entstehen zwei haploide Spermatozyten II. Ordnung, die aber immer noch über zwei am Centromer verbundene Schwesterchromatiden verfügen (1n 2C). Die zweite meiotische Reife- oder Äquationsteilung findet bereits nach wenigen Stunden statt, so dass die Spermatozyten II. Ordnung nur für kurze Zeit im Keimepithel sichtbar sind. Es entstehen die runden Spermatiden, die nun über einen haploiden Chromosomensatz und ein einzelnes Chromatid verfügen (1n 1C). Man unterscheidet zwischen Andro- und Gynospermien, die entweder ein Y- oder ein X-Chromosom tragen (Übersicht bei Weinbauer et al. 2010). Es schließt sich nun die Spermiogenese an, in der die runden zu elongierten Spermatiden werden. Dieser Prozess dauert ca. 24 Tage und die Spermatiden durchlaufen in dieser Zeit vier Phasen. In der Golgiphase bilden sich präakrosomale Granula, die vom Golgi-Apparat abgeschnürt werden. Die präakrosomalen Granula verschmelzen und bilden die spätere Akrosomenkappe. Diese umschließt in der Kappenphase den Zellkern. Gegenüber der Kappe dient eines der Zentriole als Verankerungspunkt für die Spermiengeißel, die sich von dort aus verlängert. Zeitgleich bildet sich die Spermienmanschette, eine temporäre Mikrotubulusstruktur, die den elongierenden Spermatiden die längliche Form vorgibt. Zudem beginnt die Kondensation des Zellkerns. Dafür müssen Histone, die in normalen Körperzellen die DNA locker zu Nukleosomen kondensieren, durch platzsparendere Transitionsproteine und danach Protamine ersetzt werden. Untersuchungen bei Mensch und Tier haben gezeigt, dass der Histon-Protaminaustausch essentiell für die korrekte Spermiogenese und damit für die Fertilität ist (Übersicht bei Steger 2009). Ca. 15% der Histone verbleiben in der DNA und werden nicht durch Protamine ersetzt. Diese können epigenetische Markierungen (Methylierungen und Acetylierungen) tragen, die für eine Aktivierung oder Inhibierung von Genen verantwortlich sind. Diese Markierungen sind bereits gut untersucht und lassen Rückschlüsse auf die Fertilität zu (Übersicht bei Schagdarsurengin und Steger 2016). In der Akrosom- und Reifephase werden die Umbauvorgänge an den Spermatiden abgeschlossen: Reste des Zytoplasmas und nicht benötigter Zellorganellen werden immer weiter abgeschnürt und schließlich von den Sertolizellen als *residual bodies* phagozytiert. Einzig die Mitochondrien bleiben übrig und ordnen sich um das Mittelstück der Geißel an. Die fertige Spermiengeißel kann nun in einen Halsbereich, der das Zentriol als „Gelenk" enthält, Mittel-, Haupt- und Endstück eingeteilt werden.

4.3.2. Stadien und Kinetik der Spermatogenese

Um eine kontinuierliche Spermienproduktion zu ermöglichen, laufen mehrere Keimzellgenerationen gleichzeitig an. Diese parallel ablaufenden Entwicklungswellen führen zu klar definierten Keimzellassoziationen, die als Keimzellstadien bezeichnet werden. Bei Mensch und Tier werden unterschiedlich viele Keimzellstadien beschrieben, z.B. wurden von Clermont (1963, Übersicht bei Bergmann und Kliesch 2010) beim Menschen acht Stadien identifiziert, während Russell et al. (1990) bei der Ratte 14, bei der Maus 12 und beim Hund acht Stadien beschreiben. Während der *sperm release* beim Menschen im Stadium II stattfindet, findet er bei der Maus im Stadium VIII statt. Das Stadium des *sperm release* stellt zeitgleich auch den Beginn einer neuen meiotischen Reifeteilung dar, da hier die B-Spermatogonien zu prä-leptotänen Spermatozyten I. Ordnung werden und sich von der Basalmembran lösen. Das letzte Stadium der Spermatogenese (beim Mensch Stadium VI) ist immer durch das Auftreten der Spermatozyten II. Ordnung charakterisiert, d.h. es ist das Stadium nach der ersten meiotischen Reifeteilung. Die Spermatogenesestadien des Menschen können Abb. 5 entnommen werden.

Während bei den Haussäuge- und Labortieren in einem Tubulusquerschnitt nur ein Stadium vorkommt (*single stage arrangement*, Übersicht bei Russell et al. 1990), können beim Mensch immer mehrere Spermatogenesestadien in einem Schnitt identifiziert werden, so dass man hier von einem *multi stage arrangement* (Luetjens et al. 2005) spricht. Die Spermatogenese beim Menschen dauert ca. 64 Tage. Die längsten Phasen der Spermatogenese sind die Prophase I und die Spermiogenese nach Abschluss der zweiten Reifeteilung. Das kürzeste Stadium ist bei der humanen Spermatogenese ist das Stadium VI, das nur wenige Stunden im Keimepithel zu sehen ist.

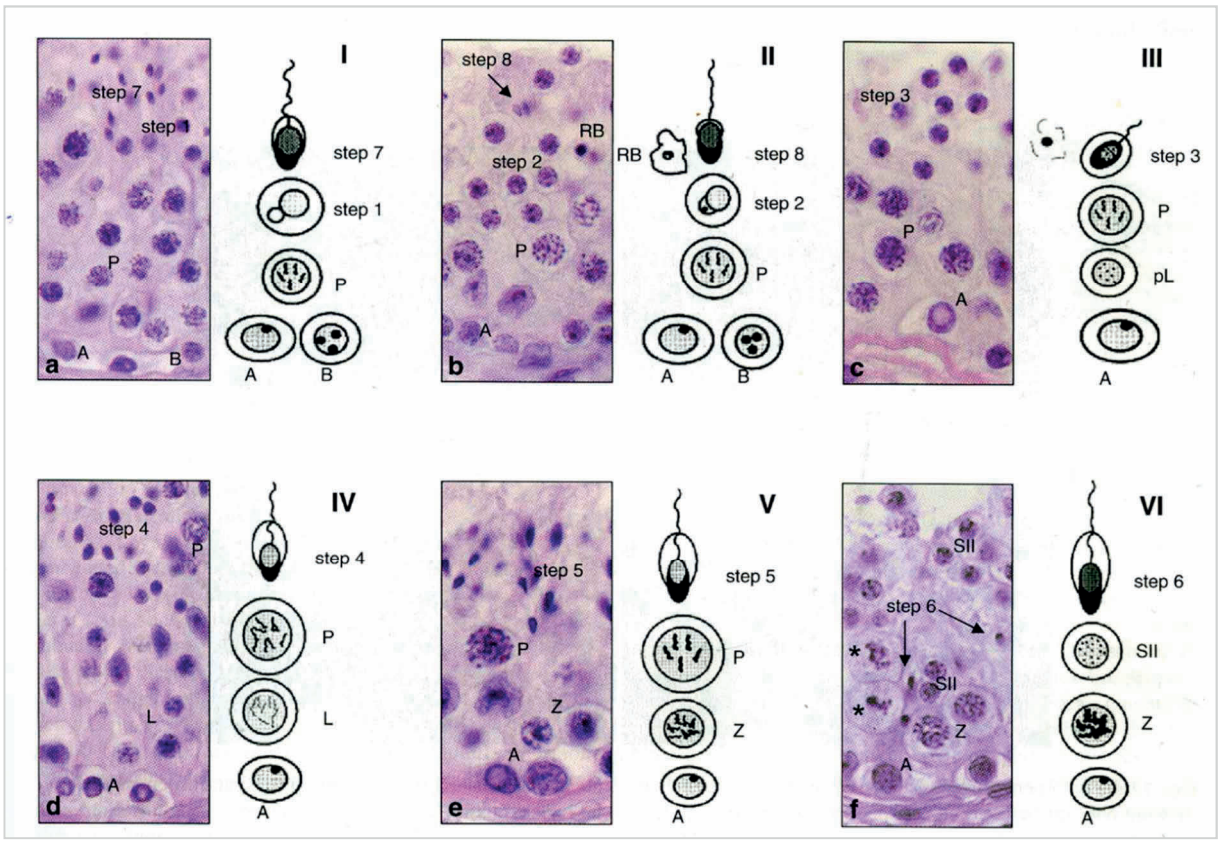

Abb. 5 Spermatogenesestadien beim Menschen (nach Bergmann und Kliesch 2010)

A A-Spermatogonie, **B** B-Spermatogonie, **pL** prä-leptotäne, **L** leptotäne, **Z** zygotäne, **P** pachytäne Spermatozyte I. Ordnung, **SII** Spermatozyte II. Ordnung, **step 1-6** verschiedene Spermatidenstadien, **RB** *residual body*

4.4. Männliche Infertilität: Störungen der Spermatogenese

In Deutschland sind ca. 15% der Paare ungewollt kinderlos. Nach Definition der World Health Organization (WHO) spricht man von Infertilität, wenn nach einem Jahr ungeschützten regelmäßigen Geschlechtsverkehrs keine Schwangerschaft eintritt. In ungefähr 50% dieser Fälle sind die Ursachen auf der Seite des Mannes (*male factor infertility)* zu suchen. Nach Vorgaben der WHO wird neben der allgemeinen und speziellen klinischen Untersuchung, Ultraschall- und Blutuntersuchungen eine Ejakulatuntersuchung durchgeführt. Die Beurteilung des Ejakulats erfolgt nach genauen Kriterien wie u.a. Anzahl der Spemien (Zahl/ml), progressiver Vorwärtsbeweglichkeit der Spermien (in %) und Anzahl an morphologisch abnormalen Spermien (in %). Bei einer verminderten Anzahl der Spermienzahl spricht man von einer Oligozoospermie, die zu Subfertilität verschiedenen Ausmaßes führt. Im Gegensatz dazu wird das vollständige Fehlen von Spermien als Azoospermie bezeichnet. Bei Vorliegen einer Azoospermie muss zwischen einer obstruktiven und nicht-obstruktiven Azoospermie unterschieden werden. Bei der obstruktiven Azoospermie (OA) liegt ein Verschluss der

samenleitenden Wege vor, z.B. eine erbliche Aplasie der Samenleiter, die meist beidseits vorkommt (*congential bilateral aplasia of vasa deferens,* CBAVD) oder auch ein iatrogener Verschluss der Samenwege durch eine Vasektomie. Bei der nicht-obstruktiven Azoospermie (NOA) dagegen ist eine mehr oder weniger schwerwiegende Störung der Spermatogenese zu erwarten. Die weitere Diagnostik erfolgt mittels einer Hodenbiopsie, für die es von der European Assoziation of Urology (EAU) klare Indikationen gibt (Übersicht bei Bergmann und Kliesch 2010). Diese sind:

1) Abklärung des Spermatogenesestatus vor einer Refertilisierung durch Vasovasostomie bzw. als therapeutische Biopsie zur Spermiengewinnung mittels testikulärer Spermienextraktion (TESE) für die assistierte Reproduktion bei CBAVD
2) Vorliegen einer NOA unklarer Genese
3) Vorliegen einer NOA auf Grund von Klinefelter Syndrom bzw. AZFc Deletion
4) Verdacht auf testikuläre Tumorerkrankungen bzw. Krebsvorstufen

Nach Vorgaben der EAU werden die Hodenbiopsien für eine gute Morphologie in Bouinscher Lösung fixiert und in Paraffin eingebettet. Für die Bewertung der Spermatogenese werden 5µm dicke Schnitte angefertigt und nach Standardprotokollen mit Hämatoxylin und Eosin gefärbt. Die Bewertung erfolgt dann nach einem semi-quantitativen Scoring-System. Beschrieben wurde bereits 1970 der Score Count von Johnsen (Johnsen 1970). Bei diesem System wird jeden Tubulusquerschnitt ein Zahlenwert zugewiesen. Dieser richtet sich nach dem letzten Keimzelltyp im Keimepithel. Der Johnsen-Score wurde v.a. für Biopsien von oligozoospermen Patienten entwickelt. Dies ist allerdings nach EAU-Vorgaben keine Indikation für Hodenbiopsien mehr. 1998 wurde deswegen von Bergmann und Kliesch (Übersicht bei Bergmann und Kliesch 2010) ein Score count-System entworfen, der die Anzahl von Tubuli mit elongierten Spermatiden in Prozent wiedergibt. So kann dann die Wahrscheinlichkeit, bei einer TESE Spermien finden zu können, vorhergesagt werden.
Bei normaler Spermatogenese (Abb. 6A) sind in allen Tubuli elongierte Spermatiden zu finden, der Score count liegt demnach bei 100% bzw. 10. Zudem können bei normaler Spermatogenese (NSP) die verschiedenen Spermatogenesestadien klar zugeordnet werden. Bei einer Hypospermatogenese (Abb. 6B) handelt es sich um eine quantitativ reduzierte, aber qualitativ erhaltene Spermatogenese. Eine klare Zuordnung der Stadien ist zwar meist nicht mehr möglich, dennoch kann man in einer größeren Anzahl der Tubuli oder sogar in allen Tubuli elongierte Spermatiden finden. Der Score count liegt zwischen 1 und 10. Diese beiden Diagnosen kommen meistens bei Männern mit einer obstruktiven Azoospermie vor, wo die Spermatogenese in größten Teilen erhalten ist. Eine der häufigsten Ursachen der NOA sind Spermatogenesearreste (*maturation arrest*, MA). Diese können auf unterschiedlichen Keimzellstufen stattfinden, z.B. auf Ebene der Spermatiden (SDA) (Abb. 6C),

(primären) Spermatozyten (SZA) (Abb. 6D) oder auch Spermatogonien (SGA) (Abb. 6E). Bei einer totalen Keimzellaplasie, dem sog. Sertoli cell only-Syndrom (SCO) (Abb. 6F), sind alle Keimzellen aus dem Keimepithel verschwunden und nur die Sertolizellen sind noch zu sehen

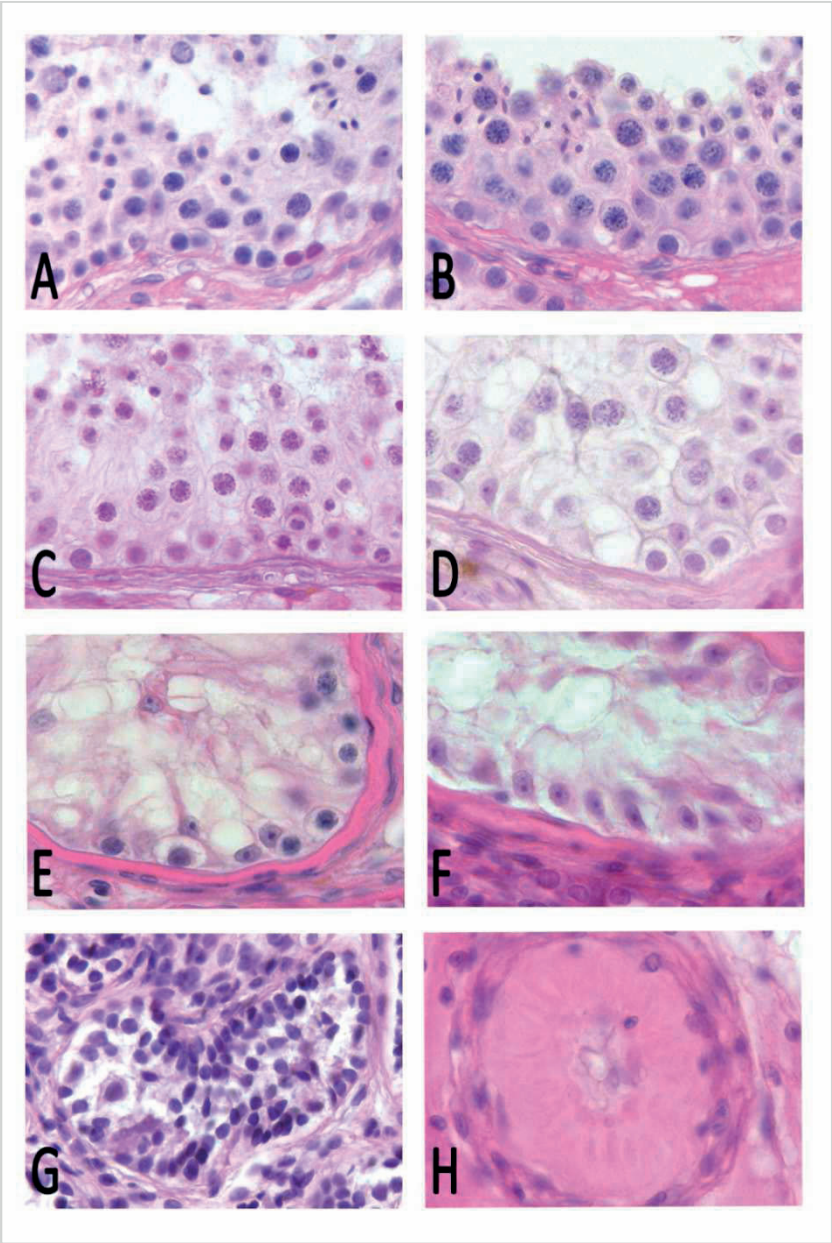

Abb. 6 Normale humane Spermatogenese und verschiedene Spermatogenesedefekte

Darstellung von normaler Spermatogenese (Stadium II/III, A) und verschiedenen Spermatogenesestörungen beim Menschen; B Hypospermatogenese, C Spermatidenarrest (SDA), D Spermatozytenarrest (SZA), E Spermatogonienarrest (SGA), F Sertoli cell only Syndrom (SCO), G unreife Sertolizellen und H Tubulusschatten. Primäre Vergrößerung x40 (A-F, H) bzw. x20 (G); Färbung Hämatoxylin und Eosin.

Bei einem SCO muss man zwischen einem totalen und einem fokalen SCO unterscheiden. Meistens erscheinen die Sertolizellen bei einem SCO morphologisch normal und zeichnen sich durch einen

mehr oder weniger dreieckigen Zellkern mit gut sichtbaren Kernkörperchen aus, ein Tubuluslumen ist vorhanden. Daraus ergibt sich, dass die Blut-Hodenschranke bei einem SCO erhalten ist. In einem solchen Fall ist von einem sekundären Keimzellverlust (z.B. durch Fieber, Bestrahlung o.ä.) auszugehen. Bei sog. immaturen Sertolizellen (ISZ) (Abb. 6G) dagegen erscheinen die Sertolizellen unreif, der Zellkern ist homogen dunkler und rund, die betroffenen Tubuli erscheinen kompakt und zeigen keine Lumenbildung. In einem solchen Fall geht man von einem primären Keimzellverlust aus. Bei sog. Tubulusschatten (TubS) (Abb. 6H), der schwersten Form der gestörten Spermatogenese, sind keinerlei Zellen mehr im Tubulus vorhanden. Die Tubuluswand ist zudem verdickt.

Alle diese Spermatogenesestörungen führen zu einer vollständigen Azoospermie, der Score count bei diesen Biopsien ist immer 0, da es keine elongierten Spermatiden mehr gibt. Eine Sonderform der gestörten Spermatogenese ist die sog. „bunte Atrophie“. Hierbei ist das Bild der Hodenbiopsie nicht einheitlich, neben Tubuli mit erhaltener Spermatogenese (HYP) kommen verschiedene Abstufungen an Spermatogenesestörungen, z.B. ein fokales SCO, Reifungsarreste und/oder Tubulusschatten vor.

Die Ursache von Spermatogenesestörungen ist größtenteils unbekannt (idiopathische Infertilität). Es gibt einige bekannte genetische und nicht-genetische Ursachen für eine Schädigung der Spermatogenese, die hier nur kurz behandelt werden sollen.

1. Klinefelter Syndrom

Eine der häufigsten genetischen Ursachen für die Schädigung der Spermatogenese ist das Klinefelter Syndrom. Durch eine fehlerhafte Trennung der homologen Chromosomen bzw. der Schwesterchromatiden des X-Chromosoms während der Spermatogenese bzw. Oogenese kommt es zu einem überzähligen X-Chromosom, so dass der Genotyp bei Klinefelter Syndrom 47,XXY ist. Mit einer Prävalenz von 1:500 ist es die häufigste numerische Chromosomenaberration, die beim präpubertären Jungen zu Lern- und Sprachschwierigkeiten, zu einem verzögerten Eintritt in die Pubertät und nach der Pubertät zu einem Hypogonadismus (mangelnde Androgenisierung, Spermatogenesedefekte und Infertilität) führt (Übersicht bei Nieschlag et al. 2010). In Hodenbiopsien können meistens ein totales oder fokales SCO, ISZ und TS zusammen mit einer mehr oder weniger schwerwiegenden Hyperplasie der interstitiellen Leydigzellen detektiert werden. Gerade bei jungen Patienten gibt es auch immer wieder Bereiche von bunter Atrophie, in denen die Spermatogenese erhalten ist (Übersicht bei Aksglaede und Juul 2013).

2. Mikrodeletionen auf dem Y-Chromosom

Auf dem langen Arm des Y-Chromosoms (Yq) finden sich drei Bereiche, die für sogenannte „Azoospermiefaktoren“ (AZF) codieren. Von diesen AZF sind drei spezielle Bereiche bekannt, die mit a-c bezeichnet werden. Die Deletion eines oder mehrerer AZFs führt zu einer mehr oder weniger schwerwiegend gestörten Spermatogenese. Es ist bekannt, dass nur bei einer AZFc-, sowie einer AZFab-Deletion einzelne Bereiche mit erhaltener Spermatogenese zu erwarten sind. Alle anderen Formen dieser Deletion(en) führen zu einer Azoospermie mit Reifungsarresten, SCO und TS (Übersicht bei Krausz und Casamonti 2017).

3. Störungen der Meiose

Die Meiose als Reduktions- und Reifeteilung spielt für die Entwicklung der haploiden Keimzellen eine essentielle Rolle (s. 4.3.1). Als erster Schritt muss sich der synaptonemale Komplex bilden, der leiterartig die homologen Chromosomen zusammenhält und eine Rekombination erst ermöglicht (Übersicht bei Fraune et al. 2012). Störungen in seiner Formation können zu einem Abbruch der Spermatogenese führen, was sich dann als Spermatozytenarrest darstellt. Untersuchungen bei Mäusen haben gezeigt, dass der totale Verlust eines am synaptonemalen Komplex beteiligten Gens (Untersuchung von knock out Mausmodellen) zu einer veränderten Rekombination und damit zu einer Störung der Spermatogenese führt (Pittman et al. 1998; Liebe et al. 2004; Judis et al. 2004; de Vries et al. 2005; Costa und Cooke 2007; Sanderson et al. 2008; Fraune et al. 2012). Die Untersuchungen beim Menschen sind im Gegensatz dazu eher widersprüchlich. Manche Arbeitsgruppen konnten den Zusammenhang zu einer vorliegenden Azoospermie herstellen, andere nicht (Miyamoto et al. 2003; Gonsalves et al. 2004; Sun et al. 2004; Sciurano et al. 2006). Eine Untersuchung von Biopsien mit einem totalen Spermatozytenarrest in Hinblick auf mehrere an der Rekombination beteiligten Gene wurde in Zusammenarbeit mit einer Master-Studentin des EUCOMOR-Programmes unter meiner Leitung durchgeführt und zeigt, dass drei Gene im besonderen Maße bei der Entstehung des Spermatozytenarrests des Menschen beteiligt zu sein scheinen (Fietz et al., in Vorbereitung).

Nicht-genetische Ursachen für Spermatogenesestörungen sind sehr vielfältig und können manchmal auch nicht eindeutig für die Entstehung von Spermatogenesedefekten verantwortlich gemacht werden (z.B. die Beteiligung von Ernährung und Umweltgiften an der Infertilität des Mannes). Gesichert ist der Zusammenhang zwischen hoch fieberhaften Erkrankungen, wie z.B. viralen Infekten (Mumps), an der Entstehung einer totalen, wenn auch häufig reversiblen Keimzellaplasie. Generell

haben Infektionen des Hodens einen Einfluss auf die Spermatogenesequalität. Zu unterscheiden sind hierbei akute und chronische Infektionen. Während akute Infektionen meistens durch Fieber einen direkten Einfluss auf die Keimzellen nehmen, stehen auch chronische Infektionen einen nicht zu vernachlässigenden Faktor für die Entstehung von Spermatogenesedefekten dar. Diese treten häufig als Zufallsbefund bei der Untersuchung von Hodenbiopsien mit einer bunten Atrophie der Spermatogenese auf und zeichnen sich durch mehr oder weniger starke Immunzellinfiltrate aus. Auch eine nicht-infektiös bedingt erhöhte Körpertemperatur im Bereich des Hodens, z.B. durch einen fehlenden oder mangelhaften Hodenabstieg (Kryptorchismus) kann zu einer Schädigung der Spermatogenese bis hin zu einer malignen Entartung der Keimzellen führen.

5. Einleitung II: Steroidhormone, Rezeptoren und Transportwege

5.1. Steroidhormone

Steroidhormone regulieren viele physiologische Prozesse, sowohl während der Entwicklung als auch im erwachsenen Wirbeltier. Steroidhormone steuern hier sowohl Reproduktion, Wachstum und beeinflussen den Energie- und Wasserhaushalt. Besonders wurde die Bedeutung der Steroidhormone als Geschlechtshormone auf die Regulation des Reproduktionsverhaltens untersucht (Thornton 2001; Lowartz et al. 2003). Alle Steroidhormone werden aus einer gemeinsamen Vorstufe, dem Cholesterin, während der Steroidogenese synthetisiert. Alle Steroidhormone zeichnen sich deswegen durch eine gemeinsame Struktur, das Sterangerüst, aus. Zu den Steroidhormonen gehören neben den Androgen, Estrogenen und Gestagenen auch Mineralokortikoide und Glukokortikoide (Übersicht bei Miller und Auchus 2011). Im Verlauf der Steroidogenese entstehen die sog. freien Steroide, die durch ihre hohe Fettlöslichkeit frei in die Zelle diffundieren und dort ihre Wirkung entfalten können. Im Gegensatz dazu können Steroide auch in einer gebundenen bzw. konjugierten Form vorkommen, in der sie an verschiedene Moleküle, wie z.B. an einen Sulfatrest gebunden sind. Diese Form der Steroidhormone ist wasser- und nicht mehr fettlöslich. Demnach können diese konjugierten Steroidhormone nicht mehr frei in die bzw. aus der Zelle diffundieren und benötigen spezifische Transportmechanismen (Döring et al. 2012).

5.1.1. Produktion von freien Steroidhormonen

Cholesterin ist die schwer lösliche Vorstufe aller Steroidhormone, die entweder aus den Nahrungsfetten aufgenommen oder *de novo* in Leber und Darm synthetisiert werden kann. An *low density lipoproteins* (LDL) gebunden, wird Cholesterol in die Zielzellen aufgenommen. Die ersten Schritte der Steroidhormonsynthese finden in den Mitochondrien statt. Da die hormonproduzierenden Zellen nur wenig bis gar keine Steroidhormone speichern können, muss die Steroidogenese auf Signal der übergeordneten endokrinen Drüsen Hypothalamus und Hypophyse sehr schnell anlaufen. Das Protein StAR (*Steroidogenic Acute Regulatory Protein*) vermittelt diesen schnellen Transport des Cholesterins von der äußeren in die innere Mitochondrienmembran (Übersicht bei Stocco 2001). Die in die Steroidogenese eingebundenen Enzyme sind entweder Cytochrom P_{450} (CYP)-Enzyme oder Hydroxysteroiddehydrogenasen (HSD). Bei den CYPs unterscheidet man den Typ 1, der in den Mitochondrien zu finden ist, und den Typ 2, der in den Mikrosomen vorkommt. Während die von CYPs vermittelten Reaktionen irreversibel sind, können Produkte der HSDs wieder zu dem Vorgängermolekül zurück katalysiert werden (Übersicht bei Miller und Auchus 2011).

Der erste Schritt der Steroidhormonsynthese ist die Konversion von Cholesterin zu Pregnenolon durch das Enzym CYP11A1 bzw. $P450_{scc}$ (Cytochrom P_{450} side-chain-cleavage wegen der Abspaltung der Seitenkette des Cholesterins) mit einer 20,22-Lyaseaktivität. Diese erste Reaktion bestimmt die Geschwindigkeit und Effizienz der weiteren Syntheseschritte und ist ihrerseits durch cAMP hormonell reguliert. Bei den weiteren Schritten in der Steroidhormonsynthese muss zwischen zwei Synthesewegen unterschieden werden, dem Δ5- und dem Δ4-Weg. Beim Menschen entstehen Androgene und Estrogene vorwiegend über den Δ5-Weg, bei der Maus dagegen über den Δ4-Weg. Die 17α-Hydroxylierung von Pregnenolon zu 17α-Hydroxypregnenolon (17α-OH-Preg) wird von der CYP17A1 bzw. P450c17 vermittelt, das dann im weiteren Verlauf der Steroidbiosynthese aus 17α-OH-Preg Dehydroepiandrosteron (DHEA) synthetisiert. Alle diese „Zwischenprodukte" (Pregnenolon, 17α-OH-Preg und DHEA) können von dem Enzym 3β-Hydroxysteroiddehydrogenase (3β-HSD) in die Hormone bzw. Hormonvorstufen des Δ4-Weges (Progesteron, 17α-OH-Progesteron und Androstenedion) konvertiert werden. Weitere HSDs vermitteln nun die Synthese von Androstenediol aus DHEA (17β-HSD1) bzw. Testosteron aus Androstenedion (17β-HSD3). Androstenediol kann durch das bekannte Enzym 3β-HSD ebenfalls in Testosteron umgewandelt werden. Testosteron wiederum kann durch das Enzym 5α-Reduktase in das aktivere Dihydrotestosteron (DHT) konvertiert werden. Die Estrogene Estron und Estradiol entstehen durch einen Aromatisierungsschritt aus Testosteron, der durch das Enzym Aromatase (CYP19A1 oder P450aro) vermittelt wird (Abb. 7). Die Syntheseschritte, die durch Cytochrome vermittelt werden, benötigen Ko-Faktoren zur Bereitstellung von Elektronen. Dies sind u.a. Cytochrome b5, Ferredoxin, Ferredoxinreduktase und POR (P450 Oxyreduktase). Die Reaktionen mit den HSDs werden dagegen von $NADH/NAD^+$ und $NADPH/NADP^+$ als Ko-Faktoren ermöglicht (Übersicht bei Miller und Auchus 2011).

Die Ausstattung mit Enzymen und Ko-Faktoren bestimmt, welche Steroide gebildet werden. Aus diesen Expressionsmustern ergeben sich dann verschiedene Synthesewege in den unterschiedlichen steroidogenen Zelltypen, wie z.B. in der Nebenniere und den Gonaden. Ähnlich wie in der *Zona reticularis* der Nebennierenrinde exprimieren die Leydigzellen P450c17 und Cytochrom b5, so dass aus Cholesterin und Pregnenolon große Mengen DHEA produziert werden. Da die Leydigzellen 3β-HSD2 und 17β-HSD3 exprimieren, aber keine SULT2A1, wird in diesen Zellen das produzierte DHEA nicht zu DHEAS sulfatiert, sondern gleich über Androstenedion und Androstenediol zu Testosteron synthetisiert. Die Menge an Androstenedion ist allerdings geringer, da der Δ5-Weg beim Menschen überwiegt (Übersicht bei Miller und Auchus 2011). Die Steuerung der Steroidogenese in den Leydigzellen erfolgt über die Ausschüttung von LH aus der Hypophyse, die wiederum durch die pulsatile Ausschüttung von *Gonadotropin Releasing Hormone* (GnRH) aus dem Hypothalamus beeinflusst wird. Die Produktion von Testosteron auf die LH-Stimulation hin führt zu einem negativen

Feedbackmechanismus und somit einer verminderten Ausschüttung von LH aus der Hypophyse (Übersicht bei Weinbauer et al. 2010).

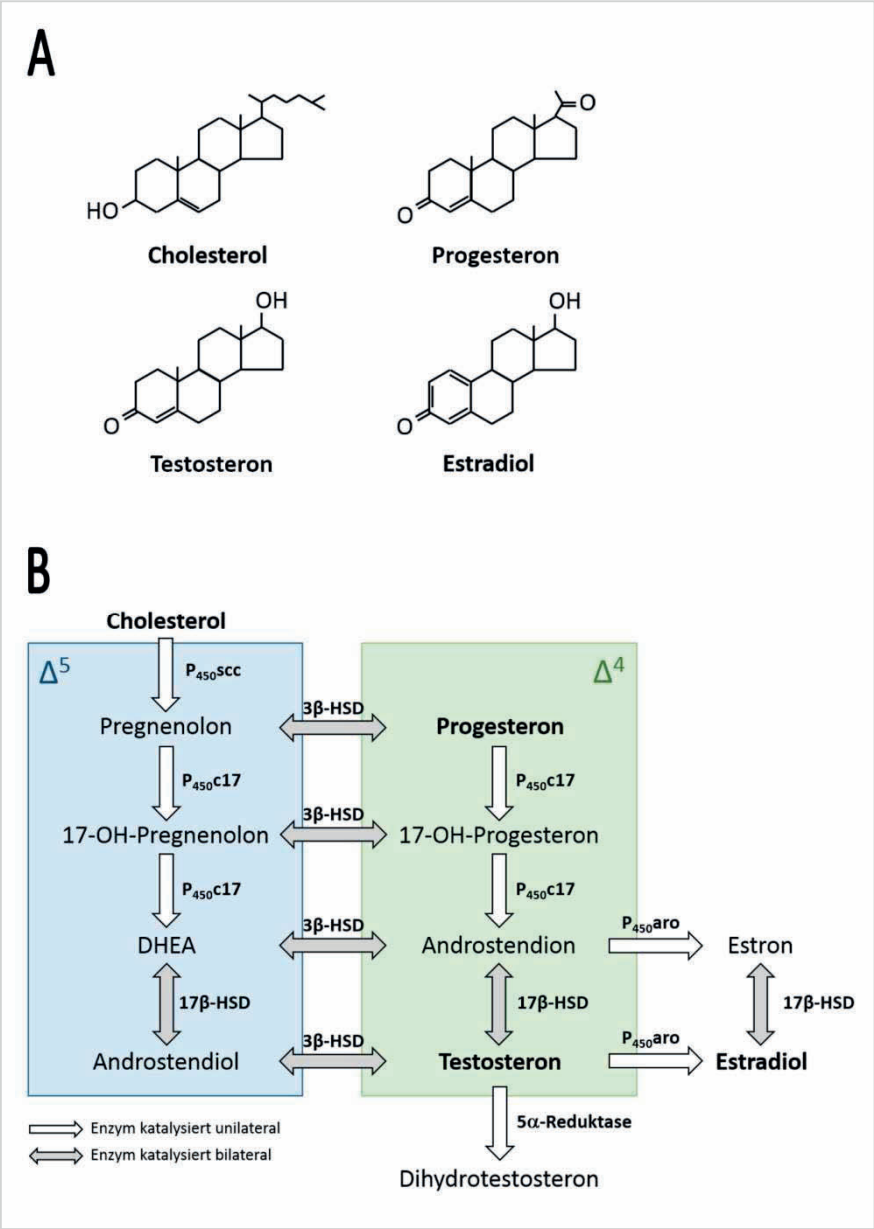

Abb. 7 Schematische Darstellung der Steroidogenese

A Strukturformeln von Cholesterol und den wichtigsten Steroidhormonen Progesteron, Testoteron und Estradiol

B Übersicht über die Hauptschritte der Steroidhormonbiosynthese, modifiziert nach Miller und Auchus (2011). Während beim Menschen die Steroidhormonsynthese auf dem sog. Δ^5-Syntheseweg (blauer Kasten) bevorzugt wird, läuft die Synthese bei der Maus v.a. über den Δ^4-Syntheseweg (grüner Kasten). Die Konversion von Testosteron in das potentere DHT über das Enzym 5α-Reduktase findet in den peripheren Androgenzielzellen statt. Die Aromatisierung des Testosterons bzw. Androstenedions in Estradiol bzw. Estron findet einmal zentral im Hoden statt, aber auch in peripheren Geweben, wie z.B. dem Fettgewebe.

P_{450}ssc *Cytochrom P_{450} side chain cleavage* (alter Name: CYP11A1), P_{450}c17 *Cytochrom P_{450}c17* (alter Name: CYP17A1), 3β-HSD *3ß-Hydroxysteroiddehydrogenase*, 17β-HSD *17ß-Hydroxysteroiddehydrogenase*; P_{450}aro *Cytochrom P_{450} aromatase* (alter Name: Aromatase, CYP19A1).

5.1.2. Produktion von konjugierten Steroidhormonen

Steroidhormone können auf verschiedene Art weiter modifiziert werden. Alle Vorgänge erhöhen die Wasserlöslichkeit der Steroide und erleichtern die Exkretion über Galle und Urin. Zwei Mechanismen, die hier beschrieben werden sollen, sind die Glucuronidierung und die Sulfatierung.

Die Glucuronidierung wird durch das Enzym Uridindiphosphoglucuronisyltransferase (UGT) katalysiert. Wie durch Hum et al. (1999) gezeigt, können zwei UGT-Familien, UGT1 und UGT2, unterschieden werden. Sie werden in vielen verschiedenen Organen exprimiert. Neben Gallensäuren, Bilirubin etc. können die UGT1 und UGT2B verschiedene Steroide modifizieren. Der Hauptort der Glucuronidierung ist die Leber, auch wenn diese Modifikation verschiedener endogener und exogener Stoffe auch in anderen Organen, wie z.B. der Prostata, dem Brustgewebe und verschiedenen Tumorzellkulturen (z.B. MCF-7 und LNCaP), nachgewiesen werden kann. Durch diese Konjugierung wird ein Gleichgewicht von aktiven und inaktiven Steroiden in den Zielgeweben bzw. -zellen dieser Hormone erreicht. Die Hauptmetaboliten, die glucuronidiert im Blut detektiert werden können, sind Androgene, z.B. 5α-reduzierte C_{19} Steroide, die dort einen Pool für die Herstellung von aktiven Androgenen darstellen. Bereits 1997 wurde deswegen postuliert, dass die Konzentration freier Steroide im Blut nicht als alleinigen Indikator für die Steroidhormonaktivität zu bestimmen sei, sondern auch die glucuronidierten Androgene und Estrogene mit zu berücksichtigen seien (Labrie et al. 1997). Während UGT1 vor allem Estrogene modifiziert, wird die UGT2B als androgenspezifisches Enzym bezeichnet (Hum et al. 1999). Die Enzyme UGT1 und UGT2B werden extrahepatisch u.a. in Hoden, Ovar, Prostata und der Brust exprimiert und können dort zur lokalen Regulation der Steroidhormonwirkung beitragen.

Da die sulfatierten Steroidhormone Gegenstand der meisten Publikationen dieser Habilitationsschrift sind, soll hier genauer auf die Bildung und Funktion der sulfonierten Steroide eingegangen werden. Wie von Strott beschrieben (Übersicht bei Strott 2002), werden die Steroidhormone über die Aktivität der Sulfotransferasen (SULTs) an einen Sulfitrest (SO_3^-) gebunden. Eigentlich müsste man das Ergebnis dieser Reaktion als „sulfoniertes Steroid“ bezeichnen, allerdings hat sich die Bezeichnung „sulfatierte Steroide“ in den Sprachgebrauch eingebürgert und soll deswegen hier auch im Weiteren verwendet werden. Die Sulfonierung ist essentiell für physiologisches Wachstum, Aufbau von Geweben und Organen und den Erhalt der Homöostase. Sulfonierte Proteoglykane zum Beispiel sind Ausgangsmoleküle für das interstitielle Bindegewebe aller Organe. Neben den Strukturproteinen der Bestandteile der extrazellulären Matrix können auch Cholesterol, Gallensäuren, Vitamin D und Steroidhormone sulfoniert werden. Man unterscheidet zwischen fünf SULT-Familien. Die ersten beiden Familien SULT1 und SULT2 sind die häufigsten, die auch Estrogene (SULT1E1) und Androgene (SULT2A1) sulfonieren können. Das Hauptsubstrat der SULT2A1 ist DHEA,

welches zu DHEAS sulfoniert wird. Es ist das häufigste Steroidsulfat im Kreislauf und wird vor allem in der Nebennierenrinde, aber auch zu einem kleineren Anteil im Hoden synthetisiert. Durch einen Abfall der DHEAS-Konzentration mit dem Alter wurde DHEAS zunehmend als „Jungbrunnen" bezeichnet. Weitere Substrate der SULT sind aber auch Pregnenolon, Estron, Estradiol und Testosteron (Übersicht bei Strott 2002).

Die Ausscheidung der sulfatierten Steroide über den Urin wurde bereits in den 1920er Jahren untersucht (Übersicht bei Bradlow 1970). Ähnlich wie bei der Glucuronidierung führt auch die Sulfonierung zu einer deutlich gesteigerten Hydrophilie der Steroide. Sehr lange galten die sulfatierten Steroide als Exkretionsprodukte ohne eigene biologische Wirkung, da sie nicht durch die Zellmembran in die Zielzellen hinein- bzw. aus den Ursprungszellen hinausdiffundieren können (Hähnel et al. 1973; Strott 1996; Kuiper et al. 1997; Hum et al. 1999). Diese Theorie wurde bereits sehr früh in Frage gestellt, da schon in den 1970er Jahren Versuche zur Synthese von Steroidsulfaten im menschlichen Hoden durchgeführt wurden. Hierbei konnte gezeigt werden, dass im Hoden des Menschen große Mengen von sulfatierten Steroiden wie Pregnenolonsulfat (PREGS), Dehydroepiandrosteronsulfat (DHEAS) und Testosteronsulfat (TS) produziert (Laatikainen et al. 1971; Ruokonen et al. 1972; Mouhadjer et al. 1989) und auch als Vorstufen für die Testosteronsynthese genutzt werden können (Payne et al. 1971; Payne et al. 1973; Payne und Jaffe 1975). Ermöglicht wird diese Reaktivierung der sulfatierten Steroide durch die Aktivität der Steroidsulfatase (STS), die den Sulfitrest abspaltet und die Steroide wieder in ihre freie, biologisch aktive Form überführt. Nach den Veröffentlichungen von Payne et al. und Ruokonen et al. zur *in vitro* Metabolisierung von DHEAS und PREGS zu Testosteron (Payne et al. 1971; Ruokonen 1978) wurde die STS als regulatorisches Enzym für die testikuläre Testosteronproduktion beschrieben (Payne und Jaffe 1970; Gosden et al. 1986; Orava et al. 1985). Die Expression der STS wurde beim Menschen in Sertoli- und Keimzellen beschrieben, bei der Ratte im gesamten Hoden mit besonderer Häufung in den Leydigzellen und beim Eber nur in den Leydigzellen (Payne et al. 1973; Bedin et al. 1988; Mouhadjer et al. 1989; Mutembei et al. 2009). Beim Menschen gibt es einen beschriebenen rezessiven Defekt im STS-Gen auf dem X-Chromosom, die sog. *recessive X-linked ichthyosis* (RXLI). Bei dieser STS-Defizienz lagern sich große Mengen Cholesterolsulfat (CS) in die Haut ein. Dies führt zu einer Bildung von Rissen und Narben in der Haut. Lange wurde bei einer STS-Defizienz eine Häufung von Kryptorchismus und Hodentumoren beschrieben (Traupe und Happle 1983; Lykkesfeldt et al. 1985; 1991), die sich allerdings nicht nach neueren Erkenntnissen nicht bestätigt haben (Elias et al. 2014).

Die Ko-Expression von SULTs und STS im Hoden impliziert das Vorhandensein eines sog. *„sulfatase pathway"* (Abb. 8). Dieser umschreibt eine Re-Aktivierung von sulfatierten Steroiden durch die STS zu ihrer aktiven, freien Form sowie auch die Möglichkeit der De-Aktivierung durch die SULTs. Das

Vorkommen beider Enzyme in einem Gewebe und so die Existenz des *„sulfatase pathway“* wurde in verschiedenen Organen beschrieben wie z.B. Plazenta, Brust, Ovar, Gehirn und auch dem Hoden (Makawiti et al. 1983; Daels et al. 1995; Hoffmann et al. 1996; Purinton und Wood 2000; Janowski et al. 2002; Schuler et al. 2008; Mutembei et al. 2009). Dieser „Recyclingprozess“ kann eine wichtige Quelle für die lokale Estrogen- und Androgenversorgung von Hormon-rezeptiven Zellen im Hoden sein, spielt aber auch eine wichtige Rolle bei der Entwicklung von hormonabhängigen Tumorerkrankungen wie Brust- oder Prostatakrebs (Labrie et al. 2001; Selcer et al. 2002; Pasqualini und Chetrite 2005). Die STS wurde bereits vor zehn Jahren als vielversprechendes therapeutisches Target angesehen (Stanway et al. 2007), da etwa 90% Brustkrebszellen STS exprimieren (Übersicht bei McNamara et al. 2015). Es können verschiedene Klassen von STS-Inhibitoren beschrieben werden. Dies sind zum Beispiel modifizierte Steroide, die an die STS binden und sie blockieren, reversible und irreversible Inhibitoren. Als besonders vielversprechend wird Coumate beschrieben, das in der ersten klinsichen Phase gute Ergebnisse bei der Inhibierung der STS bei postmenopausalen Brustkrebspatientinnen erreichen konnte (Übersicht bei Shah et al. 2016).

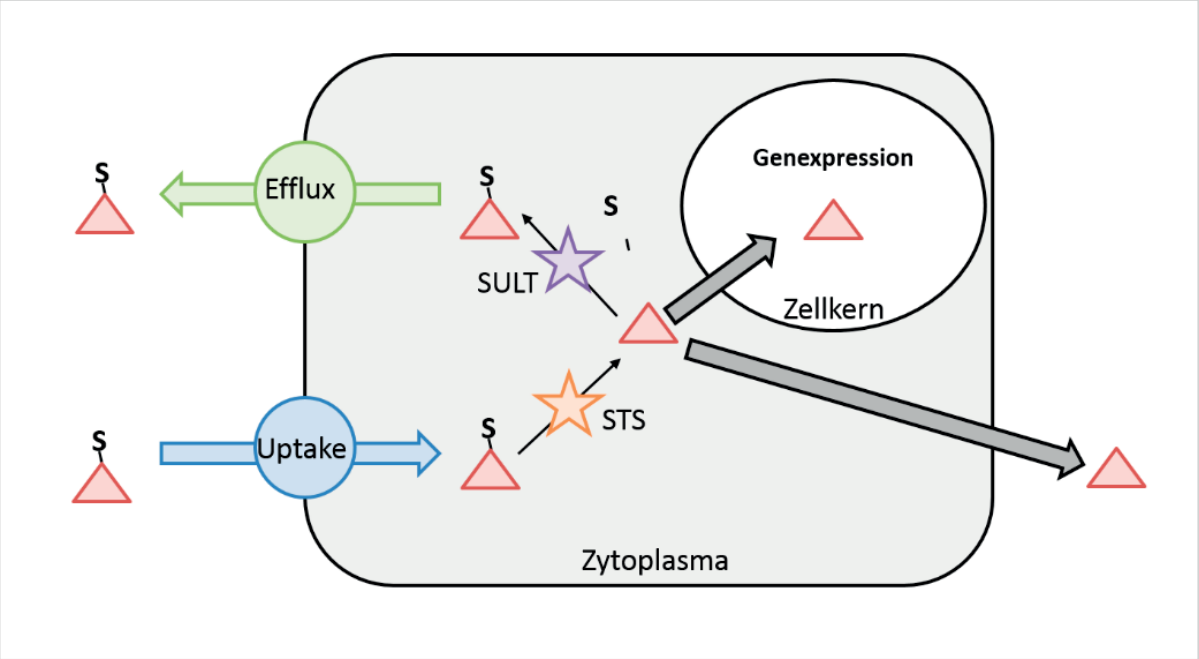

Abb. 8 Schematische Darstellung des „sulfatase pathway“

Nach der Aufnahme der sulfatierten Steroide (rotes Dreieck mit „S“) in die Zelle mittels Uptake Carriern kann der Sulfatrest durch die Steroidsulfatase (STS, oranger Stern) abgespalten werden. Die freien Steroide (rotes Dreieck“ können in der Zelle wirken oder die Zelle per Diffusion verlassen. Freie Steroide können aber auch innerhalb der Zelle durch die Sulfotransferasen (SULT, lila Stern) sulfoniert werden und durch Effluxtransporter aus der Zelle heraustransportiert werden.

5.2. Klassische und nicht-klassische Steroidhormonrezeptoren

5.2.1. Klassische (nukleäre) Steroidhormonrezeptoren

Klassische Steroidhormonrezeptoren für Androgene, Estrogene und auch Progesteron sind generell zytoplasmatisch lokalisierte nukleäre Transkriptionsfaktoren, für den Androgenrezeptor (AR) wurde allerdings auch eine nukleäre „Warteposition" beschrieben wurde (Übersicht bei Gelmann 2002). Der AR liegt an *heat shock* Proteine gebunden vor. Nach einer Ligandenbindung kommt es zu einer Konformationsänderung, die zu einer Abspaltung der *heat shock* Proteine und einer Dimerisierung der AR-Liganden-Komplexe führt. Die Translokation dieser Rezeptor-Liganden-Komplexe in den Zellkern wird durch die *hinge*-Region beeinflusst. Jenster et al. (1993) konnten zeigen, dass es Bereiche im AR-Protein gibt, die dem nukleären Lokalisationssignal Nukleoplasmin ähneln und so das Signal zur Kerntranslokation gegeben wird. Im Zellkern binden die Steroidhormonrezeptoren an *hormone responsive elements* (HREs) und fungieren dort als Transkriptionsfaktor. Beeinflusst durch Ko-Faktoren, die ihrerseits hemmend oder aktivierend sein können, wird so die Genexpression eines hormonabhängigen Gens gehemmt oder aktiviert (für den Androgenrezeptor Übersicht bei Bennett et al. 2010). Diese genomische Aktivität der klassischen Steroidhormonrezeptoren dauert mehrere Stunden bis Tage (Übersicht bei Walker 2009).

Der Androgenrezeptor (AR) ist ein klassischer Steroidhormonrezeptor, dessen Gen auf dem langen Arm des X-Chromosoms liegt (Übersicht bei Gelmann 2002; Claessens et al. 2005). Der AR wird in fast allen Organen bis auf die Milz exprimiert (Gelmann 2002). Im Hoden wird der Rezeptor in fast allen Zellpopulationen beschrieben, er wurde in Leydig- und Sertolizellen, peritubulären Myoidzellen sowie glatten Muskel- und Endothelzellen nachgewiesen (Bergh und Damber 1992; Fietz et al. 2011 (**Publikation #2**)). In Keimzellen wurde der AR nur von wenigen Arbeitsgruppen gezeigt, wie zum Beispiel von Kimura et al. (1993) in Spermatogonien und Spermatozyten (Übersicht bei Walker 2009). In Sertolizellen spielt der AR eine essentielle Rolle, wie durch die Generierung einer Knockout-Maus bei Wang et al. (2006) gezeigt werden konnte. Ein Fehlen des AR in Sertolizellen führt zu einem verminderten Hoden- und Nebenhodengewicht, einem geringeren Tubulusdurchmesser, einem Arrest der Spermatogenese auf Stufe der primären Spermatozyten und verringerte Testosteronwerte im Serum. Direkte Effekte auf die Sertolizellen sind eine Dislokation des Zellkerns im Keimepithel, eine vermehrte Expression des Zytoskelettproteins Vimentin und eine fehlende Ausbildung der BHS. Der AR ist demnach von essentieller Bedeutung für die Sertolizellbiologie und die Spermatogenese. Der AR besteht aus acht Exonen, die für eine Transaktivierungsdomäne, eine DNA-bindende Domäne, eine *hinge*-Region sowie eine Liganden-bindende Domäne kodieren (Übersicht bei Gelmann 2002). An den AR können sowohl Testosteron als auch DHT binden; letzteres bindet mit einer höheren Effizienz. Es gibt beim AR auch zwei

Transaktivierungsfunktionen (TAFs, auch *activation functions*, AFs), die maßgeblich an der Rezeptorfunktion beteiligt sind. Während bei den anderen Steroidhormonrezeptoren v.a. die AF-2 in der Liganden-bindenden Domäne hauptsächlich für die Transaktivierungsfunktion verantwortlich ist, spielt sie beim AR eine der AF-1 untergeordnete Rolle, die aber genau wie die AF-2 Liganden-abhängig ist (Brinkmann et al. 1999, Übersicht bei Sadar 2011). Der AR beinhaltet weiterhin die AF-5, die ebenfalls in der Transaktivierungsdomäne liegt. Diese ist allerdings Liganden-unabhängig, kann also auch bei einer trunkierten AR-Version ohne Liganden-Bindungsdomäne eine Transaktivierung vermitteln (Übersicht bei Gelmann 2002). Die AF-1 liegt in der Transaktivierungsdomäne des AR und ist Ziel von Ko-Faktoren wie dem aktivierenden p160 (Irvine et al. 2000; Lee und Chang 2003). Diese Domäne beinhaltet zudem ein polymorphes CAG-Repeat, das mit seiner physiologischen Länge von 9-36 Repeats und einer mittleren physiologischen Repeatlänge von 21±2 (Quigley et al. 1995; La Spada et al. 1991). Verlängerungen dieses CAG-Repeats, wie z.B. bei einer spino-bulbären Muskelatrohie (Tanaka et al. 1999) beeinflussen die Transaktivierungsfunktion des AR negativ, was zu einer verschlechterten Transaktivierung der AR-Zielgene führt (Tut et al. 1997). Das Ergebnis ist das Androgeninsensitivitätssyndrom (AIS) mit unterschiedlichen Ausprägungen (*partial AIS* mit milder Sub- bis Infertilität bis hin zum *complete AIS* mit einer testikulären Feminisierung) (Rajender et al. 2007). Es wurde lange angenommen, dass neben der pathologischen Verlängerung des CAG-Repeats auf über 40 Repeats auch geringgradig verlängerte oder verkürzte Repeats im physiologischen Rahmen Einfluss auf die AR-Transaktivierungsfunktion und somit die Physiologie des Keimepithels und der Spermatogenese nehmen können (Nenonen et al. 2010). In verschiedenen Studien in wurde das CAG-Repeat im Blut von fertilen und infertilen Patienten bestimmt (Dowsing et al. 1999; Dadze et al. 2000; Mifsud et al. 2001; Eckardstein et al. 2001; Rajpert-De Meyts et al. 2002; Casella et al. 2003). Die Ergebnisse der Studien variierten stark. Mifsud et al. konnten zum Beispiel ein siebenfach erhöhtes Risiko für das Auftreten einer Azoospermie bei einer CAG-Repeatzahl von 26 und mehr feststellen (Mifsud et al. 2001). In einer Meta-Analyse von Davis-Dao et al. (2007) wurden 33 Studien zusammengefasst und ein schwach positiver Zusammenhang zwischen verlängerten CAG-Repeatlängen und Infertilität festgestellt werden. Huhtaniemi et al. (2009) stellten die Theorie auf, dass nicht die verminderte Transaktivierungsfunktion des AR bei einem verlängerten CAG-Repeat für eine Infertilität verantwortlich gemacht werden könnte, sondern die mit den verminderen Androgenspiegeln einhergehenden erhöhten Estrogenspiegel. In unseren eigenen Untersuchungen wurde die CAG-Repeatlänge im physiologischen Bereich bei verschiedenen Patienten mit normaler und gestörter Spermatogenese untersucht. Dabei konnte kein kausaler Zusammenhang zwischen der Repeatlänge und dem Spermatogenesestatus hergestellt und auch keine verminderte AR-Genexpression ermittelt werden. Auffällig war allerdings ein Mosaik in der

CAG-Repeatlänge, das zwischen der DNA und mRNA, Blut und Hoden sowie zwischen dem rechten und linken Hoden detektiert werden konnte (Fietz et al. 2011, **Publikation #2**).

Der Grundaufbau des Estrogenrezeptors (ER, ESR) ist identisch zum AR. Es gibt allerdings zwei verschiedene Subtypen von ERs. Der sog. „klassische" ERα (ESR1) wurde bereits in den 1960ern entdeckt und in den 1980er Jahren weiter untersucht (Walter et al. 1985, Übersicht bei Prossnitz und Barton 2011). Sein Gen (*ERS1*) liegt auf Chromosom 6 (Gosden et al. 1986) und ist deutlich länger als das Gen des erst später entdeckten „nicht-klassischen" ERβ (ESR2, Gen: *ESR2*) (Mosselman et al. 1996). Dessen Gen (*ESR2*) liegt auf Chromosom 14 (Enmark et al. 1997). Beide ER-Subtypen sind in den DNA-Bindungsdomänen und der Liganden-Bindungsdomäne zu 95% bzw. 58% homolog (Marino et al. 2006). Für beide ESRs sind Isoformen bekannt (Übersicht bei Gibson und Saunders 2012) und beide binden Estradiol, Estriol und Estron mit hoher Affinität (Paech et al. 1997). Neben den weiblichen Geschlechtsorganen werden die ESRs auch im männlichen Genitaltrakt exprimiert. Anders als der AR sind die ESRs v.a. in den verschiedenen Keimzellpopulationen (Spermatogonien, Spermatozyten und Spermatiden) und auch den somatischen Zellen (Sertoli- und Leydigzellen) des Hodens zu finden; die Berichte zur zellulären Expression wird aber auf Grund sehr vieler verschiedener Antikörper sehr kontrovers diskutiert. Während einzelne Gruppen den ERα gar nicht im Hoden nachweisen konnten (Saunders et al. 2001; Mäkinen et al. 2001), detektierten die meisten Gruppen das Protein zumindest in einer Zellpopulation wie z.B. den Leydigzellen (Pelletier und El-Alfy 2000), Spermatozyten und elongierenden Spermatiden (Pentikäinen et al. 2000), Keim- und Leydigzellen (Han et al. 2009) oder nur in somatischen Zellen (Filipiak et al. 2013). Cavaco et al. (2009) konnten den ERα überall nachweisen. Der ERβ wurde ebenfalls in verschiedenen somatischen Zellen und Keimzellen beim Nager und Mensch detektiert (Saunders et al. 2001; Mäkinen et al. 2001, Übersicht bei Carreau und Hess 2010). In unserer eigenen Arbeit wurde der ERα in Spermatogonien, primären Spermatozyten und runden Spermatiden detektiert, aber nicht in Sertolizellen und nur vereinzelnt in interstitiellen Zellen. Der ERβ dagegen konnte zusätzlich zu der Expression in den bereits genannten Keimzellen auch in den Sertolizellen detektiert werden, aber nicht in Leydigzellen (Fietz et al. 2014, **Publikation #3**). Estrogene werden im Hoden (v.a. bei Hengst und Eber, aber auch beim Menschen) *de novo* in Leydig-, Sertoli- (allerdings nur fetal) und auch Keimzellen synthetisiert (Nitta et al. 1993, Übersicht bei Carreau et al. 2011). Auch über den *„sulfatase pathway"* können aus sulfatierten Steroidhormonen freie Estrogene synthetisiert werden (Schuler et al. 2014). Zudem haben beim Schwein freie und sulfatierte Steroide eine Bedeutung als Pheromone (Übersicht bei Liberles 2014). Lange war unklar, welche Rolle Estrogene und ihre Rezeptoren bei der Aufrechterhaltung der Spermatogenese spielen, da für diese Aufgabe immer nur die Androgene verantwortlich gemacht wurden. Es ist bekannt, dass Estrogene die Proliferation von

Spermatogonien beeinflussen (Pentikäinen et al. 2000; Wagner et al. 2006; Lekhkota et al. 2006). Erst durch die Untersuchung von Knockout-Mäusen für Erα (ERαKO) (Lubahn et al. 1993) und ERβ (ERβKO) wurde die Bedeutung für die männliche Fertilität deutlich. ERαKO Mäuse sind steril, da die aus dem Nebenhoden entnommenen Spermien immotil sind. Dies ist allerdings nicht auf eine Störung der Spermatogenese zurück zu führen, sondern auf mangelhafte Ansäuerung des Nebenhodenganges und Flüssigkeitsresorption. Demnach sind Estrogene und ihre Rezeptoren eher bei der Formung eines *microenvironments* in Hoden und Nebenhoden als an der Spermatogenese selbst beteiligt. Auch ERβKO-Mäuse sind steril, allerdings ist hier nicht klar, warum: Sowohl Hoden als auch Nebenhoden sind histologisch normal und die Spermien sind beweglich (Couse und Korach 1999). Berichte über Estrogenrezeptor-Defizienzen beim Menschen sind selten. Im Gegensatz zu den Versuchen bei der Maus scheint aber auch die Spermatogenese gestört zu sein, da diese Defizienzen mit einer Verschlechterung der Ejakulatparameter einhergehen (Smith et al. 1994).

Neben den genomischen Effekten der klassischen Steroidhormonrezeptoren können diese auch schnelle, nicht-genomische Effekte vermitteln (Übersicht bei Levin und Hammes 2016). Die im Zytoplasma lokalisierten Kernrezeptoren sammeln sich zu diesem Zweck in der Nähe oder sogar in der Zellmembran und können dort Liganden binden. Entgegen der Aktivität als Transkriptionsfaktoren, verlagern diese Komplexe sich nicht in den Kern und aktivieren die Genexpression. Sie aktivieren dagegen eine intrazytoplasmatische Signalkaskade, die z.B. mit einer Erhöhung des intrazellulären cAMPs oder auch einem Ca^{2+}-Anstieg einhergeht (Spaziani und Szego 1959; Szego und Davis 1967). Neben Ansammlungen von Estrogen-, Androgen- und Progesteronrezeptormolekülen in der Zellmembran können die Steroidhormonrezeptoren auch im endoplasmatischen Retikulum oder den Mitochondrien vorkommen. Vor allem in Krebszellen, wie Brust- und Prostatakrebs, kann diese Art der Steroidhormonwirkung die Pathogenese der Erkrankungen beeinflussen (Übersicht bei Hammes und Levin 2007; Levin und Hammes 2016).

5.2.2. Nicht-klassische (membran-ständige) Steroidhormonrezeptoren

Neben den klassischen Steroidrezeptoren und ihrer Lokalisation in der Zellmembran gibt es auch membran-ständige Steroidhormonrezeptoren, die allerdings nicht zur Superfamilie der nukleären Transkriptionsfaktoren gehören und deswegen als „nicht-klassisch“ bezeichnet werden. Diese häufig G-Protein gekoppelten Rezeptoren (*G protein coupled receptors*, GPCRs) vermitteln eine schnelle nicht-genomische Wirkung, wie z.B. einen Ca^{2+}-Einstrom, der von Lyng et al. (2000) bereits für Androgene und Estrogene beschrieben werden konnte. Beispiele für diese nicht-genomischen Steroidwirkungen sind die estrogen-vermittelte Vasodilatation, die Progesteron-induzierte

Akrosomenreaktion und die Hypermotorik der Spermien, die durch die Bindung von Progesteron an den CatSper-Kanal vermittelt wird (Übersicht bei Wang et al. 2014). Auch in Sertolizellen sind nicht-genomischen Signalwege bekannt (Übersicht bei Walker 2010). Wie von Wang et al. (2014) beschrieben, scheinen die GPCRs als gemeinsames Motiv die Cholesterolgrundstruktur zu erkennen. Die G-Proteine können entweder eine aktivierende oder auch eine inhibierende intrazelluläre Signalkaskade anstoßen, z.B. die Aktivierung der Adenylatzyklase-Proteinkinase A (PKA) oder der Phospholipase C-Proteinkinase C (Übersicht bei Wang et al. 2014). Das erklärt die verschiedenen nicht-genomischen Effekte, die von Steroidhormonen hervorgerufen werden können. So können zum Beispiel Progestine und Androgene die Oozytenreifung unterstützen, da beide an denselben GPCR binden. Nicht nur freie Steroidhormone können an GPCRs binden und einen nicht-genomischen Signalweg direkt initiieren, sondern auch konjugierte Steroide wie DHEAS (Shihan et al. 2014; Papadopoulos et al. 2016).

Der G-Protein gekoppelte Estrogenrezeptor GPER (auch GPR30) (Rago et al. 2014, Übersicht bei Prossnitz und Barton 2011) wurde intensiv untersucht. Zahlreiche Studien konnten nachweisen, dass GPER an ein stimulierendes G-Protein (G_S) gebunden ist und v.a. die Adenylatzyklase und den *Epidermal Growth Factor* (EGF) aktiviert (Filardo et al. 2008). Eine Aktivierung des GPER durch Ligandenbindung wird mit einer Proliferation von Krebszellen der Reproduktionsorgane in Verbindung gebracht (Übersicht bei Wang et al. 2014). Doch auch im gesunden Gewebe, z.B. dem Hoden, wurde GPER bereits in verschiedenen Zellpopulationen wie den Leydig- und den Sertolizellen lokalisiert (Übersichten bei Carreau et al. 2011; 2012; Fietz et al. 2014, **Publikation #3**). Eine Lokalisation in den Keimzellen dagegen ist umstritten. Franco et al. (2011) fanden zwar beim Mensch eine Expression in Keimzellen bei normaler Spermatogenese und auch in Seminomen, andere Gruppen dagegen nicht. Vor allem bei Tieren mit einer starken Sekretion sulfatierter Estrogene im Hoden, wie Eber und Hengst (Claus und Hoffmann 1980; Hoffmann und Landeck 1999) könnte der GPER eine Rolle für das „Fine-Tuning“ der Estrogenwirkung im Hoden sein.

In humanen Brustkrebs- und Prostatakarzinomzellen wurde ein membranständiger Androgenrezeptor, ZIP9, nachgewiesen. Er gehört zu der Zink-Transporterfamilie und kann sowohl in der Zell- und Kernmembran sowie im endoplasmatischen Retikulum und den Mitochondrien exprimiert werden. In AR-freien Krebszellen ist ZIP9 für Testosteron-induzierte Apoptose verantwortlich (Thomas et al. 2014). Wie auch GPER ist ZIP9 an ein G_S-Protein gebunden und eine Aktivierung führt zu einem cAMP-Anstieg in den Zellen. Eine Gruppe konnte zeigen, dass Testosteron spezifisch an den intrazellulär lokalisierten ZIP9 binden kann (Bulldan et al. 2017) und die von Testosteron induzierten ZIP9-vermittelten nicht-genomischen Effekte in Sertoli- und Keimzellkulturen Einfluss auf die Genexpression haben (Shihan et al. 2015; Bulldan et al. 2016a). Nach einer

chemischen Kastration von Hunden mit einem GnRH-Implantat konnte dieselbe Gruppe eine verminderte Expression von ZIP9 zeigen, welche mit verminderten Testosteronkonzentrationen in Verbindung gebracht wurde (Bulldan et al. 2016b). Neben Testosteron kann dieser Rezeptor auch Estradiol binden (Übersicht bei Thomas et al. 2017). Bisher wurde die ZIP9-Expression und -Wirkung in Krebszellkulturen und normalen Sertoli- und Keimzellkulturen untersucht, nicht aber in physiologischen Organen. Ein weiterer Rezeptor, der die nicht-genomischen Effekte von Androgenen vermittelt, ist der GPRC6A (Übersicht bei Wang et al. 2014). Dieser Rezeptor kann Aminosäuren und extrazelluläres Calcium binden. Ein *Gprc6a*-Knockout führt in männlichen Mäusen zu einer testikulären Feminisierung und deswegen wurde der Rezeptor auch auf die Bindung von Steroidhormonen hin untersucht (Pi et al. 2010). GPCR6A bindet Testosteron, aber auch andere Steroidhormone. Dies wurde in verschiedenen Zellkulturmodellen untersucht. GPCR6A wird in Leydigzellen und verschiedenen peripheren Organen exprimiert (Wellendorph et al. 2005); eine verminderte Expression in den Leydigzellen führt zu einer reduzierten Testosteronproduktion im Hoden. Vermutlich aus diesem Grund zeigten Gprc6a-negative Mäuse kleinere Samenblasendrüsen als die Kontrolltiere und ein verlangsamtes Wachstum von Prostatakarzinomen. Toni et al. (2016) berichtet von zwei Fällen inaktivierender GPCR6A-Mutationen, die mit gestörter Spermatogenese und Kryptorchismus einhergingen. Ein Polymorphismus im GPCR6A wurde des Weiteren mit Prostatakarzinomen in Verbindung gebracht.

Membranassoziierte Progesteronrezeptoren wurden in verschiedenen Organen und Zellen wie Aorta, Leber, Gehirn, Brust, Ovar und Spermien nachgewiesen. Während die Aktivierung dieser Rezeptoren in Uterus und Darm eine Relaxation der glatten Muskulatur auslöst, kommt es in Brustkrebszelllinien zu einer gesteigerten Proliferation (Übersicht bei Gadkar-Sable et al. 2005). Besonders in Spermien ist der Effekt von Progesteron gut untersucht. Durch die Bindung von Progesteron an Kationenkanäle (sog. CatSper-Kanäle) kommt es zu einem schnellen Calciumeinstrom, der wiederum die Hypermotilität der Spermiengeißel im weiblichen Genital hervorruft. Weitere nicht-genomische Effekte der Progesteronbindung sind Spermienkapazitation und Akrosomenreaktion. Dieser Effekt kann durch Estradiol gehemmt werden (Übersicht bei Gadkar-Sable et al. 2005). Ein erstmals in Fischen beschriebener membranständiger Progesteronrezeptor ist der mPRα. Dieser Rezeptor kommt vor allem im weiblichen Genitaltrakt vor, wurde aber auch auf Spermien und im Hoden von Mensch und Maus nachgewiesen. Die Expression von mPRα auf Spermien war bei hypomotilen Spermien verringert (Thomas et al. 2009, Übersicht bei Dressing et al. 2011).

5.3. Mechanismen des transmembranären Transports

Alle Zellen des Körpers werden von Lipiddoppelmembran umschlossen, die das Innere der Zelle mit den im Zytoplasma gelösten Stoffen von dem extrazellulären Milieu trennt. So findet man im extrazellulären Milieu z.B. deutlich mehr Natrium- und Chloridionen als im Inneren der Zelle. Im Gegensatz dazu ist die Konzentration von Phosphat und Aminosäuren/Proteinen im Inneren der Zelle deutlich höher als außerhalb. Durch die semipermeable Biomembran wird ein Konzentrationsgradient aufgebaut, der für die verschiedenen Mechanismen des transmembranären Transports genutzt werden kann (Abb. 9) (Übersicht bei Guyton and Hall 2006; Constanzo 2010). Physiologische Konzentrationsunterschiede sind des Weiteren essentiell für verschiedene biologische Vorgänge wie z.B. Erregungsweiterleitung.

Bei der einfachen Diffusion können lipophile Moleküle durch ihre Molekularbewegung durch die Zellmembran hindurchtreten. Dabei sind keine Transporterproteine involviert. Bei der erleichterten Diffusion sind Kanalproteine vorhanden, die durch die gesamte Zellmembran reichen und die für verschiedene Stoffe durchlässig sind. Dieser Transport ist auf das Vorhandensein eines Konzentrationsgradienten angewiesen, der die Diffusion antreibt. Sind beide Seiten der semipermeablen Membran ausgeglichen, kommt die Diffusion zum Stillstand. Freie Steroidhormone können aufgrund ihrer hohen Fettlöslichkeit einfach die Zellmembran passieren und dann intrazellulär an Rezeptoren binden. Konjugierte Steroide dagegen zeichnen sich durch eine hohe Wasserlöslichkeit aus und können demnach nicht mehr per Diffusion in die Zelle aufgenommen werden. Kleinere anorganische Moleküle wie Harnstoff oder auch nur Wasser dagegen sind war auch nicht lipophil, können aber durch Kanalproteine in die Zelle aufgenommen werden. Glukose und Aminosäuren dagegen sind größer und benötigen Transporterproteine, an die sie binden und die sie durch eine Konformationsänderung in das Innere der Zelle hineinlassen. Wie bei der einfachen Diffusion ist auch die erleichterte Diffusion ein ungerichteter Vorgang, der in beide Richtungen, je nach anliegendem Konzentrationsgradienten, funktioniert.
Beim aktiven Transport dagegen kann ein Transport entgegen einen Konzentrationsgradient auftreten. Dieser Vorgang ist *per se* energieabhängig. Der aktive Transport erhält außerdem die intra- und extrazellulären Ionenkonzentrationen und somit den Konzentrationsgradienten aufrecht. Man unterscheidet dabei den aktiven Transport und den sekundär aktiven Transport. Beim aktiven Transport wird die benötige Energie direkt durch die Spaltung von ATP gewonnen. Beim sekundär aktiven Transport dagegen muss ein durch aktiven Transport ein Ionengradient aufgebaut werden, der den sekundär aktiven Transport dann antreibt. Beide Formen des aktiven Transports sind auf Membranproteine angewiesen, die die Zellmembran durchlaufen. Die Natrium-Kalium-Pumpe ist ein

klassisches Beispiel für aktiven Transport, der zeitgleich Natrium nach außen und Kalium nach innen transportiert. Beim sekundär aktiven Transport unterscheidet man zwischen Ko-Transportern (Symportern) und Antiportern. Ein Ko-Transport von Natriumionen und hydrophilen Molekülen ist der vorherrschende Aufnahmemechanismus für sulfatierte Steroidhormone (Übersicht bei Geyer et al. 2016, **Publikation #8**).

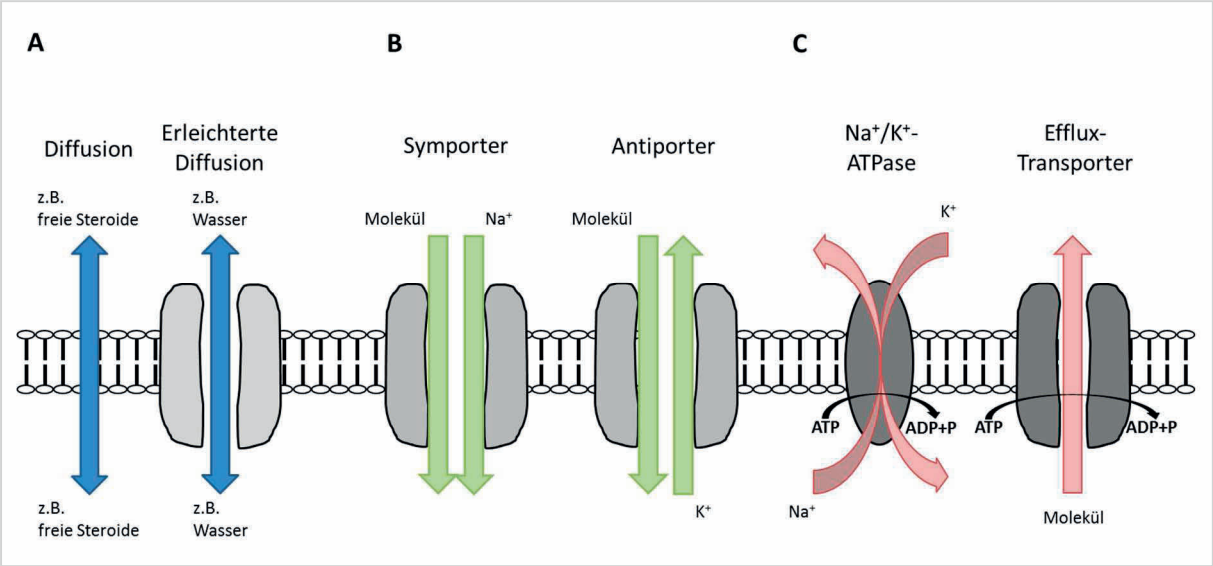

Abb. 9 Transmembranäre Transportmechanismen

A Diffusion und erleichterte Diffusion **B** sekundär aktiver Transport (Symport und Antiport) **C** aktiver Transport (Na^+/K^+-ATPase und Effluxpumpen)

5.4. *Uptake carrier* und *Efflux*-Transporter für sulfatierte Steroidhormone

Für die Aufnahme und auch die Abgabe der hydrophilen sulfatierten Steroidhormone in die Zielzellen hinein bzw. aus ihnen hinaus sind spezifische Transportsysteme nötig. Diese Transporter sind essentiell für den *„sulfatase pathway“* (Abb. 8). Besonders der Transport im Hoden über die Blut-Hodenschranke hinweg erfordert die Expression von beiden Transportsystemen in den Sertolizellen. Mitglieder von zwei Transportersuperfamilien, die *Solute Carriers* (SLC) und *ATP-binding cassette transporter* (ABC Transporter) sind hier von größter Bedeutung.

Die Mitglieder der SLC Superfamilie sind Ionen-gekoppelte Sym- oder Antiporter, die sekundär aktive Moleküle in das Innere der Zelle transportieren können. Auch Uniporter gehören in diese Superfamilie (Petzinger und Geyer 2006). Das *HUGO Nomenclature Committee* beschreibt im Jahr 2017 52 verschiedene SLC-Familien mit etwa 395 Genen (http://www.genenames.org/cgi-bin/genefamilies/set/752). Die ersten Mitglieder der SLC10-Familie waren die beiden Ko-Transporter

NTCP (*Na^+-/Taurocholate cotransporting polypeptide*; Gen: *SLC10A1*) in der Leber und ASBT (*apical sodium-dependent bile transporter*; Gen: *SLC10A2*) in der Dünndarmschleimhaut. Beide sind in den enterohepatischen Gallensäurenkreislauf eingebunden (Hagenbuch und Dawson 2004; Geyer et al. 2006). Bereits früh wurde gezeigt, dass der NTCP auch spezifisch sulfatierte Steroide transportieren kann (Schroeder et al. 1998). Weitere Mitglieder der SLC10-Familie wurden beschrieben (*SLC10A3-SLC10A7*) und in Hinblick auf ihre Spezies-spezifische Expression hin untersucht (Godoy et al. 2007; Fernandes et al. 2007; Geyer et al. 2008; Burger et al. 2011; Schmidt et al. 2015). Den meisten konnte aber noch kein spezifisches Substrat zugewiesen werden, weswegen man sie als *orphan transporter* bezeichnet (Geyer et al. 2006). Der *Slc10a6* wurde 2004 bei der Ratte und 2007 beim Menschen (*SLC10A6*) von Geyer et al. (2004; 2007) kloniert, beschrieben und als SOAT/Soat (*sodium-dependent organic anion transporter*) bezeichnet. Wie der NTCP und ASBT ist SOAT ein Membranprotein mit neun Transmembrandomänen, einem extrazellulären N-Terminus und einem intrazellulären C-Terminus (Abb. 10A). SOAT/Soat transportiert keine Gallensäuren, aber verschiedene sulfatierte Androgene und auch Estrogene. Als weiterer Unterschied zu NTCP und ABST ist SOAT nicht organ- bzw. zellspezifisch exprimiert, sondern kommt in verschiedenen Organen vor. Beim Mensch ist *SLC10A6* vor allem im Hoden exprimiert (Geyer et al. 2004; 2006), bei der Maus kann *Slc10a6* zwar auch im Hoden, aber vorrangig in der Lunge detektiert werden (Grosser et al. 2013, **Publikation #6**).
Neben dem Natrium-abhängigen Transport der SLC10 Familie, gibt es auch Natrium-unabhängige Transporter, die *Organic Anion Transporting Peptides* (OATPs); diese gehören zur SLCO-Familie (das „O“ steht hier für die OATPs). Die Mitglieder der Familie zeigen z.T. eine große Spezies- und Substratdiversität (Hagenbuch und Meier 2004; Petzinger und Geyer 2006). Im Gegensatz zur SLC10-Familie zeigen die SLCOs zwölf Transmembrandomänen mit einem extrazellulären N- und C-Terminus (Abb. 10B). Bekannt für den Transport von sulfatierten Steroiden sind alle Mitglieder der OATP1-Familie, der OATP2B- und OATP3A-Subfamilie, der OATP4A1 und der OATP4C1 (Übersicht bei Roth et al. 2011). Im Jahr 2005 wurde ein weiterer Natrium-unabhängiger Transporter beschrieben, das *Organic solute carrier protein* (OSCP) (Kobayashi et al. 2005), der in Hoden und Plazenta des Menschen exprimiert und als OSCP1 bezeichnet wird. Zwei Jahre später wurde auch in der Maus ein Homolog, *Oscp1*, beschrieben (Kobayashi et al. 2007). OSCP1 und Oscp1 transportieren ebenfalls sulfatierte Steroide und zeigen eine vollkommen andere Membranproteinstruktur mit nur drei Transmembrandomänen (Abb. 10C).
Die zweite Transporter-Superfamilie sind die ABC Transporter. Sie sind aktive Transporter (Effluxpumpen), die unter Energieverbrauch Moleküle entgegen eines Konzentrationsgradienten aus einer Zelle hinaustransportieren können (Borst und Elferink 2002). Beschrieben wurden die ABC Transporter erstmals an verschiedenen Blut-Gewebeschranken wie der Blut-Hirnschranke. Hier eliminieren die Transporter endo- und exogene Stoffe, die schadhaft für das Gewebe sein können,

indem sie sie in das Blutgefäß zurück transportieren. Dieses Phänomen wurde auch als *multidrug resistance* bezeichnet. Der erste dieser ABC-Transporter wurde in der Zellmembran von Hamsterovarien beschrieben und als P-Glycoprotein (P-gp) oder auch Multidrug-Resistance Carrier 1 (MDR1, Gen: *ABCB1*) bezeichnet (Juliano und Ling 1976). Er besteht aus zwei Hälften mit je sechs Transmembrandomänen und zwei Nukleotid-Bindungsdomänen, an die das ATP binden kann. Sowohl N- als auch C-Terminus sind intrazellulär lokalisiert (Abb. 10D). Weitere Mitglieder der ABC-Superfamilie wurden beschrieben, wie z.B. die *Multidrug resistance related proteins* 1-9 (MRP1-9; Gene *ABCC1-9*) und das *breast cancer related protein* (BCRP; Gen *ABCG2*) (Übersicht bei Schinkel und Jonker 2003). Die Transmembranstruktur der MRPs ist unterschiedlich; während MRP4 und MRP5 dem MDR1 sehr ähnlich sind, zeigen MRP1-3 eine N-terminale Verlängerung von fünf Transmembrandomänen und einen extrazellulären N-Terminus (Abb. 10E). Die Struktur von BCRP ist vollkommen anders, weswegen der Transporter auch als „Halb-Transporter“ beschrieben wird. Er besteht aus nur sechs Transmembrandomänen (Abb. 10F).

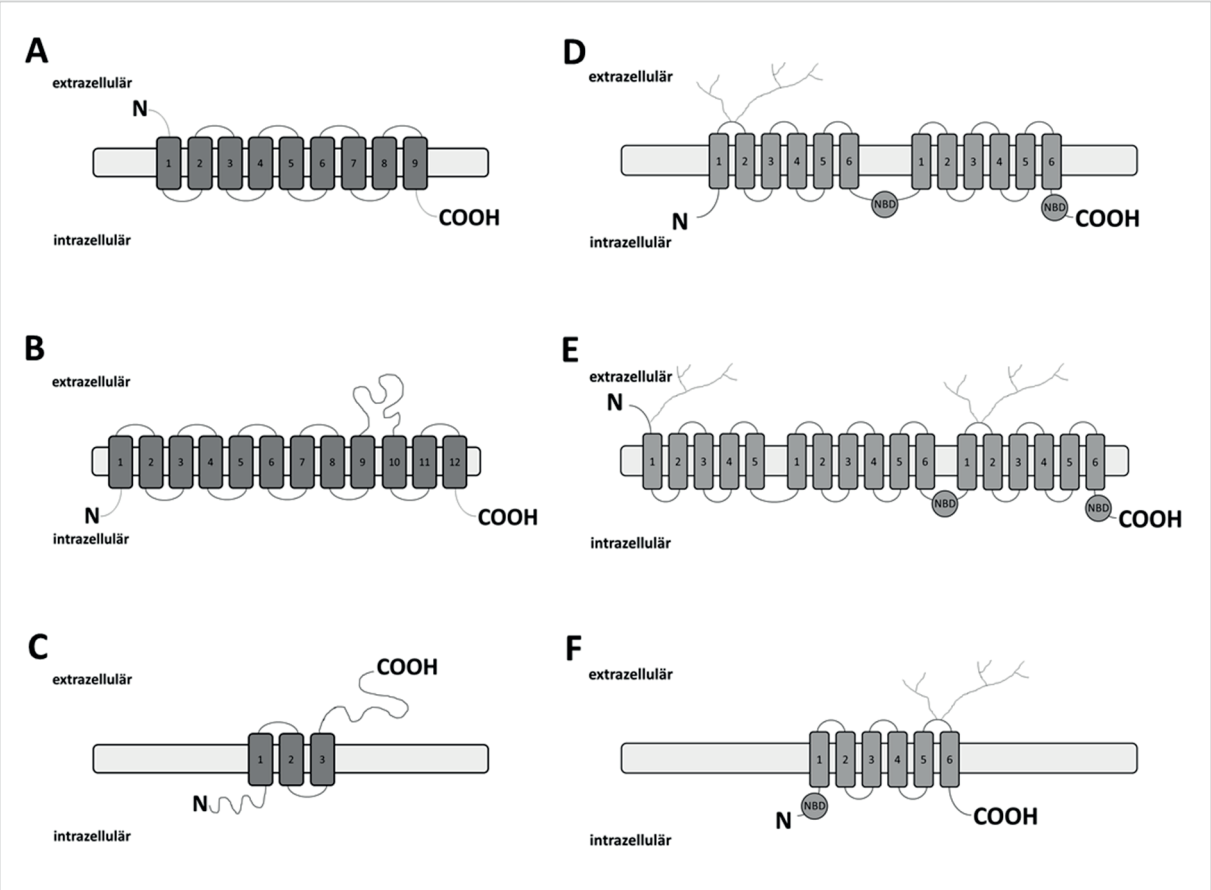

Abb. 10 Transmembranäre Transporterproteine für sulfatierte Steroide

A SOAT, **B** OATPs, **C** OSCP1, **D** MDR1, **E** MRP1-3, **F** BCRP

6. Zusammenfassende Ergebnisse und Diskussion

6.1. Das polymorphe CAG-Repeat des Androgenrezeptors und seine Bedeutung für die Spermatogenese

Die **Publikationen #1-3** befassen sich mit dem Androgenrezeptor und dem polymorphen CAG-Repeat im Exon 1 dieses klassischen Steroidhormonrezeptors. Das CAG-Repeat, welches für eine Glutaminkette kodiert, zeigt eine sehr hohe Varianz: Repeatlängen von 9-36 Repeats werden als physiologisch bezeichnet, die mittlere Länge des CAG-Repeats liegt bei 21 $\pm$ 2 Repeats (Quigley et al. 1995; La Spada et al. 1991). Krankhafte Verlängerungen oder auch Kürzungen des Repeats sind mit schwerwiegenden Störungen der allgemeinen Gesundheit, aber auch der Fruchtbarkeit assoziiert. Bei der spino-bulbären Muskeldystrophie oder auch Kennedy's Disease (La Spada et al. 1991; Tanaka et al. 1999) findet eine Verlängerung auf über 40 CAGs statt. Neben einem generalisierten Muskelschwund, mangelhaftem Muskeltonus und geistiger Retardierung treten bei dieser Krankheit auch Hodendystrophie und Infertilität auf. Eine verminderte Transaktivierungseffizienz des AR und somit eine verschlechterte Hormonwirkung konnte dafür verantwortlich gemacht werden (Tut et al. 1997). Eine verminderte Expression der Zielgene führt zu einem sog. Androgeninsensitivitäts-syndrom, welches in verschiedenen Abstufungen beschrieben wurde. Diese massive Verlängerung des CAG-Repeats ist allerdings sehr selten. Viele Studien befassen sich deswegen mit der Hypothese, dass auch schon geringgradig verlängerte bzw. verkürzte Repeats und solche an der oberen physiologischen Grenze Einfluss auf die Fruchtbarkeit haben können, bzw. bei Patienten mit einer Fertilitätsstörung detektiert werden können (Dowsing et al. 1999; Dadze et al. 2000; Mifsud et al. 2001; Eckardstein et al. 2001; Rajpert-De Meyts et al. 2002; Casella et al. 2003). Die Ergebnisse waren sehr unterschiedlich. In einer Meta-Analyse konnte eine leichte positive Korrelation der CAG-Repeatlänge und der männlichen Infertilität festgestellt werden (Übersicht bei Davis-Dao et al. 2007). Neben der gängigen Hypothese, dass eine mangelhafte Androgenwirkung zu Fertilitätsproblemen führt, vertreten Huhtaniemi et al. (2009) die Theorie, dass durch den Androgenüberschuss mehr Estrogene gebildet werden und diese für eine Infertilität verantwortlich gemacht werden könnten. Unsere Arbeiten am CAG-Repeat untersuchten die Theorie, dass ein längeres (oder kürzeres) Repeat zu einer veränderten Transaktivierungsfunktion des AR führen kann. In **Publikation #1** wurde eine Punktmutation im Bereich des CAG-Repeats untersucht, die bei Untersuchungen der CAG-Repeatlänge in einer Gruppe von 13 Patienten mit nicht-obstruktiver Azoospermie entdeckt wurde. Die histologische Untersuchung der Patienten ergab eine totale Keimzellaplasie. Entgegen des Standardprotokolls, das eine Bestimmung des CAG in der DNA von Leukozyten beschreibt (Zitzmann et al. 2001), wurde in den Arbeiten zu den **Publikationen #1 und 2** das Repeat in der Hoden-mRNA

bestimmt. Mittels laser-assistierter Mikrodissektion (LAM) konnte bei diesen Patienten aus Bouin-fixiertem Hodenmaterial Keimepithel gewonnen werden, so dass es keine „Kontamination“ mit dem AR in Leydigzellen gab. Nach erfolgter mRNA-Extraktion, reverser Transkription und RT-PCR wurde das PCR-Produkt mit dem CAG-Repeat in einen Vektor verbracht und das entstandene Plasmid in chemisch-kompetenten E. coli-Bakterien (JM109, Promega) vermehrt. Bei einem Patienten konnte bei der anschließenden Sequenzierung des Plasmids eine Punktmutation im CAG-Repeat festgestellt werden. Der betreffende Patient war 20 Jahre alt und wurde auf Grund einer hypergonadotropen Azoospermie zur Hodenbiopsie vorgestellt. Im Universitätsklinikum Münster wurde das CAG-Repeat des Mannes aus Leukozyten auf DNA-Ebene auf 22 Repeats bestimmt. In Gießen konnten drei verschiedene Klone, die jeweils auf eine Sertolizelle zurückzuführen waren, gewonnen werden. Die Sequenzierung dieser Klone zeigte eine Varianz in der Repeatlänge (21, 22 und 23). Dieses Ergebnis zeigte zum ersten Mal, dass das Standardprotokoll der CAG-Bestimmung aus der Leukozyten-DNA nicht ausreichend ist, um das CAG-Repeat im Hoden korrekt darzustellen. In zwei dieser Klone konnte die Punktmutation (212A→G) festgestellt werden. Diese führt zu einem Aminosäureaustausch von Glutamin zu Arginin und somit einer ultrastrukturellen Verlängerung des CAG-Repeats von 34Å auf 43Å (Abb. 11).

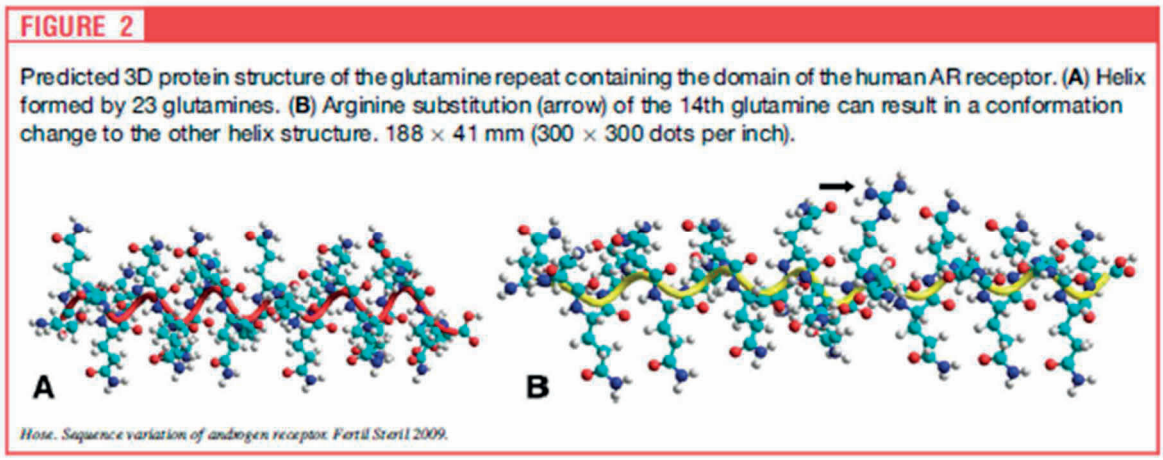

Abb. 11 Strukturänderung des CAG-Repeats bei Glutamin→Arginin-Austausch (Publikation #1)

Mit dieser Strukturänderung kann eine Effizienzminderung der Transaktivierungsdomäne des Androgenrezeptors einhergehen, was eine mögliche Ursache für die Azoospermie des Patienten sein könnte. Zhu et al. (1999) konnten ebenfalls zeigen, dass eine Insertion von zwei Adenosinmolekülen in das CAG-Repeat zu einem *frame shift* und somit zu einem zusätzlichen Stopcodon führt; Männer mit dieser Mutation zeigten das Bild eines kompletten AIS mit einen weiblichen Phänotyp. In

Publikation #2 sollte weiterführend untersucht werden, inwiefern das CAG-Repeat Einfluss auf die Expression eines AR-abhängigen Gens (*Androgen binding protein*, ABP) und die Spermatogenese hat. Hier wurde auch die Repeatlänge bei Patienten mit normaler Spermatogenese bestimmt, da unterschiedliche Repeatlängen auch bei fertilen Männern zu unterschiedlicher Androgensensitivität führen können (Zitzmann 2009). Neben histologisch einheitlichen Hodenbiopsien mit normaler Spermatogenese, Spermatogenesearresten und SCO, wurden bei dieser Studie zudem Biopsien mit einer bunten Atrophie untersucht. In diesem Probenmaterial findet man neben Tubuli mit intakter Spermatogenese auch solche mit SCO oder anderen Spermatogenesestörungen (Sigg 1979, Übersicht bei Bergmann und Kliesch 2010). Das CAG-Repeat wurde einmal in der kompletten Biopsie (Homogenat) und in mittels LAM gewonnenen Keimepithelien bestimmt. Anders als in **Publikation #1** wurde das CAG-Repeat hier mittels hochauflösender Polyacrylamidgelelektrophorese (PAGE) ermittelt (Abb. 12).

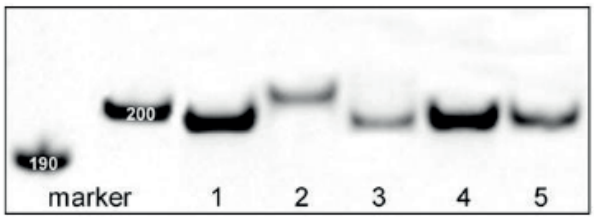

Abb. 12 Bestimmung des CAG-Repeats mittels PAGE (Publikation #2)

Mittels PAGE konnte bei einem Patienten mit einem SZA unterschiedliche CAG-Repeatlängen auf DNA und mRNA Ebene in Blut und Hoden nachgewiesen werden.

1 Blut DNA, 2 Hoden (Homogenat) DNA, 3 Hoden (Homogenat) mRNA, 4 Sertolizellen (nach LACP) mRNA, 5 Interstitium (nach LACP) mRNA

Durch die Verwendung eines 6,5%igen Gels konnten die PCR-Produkte so aufgetrennt werden, dass mittels DNA-Marker basierter Eichkurven Repeatunterschiede von 1-2 Repeats gezeigt werden konnten. Die CAG-Repeatlänge lag bei allen untersuchten Patientenproben im physiologischen Bereich von 18 bis 27 Repeats und war damit unabhängig von Histologie und Spermatogenesestatus. Unterschiede von bis zu drei Repeats konnten bei diesen Patienten je nach Quelle (Homogenat, mikrodissektiertes Material, DNA/mRNA) festgestellt werden (Abb. 12). Bei Patienten mit einer bunten Atrophie der Spermatogenese konnten zwar ebenfalls nur physiologische Repeatlängen (12 bis 24 Repeats) festgestellt werden, hier konnten aber z.T. deutliche Unterschiede in der Repeatlänge von bis zu 11 Repeats zwischen den Tubuli mit Hypospermatogenese und solchen mit SCO oder Spermatogenesearrest detektiert werden (Abb. 13). Die quantitative Expression des AR selbst und des gewählten AR-Zielgens ABP war unabhängig von der Repeatlänge. Dagegen konnte eine statistisch signifikant verminderte Expression von ABP bei Patienten mit gestörter Spermatogenese gezeigt werden (Abb. 14). Obwohl kein Zusammenhang zwischen der Spermatogenese und der CAG-Repeatlänge festgestellt werden konnte, konnte mittels verschiedener Methoden

(Fragmenlängenanalyse nach Zitzmann et al. 2001, PAGE und Klonierung) gezeigt werden, dass das Repeat sowohl innerhalb verschiedener Gewebe und Zelltypen (Blut vs. Hoden, Sertoli- vs. Leydigzellen), aber auch innerhalb eines Patienten variieren kann.

Table 2 CAG repeat length in patients showing mixed atrophy of spermatogenesis

Patient no.	Histology	Hormone concentration in blood		Method	CAG assessed from testes homogenates at the level of mRNA	CAG assessed from RNA of Sertoli cells in seminiferous epithelia showing	
		T (nmol/L)	LH (IU)			hyp	SCO/maturation arrest
23	hyp/SCO	14.0	0.3	PAGE	24	23	23
24		11.0	4.5		21	14	20
25		9.2	6.2		24	22	24
26		22.5	5.5		19	20	18
27		23.0	7.2		27	25	22
28	hyp/maturation arrest	14.2	3.7	PAGE	22	20	17
29		16.6	4.1		21	12	23
30		13.5	4.2		21	19	20
31		12.8	5.8		24	–	23
32		9.0	3.6		20	17	–

Abb. 13 CAG-Repeatlänge in Patienten mit einer bunten Atrophie der Spermatogenese (Publikation #2)

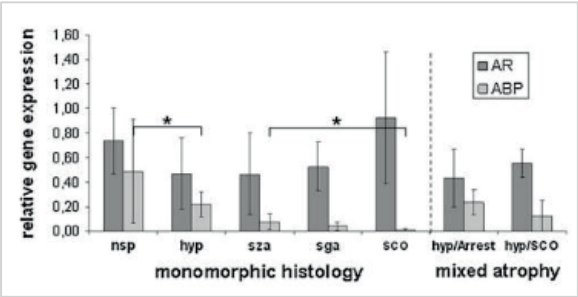

Abb. 14 Relative Genexpression von AR und ABP bei Patienten mit normaler und gestörter Spermatogenese (Publikation #2)

Eine mögliche Erklärung für verschiedene CAG-Repeatlängen in einer Hodenbiopsie ist die Entstehung von DNA-Sekundärstrukturen wie Haarnadel- und Loopstrukturen, die bei CG-reichen DNA-Abschnitten bereits beschrieben wurden. Diese Sekundärstrukturen können ein Gleiten der Polymerase auf dem Leit- bzw. Folgestrang und damit ein vermehrtes Auftreten von Lesefehlern verursachen (Shimizu et al. 1996). Die Transfektion von Bakterien mit unterschiedlichen Trinukleotiden kann zu einer veränderten Replikation (Bowater et al. 1996; Pearson und Sinden 1996; Chastain und Sinden 1998; Pearson und Sinden 1998) und damit zu einer Verlängerung oder Verkürzung der Repeats führen (Samadashwily et al. 1997). Letzteres sei auch auf tierische Zellen übertragbar; die Repeatunterschiede in unseren Versuchen könnten demnach auf einen Polymerasefehler zurückgeführt werden. Bei den Trinukleotiderkrankungen wie der spino-bulbären Muskeldystrophie wird auch die Bildung von somatischen, u.a. testikulären, Mosaiken beschrieben

(Ito et al. 1998; Tanaka et al. 1999; Taylor et al. 1999). Es stellt sich die Frage, ob die Ergebnisse der Arbeit zu den **Publikationen #1 und #2** durch Polymerase- bzw. Replikationsschwierigkeiten beeinflusst wurden. Für alle Untersuchungen der beiden ersten Publikationen wurde eine Taq-Polymerase von Qiagen mit einem speziellen Puffer für CG-reiche Gene verwendet. Allerdings wurden in den Versuchen zur **Publikation #1** allein die chemisch-kompetenten JM109 *E. coli* verwendet, bei den Arbeiten zur **Publikation #** zusätzlich auch die SURE®2 *E. coli*. Letztere konnten im Gegensatz zu den JM109 replizierbare Klonierungs- und Sequenzierergebnisse erzeugen.

Parallel zu diesen Untersuchungen wurden die Versuche für **Publikation #3** durchgeführt. Um den Einfluss des physiologischen CAG-Repeats auf die Transaktivierungseffizienz weiter untersuchen zu können, wurden AR-Moleküle mit unterschiedlich langem CAG-Repeat in Sertolizellen exprimiert und die Expression des androgenabhängigen Zielgens Clusterin bei unterschiedlichen (physiologischen) Testosteronkonzentrationen ermittelt. Hierfür wurden insgesamt vier Sertolizelllinien von Maus (WL3, SK-11) und Ratte (SCIT-C8, 93RS2) auf die intrinsische *Ar*-Expression untersucht. Verwendet wurden 93RS2-Zellen der Ratte, da diese keinen eigenen *Ar* exprimierten. Wir transfizierten die Zellen mittels Mikroporation mit einem kommerziell erhältlichen *full length* humanen AR, der 17 CAG-Repeats beinhaltet. Um den Effekt eines CAG-Repeats am oberen Ende der physiologischen Grenze untersuchen zu können, exprimierten wir in einer anderen Zelllinie ein Repeat mit 33 Repeats. Um die Transfektionseffizienz leicht detektieren zu können, wurde ein GFP-Fragment an den AR gebunden; die Effizienz ermittelten wir dann mittels Immunfluoreszenz. Diese drei Zelllinien (nicht-transfiziert, 93RS2hAR17, 93RS2hAR33) wurden in Vorversuchen mit verschiedenen Testosteronkonzentrationen sowie dem Lösungsmittel Methanol inkubiert. Bei der endgültig verwendeten Testosteronkonzentration von 10^{-7} M zeigten sich keine signifikanten Unterschiede in der Clusterinexpression (Lang 2017). Um die Genexpressionsunterschiede zwischen den verschiedenen Zelllinien globaler darstellen zu können, wurde in Zusammenarbeit mit dem Institut für Mikrobiologie der JLU ein Microarray (Code-Link Rat Whole Genome Assay) durchgeführt. Dabei ergaben sich keine signifikanten Unterschiede zwischen den 93RS2hAR17 und 93RS2hAR33 (nicht veröffentliche Daten), aber überraschenderweise Unterschiede zwischen den nicht-transfizierten und 93RS2hAR17-Zellen. Mittels Microarray identifizierten wir 672 signifikant regulierte Gene (Abb. 15). Von diesen waren 200 Gene hoch- und die anderen 472 Gene signifikant herunterreguliert; 142 hoch- bzw. 370 herunterregulierte Gene waren annotiert und 124 bzw. 330 Genen konnte eine funktionelle DAVID-Kategorie zugewiesen werden. Bei den herunterregulierten Genen konnten die meisten den Kategorien Zellentwicklung und -kontakt, Hormonantwort und Energiemetabolismus zugeordnet werden.

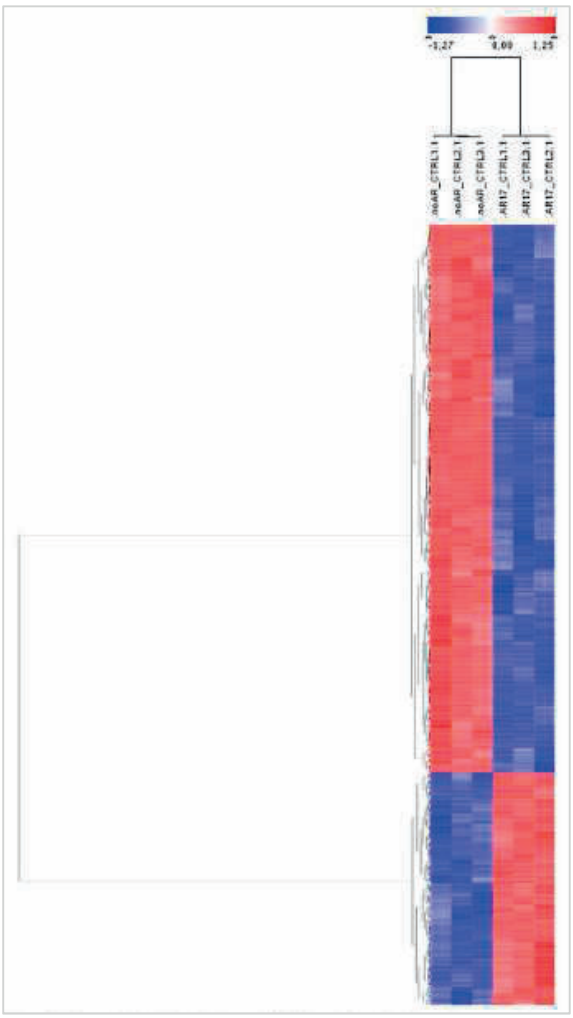

Abb. 15 Hierarchische Clusteranalyse der 672 signifikant veränderten Gene (Publikation #3)

Gene sind hier in Säulen (1-3 untransfizierte Zellen, 4-6 93RS2hAR17-Zellen) und Gene in Reihen dargestellt. Blau zeigt eine Down-Regulation, rot dagegen eine Up-Regulation von Genen. Der Baum auf der linken Seite reflektiert die Abstände zwischen den Genprofilen.

Die Ergebnisse aus **Publikation #3** konnten zwar nicht beleuchten, ob die Transaktivierungseffizienz des AR von unterschiedlichen, wenn auch physiologischen, Längen des CAG-Repeats beeinflusst wird, aber es konnte gezeigt werden, dass die Transfektion AR-freier Sertolizellen allein zu einer Veränderung der Genexpression und zu einer verminderten Sertolizellfunktion führt. Versuche mit verschiedenen Testosteronkonzentrationen hätten u. U. zu falsch-positiven oder falsch-negativen Ergebnissen geführt. **Publikation #3** zeigt deswegen deutlich, dass Transfektionsversuchen in Zellkulturen als Negativkontrolle nicht nur die mit Leervektor-transfizierten (*mock transfected*) Zellen erfordern, sondern auch die nicht-transfizierten Zellen. Ein ähnliches Phänomen wurde von Xiao et al. (2012) beschrieben. Diese Gruppe konnte zeigen, dass die Cre-Expression in Sertolizellen selbst zu einem erhöhten oxidativen Stress in diesen Zellen führte, was die eigentlichen Versuche mit einem Amh-Cre-Knockout verfälschte. Aus diesem Grund müssen die Expressionsdaten der untransfizierten Zellen immer bei einer Interpretation der Daten mit berücksichtigt werden.

6.2. Die Expression von Estrogenrezeptor α und β (ERα, Erβ) sowie dem membranständigen Estrogenrezeptor GPER30 im humanen Hoden

Im Fokus von **Publikation #4** standen die Estrogenrezeptoren. Estrogene spielen für das hormonelle Gleichgewicht des Hodens eine große Rolle, da sie sowohl in Leydig-, Sertoli und auch Keimzellen *de novo* synthetisiert werden können (Carreau und Hess 2010; Carreau et al. 2011; 2012). Zwei nukleäre Estrogenrezeptoren sind bekannt, der Estrogenrezeptor α (ERα oder auch ESR1) (Walter et al. 1985) und β (ERβ oder ESR2) (Mosselman et al. 1996). Die Lokalisation dieser Rezeptoren wurde von vielen verschiedenen Gruppen untersucht, allerdings mit z.T. gravierenden Unterschieden und die beschriebenen Expressionsmuster sind sehr variabel. In einzelnen Studien konnte der ERα in keiner Zellfraktion des humanen Hodens detektiert werden (Saunders et al. 2001; Mäkinen et al. 2001), andere Gruppen zeigten die Estrogenrezeptoren auch in Keimzellen (Lekhkota et al. 2006; Wagner et al. 2006; Pentikäinen et al. 2000; Cavaco et al. 2009). Der ERβ wurde im Gegensatz dazu in den somatischen Zellen des Hodens und auch in den Keimzellen nachgewiesen (Saunders et al. 2001; Mäkinen et al. 2001). Auch der membranständige Estrogenrezeptor GPER wurde bereits in einzelnen humanen Keimzellpopulationen nachgewiesen, v.a. aber in Keimzelltumoren (Franco et al. 2011) bzw. in reifen Spermien von Mensch und Schwein (Rago et al. 2014). Die Unterschiede in der zellulären Lokalisation können auf die Verwendung verschiedener Antikörper mit unterschiedlicher Spezifität und die Verwendung einer einzelnen Technik, der Immunhistochemie bzw. Immunfluoreszenz, zurückzuführen sein. Ziel der Studie, die zu **Publikation #4** führte, war, die Expression der ESRs auf zellulärer Ebene im menschlichen Hoden mit verschiedenen komplementären Methoden zu untersuchen. Aus diesem Grund wurden sowohl Hodenbiopsien mit normaler und gestörter Spermatogenese mittels RT-PCR, quantitativer RT-PCR, *in situ* Hybridisierung (ISH) auf mRNA-Ebene sowie mittels Immunhistochemie (IHC) und Western Blot (WB) auf Proteinebene untersucht. Alle ERs konnten in Homogenaten sowie in mittels LAM isolierten Keimepithelien (ERα, ERβ, schwach GPER) und/oder Interstitiumsbereichen (GPER) nachgewiesen werden (Abb. 16A). Auch bei verschiedenen Spermatogenesestörungen konnte die Expression von ERα, ERβ und GPER nachgewiesen werden. Dabei fiel auf, dass die Expression von ERα bei Patienten mit Spermatozytenarrest am geringsten war. Dies war auch für ERβ der Fall, nur die Expression von GPER dagegen schwankte kaum zwischen den verwendeten Arresten (Abb. 16B). Auch dies lässt auf eine Expression von ERα hauptsächlich in Keimzellen, von ERβ in Keim- und Sertolizellen und von GPER vorwiegend in interstitiellen Zellen schließen.

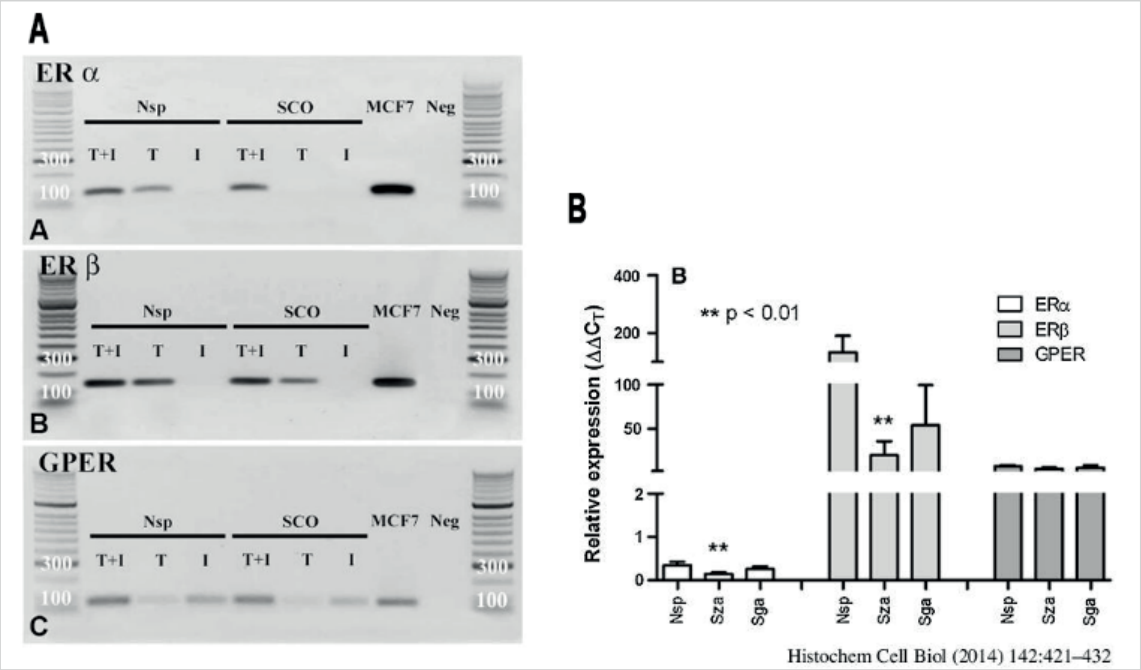

Abb. 16 Genexpressionsanalyse von ERα, ERβ und GPER im humanen Hoden (Publikation #4)

A Qualitative RT-PCR zur Detektion von ERα (A), ERβ (B) und GPER (C) bei Patienten mit normaler Spermatogenese (Nsp) und SCO. Die humane Brustkrebszelllinie MCF7 diente als Positivkontrolle. Neg Negativkontrolle

B Quantitative RT-PCR zur Darstellung der relativen Genexpression von ERα (weiß), ERβ (hellgrau) und GPER (dunkelgrau) in Hodenbiopsien mit normaler Spermatogenese (Nsp), Spermatozyten- (Sza) und Spermatogonienarrest (Sga). ** statistisch signifikanter Unterschied in der Genexpression mit $p < 0,01$

Durch die Verwendung von Biopsien mit normaler Spermatogenese und SCO sowie die Verwendung von Hodenhomogenaten und gepickten Tubulus- und Interstitiumarealen für die mRNA-Detektion kann relativ schnell eine Aussage über die Expression in den verschiedenen Zellpopulation des Hodens getroffen werden (Abb. 17).

Die tatsächliche zelluläre Lokalisierung erfolgte dann mittels ISH und bestätigte die vorherigen Versuche. ERα-mRNA konnte in Spermatogonien und Spermatozyten detektiert werden, was die Ergebnisse für Schwein und Mensch bestätigte (Lekhkota et al. 2006; 2007, Kongressbeitrag). Die Detektion von ERα auf Proteinebene mittels IHC stellte sich als schwierig heraus. Es wurden sechs verschiedene Antikörper getestet, von denen aber nur zwei reproduzierbare, mit den anderen Methoden nachvollziehbare Ergebnisse brachten (Ratzenböck 2014). Verwendet wurden dann zwei Antikörper, F-10 (Rago et al. 2006; Han et al. 2009; Madak-Erdogan et al. 2011) und HC-20 (Pelletier und El-Alfy 2000). Diese detektieren ERα in primären Spermatozyten und frühen runden Spermatiden (F-10) bzw. zusätzlich in Sertoli- und interstitiellen Zellen (HC-20) (Abb. 18A, B, F). ERβ konnte in primären Spermatozyten und Sertolizellen mittels ISH und in Spermatogonien, Spermatozyten,

runden Spermatiden und Sertolizellen in der IHC (ERβ503) detektiert werden (Abb. 18C, D). ERβ503 ist ein polyklonaler Antikörper, der für die Detektion von ERβ in der Prostata der Ratte synthetisiert (Saji et al. 2000) und dann auch in humanen Brustkrebszellen eingesetzt wurde (Roger et al. 2001). In diesen Veröffentlichungen wurde die Spezifität mittels einer Präinkubation mit rekombinantem ERβ gezeigt. Die GPER-Expression wurde nur mittels ISH untersucht und zeigte eine Expression in den Leydigzellen und einzelnen Sertolizellen (Abb. 18E). Ein Antikörper stand zur damaligen Zeit nicht zur Verfügung. Als Positivkontrolle für die Immunhistochemie wurde die Brustkrebszelllinie MCF-7 (*Michigan Cancer Foundation 7*) verwendet, da diese Zellen sehr viel ERα, nur wenig GPER und sehr wenig ERβ exprimieren (Filardo et al. 2000). Als Negativkontrolle wurde für beide ERα-Antikörper eine Präinkubation mit dem *blocking peptide* durchgeführt, für den ERβ-Antikörper ERβ503 stand kein *blocking peptide* zur Verfügung.

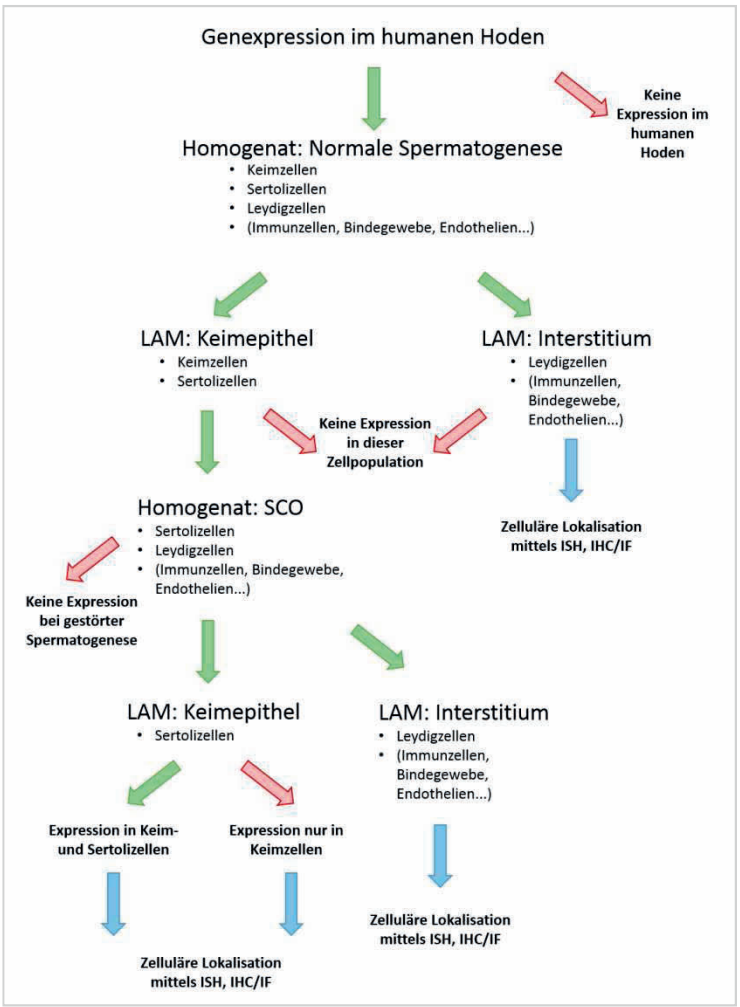

Abb. 17 Fließdiagramm zur Untersuchung von Genexpression im humanen Hoden

Darstellung der Genexpressionanalyse mit Hilfe von Proben mit normaler Spermatogenese und SCO. Verwendet werden sowohl Hodenhomogenate als auch mittels LAM gewonnene Keimepithel- und Interstitiumsbereiche. Die Durchführung einer RT-PCR-Analyse mit diesen Proben ermöglicht die schnelle, einfache und auch kostengünstige Differenzierung der Genexpression in den verschiedenen testikulären Zellpopulationen.

grün: vorhandene Expression, rot: keine Expression, blau: weiteres Vorgehen

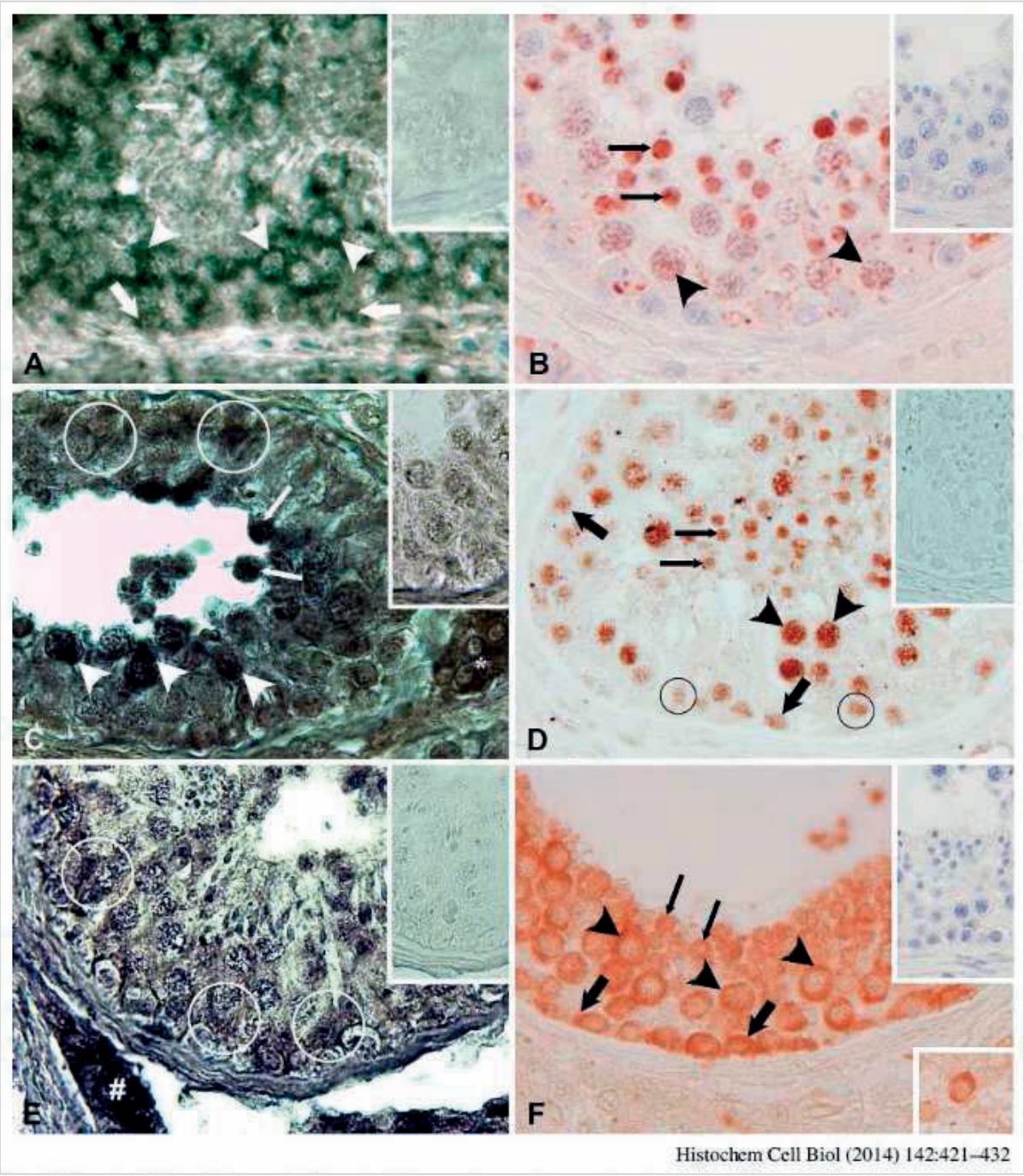

Abb. 18 Zelluläre Lokalisation von ERα, ERβ und GPER in normaler humaner Spermatogenese mittels ISH und IHC (Publikation #4)

A, B, F Zelluläre Lokalisation von ERα mRNA (A) und Protein (B, F) in Spermatogonien, Spermatozyten und Spermatiden. Einzelne interstitielle Zellen konnten mit einem der beiden ERα-Antikörper ebenfalls gefärbt werden.

C, D Lokalisation von ERβ mRNA (C) und Protein (D) in Spermatogonien, Spermatozyten, Spermatiden und Sertolizellen

E GPER mRNA ist in Sertoli- und Leydigzellen exprimiert.

dicker Pfeil = Spermatogonien, Pfeilspitze = Spermatozyten, dünner Pfeil = Spermatiden, Kreis = Sertolizellen, Doppelkreuz = Leydigzellen

Die Spezifität von Antikörpern sowie die Verwendung von Zelllinien als Positiv- oder auch Negativkontrolle werden momentan kontrovers diskutiert. So konnte nach neuesten Erkenntnissen ERβ in den MCF-7 Zellen mit validierten Antikörpern nicht mehr nachgewiesen werden (Nelson et al. 2017). Außerdem testete diese Gruppe acht standardmäßig eingesetzte ERβ-Antikörper auf ihre Spezifität und konnte bei dem am häufigsten eingesetzten Antikörper (NCL-ER-BETA) zeigen, dass dieser ERβ nicht spezifisch detektiert. In **Publikation #4** konnten wir zeigen, wie wichtig es ist, verschiedene Methoden miteinander zu kombinieren. Nur so kann ein möglichst komplettes und lückenloses Bild der ER-Expression auf mRNA- und Proteinebene gezeigt werden. Zudem haben wir die Expression der ERs nicht nur auf die Expression in Zelllinien gestützt, sondern auch eine Expressionanalyse auf testikulärer Ebene durchgeführt.

6.3. Expression von Transportern für sulfatierte Steroide im Hoden von Maus und Mensch

Die **Publikationen #5-11** befassten sich dann nicht mehr mit den klassischen Steroidhormonen, sondern mit den sulfo-konjugierten Steroiden. Im Rahmen der DFG-Forschergruppe 1369 „Sulfated Steroids in Reproduction“ (2010-2016) wurde die Bedeutung und das Vorkommen dieser Steroidsulfate und ihrer Transportsysteme untersucht.

Die Expression von spezifischen Transportsystemen für sulfatierte Steroidhormone ist essentiell für die Funktion dieser Moleküle, da sie nicht per Diffusion in die Zielzellen aufgenommen werden können. Arbeiten von Geyer et al. beschreiben den Uptake Carrier SOAT (Gen: *SLC10A6*), der spezifisch sulfatierte Steroide wie Estronsulfat, DHEAS und PREGS transportiert (Geyer et al. 2004; 2006; 2007). Die Expression von *SLC10A6* in verschiedenen humanen Organen wurde bei Geyer et al. (2007) und in **Publikation #5** untersucht. Hier zeigte sich eine sehr hohe Expression im Hoden, aber auch eine deutliche Expression in Plazenta, Brust, Pankreas und Lunge. Im Gehirn dagegen konnte keine Expression festgestellt werden. Die Expression von *SLC10A6* im humanen Hoden scheint die Publikationen aus den 1970er Jahren zu unterstützen, in denen bereits eine Synthese von sulfatierten Steroiden sowie deren Metabolisierung in den Keimepithelien beschrieben wurde (Payne und Jaffe 1970; Payne et al. 1971; Payne et al. 1973; Payne und Jaffe 1975). Zusammen mit einer sehr frühen Beschreibung der STS im Hoden (Payne et al. 1969) sollte in den **Publikationen #5 und 6** die zelluläre Lokalisation von SOAT auf mRNA- und Proteinebene beschrieben werden um das Vorhandensein eines funktionellen „*sulfatase pathway*“ (Abb. 8) zu untersuchen. Neben SOAT wurde auch die Expression und Lokalisation von drei weiteren, Natrium-unabhängigen Transportern aus der SLCO Superfamilie (OATP6A1 (Gen: *OATP6A1*), OATP1C1 (Gen: *OATP1C1*) und OSCP1 (Gen: *OSCP1*))

untersucht. Während OATP1C1 nur in sehr geringen Mengen im Hoden exprimiert ist und deswegen in der weiteren zellulären Lokalisation nicht mehr weiter untersucht wurde, konnten OATP6A1 und OSCP1 ebenfalls im Hoden detektiert werden. Die zelluläre Lokalisation der drei Uptake carrier wurde, wie in Abb. 17 beschrieben auf mRNA- und Proteinebene untersucht. Mit RT-PCR nach LACP konnte gezeigt werden, dass alle drei Uptake carrier allein in Keimzellen exprimiert werden (Abb. 19).

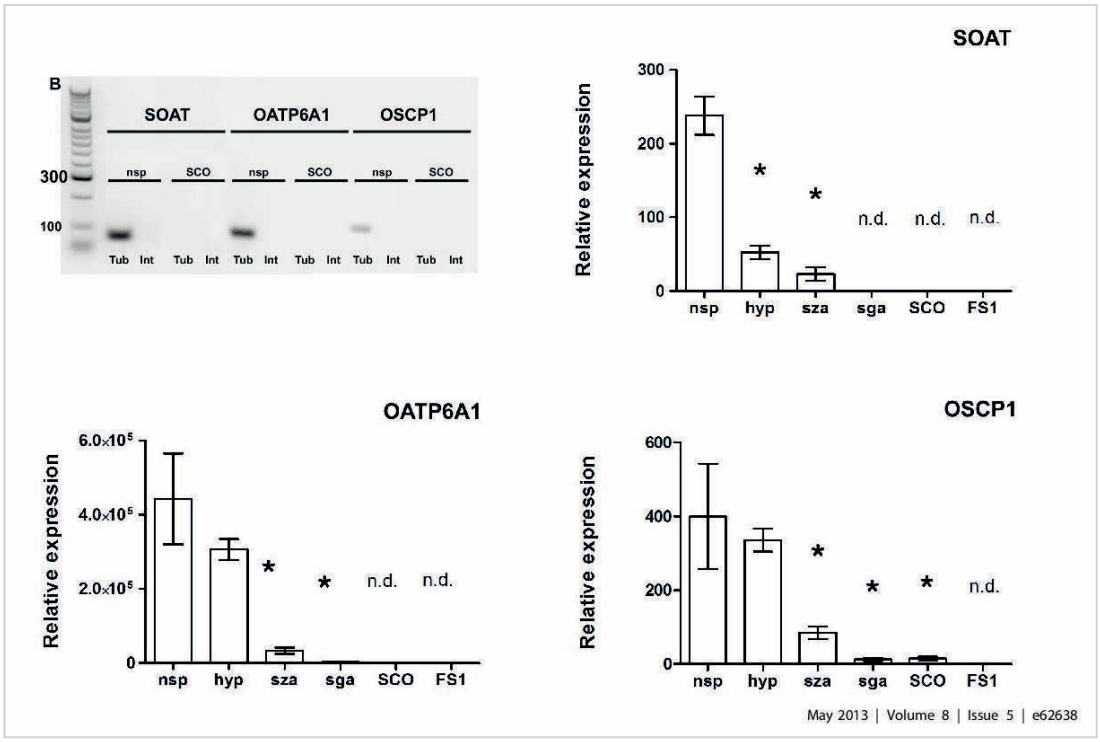

Abb. 19 Detektion der Uptake carrier SOAT, OATP6A1 und OSCP1 in Keimzellen mittels RT-PCR nach LACP und Expressionsanalyse der Transporter bei normaler und gestörter Spermatogenese mittels qRT-PCR (Publikation #5)

Für SOAT wurde eine ISH-Sonde generiert, die *SLC10A6* in pachytänen Spermatozyten detektierte. Die Proteinlokalisation stellte sich wie bei den Estrogenrezeptoren als problematisch heraus, da sehr viele verschiedene SOAT-Antikörper auf dem Markt erhältlich waren. Insgesamt wurden sechzehn verschiedene, z.T. auch selbst generierte Antikörper verwendet. Keiner dieser Antikörper konnte ein spezifisches Färbesignal im Hoden erzeugen, welches mit ISH, RT-PCR und LAM bestätigt werden konnte (Wapelhorst 2014). In den **Publikationen #5 und 6** wurde dann ein Antikörper verwendet, der sich gegen die 16 C-terminalen Aminosäuren des murinen Soat-Proteins (IHC, $Soat_{329-344}$) bzw. gegen den gesamten C-Terminus des humanen SOAT richtete (WB, $SOAT_{311-377}$), da nur diese Antikörper Ergebnisse erzeugten, die mit anderen Methoden bestätigt werden konnten und wiederholbar waren. SOAT konnte mit diesem Antikörper stadienspezifisch von zygotänen Spermatozyten (Stadium V) bis in runde Spermatiden Step 2 (Stadium II) detektiert werden (Abb. 20). Besonders stark war die Färbung in den pachytänen Spermatozyten im Golgifeld. Diese runde bis ovale Struktur liegt neben

dem Zellkern und stellt die Verschmelzung proakrosomaler Granula aus dem Golgi-Apparat und damit die Vorstufe der Akrosomenkappe dar. Die Lokalisation dort konnte mit einer Doppel-Immunfluoreszenz mit dem Golgi-Marker GOLGINA2 bestätigt werden (Abb. 21).

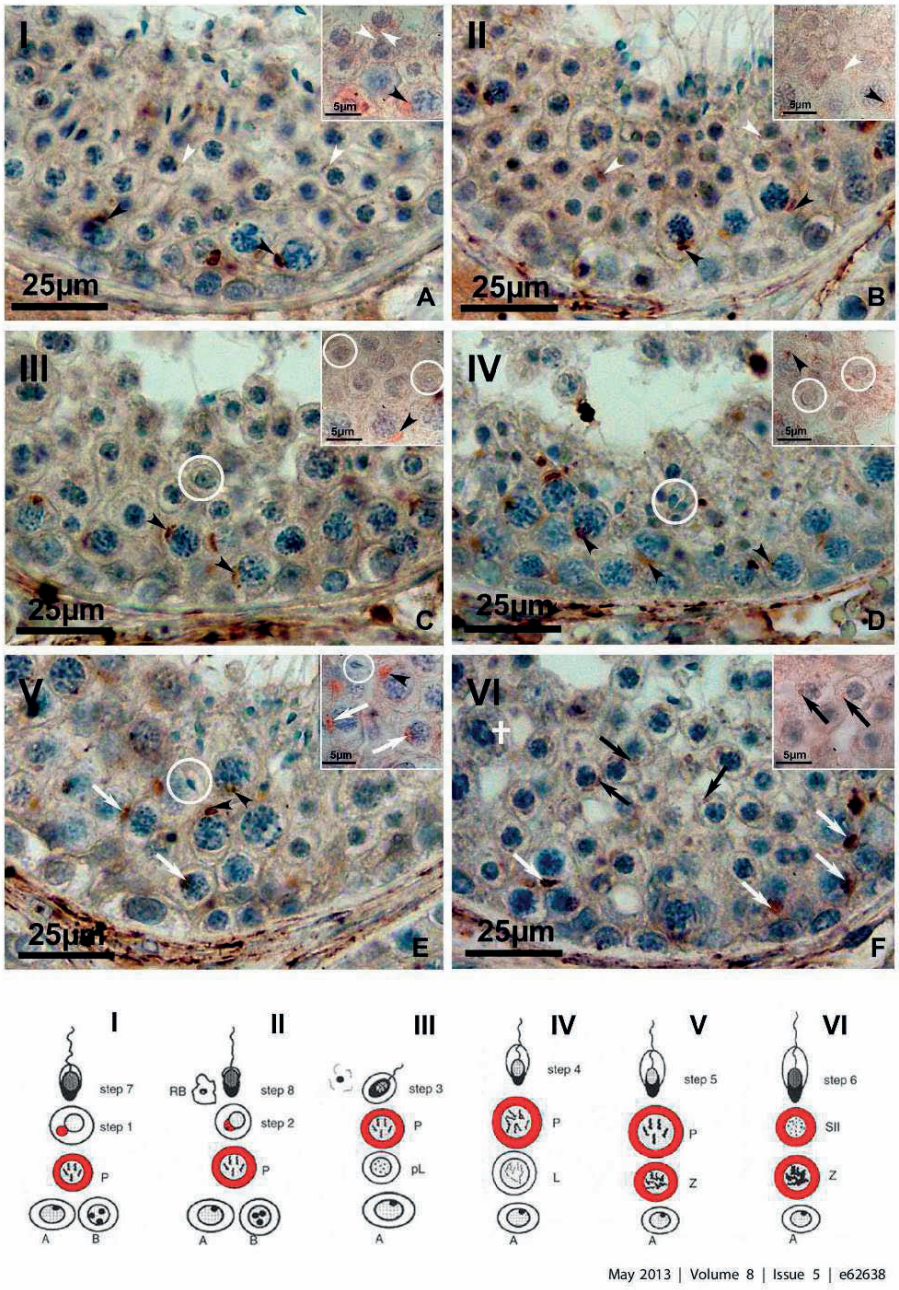

Abb. 20 Zelluläre Lokalisation von SOAT im humanen Hoden (Publikation #5)

Mittels IHC an Biopsien mit einer normalen Spermatogenese konnte der Uptake Carrier SOAT von den zygotänen Spermatozyten in Stadium V bis hin zu runden Step 2 Spermatiden in Stadium II detektiert werden. Besonders auffallend ist die starke Färbung des Golgifelds in den pachytänen Spermatozyten.

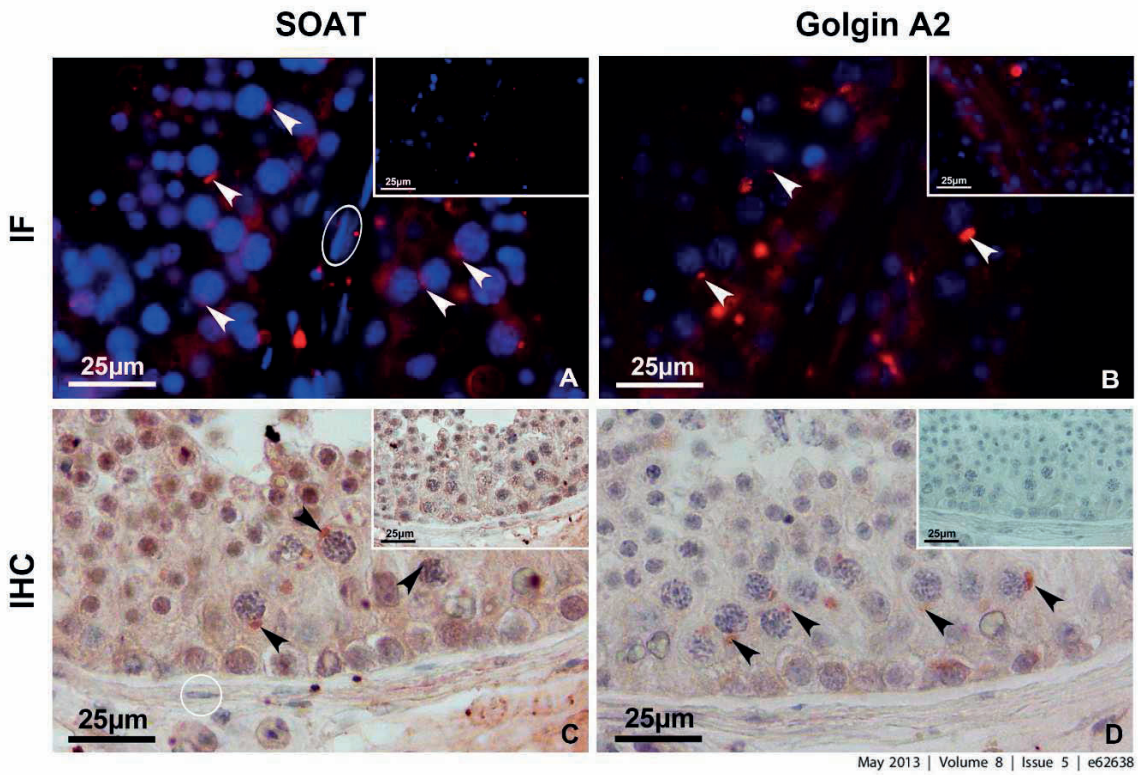

Abb. 21 Doppelfärbung von SOAT und GOLGIN A2 zeigt die Lokalisation von SOAT im Golgifeld in pachytänen Spermatozyten (Publikation #5)

Außerdem wurde SOAT in humanen HEK293-Zellen transfiziert und überexprimiert. In diesen Zellen konnte SOAT in der Zellmembran mittels IF detektiert und das Transportspektrum von SOAT noch einmal um Estradiolsulfat und Androstendiolsulfat erweitert werden (Arbeiten aus dem Institut für Veterinär-Pharmakologie und -Toxikologie). Im Gegensatz zu der dominanten testikulären Expression von SOAT beim Mensch, konnte Soat bei der Maus (mSoat) vor allem in der Lunge detektiert werden (**Publikation #6**). Im Hoden konnte mSoat in leptotänen und pachytänen Spermatozyten bis hin zu elongierenden Spermatiden nachgewiesen werden. In pachytänen Spermtozyten zeigte sich wieder die Färbung im Golgi-Vesikel. Im Gegensatz zu SOAT transportiert mSoat auch PREGS.

Durch die Lokalisation von SOAT in den Keimzellen konnte die Frage nach einen funktionellen *„sulfatase pathway“* im Hoden nicht abschließend beantwortet werden, da für den Transport von sulfatierten Steroiden aus dem Blut in das Keimepithel die Blut-Hodenschranke und somit die Sertolizellen eine essentielle Rolle spielen. Außerdem wurden in den **Publikationen #5 und 6** nur Uptake Carrier und keine Effluxtransporter untersucht. In den Arbeiten zu **Publikation #7** wurden deswegen weitere Uptake Carrier (OATP2B1 (Gen: *OATP2B1*) und OATP3A1 (Gen: *OATP3A1)*) und zum ersten Mal Effluxtransporter (MRP1 (Gen: *ABCC1*) und MRP4 (Gen: *ABCC4*)) untersucht. Alle

diese Transporter wurden bereits in der Literatur im Hoden beschrieben und können sulfatierte Steroide, meistens Estronsulfat und/oder DHEAS, transportieren. Diese Transporter sollten vor allem im Hinblick auf eine mögliche Expression in den Sertolizellen hin untersucht werden. Neben der Verwendung von Hodenbiopsien mit normaler Spermatogenese wurden deswegen auch zwei Sertolizelllinien verwendet: FS1-Zellen (mit freundlicher Genehmigung von V. Schumacher, Children's Hospital Boston, Boston, MA, USA) und HSEC-Zellen (Lonza®). OATP2B1 und OATP3A1 konnten in Sertoli- und Keimzellen nachgewiesen werden, MRP1 dagegen nur in Sertolizellen. Durch die Ausstattung mit Uptake Carriern und Effluxtransportern zusammen mit der ubiquitäten Expression von STS konnte erstmals im humanen Hoden ein funktioneller *„sulfatase pathway"* beschrieben werden (**Publikationen #8 und #11**) (Abb. 22).

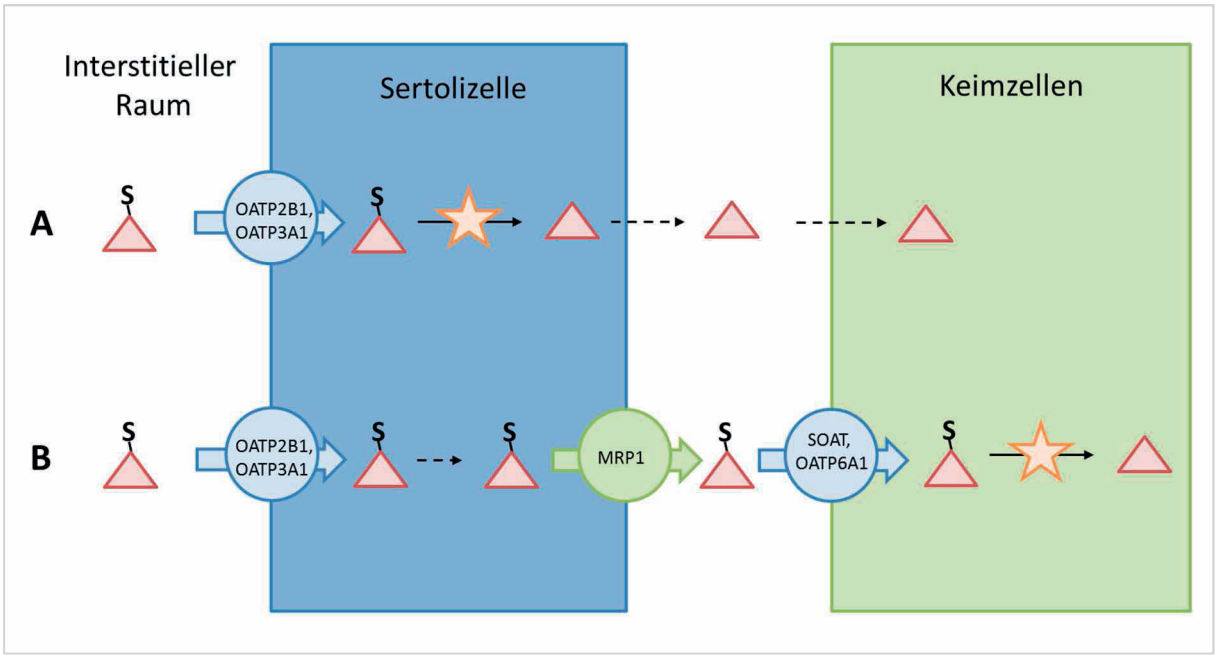

Abb. 22 **Möglichkeiten für den *sulfatase pathway* in Sertolizellen (A) oder Keimzellen (B)**

A Mittels OATPs in die Sertolizelle aufgenommene sulfatierte Steroide werden dort über die Steroidsulfatase (STS, Stern) desulfatiert und können dann durch Diffusion (gestrichelter Pfeil) aus der Sertolizelle heraus in die Keimzelle transportiert werden.

B Es besteht auch die Möglichkeit, dass die sulfatierten Steroide durch die Sertolizelle hindurch und aus diesen heraus transportiert werden. Im Interzellularraum zwischen Sertoli- und Keimzellen können diese dann wieder von Uptake carriern in die Keimzellen aufgenommen werden. Dort ist ebenfalls die STS exprimiert.

Abgeschlossen wurden die Versuche aus den **Publikationen #5-7** durch ein Review von Geyer et al. (2016, **Publikation #8**). In diesem wurden die bisherigen Ergebnisse zur Untersuchung der

sulfatierten Steroide und ihrer biologischen Bedeutung für die Reproduktion aus der ersten Förderperiode der DFG-Forschergruppe „Sulfated Steroids in Reproduction“ zusammengestellt.

6.4. Biologische Bedeutung der sulfatierten Steroide und des Transporters SOAT für die Reproduktion

Die Konzentration einiger sulfatierter Steroide wie zum Beispiel DHEAS übersteigt die Konzentration der unkonjugierten Steroide im Blut um ein Vielfaches. DHEAS ist deswegen als „Jungbrunnen“ in den Fokus der Medizin gerückt und wird vielen Nahrungsergänzungsmitteln hinzugefügt. Die Auswirkung dieser künstlichen DHEAS-Quelle auf die Steroidhormonsynthese wurde von Neunzig und Bernhardt genauer untersucht (2014). Sie konnten zeigen, dass die Anwesenheit von DHEAS die Effizienz des Enzyms CYP11A1 steigert. CYP11A1 ist das erste Enzym in der Steroidogenese, welches aus Cholesterol Pregnenolon synthetisiert. Die Anwesenheit von DHEAS steigert die Bindungsaffinität des Enzyms an Cholesterol, erhöht die Effizienz des Enzyms um 80% und damit die Menge an produziertem Pregnenolon. Im Gegensatz zum Effekt von DHEAS auf CYP11A1 wird die Effizienz von CYP17A1 nicht durch die Anwesenheit von DHEAS beeinflusst (Neunzig 2014). Die sulfatierten Steroide selbst, zum Beispiel PREGS, sind keine direkten Substrate der steroidogenen Enzyme. So kann PREGS von CYP17A1 zu 17-OH-PREGS, aber nicht zu DHEAS metabolisiert werden (Neunzig et al. 2014). DHEAS kann aber nicht nur Einfluss auf die Steroidogenese nehmen, sondern auch direkt an Rezeptoren in Zielzellen des Reproduktionstraktes binden und direkt eine Hormonwirkung entfalten. Demnach dienen sie nicht nur als Vorläufermoleküle und lokaler Speicher in den Zellen und dem Blut, sondern auch selbst als Hormon. Die Bindung von DHEAS an G-Protein-gekoppelte membranständige Rezeptoren von Keimzellen in Kultur löst einen ähnlichen intrazellulären Signaltransduktionsweg aus wie die Bindung von freien Androgenen an die Rezeptoren, d.h. es findet eine Aktivierung von Transkriptionsfaktoren wie CREB und ATF-1 statt (Shihan et al. 2013).

Publikation #8 beschreibt neben der Expression von SOAT/Soat im Hoden von Maus und Mensch auch die Expression des Transporters in der humanen Plazenta und die Effekte der sulfatierten Steroide auf die Follikulogenese sowie den Einfluss der konjugierten Steroidhormone auf die Steroidbiosynthese selbst. In der Plazenta dienen sulfatierte Steroidhormone wie DHEAS und 16-hydroxy-DHEAS (16-OH-DHEAS) aus dem Endometrium als Vorstufen für die plazentäre Estrogensynthese im Synzytotrophoblasten. Dies war einer der ersten beschriebenen *„sulfatase pathways“*, dem auch eine Funktion zugeordnet werden konnte und im Rahmen des fetomaternalen Kontakts die Hormonproduktion der Plazenta beeinflusst (Kuss 1994). Die Transportsysteme waren

allerdings unbekannt. Erst durch die Arbeiten von Schweigmann et al. (2014) konnte diese Lücke geschlossen und Uptake Carrier wie SOAT und OAT4 lokalisiert werden.

Durch den Nachweis verschiedener Transporter (SLCs, SLCOs, ABCs) für sulfatierte Steroide sowie der Enzyme für Sulfonierung (SULTs) und Desulfonierung (STS) in verschiedenen Zellpopulationen des Hodens bei Mensch und Nagern sowie der Plazenta, können die sulfatierten Steroide schon lange nicht mehr nur als inaktive Metabolite bezeichnet werden, sondern auch als Vorläufermoleküle für freie Steroidhormone (Pasqualini et al. 1989; Labrie 2003; van Luu-The 2013). Zusammen mit der Expression von klassischen Steroidrezeptoren im Hoden (**Publikationen ##2 und 4**) sowie der direkten Aktivierung membran-gebundener Rezeptoren durch DHEAS (Papadopoulos et al. 2016) haben sulfatierte Steroide im Hoden eine klare biologische Rolle, da sie sowohl para- als auch intrakrin wirken können. Für die verschiedenen Steroide (Testosteron, DHT und Estron) wurden sog. „*front-door*" und „*back-door*" Mechanismen beschrieben (van Luu-The 2013) und unter dem Begriff „Intrakrinologie" zusammengefasst. Eine Übersicht der biologischen Bedeutung der sulfatierten Steroide kann **Publikation #11** entnommen werden. Nachdem in **Publikation #7** gezeigt werden konnte, dass alle Voraussetzungen für einen *„sulfatase pathway"* im Hoden erfüllt sind, sollte dieser auch funktionell in der Sertolizelllinie HSEC untersucht werden. Diese Zelllinie exprimiert die im Hoden untersuchten Uptake carrier und Effluxtransporter, OATP2B1, OATP3A1 und MRP1 und wurde deswegen zu *in vitro* Transportversuchen verwendet. In einem Transwellsystem wurde ein zwar geringer, aber messbarer Transport von DHEAS vom apikalen in das basale Kompartiment nachgewiesen. Eine biologische Bedeutung von sulfatierten Steroiden *in vivo* kann deswegen als gesichert angesehen werden. Neben der Verwendung von Proben mit normaler Spermatogenese wurden in den **Publikationen #5 und #7** auch Spermatogenesestörungen untersucht. Die *STS*-Expression war unabhängig vom Spermatogenesestatus, da das Enzym in den interstitiellen Leydigzellen hoch exprimiert ist und diese sich bei Spermatogenesestörungen meist nicht in Anzahl oder Differenzierungsgrad verändern. Im Gegensatz dazu wurde in **Publikation #5** die Expression von *SLC10A6, OATP6A1* und *OSCP1* quantitativ in Proben mit verschiedenen Spermatogenesestörungen bis hin zu einem SCO untersucht. Interessant war die verminderte Expression der Transporter in Proben mit einer quantitativ verminderten Spermatogenese (*SLC10A6*) und/oder Spermatozytenarresten (*SLC10A6, OATP6A1, OSCP1*).

Welche biologische Rolle SOAT/mSoat im Hoden hat, konnte bisher noch nicht abschließend geklärt werden. Die Expression von *SLC10A6/Slc10a6* im Golgi- Vesikel der pachytänen Spermatozyten und in runden Spermatiden (**Publikationen ##5 und 6**) lässt eine mögliche Funktion von SOAT/mSoat beim Transport von Cholesterolsulfat (CS) in die Akrosomenkappe vermuten. Die Anreicherung von CS in Hoden und Nebenhoden bzw. die Einlagerung von CS in das Akrosom wurde bereits sehr früh

beschrieben (Lalumière et al. 1976; Cheetham et al. 1990). Durch diesen Vorgang wird eine vorzeitige Kapazitation und Akrosomenreaktion der Spermien verhindert, da CS die Akrosomenmembran stabilisiert und die Aktivität des Enzyms Akrosin hemmt (Bleau et al. 1974; Burck und Zimmerman 1980; Langlais et al. 1981; Roberts 1987). Erst im weiblichen Genitaltrakt wird CS durch die STS-Aktivität abgespalten und die Akrosomenreaktion kann stattfinden. Außerdem kann CS eine direkte Vorstufe für andere sulfatierte Steroide wie PREGS und DHEAS sein und könnte somit in der Akrosomenkappe auch als lokales Reservoir für die Steroidhormonsynthese dienen. Um die Bedeutung von SOAT/mSoat weiter zu ergründen, wurde im Institut für Veterinärpharmakologie eine *Slc10a6*$^{-/-}$ KO Maus generiert (**Publikation #9**). Die männlichen Mäuse zeigen eine vollkommen normale Spermatogenese mit einer identischen Verteilung der Spermatogenesestadien, Hodengewichte und Spermatogenesestörungen bei Wildtyp- und *Slc10a6*$^{-/-}$-Mäusen (Abb. 23). Auch das Reproduktionsverhalten ist normal, was eine direkte biologische Bedeutung von mSoat für die Fertilität auszuschließen scheint. Es ist wahrscheinlich, dass das Fehlen von mSoat durch andere Uptake carrier ausgeglichen werden kann. In dieser Studie wurde allerdings zum ersten Mal auch das Steroidmetabolom der Mäuse untersucht. Mittels GC-MS/MS und LC-MS/MS (Galuska et al. 2013; Dury et al. 2015; Sánchez-Guijo et al. 2015) wurde im Serum der *Slc10a6*$^{-/-}$ Mäuse ein Profil für zehn freie und 12 sulfatierte Steroide erstellt. Erstaunlicherweise konnten überhaupt nur sehr geringe Mengen CS, Kortikosteron und Testosteron detektiert werden. Im Vergleich zu den Wildtypen zeigten die Knockout-Mäuse statistisch signifikant höhere CS-Mengen im Serum. Dies könnte auf eine verminderte CS-Aufnahme in das Akrosom durch den fehlenden mSoat sprechen. Weitere Effekte des Soat-Mangels auf den CS-Stoffwechsel, z.B. in der Haut, müssen noch weiter untersucht werden.

Zusätzlich zur Untersuchung der *SLC10A6*-Expression bei gestörter Spermatogenese und der Untersuchung mittels Knockout-Mausmodells wurden verschiedene *single nucleotide polymorphisms* (SNPs) im humanen SOAT-Gen untersucht. Diese SNPs sind in der SNP-Datenbank gesammelt dargestellt. Die Plattform des *National Center for Biotechnology Information* beschreibt 350 genetische Varianten des *SLC10A6*-Gens (Stand: September 2015). Die meisten SNPs im SOAT-Gen sind in der nicht-kodierenden Region, aber 148 dieser SNPs liegen in der kodierenden Sequenz. Von besonderem Interesse waren die Varianten, die zu einer veränderten Aminosäuresequenz führen. Diese werden als „nicht-synonym“ bezeichnet. In Vorversuchen wurden sechs verschiedene, natürlich auftretende SNPs untersucht: S6F, L204F, V199I, I196T, R185T und I114V (Bakhaus 2014).

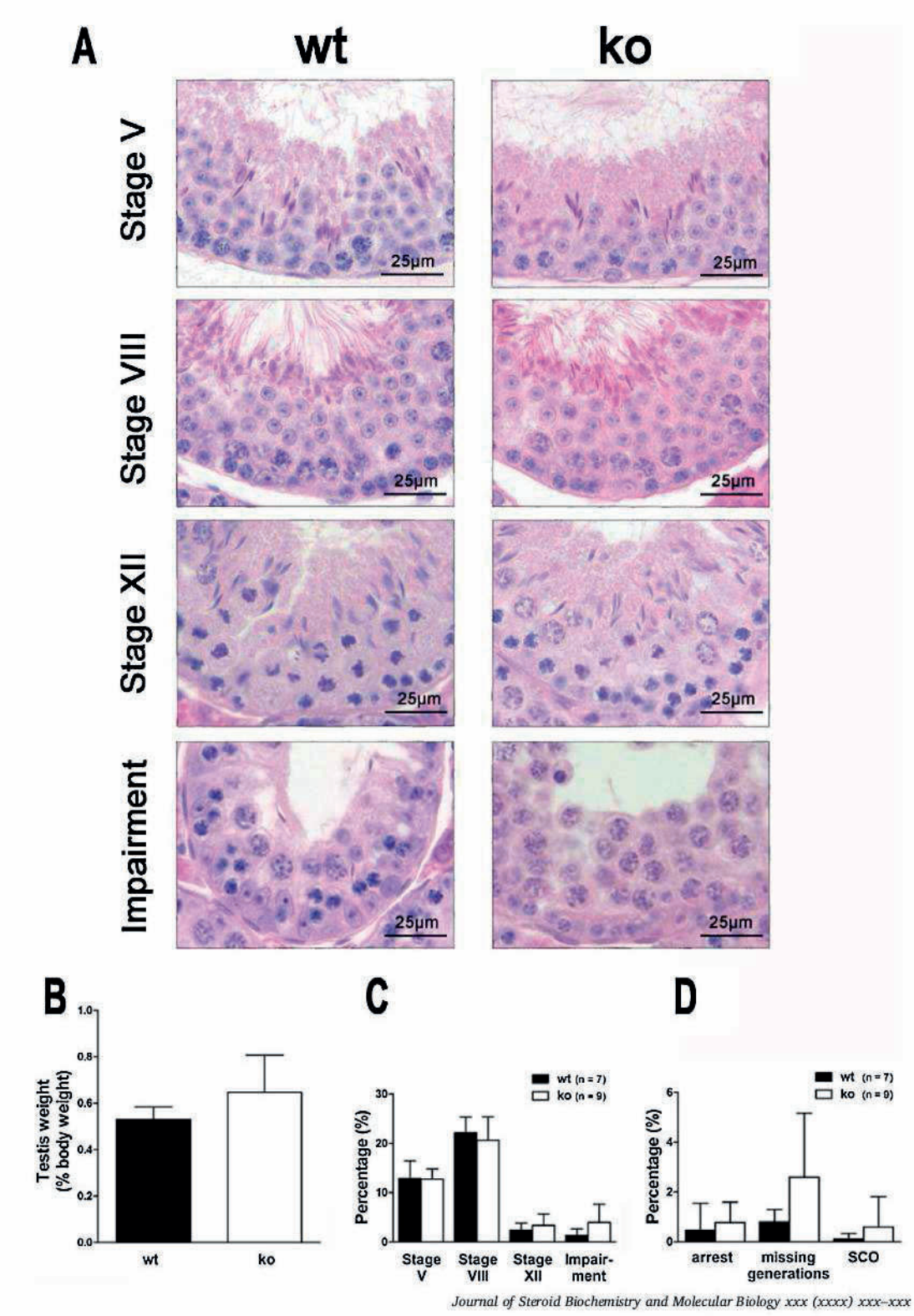

Abb. 23 Histologie des Hodens bei Wildtyp-Mäusen, hetero- und homozygoten Slc10a6$^{-/-}$ Mäusen (Publikation #9)

Von diesen SNPs zeigte nur L204F eine signifikant reduzierte Transportaktivität für DHEAS in transfizierten HEK293-Zellen und wurde deswegen in den Arbeiten zu **Publikation #10** genauer

untersucht. Dieser SNP ist direkt in der Bindungstasche des SOAT lokalisiert und stört so wahrscheinlich die Substratbindung. Mittels Immunfluoreszenz (IF) und unter Verwendung von zwei verschiedenen Antikörpern gegen den extrazellulären N- und den intrazellulären C-Terminus wurde die Internalisierung des L204F in die Membran im Vergleich zum Wildtyp-SOAT untersucht. L204F-SOAT war im Vergleich zum Wildtyp-SOAT in der Zellmembran der HEK293-Zellen vermindert, was die geringere Transporteffizienz erklärt (Abb. 24A). Die Hypothese, dass L204F bei Patienten mit Hypospermatogenese im Vergleich zur normalen Spermatogenese überrepräsentiert sein könnte, hat sich aber nicht bestätigt. Tatsächlich liegt die Häufigkeit eines homozygoten L204F SNP sowohl bei normaler Spermtogenese als auch bei Hypospermatogenese bei 4-5% und die eines heterozygoten L204F bei 8-10%. Der Großteil aller untersuchten Proben (normale Spermatogenese n=20, Hypospermatogenese n=26) zeigte den SOAT-Wildtyp (85-88%) (Abb. 24B).

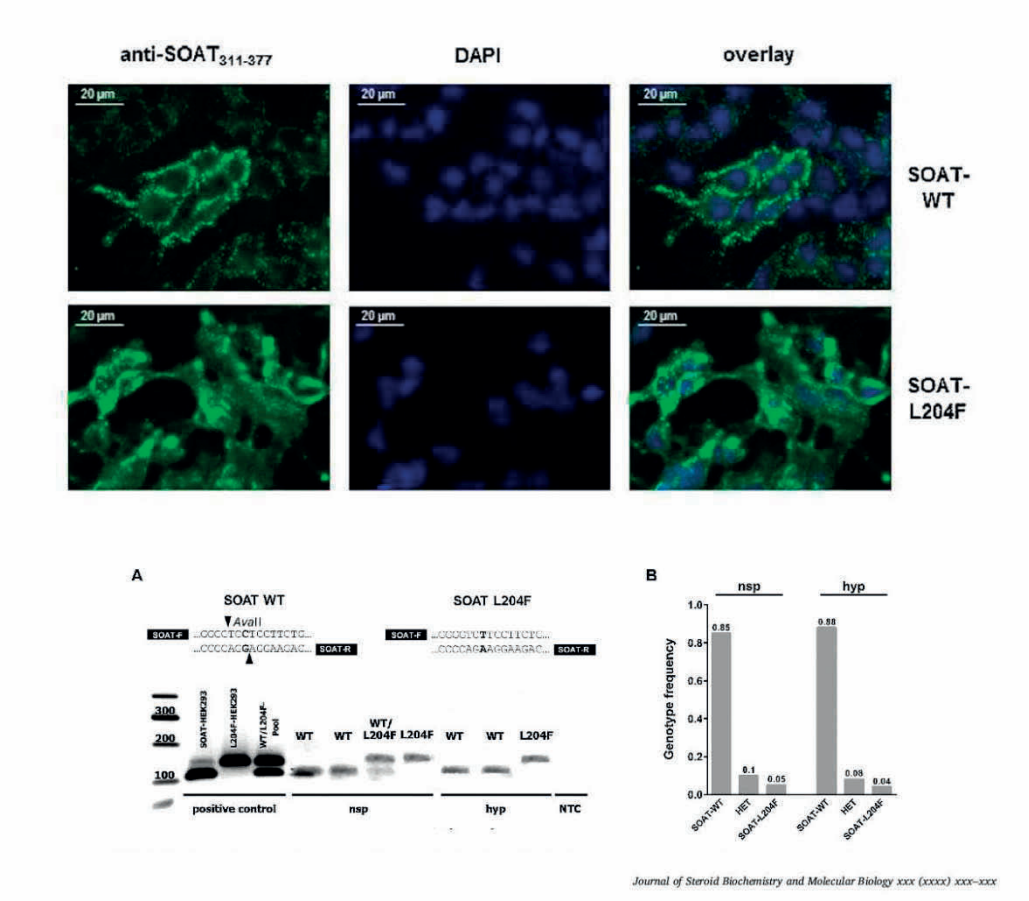

Abb. 24 Untersuchung des SNP L204F im humanen SLC10A6-Gen (Publikation #10)

A Eine membranständige Expression von SOAT konnte nur in Wildtyp-, nicht aber in L204F-HEK-Zellen gezeigt werden.

B Die Analyse des L204F-SNP in humanen Hodenbiopsien mit normaler Spermatogenese (NSP) und Hypospermatogenese (HYP) zeigte keine Häufung hetero- oder homozygoter SNPs

Neben L204F sind noch viel mehr nicht-synonyme SNPs im *SLC10A6*-Gen bekannt, von denen einige in einer weiterführenden Studie von Bennien et al. (2017) untersucht wurden. Die 148 SNPs in der kodierenden Sequenz wurden durch zwei Bioinformatik-Softwares (PolyPhen und SIFT *algorithms*) evaluiert; 24 SNPs wurden als potentiell schädigend eingeschätzt und bei sieben SNPs konnte ein *frame shift* vorhergesagt werden. Von diesen 31 untersuchten SNPs zeigten nur zwei SNPs eine ähnliche Transportaktivität wie der Wildtyp-SOAT. Im Gegensatz dazu, zeigten 11 SNPs überhaupt keine Transportaktivität für DHEAS. Ähnlich wie L204F lag das bei fünf SNPs (A83V, P107L, G241D, G263E und Y308N) ebenfalls an einer reduzierten Expression in der Zellmembran der stabil transfizierten HEK293-Zellen. Sechs dieser SNPs konnten direkt in (Q75R, S112F und N113K) oder in unmittelbarer Nähe der Natriumionen-Bindungsstelle des SOAT detektiert werden. Bisher wurden diese SNPs noch nicht in humanen Proben bzw. bei normaler und gestörter Spermatogenese untersucht. Eine mögliche biologische Bedeutung *in vivo* ist demnach noch unbekannt.

Zusätzlich zu SOAT/Soat wurden auch andere Transporter für sulfatierte Steroide im Hoden bei gestörter Spermatogenese untersucht und es konnte eine verminderte Expression für einzelne OATPs bei Spermatogenesearresten gezeigt werden. Während von SOAT verschiedene genetische Varianten, die zu einer Beeinflussung der Transportaktivität führen und so kausal mit Spermatogenesegestörungen verbunden sein können, bekannt sind, ist das bei OATPs anders. Die biologische Bedeutung der OATPs wurde v.a. in Hinblick auf Pharmakokinetik und die Wirkung von Pharmaka im normalen und entarteten Gewebe untersucht (**Publikation #11**). Sowohl OATP2B1 und OATP3A1 wurden in Brustkrebsgewebe detektiert (Kindla et al. 2011; Matsumoto et al. 2015). Die biologische Bedeutung von Effluxtransportern ist im Gegensatz dazu besser untersucht, da sie als Transporter an der Blut-Hirn- sowie auch Blut-Hodenschranke in das Phänomen der Arzneimittelresistenz eingebunden sind. Schinkel et al. (1994) generierten z.B. eine *Mdr1*$^{-/-}$ Knockout-Maus, die eine erhöhte Sensitivität gegen Ivermectin und andere Wirkstoffe zeigte, vom Reproduktionsphänotyp her aber normal war (Schinkel et al. 1994; Schinkel und Jonker 2003). Auch andere Knockout-Mäuse für *Abcc1* (Mrp1), *Abcc4* (Mrp4) und *Abcg2* (Bcrp) zeigen ein weitgehend normales Reproduktionsverhalten (Lorico et al. 1997; Wijnholds et al. 1998; Jonker et al. 2002; Zhou et al. 2002; Morgan et al. 2012), wobei die Spermatogenese selbst nicht explizit untersucht wurde. Wijnholds et al. (1997) konnten zeigen, dass *Abcc1* Knockout-Mäuse eine erhöhte Sensitivität gegenüber bestimmten Pharmaka aufwiesen. Allerdings waren die homo- und heterozygoten Mäuse vollkommen fertil und selbst „umfangreiche histologische Untersuchungen“ konnten keine histologischen Unterschiede zwischen Wildtyp- und Knockout-Mäusen gezeigt werden. In der Folgestudie wurde dann allerdings die Spermatogenese der Wildtyp und *Mrp1*$^{-/-}$ Mäuse nach einer Behandlung mit Etopophos, einem Wirkstoff in der Krebstherapie, genauer untersucht (Wijnholds et

al. 1998). Obwohl in dieser Studie die Mäuse immer noch als fertil bezeichnet werden, konnte gezeigt werden, dass die Behandlung mit Etopophos bei Knockout-Mäusen zu einer stärker veränderten Hodenhistologie und auch zu gravierenderen Spermatogenesestörungen (Meiosearrest, SCO) führt. Bei diesen Tieren konnte außerdem deutlich niedrigere Hormonspiegel für Testosteron, DHEA, Estradiol, Androstendion im Hoden ermittelt werden (Sivils et al. 2010). Auch bei einem *Abcc4* Knockout gibt es keine Hinweise auf eine Einschränkung der Reproduktion. Assem et al. (2004) beschrieben zwar einen Zusammenhang zwischen Mrp4 und Sult2a1 in der Leber, aber keinen Reproduktionsphänotyp. Morgan et al. (2012) konnten zeigen, dass *Mrp4* in den Leydigzellen exprimiert wird. Bei jungen Tieren mit einem *Abcc4* Defekt wurde eine veränderte Spermatogenese und reduzierte Testosteronkonzentrationen im Hoden beschrieben; letzteres lag an einer verminderten Testosteronproduktion in den Leydigzellen. Ebenso wie *Abcc1* Knockout-Mäuse zeigten *Abcg2* keine Einschränkungen hinsichtlich Wachstum, Lebensspanne etc. (Jonker et al. 2002; Zhou et al. 2002). In einer anderen Studie wurde die hodenspezifische Lokalisation von Abcg2 in der Ratte genauer untersucht und beschrieben. Qian et al. (2013) konnten zeigen, dass Abcg2 bei der Ratte kein klassisches BHS-Protein ist, sondern in den Gefäßendothelien und von den peritubulären Myoidzellen exprimiert wird. Eine Lokalisation im basalen Drittel zwischen Sertolizellen konnte nicht gezeigt werden, aber eine stadienspezifische *Abcg2*-Expression im Stadium VIII kurz vor dem *sperm release* im Bereich der apikalen ektoplasmatischen Spezialisierungen. Ein Knockdown von *Abcg2* mittels RNAi führte zu einem Verlust von Adhäsion und Polarität der Spermatiden in den Sertolizellen, so dass hier ein funktioneller Zusammenhang bestätigt werden konnte.

7. Nachbemerkungen und Ausblick

Mit den Untersuchungen zur Expression und Lokalisation klassischer und nicht-klassischer Steroidhormonrezeptoren sowie deren Transportsystemen im Hoden von Mensch und Tier konnten wir einen guten Überblick über die verschiedenen Wirkungswege von freien und konjugierten Steroiden gewinnen und die Hypothese eines funktionellen *„sulfatase pathway“* im Hoden konnte bestätigt werden. Allerdings konnten die Untersuchungen der **Publikationen ##1-11** keinen kausalen Zusammenhang zwischen den untersuchten Rezeptoren bzw. Transportern und Störungen der humanen Spermatogenese aufdecken.

Nur selten führt eine verminderte bzw. fehlende Expression oder die Variation eines einzelnen Gens zu einem Totalausfall der Spermatogenese, da dieser essentielle Prozess vielfach abgesichert ist. Nur wenige Gegenbeispiele sind bekannt. Ein Fehlen des Transkriptionsfaktors CREM (*cyclic AMP responsive element modulator*) führt zum Beispiel bei der Maus zu Infertilität (Blendy et al. 1996; Nantel et al. 1996) und auch beim Menschen zu einer schwerwiegenden Störung der Spermatogenese (Weinbauer et al. 1998; Steger et al. 1999; Blöcher et al. 2003; 2005). Ein weiteres Beispiel ist ein konditioneller Knockout von Connexin 43 in Sertolizellen der Maus, der zu einer totalen Keimzellaplasie führt (Brehm et al. 2007, Übersicht bei Weider et al. 2011). Eine verminderte Expression von Connexin 43 ist beim Menschen ebenfalls mit Infertilität assoziiert und wird als Marker für unreife Sertolizellen beschrieben (Defamie et al. 2003), da das Protein eine essentielle Komponente der Blut-Hodenschranke ist (Li et al. 2010). Wie die *Slc10a6*$^{-/-}$ Maus beweist, ist mSoat kein für die Spermatogenese essentielles Gen (**Publikation #9**). Dasselbe gilt für die anderen untersuchten Transporter aus den **Publikationen #5 und# 7**. Wie in **Publikation #11** zusammengefasst wurde, sind im Hoden sehr viele verschiedene Transporter für sulfatierte Steroide exprimiert, die den Verlust einzelner Gene ausgleichen können.

7.1. „Neue Steroide“ und ihre biologische Signifikanz

Neben der Untersuchung von lang bekannten freien und konjugierten Steroiden rücken die „neuen“ Steroide und Wirkungsmechanismen dieser Hormone immer mehr in den Fokus der Wissenschaft. Von besonderer Bedeutung sind hierbei die bisher unbekannten Substrate bzw. Synthesewege bekannter Enzyme. Erschwert werden die Untersuchung dieser neuen Steroide durch starke alters- und auch geschlechtsabhängige Schwankungen, sowie verschiedene Wirkungsmechanismen dieser Metabolite im Körper über klassische oder membran-ständige Steroidhormonrezeptoren. Durch Optimierung der LC-MS/MS im Rahmen der Forschergruppe FOR1369 ist es nun auch möglich,

verschiedene freie und konjugierte Steroide simultan und auch in verschiedenen Körperflüssigkeiten (Serum, Urin, Follikelflüssigkeit), Gewebe und Zellkulturen zu bestimmen (Sánchez-Guijo et al. 2015; 2016). Auch in einer Übersicht von Marcos und Pozo (2016) wird die LC-MS/MS als Methode der Wahl zur Identifikation neuer Steroide beschrieben.

Neue endogene Steroidhormonmetabolite entstehen durch erweiterte Substratspektren bekannter steroidogener Enzyme. So konnten Neunzig et al. (2017) zeigen, dass CYP21A2 nicht nur, wie bisher bekannt, Progesteron und 17-OH-Progesteron, sondern auch noch Androstendion und Testosteron binden und verstoffwechseln kann. Ein neuer Metabolit (16β-OH-Androstendion, 16β-OH-A4) mit androgener Wirkung wurde hier beschrieben und dieser ist, wie A4 alleine auch schon, in der Lage den AR zu aktivieren. Außerdem kann 16β-OH-A4 ebenso wie A4 an das Enzym Aromatase (CYP19A1) binden und ihr als Substrat dienen. Das dabei entstehende 16βOH-Estron (16β-OH-E) kann allerdings nur geringfügig an die ERs binden, verglichen mit den freien Estrogenen Estron und Estradiol. Außerdem konnte dieser Metabolit in seiner sulfatierten Form im Urin von Patienten mit einer 11-Hydroxylasedefizienz festgestellt werden. Eine physiologische Bedeutung von 16β-OH-A4 liegt also nahe. Neben den neuen Substraten für CYP21A2, konnten Mosa et al. (2015) auch neue Aktivitäten für CYP11A1 zeigen. Neben der „üblichen“ 6β-Hydroxylaseaktivität können durch dieses Enzym auch 2β- und 6β-OH-DOC, 2β- und 6β-OH-A4, 6β-OH-Testosteron und 16β-OH-DHEA entstehen. Letzteres wurde ebenfalls im Urin und Blutplasma von Erwachsenen detektiert. Während junge Erwachsene sehr hohe 16β-OH-DHEA Werte haben, sinken diese wieder mit steigendem Alter. Vor allem die Nebenniere, aber wahrscheinlich auch die Gonaden produzieren dieses Hormon (Sekihara et al. 1976). Allerdings kann 16β-OH-DHEA nur in geringen Mengen im humanen Serum nachgewiesen werden, da es schnell zu anderen Steroidmetaboliten verstoffwechselt wird (Ke et al. 2016). Der sulfatierte Metabolit 16β-OH-DHEAS konnte in fetalen Leberpräparationen nachgewiesen werden (Wynne und Renwick 1976). Henríquez et al. (2016) konnten verschiedene physiologische Estrogenmetabolite in den Gelbkörpern gesunder Frauen als parakrine Modulatoren der Gelbkörperfunktion identifizieren. Besondere Bedeutung können diese neuen Steroidmetabolite für verschiedene Krankheiten, wie zum Beispiel dem androgen-unabhängigen (oder Kastrations-resistenten) Prostatakarzinom (*castration-resistent prostata carcinoma*, CRPC) haben. Bloem et al. (2013) beschreiben in einem Review die Synthese von 11-Hydroxyandrostendion (11-OH-A4) in der Nebenniere und dessen Metabolisierung zu klassischen und auch neuen Steroiden in rezeptiven Organen durch die Anwesenheit verschiedener Enzyme wie 17β-, 11β-HSD und SRD5α, z.B. auch in der Prostata und einer Prostatakarzinomzelllinie (LNCaP). So entstehen verschiedene Metabolite, die an den AR binden und auch eine androgene Wirkung entfalten können. 11-Ketodihydrotestosteron (11-K-DHT) zum Beispiel hat dieselbe Bindungsaffinität zu AR wie Testosteron und auch die Wirkung

von 11-K-DHT ist vergleichbar mit Testosteron. Dies kann erklären, warum auch nach einer Androgendeprivation das Wachstum der Prostatakarzinomzellen nicht gestoppt werden bzw. der Tumor rezidivieren kann. Auch in einem Review von Mostaghel (2014) wird von alternativen Wirkungsmechanismen bei CRPC berichtet. Dazu zählen u.a. DHEA(S) aus der Nebenniere als klassisches adrenales Steroidhormon sowie auch DOC, 5α-DHDOC, und 11OHA4. Diese können ebenfalls den AR aktivieren. Weitere biologische Funktionen dieser bisher „neuen" Metabolite sind noch unklar und auch die Bedeutung für die Reproduktion ist noch nicht untersucht. Die Erweiterung des Substratspektrums der LC-MS/MS, wie von Galuska et al. (2013) veröffentlicht, eröffnet jedoch vollkommen neue Möglichkeiten.

Von steigender Bedeutung sind auch exogene Steroidmetabolite, die sogenannten *endocrine disruptors* (EDs). Es handelt sich dabei um hormonartige Substanzen, wie sie zum Beispiel in Pflanzen (Phytoestrogene in Mais und Soja) oder auch in der Industrie (Weichmacher in Plastik, Pflanzenschutzmittel etc.) vorkommen. Hampl et al. (2014) gaben einen guten Überblick über die verschiedenen Wirkmechanismen dieser EDs. Sie können nicht einfach „nur" an die verschiedenen klassischen und auch nicht-klassischen Steroidrezeptoren binden und dort eine genomische oder nicht-genomische Zellantwort initiieren, sondern sie können diese Rezeptoren auch für endogene Steroide blockieren. Des Weiteren können EDs die Steroidbiosynthese (über CYP19A1, 3β- und 17β-HSD), den Metabolismus der Steroide (z.B. Hemmung der SULTs) und den Transport der Steroide im Körper (z.B. des mitochondrialen Cholesteroltransports durch StAR) beeinflussen und stören.

7.2. Bedeutung neuer Wirkmechanismen für freie und konjugierte Steroide

Neben den verschiedenen „neuen" endo- und exogenen Steroidmetaboliten können auch bekannte Metabolite wie DHEA(S) und E1S an AR und ERs binden und eine Transaktivierung herbeiführen (Bjerregaard-Olesen et al. 2016). Während die Bindung von DHEAS eine aktive STS in den Zellen erfordert, kann E1S auch ohne STS binden. An die ERs können beide Hormone ohne Anwesenheit von STS binden. Dies unterstützt zum einen die Hypothese des *„sulfatase pathway"* in den Zielzellen (**Publikation ## 5-8**), kann aber auch auf nicht-genomische AR-Wirkung bzw. membran-ständige Androgenrezeptoren hinweisen. Eine Bindung von DHEAS an membran-ständige ARs mit nachfolgender Aktivierung der nicht-genomischen Signalkaskade wurde bei Shihan et al. (2013) beschrieben.

Intensiv untersucht wurden diese neuen Wirkmechanismen für Steroidhormone u.a. im Zusammenhang mit dem CRCP. In Reviews von Mostaghel (2014) und Ho und Dehm (2017) wird auf

die Möglichkeit von AR-Mutationen, Splicingvarianten und Abwandlungen der Co-Aktivator- bzw. Co-Repressorexpression hingewiesen, die zu einer veränderten Transaktivierungsfähigkeit des AR führen können. Vor allem Amplifikationen des AR sind besonders häufig bei CRCP, vermutlich als Anpassung auf die Antiandrogentherapie (Übersicht bei Ho und Dehm 2017). Auch eine androgen-unabhängige Aktivierung des AR ist möglich und macht vor allem die AF-1 des AR zu einem vielversprechenden therapeutischen Ziel (Sadar 2011). Polymorphismen im CAG-Repeat des AR stehen immer noch im Fokus des wissenschaftlichen Interesses (Übersicht bei Tirabassi et al. 2015) und es gibt aktuelle Studien zur Beteiligung des CAG-Repeats bei peripheren Testosteroneffekten (Khan et al. 2017). Bei Patienten mit einem Prostatakarzinom wurde häufig kein verlängertes, sondern ein verkürztes CAG-Repeat gefunden, welches mit einer gesteigerten Transaktivierungsfähigkeit assoziiert sein soll. Außerdem wurde bei diesen Patienten auch ein somatisches Mosaik mit Repeatunterschiede von bis zu 11 Repeats in den betroffenen Bereichen der erkrankten Prostata nachgewiesen (Alvarado et al. 2005). Dasselbe Phänomen wurde auch für die Kennedy's Disease beschrieben (Ito et al. 1998; Tanaka et al. 1999). Auch für die klassichen ERs sind verschiedene Isoformen und trunkierte Rezeptorformen bekannt (**Publikation #3**). Außerdem können klassische Rezeptoren auch in die Zellmembran integriert werden und dort direkt über freie (oder auch sulfatierte) Estrogene stimuliert werden. Der Effekt ist dann nicht-genomisch und es kommt über eine intrazelluläre Signalkaskade zu einem cAMP-Anstieg (Übersicht bei Luconi et al. 2002; Levin und Hammes 2016).

Neben den klassischen Steroidhormonrezeptoren rücken immer mehr die membran-ständigen Steroidhormonrezeptoren in den Fokus. In **Publikation #3** untersuchten wir deswegen nicht nur die Expression von ERα und ERβ im humanen Hoden, sondern auch die Expression des G-Proteingekoppelten Estrogenrezeptors GPER. Die Untersuchung dieser nicht-genomischen Wirkungsmechanismen gewinnt v.a. an Bedeutung, wenn es keine Unterschiede bei der Expression der klassischen Rezeptoren, z.B. bei Spermatogenesestörungen gibt (**Publikation #2**). Shihan et al. (2014; 2015) konnten zeigen, dass Steroide an die membran-ständigen Rezeptoren Gnα11 und ZIP9 binden können. Untersucht wurden hier Spermatozyten-ähnliche GC-2 Zellen. Dieselbe Arbeitsgruppe konnte in einer Rattensertolizelllinie, die auch schon in **Publikation #4** verwendet wurde, ebenfalls die Wirkung von DHEAS auf membranständige Rezeptoren und den Effekt auf Sertolizell-spezifische Gene wie Claudine beschreiben (Papadopoulos et al. 2016). Diese nicht-genomischen Signalwege wurden schon früher in Sertolizellen beschrieben (Übersicht bei Walker 2010). GPER könnte vor allem bei Tieren mit einer sehr hohen testikulären Estrogenproduktion wie dem Schwein und dem Hengst eine wichtige Rolle für die Erhaltung der Spermatogenese spielen. Aus diesem Grund untersuchen wir zur Zeit die Expression und Lokalisation von GPER und anderen membran-ständigen Steroidhormonrezeptoren bei Bullen, Ebern, Hengst und Hunden. Vor allem die

GPER Lokalisation weicht bei unseren Haussäugetieren von der des Menschen ab (Hartmann et al., in Vorbereitung).

7.3. Untersuchung der humanen Spermatogenese – Schwierigkeiten bei Klonierung, Auswahl von Antikörpern und Übertragbarkeit von Tiermodellen auf den Mensch

In den **Publikationen #1-10** wurden entweder transfizierte Bakterien (**Publikationen ##1-2**), tierische bzw. humane Zellen (**Publikationen ##3-4**) oder beides (**Publikationen ##5-6, 8 und 10**) verwendet. In **Publikation #9** wurde für die Untersuchung der biologischen Signifikanz von mSoat eine genetisch veränderte Maus generiert. Bei den **Publikationen ##3 und 5-11** wurden Antikörper gegen die Estrogenrezeptoren oder Transporter verwendet. Die Verwendung von Zellkulturen, Tiermodellen und auch Antikörpern ist häufig problembehaftet. Beispielhaft sollen hier die Schwierigkeiten bei der Untersuchung der klassischen Steroidhormone und das SOAT-Tiermodell erwähnt werden.

Für die Versuche aus **Publikation #1** wurde ein E. coli-Stamm (JM109, Promega) verwendet, um das CAG-Repeat verschiedener Patienten zu klonieren und zu sequenzieren. Bei den Versuchen zu **Publikation #2** zeigte sich, dass diese Bakterien keine verlässlichen, replizierbaren Ergebnisse generieren können, so dass noch ein weiterer Bakterienstamm (SURE, Invitrogen) verwendet wurde. Auch mit den transfizierten Sertolizellen der Ratte aus **Publikation #4** kam es zu Schwierigkeiten, da schon zwischen den untransfizierten und einer transfizierten Zelllinie signifikante Expressionsunterschiede gezeigt werden konnten. Das deutet darauf hin, dass die Transfektion an sich Einfluss auf die Zellen nimmt. Das konnte auch von Xiao et al. (2012) in Cre-transfizierten Zellen gezeigt werden.

Als Positivkontrolle wurden in den Versuchen zur **Publikation #3** Brustkrebszellen, MCF-7 und T47D Zellen verwendet. Die MCF7-Zellen gelten schon lange als Positivkontrolle für die Expression von ERs. Neue Erkenntnisse zeigen allerdings, dass die MCF7-Zellen keinen bzw. kaum ERβ exprimieren (Nelson et al. 2017). Diese Ergebnisse konnten wir bestätigen, da die MCF-7 Zellen sowohl im Western Blot als auch in der qRT-PCR nur sehr wenig ERβ exprimierten. Insgesamt wurden für die Doktorarbeit von C. Ratzenböck (Ratzenböck 2014) sechs verschiedene Antikörper für ERα verwendet; nur zwei Antikörper (F-10 und HC-20) zeigten Ergebnisse, die nach Verwendung einer spezifischen Positivkontrolle (Nebenhoden, Western Blot), Negativkontrolle (Peptidpräinkubation) und nach Absicherung auf molekularbiologischer Ebene (RT-PCR, RT-PCR nach LACP, qRT-PCR) sicher als richtig eingestuft werden konnten. Für die Detektion des ERβ wurde ein Antikörper verwendet, dessen Spezifität ebenfalls mit verschiedenen Methoden belegt werden konnte. Nelson et al. (2017)

konnten dagegen zeigen, dass die meisten gegen den ERβ verwendeten Antikörper den Estrogenrezeptor dagegen nicht spezifisch detektieren.

Die Verwendung von Tiermodellen für die Untersuchung der humanen Spermatogenese ist ebenfalls problembehaftet, da die Spermatogenese bei allen Spezies eine eigene Kinetik und Stadienverteilung zeigt (Clermont 1963, Übersicht bei Russell et al. 1990; Russell 1990; Bergmann und Kliesch 2010). Außerdem müssen wir zwischen einem *single-stage arrangement* bei Tieren und einem *multi-stage arrangement* beim Menschen unterscheiden. Rückschlüsse von Mausmodellen auf die Spermatogenese oder die Entstehung von Infertilität beim Mensch sind demnach nur dann möglich, wenn sie parallel an Tier und Mensch durchgeführt werden und sich gegenseitig ergänzen. Im Rahmen des deutsch-australischen Graduiertenkollegs (*International Research Training Group*, IRTG) DFG GRK1871 "Molecular Pathogenesis of Male Reproductive Disorders" werden deshalb in Zusammenarbeit zwischen der JLU Gießen und Monash Universtiy Melbourne, Australien in komplementären und ergänzenden Versuchen Mausmodelle mit einem Reproduktionsphänotyp und die Spermatogenese beim Menschen untersucht. Auch im Rahmen der DFG Forschergruppe FOR1369 „Sulfated Steroids in Reproduction" wurden vor der Generierung der *Slc10a6*$^{-/-}$ Maus umfassende Vorversuche zur *Slc10a6* Expression in Wildtyp-Mäusen durchgeführt. Beim Mensch konnte eine signifikant reduzierte SOAT-Expression bei Spermatogenesestörungen nachgewiesen werden, im Mausmodell dagegen nicht. Dass Mausmodell und die Situation im Mensch nicht übereinstimmen müssen, konnte schon an verschiedenen Beispielen in unserer Arbeitsgruppe gezeigt werden, z.B. bei der *Kif4* Knockout Maus und der *Cbe1* Knockout Maus; während diese beiden Mausmodelle keinen Reproduktionsphäntotyp zeigten, konnte durchaus eine Beteiligung der Gene an der Entstehung von Spermatogenesestörungen beim Menschen nachgewiesen werden (KIF4/Kif4) (Behr et al. 2007; Godmann et al. 2009) und CBE1/Cbe1 (Pleuger et al. 2017; Miyata et al. 2016).

8. Zusammenfassung

Fertilitätsstörungen sind ein Problem mit steigender Inzidenz, ca. 15% deutscher Paare sind ungewollt kinderlos. In etwa 50% der Fälle ist die Ursache hierfür auf der Seite des Mannes zu suchen (*male factor infertility*). Spermatogenesestörungen wie Arreste, totale Keimzellaplasie oder auch eine bunte Atrophie können durch morphologische und z.T. auch molekularbiologische Methoden gut untersucht werden - die Gründe für die Spermatogenesestörungen bleiben dennoch bis auf wenige Fälle unklar.

Die Bedeutung von klassichen Steroidhormonen wie Androgenen und Estrogenen für das Reproduktionsgeschehen ist gut untersucht, ebenso wie die Aktivierung oder Inhibierung der Genexpession durch die klassischen Steroidhormonrezeptoren. Besonders Mutationen, Splicingvarianten und Polymorphismen dieser wurden in Hinsicht auf die humane Reproduktion intensiv untersucht. Mutationen im Androgenrezeptor können zu einer teilweisen oder auch kompletten Insensitivität gegenüber Androgenen und damit zu schwerwiegenden Fertilitätsstörungen führen. Eine Beteiligung des polymorphen CAG-Repeats an der Entstehung dieser Androgeninsensitivität ist eine Hypothese, die bereits von vielen Arbeitsgruppen mit sehr unterschiedlichen Ergebnissen untersucht wurde.

Neben diesen klassischen Steroidhormonen und ihren Rezeptoren können auch membran-ständige Rezeptoren, sowie neue Steroidhormone und deren Metabolite eine Bedeutung für die männliche Reproduktion haben. Für Androgene und Estrogene sind verschiedene membran-ständige Rezeptoren bekannt, diese sind meistens an G-Proteine gekoppelt und können schnelle, nicht-genomische Effekte hervorrufen. Während bei klassischen Rezeptoren das Steroidhormon in die Zelle gelangen muss, um an den Rezeptor zu binden, können membran-ständige Rezeptoren auch von extrazellulär lokalisierten freien Steroiden oder hydrophilen Steroidhormonmetaboliten aktiviert werden. Obwohl bereits seit Jahrzehnten bekannt ist, dass konjugierte (v.a. sulfatierte) Steroidhormone in großen Mengen im humanen und tierischen Hoden synthetisiert werden, wurde ihnen bis vor zehn Jahren keine größere biologische Bedeutung zugewiesen, sondern sie wurden als wasserlösliche Exkretionsprodukte angesehen. Die biologische Bedeutung der sulfatierten Steroide als intrazelluläre Speicherform für die Steroidhormonsynthese in verschiedenen Organen wie der Plazenta, der Brust und auch dem Hoden konnte allerdings nicht weiter geklärt werden, bis spezifische Transporter für diese hydrophilen Moleküle entdeckt wurden. Nur über diese können die Steroidsulfate in verschiedene Zielzellen aufgenommen und auch wieder aus diesen Zellen heraus transportiert werden. In den Zielgeweben können sulfatierte Steroide über die Aktivität der Steroidsulfatase STS reaktiviert werden. Dies bezeichnet man als *„sulfatase pathway“.* Sie können so

in den Zielgeweben zu einer lokalen Steroidsynthese und zur auto-, para- und intrakrinen Steuerung beitragen.

Die vorliegende Habilitationsschrift fasst 11 Publikationen zusammen, die sich mit der Expression und Lokalisation von klassischen und membran-ständigen Steroidhormonrezeptoren sowie von Transportsystemen für sulfatierte Steroide im humanen und tierischen Hoden befassen. In den zu Grunde liegenden Untersuchungen konnte gezeigt werden, dass die Länge des polymorphen CAG-Repeats im humanen Androgenrezeptor nicht mit Spermatogenesestörungen und einer verminderten Expression von zwei androgenabhängigen Genen (*Androgen binding protein* und Clusterin) in Verbindung gebracht werden kann. In Arbeiten zu den klassischen und einem membran-ständigen Estrogenrezeptor(en) wurde die Lokalisation in den Keim-, Sertoli- und Leydigzellen und die Bedeutung dieser Rezeptoren in der normalen und gestörten Spermatogenese untersucht. Die verschiedenen Veröffentlichungen zur zellulären Lokalisation konnten durch den Einsatz mehrerer, sich ergänzender Methoden von uns zum Teil bestätigt werden. Als gesichert gilt nun die Expression der Estrogenrezeptoren in Keim-, Sertoli-, peritubulären Myoid- und Leydigzellen. Ein Großteil der Publikationen befasst sich mit der Lokalisation und biologischen Bedeutung von sulfatierten Steroidhormonen und ihren Transportsystemen im humanen und murinen Hoden. Durch diese Untersuchungen konnte gezeigt werden, dass es einen *„sulfatase pathway“* im Hoden gibt, da verschiedene Uptake Carrier und Effluxtransporter in Keim- und Sertolizellen detektiert werden konnten. Durch *in vitro* Versuche wurde gezeigt, dass ein Transport von sulfatierten Steroiden über die Sertolizellen stattfinden kann. Eine biologische Bedeutung der sulfatierten Steroide für die männliche Reproduktion ist demnach unstrittig. In weiteren Untersuchungen mit einem *Soat*-Knockoutmausmodell und verschiedenen SOAT-Punktmutationen sollte der Einfluss von SOAT auf die Entstehung von humanen Spermatogenesestörungen weiter untersucht werden. Bisherige Ergebnisse zeigen, dass ein totaler Knockout bzw. verschiedene Punktmutationen nicht kausal für die Entstehung der Spermatogenesestörung verantwortlich gemacht werden können.

9. Literaturverzeichnis

Ahmed EA, Barten-van Rijbroek AD, Kal HB, Sadri-Ardekani H, Mizrak SC, van Pelt AMM, Rooij DG de (2009) Proliferative activity in vitro and DNA repair indicate that adult mouse and human Sertoli cells are not terminally differentiated, quiescent cells. Biol. Reprod 80(6):1084–1091

Aksglaede L, Juul A (2013) Testicular function and fertility in men with Klinefelter syndrome: a review. Eur. J. Endocrinol 168(4):76

Albrecht M (2009) Insights into the nature of human testicular peritubular cells. Ann. Anat 191(6):532–540. doi:10.1016/j.aanat.2009.08.002

Alvarado C, Beitel LK, Sircar K, Aprikian A, Trifiro M, Gottlieb B (2005) Somatic mosaicism and cancer: a micro-genetic examination into the role of the androgen receptor gene in prostate cancer. Cancer Res 65(18):8514–8518. doi:10.1158/0008-5472.CAN-05-0399

Amann RP, Veeramachaneni DNR (2007) Cryptorchidism in common eutherian mammals. Reproduction 133(3):541–561

Assem M, Schuetz EG, Leggas M, Sun D, Yasuda K, Reid G, Zelcer N, Adachi M, Strom S, Evans RM, Moore DD, Borst P, Schuetz JD (2004) Interactions between hepatic Mrp4 and Sult2a as revealed by the constitutive androstane receptor and Mrp4 knockout mice. J. Biol. Chem 279(21):22250–22257

Bakhaus K (2014) Membrantransporter für sulfatierte Steroidhormone im Hoden: Die Bedeutung des Sodium-dependent Organic Anion Transporter (SOAT) im Reproduktionsgeschehen. Dissertation, Justus Liebig Universität Gießen

Bedin M, Fournier T, Mouhadjer N, Pointis G (1988) Ontogenesis and regulation of steroid sulfatase activity in Leydig cells and seminiferous tubules in the Long-Evans rat. J. Steroid Biochem 30(1-6):439–441

Behr R, Deller C, Godmann M, Müller T, Bergmann M, Ivell R, Steger K (2007) Kruppel-like factor 4 expression in normal and pathological human testes. Mol. Hum. Reprod. 13(11):815–820

Bennett NC, Gardiner RA, Hooper JD, Johnson DW, Gobe GC (2010) Molecular cell biology of androgen receptor signalling. Int. J. Biochem. Cell Biol 42(6):813–827. doi:10.1016/j.biocel.2009.11.013

Bennien J, Fischer T, Geyer J (2017) Rare genetic variants in the sodium-dependent organic anion transporter SOAT (SLC10A6): Effects on transport function and membrane expression. J. Steroid Biochem. Mol. Biol 2017 Sep 8. pii: S0960-0760(17)30252-2. doi: 10.1016/j.jsbmb.2017.09.004

Bergh A, Damber JE (1992) Immunohistochemical demonstration of androgen receptors on testicular blood vessels. Int. J. Androl 15(5):425–434

Bergmann M, Dierichs R (1983) Postnatal formation of the blood-testis barrier in the rat with special reference to the initiation of meiosis. Anat. Embryol 168(2):269–275

Bergmann M, Nashan D, Nieschlag E (1989) Pattern of compartmentation in human seminiferous tubules showing dislocation of spermatogonia. Cell Tissue Res 256(1):183–190

Bergmann M, Kliesch S (1994) The distribution pattern of cytokeratin and vimentin immunoreactivity in testicular biopsies of infertile men. Anat. Embryol 190(6):515–520

Bergmann M, Kliesch S (2010) Testicular biopsy and histology. In: Nieschlag E, Behre HM, Nieschlag S (Eds.) Andrology. Male Reproductive Health and Dysfunction. Springer, Berlin, Heidelberg, pp 155–167

Berney DM, Looijenga LHJ, Idrees M, Oosterhuis JW, Rajpert-De Meyts E, Ulbright TM, Skakkebaek NE (2016) Germ cell neoplasia in situ (GCNIS): evolution of the current nomenclature for testicular pre-invasive germ cell malignancy. Histopathology 69(1):7–10

Berruti G, Paiardi C (2014) The dynamic of the apical ectoplasmic specialization between spermatids and Sertoli cells: the case of the small GTPase Rap1. BioMed Res. Int 2014:635979

Bickhardt K, Heinritzi K, Lahrmann K-H (2004) Lehrbuch der Schweinekrankheiten. 63 Tabellen, 4th edn. Parey, Stuttgart

Bjerregaard-Olesen C, Ghisari M, Kjeldsen LS, Wielsøe M, Bonefeld-Jørgensen EC (2016) Estrone sulfate and dehydroepiandrosterone sulfate. Transactivation of the estrogen and androgen receptor. Steroids 105:50–58

Bleau G, Bodley FH, Longpré J, Chapdelaine A, Roberts KD (1974) Cholesterol sulfate. I. Occurrence and possible biological function as an amphipathic lipid in the membrane of the human erythrocyte. Biochim. Biophys. Acta 352(1):1–9

Blendy JA, Kaestner KH, Weinbauer GF, Nieschlag E, Schütz G (1996) Severe impairment of spermatogenesis in mice lacking the CREM gene. Nature 380(6570):162–165

Blöcher S, Behr R, Weinbauer GF, Bergmann M, Steger K (2003) Different CREM-isoform gene expression between equine and human normal and impaired spermatogenesis. Theriogenology 60(7):1357–1369

Blöcher S, Fink L, Bohle RM, Bergmann M, Steger K (2005) CREM activator and repressor isoform expression in human male germ cells. Int. J. Androl 28(4):215–223

Bloem LM, Storbeck K-H, Schloms L, Swart AC (2013) 11β-hydroxyandrostenedione returns to the steroid arena. Biosynthesis, metabolism and function. Molecules 18(11):13228–13244

Borst P, Elferink RO (2002) Mammalian ABC transporters in health and disease. Annu. Rev. Biochem 71:537–592

Bowater RP, Rosche WA, Jaworski A, Sinden RR, Wells RD (1996) Relationship between Escherichia coli growth and deletions of CTG.CAG triplet repeats in plasmids. J. Mol. Biol 264(1):82–96. doi:10.1006/jmbi.1996.0625

Bradlow HL (1970) The Hydrolysis of Steroid Conjugates. In: Bernstein S, Solomon S (ed) Chemical and Biological Aspects of Steroid Conjugation. Springer Berlin Heidelberg, Berlin, Heidelberg, pp 131–181

Brehm R, Rey R, Kliesch S, Steger K, Marks A, Bergmann M (2006) Mitotic activity of Sertoli cells in adult human testis: an immunohistochemical study to characterize Sertoli cells in testicular cords from patients showing testicular dysgenesis syndrome. Anat. Embryol 211(3):223–236. doi:10.1007/s00429-005-0075-8

Brehm R, Zeiler M, Rüttinger C, Herde K, Kibschull M, Winterhager E, Willecke K, Guillou F, Lécureuil C, Steger K, Konrad L, Biermann K, Failing K, Bergmann M (2007) A sertoli cell-specific knockout of connexin43 prevents initiation of spermatogenesis. Am. J. Pathol 171(1):19–31

Brinkmann AO, Blok LJ, Ruiter PE de, Doesburg P, Steketee K, Berrevoets CA, Trapman J (1999) Mechanisms of androgen receptor activation and function. J. Steroid Biochem. Mol. Biol 69(1-6):307–313

Bruning G, Dierichs R, Stümpel C, Bergmann M (1993) Sertoli cell nuclear changes in human testicular biopsies as revealed by three dimensional reconstruction. Andrologia 25(6):311–316

Bulldan A, Dietze R, Shihan M, Scheiner-Bobis G (2016a) Non-classical testosterone signaling mediated through ZIP9 stimulates claudin expression and tight junction formation in Sertoli cells. Cell. Signal 28(8):1075–1085

Bulldan A, Shihan M, Goericke-Pesch S, Scheiner-Bobis G (2016b) Signaling events associated with gonadotropin releasing hormone-agonist-induced hormonal castration and its reversal in canines. Mol. Reprod. Dev 83(12):1092–1101

Bulldan A, Malviya VN, Upmanyu N, Konrad L, Scheiner-Bobis G (2017) Testosterone/bicalutamide antagonism at the predicted extracellular androgen binding site of ZIP9. Biochim. Biophys. Acta 1864:2402–2414. doi: 10.1016/j.bbamcr.2017.09.012

Burck PJ, Zimmerman RE (1980) The inhibition of acrosin by sterol sulphates. J. Reprod. Fertil 58(1):121–125

Burger S, Doring B, Hardt M, Beuerlein K, Gerstberger R, Geyer J (2011) Co-expression studies of the orphan carrier protein Slc10a4 and the vesicular carriers VAChT and VMAT2 in the rat central and peripheral nervous system. Neuroscience 193:109–121

Carreau S, Hess RA (2010) Oestrogens and spermatogenesis. Phil. Trans. R. Soc. London. Series B, Biol. Sci 365(1546):1517–1535

Carreau S, Bouraima-Lelong H, Delalande C (2011) Estrogens: new players in spermatogenesis. Reprod. Biol 11(3):174–193

Carreau S, Bouraima-Lelong H, Delalande C (2012) Estrogen, a female hormone involved in spermatogenesis. Adv. Med. Sci 57(1):31–36

Casella R, Maduro MR, Misfud A, Lipshultz LI, Yong EL, Lamb DJ (2003) Androgen receptor gene polyglutamine length is associated with testicular histology in infertile patients. J. Urol 169(1):224–227. doi:10.1097/01.ju.0000035361.18870.6e

Cavaco JEB, Laurentino SS, Barros A, Sousa M, Socorro S (2009) Estrogen receptors alpha and beta in human testis: both isoforms are expressed. Syst. Biol. Reprod. Med 55(4):137–144

Chastain PD, Sinden RR (1998) CTG repeats associated with human genetic disease are inherently flexible. J. Mol. Biol 275(3):405–411. doi:10.1006/jmbi.1997.1502

Cheetham JJ, Chen RJ, Epand RM (1990) Interaction of calcium and cholesterol sulphate induces membrane destabilization and fusion. Implications for the acrosome reaction. Biochim. Biophys. Acta 1024(2):367–372

Claessens F, Verrijdt G, Haelens A, Callewaert L, Moehren U, d'Alesio A, Tanner T, Schauwaers K, Denayer S, van Tilborgh N (2005) Molecular biology of the androgen responses. Andrologia 37(6):209–210. doi:10.1111/j.1439-0272.2005.00698.x

Claus R, Hoffmann B (1980) Oestrogens, compared to other steroids of testicular origin, in blood plasma of boars. Acta Endocrinol 94(3):404–411

Clermont Y (1963) The cycle of the seminiferous epithelium in man. Am. J. Anat 112:35–51. doi:10.1002/aja.1001120103

Constanzo LS (2010) Cellular Physiology. In: Costanzo LS (ed) Physiology, 4th edn. Saunders, Philadelphia Pa., London, pp 1–43

Costa Y, Cooke HJ (2007) Dissecting the mammalian synaptonemal complex using targeted mutations. Chromosome Res 15(5):579–589

Couse JF, Korach KS (1999) Estrogen receptor null mice: what have we learned and where will they lead us? Endocr. Rev 20(3):358–417

Cupp AS, Skinner MK (2005) Embryonic Sertoli Cell Differentiation. In: Skinner MK, Griswold MD (Eds.) Sertoli cell biology. Elsevier Academic Press, Amsterdam, Boston, pp 43–70

Dadze S, Wieland C, Jakubiczka S, Funke K, Schröder E, Royer-Pokora B, Willers R, Wieacker PF (2000) The size of the CAG repeat in exon 1 of the androgen receptor gene shows no significant relationship to impaired spermatogenesis in an infertile Caucasoid sample of German origin. Mol. Hum. Reprod 6(3):207–214

Daels PF, Albrecht BA, Mohammed HO (1995) In vitro regulation of luteal function in mares. Reprod. Domest. Anim 30(4):211–217

Davidoff MS, Middendorff R, Müller D, Holstein AF (2009) Fetal and Adult Leydig Cells Are of Common Orign. In: Davidoff MS, Middendorff R, Müller D et al. (Eds.) The Neuroendocrine Leydig Cells and their Stem Cell Progenitors, the Pericytes. Springer Berlin Heidelberg, Berlin, Heidelberg, pp 89–103

Davis-Dao CA, Tuazon ED, Sokol RZ, Cortessis VK (2007) Male infertility and variation in CAG repeat length in the androgen receptor gene: a meta-analysis. J. Clin. Endocrinol. Metab 92:4319–4326. doi: 10.1210/jc.2007-1110

de Vries, Femke AT, Boer E de, van den Bosch M, Baarends WM, Ooms M, Yuan L, Liu J-G, van Zeeland AA, Heyting C, Pastink A (2005) Mouse Sycp1 functions in synaptonemal complex assembly, meiotic recombination, and XY body formation. Genes Dev 19(11):1376–1389

Defamie N, Berthaut I, Mograbi B, Chevallier D, Dadoune J-P, Fénichel P, Segretain D, Pointis G (2003) Impaired gap junction connexin43 in Sertoli cells of patients with secretory azoospermia: a marker of undifferentiated Sertoli cells. Lab. Invest 83(3):449–456

Donner J, Kliesch S, Brehm R, Bergmann M (2004) From carcinoma in situ to testicular germ cell tumour. APMIS 112(2):79–88

Döring B, Lütteke T, Geyer J, Petzinger E (2012) The SLC10 carrier family: transport functions and molecular structure. Curr. Top. Membr 70:105–168

Dowsing AT, Yong EL, Clark M, McLachlan RI, Kretser DM de, Trounson AO (1999) Linkage between male infertility and trinucleotide repeat expansion in the androgen-receptor gene. Lancet 354(9179):640–643

Dressing GE, Goldberg JE, Charles NJ, Schwertfeger KL, Lange CA (2011) Membrane progesterone receptor expression in mammalian tissues: a review of regulation and physiological implications. Steroids 76(1-2):11–17

Dury AY, Ke Y, Gonthier R, Isabelle M, Simard J-N, Labrie F (2015) Validated LC-MS/MS simultaneous assay of five sex steroid/neurosteroid-related sulfates in human serum. J. Steroid Biochem. Mol. Biol 149:1–10

Dyce KM, Sack WO, Wensing CJG (2002) The Urogenital Apparatus. In: Dyce KM, Sack WO, Wensing CJG (Eds.) Textbook of veterinary anatomy. Saunders, Philadelphia,PA, pp 166–209

Dym M, Fawcett DW (1970) The blood-testis barrier in the rat and the physiological compartmentation of the seminiferous epithelium. Biol. Reprod 3(3):308–326

Eckardstein S von, Syska A, Gromoll J, Kamischke A, Simoni M, Nieschlag E (2001) Inverse correlation between sperm concentration and number of androgen receptor CAG repeats in normal men. J. Clin. Endocrinol. Metab 86(6):2585–2590

Ehmcke J, Schlatt S (2006) A revised model for spermatogonial expansion in man: lessons from non-human primates. Reproduction 132(5):673–680. doi:10.1530/rep.1.01081

Elias PM, Williams ML, Choi E-H, Feingold KR (2014) Role of cholesterol sulfate in epidermal structure and function: lessons from X-linked ichthyosis. Biochim. Biophys. Acta 1841(3):353–361

Enmark E, Pelto-Huikko M, Grandien K, Lagercrantz S, Lagercrantz J, Fried G, Nordenskjöld M, Gustaffson J-A (1997) Human Estrogen Receptor β-Gene Structure, Chromosomal Localization, and Expression Pattern. J. Clin. Endocrinol. Metab 82(12):4258–4265

Felici M de (2016) The Formation and Migration of Primordial Germ Cells in Mouse and Man. Res. Prob. Cell Diff 58:23–46

Ferlin A, Arredi B, Zuccarello D, Garolla A, Selice R, Foresta C (2006) Paracrine and endocrine roles of insulin-like factor 3. J. Endocrinol. Invest 29(7):657–664

Fernandes CF, Godoy JR, Döring B, Cavalcanti MCO, Bergmann M, Petzinger E, Geyer J (2007) The novel putative bile acid transporter SLC10A5 is highly expressed in liver and kidney. Biochem. Biophys. Res. Commun 361(1):26–32. doi:10.1016/j.bbrc.2007.06.160

Fietz D, Geyer J, Kliesch S, Gromoll J, Bergmann M (2011) Evaluation of CAG repeat length of androgen receptor expressing cells in human testes showing different pictures of spermatogenic impairment. Histochem. Cell Biol 136(6):689–697

Fietz D, Ratzenböck C, Hartmann K, Raabe O, Kliesch S, Weidner W, Klug J, Bergmann M (2014) Expression pattern of estrogen receptors α and β and G-protein-coupled estrogen receptor 1 in the human testis. Histochem. Cell Biol 142(4):421-432. doi: 10.1007/s00418-014-1216-z

Fietz D, Bergmann M, Hartmann K (2016) In Situ Hybridization of Estrogen Receptors alpha and beta and GPER in the Human Testis. Meth. Mol. Biol. (Clifton, N.J.) 1366:189–205. doi: 10.1007/978-1-4939-3127-9_15

Fijak M, Bhushan S, Meinhardt A (2011) Immunoprivileged sites: the testis. Meth. Mol. Biol 677:459–470

Filardo EJ, Quinn JA, Bland KI, Frackelton AR (2000) Estrogen-induced activation of Erk-1 and Erk-2 requires the G protein-coupled receptor homolog, GPR30, and occurs via trans-activation of the epidermal growth factor receptor through release of HB-EGF. Mol. Endocrinol 14(10):1649–1660

Filardo EJ, Quinn JA, Sabo E (2008) Association of the membrane estrogen receptor, GPR30, with breast tumor metastasis and transactivation of the epidermal growth factor receptor. Steroids 73(9-10):870–873

Filipiak E, Suliborska D, Laszczynska M, Walczak-Jedrzejowska R, Oszukowska E, Marchlewska K, Kula K, Slowikowska-Hilczer J (2013) Estrogen receptor alpha localization in the testes of men with normal spermatogenesis. Folia Histochem. Cytobiol 50(3):340–345

Franco R, Boscia F, Gigantino V, Marra L, Esposito F, Ferrara D, Pariante P, Botti G, Caraglia M, Minucci S, Chieffi P (2011) GPR30 is overexpressed in post-puberal testicular germ cell tumors. Cancer Biol. Therapy 11(6):609–613

Fraune J, Schramm S, Alsheimer M, Benavente R (2012) The mammalian synaptonemal complex: protein components, assembly and role in meiotic recombination. Exp. Cell Res 318(12):1340–1346

Gadkar-Sable S, Shah C, Rosario G, Sachdeva G, Puri C (2005) Progesterone receptors: various forms and functions in reproductive tissues. Front. Biosci 10:2118–2130

Galuska CE, Hartmann MF, Sánchez-Guijo A, Bakhaus K, Geyer J, Schuler G, Zimmer K-P, Wudy SA (2013) Profiling intact steroid sulfates and unconjugated steroids in biological fluids by liquid chromatography-tandem mass spectrometry (LC-MS-MS). Analyst 138(13):3792–3801

Gasse H (2004) Männliche Geschlechtsorgane, Organa genitalia masculina. In: Nickel R (Ed.) Lehrbuch der Anatomie der Haustiere. Parey, Berlin [u.a.], pp 341–391

Gelmann EP (2002) Molecular biology of the androgen receptor. J. Clin. Oncol 20(13):3001–3015

Geyer J, Godoy JR, Petzinger E (2004) Identification of a sodium-dependent organic anion transporter from rat adrenal gland. Biochem. Biophys. Res. Commun 316(2):300–306

Geyer J, Wilke T, Petzinger E (2006) The solute carrier family SLC10: more than a family of bile acid transporters regarding function and phylogenetic relationships. Naunyn Schmiedebergs Arch. Pharmacol 372(6):413–431. doi:10.1007/s00210-006-0043-8

Geyer J, Döring B, Meerkamp K, Ugele B, Bakhiya N, Fernandes CF, Godoy JR, Glatt H, Petzinger E (2007) Cloning and functional characterization of human sodium-dependent organic anion transporter (SLC10A6). J. Biol. Chem 282(27):19728–19741. doi:10.1074/jbc.M702663200

Geyer J, Fernandes CF, Doring B, Burger S, Godoy JR, Rafalzik S, Hubschle T, Gerstberger R, Petzinger E (2008) Cloning and molecular characterization of the orphan carrier protein Slc10a4: expression in cholinergic neurons of the rat central nervous system. Neuroscience 152(4):990–1005

Geyer J, Bakhaus K, Bernhardt R, Blaschka C, Dezhkam Y, Fietz D, Grosser G, Hartmann K, Hartmann MF, Neunzig J, Papadopoulos D, Sánchez-Guijo A, Scheiner-Bobis G, Schuler G, Shihan M, Wrenzycki C, Wudy SA, Bergmann M (2016) The role of sulfated steroid hormones in reproductive processes. J. Steroid Biochem. Mol. Biol. Jul 15; pii: S0960-0760(16)30201-1

Gibson DA, Saunders PTK (2012) Estrogen dependent signaling in reproductive tissues - a role for estrogen receptors and estrogen related receptors. Mol. Cell. Endocrinol 348(2):361–372

Godmann M, Gashaw I, Katz JP, Nagy A, Kaestner KH, Behr R (2009) Krüppel-like factor 4, a "pluripotency transcription factor" highly expressed in male postmeiotic germ cells, is dispensable for spermatogenesis in the mouse. Mech. Dev 126(8-9):650–664

Godoy JR, Fernandes C, Döring B, Beuerlein K, Petzinger E, Geyer J (2007) Molecular and phylogenetic characterization of a novel putative membrane transporter (SLC10A7), conserved in vertebrates and bacteria. Eur. J. Cell Biol 86(8):445–460. doi:10.1016/j.ejcb.2007.06.001

Gonsalves J, Sun F, Schlegel PN, Turek PJ, Hopps CV, Greene C, Martin RH, Pera RAR (2004) Defective recombination in infertile men. Hum. Mol. Genet 13(22):2875–2883

Gores PF, Hayes DH, Copeland MJ, Korbutt GS, Halberstadt C, Kirkpatrick SA, Rajotte RV (2003) Long-term survival of intratesticular porcine islets in nonimmunosuppressed beagles. Transplantation 75(5):613–618

Gosden JR, Middleton PG, Rout D (1986) Localization of the human oestrogen receptor gene to chromosome 6q24----q27 by in situ hybridization. Cytogen. Cell Genet 43(3-4):218–220

Goto T, Adjaye J, Rodeck CH, Monk M (1999) Identification of genes expressed in human primordial germ cells at the time of entry of the female germ line into meiosis. Mol. Hum. Reprod 5:851–860. doi: 10.1093/molehr/5.9.851

Gray H (ed) (1918) Anatomy of the Human Body, 20th edn., Philadelphia, PA über www.bartleby.com/107/

Greenbaum MP, Iwamori T, Buchold GM, Matzuk MM (2011) Germ cell intercellular bridges. Cold Spring Harb. Perspec. Biol 3(8):a005850

Griswold MD (1998) The central role of Sertoli cells in spermatogenesis. Semin. Cell Dev. Biol. 9(4):411–416. doi:10.1006/scdb.1998.0203

Grosser G, Fietz D, Günther S, Bakhaus K, Schweigmann H, Ugele B, Brehm R, Petzinger E, Bergmann M, Geyer J (2013) Cloning and functional characterization of the mouse sodium-dependent organic anion transporter Soat (Slc10a6). J. Steroid Biochem. Mol. Biol 138:90–99

Guyton AC, Hall JE (2006) Transport of Substances Through the Cell Membrane. In: Guyton AC, Hall JE (Eds.) Textbook of medical physiology. [online access + interactive extras: studentconsult.com]. Elsevier Saunders, Philadelphia, Pa., pp 45–56

Hagenbuch B, Dawson P (2004) The sodium bile salt cotransport family SLC10. Pflugers Arch 447(5):566–570

Hagenbuch B, Meier PJ (2004) Organic anion transporting polypeptides of the OATP/ SLC21 family: phylogenetic classification as OATP/ SLCO superfamily, new nomenclature and molecular/functional properties. Pflugers Arch 447(5):653–665

Hähnel R, Twaddle E, Ratajczak T (1973) The specificity of the estrogen receptor of human uterus. J. Steroid Biochem 4(1):21–31

Hammes SR, Levin ER (2007) Extranuclear steroid receptors: nature and actions. Endocr. Rev. 28(7):726–741

Hampl R, Kubatova J, Starka L (2014) Steroids and endocrine disruptors--History, recent state of art and open questions. J. Steroid Biochem. Mol. Biol 155(Pt B):217–223

Han Y, Feng HL, Sandlow JI, Haines CJ (2009) Comparing expression of progesterone and estrogen receptors in testicular tissue from men with obstructive and nonobstructive azoospermia. J. Androl 30(2):127–133

Hatano O, Takakusu A, Nomura M, Morohashi K-i (1996) Identical origin of adrenal cortex and gonad revealed by expression profiles of Ad4BP/SF-1. Genes Cells 1(7):663–671

Henríquez S, Kohen P, Xu X, Veenstra TD, Muñoz A, Palomino WA, Strauss JF, Devoto L (2016) Estrogen metabolites in human corpus luteum physiology. Differential effects on angiogenic activity. Fertil. Steril 106(1):230-237.e1

Hess RA, França LR (2005) Structure of the Sertoli Cell. In: Skinner MK, Griswold MD (Eds.) Sertoli cell biology. Elsevier Academic Press, Amsterdam, Boston, pp 19–40

Ho Y, Dehm SM (2017) Androgen Receptor Rearrangement and Splicing Variants in Resistance to Endocrine Therapies in Prostate Cancer. Endocrinology 158(6):1533–1542

Hoffmann B, Gentz F, Failing K (1996) Investigations into the Course of Progesterone-, Oestrogen- and eCG-concentrations During Normal and Impaired Pregnancy in the Mare. Reprod. Domest. Anim. 31(3):717–723

Hoffmann B, Landeck A (1999) Testicular endocrine function, seasonality and semen quality of the stallion. Anim. Reprod. Sci 57(1-2):89–98

Holstein AF, Roosen-Runge EC (1981) Atlas of human spermatogenesis. Grosse, Berlin

Huhtaniemi IT, Pye SR, Limer KL, Thomson W, O'Neill TW, Platt H, Payne D, John SL, Jiang M, Boonen S, Borghs H, Vanderschueren D, Adams JE, Ward KA, Bartfai G, Casanueva F, Finn JD, Forti G, Giwercman A, Han TS, Kula K, Lean MEJ, Pendleton N, Punab M, Silman AJ, Wu FCW (2009) Increased estrogen rather than decreased androgen action is associated with longer androgen receptor CAG repeats. J. Clin. Endocrinol. Metab 94:277–284. doi: 10.1210/jc.2008-0848

Hum DW, Bélanger A, Lévesque E, Barbier O, Beaulieu M, Albert C, Vallée M, Guillemette C, Tchernof A, Turgeon D, Dubois S (1999) Characterization of UDP-glucuronosyltransferases active on steroid hormones. J. Steroid Biochem. Mol. Biol 69(1-6):413–423

Hutson JM, Hasthorpe S, Heyns CF (1997) Anatomical and functional aspects of testicular descent and cryptorchidism. Endocr. Rev. 18(2):259–280

Irvine RA, Ma H, Yu MC, Ross RK, Stallcup MR, Coetzee GA (2000) Inhibition of p160-mediated coactivation with increasing androgen receptor polyglutamine length. Hum. Mol. Genet 9(2):267–274

Isaac JR, Skinner S, Elliot R, Salto-Tellez M, Garkavenko O, Khoo A, Lee KO, Calne R, Wang DZ (2005) Transplantation of neonatal porcine islets and sertoli cells into nonimmunosuppressed nonhuman primates. Transpl. Proc 37(1):487–488

Ito Y, Tanaka F, Yamamoto M, Doyu M, Nagamatsu M, Riku S, Mitsuma T, Sobue G (1998) Somatic mosaicism of the expanded CAG trinucleotide repeat in mRNAs for the responsible gene of Machado-Joseph disease (MJD), dentatorubral-pallidoluysian atrophy (DRPLA), and spinal and bulbar muscular atrophy (SBMA). Neurochem. Res 23(1):25–32

Janowski T, Zduńczyk S, Malecki-Tepicht J, Barański W, Raś A (2002) Mammary secretion of oestrogens in the cow. Domes. Anim. Endocrinol 23(1-2):125–137

Jenster G, Trapman J, Brinkmann AO (1993) Nuclear import of the human androgen receptor. Biochem J 293 (Pt 3):761–768

Johnsen SG (1970) Testicular biopsy score count--a method for registration of spermatogenesis in human testes: normal values and results in 335 hypogonadal males. Hormones 1(1):2–25

Johnson MH (1970) An immunological barrier in the guinea-pig testis. J. Pathol 101(2):129–139

Jonker JW, Buitelaar M, Wagenaar E, Van Der Valk, Martin A, Scheffer GL, Scheper RJ, Plosch T, Kuipers F, Elferink, Ronald P J Oude, Rosing H, Beijnen JH, Schinkel AH (2002) The breast cancer resistance protein protects against a major chlorophyll-derived dietary phototoxin and protoporphyria. Proc. Natl. Acad. Sci. USA 99(24):15649–15654

Judis L, Chan ER, Schwartz S, Seftel A, Hassold T (2004) Meiosis I arrest and azoospermia in an infertile male explained by failure of formation of a component of the synaptonemal complex. Fertil. Steril 81(1):205–209

Juliano RL, Ling V (1976) A surface glycoprotein modulating drug permeability in Chinese hamster ovary cell mutants. Biochim. Biophys. Acta 455(1):152–162

Ke Y, Gonthier R, Labrie F (2016) The conversion of 16β hydroxyldehydroepiandrosterone in human serum. Steroids 109:50–55. doi: 10.1016/j.steroids.2016.02.007

Khan HL, Bhatti S, Abbas S, Khan YL, Aslamkhan M, Gonzalez RMM, Gonzalez GR, Aydin HH, Trinidad MS (2017) Tri-nucleotide consortium of androgen receptor is associated with low serum FSH and testosterone in asthenospermic men. Syst. Biol. Reprod. Med 30:1–10. doi: 10.1080/19396368.2017.1384080

Kimura N, Mizokami A, Oonuma T, Sasano H, Nagura H (1993) Immunocytochemical localization of androgen receptor with polyclonal antibody in paraffin-embedded human tissues. J. Histochem. Cytochem 41(5):671–678

Kindla J, Rau TT, Jung R, Fasching PA, Strick R, Stoehr R, Hartmann A, Fromm MF, Konig J (2011) Expression and localization of the uptake transporters OATP2B1, OATP3A1 and OATP5A1 in non-malignant and malignant breast tissue. Cancer Biol. Ther 11(6):584–591

Klein B, Haggeney T, Fietz D, Indumathy S, Loveland K, Hedger M, Kliesch S, Weidner W, Bergmann M, Schuppe H (2016) Specific immune cell and cytokine characteristics of human testicular germ cell neoplasia. Hum. Reprod 31(10):2192–202 doi: 10.1093/humrep/dew211

Kliesch S, Behre HM, Hertle L, Bergmann M (1998) Alteration of Sertoli cell differentiation in the presence of carcinoma in situ in human testes. J. Urol 160(5):1894–1898

Kobayashi Y, Shibusawa A, Saito H, Ohshiro N, Ohbayashi M, Kohyama N, Yamamoto T (2005) Isolation and functional characterization of a novel organic solute carrier protein, hOSCP1. J. Biol. Chem 280(37):32332–32339 doi:10.1074/jbc.M504246200

Kobayashi Y, Tsuchiya A, Hayashi T, Kohyama N, Ohbayashi M, Yamamoto T (2007) Isolation and characterization of polyspecific mouse organic solute carrier protein 1 (mOscp1). Drug Metab. Dispos 35(7):1239–1245

Krausz C, Casamonti E (2017) Spermatogenic failure and the Y chromosome. Hum. Genet 136(5):637–655

Kuiper GG, Carlsson B, Grandien K, Enmark E, Häggblad J, Nilsson S, Gustafsson JA (1997) Comparison of the ligand binding specificity and transcript tissue distribution of estrogen receptors alpha and beta. Endocrinology 138(3):863–870

Kuss E (1994) The fetoplacental unit of primates. Exp. Clin. Endocrinol 102(3):135–165

La Spada AR, Wilson EM, Lubahn DB, Harding AE, Fischbeck KH (1991) Androgen receptor gene mutations in X-linked spinal and bulbar muscular atrophy. Nature 352(6330):77–79. doi:10.1038/352077a0

Laatikainen T, Laitinen EA, Vihko R (1971) Secretion of free and sulfate-conjugated neutral steroids by the human testis. Effect of administration of human chorionic gonadotropin. J. Clin. Endocrinol. Metab 32(1):59–64

Labrie F, Bélanger A, Cusan L, Candas B (1997) Physiological changes in dehydroepiandrosterone are not reflected by serum levels of active androgens and estrogens but of their metabolites. Intracrinology. J. Clin. Endocrinol. Metab 82:2403–2409. doi: 10.1210/jcem.82.8.4161

Labrie F, Luu-The V, Labrie C, Simard J (2001) DHEA and its transformation into androgens and estrogens in peripheral target tissues: intracrinology. Front. Neuroendocrinol 22(3):185–212

Labrie F (2003) Extragonadal synthesis of sex steroids: intracrinology. Ann. Endocrinol 64(2):95–107

Lalumière G, Bleau G, Chapdelaine A, Roberts KD (1976) Cholesteryl sulfate and sterol sulfatase in the human reproductive tract. Steroids 27(2):247–260

Lang D (2017) Klonierung zweier Rattensertolizelllinien mit stabiler Expression eines humanen Androgenrezeptors unterschiedlicher CAG-Repeat-Länge als in vitro Modell zur Untersuchung testosteronabhängiger, mit der Spermatogenese assoziierter Gene. Dissertation, Justus Liebig Universität Gießen

Langlais J, Zollinger M, Plante L, Chapdelaine A, Bleau G, Roberts KD (1981) Localization of cholesteryl sulfate in human spermatozoa in support of a hypothesis for the mechanism of capacitation. Proc. Natl. Acad. Sci. USA 78(12):7266–7270

Lee H-J, Chang C (2003) Recent advances in androgen receptor action. Cell. Mol. Life Sci 60(8):1613–1622 doi:10.1007/s00018-003-2309-3

Lekhkota O, Brehm R, Claus R, Wagner A, Bohle RM, Bergmann M (2006) Cellular localization of estrogen receptor-alpha (ERalpha) and -beta (ERbeta) mRNA in the boar testis. Histochem. Cell Biol 125(3):259–264

Lekhkota O, Bergmann M (2007) Expression and cellular localization of estrogen receptor α in the testis of different mammals. AnatGes Poster Abstract booklet:67. doi: 10.3337/anatges.2007.0001

Levin ER, Hammes SR (2016) Nuclear receptors outside the nucleus: extranuclear signalling by steroid receptors. Nature Rev. Mol. Cell Biol 17(12):783–797

Li MWM, Mruk DD, Lee WM, Cheng CY (2010) Connexin 43 is critical to maintain the homeostasis of the blood-testis barrier via its effects on tight junction reassembly. Proc. Natl. Acad. Sci. USA 107(42):17998–18003 doi:10.1073/pnas.1007047107

Liberles SD (2014) Mammalian pheromones. Ann. Rev. Physiol 76:151–175. doi: 10.1146/annurev-physiol-021113-170334

Liebe B, Alsheimer M, Höög C, Benavente R, Scherthan H (2004) Telomere attachment, meiotic chromosome condensation, pairing, and bouquet stage duration are modified in spermatocytes lacking axial elements. Mol. Biol. Cell 15(2):827–837

Lorico A, Rappa G, Finch RA, Yang D, Flavell RA, Sartorelli AC (1997) Disruption of the murine MRP (multidrug resistance protein) gene leads to increased sensitivity to etoposide (VP-16) and increased levels of glutathione. Cancer Res 57(23):5238–5242

Lowartz S, Petkam R, Renaud R, Beamish FWH, Kime DE, Raeside J, Leatherland JF (2003) Blood steroid profile and in vitro steroidogenesis by ovarian follicles and testis fragments of adult sea lamprey, Petromyzon marinus. Comp. Biochem. Physiol 134:365–376.

Lubahn DB, Moyer JS, Golding TS, Couse JF, Korach KS, Smithies O (1993) Alteration of reproductive function but not prenatal sexual development after insertional disruption of the mouse estrogen receptor gene. Proc. Natl. Acad. Sci. USA 90(23):11162–11166

Luconi M, Forti G, Baldi E (2002) Genomic and nongenomic effects of estrogens. Molecular mechanisms of action and clinical implications for male reproduction. J. Steroid Biochem. Mol. Biol 80(4-5):369–381

Luetjens CM, Weinbauer GF, Wistuba J (2005) Primate spermatogenesis: new insights into comparative testicular organisation, spermatogenic efficiency and endocrine control. Biol. Rev. Camb. Phil. Soc 80(3):475–488

Lykkesfeldt G, Müller J, Skakkebaek NE, Bruun E, Lykkesfeldt AE (1985) Absence of testicular steroid sulphatase activity in a boy with recessive X-linked ichthyosis and testicular maldescent. Eur. J. Pediatr 144(3):273–274

Lykkesfeldt G, Bennett P, Lykkesfeldt AE, Micic S, Rorth M, Skakkebaek NE, Svenstrup B (1991) Testis cancer. Ichthyosis constitutes a significant risk factor. Cancer 67(3):730–734

Lyng FM, Jones GR, Rommerts FF (2000) Rapid androgen actions on calcium signaling in rat sertoli cells and two human prostatic cell lines. Similar biphasic responses between 1 picomolar and 100 nanomolar concentrations. Biol. Reprod 63(3):736–747

Madak-Erdogan Z, Lupien M, Stossi F, Brown M, Katzenellenbogen BS (2011) Genomic collaboration of estrogen receptor alpha and extracellular signal-regulated kinase 2 in regulating gene and proliferation programs. Mol. Cell. Biol 31(1):226–236

Makawiti DW, Allen WE, Kilpatrick MJ (1983) Changes in oestrone sulphate concentrations in peripheral plasma of Pony mares associated with follicular growth, ovulation and early pregnancy. J. Reprod. Fertil 68(2):481–487

Mäkinen S, Mäkelä S, Weihua Z, Warner M, Rosenlund B, Salmi S, Hovatta O, Gustafsson JA (2001) Localization of oestrogen receptors alpha and beta in human testis. Mol. Hum. Reprod 7(6):497–503

Mamoulakis C, Antypas S, Sofras F, Takenaka A, Sofikitis N (2015) Testicular Descent. Hormones 14(4):515–530

Marcos J, Pozo OJ (2016) Current LC-MS methods and procedures applied to the identification of new steroid metabolites. J. Steroid Biochem. Mol. Biol 162:41–56

Marino M, Galluzzo P, Ascenzi P (2006) Estrogen Signaling Multiple Pathways to Impact Gene Transcription. Curr. Genom 7(8):497–508

Matsumoto J, Ariyoshi N, Sakakibara M, Nakanishi T, Okubo Y, Shiina N, Fujisaki K, Nagashima T, Nakatani Y, Tamai I, Yamada H, Takeda H, Ishii I (2015) Organic anion transporting polypeptide 2B1 expression correlates with uptake of estrone-3-sulfate and cell proliferation in estrogen receptor-positive breast cancer cells. Drug Metab. Pharmacokin 30(2):133–141

McNamara KM, Sasano H (2015) The intracrinology of breast cancer. J. Steroid Biochem. Mol. Biol 145:172–178. doi: 10.1016/j.jsbmb.2014.04.004

Mifsud A, Sim CK, Boettger-Tong H, Moreira S, Lamb DJ, Lipshultz LI, Yong EL (2001) Trinucleotide (CAG) repeat polymorphisms in the androgen receptor gene: molecular markers of risk for male infertility. Fertil. Steril 75(2):275–281

Migaleddu V, Virgilio G, Del Prato A, Bertolotto M (2012) Sonographic Scrotal Anatomy. In: Trombetta C (Ed.) Scrotal Pathology. Springer Berlin Heidelberg, Berlin, Heidelberg, pp 41–54

Miller WL, Auchus RJ (2011) The molecular biology, biochemistry, and physiology of human steroidogenesis and its disorders. Endocr. Rev 32(1):81–151

Miyamoto T, Hasuike S, Yogev L, Maduro MR, Ishikawa M, Westphal H, Lamb DJ (2003) Azoospermia in patients heterozygous for a mutation in SYCP3. Lancet 362(9397):1714–1719

Miyata H, Castaneda JM, Fujihara Y, Yu Z, Archambeault DR, Isotani A, Kiyozumi D, Kriseman ML, Mashiko D, Matsumura T, Matzuk RM, Mori M, Noda T, Oji A, Okabe M, Prunskaite-Hyyrylainen R, Ramirez-Solis R, Satouh Y, Zhang Q, Ikawa M, Matzuk MM (2016) Genome engineering uncovers 54 evolutionarily conserved and testis-enriched genes that are not required for male fertility in mice. Proc. Natl. Acad. Sci. USA 113(28):7704–7710

Morgan JA, Cheepala SB, Wang Y, Neale G, Adachi M, Nachagari D, Leggas M, Zhao W, Boyd K, Venkataramanan R, Schuetz JD (2012) Deregulated hepatic metabolism exacerbates impaired testosterone production in Mrp4-deficient mice. J. Biol. Chem 287(18):14456–14466

Mosa A, Neunzig J, Gerber A, Zapp J, Hannemann F, Pilak P, Bernhardt R (2015) 2β- and 16β-hydroxylase activity of CYP11A1 and direct stimulatory effect of estrogens on pregnenolone formation. J. Steroid Biochem. Mol. Biol 150:1–10

Mosselman S, Polman J, Dijkema R (1996) ERβ. Identification and characterization of a novel human estrogen receptor. FEBS Letters 392(1):49–53

Mostaghel EA (2014) Beyond T and DHT - novel steroid derivatives capable of wild type androgen receptor activation. Int. J. Biol. Sci 10(6):602–613

Mouhadjer N, Bedin M, Pointis G (1989) Steroid sulfatase activity in homogenates, microsomes and purified Leydig cells from adult rat testis. Reprod. Nutr. Dev 29(3):277–282

Mutembei HM, Kowalewski MP, Ugele B, Schuler G, Hoffmann B (2009) Expression and activity of steroid sulphatase in the boar testis. Reprod. Domest. Anim 44(1):17–23. doi:10.1111/j.1439-0531.2007.00983.x

Naito M, Itoh M (2008) Patterns of infiltration of lymphocytes into the testis under normal and pathological conditions in mice. Am. J. Reprod. Immunol 59(1):55–61

Nantel F, Monaco L, Foulkes NS, Masquilier D, LeMeur M, Henriksén K, Dierich A, Parvinen M, Sassone-Corsi P (1996) Spermiogenesis deficiency and germ-cell apoptosis in CREM-mutant mice. Nature 380(6570):159–162

Nelson AW, Groen AJ, Miller JL, Warren AY, Holmes KA, Tarulli GA, Tilley WD, Katzenellenbogen BS, Hawse JR, Gnanapragasam VJ, Carroll JS (2017) Comprehensive assessment of estrogen receptor beta antibodies in cancer cell line models and tissue reveals critical limitations in reagent specificity. Mol. Cell. Endocrinol 440:138–150

Nenonen HA, Giwercman A, Hallengren E, Giwercman YL (2010) Non-linear association between androgen receptor CAG repeat length and risk of male subfertility - a meta-analysis. Int. J. Androl 34:327–332. doi: 10.1111/j.1365-2605.2010.01084.x

Neunzig J (2014) Die Rolle sulfonierter Steroide und pharmazeutischer Substanzen in der Steroidhormonbiosynthese. Dissertation, Universität des Saarlandes

Neunzig J, Bernhardt R (2014) Dehydroepiandrosterone sulfate (DHEAS) stimulates the first step in the biosynthesis of steroid hormones. PLoS ONE 9(2):e89727

Neunzig J, Sánchez-Guijo A, Mosa A, Hartmann MF, Geyer J, Wudy SA, Bernhardt R (2014) A steroidogenic pathway for sulfonated steroids. The metabolism of pregnenolone sulfate. J. Steroid Biochem. Mol. Biol 144(B):324–333

Neunzig J, Milhim M, Schiffer L, Khatri Y, Zapp J, Sánchez-Guijo A, Hartmann MF, Wudy SA, Bernhardt R (2017) The steroid metabolite 16(β)-OH-androstenedione generated by CYP21A2 serves as a substrate for CYP19A1. J. Steroid Biochem. Mol. Biol 167:182–191

Nieschlag E, Behre HM, Wieacker P, Meschede D, Kamischke A, Kliesch S (2010) Disorders at the Testicular Level. In: Nieschlag E, Behre HM, Nieschlag S (Eds.) Andrology. Male Reproductive Health and Dysfunction. Springer, Berlin, Heidelberg, pp 194–238

Nitta H, Bunick D, Hess RA, Janulis L, Newton SC, Millette CF, Osawa Y, Shizuta Y, Toda K, Bahr JM (1993) Germ cells of the mouse testis express P450 aromatase. Endocrinology 132(3):1396–1401

Orava M, Haour F, Leinonen P, Ruokonen A, Vihko R (1985) Relationships between unconjugated and sulphated steroids in porcine primary Leydig cell culture. J. Steroid Biochem 22(4):507–512

Paech K, Webb P, Kuiper GG, Nilsson S, Gustafsson J, Kushner PJ, Scanlan TS (1997) Differential ligand activation of estrogen receptors ERalpha and ERbeta at AP1 sites. Science 277(5331):1508–1510

Papadopoulos D, Dietze R, Shihan M, Kirch U, Scheiner-Bobis G (2016) Dehydroepiandrosterone Sulfate Stimulates Expression of Blood-Testis-Barrier Proteins Claudin-3 and -5 and Tight Junction Formation via a Gnalpha11-Coupled Receptor in Sertoli Cells. PLoS ONE 11(3):e0150143

Pasqualini JR, Gelly C, Nguyen BL, Vella C (1989) Importance of estrogen sulfates in breast cancer. J. Steroid Biochem 34(1-6):155–163

Pasqualini JR, Chetrite GS (2005) Recent insight on the control of enzymes involved in estrogen formation and transformation in human breast cancer. J. Steroid Biochem. Mol. Biol 93(2-5):221–236

Payne AH, Mason M, Jaffe RB (1969) Testicular steroid sulfatase. Substrate specificity and inhibition. Steroids 14(6):685–704

Payne AH, Jaffe RB (1970) Comparative roles of dehydroepiandrosterone sulfate and androstenediol sulfate as precursors of testicular androgens. Endocrinology 87(2):316–322

Payne AH, Jaffe RB, Abell MR (1971) Gonadal steroid sulfates and sulfatase. 3. Correlation of human testicular sulfatase, 3beta-hydroxysteroid dehydrogenase-isomerase, histologic structure and serum testosterone. J. Clin. Endocrinol. Metab 33(4):582–591

Payne AH, Kawano A, Jaffe RB (1973) Formation of dihydrotestosterone and other 5 alpha-reduced metabolites by isolated seminiferous tubules and suspension of interstitial cells in a human testis. J. Clin. Endocrinol. Metab 37(3):448–453

Payne AH, Jaffe RB (1975) Androgen formation from pregnenolone sulfate by fetal, neonatal, prepubertal and adult human testes. J. Clin. Endocrinol. Metab 40(1):102–107

Pearson CE, Sinden RR (1996) Alternative structures in duplex DNA formed within the trinucleotide repeats of the myotonic dystrophy and fragile X loci. Biochemistry 35(15):5041–5053. doi:10.1021/bi9601013

Pearson CE, Sinden RR (1998) Trinucleotide repeat DNA structures: dynamic mutations from dynamic DNA. Curr. Opin. Struct. Biol 8(3):321–330

Pelletier G, El-Alfy M (2000) Immunocytochemical localization of estrogen receptors alpha and beta in the human reproductive organs. J. Clin. Endocrinol. Metab 85(12):4835–4840

Pentikäinen V, Erkkilä K, Suomalainen L, Parvinen M, Dunkel L (2000) Estradiol acts as a germ cell survival factor in the human testis in vitro. J. Clin. Endocrinol. Metab 85(5):2057–2067

Petzinger E, Geyer J (2006) Drug transporters in pharmacokinetics. Naunyn Schmiedebergs Arch. Pharmacol 372(6):465–475

Pi M, Parrill AL, Quarles LD (2010) GPRC6A mediates the non-genomic effects of steroids. J. Biol. Chem 285(51):39953–39964

Pittman DL, Cobb J, Schimenti KJ, Wilson LA, Cooper DM, Brignull E, Handel MA, Schimenti JC (1998) Meiotic prophase arrest with failure of chromosome synapsis in mice deficient for Dmc1, a germline-specific RecA homolog. Mol. Cell 1(5):697–705

Pleuger C, Fietz D, Hartmann K, Schuppe H-C, Weidner W, Kliesch S, Baker M, O'Bryan MK, Bergmann M (2017) Expression of ciliated bronchial epithelium 1 during human spermatogenesis. Fertil. Steril 108(1):47–54

Prossnitz ER, Barton M (2011) The G protein-coupled estrogen receptor GPER in health and disease. Nature reviews. Endocrinology 7(12):715–726

Purinton SC, Wood CE (2000) Ovine fetal estrogen sulfotransferase in brain regions important for hypothalamus-pituitary-adrenal axis control. Neuroendocrinology 71(4):237–242

Qian X, Mruk DD, Wong EWP, Cheng CY (2013) Breast cancer resistance protein regulates apical ectoplasmic specialization dynamics stage specifically in the rat testis. Am. J. Physiol. Endocrinol. Metab 304(7):69

Quigley CA, Bellis A de, Marschke KB, el-Awady MK, Wilson EM, French FS (1995) Androgen receptor defects: historical, clinical, and molecular perspectives. Endocr. Rev 16(3):271–321

Rago V, Siciliano L, Aquila S, Carpino A (2006) Detection of estrogen receptors ER-alpha and ER-beta in human ejaculated immature spermatozoa with excess residual cytoplasm. Reprod. Biol. Endocrinol 4:36

Rago V, Giordano F, Brunelli E, Zito D, Aquila S, Carpino A (2014) Identification of G protein-coupled estrogen receptor in human and pig spermatozoa. J. Anat 224(6):732–736

Rajender S, Singh L, Thangaraj K (2007) Phenotypic heterogeneity of mutations in androgen receptor gene. Asian J. Androl 9(2):147–179. doi:10.1111/j.1745-7262.2007.00250.x

Rajpert-De Meyts E, Leffers H, Petersen JH, Andersen AG, Carlsen E, Jørgensen N, Skakkebaek NE (2002) CAG repeat length in androgen-receptor gene and reproductive variables in fertile and infertile men. Lancet 359(9300):44–46

Ratzenböck C (2014) Lokalisation und Expression des Östrogenrezeptors alpha und Zusammenhang zwischen der mitotischen Aktivität der Spermatogonien und dem peripheren Östrogenwert im menschlichen Hoden mit normaler und gestörter Spermatogenese. Dissertation, Justus Liebig Universität Gießen

Roberts KD (1987) Sterol sulfates in the epididymis; synthesis and possible function in the reproductive process. J. Steroid Biochem 27(1-3):337–341

Roger P, Sahla ME, Mäkelä S, Gustafsson JA, Baldet P, Rochefort H (2001) Decreased expression of estrogen receptor beta protein in proliferative preinvasive mammary tumors. Cancer Res 61(6):2537–2541

Roth M, Obaidat A, Hagenbuch B (2011) OATPs, OATs and OCTs: The organic anion and cation transporters of the SLCO and SLC22A gene superfamilies. Br. J. Pharmacol Mar;165(5):1260–1287. doi: 10.1111/j.1476-5381.2011.01724.x

Ruokonen A, Laatikainen T, Laitinen EA, Vihko R (1972) Free and sulfate-conjugated neutral steroids in human testis tissue. Biochemistry 11(8):1411–1416

Ruokonen A (1978) Steroid metabolism in testis tissue: the metabolism of pregnenolone, pregnenolone sulfate, dehydroepiandrosterone and dehydroepiandrosterone sulfate in human and boar testes in vitro. J. Steroid Biochem 9(10):939–946

Russell LD (Ed.) (1990) Histological and histopathological evaluation of the testis. Cache River Press, Clearwater, Fl

Russell LD, Ettlin RA, Sinha Hikim AP, Clegg ED (1990) Staging for Laboratory Species. In: Russell LD (Ed.) Histological and histopathological evaluation of the testis. Cache River Press, Clearwater, Fl, pp 162–194

Sadar MD (2011) Small Molecule Inhibitors Targeting the 'Achilles' Heel of Androgen Receptor Activity. Cancer Res 71(4):1208–1213

Saji S, Jensen EV, Nilsson S, Rylander T, Warner M, Gustafsson J-A (2000) Estrogen receptors alpha and beta in the rodent mammary gland. Proc. Natl. Acad. Sci. USA 97(1):337–342

Samadashwily GM, Raca G, Mirkin SM (1997) Trinucleotide repeats affect DNA replication in vivo. Nat. Genet 17(3):298–304. doi:10.1038/ng1197-298

Sánchez-Guijo A, Oji V, Hartmann MF, Traupe H, Wudy SA (2015) Simultaneous quantification of cholesterol sulfate, androgen sulfates, and progestagen sulfates in human serum by LC-MS/MS. J. Lipid Res. 56(9):1843–1851

Sánchez-Guijo A, Neunzig J, Gerber A, Oji V, Hartmann MF, Schuppe H-C, Traupe H, Bernhardt R, Wudy SA (2016) Role of steroid sulfatase in steroid homeostasis and characterization of the sulfated steroid pathway. Evidence from steroid sulfatase deficiency. Mol. Cell. Endocrinol 437:142–153

Sanderson ML, Hassold TJ, Carrell DT (2008) Proteins involved in meiotic recombination: a role in male infertility? Syst. Biol. Reprod. Med 54(2):57–74

Sartorius GA, Handelsman DJ (2010) Testicular Dysfunction in Systemic Diseases. In: Nieschlag E, Behre HM, Nieschlag S (Eds.) Andrology. Male Reproductive Health and Dysfunction. Springer, Berlin, Heidelberg, pp 339–364

Sato Y, Nozawa S, Iwamoto T (2008) Study of spermatogenesis and thickening of lamina propria in the human seminiferous tubules. Fertil. Steril 90(4):1310–1312

Saunders PT, Sharpe RM, Williams K, Macpherson S, Urquart H, Irvine DS, Millar MR (2001) Differential expression of oestrogen receptor alpha and beta proteins in the testes and male reproductive system of human and non-human primates. Mol. Hum. Reprod 7(3):227–236

Schagdarsurengin U, Steger K (2016) Epigenetics in male reproduction. Effect of paternal diet on sperm quality and offspring health. Nat. Rev. Urol 13:584–595. doi: 10.1038/nrurol.2016.157

Schinkel AH, Smit JJ, van Tellingen O, Beijnen JH, Wagenaar E, van Deemter L, Mol CA, van der Valk MA, Robanus-Maandag EC, te Riele HP (1994) Disruption of the mouse mdr1a P-glycoprotein gene leads to a deficiency in the blood-brain barrier and to increased sensitivity to drugs. Cell 77(4):491–502

Schinkel AH, Jonker JW (2003) Mammalian drug efflux transporters of the ATP binding cassette (ABC) family: an overview. Adv. Drug Deliv. Rev 55(1):3–29

Schmidt S, Moncada M, Burger S, Geyer J (2015) Expression, sorting and transport studies for the orphan carrier SLC10A4 in neuronal and non-neuronal cell lines and in Xenopus laevis oocytes. BMC Neuroscience 16:35

Schroeder A, Eckhardt U, Stieger B, Tynes R, Schteingart CD, Hofmann AF, Meier PJ, Hagenbuch B (1998) Substrate specificity of the rat liver Na(+)-bile salt cotransporter in Xenopus laevis oocytes and in CHO cells. Am. J. Physiol 274(2-1):5

Schuler G, Greven H, Kowalewski MP, Döring B, Ozalp GR, Hoffmann B (2008) Placental steroids in cattle: hormones, placental growth factors or by-products of trophoblast giant cell differentiation? Exp. Clin. Endocrinol. Diabetes 116(7):429–436

Schuler G, Dezhkam Y, Bingsohn L, Hoffmann B, Failing K, Galuska CE, Hartmann MF, Sánchez-Guijo A, Wudy SA (2014) Free and sulfated steroids secretion in postpubertal boars (Sus scrofa domestica). Reproduction 148(3):303–314

Schuppe H-C, Meinhardt A (2005) Immune privilege and inflammation of the testis. Chem. Immunol. Allergy 88:1–14

Schuppe H-C, Meinhardt A, Allam JP, Bergmann M, Weidner W, Haidl G (2008) Chronic orchitis: a neglected cause of male infertility? Andrologia 40(2):84–91

Schweigmann H, Sánchez-Guijo A, Ugele B, Hartmann K, Hartmann MF, Bergmann M, Pfarrer C, Döring B, Wudy SA, Petzinger E, Geyer J, Grosser G (2014) Transport of the placental estriol precursor 16α-hydroxy-dehydroepiandrosterone sulfate (16α-OH-DHEAS) by stably transfected OAT4-, SOAT-, and NTCP-HEK293 cells. J. Steroid Biochem. Mol. Biol 143:259–265

Sciurano RB, Rahn MI, Pigozzi MI, Olmedo SB, Solari AJ (2006) An azoospermic man with a double-strand DNA break-processing deficiency in the spermatocyte nuclei: case report. Hum. Reprod 21(5):1194–1203

Sekihara H, Sennett JA, Liddle GW, McKenna TJ, Yarbro LR (1976) Plasma 16 beta-hydroxydehydroepiandrosterone in normal and pathological conditions in man. J. Clin. Endocrinol. Metab 43(5):1078–1084

Selcer KW, Kabler H, Sarap J, Xiao Z, Li P-K (2002) Inhibition of steryl sulfatase activity in LNCaP human prostate cancer cells. Steroids 67(10):821–826

Sertoli E (1865) Dell' esistenza di particolari cellule ramificante nei cunalicoli seminiferi del testicoli umano. Morgagni 7:31–40

Setchell BB, Breed WG (2006) Anatomy, Vasculature, and Innervation of the Male Reproductive Tract. In: Knobil and Neill's physiology of reproduction. Elsevier/Academic Press, Amsterdam [u.a.], pp 771–825

Shafik A (1977) Anatomy and function of scrotal ligament. Urology 9(6):651–655

Shah R, Singh J, Singh D, Jaggi AS, Singh N (2016) Sulfatase inhibitors for recidivist breast cancer treatment. A chemical review. Eur. J. Med. Chem 114:170–190. doi: 10.1016/j.ejmech.2016.02.054

Sharpe RM, McKinnell C, Kivlin C, Fisher JS (2003) Proliferation and functional maturation of Sertoli cells, and their relevance to disorders of testis function in adulthood. Reproduction 125(6):769–784

Shihan M, Kirch U, Scheiner-Bobis G (2013) Dehydroepiandrosterone sulfate mediates activation of transcription factors CREB and ATF-1 via a Gα11-coupled receptor in the spermatogenic cell line GC-2. Biochim. Biophys. Acta 1833(12):3064–3075

Shihan M, Bulldan A, Scheiner-Bobis G (2014) Non-classical testosterone signaling is mediated by a G-protein-coupled receptor interacting with Gnalpha11. Biochim. Biophys. Acta 1843(6):1172–1181

Shihan M, Chan K-H, Konrad L, Scheiner-Bobis G (2015) Non-classical testosterone signaling in spermatogenic GC-2 cells is mediated through ZIP9 interacting with Gnα11. Cell. Signal 27(10):2077–2086

Shimizu M, Gellibolian R, Oostra BA, Wells RD (1996) Cloning, characterization and properties of plasmids containing CGG triplet repeats from the FMR-1 gene. J. Mol. Biol 258(4):614–626. doi:10.1006/jmbi.1996.0273

Shimizu S, Tsounapi P, Dimitriadis F, Higashi Y, Shimizu T, Saito M (2016) Testicular torsion-detorsion and potential therapeutic treatments: A possible role for ischemic postconditioning. Int. J. Urol 23(6):454–463

Sigg C (1979) [Classification of tubular testicular atrophies in the diagnosis of sterility. Significance of the so-called "bunte Atrophie"]. Schweiz. Med. Wochenschr 109(35):1284–1293

Singh I (2011) The Male Reproductive Organs. In: Singh I (Ed.) Textbook of human histology. (with colour atlas & practical guide). Jaypee Brothers Medical Publishers, New Delhi, St. Louis, pp 290–303

Singh V (Ed.) (2014) Textbook of Anatomy. Abdomen and Lower Limb. Elsevier, New Delhi India

Sivils JC, Gonzalez I, Bain LJ (2010) Mice lacking Mrp1 have reduced testicular steroid hormone levels and alterations in steroid biosynthetic enzymes. Gen. Comp. Endocrinol 167(1):51–59

Smith EP, Boyd J, Frank GR, Takahashi H, Cohen RM, Specker B, Williams TC, Lubahn DB, Korach KS (1994) Estrogen resistance caused by a mutation in the estrogen-receptor gene in a man. New Engl. J. Med 331(16):1056–1061

Spaziani E, Szego CM (1959) Early effects of estradiol and cortisol on water and electrolyte shifts in the uterus of the immature rat. Am. J. Physiol 197:355–359

Stanway SJ, Delavault P, Purohit A, Woo LWL, Thurieau C, Potter BVL, Reed MJ (2007) Steroid sulfatase: a new target for the endocrine therapy of breast cancer. Oncologist 12(4):370–374

Steger K, Aleithe I, Behre H, Bergmann M (1998) The proliferation of spermatogonia in normal and pathological human seminiferous epithelium: an immunohistochemical study using monoclonal antibodies against Ki-67 protein and proliferating cell nuclear antigen. Mol. Hum. Reprod 4(3):227–233

Steger K, Klonisch T, Gavenis K, Behr R, Schaller V, Drabent B, Doenecke D, Nieschlag E, Bergmann M, Weinbauer GF (1999) Round spermatids show normal testis-specific H1t but reduced cAMP-responsive element modulator and transition protein 1 expression in men with round-spermatid maturation arrest. J. Androl 20(6):747–754

Steger K (2009) Role of histone to protamine exchange in male fertility. In: Glander H-J, Grunewald S, Paasch U (Eds.) Biology of male germ cells. Shaker, Aachen, pp 51–70

Stocco DM (2001) StAR protein and the regulation of steroid hormone biosynthesis. Annu. Rev. Physiol 63:193-213

Strott CA (1996) Steroid sulfotransferases. Endocr. Rev 17(6):670–697

Strott CA (2002) Sulfonation and molecular action. Endocr. Rev 23(5):703–732

Sun F, Kozak G, Scott S, Trpkov K, Ko E, Mikhaail-Philips M, Bestor TH, Moens P, Martin RH (2004) Meiotic defects in a man with non-obstructive azoospermia: case report. Hum. Reprod 19(8):1770–1773

Svechnikov K, Landreh L, Weisser J, Izzo G, Colón E, Svechnikova I, Söder O (2010) Origin, development and regulation of human Leydig cells. Horm. Res. Paediatr 73(2):93–101. doi:10.1159/000277141

Szego CM, Davis JS (1967) Adenosine 3',5'-monophosphate in rat uterus: acute elevation by estrogen. Proc. Natl. Acad. Sci. USA 58(4):1711–1718

Tanaka F, Ito Y, Sobue G (1999) [Somatic mosaicism of expanded CAG trinucleotide repeat in spinal and bulbar muscular atrophy (SBMA)]. Nippon Rinsho 57(4):862–868

Tarulli GA, Stanton PG, Meachem SJ (2012) Is the Adult Sertoli Cell Terminally Differentiated? Biol. Reprod 87(1):13,1–11 doi: 10.1095/biolreprod.111.095091.

Taylor AK, Tassone F, Dyer PN, Hersch SM, Harris JB, Greenough WT, Hagerman RJ (1999) Tissue heterogeneity of the FMR1 mutation in a high-functioning male with fragile X syndrome. Am. J. Med. Genet 84(3):233–239

Thomas P, Tubbs C, Garry VF (2009) Progestin functions in vertebrate gametes mediated by membrane progestin receptors (mPRs). Identification of mPRalpha on human sperm and its association with sperm motility. Steroids 74(7):614–621

Thomas P, Pang Y, Dong J, Berg AH (2014) Identification and characterization of membrane androgen receptors in the ZIP9 zinc transporter subfamily: II. Role of human ZIP9 in testosterone-induced prostate and breast cancer cell apoptosis. Endocrinology 155(11):4250–4265

Thomas P, Converse A, Berg HA (2017) ZIP9, a novel membrane androgen receptor and zinc transporter protein. Gen. Comp. Endocrinol pii: S0016-6480(17)30341-6 doi:10.1016/j.ygcen.2017.04.016.

Thornton JW. 2001 Evolution of vertebrate steroid receptors from an ancestral estrogen receptor by ligand exploitation and serial genome expansions. Proc. Natl. Acad. Sci. USA 98:5671–5676

Tirabassi G, Cignarelli A, Perrini S, Delli Muti N, Furlani G, Gallo M, Pallotti F, Paoli D, Giorgino F, Lombardo F, Gandini L, Lenzi A, Balercia G (2015) Influence of CAG Repeat Polymorphism on the Targets of Testosterone Action. Int. J. Endocrinol 2015:298107. doi: 10.1155/2015/298107

Toni L de, Di Nisio A, Speltra E, Rocca MS, Ghezzi M, Zuccarello D, Turiaco N, Ferlin A, Foresta C (2016) Polymorphism rs2274911 of GPRC6A as a Novel Risk Factor for Testis Failure. J. Clin. Endocrinol. Metab 101(3):953–961

Traupe H, Happle R (1983) Clinical spectrum of steroid sulfatase deficiency: X-linked recessive ichthyosis, birth complications and cryptorchidism. Eur. J. Pediat 140(1):19–21

Tu J, Fan L, Tao K, Zhu W, Li J, Lu G (2007) Stem cell factor affects fate determination of human gonocytes in vitro. Reproduction 134(6):757–765

Tut TG, Ghadessy FJ, Trifiro MA, Pinsky L, Yong EL (1997) Long polyglutamine tracts in the androgen receptor are associated with reduced trans-activation, impaired sperm production, and male infertility. J. Clin. Endocrinol. Metab 82(11):3777–3782

van Luu-The (2013) Assessment of steroidogenesis and steroidogenic enzyme functions. J. Steroid Biochem. Mol. Biol 137:176–182

Wagner A, Messe N, Bergmann M, Lekhkota O, Claus R (2006) Effects of estradiol infusion in GnRH immunized boars on spermatogenesis. J. Androl 27(6):880–889

Walker WH (2009) Molecular mechanisms of testosterone action in spermatogenesis. Steroids 74(7):602–607 doi:10.1016/j.steroids.2008.11.017

Walker WH (2010) Non-classical actions of testosterone and spermatogenesis. Philos. Trans. R. Soc. Lond., B, Biol. Sci 365(1546):1557–1569 doi:10.1098/rstb.2009.0258

Walter P, Green S, Greene G, Krust A, Bornert JM, Jeltsch JM, Staub A, Jensen E, Scrace G, Waterfield M (1985) Cloning of the human estrogen receptor cDNA. Proc. Natl. Adad. Sci. USA 82(23):7889–7893

Wang C, Liu Y, Cao J-M (2014) G protein-coupled receptors. Extranuclear mediators for the non-genomic actions of steroids. Int. J. Mol. Sci 15(9):15412–15425

Wang R-S, Yeh S, Chen L-M, Lin H-Y, Zhang C, Ni J, Wu C-C, Di Sant'Agnese PA, deMesy-Bentley KL, Tzeng C-R, Chang C (2006) Androgen receptor in sertoli cell is essential for germ cell nursery and junctional complex formation in mouse testes. Endocrinology 147(12):5624–5633. doi:10.1210/en.2006-0138

Wapelhorst B (2014) SOAT, Membrantransporter für sulfatierte Steroide - Expression und zelluläre Lokalisation im humanen Hoden. Dissertation, Justus Liebig Universität Gießen

Wartenberg H, Breucker H, Holstein AF, Dvorák M, Tesarík J (1993) Entwicklung der Genitalorgane und Bildung der Gameten. In: Hinrichsen KV, Beier HM (Eds.) Humanembryologie. Lehrbuch und Atlas der vorgeburtlichen Entwicklung des Menschen ; mit 41 Tabellen. Springer, Berlin, Heidelberg, New York, London, Paris, Tokyo, Hong Kong, Barcelona, pp 745–822

Weber JE, Russell LD (1987) A study of intercellular bridges during spermatogenesis in the rat. Am. J. Anat 180(1):1–24

Weider K, Bergmann M, Brehm R (2011) Connexin 43: its regulatory role in testicular junction dynamics and spermatogenesis. Histol. Histopathol 26(10):1343–1352

Weinbauer GF, Behr R, Bergmann M, Nieschlag E (1998) Testicular cAMP responsive element modulator (CREM) protein is expressed in round spermatids but is absent or reduced in men with round spermatid maturation arrest. Mol. Hum. Reprod 4:9–15

Weinbauer G, Luetjens C, Simoni M, Nieschlag E (2010) Physiology of Testicular Function. In: Nieschlag E, Behre HM, Nieschlag S (Eds.) Andrology. Male Reproductive Health and Dysfunction. Springer, Berlin, Heidelberg, pp 11–59

Wellendorph P, Hansen KB, Balsgaard A, Greenwood JR, Egebjerg J, Bräuner-Osborne H (2005) Deorphanization of GPRC6A. A promiscuous L-alpha-amino acid receptor with preference for basic amino acids. Mol. Pharmacol 67(3):589–597

Wen Q, Cheng CY, Liu Y-X (2016) Development, function and fate of fetal Leydig cells. Sem. Cell Dev. Biol 59:89–98

Wijnholds J, Evers R, van Leusden MR, Mol CA, Zaman GJ, Mayer U, Beijnen JH, van der Valk M, Krimpenfort P, Borst P (1997) Increased sensitivity to anticancer drugs and decreased inflammatory response in mice lacking the multidrug resistance-associated protein. Nat. Med 3(11):1275–1279

Wijnholds J, Scheffer GL, van der Valk M, van der Valk P, Beijnen JH, Scheper RJ, Borst P (1998) Multidrug resistance protein 1 protects the oropharyngeal mucosal layer and the testicular tubules against drug-induced damage. J. Exp. Med 188(5):797–808

Windschüttl S, Nettersheim D, Schlatt S, Huber A, Welter H, Schwarzer JU, Köhn FM, Schorle H, Mayerhofer A (2014) Are testicular mast cells involved in the regulation of germ cells in man? Andrology 2(4):615–622

Wynne KN, Renwick AG (1976) 16Beta-hydroxylation of dehydroepiandrosterone sulphate by homogenates of human foetal liver. Biochem. J 156:419–425

Xiao Y, Karnati S, Qian G, Nenicu A, Fan W, Tchatalbachev S, Höland A, Hossain H, Guillou F, Lüers GH, Baumgart-Vogt E, Bonini MG (2012) Cre-Mediated Stress Affects Sirtuin Expression Levels, Peroxisome Biogenesis and Metabolism, Antioxidant and Proinflammatory Signaling Pathways. PLoS ONE 7(7):e41097

Zhang S-X (1999) Male Reproductive System. In: Zhang S-X (Ed.) An atlas of histology. Springer, New York, pp. 271–296

Zhengwei Y, McLachlan RI, Bremner WJ, Wreford NG (1997) Quantitative (stereological) study of the normal spermatogenesis in the adult monkey (Macaca fascicularis). J. Androl 18(6):681–687

Zhengwei Y, Wreford NG, Royce P, Kretser DM de, McLachlan RI (1998) Stereological evaluation of human spermatogenesis after suppression by testosterone treatment: heterogeneous pattern of spermatogenic impairment. J. Clin. Endocrinol. Metab 83(4):1284–1291

Zhou S, Morris JJ, Barnes Y, Lan L, Schuetz JD, Sorrentino BP (2002) Bcrp1 gene expression is required for normal numbers of side population stem cells in mice, and confers relative protection to mitoxantrone in hematopoietic cells in vivo. Proc. Natl. Acad. Sci. USA 99(19):12339–12344

Zhu YS, Cai LQ, Cordero JJ, Canovatchel WJ, Katz MD, Imperato-McGinley J (1999) A novel mutation in the CAG triplet region of exon 1 of androgen receptor gene causes complete androgen insensitivity syndrome in a large kindred. J. Clin. Endocrinol. Metab 84(5):1590–1594

Zitzmann M, Brune M, Kornmann B, Gromoll J, Eckardstein S von, Eckardstein A von, Nieschlag E (2001) The CAG repeat polymorphism in the AR gene affects high density lipoprotein cholesterol and arterial vasoreactivity. J. Clin. Endocrinol. Metab 86(10):4867–4873

Zitzmann M (2009) The role of the CAG repeat androgen receptor polymorphism in andrology. Front. Horm. Res 37:52–61 doi:10.1159/000175843

10. Danksagung

An dieser Stelle möchte ich nun allen danken, die an dieser Arbeit bzw. meinem bisherigen Werdegang im Institut für Veterinäranatomie beteiligt waren.

Als Erster soll hier **Prof. Dr. Martin Bergmann** erwähnt werden. Ihm habe ich tatsächlich am meisten zu verdanken – er übernahm meine Doktorarbeit bzw. gab mir ein neues Thema und kurz darauf bereits meine erste Stelle. Dank seiner unermüdlichen Unterstützung und Hilfe bin ich nun hier angekommen. Mit einer guten Portion Bissigkeit und Humor („Wenn Sie meinen, Sie können es sich leisten in Urlaub zu gehen… ☺!“) war er mir immer ein toller Chef. Martin, danke für alles und ich hoffe, ich werde noch viele „Geht doch!“s von Dir zu hören kriegen.

Als nächstes möchte ich nun den Mitgliedern unserer Arbeitsgruppe danken. Meiner lieben Kollegin **Dr. Katja Hartmann**, mit der ich viele nette, lustige und ernste Unterhaltungen hatte und haben werde und die mir bei der der Umsetzung der Projekte immer hilfreich unter die Arme greift; unseren „Labordamen“ **Jutta Dern-Wieloch**, **Alex Hax** und **Susi Schubert-Porth**, die ich immer für meine Versuche und Lehre einspannen durfte und die mir mit Rat und Tat zu Seite standen und stehen; den Doktoranden, die ich bisher in der Arbeitsgruppe (mit)betreuen durfte **Clara Ratzenböck, Britta Wapelhorst, Dennis Lang, Anna-Lena Hempfling, Britta Klein, Christiane Pleuger, Dana Püschl** und **Lisa Bertl** – es war/ist schön mit euch!

Ein großes Dankeschön soll an dieser Stelle auch die anderen Mitarbeiter des Instituts, die mich unterstützt haben und bei denen ich immer mit offenen Armen und Ohren empfangen wurde, gehen: **Prof. Dr. Stefan Arnhold**, **Prof. Dr. Monika Kressin**, **Prof. Dr. Carsten Staszyk**, **Prof. Dr. Sabine Wenisch**, **Dr. Antje Pöschke**, **Bastian Krähling**, **Jörg Vogelsberg**, **Veronika Kowalewski, Eva Kammer**, die „Jungs aus dem Keller“ und alle, mit denen ich über die Jahre ein so herzliches Verhältnis hatte.

Doch nicht nur die Mitarbeiter unseres Instituts sollen hier Erwähnung finden. Auch institutsübergreifend habe ich viel Unterstützung und Freundschaft erfahren: **Prof. Dr. Joachim Geyer**, **Dr. Barbara Döring** und **Dr. Katharina Bakhaus** aus der Pharmakologie, **Prof. Dr. Christine Wrenzycki** und **Prof. Dr. Gerhard Schuler** aus der Geburtshilfe und viele weitere Instituts- und Kliniksmitarbeiter haben mir geholfen, mich unterstützt – sei es mit Proben, Wissen oder Cappuchino (Danke, Rina!).

DANKSAGUNG

Ich wäre nicht da, wo ich jetzt bin, wenn ich nicht an so vielen großartigen Forschergruppeninitiativen hätte teilnehmen dürfen. Den „Strippenziehern“ möchte ich hier danken: **Prof. Dr. Klaus Steger**, **Prof. Dr. Joachim Geyer**, **Prof. Dr. Andreas Meinhardt** und **Pia Jürgens**. Für die viele Arbeit, die gute Koordination und nicht zuletzt für die Chance, Teil des großen Ganzen zu sein. Der **Deutschen Forschungsgemeinschaft** möchte ich an dieser Stelle ebenfalls für die Unterstützung finanzieller Art danken.

Für die vielen Hoden- und Ejakulatproben, die in meinen Versuchen Verwendung gefunden haben, möchte ich **Prof. Dr. Florian Wagenlehner**, **Prof. Dr. Hans-Christian Schuppe** und **Prof. Dr. Wolfgang Weidner** aus der Urologie des UKGM und **Prof. Dr. Sabine Kliesch** aus dem CERA Münster danken.

Und – wie immer am Schluss, denn das Wichtigste kommt bekanntlich zum Schluss – möchte ich meiner Familie danken. **Christine**, Du bist meine beste Freundin und wir haben alle Höhen und Tiefen seit dem Studium zusammen durchlebt, im Job und privat. Du bist immer für mich da und ich für Dich und das macht mich froh. Meiner **Mutter Christa** und ihrem Lebensgefährten **Pergrin**, meinen **Schwiegereltern Heidi und Klaus** und natürlich meinem Ehemann **Sebastian** möchte ich für die Unterstützung danken, die ich die ganzen Jahre erfahren durfte. Besonders für meinen Mann war es sicherlich nicht immer einfach, eine übermüdete und knatschige Frau, die fast an ihrem Laptop einschläft, zu ertragen. Danke für alles! Ich liebe Dich.

11. Anhang – Publikationen

Im Folgenden wird der Eigenanteil an den elf Publikationen, die Teil dieser Habilitationsschrift sind, angegeben. Dabei möchte ich zwischen *Idee und Planung* (Pla), *experimenteller Arbeit* (Exp) und der *Publikation* (Pub) differenzieren. Der Eigenanteil wird in Prozent angegeben.

		Pla	Exp	Pub
1.	K.A. Hose, K. Häffner, **D. Fietz**, J. Gromoll, T. Eckert, S. Kliesch, H. Siebert, M. Bergmann. A novel sequence variation in the transactivation regulating domain of the human androgen receptor. Fertil Steril 2009 92:390.e9-390.e11.	20	50	10
2.	**D. Fietz**, J. Geyer, S. Kliesch, J. Gromoll, M. Bergmann. Evaluation of CAG repeat length of Androgen Receptor expressing cells in human testes showing different pictures of spermatogenic impairment. Histochem Cell Biol 2011 136:689-697.	90	100	95
3.	**D. Fietz***, M. Markmann*, D. Lang, L. Konrad, S. Kliesch, T. Chakraborty, H. Hossain*, M. Bergmann. Transfection of Sertoli cells with Androgen Receptor alters gene expression without androgen stimulation. BMC Mol Biol 2015 Dec 29;16(1):23. doi: 10.1186/s12867-015-0051-7.	90	60	95
4.	**D. Fietz***, C. Ratzenböck*, O. Raabe, K. Hartmann, S. Kliesch, W. Weidner, J. Klug, M. Bergmann. Expression pattern of estrogen receptors α and β and G-protein-coupled estrogen receptor 1 in the human testis. Histochem Cell Biol 2014 142(4):421-432.	40	10	50
5.	**D. Fietz***, K. Bakhaus*, B. Wapelhorst, G. Grosser, S. Günther, J. Alber, B. Döring, S. Kliesch, W. Weidner, C.E. Galuska, M.F. Hartmann, S.A. Wudy, M. Bergmann, J. Geyer. Membrane transporters for sulfated steroids in the human testis - Cellular localization, expression pattern and functional analysis. PLoS One 2013 8(5): e62638	75	10	90
6.	G. Grosser, **D. Fietz**, S. Günther, K. Bakhaus, H. Schweigmann, B. Ugele, R. Brehm, E. Petzinger, M. Bergmann, J. Geyer. Cloning and functional characterization of the mouse sodium-dependent organic anion transporter Soat (Slc10a6). J Ster Biochem Mol Biol 2013 138C:90-99.	10	25	25
7.	K. Hartmann, J. Bennien, B. Wapelhorst, K. Bakhaus, V. Schumacher, S. Kliesch, W. Weidner, M. Bergmann, J. Geyer, **D. Fietz**. Current insights into the sulfatase pathway in human testis and cultured Sertoli cells. Histochem Cell Biol 2016 Dec;146(6):737-748.	95	10	75
8.	J. Geyer, K. Bakhaus, R. Bernhardt, C. Blaschka, Y. Dezhkam, **D. Fietz**, G. Grosser, K. Hartmann, M.F. Hartmann, J. Neunzig, D. Papadopoulos, A. Sánchez-Guijo, G. Scheiner-Bobis, G. Schuler, M. Shihan, C. Wrenzycki, S.A. Wudy, M. Bergmann. The role of sulfated steroid hormones in reproductive processes. J Steroid Biochem Mol Biol 2016 Jul 15; pii: S0960-0760(16)30201-1.	30	–	10

9.	K. Bakhaus*, J. Bennien*, **D. Fietz**, A. Sánchez-Guijo, M. Hartmann, R. Serafini, C.C. Love, A. Golovko, S.A. Wudy, M. Bergmann, J. Geyer. Sodium-dependent organic anion transporter (Slc10a6-/-) knockout mice show normal spermatogenesis and reproduction, but elevated serum levels for cholesterol sulfate. J Steroid Biochem Mol Biol 2017 Jul 22. pii: S0960-0760(17)30184-X.	40	10	25
10.	K. Bakhaus, **D. Fietz**, S. Kliesch, W. Weidner, M. Bergmann, J. Geyer. The polymorphism L204F affects transport and membrane expression of the sodium-dependent organic anion transporter SOAT (SLC10A6). J Steroid Biochem Mol Biol 2017 Sep 23. pii: S0960-0760(17)30265-0. doi: 10.1016/j.jsbmb.2017.09.017	25	25	30
11.	**D. Fietz**. Transporter for sulfated steroid hormones in the testis - expression pattern, biological significance and implications for fertility in men and rodents. J Steroid Biochem Mol Biol 2017 Oct 7. pii: S0960-0760(17)30270-4. doi: 10.1016/j.jsbmb.2017.10.001	100	–	100
	* gleichwertige Erstautoren			

Zusätzlich zu den im Anhang aufgelisteten Publikationen habe ich verschiedene Veröffentlichungen zum Thema Hodenhistologie oder zur molekularbiologischen Untersuchung von Hodenbiopsien von Mensch und Tier angefertigt.

Der veröffentlichte klinische Fallbericht zu Stumpf et al. (2012) beschreibt die Identifikation von gonadalem Gewebe, das mittels Laparoskopie einem kryptorchiden Hengst entnommen wurde. Rein morphologisch war eine Identifizierung des veränderten Gewebes nicht mehr sicher möglich und auch histologisch konnte keine abschließende Diagnose gestellt werden. Mittels Immunhistochemie konnten einzelne Tubulus-artige Strukturen und große, weit verstreute Zellen in Bindegewebe gezeigt werden. Erst durch molekularbiologische Untersuchung des entnommenen Gewebes (RNA-Extraktion aus formalin-fixiertem und paraffineingebetteten Material, RT-PCR) auf die Expression von *Star* als Leydigzellmarker konnte die definitive Diagnose „Hodengewebe“ gestellt werden. Weitere Arbeiten, die die molekularbiologische Untersuchung von Hodenmaterial von Mensch und Tier als Grundlage haben sind Günther et al. 2013, Noelke et al. 2015, Klein et al. 2016, Schneider et al. 2016, Pleuger et al. 2016 und Pleuger et al. 2017.

Die **Publikation #4** führte zu einer Einladung zu einem Buchkapitel in der Springer Serie *Methods in Molecular Biology* über die Anwendung der *in situ* Hybridisierung in Hodenbiopsien (Fietz et al. 2016). In einem Buch zur Endokrinologie und Männlichen Reproduktion wurde ein Kapitel zur Funktionellen Anatomie und Histologie des Hodens veröffentlicht (Fietz und Bergmann 2017).

G. Stumpf*, **D. Fietz***, J. Ezer*, L.-F. Litzke, M. Bergmann. Identification of gonadal tissue in cryptorchid stallion can be improved by molecular biological analysis - a case report. Anat Histol Embryol 2012; 41:311-315.

S. Günther, **D. Fietz**, K. Weider, M. Bergmann, R. Brehm. Effects of a murine germ cell-specific knockout of Connexin 43 on Connexin expression in testis and fertility. Transgenic Res 2013; 22(3):631-641.

Noelke J, Wistuba J, Damm OS, **Fietz D**, Gerber J, Gaehle M, Brehm R. A Sertoli cell-specific connexin43 knockout leads to altered interstitial connexin expression and increased Leydig cell numbers. Cell Tis Res 2015; 361(2):633-644.

C. Pleuger, **D. Fietz**, K. Hartmann, W. Weidner, S. Kliesch, M.K. O'Bryan, A. Dorresteijn, M. Bergmann. The expression of Katanin p80 (KATNB1) in the human testis. Fertil Steril 2016 Oct 4. pii: S0015-0282(16)62769-3.

B. Klein, T. Haggeney, **D. Fietz**, S. Indumathy, K. Loveland, M. Hedger, S. Kliesch, W. Weidner, M. Bergmann, H.C. Schuppe. Specific immune cell and cytokine characteristics of human testicular germ cell neoplasia. Hum Reprod 2016; Sept. 8

D. Fietz, M. Bergmann, K. Hartmann. In situ Hybridization of Estrogen receptors α and β and GPER in the Human Testis. Methods Mol. Biol. 2016; 1366:189-205.

S. Schneider, M. Balbach, J. Jikeli, **D. Fietz**, D. Nettersheim, S. Jostes, R. Schmidt, M. Kressin, M. Bergmann, D. Wachten, K. Steger, H. Schorle. Re-visiting the Protamine-2 locus: deletion, but not haplosufficiency, renders male mice infertile. Sci Rep 2016 6:36764

D. Fietz, M. Bergmann. Functional Anatomy and Histology of the Testis. In: Simoni M, Huhtaniemi IT (ed) Endocrinology of the testis and male reproduction, 1st edn. Springer 2017, pp 313–341

C. Pleuger, **D. Fietz**, K. Hartmann, H.-C. Schuppe, W. Weidner, S. Kliesch, M. Baker, M.K. O'Bryan, M. Bergmann. Expression of CBE1 (Ciliated Bronchial Epithelium 1) during Human Spermatogenesis. Fertil Steril 2017 Jul;108(1):47-54.

1. K.A. Hose, K. Häffner, D. Fietz, J. Gromoll, T. Eckert, S. Kliesch, H. Siebert, M. Bergmann. Fertil Steril 2009 92:390.e9-390.e11.

CASE REPORT

A novel sequence variation in the transactivation regulating domain of the human androgen receptor

Katja Anette Hose, M.D.,[a] *Kristina Häffner, D.V.M.,*[a] *Daniela Fietz, D.V.M.,*[a] *Jörg Gromoll, Ph.D.,*[b] *Thomas Eckert, M.D.,*[c] *Sabine Kliesch, Ph.D.,*[b] *Hans-Christian Siebert, Ph.D.,*[c] *and Martin Bergmann, Ph.D.*[a]

[a] Institute of Veterinary Anatomy, University of Giessen, Giessen; [b] Centre of Reproductive Medicine and Andrology, University of Münster, Münster; and [c] Institute of Biochemistry und Endocrinology, University of Giessen, Giessen, Germany

Objective: To study a novel sequence variation within the androgen receptors' N-terminal CAG repeat region and possible resulting consequences for the receptors' three-dimensional (3D) protein structure.
Design: Controlled clinical study.
Setting: University research and andrology clinic.
Patient(s): Twenty-one adult infertile men.
Intervention(s): Ultraviolet laser–assisted microdissection (PALM, Microlaser Technology AG, Bernried, Germany), cloning into pGEM-T vector (Promega, Madison, WI), automated sequencing (Gene Scan 3.7 ABI Prim, Applied Biosystems, Foster City, CA), and Assisted Model Building with Energy Refinement (AMBER).
Main Outcome Measure(s): Determination of the sequence of the CAG repeat of the androgen receptor gene and analysis of the 3D protein structure.
Results(s): In one hypergonadotropic azoospermic patient with Sertoli-cell-only syndrome, we found a punctual sequence variation of 212A→G in the CAG repeat resulting in a glutamine-arginine substitution, which leads to a moderate conformational change of the α-helix from 34 Å in length and 16 Å in diameter (without mutation) to a slightly longer helix (43 Å) with a smaller diameter (15 Å).
Conclusion(s): Whether the novel 212A→G exchange in the CAG repeat leading to a glutamine→arginine substitution and a change in α-helix structure may causally be related to the Sertoli-cell-only phenotype of the patient remains to be elucidated. (Fertil Steril® 2009;92:390.e9–e11. ©2009 by American Society for Reproductive Medicine.)

Key Words: Sertoli-cell-only syndrome, androgen receptor, sequence variation

The human androgen receptor (AR) is a ligand-activated transcription factor belonging to the nuclear receptor superfamily (1). Being located at the X-chromosome (Xq11-12) (2), the AR gene encodes a 110 kDa protein of 918 amino acids (3–5). The gene comprises eight exons (6): exon 1 encodes the N-terminal activation domain, exons 2 and 3 encode a highly conserved DNA-binding domain, exon 4 encodes for the hinge domain, and exons 5–8 encode for the ligand-dependent binding domain.

The 5-terminal region of exon 1 contains a polymorph polyglutamine repeat consisting of multiple repeats of the triplet CAG. The physiological number of CAG repeats is 21 ± 2 (7), with a range of 9–36 (8). The CAG repeat region plays an important role in the fine-tuning of the transcriptional activity of the AR (9–11). The region of CAG triplet repeats is genetically unstable, and this instability is greater in male than in female meiosis (7). Mutations in the AR gene usually lead to X-linked recessive androgen insensitivity syndrome (AIS) with moderate or severe virilization deficit in karyotypic males (testicular feminization). Genetic aberrations with partial AIS due to residual AR function are mostly point mutations and are characterized by sub- or infertility but a normal male phenotype (12). In analogy to the fragile mental retardation protein-1 (13), we investigate possible CAG repeat mosaics, which have already been suggested to be present in the testis (14), at the level of AR-expressing Sertoli cells.

Received November 6, 2008; revised February 19, 2009; accepted February 25, 2009; published online April 9, 2009.
K.A.H. has nothing to disclose. K.H. has nothing to disclose. D.F. has nothing to disclose. J.G. has nothing to disclose. T.E. has nothing to disclose. S.K. has nothing to disclose. H.-C.S. has nothing to disclose. M.B. has nothing to disclose.
Supported by Deutsche Forschungsgemeinsachaft grant no. DFG KFO 181, BE 1016/7-1.
Reprint requests: Professor Martin Bergmann, Institute of Veterinary Anatomy, Frankfurterstrasse 98, D-35392 Giessen, Germany (FAX: 641-99-38109; E-mail: Martin.Bergmann@vetmed.uni-giessen.de).

CASE REPORT

Testis samples were obtained during routine diagnostic biopsy after written informed consent of the patients. The study has been approved by the Ethics Committee of the medical faculty of the Justus Liebig University, Giessen (decision 75/00 and 56/05). Biopsies are routinely divided into two

0015-0282/09/$36.00
doi:10.1016/j.fertnstert.2009.02.068

FIGURE 1

(**A**) SCO syndrome showing AR immunoreactive nuclei of Sertoli cells and peritubular cells. (**B**) Magnification of rectangle in A. Primary magnification: (**A**) ×10; (**B**) ×40.

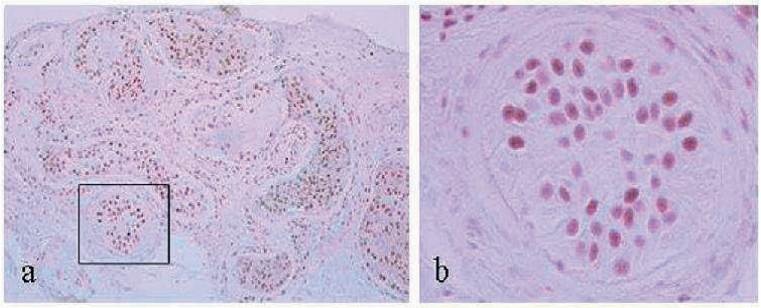

Hose. Sequence variation of androgen receptor. Fertil Steril 2009.

halves and either fixed in Bouin's solution and paraffin embedded or snap frozen. We used ultraviolet laser–assisted microdissection to extract seminiferous epithelia from frozen slices of patients showing either qualitatively intact (n = 9) or impaired (n = 13, Sertoli-cell-only syndrome [SCO]) spermatogenesis (manuscript in preparation). Extracted RNA was transcribed into cDNA and cloned into *Escherichia coli*. Plasmids were isolated and sequenced by Scientific Research Development (SRD) (Bad Homburg, Germany) from frozen slices of 19 patients. In one patient with hypergonadotropism and azoospermia due to SCO with regularly differentiated Sertoli cells as shown by AR immunoreactive nuclei (Fig. 1) and a CAG repeat length of 22 in DNA of blood lymphocytes (Table 1), we got five different clones representing mRNA/cDNA from five single Sertoli cells showing CAG repeat lengths of 20, 21, and 23 (three clones). Two clones containing a punctual sequence variation 212A→G in the CAG repeat could be found, resulting in a glutamine-arginine substitution. The structure and dynamics of the linear peptides (polyglutamine repeat without and with the glutamine-arginine substitution; Fig. 1A, 1B) were analyzed with molecular dynamics simulations using the Assisted Model Building with Energy Refinement (AMBER) force field (15).

TABLE 1

Patient data.

Age	20 years
Karyotype	46,XY
Microdeletion of Y chromosome	None
CAG repeat in blood lymphocytes	22
LH (2–10 IU/L)	11.3 IU/L
FSH (1–7 IU/L)	33.0 IU/L
T (>12 nmol/L)	11.6 nmol/L
SHBG (11–71 nmol/L)	39.0 nmol/L
Free T (>250 pmol/L)	210 pmol/L

Hose. Sequence variation of androgen receptor. Fertil Steril 2009.

In this patient, the overall length of repeats including the variation was 23, thus, in the physiological range (21 ± 2). The glutamine-arginine substitution leads to a moderate change of the predicted three-dimensional (3D) protein structure in the N-terminal domain of the AR. The α-helix with 34 Å length and 16 Å diameter is an energetically advantageous structure for the "clean" glutamine repeat (Fig. 2A). In contrast, the glutamine-arginine substitution at position 14 within the repeat (Fig. 2B, arrow) can support a moderate conformational change to another helix structure. The other helix is longer (43 Å) than the α-helix and has a slightly smaller diameter, 15 Å.

DISCUSSION

Our patient, in whom SCO was histologically confirmed, showed an increased level of FSH (33 IU/L; normal range, 1–7 IU/L). Elevated FSH has long been known to be associated with SCO (16, 17). AR immunoreactivity of nuclei and lumen formation within seminiferous tubules indicate the expression of a functional blood-testis barrier and Sertoli cell fluid secretion suggesting androgen responsiveness. In this patient, a subpopulation of Sertoli cells reveals a glutamine-arginine substitution on mRNA level of single androgen expressing Sertoli cells and not on the level of DNA deriving from blood cells. The difference between 22 CAG repeats found in blood lymphocyte DNA and 21–23 repeats found in Sertoli cell mRNA indicates possible tissue heterogeneity. Additionally, the mutation leads to a moderate change of the predicted 3D protein structure in the transactivation domain of the AR. This region is known to interact with cofactors like transcription complexes amino-terminal enhancer of split (corepressor) and AR-associated protein 24 (coactivator) (18, 19).

Aberrations within the CAG region published so far comprise variations in the numbers of triplet repeats (20) and two point mutations. With respect to the latter, the insertion of a single adenine into the CAG trinucleotide region results in a frame shift and thus a premature termination of the

FIGURE 2

Predicted 3D protein structure of the glutamine repeat containing the domain of the human AR receptor. (**A**) Helix formed by 23 glutamines. (**B**) Arginine substitution (arrow) of the 14th glutamine can result in a conformation change to the other helix structure. 188 × 41 mm (300 × 300 dots per inch).

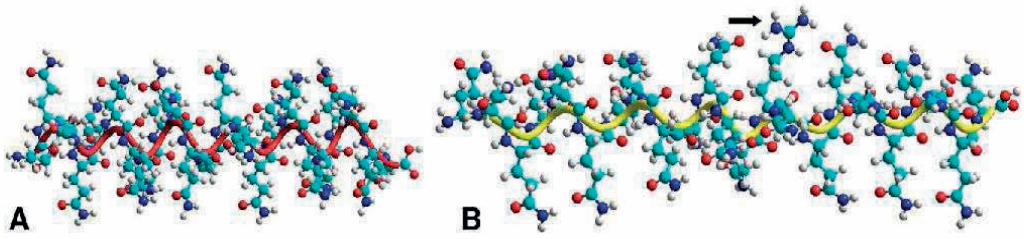

Hose. Sequence variation of androgen receptor. Fertil Steril 2009.

protein downstream of the mutation (21). Men revealing this mutation show female phenotype and lack secondary sexual hair. Lund et al. reported a point mutation at the start of the CAG repeat changing the first CAG to CTG. This mutation probably is responsible for impaired spermatogenesis in two Finnish males (22).

This is the third point mutation within the AR CAG region reported so far, however, it is on the level of Sertoli cell AR mRNA. Whether the tissue heterogeneity and the described change of the 3D protein structure due to arginine substitution leading to a transcriptional disturbance of AR target genes in a subpopulation of testicular Sertoli cells is causally related to the SCO phenotype of our patient remains to be elucidated.

Acknowledgments: The authors thank M. Fink, A. Hax, and G. Erhardt for their skillful technical assistance.

REFERENCES

1. Collins LL, Lee HJ, Chen YT, Chang M, Hsu HY, Yeh S, et al. The androgen receptor in spermatogenesis. Cytogenet Genome Res 2003;103:299–301.
2. Brown CJ, Goss S, Lubahn DB, Joseph DR, Wilson EM, French FS, et al. Androgen receptor locus on the human X chromosome: regional localization to Xq11-12 and description of a DNA polymorphism. Am J Hum Genet 1989;44:264–9.
3. Chang C, Kokontis J. Identification of a new member of the steroid receptor super-family by cloning and sequence analysis. Biochem Biophys Res Commun 1988;155:971–7.
4. Chang CS, Kokontis J, Liao ST. Structural analysis of complementary DNA and amino acid sequences of human and rat androgen receptors. Proc Natl Acad Sci USA 1988;85:7211–5.
5. Lubahn DB, Joseph DR, Sullivan PM, Willard HF, French FS, Wilson EM. Cloning of human androgen receptor complementary DNA and localization to the X chromosome. Science 1988;240:327–30.
6. Tsai MJ, O'Malley BW. Molecular mechanisms of action of steroid/thyroid receptor superfamily members. Ann Rev Biochem 1994;63:451–86.
7. Quigley CA. The androgen receptor: Physiology and pathophysiology. In: Nieschlag E, Behre HM, eds. Testosterone, Action, Deficiency, Substitution. Berlin, Heidelberg: Springer-Verlag, 1998:33–106.
8. Andrew SE, Goldberg YP, Hayden MR, Krause W. Rethinking genotype and phenotype correlations in polyglutamine expansion disorders. Hum Mol Genet 1997;6:2005–10.
9. Sleddens HF, Oostra BA, Brinkmann AO, Trapman J. Trinucleotide repeat polymorphism in the androgen receptor gene (AR). Nucleic Acids Res 1992;20:1427.
10. Gao T, Marcelli M, McPhaul MJ. Transcriptional activation and transient expression of the human androgen receptor. J Steroid Biochem Mol Biol 1996;59:9–20.
11. Tut TG, Ghadessy FJ, Trifiro MA, Pinsky L, Yong EL. Long polyglutamine tracts in the androgen receptor are associated with reduced transactivation, impaired sperm production, and male infertility. J Clin Endocrinol Metab 1997;82:3777–82.
12. Lobaccaro JM, Belon C, Chaussain JL, Job JC, Toublanc JE, Battin J, et al. Molecular analysis of the androgen receptor gene in 52 patients with complete or partial androgen insensitivity syndrome: a collaborative study. Horm Res 1992;37:54–9.
13. Taylor AK, Tassone F, Dyer PN, Hersch SM, Harris JB, Greenough WT, et al. Tissue heterogeneity of the FMR1 mutation in a high-functioning male with fragile X syndrome. Am J Med Genet 1999;84:233–9.
14. Tanaka F, Reeves MF, Ito Y, Matsumoto M, Li M, Miwa S, et al. Tissue-specific somatic mosaicism in spinal and bulbar muscular atrophy is dependent on CAG-repeat length and androgen receptor-gene expression level. Am J Hum Genet 1999;65:966–73.
15. Case DA, Cheatham TE III, Darden T, Gohlke H, Luo R, Merz KM Jr, et al. The Amber biomolecular simulation programs. J Comput Chem 2005;26:1668–88.
16. Bergmann M, Behre HM, Nieschlag E. Serum FSH and testicular morphology in male infertility. Clin Endocrinol 1994;40:133–6.
17. Sharpe RM, McKinnell C, Kivlin C, Fisher S. Proliferation and functional maturation of Sertoli cells, and their relevance to disorders of testis function in adulthood. Reproduction 2003;125:769–84.
18. Yu X, Li P, Roeder RG, Wang Z. Inhibition of androgen receptor-mediated transcription by amino-terminal enhancer of split. Mol Cell Biol 2001;21:4614–25.
19. Hsiao PW, Lin DL, Nakao R, Chang C. The linkage of Kennedy's neuron disease to ARA24, the first identified androgen receptor polyglutamine region-associated coactivator. J Biol Chem 1999;274:20229–35.
20. Davis-Dao CA, Tuazon ED, Sokol RZ, Cortessis VK. Male infertility and variation in CAG repeat length in the androgen receptor gene: a meta-analysis. J Clin Endocrinol Metab 2007;92:3419–26.
21. Zhu YS, Cai LQ, Cordero JJ, Canovatchel WJ, Katz MD, Imperato-McGinley J. A novel mutation in the CAG triplet region of exon 1 of androgen receptor gene causes complete androgen insensitivity syndrome in a large kindred. J Clin Endocrinol Metab 1999;84:1590–4.
22. Lund A, Juvonen V, Lähdetie J, Aittomäki K, Tapanainen JS, Savontaus ML. A novel sequence variation in the transactivation regulating domain of the androgen receptor in two infertile Finnish men. Fertil Steril 2003;79:1947–8.

11. Anhang – Publikationen

2. D. Fietz, J. Geyer, S. Kliesch, J. Gromoll, M. Bergmann. Histochem Cell Biol 2011 136:689-697.

Histochem Cell Biol (2011) 136:689–697
DOI 10.1007/s00418-011-0871-6

ORIGINAL PAPER

Evaluation of CAG repeat length of androgen receptor expressing cells in human testes showing different pictures of spermatogenic impairment

Daniela Fietz · Joachim Geyer · Sabine Kliesch · Jörg Gromoll · Martin Bergmann

Accepted: 1 October 2011 / Published online: 25 October 2011

Abstract The androgen receptor (AR) is a ligand-activated transcriptional factor with crucial importance for spermatogenesis. Its transactivation domain consists of a polymorphic sequence of 9–36 cytosin-adenin-guanin (CAG) repeats. Within the physiological range an increased CAG repeat length is assumed to correlate with the reduced androgen sensitivity resulting in impaired spermatogenesis. In 33 testes of 32 patients showing different histological pictures ranging from normal spermatogenesis, hypospermatogenesis to severe spermatogenetic impairment such as maturation arrest, Sertoli cell only Syndrome (SCO) and mixed atrophy, CAG repeat length was assessed in lymphocyte DNA, DNA/mRNA from testis homogenate and in mRNA of AR expressing Sertoli cells within the seminiferous tubules, and interstitial Leydig cells collected by the laser-assisted cell picking. The latter examination was performed to detect a possible somatic mosaicism of CAG repeat length in different testicular cell populations. CAG repeat lengths varied from 12 to 27 repeats, i.e., within the physiological range. We found deviating CAG repeat numbers in different fractions of AR expressing Sertoli and Leydig cells indicating tissue heterogeneity. We did not find a correlation of CAG repeat length to testicular histology or AR expression, and testosterone or luteinizing hormone levels even in biopsies showing mixed atrophy. Additionally, we evaluated the expression pattern of the AR-dependent gene androgen binding protein (ABP), and did not find a correlation to CAG repeat, but a significant reduction of ABP mRNA related to severe spermatogenic impairment in the monomorphic histologies. These data suggest other factors than CAG repeat to be responsible for severe spermatogenic impairment including mixed atrophy.

Keywords Human testis · Androgen receptor · CAG repeat · Histological status of spermatogenesis · Somatic mosaicism

Electronic supplementary material The online version of this article (doi:10.1007/s00418-011-0871-6) contains supplementary material, which is available to authorized users.

D. Fietz (✉) · M. Bergmann
Institute of Veterinary Anatomy, Histology and Embryology, Justus-Liebig-University Giessen, Frankfurter Str. 98, 35392 Giessen, Germany
e-mail: Daniela.Fietz@vetmed.uni-giessen.de

J. Geyer
Institute of Veterinary Pharmacology, Giessen, Germany

S. Kliesch · J. Gromoll
Centre of Andrology and Reproductive Medicine, Munster, Germany

Introduction

The androgen receptor (AR) is a ligand-activated transcriptional factor belonging to the nuclear receptor superfamily, located on the long arm of the X-chromosome (Gelmann 2002). The 5-terminal region of exon 1 contains a median number of 21 ± 2 CAG repeats (Quigley et al. 1995) with a range of 11–31 (La Spada et al. 1991) or 9–36 repeats (Andrew et al. 1997), respectively. The respective sequence encodes a polyglutamine tract, and the number of CAG repeats is supposed to play an important role in "fine-tuning" of AR transcriptional activity (Gottlieb et al. 1999; Ferlin et al. 2005).

Current studies investigating the correlation between CAG length, fertility and impaired sperm production do (Tut et al. 1997; Dowsing et al. 1999; Mifsud et al. 2001; von Eckardstein et al. 2001; Claessens et al. 2005) or do

not (Dadze et al. 2000; Rajpert-De Meyts et al. 2002; Westerveld et al. 2008; Badran et al. 2009) find a connection. Davis-Dao et al. (2007) identified a mild association of AR–CAG length on male idiopathic infertility by comparing 33 reports in a meta-analysis. All these studies are based on the CAG repeat length determination in blood lymphocytes. To the author's knowledge, there are only two studies comparing CAG repeat length and testicular histology. Casella et al. (2003) found a significant difference of one repeat in patients showing hypospermatogenesis compared to normal controls (22 vs. 21 repeats), but no correlation with Sertoli cell only Syndrome (SCO) or maturation arrest. On the other hand, Dakouane-Giudicelli et al. (2006) did not find a difference of CAG repeat length between preserved spermatogenesis (hypospermatogenesis) and maturation arrest in aged men. Testicular biopsies of many patients with oligozoospermia or non-obstructive azoospermia reveal mixed atrophy, i.e., showing seminiferous tubules with at least qualitatively preserved spermatogenesis adjacent to tubules showing different signs of spermatogenic impairment including SCO (Sigg 1979, for review see Bergmann and Kliesch 2010). Additionally, spermatogenic defects are regularly associated with the Sertoli cell differentiation deficiency (Bruning et al. 1993; Sharpe et al. 2003; Brehm et al. 2006) and the reduced AR expression in patients showing cryptorchidism (Regadera et al. 2001). Sertoli cell specific proteins like androgen binding protein (ABP) are directly correlated to AR expression (for review see Dohle et al. 2003) and can therefore be used to show the efficiency of Sertoli cell function.

Increasing CAG repeat lengths are suggested to lead to a reduced trans-activational function due to three dimensional alteration of the transactivation domain of the AR (Tut et al. 1997). Also point mutations on DNA level are shown to induce androgen insensitivity Syndrome (AIS) (Rajender et al. 2007) with a gradation from partial AIS with normal phenotype and "idiopathic" sub- or infertility up to a complete AIS with female external genitals and complete infertility (Irvine et al. 2000; Ferlin et al. 2005) or on mRNA level resulting in alterations of the receptor protein (Hose et al. 2009). An excessive extension of CAG repeat length of more than 40 repeats results in spinal and bulbar muscular atrophy (SBMA) (La Spada et al. 1991; Choong et al. 1996). In patients with SBMA or fragile mental retardation (Fragile X Syndrome), tissue heterogeneity of the mutation was demonstrated (de Vries et al. 1998; Tanaka et al. 1999b; Taylor et al. 1999) and also Bettencourt et al. (2010) showed, that a difference in CAG repeat length between DNA and cDNA level is possible in ATXN3 gene of Machado-Jopseph disease due to the transcriptional discrepancies. Alvarado et al. (2005) found a genetic tissue heterogeneity in respect of AR–CAG repeat in prostate cancer tissue after LACP. The aim of the study was to examine a possible relation between Sertoli cell differentiation deficiency and mixed atrophy of spermatogenesis considering the aspect of a possible somatic mosaicism of CAG repeat length within the human testis. We therefore examined the repeat in the testes of patients showing normal or severely impaired spermatogenesis, not only based on the lymphocyte DNA, but also on mRNA of AR expressing Sertoli and Leydig cells within the testis itself.

Materials and methods

Testicular tissue

We evaluated 33 testis biopsies of 32 patients. Testicular biopsy was indicated because of normo- or hypergonadotropic azoospermia (for review see Bergmann and Kliesch 2010) including the patients with obstructive azoospermia after vasectomy. After written informed consent, biopsies were taken under general anesthesia. The reported study has been approved by the Ethic's committee of the Medical Faculty of the Justus-Liebig University Giessen (decision 75/00 and 56/05). In blood samples of 16 patients, CAG repeat length was detemined from the blood lymphocyte DNA. Because of lacking blood samples of the missing 16 patients, CAG repeat length was only assessed in testicular tissue. In 28 of 32 patients, testosterone and LH levels have been determined following the standard protocols.

CAG repeat length determination

CAG repeat length was determined in blood lymphocyte DNA as described before (Zitzmann et al. 2001).

Genomic DNA from testis homogenate was extracted from whole histological slides by using QIAamp DNA FFPE Kit (Qiagen, Hilden, Germany) and mRNA from testis homogenate was extracted from whole slides using RNeasy Micro FFPE Kit (Qiagen). mRNA was incubated with RNase-free DNase I (10 U/L; Roche, Mannheim, Germany) and RNase Inhibitor (40 U/L; Ambion via Applied Biosystems) to digest genomic DNA. cDNA was synthesized from 1.5 µl total mRNA using 8.5 µl of the RT-mix (GeneAmp® Gold RNA PCR Core Kit, Applied Biosystems, Foster City, CA, USA). PCR and RT-PCR were performed by using following primer pairs (derived from GenBank accession number NM_000044.2): 5′-AGT GAT CCA GAA CCC GGG C-3′ as forward and 5′-TTG GGG AGA ACC ATC CTC A-3′ as reverse primer, resulting in a 200 bp amplicon. For PCR analysis, *Taq* DNA Polymerase (Qiagen) and, additionally, Q solution (5×) were used according to the manufacturer's protocols.

Q solution is recommended for amplification of templates containing GC-rich sequences with an affinity to forming of secondary DNA structures. By influencing the melting behavior of DNA, Q solution is able to unbend the DNA strand and diminish the polymerase failure due to hairpin structures and loops.

We collected seminiferous epithelia and interstitial tissue predominantly containing Leydig cells by laser-assisted cell picking (LACP) using either frozen or paraffin-embedded tissue. Slices mounted on PALM® membrane slides (MembranSlide 0.1 PEN, Zeiss, Oberkochen, Germany) were stained with Mayers Hematoxylin, the tissue of interest was excised and catapulted by PALM MicroBeam® system and PALM Robo® Software (Zeiss, Oberkochen, Germany). Specimen of tubules showing normal and impaired spermatogenesis in the same histological section and interstitial Leydig cells, respectively, were picked and stored separately as can be seen in Online resource 1. At least 50 tubules and 20 areas containing interstitial tissue were collected. mRNA extraction was performed using the RNeasy Micro Kit (Qiagen) or RNeasy FFPE Kit (Qiagen) for paraffin-embedded specimen, respectively. Because of the fact that in the testis, only the Sertoli cells, Leydig cells and peritubular cells express the AR, but not germ cells (Walker 2009), AR mRNA has to be derived from Sertoli cells when tubules are assessed separately. In the interstitial tissue, Leydig cells and endothelial cells (Bergh and Damber 1992) express AR mRNA. As only Leydig cells, but not blood vessels, were assessed via LACP, AR mRNA has to originate from Leydig cells. Digestion of genomic DNA, first strand cDNA synthesis and RT-PCR were performed as mentioned above.

To separate the PCR products with different CAG counts, high resolution native PAGE was performed. Using a 6.5% polyacrylamide gel, we were able to disperse different CAG numbers for counting. To validate the CAG repeat number assessed, several PCR products were purified using QIAquick PCR Purification Kit (Qiagen) and sequenced by SRD (Scientific Research Development, Oberursel, Germany). Due to methodological failure, a possible variability of ±1–2 repeat has to be mentioned. As positive control, mRNA from testis homogenate, assessed after orchiectomy showing normal spermatogenesis was used.

AR and ABP gene expression

qPCR was performed to examine AR and ABP expression in testis homogenate on mRNA level of 31 patients. For the detection of AR and ABP expression, iQ SYBR Green Supermix (Bio-Rad Laboratories, Inc., Hercules, CA, USA) was used with following primer pairs: humAR_forward (GenBank accession number NM_000044.2) 5′-GCT TCT ACC AGC TCA CCA AGC T-3′ and humAR_reverse 5′-CTT GAT TAG CAG GTC AAA AGT GAA CT-3′ (amplicon 85 bp) and humABP_forward (GenBank accession number NM_001040.3) 5′-CCT GGG CCT TCT CTT TGG A-3′ and humABP_reverse 5′-GGT GGA GAC TGA GCC AAG ATG-3′ (amplicon 102 bp). As a housekeeping gene, β-actin was used to normalize the AR expression with $\Delta\Delta C_t$ method (Bio-Rad CFX Manager Software 2.0, Bio-Rad). For statistical analysis, a Levene test was used to assess the equality of variances in different samples, followed by an unpaired two-sample t test (SPSS 16.0, IBM Germany GmbH, Munich).

Molecular cloning procedure

In order to evaluate the cellular replication machinery, PCR products of eight patients (patient 1, 7, 11, 13, 14, 19, 20 and 22, see Table 1) were cloned into pGEM®-T vector system (Promega, Madison, WI, USA) by T/A cloning and transformed into JM109 *E. coli* (Promega). A total of 39 clones were assessed by sequencing and showed varying CAG repeat lengths. After re-cloning of a sequenced clone, CAG repeat lengths varied again. To identify the failure to be a problem of polymerase error, plasmid DNA of a sequenced clone was transformed into SURE(R)2 Supercompetent cells (Stratagene, La Jolla, CA, USA). All ten clones examined showed the same CAG count as determined via PAGE.

Results

Fragment length analysis (FLA) and PAGE analysis of patients showing a monomorphic histology revealed identical results with a variation of 1–2 repeats. Only in one case (patient 2), a deviation of six repeats between both methods occurred. Comparing the CAG values found in the different testis fractions, i.e., DNA, and mRNA from testis homogenate and mRNA from AR expressing Sertoli and Leydig cells assessed by LACP, we found identical repeat lengths within the samples in nine cases (patients 2, 5, 6, 7, 8, 13, 14, 17, 20). In 13 cases (patients 1, 3, 4, 9, 10, 11, 12, 15, 16, 18, 19, 21, 22), CAG length differences of up to two or three repeats occurred between the different fractions. Exemplarily (patient 10, Fig. 1) the difference of two repeats was confirmed by sequencing. Data are summarized in Table 1. Within the group of patients revealing monomorphic histology, CAG counts varied with a wide range from 18 to 27 repeats irrespective of normal or impaired spermatogenesis, and CAG repeat length did not correlate with the histology (Fig. 2). Biopsies of patients showing mixed atrophy, i.e., different spermatogenic impairment in adjacent tubules, revealed CAG repeats from

Table 1 CAG repeat length determination in biopsies with monomorphic histology

Patient no.	Histology	Hormone concentration in blood		Method FLA/ PAGE	CAG assessed from lymphocyte DNA	CAG assessed from testes homogenates at the level of		CAG assessed from RNA of	
		T (nmol/L)	LH (IU)			DNA	mRNA	Sertoli cells	Leydig cells
1	nsp	17.5	8.8	FLA	25	–	–	–	–
				PAGE	–	25	25	23	25
2		30.3	3.2	FLA	21	–	–	–	–
				PAGE	27	25	–	25	25
3		14.8	4.9	FLA	24	–	–	–	–
				PAGE	–	23	22	23	23
4		22.9	4.2	FLA	26	–	–	–	–
				PAGE	24	24	21	24	24
5		19.7	11.7	FLA	–	–	–	–	–
				PAGE	–	18	18	18	18
6	hyp	12.7	2.3	FLA	24	–	–	–	–
				PAGE	–	23	23	23	23
7		–	–	FLA	–	–	–	–	–
				PAGE	–	–	–	27	27
8		26.2	0.2	FLA	–	–	–	–	–
				PAGE	–	20	20	20	20
9	sza	10.5	7.2	FLA	22	–	–	–	–
				PAGE	–	22	21	21	21
10		14.2	2.7	FLA	22	22	17	22	22
				PAGE	21	23	21	21	21
11		17.2	4.6	FLA	25	–	–	–	–
				PAGE	24	24	22	21	18
12		7.1	2.7	FLA	21	–	–	21	21
				PAGE	20	22	22	20	20
13	sga	12.8	6.5	FLA	19	19	–	–	19
				PAGE	19	18	18	18	18
14		1.1	0.5	FLA	23	–	–	–	–
				PAGE	–	23	23	23	23
15		12.4	12.3	FLA	23	–	–	–	–
				PAGE	21	21	23	20	23
16		–	–	FLA	–	–	–	–	–
				PAGE	–	23	–	22	22
17		–	–	FLA	–	–	–	–	–
				PAGE		23	23	23	23
18	SCO	23.1	7.8	FLA	21	–	–	–	–
				PAGE	–	21	21	19	21
19		10.0	13.3	FLA	24 + 20	–	–	–	–
				PAGE	23 + 19	20	19	19	19
20		15.8	4.6	FLA	25	–	–	–	–
				PAGE	–	24	–	24	24
21		19.7	4.2	FLA	22	23	23	23	23
				PAGE	21	22	21	21	21

Table 1 continued

Patient no.	Histology	Hormone concentration in blood		Method FLA/PAGE	CAG assessed from lymphocyte DNA	CAG assessed from testes homogenates at the level of		CAG assessed from RNA of	
		T (nmol/L)	LH (IU)			DNA	mRNA	Sertoli cells	Leydig cells
22	SCO^{+}	–	–	FLA	–	–	–	–	–
				PAGE	–	19	19	18	18
	hyp^{++}			FLA	–	–	–	–	–
				PAGE	–	23	23	18	23

Multiple CAG repeat within lymphocyte DNA of patient 19 is due to Klinefelter syndrome, resulting into 47 XXY karyotype and therefore two AR copies on both X chromosomes

nsp quantitative and qualitative normal spermatogenesis, *hyp* qualitative normal but quantitative reduced spermatogenesis, *sza* arrest of spermatogenesis at the level of primary spermatocytes, *sga* arrest of spermatogenesis at the level of spermatogonia, *SCO* sertoli cell only syndrome, *FLA* fragment length analysis, *PAGE* polyacrylamide gel electrophoresis, – non-detected CAG repeat, + right testis of patient 22, ++ left testis of patient 22

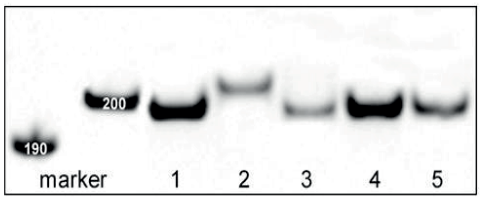

Fig. 1 PAGE; differing CAG repeat lengths in DNA and mRNA fractions within patient 10 (CAG repeat numbers were proved by sequencing). marker = 100 bp DNA ladder. CAG repeat length was assessed in *1* blood lymphocyte DNA (21 CAG counts), *2* testis homogenate on DNA level (23 CAG counts), *3* testis homogenate on mRNA level (21 CAG counts), *4* separately picked Sertoli cells on mRNA level (21 CAG counts), *5* separately picked Leydig cells on mRNA level (21 CAG counts)

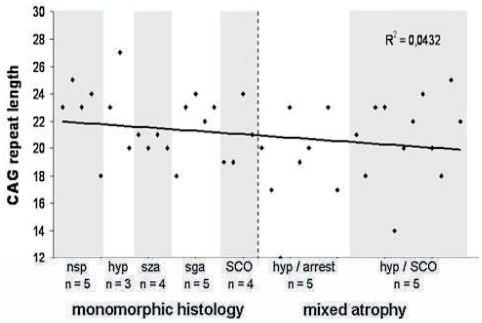

Fig. 2 Correlation between CAG repeat length assessed in Sertoli cell mRNA and histology

12 to 24 repeats, and in 5 of 10 patients, differences in CAG repeat length of up to 11 repeats were counted in testis homogenate and Sertoli cell mRNA showing hypospermatogenesis or impaired spermatogenesis, respectively. Data are summarized in Table 2.

qPCR in tissue homogenate showing monomorphic histology analysis revealed that neither AR nor ABP expression shows any relation to CAG repeat length (Fig. 3). In contrast to AR expression that did not change in relation to histology, there was a significant downregulation of the AR-dependent gene ABP mRNA in biopsies with maturation arrest or SCO ($p = 0.028$) compared to biopsies showing normal or hypospermatogenesis (Fig. 4). In tissue homogenates showing mixed atrophy, the decrease of ABP expression did not reach the statistical significance due to the combination of tubules showing normal or hypospermatogenesis and maturation arrest or SCO.

Testosterone concentration was found to range from 1.1 to 30.3 nmol/L (reference values: 12–40 nmol/L) with two patients (patient 12 and 14, see Table 1) below 8 nmol/L. LH concentration ranged from 0.2 to 13.6 U/L (reference values: 0.8–8.3 U/L) with three patients below 0.8 U/L (patient 8, 14 and 23, see Table 1, 2). There was no correlation between CAG repeat length and histology neither with testosterone nor with LH levels (Fig. 5).

Discussion

In the present study, all CAG counts assessed were within the physiological range of 9–36 (Andrew et al. 1997) or 11–31 repeats (La Spada et al. 1991), respectively. These data are in line with all previous studies that evaluated a possible relationship between CAG repeat length and fertility (for meta-analyses see Davis-Dao et al. 2007; Nenonen et al. 2010).

CAG repeat length has either been determined via fragment length analysis (Zitzmann et al. 2001; Schneider et al. 2009) or using high resolution PAGE (Geyer et al.

Table 2 CAG repeat length in patients showing mixed atrophy of spermatogenesis

Patient no.	Histology	Hormone concentration in blood		Method	CAG assessed from testes homogenates at the level of mRNA	CAG assessed from RNA of Sertoli cells in seminiferous epithelia showing	
		T (nmol/L)	LH (IU)			hyp	SCO/maturation arrest
23	hyp/SCO	14.0	0.3	PAGE	24	23	23
24		11.0	4.5		21	14	20
25		9.2	6.2		24	22	24
26		22.5	5.5		19	20	18
27		23.0	7.2		27	25	22
28	hyp/maturation arrest	14.2	3.7	PAGE	22	20	17
29		16.6	4.1		21	12	23
30		13.5	4.2		21	19	20
31		12.8	5.8		24	–	23
32		9.0	3.6		20	17	–

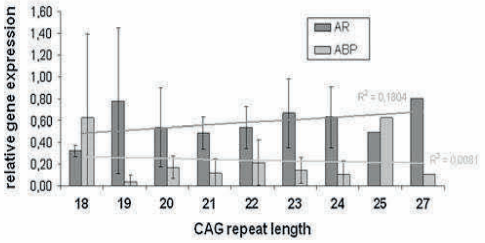

Fig. 3 Quantitative AR and ABP expression in testis homogenate compared to CAG repeat length

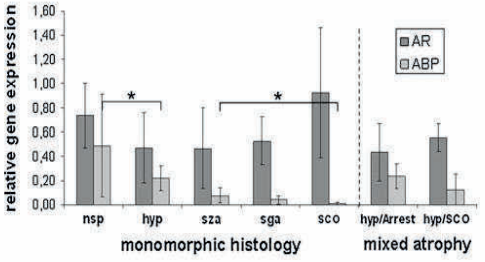

Fig. 4 Quantitative AR and ABP expression in testis homogenate compared to spermatogenic status

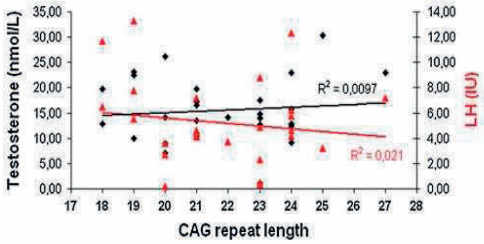

Fig. 5 Free testosterone (*rhombus*) and LH (*triangle*) concentration compared to CAG repeat length

2005) after PCR, due to different technical equipment in both laboratories. With both techniques, we did not find major differences between CAG repeat length in DNA of blood lymphocytes and the testis, as well as between DNA and mRNA of AR expressing cells within the testis, despite, one patient showing a monomorphic histology and five patients with a mixed atrophy of spermatogenesis. Considering these data, we were able to show that the CAG repeat length found in peripheral blood reflects the situation in the testis quite well. CAG repeat differences found in the different fractions examined might be explained by replication difficulties. Knoke et al. (1999b) also reported the differences of ±1 repeat after repeated examination of blood lymphocyte DNA in a patient with severe oligozoospermia, and similar data were shown by Bettencourt et al. (2010) in a patient with Machado-Joseph disease, where differences with an average of one repeat occurred between DNA and cDNA samples. Alvarado et al. (2005) examined different areas of prostate cancer samples, assessed via LACP method. They found deviating CAG repeat counts in separately assessed areas from one patient and also multiple CAG repeat lengths within one sample, each consisting of about 2,500–4,000 cells. In our study, we also found deviating CAG repeat lengths within LACP samples of different areas of AR expressing Sertoli and Leydig cells. However, in the respective testicular homogenate, only one CAG value was measured. Tanaka et al. (1999b) found a somatic mosaicism of CAG repeat length in different tissues including testes in the patients showing SBMA via ALFred technique. They were able to

display multiple peaks, each one representing one CAG repeat length within the tissue, with one CAG repeat length predominantly expressed. While fractionation of amplificates is comparable in ALFred and PAGE technique, PAGE after RT-PCR might only be able to display the predominantely expressed CAG repeat length in a sample.

It is known that trinucleotide repeats are not easy to replicate because of strong base-to-base interactions leading to secondary DNA structures like hairpins and loops (Richards and Sutherland 1994; Yu et al. 1995; Pearson and Sinden 1998). These secondary structures are responsible for stopping the replication process, like it has been shown in *E. coli* (Bowater et al. 1996). Knoke et al. (1999a) observed varying CAG repeat sequences in artificially generated plasmid constructs containing 3, 23, 45 or 62 CAG repeats, respectively. Samadashwily et al. (1997) stated that mainly long trinucleotide repeats form secondary structures and affect DNA replication in yeast and bacteria, suggesting this problem to be transmittable to humans. In contrast to that, Pelletier et al. (2003) showed that also large CAG_n–CTG_n sequences did not influence replication fork formation in yeasts. We were able to show with cloning experiments that also a CAG repeat within the physiological range may be incorrectly replicated by *E. coli*. The usage of SURE cells provided a good result, since these bacteria are recommended for PCR templates tending to form secondary DNA structures. Moe et al. (2008) tried to explain mutations in Huntingtin Fen1 gene with (a) a slippage of polymerases, (b) forming of hairpin structures, or (c) problems in DNA reparation mechanisms in the cells.

Since the existence of somatic mosaicism is known in trinucleotide repeat diseases (Tanaka et al. 1999a; Moe et al. 2008), we analysed the CAG repeat in mRNA of AR expressing Sertoli and Leydig cells. Here, we were especially interested in Sertoli cell mRNA associated with extremely different spermatogenic impairment not only between different patients, but also with respect to the phenomenon of mixed atrophy (Sigg 1979), which is regularly found in infertile men with oligozoospermia or non-obstructive azoospermia (for review see Bergmann and Kliesch 2010). To date, only two other studies provided an evaluation of CAG repeat length and testicular histology. Casella et al. (2003) showed a small but significant difference of CAG repeat lengths assessed in blood DNA between the patients revealing hypospermatogeneis (23.0 ± 3.63 repeats) and control patients (21.0 ± 3.9 repeats). No correlation was found between the control group and severe spermatogenic impairment as maturation arrests or SCO, implying other factors to be involved into the formation of severe spermatogenic defects as CAG repeat length. In contrast to Casella et al., the study by Dakouane-Giudicelli et al. (2006) was conducted with DNA from testis homogenate. Consensually, no correlation between CAG repeat length and histological status in aged men could be found. Supporting the study by Dakouane-Giudicelli et al., we were not able to show a correlation between CAG repeat length and histological status of spermatogenesis within our samples. A somatic mosaicism of CAG repeat length as observed in SBMA (Tanaka et al. 1999a), Fragile X Syndrome (Vries et al. 1998) and Huntington's disease (Gusella and MacDonald 1995) could be shown in five of ten patients showing mixed atrophy of spermatogenesis.

So, even if an elongated CAG repeat is not causally responsible for severe spermatogenic defects, it seems to be able to influence spermatogenesis. Since spermatogenic defects are regularly associated with Sertoli cell differentiation deficiency (Bruning et al. 1993; Sharpe et al. 2003; Brehm et al. 2006), we examined AR expression in dependence to histological picture and CAG repeat length. Additionally, the expression of the Sertoli cell specific protein ABP was examined to evaluate the Sertoli cell function. We were able to show that AR expression is not correlated to histology and CAG repeat length. AR expression seems to be retained with CAG repeat length within the physiological range, confirming the data of Irvine et al. (2000). ABP expression could be shown to be significantly altered in patients with impaired spermatogenesis, showing a monomorphic histology. ABP is an AR-dependent gene, which is upregulated concomitantly with AR expression itself. A significant downregulation of ABP in patients showing spermatogenic arrest and SCO confirms the theory of Sertoli cell function deficiency in patients with impaired spermatogenesis. Nevertheless, the ABP expression is independent from CAG repeat length, which supports the findings of Huhtaniemi et al. (2009). In this study, sex hormone binding globulin (SHBG) levels in peripheral blood were correlated to CAG repeat length assessed in blood lymphocyte DNA, but no significant relationship was found.

In this study, we did not find a correlation among CAG repeat length, testosterone and LH levels. Huhtaniemi et al. (2009, 2010) stated that a decreased AR transcriptional activity due to elongated CAG repeats and therefore lowered testosterone sensitivity is compensated by higher serum testosterone levels, which are associated with higher estrogen levels because of a constant testosterone/estrogen ratio. This suggests that higher estrogen levels may be responsible for the observed phenotypic effect of longer CAG repeat sequences. Nenonen et al. (2010) stated, that outliers in CAG repeat length—even within the physiological range—result in an altered AR function and therefore in male reproductive disorders. These may even be more important than an influence by an increased CAG length. These results can be supported by the study of Hose et al. (2009), who showed an alteration in the three dimensional structure of AR, caused by a point mutation.

In conclusion, this is the first study examining CAG repeat length at the testicular level in AR expressing Sertoli cells associated with histologically clearly defined spermatogenic impairments including mixed atrophy of spermatogenesis. We were able to show a difference in CAG repeat length originating from Sertoli cells of tubules showing hypospermatogenesis or SCO/maturation arrest, respectively, supporting the existence of tissue hetereogeneity as stated by other groups. CAG repeat length could not be correlated to histologically defined pictures of severe spermatogenic impairment, such as maturation arrest or SCO, AR and androgen-dependent ABP expression and hormone levels in blood, and suggest other factors than CAG repeat to be responsible for severe spermatogenic impairment including mixed atrophy.

Acknowledgements The authors thank E. Lahrmann, R. Leidolf and M. Fink for their skillful technical assistance as well as B. Döring and J. Alber for scientific support. The study was supported by grant BE 1016/7-1, German Research Foundation.

References

Alvarado C, Beitel LK, Sircar K, Aprikian A, Trifiro M, Gottlieb B (2005) Somatic mosaicism and cancer: a micro-genetic examination into the role of the androgen receptor gene in prostate cancer. Cancer Res 65(18):8514–8518. doi:10.1158/0008-5472.CAN-05-0399

Andrew SE, Goldberg YP, Hayden MR (1997) Rethinking genotype and phenotype correlations in polyglutamine expansion disorders. Hum Mol Genet 6(12):2005–2010

Badran WA, Fahmy I, Abdel-Megid WM, Elder K, Mansour R, Kent-First M (2009) Length of androgen receptor-CAG repeats in fertile and infertile Egyptian men. J Androl 30(4):416–425. doi:10.2164/jandrol.108.005843

Bergh A, Damber JE (1992) Immunohistochemical demonstration of androgen receptors on testicular blood vessels. Int J Androl 15(5):425–434. doi:10.1111/j.1365-2605.1992.tb01357.x

Bergmann M, Kliesch S (2010) Testicular biopsy and histology. In: Nieschlag E, Behre HM, Nieschlag S (eds) Andrology. Male reproductive health and dysfunction, 3rd edn. Springer, Berlin Heidelberg, pp 155–167

Bettencourt C, Santos C, Montiel R, Kay T, Vasconcelos J, Maciel P, Lima M (2010) The (CAG)n tract of Machado-Joseph disease gene (ATXN3): a comparison between DNA and mRNA in patients and controls. Eur J Hum Genet 18(5):621–623. doi:10.1038/ejhg.2009.215

Bowater RP, Rosche WA, Jaworski A, Sinden RR, Wells RD (1996) Relationship between *Escherichia coli* growth and deletions of CTG. CAG triplet repeats in plasmids. J Mol Biol 264(1):82–96. doi:10.1006/jmbi.1996.0625

Brehm R, Rey R, Kliesch S, Steger K, Marks A, Bergmann M (2006) Mitotic activity of Sertoli cells in adult human testis: an immunohistochemical study to characterize Sertoli cells in testicular cords from patients showing testicular dysgenesis syndrome. Anat Embryol 211(3):223–236. doi:10.1007/s00429-005-0075-8

Bruning G, Dierichs R, Stümpel C, Bergmann M (1993) Sertoli cell nuclear changes in human testicular biopsies as revealed by three dimensional reconstruction. Andrologia 25(6):311–316

Casella R, Maduro MR, Misfud A, Lipshultz LI, Yong EL, Lamb DJ (2003) Androgen receptor gene polyglutamine length is associated with testicular histology in infertile patients. J Urol 169(1):224–227. doi:10.1097/01.ju.0000035361.18870.6e

Choong CS, Kemppainen JA, Zhou ZX, Wilson EM (1996) Reduced androgen receptor gene expression with first exon CAG repeat expansion. Mol Endocrinol 10(12):1527–1535

Claessens F, Verrijdt G, Haelens A, Callewaert L, Moehren U, d'Alesio A, Tanner T, Schauwaers K, Denayer S, van Tilborgh N (2005) Molecular biology of the androgen responses. Andrologia 37(6):209–210. doi:10.1111/j.1439-0272.2005.00698.x

Dadze S, Wieland C, Jakubiczka S, Funke K, Schröder E, Royer-Pokora B, Willers R, Wieacker PF (2000) The size of the CAG repeat in exon 1 of the androgen receptor gene shows no significant relationship to impaired spermatogenesis in an infertile Caucasoid sample of German origin. Mol Hum Reprod 6(3):207–214

Dakouane-Giudicelli M, Legrand B, Bergere M, Giudicelli Y, Cussenot O, Selva J (2006) Association between androgen receptor gene CAG trinucleotide repeat length and testicular histology in older men. Fertil Steril 86(4):873–877. doi:10.1016/j.fertnstert.2006.03.035

Davis-Dao CA, Tuazon ED, Sokol RZ, Cortessis VK (2007) Male infertility and variation in CAG repeat length in the androgen receptor gene: a meta-analysis. J Clin Endocrinol Metab 92(11):4319–4326. doi:10.1210/jc.2007-1110

de Vries BB, Halley DJ, Oostra BA, Niermeijer MF (1998) The fragile X syndrome. J Med Genet 35(7):579–589

Dohle GR, Smit M, Weber RFA (2003) Androgens and male fertility. World J Urol 21(5):341–345. doi:10.1007/s00345-003-0365-9

Dowsing AT, Yong EL, Clark M, McLachlan RI, Kretser DM, de Trounson AO (1999) Linkage between male infertility and trinucleotide repeat expansion in the androgen-receptor gene. Lancet 354(9179):640–643

Ferlin A, Garolla A, Bettella A, Bartoloni L, Vinanzi C, Roverato A, Foresta C (2005) Androgen receptor gene CAG and GGC repeat lengths in cryptorchidism. Eur J Endocrinol 152(3):419–425. doi:10.1530/eje.1.01860

Gelmann EP (2002) Molecular biology of the androgen receptor. J Clin Oncol 20(13):3001–3015

Geyer J, Döring B, Godoy JR, Moritz A, Petzinger E (2005) Development of a PCR-based diagnostic test detecting a nt230(del4) MDR1 mutation in dogs: verification in a moxidectin-sensitive Australian Shepherd. J Vet Pharmacol Ther 28(1):95–99. doi:10.1111/j.1365-2885.2004.00625.x

Gottlieb B, Pinsky L, Beitel LK, Trifiro M (1999) Androgen insensitivity. Am J Med Genet 89(4):210–217

Gusella JF, MacDonald ME (1995) Huntington's disease: CAG genetics expands neurobiology. Curr Opin Neurobiol 5(5):656–662

Hose KA, Häffner K, Fietz D, Gromoll J, Eckert T, Kliesch S, Siebert H, Bergmann M (2009) A novel sequence variation in the transactivation regulating domain of the human androgen receptor. Fertil Steril 92(1):390.e9–390.e11. doi:10.1016/j.fertnstert.2009.02.068

Huhtaniemi IT, Pye SR, Limer KL, Thomson W, O'Neill TW, Platt H, Payne D, John SL, Jiang M, Boonen S, Borghs H, Vanderschueren D, Adams JE, Ward KA, Bartfai G, Casanueva F, Finn JD, Forti G, Giwercman A, Han TS, Kula K, Lean MEJ, Pendleton N, Punab M, Silman AJ, Wu FCW et al (2009) Increased estrogen rather than decreased androgen action is associated with longer androgen receptor CAG repeats. J Clin Endocrinol Metab 94(1):277–284. doi:10.1210/jc.2008-0848

Huhtaniemi IT, Pye SR, Holliday KL, Thomson W, O'Neill TW, Platt H, Payne D, John SL, Jiang M, Bartfai G, Boonen S, Casanueva FF, Finn JD, Forti G, Giwercman A, Han TS, Kula K, Lean MEJ,

Pendleton N, Punab M, Silman AJ, Vanderschueren D, Labrie F, Wu FCW et al (2010) Effect of polymorphisms in selected genes involved in pituitary-testicular function on reproductive hormones and phenotype in aging men. J Clin Endocrinol Metab 95(4):1898–1908. doi:10.1210/jc.2009-2071

Irvine RA, Ma H, Yu MC, Ross RK, Stallcup MR, Coetzee GA (2000) Inhibition of p160-mediated coactivation with increasing androgen receptor polyglutamine length. Hum Mol Genet 9(2):267–274

Knoke I, Allera A, Wieacker P (1999a) Significance of the CAG repeat length in the androgen receptor gene (AR) for the transactivation function of an M780I mutant AR. Hum Genet 104(3):257–261

Knoke I, Jakubiczka S, Lehnert H, Wieacker P (1999b) A new point mutation of the androgen receptor gene in a patient with partial androgen resistance and severe oligozoospermia. Andrologia 31(4):199–201

La Spada AR, Wilson EM, Lubahn DB, Harding AE, Fischbeck KH (1991) Androgen receptor gene mutations in X-linked spinal and bulbar muscular atrophy. Nature 352(6330):77–79. doi:10.1038/352077a0

Mifsud A, Sim CK, Boettger-Tong H, Moreira S, Lamb DJ, Lipshultz LI, Yong EL (2001) Trinucleotide (CAG) repeat polymorphisms in the androgen receptor gene: molecular markers of risk for male infertility. Fertil Steril 75(2):275–281

Moe SE, Sorbo JG, Holen T (2008) Huntingtin triplet-repeat locus is stable under long-term Fen1 knockdown in human cells. J Neurosci Methods 171(2):233–238. doi:10.1016/j.jneumeth.2008.03.012

Nenonen HA, Giwercman A, Hallengren E, Giwercman YL (2010) Non-linear association between androgen receptor CAG repeat length and risk of male subfertility—a meta-analysis. Int J Androl 34:327–332. doi:10.1111/j.1365-2605.2010.01084.x

Pearson CE, Sinden RR (1998) Trinucleotide repeat DNA structures: dynamic mutations from dynamic DNA. Curr Opin Struct Biol 8(3):321–330

Pelletier R, Krasilnikova MM, Samadashwily GM, Lahue R, Mirkin SM (2003) Replication and expansion of trinucleotide repeats in yeast. Mol Cell Biol 23(4):1349–1357

Quigley CA, de Bellis A, Marschke KB, el-Awady MK, Wilson EM, French FS (1995) Androgen receptor defects: historical, clinical, and molecular perspectives. Endocr Rev 16(3):271–321

Rajender S, Singh L, Thangaraj K (2007) Phenotypic heterogeneity of mutations in androgen receptor gene. Asian J Androl 9(2):147–179. doi:10.1111/j.1745-7262.2007.00250.x

Rajpert-De Meyts E, Leffers H, Petersen JH, Andersen AG, Carlsen E, Jørgensen N, Skakkebaek NE (2002) CAG repeat length in androgen-receptor gene and reproductive variables in fertile and infertile men. Lancet 359(9300):44–46

Regadera J, Martínez-García F, González-Peramato P, Serrano A, Nistal M, Suárez-Quian C (2001) Androgen receptor expression in Sertoli cells as a function of seminiferous tubule maturation in the human cryptorchid testis. J Clin Endocrinol Metab 86(1):413–421

Richards RI, Sutherland GR (1994) Simple repeat DNA is not replicated simply. Nat Genet 6(2):114–116. doi:10.1038/ng0294-114

Samadashwily GM, Raca G, Mirkin SM (1997) Trinucleotide repeats affect DNA replication in vivo. Nat Genet 17(3):298–304. doi:10.1038/ng1197-298

Schneider G, Nienhaus K, Gromoll J, Heuft G, Nieschlag E, Zitzmann M (2009) Aging males' symptoms in relation to the genetically determined androgen receptor CAG polymorphism, sex hormone levels and sample membership. Psychoneuroendocrinology 35(4):578–587. doi:10.1016/j.psyneuen.2009.09.008

Sharpe RM, McKinnell C, Kivlin C, Fisher JS (2003) Proliferation and functional maturation of Sertoli cells, and their relevance to disorders of testis function in adulthood. Reproduction 125(6):769–784

Sigg C (1979) Classification of tubular testicular atrophies in the diagnosis of sterility. Significance of the so-called "bunte Atrophie". Schweiz Med Wochenschr 109(35):1284–1293

Tanaka F, Ito Y, Sobue G (1999a) Somatic mosaicism of expanded CAG trinucleotide repeat in spinal and bulbar muscular atrophy (SBMA). Nippon Rinsho 57(4):862–868

Tanaka F, Reeves MF, Ito Y, Matsumoto M, Li M, Miwa S, Inukai A, Yamamoto M, Doyu M, Yoshida M et al (1999b) Tissue-specific somatic mosaicism in spinal and bulbar muscular atrophy is dependent on CAG-repeat length and androgen receptor–gene expression level. Am J Hum Genet 65(4):966–973

Taylor AK, Tassone F, Dyer PN, Hersch SM, Harris JB, Greenough WT, Hagerman RJ (1999) Tissue heterogeneity of the FMR1 mutation in a high-functioning male with fragile X syndrome. Am J Med Genet 84(3):233–239

Tut TG, Ghadessy FJ, Trifiro MA, Pinsky L, Yong EL (1997) Long polyglutamine tracts in the androgen receptor are associated with reduced trans-activation, impaired sperm production, and male infertility. J Clin Endocrinol Metab 82(11):3777–3782

von Eckardstein S, Syska A, Gromoll J, Kamischke A, Simoni M, Nieschlag E (2001) Inverse correlation between sperm concentration and number of androgen receptor CAG repeats in normal men. J Clin Endocrinol Metab 86(6):2585–2590

Walker WH (2009) Molecular mechanisms of testosterone action in spermatogenesis. Steroids 74(7):602–607. doi:10.1016/j.steroids.2008.11.017

Westerveld H, Visser L, Tanck M, van der Veen F, Repping S (2008) CAG repeat length variation in the androgen receptor gene is not associated with spermatogenic failure. Fertil Steril 89(1):253–259. doi:10.1016/j.fertnstert.2007.02.001

Yu A, Dill J, Mitas M (1995) The purine-rich trinucleotide repeat sequences d(CAG)15 and d(GAC)15 form hairpins. Nucleic Acids Res 23(20):4055–4057

Zitzmann M, Brune M, Kommann B, Gromoll J, von Eckardstein S, von Eckardstein A, Nieschlag E (2001) The CAG repeat polymorphism in the AR gene affects high density lipoprotein cholesterol and arterial vasoreactivity. J Clin Endocrinol Metab 86(10):4867–4873

11. Anhang – Publikationen

3. D. Fietz, C. Ratzenböck, O. Raabe, K. Hartmann, S. Kliesch, W. Weidner, J. Klug, M. Bergmann. Histochem Cell Biol 2014 142(4):421-432.

Histochem Cell Biol (2014) 142:421–432
DOI 10.1007/s00418-014-1216-z

ORIGINAL PAPER

Expression pattern of estrogen receptors α and β and G-protein-coupled estrogen receptor 1 in the human testis

Daniela Fietz · Clara Ratzenb ck · Katja Hartmann · Oksana Raabe · Sabine Kliesch · Wolfgang Weidner · J rg Klug · Martin Bergmann

Accepted: 19 March 2014 / Published online: 2 April 2014

Abstract Estrogen signaling is considered to play an important role in spermatogenesis, spermiogenesis and male fertility. Estrogens can act via the two nuclear estrogen receptors ESR1 (ERα) and ESR2 (ERβ) or via the intracellular G-protein-coupled estrogen receptor 1 (GPER, formerly GPR30). Several reports on the localization and expression of all three receptors in the human testis have been published but are controversial particularly in case of ERα. Contrary to previous studies, we decided therefore to evaluate expression of all three receptors in the testis by a number of different methods and in comparison with MCF-7 cells. Using qPCR, we could show that mRNA expression of ERα is considerably lower and expression of ERβ and GPER much higher in the testis than in MCF-7 cells. RT-PCR after laser-assisted microdissection of tubular and interstitial compartments from normal and Sertoli cell only syndrome testes plus in situ hybridization and immunohistochemical analyses of the same samples demonstrated that there is very low expression of ERα in germ cells and in single interstitial cells, very high expression of ERβ in germ cells and Sertoli cells and high expression of GPER in interstitial cells and less in Sertoli cells.

Keywords Estrogen receptor α · Estrogen receptor β · G-protein-coupled estrogen receptor 1 · Human testis · MCF-7 cells

Daniela Fietz, Clara Ratzenb ck, J rg Klug and Martin Bergmann have contributed equally in this work.

Electronic supplementary material The online version of this article (doi:10.1007/s00418-014-1216-z) contains supplementary material, which is available to authorized users.

D. Fietz · C. Ratzenb ck · K. Hartmann · O. Raabe · M. Bergmann
Institute of Veterinary Anatomy, Histology and Embryology, University of Giessen, Giessen, Germany

S. Kliesch
Center of Andrology and Reproductive Medicine, University of M nster, M nster, Germany

W. Weidner
Clinic for Urology, Pediatric Urology and Andrology, University of Giessen, Giessen, Germany

J. Klug (✉)
Institute of Anatomy and Cell Biology, University of Giessen, 35392 Giessen, Germany
e-mail: Joerg.Klug@anatomie.med.uni-giessen.de

Introduction

Estrogens are steroid hormones that are irreversibly transformed from androgens. The terminal enzyme catalyzing this process is the cytochrome P450 aromatase. In the human testis, estrogens are produced in Leydig cells, Sertoli cells and germ cells (Carreau and Hess 2010; Carreau et al. 2011, 2012). They interact with specific receptors, which belong to the nuclear receptor superfamily (Beato and Klug 2000). Two ERs displaying high sequence homology in their DNA- and ligand-binding domains (Enmark et al. 1997) have been identified, ERα (Walter et al. 1985) and ERβ (Mosselman et al. 1996).

ERα and ERβ are expressed throughout the mouse male genital tract, and numerous studies have demonstrated that male fertility is impaired in mice lacking ERα (ERKO mice) (Chen et al. 2009; Dupont et al. 2000; Eddy et al. 1996; Lubahn et al. 1993). In efferent ductules, expressing even higher amounts of ERα than uterine tissues, ERα is important for the resorption of water (Hess et al. 1997). Its absence also leads to an inability to properly acidify the

epididymal fluid (Joseph et al. 2010a) and to a decrease in its osmolality (Joseph et al. 2010b). Sperm recovered from the cauda epididymis of ERKO mice show reduced motility and fail to fertilize eggs in vitro (Eddy et al. 1996). At 2–3 months of age, this leads to dilatation of the seminiferous tubules (Weiss et al. 2008). When at this stage $ER\alpha^{-/-}$ germ cells were transplanted into wild-type testes depleted of germ cells, the recipient mice sired heterozygous offspring (Mahato et al. 2000) demonstrating that spermatogenesis in the ERKO males was not impaired. By 3–4 months of age, some 40 % of tubules from ERKO mice are damaged which is considered to be a secondary effect of the malfunctioning efferent ductules and epididymis (Weiss et al. 2008). In man, there is only one case report of a patient showing estrogen resistance caused by a mutation in the ERα gene, who revealed subnormal sperm counts and severely reduced sperm viability (Smith et al. 1994). The importance of non-classical estrogen action mediated by ERα was elegantly shown in a mouse model exclusively expressing an ERα mutant (AA) defective in DNA binding (Weiss et al. 2008). Compared with ERKO mice, AA mice had greatly reduced or absent tubular defects and normal sperm counts and motility.

Although there appears to be no clear testis phenotype in ERKO mice, there is increasing evidence that estrogens are involved in triggering spermatogonial mitotic activity within mammals, like inhibiting apoptosis of spermatogonia in human seminiferous tubules in vitro (Pentikainen et al. 2000) and stimulating the proliferation of spermatogonia in frogs (Minucci et al. 1997) and cryptorchid mice (Li et al. 2007), and of rat gonocytes (Li et al. 1997) as well as stimulating pre-mitotic DNA synthesis in rats via the ERβ pathway (Wahlgren et al. 2008). These findings were also confirmed in the boar where ERα expression was localized in spermatogonia and primary spermatocytes on the mRNA and protein level (Lekhkota et al. 2006; Wagner et al. 2006). GnRH immunization leads to a decrease in testosterone and estrogen levels resulting in compromised spermatogenesis. Subsequent infusion of estrogens resulted in the re-establishment of spermatogenesis due to increased mitotic activity (Wagner et al. 2006).

Whereas there is a plethora of studies on estrogen action and expression of estrogen receptors in the male genital tract of mice, rats and other animals, the number of studies in humans is rather limited. ERα has been localized in the nuclei of Leydig cells (Pelletier and El-Alfy 2000) and in the cytoplasm of early meiotic germ cells and early elongating spermatids (Pentikainen et al. 2000), whereas Han et al. (2009) detected ERα in the nuclei of germ cells and the cytoplasm of Leydig cells. Cavaco et al. (2009) found the receptor in the nuclei of Sertoli and Leydig cells as well as in the nuclei of all germ cell stages. In contrast, Saunders et al. (2001) and M kinen et al. (2001) could not find any ERα expression in the human testis. Additionally, ERα expression was demonstrated in immature germ cells and spermatozoa in semen samples of healthy men (Aquila et al. 2004; Lambard et al. 2004; Solakidi et al. 2005).

A number of non-genomic and rapid estrogen effects have been reported and are thought to be mediated either by membrane-associated classical ERs [for review see (Luconi et al. 2002; Matthews and Gustafsson 2003)] or by the G-protein-coupled estrogen receptor GPER [for review see (Prossnitz and Barton 2011)] Like classical ERs, GPER is a predominantly intracellular protein. Signaling via GPER occurs through activation of metalloproteinases and the release of heparin-binding EGF, which binds and activates the EGF receptor like it was described for other G-protein-coupled receptors. GPER is also able to indirectly initiate transcriptional responses. GPER, like ERα and ERβ, acts pro-proliferative and anti-apoptotic in spermatogenesis. One example is the GPER-mediated estradiol-induced proliferation of the mouse spermatogonial cell line GC-1 (Sirianni et al. 2008). GPER has been demonstrated to be faintly expressed in normal human germ cells and overexpressed in testicular germ cell tumors (Franco et al. 2011), whereas Rago et al. (2011) found human Sertoli and Leydig cells immunopositive while germ cells were negative [for reviews see (Carreau et al. 2011, 2012; Carreau and Hess 2010)]. In the rat, there is evidence that estrogens induce Sertoli cell proliferation via ERα and ERβ as well as via GPER (Lucas et al. 2011).

The conflicting data on expression and cellular localization of estrogen receptors in the human testis, particularly of ERα, are mainly due to the fact that many studies were employing only a single methodology, mainly immunohistochemistry. Often a single antibody had been used, and different studies had used different antibodies. Therefore, we decided to use a combination of Western blotting, laser-capture-assisted cell picking, quantitative and qualitative RT-PCR, in situ hybridization in addition to immunostaining in order to obtain a conclusive picture.

Materials and methods

Ethics statement

The use of biopsies had been approved by the ethics committee of the Medical Faculty of the Justus Liebig University Giessen (decision 187b/09). All testicular biopsies were taken after written informed consent at the Department for Clinical Andrology, Center for Reproductive Medicine and Andrology at the University of M nster or at the Department of Urology at UKGM Giessen.

Testis biopsies and histological evaluation

Human testis samples were obtained from 18 men, aged 27–47 years, who underwent diagnostic testicular biopsies because of normo- or hypergonadotropic azoospermia or for collecting testis tissue for cryopreservation during vasectomy (McLachlan et al. 2007), for review see (Bergmann and Kliesch 2010). Some biopsies also contained efferent ductules. Testicular biopsies were fixed by immersion in Bouin's solution and embedded in paraffin. For histological evaluation, 5-μm-thick sections were cut, stained with hematoxylin and eosin and evaluated following score count analysis according to Bergmann and Kliesch (2010). Testicular biopsies were revealing normal spermatogenesis (Nsp, $n = 4$), arrest at the level of primary spermatocytes (Sza, $n = 5$) or spermatogonia (Sga, $n = 5$) as well as Sertoli cell only syndrome (SCO, $n = 4$). Gonadal hormones were measured and found to be in the normal range.

Immunohistochemistry

Paraffin sections were mounted on slides coated with 3-aminopropyltriethoxysilane (Merck KGaA, Hohenbrunn, Germany). After deparaffinization and rehydration, heat-mediated antigen retrieval was performed in citrate buffer solution (pH 6) for 15 min at 465 W in a microwave oven. For inhibition of endogenous peroxidase activity, sections were incubated in 3 % H_2O_2 for 30 min. In order to block non-specific binding, sections were treated with 5 % bovine serum (Merck KGaA) for 30 min. Sections were incubated with (1) mouse monoclonal antibody F-10 (sc-8002, Santa Cruz Biotechnology) raised against an epitope that maps to amino acids 570–595 at the C-terminus of human ERα, (2) rabbit polyclonal antibody HC-20 (sc-543, Santa Cruz Biotechnology) also raised against an epitope that maps to the C-terminus or (3) chicken ERβ 503 antibody (Roger et al. 2001; Saji et al. 2000) raised against human ERβ, that was missing the N-terminus, for overnight at 4 °C and at a dilution of 1:50 (F-10) or 1:100 (HC-20 and ERβ 503). Biotinylated goat anti-mouse (E0433, 1:300, DAKO Cytomation), goat anti-rabbit (E0466, 1:300, DAKO Cytomation) or goat anti-chicken antibodies (sc-2430, 1:200, Santa Cruz Biotechnology) were applied as secondary antibodies for 1 h at room temperature. Antibody treatment was followed by application of peroxidase-conjugated streptavidin (VECTASTAIN Elite ABC Kit (Standard), Biologo, Kronshagen, Germany) for 1 h at room temperature. After each treatment, sections were washed with Tris-buffered saline (TBS) pH 7.4. The immunoreaction was visualized with AEC (Biologo) for maximally 30 min. Finally, sections were mounted in Glycergel (Sigma-Aldrich). Specimens exhibiting efferent ductules were used as positive controls (Hess 2003). Negative controls were performed by substituting buffer for the primary antibody or using a blocking peptide [Santa Cruz Biotechnology, sc-8002 P (F-10) or sc-543 P (HC-20)] at a dilution of 1:10 (F-10) or 1:20 (HC-20).

Immunoblot analyses

Protein extracts were prepared from cryopreserved testis biopsy samples of patients showing normal spermatogenesis and from MCF-7 and T47D breast cancer cell lines (positive controls). 70–80 mg testis tissue samples were homogenized in 500 μl RIPA buffer (50 mM Tris (pH 7.5), 150 mM NaCl, 10 mM K_2HPO4, 10 % (v/v) glycerol, 1 % (v/v) Igepal CA-630, 0.15 % (w/v) SDS, 1 mM Na_3VO_4, 1 mM sodium molybdate, 20 mM NaF, 0.1 mM phenylmethylsulfonyl fluoride) containing an additional proteinase inhibitor cocktail (Sigma, P8340) using a bead mill (Tissue Lyser LT, Qiagen). Lysates were centrifuged at 13,000*g* for 10 min at 4 °C.

MCF-7 and T47D cells were washed and lysed in 500 μl of RIPA lysis buffer, passed through a 24-gauge needle and centrifuged at 13,000*g* for 10 min at 4 °C. The supernatant was recovered, and its protein concentration determined by Bradford assay (Bradford 1976). Samples containing 65 μg protein were mixed with 3× SDS sample buffer and incubated for 10 min at 95 °C. The denatured samples were separated on standard 10 % SDS polyacrylamide gels and blotted onto nitrocellulose membranes (GE Healthcare). The membranes were blocked with 5 % non-fat dry milk (Bio-Rad) in Tris-buffered saline (pH 7.4) containing 0.05 % Tween 20 and incubated with primary antibody F-10 (sc-8002, 1:200, Santa Cruz Biotechnology) or antibody plus blocking peptide (200 μg/ml, 1:80, sc-8002 P, Santa Cruz Biotechnology) overnight. Primary antibodies were decorated with horseradish peroxidase-conjugated sheep anti-mouse (1:10,000, Sigma) secondary antibody. Bound secondary antibodies were visualized using the SuperSignal West Femto enhanced chemiluminescence substrate (Thermo Scientific).

In situ hybridization (ISH)

DIG-labeled cRNA probes were generated as described previously (Steger et al. 1998). For ERα, a 183-bp PCR product of the human ERα gene was subcloned into the pGEM-T vector (Promega), and for ERβ and GPER, a 329- and a 310-bp PCR product of the human ERβ gene and the human GPER gene, respectively, were subcloned into the pCRII-TOPO vector (Invitrogen).

All plasmids were validated by sequencing (Scientific Research Development GmbH, Bad Homburg, Germany). Primers were obtained from Eurofins MWG GmbH (Ebersberg, Germany) (Table 1). For the synthesis of cRNAs,

plasmids were digested with NcoI (sense) and NotI (antisense) for the ERα probes and BamHI (sense/antisense) and NotI (antisense/sense) for the ERβ and GPER probes (all restriction enzymes were from New England Biolabs). Subsequently, in vitro transcription was performed using the RNA-DIG Labeling Mix (Boehringer Mannheim) and RNA polymerases T7 and SP6 (Promega).

ISH was performed with minor changes as described previously (Lekhkota et al. 2006). Deparaffinized and rehydrated tissue sections (6 μm) were digested with proteinase K (15 μg/ml in 1× PBS) for 30 min at 37 °C (ERα) or at room temperature for 15 min (ERβ and GPER), post-fixed in 4 % paraformaldehyde for 10 min, exposed to 20 % acetic acid and pre-hybridized in 20 % glycerol for 30 min. Sections were then incubated with the DIG-labeled sense or antisense cRNA probes. Both cRNAs were used at a dilution of 1:25 (ERα) or 1:50 (ERβ and GPER) in hybridization buffer containing 50 % deionized formamide, 10 % dextran sulfate, 2× standard saline citrate (SSC), 1× Denhardt's solution, 10 μg/ml salmon sperm DNA (Sigma-Aldrich) and 10 μg/ml yeast tRNA (Sigma-Aldrich). Hybridization was performed overnight at 40 °C (ERα), 45 °C (GPER) or 48 °C (ERβ) in a humidified chamber containing 50 % formamide in 2× SSC. Post-hybridization washes were performed in 4× SSC at 37 °C (ERα) or 55 °C (ERβ and GPER). Subsequently, sections were incubated with an anti-DIG Fab antibody conjugated to alkaline phosphatase (Boehringer Mannheim) overnight at 4 °C. Hybridization was visualized by developing sections with nitroblue–tetrazolium/5-bromo-4-chloro-3-indolyl-phosphate (NBT from KPL, Gaithersburg MA, USA) in a humidified chamber protected from light. Finally, sections were mounted in Glycergel. For each test, negative controls were performed using DIG-labeled cRNA sense probes. ISH was repeated at least twice.

Detection of ERα, ERβ and GPER in testis homogenates as well as in separated seminiferous tubules and the interstitial compartment by qualitative RT-PCR

Total mRNA from the testis was extracted from Bouin fixed, paraffin-embedded tissue using the RNeasy Micro FFPE Kit (Qiagen) as recommended by the manufacturer. For the preparation of mRNA from isolated tubules and interstitium, paraffin sections were mounted on PALM® membrane slides (Carl Zeiss MicroImaging GmbH). UV-LACP was then performed using a PALM® MicroBeam system and PALM® Robo software (Carl Zeiss MicroImaging GmbH) in order to isolate tubules and interstitium individually. mRNA was prepared from these samples using again the RNeasy Micro FFPE Kit (see above). Samples were incubated with RNase-free DNase I (10 U/l; Roche) and RNase Inhibitor (40 U/l, LifeTechnologies) to remove contaminating traces of genomic DNA. cDNA was synthesized from 1.5 μl of total mRNA using 8.5 μl of RT-mix (GeneAmp Gold RNA PCR Core Kit, LifeTechnologies). Negative controls were performed by omitting the reverse transcriptase (RT) reaction. For RT-PCR, 5 μl of cDNA were added to 2 μl $MgCl_2$, 2.5 μl 10× PCR Gold Buffer, 1 μl dNTP blend (10 mM), 0.13 μl GOLDAmplitaq, 1 μl of each primer (10 μmol/l) and aqua bidest to a final volume of 20 μl. RT-PCR was performed using specific primers (Eurofins MWG Operon) for ERα, ERβ and GPER (for sequences see Table 1). To control cDNA quality and success of genomic DNA digestion, primers for β actin were used with cDNA samples as well as samples without reverse transcriptase. RT-PCR conditions were 1 × 95 °C for 9 min, 40 × (94 °C for 45 s, 60 °C for 45 s and 72 °C for 45 s) and 72 °C for 7 min. PCR products were separated by 2 % agarose gel electrophoresis and visualized by SYBR Green I staining (Sigma-Aldrich).

Quantitative real-time PCR with cDNA from testicular biopsies

For quantitative analyses of ERα, ERβ and GPER mRNA expression in testis homogenates, quantitative real-time PCR amplification was performed using human β-actin and glyceraldehyde 3-phosphate dehydrogenase (GAPDH) mRNAs as reference standards. Detection of ERα, ERβ and GPER expression levels was performed with the same primer pairs that were also used for RT-PCR (Table 1). Melting curve analyses ensured the specificity of PCR products. All amplicons were sequenced for confirming sequence identity. For each specimen, triplicate determinations were performed using 1 μl of cDNA, 10 μl of iQ SYBR Green Supermix (Bio-Rad), 0.6 μl of each primer and aqua bidest to a final volume of 20 μl. Quantitative real-time PCR was performed on a CFX96 RealTime Cycler (Bio-Rad). Conditions were 1 × 95 °C for 3 min and 40 × (95 °C for 15 s, 60 °C for 30 s) and melting curve analysis (1 × 95 °C for 10 s, 65 °C to 95 °C, increment 0.5 °C for 5 s). Relative gene expression was calculated using CFX Manager Software 2.0 (Bio-Rad). For statistical analyses, ANOVA was performed followed by a Student's *t*-test (SPSS 19.0, IBM).

Results

The mRNAs of both estrogen receptors and of GPER are expressed in different compartments of the human testis

The human testis largely consists of seminiferous tubules (T) and the interstitial tissue (I) between them. Using laser-assisted microdissection, both compartments were dissected on tissue slides from testis biopsies showing normal spermatogenesis (Nsp) and from biopsies of

Table 1 List of PCR primers used

Target	NCBI RefSeq accession	Primer sequence (5′ → 3′)	Amplicon length (bp)
ERα (PCR)	NM_000125.2	GGAGGGCAGGGGTGAA for GGCCAGGCTGTTCTTCTTAG rev	102
ERβ (PCR)	NM_001040275	AGAGTCCCTGGTGTGAAGCAAG for GACAGCGCAGAAGTGAGCATC rev	143
ERα (ISH)	NM_000125	TCCTACCAGACCCTTCAGTG for CAGACGAGACCAATCATCAG rev	183
ERβ (ISH)	NM_001040275	AGAGTCCCTGGTGTGAAGCAAG for TCCCACTTCGTAACACTTCCG rev	329
GPER (PCR)	NM_001505.2	CGTCCTGTGCACCTTCATGT for AGCTCATCCAGGTGAGGAAGAA rev	77
GPER (ISH)	NM_001505.2	CAGTACGTGATCGGCCTGTT for TGTAGCGGTCGAAGCTCA rev	310
β Actin (PCR)	NM_001101.3	TTCCTTCCTGGGCATGGAGT for TACAGGTCTTTGCGGATGTC rev	89
GAPDH (PCR)	NM_002046.3	CCAGGTGGTCTCCTCTGACTTC for GTGGTCGTTGAGGGCAATG rev	81

The primers for ERα (PCR) are located in exon 4 and are picking up most ERα variants, except ERαΔ2 and ERαΔ4. The primers for ERα (ISH) are intron spanning (exons 4 and 5). The primers for ERβ (PCR) and ERβ (ISH) are intron spanning as well (exon 1 and 2 for PCR and exons 2 and 4 for ISH) and are picking up all ERβ variants, except ERβΔ2. The primers for GPER (PCR and ISH) are not intron spanning (exon 2 in transcript variant 2) and are picking up all three transcript variants

ISH in situ hybridization

patients with Sertoli cell only (SCO) syndrome. SCO tubules do not contain germ cells but only somatic cells (Sertoli cells). Sertoli cells in SCO testes show a very similar gene expression profile than Sertoli cells in normal testes [see Online Resources 1 and 2 and (Fietz et al. 2011)]. We isolated RNA from these samples as well as from whole testes (Nsp and SCO) and MCF-7 cells and amplified the messages for both estrogen receptors and GPER by RT-PCR (Fig. 1). Throughout our study, we used MCF-7 cells as positive control and standard alike because they are known to express large amounts of ERα, very low amounts of ERβ as well as moderate amounts of GPER [see e.g., (Filardo et al. 2000)]. As a number of factors can modify the levels of estrogen receptors in MCF-7 cells, they are unsuitable for serving as a bona fide reference. Nevertheless, we consider the comparison with a well-known cell line expressing all three receptors as instructive in order to classify expression levels. Using this combination of samples, we were able to localize the expression of all three receptors within these two compartments. Expression of ERα was detectable in whole (T + I) normal and SCO testes as well as in normal tubules (T) but neither in SCO tubules nor interstitium (I) indicating expression mainly in germ cells and weak expression in the interstitium (Fig. 1a, see also Fig. 3f and discussion). Contrary to ERα, expression of ERβ was strong in whole (T + I) normal and SCO testes, as well as in isolated seminiferous tubules from normal and SCO testes. Expression in the interstitium was not detectable (Fig. 1b). Because expression in seminiferous tubules from SCO testes was slightly reduced compared with expression in tubules from testes showing normal spermatogenesis, we conclude that ERβ is expressed in Sertoli cells and germ cells. GPER expression was detectable in whole (T + I) normal and SCO testes as well as in normal and SCO tubules (T) and interstitium (I) (Fig. 1c). Because there was virtually no difference between samples from testes showing normal spermatogenesis and SCO testes, GPER appears to be weakly expressed in Sertoli cells and moderately in the interstitial compartment.

qPCR analyses indicate that germ cells weakly express ERα mRNA, Sertoli cells moderately express ERβ mRNA and GPER, and GPER mRNA is strongly synthesized in interstitial cells

The results obtained by RT-PCR analyses could be confirmed by quantitative PCR of both estrogen receptors and of GPER from whole testis cDNA prepared from normal and SCO testes (Fig. 2a). ERα mRNA expression in normal testes is strongly reduced compared with the expression level in MCF-7 cells (high expression of ERα). In SCO testes only background expression was detectable indicating that there is only weak expression of ERα mRNA in germ cells and/or interstitial cells. On the other hand, ERβ was expressed 133-fold stronger in normal testes than in MCF-7 cells (low expression of ERβ).

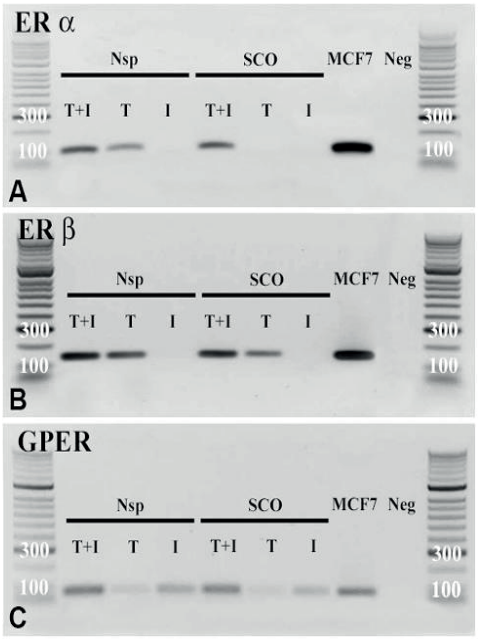

Fig. 1 The mRNAs of both estrogen receptors and GPER are expressed in different compartments of the human testis. RT-PCRs were performed with cDNAs obtained from whole tissue lysates (T + I) as well as from tubuli (T) and interstitium (I) collected by ultraviolet laser-assisted cell picking. Sample sets were obtained from three testes showing normal spermatogenesis (Nsp) and Sertoli cell only (SCO) syndrome each. Three different PCR reactions were performed using primers (see Table 1) for ERα (**a**), ERβ (**b**) and GPER (**c**). MCF-7 cDNA was used as positive control; a negative control (Neg) was performed without cDNA. One representative data set for one Nsp and SCO testis each is shown

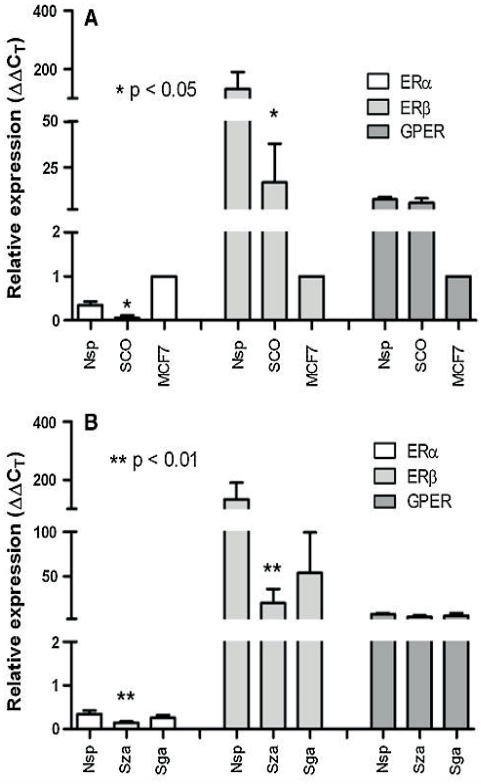

Fig. 2 qPCR analyses show that germ cells weakly express ERα mRNA and strongly express ERβ and that GPER mRNA is synthesized in Sertoli (weak) and interstitial cells. qRT-PCRs for ERα, ERβ and GPER were carried out using cDNAs from four normal (Nsp) and SCO testes each and from MCF-7 cells (**a**). Relative expression of the receptor mRNAs was normalized for expression in MCF-7 cells (set to one). In addition, four testes with spermatocyte (sza) or spermatogonial arrest (sga) each were used for comparing the expression of the three messages with expression in testes showing normal spermatogenesis (**b**). The mean ± SD of the results from the four qRT-PCRs for each receptor gene is shown. In (**b**), the expression levels were normalized for the expression levels in testes with normal spermatogenesis that had been normalized for expression in MCF-7 cells before. For statistical analyses, ANOVA was performed followed by student's *t*-test

In SCO testes, expression was reduced down to 27-fold confirming that ERβ is expressed in Sertoli cells and germ cells. GPER mRNA expression was 5.6- and 7.4-fold higher in normal and SCO testes, respectively, than in MCF-7 cells (moderate expression of GPER) which can be explained by expression of GPER mRNA either in the interstitial compartment or in Sertoli cells or in both. Together with the results shown in Fig. 1, it can be concluded that expression of GPER mRNA is weak in Sertoli cells and strong in the interstitium.

The use of RNA samples from testes with spermatogenic maturation arrest for qPCR revealed that expression of ERα and ERβ was significantly reduced in samples obtained from testes with spermatogenic arrest on the primary spermatocyte level. The reduction in expression in samples with spermatogonial arrest did not reach significance level (Fig. 2b). Therefore, these results indicate that ERα and ERβ are expressed by germ cells up to the spermatid stage. In order to more precisely localize expression of the two receptors in the seminiferous epithelium, we performed in situ hybridizations and immunohistochemical analyses for ERα and ERβ as well as for GPER (in situ hybridization only).

In situ hybridizations and immunohistochemical analyses confirm ERα and ERβ mRNA expression in germ cells, ERβ and GPER expression in Sertoli cells, and expression of GPER in Leydig cells

In situ hybridization experiments revealed ERα mRNA expression in spermatogonia and primary spermatocytes

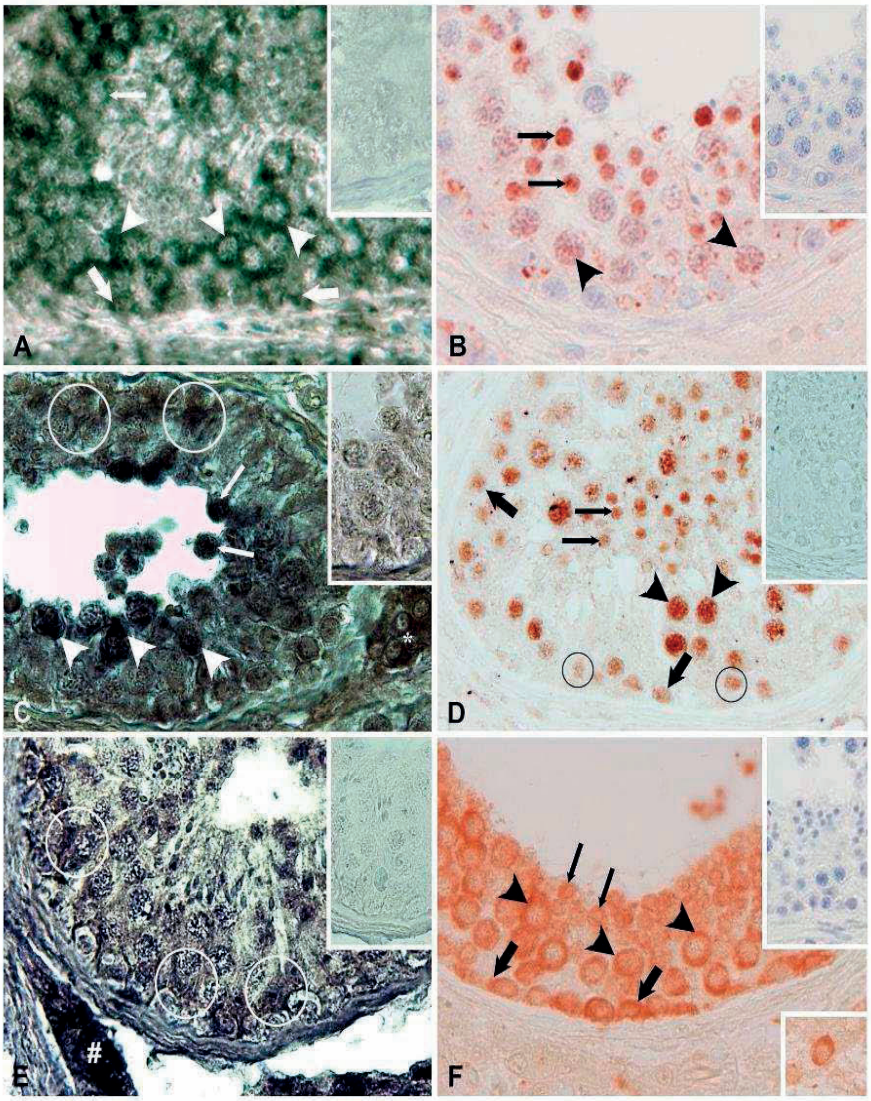

Fig. 3 ERα, ERβ and GPER mRNAs and ERα and ERβ proteins can be detected by in situ hybridization and immunostaining in the human testis. Tissue sections of a testis with normal spermatogenesis were hybridized in situ with a DIG-labeled ERα cRNA (**a**), a ERβ cRNA probe (**c**) or a GPER cRNA probe (**e**) and stained with NBT. *Insets* show the negative control of a tissue section hybridized with the cognate antisense probe. *Asterisk* in (**c**) = unspecific labeling of interstitial Leydig cells which is also seen in the control. Immunohistochemical staining of ERα with antibody F-10 (**b**), ERβ with chicken ERβ 503 antibody (**d**) and ERα with antibody HC-20 (**f**). *Insets* in (**b**), (**d**) and (**f**) show negative controls without cognate primary antibodies. The *inset* in the *lower right corner* in (**f**) shows a single interstitial cell stained by HC-20. *Bold arrows* = spermatogonia, *arrowheads* = pachytene spermatocytes, *thin arrows* = early round spermatids, *circles* = Sertoli cells, *hash* = Leydig cells in (**e**). All original magnifications were 40×

but not in spermatids and Sertoli cells (Fig. 3a), whereas immunohistochemical staining using the monoclonal antibody F-10 demonstrated nuclear staining of primary spermatocytes and early round spermatids, but not of spermatogonia, Sertoli cells or interstitial cells (Fig. 3b). Antibody HC-20 immunostained the same cell types but additionally spermatogonia (Fig. 3f) and single interstitial cells (Fig. 3f, lower inset) became positive.

ERβ mRNA expression could be detected in primary spermatocytes and Sertoli cells by in situ hybridization

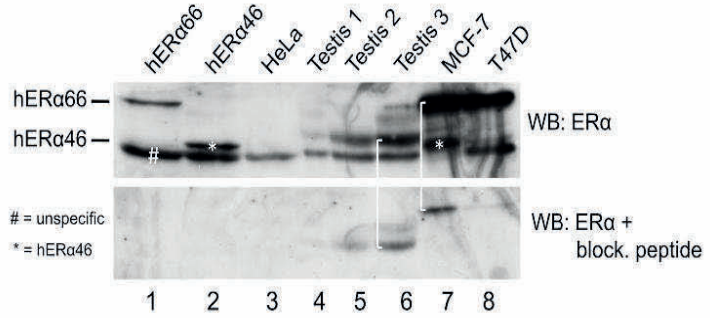

Fig. 4 ERα protein cannot be detected in the human testis using Western blotting. (*Upper panel*) Expression of ERα in the testis as well as in control cell lines was investigated by immunoblotting using monoclonal antibody F-10 directed against the C-terminal end of ERα. Lysates of HeLa cells ectopically expressing either hERα66 (*lane 1*) or isoform hERα46 (*, *lane 2*) were used as markers (Flouriot et al. 2000). *Hash* = unspecific band. In the *lower panel*, a duplicate gel was immunoblotted using the cognate ERα blocking peptide together with antibody F-10

(Fig. 3c), whereas immunohistochemical analysis showed nuclear staining in spermatogonia, primary spermatocytes, early round spermatids as well as in Sertoli cells. The interstitial compartment was negative with both methods (Fig. 3d).

Strong expression of GPER mRNA expression in Leydig cells is evident by in situ hybridization (Fig. 3e). Sertoli cells were also moderately stained, whereas germ cells showed a faint staining in some hybridizations only (data not shown). For Western blotting and immunohistochemistry, the anti-GPER antibody that had been used by Rago et al. (2011) did not work on our material.

Estrogen receptor α and its 46-kDa isoform cannot be detected in the human testis by Western blotting

Before performing immunoblotting experiments with testis lysates, we tested a total of six different anti-ERα antibodies in Western blotting and immunohistochemical staining of testis including epididymal sections. It turned out that the two antibodies F-10 (monoclonal) and HC-20 (polyclonal) that had been used in a number of studies before (Han et al. 2009; Madak-Erdogan et al. 2011; Pelletier and El-Alfy 2000; Rago et al. 2006) were the most sensitive ones. As specific molecular weight markers, we used lysates of HeLa cells that were ectopically expressing human ERα66 or ERα46 from transfected pSG constructs (Flouriot et al. 2000) (Fig. 4, lanes 1–2). Immunoblotting analyses of three testis lysates with ERα antibody F-10 detected two (Fig. 4, lane 5) or three bands (lanes 4 and 6). The low-molecular-weight band at approximately 44 kDa is unspecific because it also appeared in the ER-negative HeLa cell lysate (lane 3). The other two bands represent proteins with a molecular weight larger than 46 and lower than 66 kDa indicating that these bands are neither ERα66 nor ERα46. Moreover, these bands could not be efficiently competed with a blocking peptide for F-10 (Fig. 4, lanes 4–6, lower panel) strongly indicating that they are unspecific. In the positive controls (lanes 7–8), antibody F-10 detects large amounts of ERα66 in the ERα-positive breast cancer cell lines MCF-7 and T47D as well as smaller amounts of ERα46 in MCF-7 as described (Flouriot et al. 2000).

Discussion

Conflicting data concerning the cellular expression of ERα in the testis can be explained by the use of different antibodies and the lack of combined mRNA and protein analysis on the cellular level in many previous studies. Therefore, we used a combination of PCR analyses of cDNAs obtained from whole testes and from cells obtained by laser-assisted cell picking (LACP), in situ hybridization and immunohistochemistry.

PCR analyses indicated expression of ERα mainly in germ cells and weak expression in the interstitium. For immunohistochemical stainings, we used the antibodies F-10 (Han et al. 2009; Madak-Erdogan et al. 2011; Rago et al. 2006) and HC-20 (Madak-Erdogan et al. 2011; Pelletier and El-Alfy 2000) that had been used previously in other studies as well. F-10 detected wild-type ERα66 in the ERα-positive breast cancer lines MCF-7 and T47D as well as the shorter isoform ERα46 in MCF-7 cells (Flouriot et al. 2000) and intensely immunostained the efferent ductule epithelium (not shown). Using F-10 for IHC, we detected ERα expression in primary spermatocytes and early round spermatids but not in Sertoli or interstitial Leydig cells. The HC-20 antibody additionally stained spermatogonia and single interstitial cells. The latter explains amplification of ERα from cDNA prepared from whole

SCO testes (Fig. 1a, SCO (T + I)) that are devoid of germ cells. Whereas the cDNA for the T + I samples (whole testis) was prepared from a few tissue slides per sample providing relatively large amounts of cDNA, the T or I samples were prepared from a few tubules (T) or interstitial compartments (I) picked by LACP and provided only very little cDNA so that the number of PCR cycles had to be increased in order to reliably amplify even frequent cDNAs. This technical constraint explains why all cDNAs from the interstitial space remained negative for ERα although the HC-20 antibody did stain single interstitial cells. Contrary to IHC, we could not detect ERα in the F-10 immunoblot of three testis samples indicating that the concentration of ERα must be very low. Using extracts from HeLa cells ectopically expressing either ERα66 or isoform ERα46 as specific ERα size markers, we could unequivocally show that all bands detected in the testis samples were neither ERα66 nor ERα46. This result is not surprising as the concentration of steroid hormone receptors in tissues is very low in general so that they have to be enriched in order to being detectable on immunoblots (Margaret Warner, personal communication). Therefore, the concentration of ERα must be very low in the whole testis and extremely low in the interstitial space. This again explains why ERα message could not be detected in interstitial cells picked by LACP. Contrary to us, Han et al. (2009) and Pentikainen et al. (2000) claimed to have detected ERα in testis samples using immunoblotting, but both studies did not include proper (size) controls.

Like M kinen et al. (2001), we detected ERβ mRNA expression in primary spermatocytes and early round spermatids but not in elongated spermatids or Leydig cells by in situ hybridization. Immunohistochemical staining in addition revealed expression in spermatogonia. But contrary to M kinen et al., we also detected ERβ nuclear immunoreactivity in Sertoli cells using in situ hybridization as well as immunohistochemistry like it was reported by a couple of groups for rodents (for review see Carreau and Hess 2010). Whereas M kinen et al. could investigate only a single SCO testis that showed no immunoreaction, we looked at three SCO testes, from which tubules were isolated by LACP, by RT-PCR and at four SCO testes by qPCR. All tested SCO samples turned out to be ERβ positive in both assays although the four samples investigated by qPCR showed large quantitative differences. Therefore, it is possible that the sample investigated by M kinen et al. (2001) belonged to the low expression group.

In case of ERβ, it was particularly difficult to choose a truly specific antibody because Snyder et al. (Snyder et al. 2010) demonstrated that many out of nine anti-ERβ antibodies tested do recognize recombinant ERβ and ERβ expressed in cultured and transfected cells. But in tissues, no matter if obtained from wild-type mice or two ERβ knockout mouse strains, they detected other protein(s) that were not known ERβ proteins or variants but only had a similar molecular weight. The non-ERβ proteins in the two knockout strains appeared to be "specific" because their bands on the immunoblots were eliminated by pre-adsorption of the antiserum with the antigenic peptide. Unfortunately, the antibodies Z8P (Shughrue et al. 2002), Ab14021 (Abcam) and AP-ERβ1 and AP-ERβ2/cx (from M. Younes, Baylor College of Medicine, Houston, TX, USA) that had been shown to specifically detect ERβ or ERβ isoforms were no longer available. Therefore, we used the chicken polyclonal anti-ERβ 503 IgY that is directed against a slightly modified recombinant human ERβ1 protein that is known to pick up most ERβ isoforms except ERβ2 (Margaret Warner, personal communication) and had been used already in a similar study (M kinen et al. 2001). ERβ 503 showed strong immunoreactivity in the nuclei of rat ventral prostate epithelial cells, which was almost completely abolished when the antiserum was pre-adsorbed to recombinant ERβ protein coupled to Sepharose (Saji et al. 2000).

Table 2 Expression pattern of estrogen receptors in the testis—summary

Gene/protein	Sertoli cells	Germ cells	Interstitial cells
ERα			
mRNA	n.d.	+	n.d.
Protein	n.d.	+	(+)[a]
ERβ			
mRNA	+++	++	n.d.
Protein	++	++	n.d.
GPER			
mRNA	+	−	++
Protein	n.a.	n.a.	n.a.

Cellular localization and expression levels of both estrogen receptors and GPER in the compartments of the human testis

n.d. not detected, *a* detected by HC-20 antibody, *n.a.* not analyzed

In quantitative terms, ERβ and GPER turned out to be the dominant receptors in the human testis (see Table 2). But when analyzing mouse knockout models, there seemed to be no functional correlation, because ERβKO$_{CH}$ (Krege et al. 1998) and ERβKO$_{ST}$ (Dupont et al. 2000) males were reported to be fertile. But in all ERβ-null mutant mouse lines published before 2008, several ERβ transcript variants were still found, encoding putative truncated peptides lacking the DNA-binding domain (DBD) and ligand-binding domain or the DBD only. Therefore, Antal et al. (2008) generated the ERβ$_{ST}^{L-/L-}$ mouse mutant that is devoid of ERβ mRNAs containing sequences downstream of exon 3. Interestingly, males and females of this genuine ERβ-null mutant are infertile. But the underlying reason is not

known because males appear to exhibit a normal testis and epididymis histology, and their spermatozoa show regular motility.

Considering published reports with clear data and our own results (see Table 2), the following picture emerges for ERα. Using RT-PCR or qPCR, the message for ERα is consistently detected in the testis by many groups. But compared with MCF-7 cells, which contain a high amount of ERα mRNA and protein, the message is detectable in the testis only on a very low level in the germ cell fraction and in single interstitial cells. Using in situ hybridization, it is only detectable in spermatogonia and primary spermatocytes, but not in early round spermatids. This can be explained by the temporal uncoupling of transcription and translation in haploid spermatids because of the nuclear histone to protamine exchange leading to a stop of gene expression (Kotaja and Sassone-Corsi 2007; Steger 2001). In the case of the cAMP responsive element modulator (CREM), for example, its mRNA has been shown to be expressed in pachytene primary spermatocytes up to early round spermatids, while the protein was only found in spermatids (Steger et al. 1999). Compared with its message, ERα protein is not at all or at least hardly detectable by immunoblotting, whereas its detection and cellular localization by IHC is very much dependent on the antibody used. When mature or immature germ cells are "enriched" by ejaculation, ERα can also be detected by immunoblotting (Aquila et al. 2004; Lambard et al. 2004). But as sperm cells are stored in the epididymis, it cannot be fully excluded that they pick up ERα from the epididymal epithelium that is strongly expressing ERα (Hess 2003) like it is known for glycoproteins (Schr ter et al. 1999).

Although (1) estrogens are considered to play an important role in spermatogenesis and spermiogenesis and (2) both estrogen receptors and GPER are expressed in the human testis, ERα- and $ER\beta_{ST}^{L-/L-}$-null mutant male mice are infertile but show no direct testis phenotype, and GPER-null mutant male mice are fertile and show no overt reproductive anomalies. As there is a high evolutionary pressure on successful spermatogenesis, it appears that all three receptors have predominantly overlapping roles in the testis in order to assure normal spermatogenesis. Functional studies with receptor-specific agonists and antagonists or a conditional triple knockout are needed for testing this hypothesis.

Acknowledgments The skillful technical assistance of J. Dern-Wieloch, S. Fr hlich, A. Hax, A. Hild, S. Schubert-Porth, J. Vogelsberg and R. Weigel is gratefully acknowledged. MCF-7 cells were provided by Uta Bauer, Marburg, and T47D cells by Lutz Konrad, Giessen. Expression constructs pSG hER-α66 and pSG hER-α46 were kindly provided by Gilles Flouriot (University of Rennes, France) and the chicken ERβ 503 antibody by Margaret Warner (University of Houston, Texas, USA).

References

Antal MC, Krust A, Chambon P, Mark M (2008) Sterility and absence of histopathological defects in nonreproductive organs of a mouse ERbeta-null mutant. Proc Natl Acad Sci USA 105(7):2433–2438

Aquila S, Sisci D, Gentile M, Middea E, Catalano S, Carpino A, Rago V, Ando S (2004) Estrogen receptor (ER) alpha and ER beta are both expressed in human ejaculated spermatozoa: evidence of their direct interaction with phosphatidylinositol-3-OH kinase/Akt pathway. J Clin Endocrinol Metab 89(3):1443–1451

Beato M, Klug J (2000) Steroid hormone receptors: an update. Hum Reprod Update 6(3):225–236

Bergmann M, Kliesch S (2010) Testicular Biopsy and Histology. In: Nieschlag E, Behre HM, Nieschlag S (eds) Andrology - Male Reproductive Health and Dysfunction. Springer, Stuttgart, pp 155–168

Bradford MM (1976) A rapid and sensitive method for the quantitation of microgram quantities of protein utilizing the principle of protein-dye binding. Anal Biochem 72:248–254

Carreau S, Hess RA (2010) Oestrogens and spermatogenesis. Philos Trans R Soc Lond B Biol Sci 365(1546):1517–1535

Carreau S, Bouraima-Lelong H, Delalande C (2011) Estrogens: new players in spermatogenesis. Reprod Biol 11(3):174–193

Carreau S, Bouraima-Lelong H, Delalande C (2012) Estrogen, a female hormone involved in spermatogenesis. Adv Med Sci 57(1):31–36

Cavaco JE, Laurentino SS, Barros A, Sousa M, Socorro S (2009) Estrogen receptors alpha and beta in human testis: both isoforms are expressed. Syst Biol Reprod Med 55(4):137–144

Chen M, Hsu I, Wolfe A, Radovick S, Huang K, Yu S, Chang C, Messing EM, Yeh S (2009) Defects of prostate development and reproductive system in the estrogen receptor-alpha null male mice. Endocrinology 150(1):251–259

Dupont S, Krust A, Gansmuller A, Dierich A, Chambon P, Mark M (2000) Effect of single and compound knockouts of estrogen receptors alpha (ERalpha) and beta (ERbeta) on mouse reproductive phenotypes. Development 127(19):4277–4291

Eddy EM, Washburn TF, Bunch DO, Goulding EH, Gladen BC, Lubahn DB, Korach KS (1996) Targeted disruption of the estrogen receptor gene in male mice causes alteration of spermatogenesis and infertility. Endocrinology 137(11):4796–4805

Enmark E, Pelto HM, Grandien K, Lagercrantz S, Lagercrantz J, Fried G, Nordenskjold M, Gustafsson J (1997) Human estrogen receptor beta-gene structure, chromosomal localization, and expression pattern. J Clin Endocrinol Metab 82(12):4258–4265

Fietz D, Geyer J, Kliesch S, Gromoll J, Bergmann M (2011) Evaluation of CAG repeat length of androgen receptor expressing cells in human testes showing different pictures of spermatogenic impairment. Histochem Cell Biol 136(6):689–697

Filardo EJ, Quinn JA, Bland KI, Frackelton AR Jr (2000) Estrogen-induced activation of Erk-1 and Erk-2 requires the G protein-coupled receptor homolog, GPR30, and occurs via trans-activation of the epidermal growth factor receptor through release of HB-EGF. Mol Endocrinol 14(10):1649–1660

Flouriot G, Brand H, Denger S, Metivier R, Kos M, Reid G, Sonntag-Buck V, Gannon F (2000) Identification of a new isoform of the human estrogen receptor-alpha (hER-alpha) that is encoded by distinct transcripts and that is able to repress hER-alpha activation function 1. EMBO J 19(17):4688–4700

Franco R, Boscia F, Gigantino V, Marra L, Esposito F, Ferrara D, Pariante P, Botti G, Caraglia M, Minucci S, Chieffi P (2011) GPR30 is overexpressed in post-puberal testicular germ cell tumors. Cancer Biol Ther 11(6):609–613

Han Y, Feng HL, Sandlow JI, Haines CJ (2009) Comparing expression of progesterone and estrogen receptors in testicular tissue

from men with obstructive and nonobstructive azoospermia. J Androl 30(2):127–133
Hess RA (2003) Estrogen in the adult male reproductive tract: a review. Reprod Biol Endocrinol 1:52
Hess RA, Gist DH, Bunick D, Lubahn DB, Farrell A, Bahr J, Cooke PS, Greene GL (1997) Estrogen receptor (alpha and beta) expression in the excurrent ducts of the adult male rat reproductive tract. J Androl 18(6):602–611
Joseph A, Hess RA, Schaeffer DJ, Ko C, Hudgin-Spivey S, Chambon P, Shur BD (2010a) Absence of estrogen receptor alpha leads to physiological alterations in the mouse epididymis and consequent defects in sperm function. Biol Reprod 82(5):948–957
Joseph A, Shur BD, Ko C, Chambon P, Hess RA (2010b) Epididymal hypo-osmolality induces abnormal sperm morphology and function in the estrogen receptor alpha knockout mouse. Biol Reprod 82(5):958–967
Kotaja N, Sassone-Corsi P (2007) The chromatoid body: a germ-cell-specific RNA-processing centre. Nat Rev Mol Cell Biol 8(1):85–90
Krege JH, Hodgin JB, Couse JF, Enmark E, Warner M, Mahler JF, Sar M, Korach KS, Gustafsson J , Smithies O (1998) Generation and reproductive phenotypes of mice lacking estrogen receptor beta. PNAS 95(26):15677–15682
Lambard S, Galeraud-Denis I, Saunders PT, Carreau S (2004) Human immature germ cells and ejaculated spermatozoa contain aromatase and oestrogen receptors. J Mol Endocrinol 32(1):279–289
Lekhkota O, Brehm R, Claus R, Wagner A, Bohle RM, Bergmann M (2006) Cellular localization of estrogen receptor-alpha (ERalpha) and -beta (ERbeta) mRNA in the boar testis. Histochem Cell Biol 125(3):259–264
Li H, Papadopoulos V, Vidic B, Dym M, Culty M (1997) Regulation of rat testis gonocyte proliferation by platelet-derived growth factor and estradiol: identification of signaling mechanisms involved. Endocrinology 138(3):1289–1298
Li EZ, Li DX, Zhang SQ, Wang CY, Zhang XM, Lu JY, Duan CM, Yang XZ, Feng LX (2007) 17beta-estradiol stimulates proliferation of spermatogonia in experimental cryptorchid mice. Asian J Androl 9(5):659–667
Lubahn DB, Moyer JS, Golding TS, Couse JF, Korach KS, Smithies O (1993) Alteration of reproductive function but not prenatal sexual development after insertional disruption of the mouse estrogen receptor gene. Proc Natl Acad Sci USA 90:11162–11166
Lucas TF, Pimenta MT, Pisolato R, Lazari MF, Porto CS (2011) 17beta-estradiol signaling and regulation of Sertoli cell function. Spermatogenesis 1(4):318–324
Luconi M, Forti G, Baldi E (2002) Genomic and nongenomic effects of estrogens: molecular mechanisms of action and clinical implications for male reproduction. J Steroid Biochem Mol Biol 80(4–5):369–381
Madak-Erdogan Z, Lupien M, Stossi F, Brown M, Katzenellenbogen BS (2011) Genomic collaboration of estrogen receptor alpha and extracellular signal-regulated kinase 2 in regulating gene and proliferation programs. Mol Cell Biol 31(1):226–236
Mahato D, Goulding EH, Korach KS, Eddy EM (2000) Spermatogenic cells do not require estrogen receptor-alpha for development or function. Endocrinology 141(3):1273–1276
M kinen S, Makela S, Weihua Z, Warner M, Rosenlund B, Salmi S, Hovatta O, Gustafsson JA (2001) Localization of oestrogen receptors alpha and beta in human testis. Mol Hum Reprod 7(6):497–503
Matthews J, Gustafsson JA (2003) Estrogen signaling: a subtle balance between ER alpha and ER beta. Mol Interv 3(5):281–292
McLachlan RI, Rajpert-De Meyts E, Hoei-Hansen CE, de Kretser DM, Skakkebaek NE (2007) Histological evaluation of the human testis - approaches to optimizing the clinical value of the assessment: mini review. Hum Reprod 22(1):2–16
Minucci S, Di Matteo L, Chieffi P, Pierantoni R, Fasano S (1997) 17 beta-estradiol effects on mast cell number and spermatogonial mitotic index in the testis of the frog. Rana esculenta. J Exp Zool 278(2):93–100
Mosselman S, Polman J, Dijkema R (1996) ER beta: identification and characterization of a novel human estrogen receptor. FEBS Lett 392(1):49–53
Pelletier G, El-Alfy M (2000) Immunocytochemical localization of estrogen receptors alpha and beta in the human reproductive organs. J Clin Endocrinol Metab 85(12):4835–4840
Pentikainen V, Erkkila K, Suomalainen L, Parvinen M, Dunkel L (2000) Estradiol acts as a germ cell survival factor in the human testis in vitro. J Clin Endocrinol Metab 85(5):2057–2067
Prossnitz ER, Barton M (2011) The G-protein-coupled estrogen receptor GPER in health and disease. Nat Rev Endocrinol 7(12):715–726
Rago V, Siciliano L, Aquila S, Carpino A (2006) Detection of estrogen receptors ER-alpha and ER-beta in human ejaculated immature spermatozoa with excess residual cytoplasm. Reprod Biol Endocrinol 4:36
Rago V, Romeo F, Giordano F, Maggiolini M, Carpino A (2011) Identification of the estrogen receptor GPER in neoplastic and non-neoplastic human testes. Reprod Biol Endocrinol 9:135
Roger P, Sahla ME, Makela S, Gustafsson JA, Baldet P, Rochefort H (2001) Decreased expression of estrogen receptor beta protein in proliferative preinvasive mammary tumors. Cancer Res 61(6):2537–2541
Saji S, Jensen EV, Nilsson S, Rylander T, Warner M, Gustafsson JA (2000) Estrogen receptors alpha and beta in the rodent mammary gland. Proc Natl Acad Sci U S A 97(1):337–342
Saunders PT, Sharpe RM, Williams K, Macpherson S, Urquart H, Irvine DS, Millar MR (2001) Differential expression of oestrogen receptor alpha and beta proteins in the testes and male reproductive system of human and non-human primates. Mol Hum Reprod 7(3):227–236
Schr ter S, Osterhoff C, McArdle W, Ivell R (1999) The glycocalyx of the sperm surface. Hum Reprod Update 5(4):302–313
Shughrue PJ, Askew GR, Dellovade TL, Merchenthaler I (2002) Estrogen-binding sites and their functional capacity in estrogen receptor double knockout mouse brain. Endocrinology 143(5):1643–1650
Sirianni R, Chimento A, Ruggiero C, De Luca A, Lappano R, Ando S, Maggiolini M, Pezzi V (2008) The novel estrogen receptor, G protein-coupled receptor 30, mediates the proliferative effects induced by 17beta-estradiol on mouse spermatogonial GC-1 cell line. Endocrinology 149(10):5043–5051
Smith EP, Boyd J, Frank GR, Takahashi H, Cohen RM, Specker B, Williams TC, Lubahn DB, Korach KS (1994) Estrogen resistance caused by a mutation in the estrogen-receptor gene in a man [published erratum appears in N Engl J Med 1995 Jan 12;332(2):131]. N Engl J Med 331(16):1056–1061
Snyder MA, Smejkalova T, Forlano PM, Woolley CS (2010) Multiple ERbeta antisera label in ERbeta knockout and null mouse tissues. J Neurosci Methods 188(2):226–234
Solakidi S, Psarra AM, Nikolaropoulos S, Sekeris CE (2005) Estrogen receptors alpha and beta (ERalpha and ERbeta) and androgen receptor (AR) in human sperm: localization of ERbeta and AR in mitochondria of the midpiece. Hum Reprod 20(12):3481–3487
Steger K (2001) Haploid spermatids exhibit translationally repressed mRNAs. Anat Embryol (Berl) 203(5):323–334
Steger K, Klonisch T, Gavenis K, Drabent B, Doenecke D, Bergmann M (1998) Expression of mRNA and protein of nucleoproteins during human spermiogenesis. Mol Hum Reprod 4(10):939–945
Steger K, Klonisch T, Gavenis K, Behr R, Schaller V, Drabent B, Doenecke D, Nieschlag E, Bergmann M, Weinbauer GF (1999) Round spermatids show normal testis-specific H1t but reduced

cAMP-responsive element modulator and transition protein 1 expression in men with round-spermatid maturation arrest. J Androl 20(6):747–754

Wagner A, Messe N, Bergmann M, Lekhkota O, Claus R (2006) Effects of estradiol infusion in GnRH immunized boars on spermatogenesis. J Androl 27(6):880–889

Wahlgren A, Svechnikov K, Strand ML, Jahnukainen K, Parvinen M, Gustafsson JA, Soder O (2008) Estrogen receptor beta selective ligand 5alpha-Androstane-3beta, 17beta-diol stimulates spermatogonial deoxyribonucleic acid synthesis in rat seminiferous epithelium in vitro. Endocrinology 149(6):2917–2922

Walter P, Green S, Greene G, Krust A, Bornert JM, Jeltsch JM, Staub A, Jensen E, Scrace G, Waterfield M et al (1985) Cloning of the human estrogen receptor cDNA. Proc Natl Acad Sci U S A 82(23):7889–7893

Weiss J, Bernhardt ML, Laronda MM, Hurley LA, Glidewell-Kenney C, Pillai S, Tong M, Korach KS, Jameson JL (2008) Estrogen actions in the male reproductive system involve estrogen response element-independent pathways. Endocrinology 149(12):6198–6206

11. Anhang – Publikationen

4. D. Fietz, M. Markmann, D. Lang, L. Konrad, S. Kliesch, T. Chakraborty, H. Hossain, M. Bergmann. BMC Mol Biol 2015 Dec 29;16(1):23.

Fietz et al. BMC Molecular Biol (2015) 16:23
DOI 10.1186/s12867-015-0051-7

BMC Molecular Biology

RESEARCH ARTICLE Open Access

Transfection of Sertoli cells with androgen receptor alters gene expression without androgen stimulation

D. Fietz[1*†], M. Markmann[2†], D. Lang[1†], L. Konrad[3], J. Geyer[1], S. Kliesch[4], T. Chakraborty[2], H. Hossain[2] and M. Bergmann[1]

Abstract

Background: Androgens play an important role for the development of male fertility and gained interest as growth and survival factors for certain types of cancer. Androgens act via the androgen receptor (AR/*Ar*), which is involved in various cell biological processes such as sex differentiation. To study the functional mechanisms of androgen action, cell culture systems and AR-transfected cell lines are needed. Transfection of AR into cell lines and subsequent gene expression analysis after androgen treatment is well established to investigate the molecular biology of target cells. However, it remains unclear how the transfection with AR itself can modulate the gene expression even without androgen stimulation. Therefore, we transfected *Ar*-deficient rat Sertoli cells 93RS2 by electroporation using a full length human AR.

Results: Transfection success was confirmed by Western Blotting, immunofluorescence and RT-PCR. AR transfection-related gene expression alterations were detected with microarray-based genome-wide expression profiling of transfected and non-transfected 93RS2 cells without androgen stimulation. Microarray analysis revealed 672 differentially regulated genes with 200 up- and 472 down-regulated genes. These genes could be assigned to four major biological categories (development, hormone response, immune response and metabolism). Microarray results were confirmed by quantitative RT-PCR analysis for 22 candidate genes.

Conclusion: We conclude from our data, that the transfection of *Ar*-deficient Sertoli cells with AR has a measurable effect on gene expression even without androgen stimulation and cause Sertoli cell damage. Studies using AR-transfected cells, subsequently stimulated, should consider alterations in AR-dependent gene expression as off-target effects of the AR transfection itself.

Keywords: Transfection, Gene expression analysis, Androgen receptor, Sertoli cells

Background

Androgens play a pivotal role for the development of the male phenotype, the initiation and maintenance of spermatogenesis and therefore male fertility (for review see [1]). The action of the most important androgens testosterone (T) and dihydrotestosterone (DHT) is mediated by the androgen receptor (AR/*Ar*). It is a ligand-activated transcriptional factor belonging to the nuclear receptor superfamily. The AR/*Ar* gene is located on the X chromosome and consists of eight exons, coding for the N-terminal transcription regulation domain, the DNA binding domain (DBD) in the middle of the protein and the C-terminal ligand binding domain (LBD). The DBD as well as the LBD are highly conserved throughout species (for review see [2]). Bound to its ligand, the androgen-AR complex is translocated into the nucleus, binds to the DNA (androgen responsive elements, AREs) and is able to activate or repress gene expression by recruiting co-activators or co-repressors (for review see [3]). The

*Correspondence: Daniela.Fietz@vetmed.uni-giessen.de
†D. Fietz, M. Markmann, D. Lang contributed equally to the study
[1] Institute of Veterinary Anatomy, Histology and Embryology, Justus Liebig University, Frankfurter Straße 98, 35392 Giessen, Germany
Full list of author information is available at the end of the article

activity of steroid hormone receptors is also regulated by post-transcriptional modifications. In case of AR/*Ar*, a great variety of these modifications has been described, i.e. phosphorylation, acetylation, ubiquitination and also methylation (for review see [4]).

The AR/*Ar* is expressed in all tissues except the spleen (for review see [2]). In the testis, it is expressed in interstitial Leydig cells and endothelial cells, as well as in peritubular myoid cells and tubular Sertoli cells [5], for review see [1]. Since germ cells do not express AR/*Ar*, the androgen action has to be mediated towards the germ cells by Sertoli cells. These somatic cells have been described as branched cells surrounding all germ cell stages [6, 7]. As was shown by Willems et al. [8], a selective ablation of *Ar* in mouse Sertoli cells (SCARKO) leads to a disturbed Sertoli cell maturation including a delayed and defective establishment of the blood-testis barrier. Moreover, no meiotic germ cells were observed in SCARKO mice, showing the importance of a functional AR/*Ar* on Sertoli cell biology and for the development of germ cells.

To examine the role of the AR/*Ar* in different biological processes such as cell growth and survival as well as AR/*Ar*-dependent gene expression, cell culture systems are needed. Therefore, administration of T and/or the more efficient metabolite DHT has widely been used to investigate the effect of androgens and AR/*Ar*, respectively, in diverse cultured cells such as human breast cancer cells, adrenocortical carcinoma cells, murine skeletal muscle cells or liver carcinoma cells [9–12]. Additionally, AR/*Ar*-deficient cell lines were used, e.g. AR-deficient MCF-7 breast cancer cells, to examine the effect on estrogen administration in a system lacking AR [13]. Szelei et al. [14] transfected AR-deficient MCF-7 breast cancer cells with human AR and showed an inhibition of proliferation. Also prostate cancer cells devoid of AR were transfected with human AR and showed a decreased proliferation rate [15]. The question is, whether the transfection procedure itself might have led to an altered expression of AR/*Ar*-dependent and AR/*Ar*-independent genes. Xiao et al. [16] demonstrated equal concerns in *Amh*-Cre-transfected mouse, where an increase of oxidative stress and lipid peroxidation in Sertoli cells was detected even without stimulation.

Beside "classical" androgen-dependent prostate cancer development, also androgen-independent signalling pathways gained increasing interest as shown recently by Li et al. [17]. The authors describe a persistent transcriptional activity in castration-resistant prostate cancer cell lines in the absence of androgens. This transcriptional activity was mediated by a truncated AR protein lacking the LBD. This raises the question, whether an androgen-independent AR/*Ar* action is always important in cell biology and which genes might be expressed or repressed by AR/*Ar* presence alone.

For this purpose, we transfected rat Sertoli cells which have been shown to be deficient of *Ar* with full length human AR DNA. After transfection, we performed genome-wide microarray analysis and compared the gene expression pattern with non-transfected Sertoli cells to identify a possible "intrinsic" activity of AR/*Ar* without androgen administration. We found significantly altered gene expression in transfected compared with non-transfected cells, possibly influencing Sertoli cell function.

Results

Transfection of 93RS2 cells with the human AR

Performing RT-PCR with primers specific for mouse and rat *Ar*, respectively, rat Sertoli cells (93RS2, [18]) proved to lack endogenous *Ar* (Fig. 1) and were therefore chosen for further experiments.

Success of transfection with full length human AR CDS was validated by immunofluorescence (IF, Fig. 2a), Western Blot (Fig. 2b) and RT-PCR (Fig. 2c). As the commercially available human AR was introduced in a GFP-coupled vector system, we used a rabbit anti-GFP antibody for IF experiments in transfected cells whereas non-transfected cells were used as internal negative control. Using PAGE, we were able to show the CAG repeat length of 17 to be stable throughout different settings (Fig. 2d).

Microarray analysis revealed an altered gene expression in transfected 93RS2 cells

Microarray analysis revealed 672 significantly regulated genes ($p < 0.01$ and fold change (FC) ≥ 2.0). Of these, 200

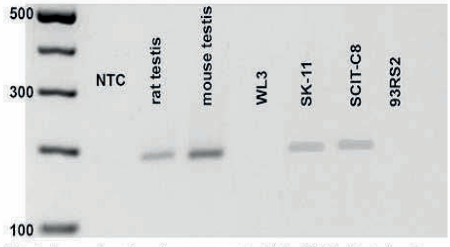

Fig. 1 Expression of androgen receptor (*Ar*) mRNA in Sertoli cell cultures. To find an appropriate cell culture system for our planned transfection studies, RT-PCR with specific primers for mouse and rat *Ar* was performed. Testis homogenate from rat and mouse served as positive control, whereas water was used as no template control (NTC) samples. We tested two mouse (WL3 and SK-11) as well as two rat Sertoli cell lines (SCIT-C8 and 93RS2). The latter revealed no expression of intrinsic *Ar* and were therefore used for further experiments

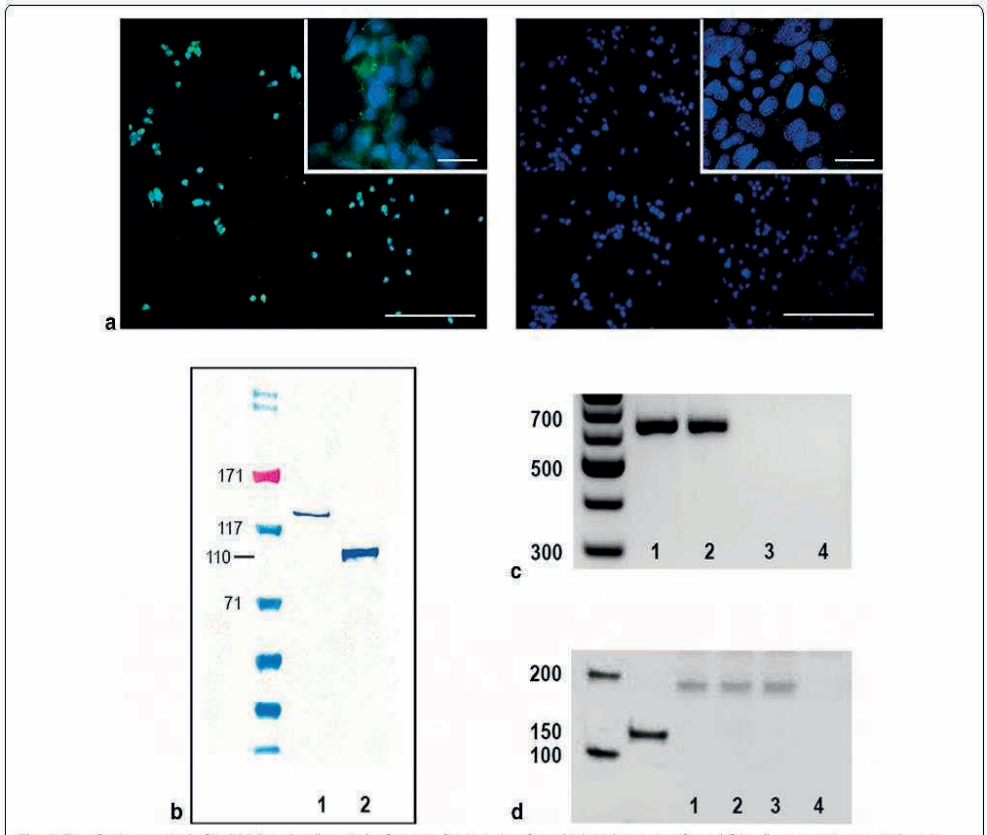

Fig. 2 Transfection control of 93RS2 Sertoli cells. **a** 24 h after transfection, transfected (**a**) and non-transfected (**b**) cells as negative control were fixed for IF experiments. *left* Incubation with rabbit anti-GFP antibody showed successful transfection of almost 80 % of cells. *right* No staining signal was detectable in non-transfected cells. *Scale bars* in main image: 200 µm, detail: 25 µm. DAPI counterstain. **b** Western Blot analysis revealed AR protein in transfected Sertoli cells at approx. 135 kDa (*1*) and in human testis tissue at the expected molecular weight of 110 kDa (*2*). The higher protein weight measured in transfected cells is due to coupling of AR with GFP. **c** Expression of human AR mRNA was tested in human testis homogenate (*1*), transfected (*2*) and non-transfected cells (*3*). AR mRNA was detected in the positive control and transfected 93RS2hAR17 cells, but not in non-transfected cells and the NTC (*lane 4*). **d** To control the CAG repeat length in transfected 93RS2 cells, we performed high-resolution PAGE. Three different passages of 93RShAR17 cells (*lanes 1–3*) were analysed and revealed a band for human AR at 185 bp by using two different DNA ladders. By sequencing, 185 bp was shown to be typical for the presence of 17 CAG repeats. *Lane 4* no template control (NTC)

genes showed higher gene expression values, whereas 472 revealed a lower gene expression in 93RShAR17 cells compared with non-transfected cells.

Hierarchical clustering of the 672 significantly regulated genes shows two clusters clearly differentiating between transfected and non-transfected cells (Fig. 3). Three biological replicates have been tested and show a homogeneous expression pattern, indicating high reproducibility of microarray results. An overview of the ten highest regulated genes for down- and up-regulation is given in Table 1. Complete array data may be found following the link provided [19].

"Development", "Hormone response" and "Immune response" are the predominant functions of the differently regulated genes

Of 370 annotated down-regulated genes, 330 could be assigned to DAVID functional categories, and 124 out of 142 annotated up-regulated genes, respectively.

An overview of the functional categories that have been inferred with DAVID is given in Table 2. Down-regulation is predominant in "Cell development/Cell contact", "Response to hormone stimulus" and "Nucleotide catabolic process", whereas regulation is evenly distributed in "Immune response". The highest score values are achieved by four

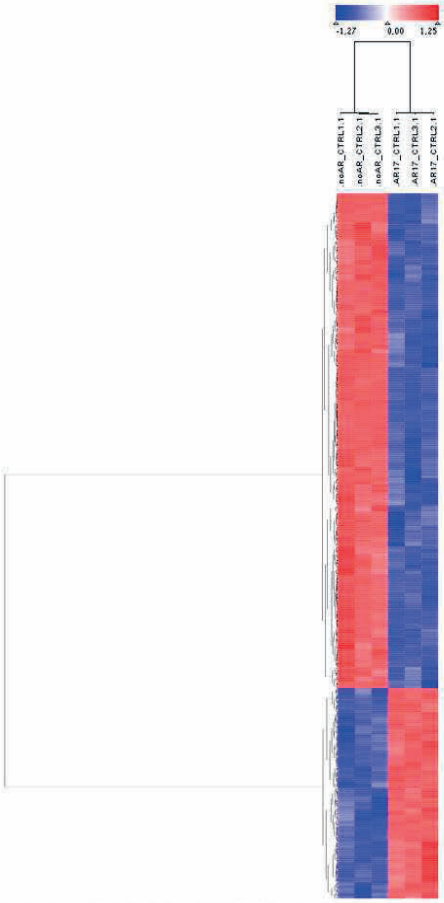

Fig. 3 Hierarchical clustering of 672 significantly altered genes. *Genes* are depicted in *rows* and samples in *columns*. *Blue* indicates down-regulation whereas red shows upregulation. Clustering was done using "Pearson correlation" and "complete linkage". The tree on the *left* reflects the distances between gene profiles based on this algorithm

significantly overrepresented gene ontology (GO) categories clustered under "Biological adhesion", whereas the highest number of genes is assigned to 15 GO categories grouped as a cluster named "Epithelium development". More than half of the functional assigned groups belong to cell development and cell contact while 25 % of the functionally assigned genes are related to immune response. 36 genes can be attributed to "Hormone stimulus" and a minority of 12 genes contributes to "Nucleotide catabolic process".

Upstream regulation analysis identified more activation than de-activation

Upstream regulation analysis with IPA is based on gene expression patterns and predicts activation or deactivation of regulators of the differentially regulated genes. The results show that more upstream regulators are predicted to be activated (n = 51) than inhibited (n = 20).

These predictions are based on 220 genes from which 95 contributed to activation as well as to deactivation. The proportion of overall down- and up-regulation is mirrored in these genes with more down-regulation in inhibition as well as in activation (Tables 3, 4, 5, 6). The majority of deactivated upstream regulators (8 out of 20) are classified as transcription regulators. Activation is mainly predicted for cytokines (14 out of 51).

Validation of microarray data by RT-qPCR

For validation of microarray results we performed RT-qPCR for 22 candidate genes, showing different ranges of regulation (up, down). Among the chosen genes, some are mainly associated with development and are known Sertoli cell markers, such as *Dhh* [20], *Gja1* [21], *Inhbb* [22], and *Tf* [23]. Other genes are markers for differentiation and proliferation (e.g. *Bambi* and *Tgfb1i1* [24]) and some are involved in apoptosis, such as *Myc* and *Tnfrsf1a* [25]. Results from RT-qPCR were mostly consistent with data from microarray analysis (Fig. 4). Relative gene expression was lower in transfected compared to non-transfected Sertoli cells in 13 of 22 cases. Gene expression of *Cdkn1a*, *Egr1*, *Fst*, *Gja1*, *Myc*, *Pmepa1*, *Ptsg2*, *Rarg* and *Tnfrsf1a* was higher in 93RShAR17 cells compared to *Ar*-deficient 93RS2 cells. In the latter case, it has to be mentioned, that differences of the means did not reach significance in four genes, due to high variability of C_q.

Discussion

To study the effects of androgens and AR/*Ar* on diverse cell culture systems and the relevance for cell biology, cell culture experiments were conducted in different human cell lines (e.g. breast cancer cells, adrenocortical carcinoma cells, murine skeletal muscle cells or liver carcinoma cells [9–12]). Also AR-deficient cell lines have been used, either transfected with AR [14, 15] or without [13]. Both groups working with transfected cell lines performed their experiments using either not stimulated [14] or mock-transfected cells [15] as negative controls. Moreover, Jacobsen et al. [26] showed, that transfection of MCF-7 breast cancer cells lead to severe differences in gene expression levels in distinct genes, depending on the transfection reagent used. Interestingly, transfection with a vector encoding for a reporter gene and a vector without insert, respectively, revealed no differences in gene expression. This implies, that the transfection procedure itself might alter gene expression in these cells. Therefore, we performed gene expression analysis with AR-transfected rat Sertoli cells using non-transfected

Table 1 Overview of ten highest ranked up- and down-regulated genes

Regulation	Identifier	Symbol	EntrezID	FDR	FC	Gene name	Comment
Down	Idx_R307_C32	*Cybrd1*	295,669	0.001	−107,712	Cytochrome b reductase 1	Expression of the ferric reductase is regulated by intracellular iron concentration and other facilitators of iron absorption, indicating that it responds to iron demand
Down	Idx_R293_C42	*Tmsbl1*	286,978	0.003	−71,936	Thymosin beta-like protein 1	Actin cytoskeleton organization
Down	Idx_R29_C52	*Nnat*	94,270	0.001	−50,214	Neuronatin	The effects of Nnat on inflammatory pathways in vitro and in vivo suggest a pathophysiological role of this new gene in diabetic vascular diseases
Down	Idx_R245_C71	*Fam46a*	300,870	0.006	−42,921	Family with sequence similarity 46, member A	
Down	Idx_R259_C49	*Ctsz*	252,929	0.003	−39,163	Cathepsin Z	Accounts for the lysosome's capacity to digest polyQ sequences. Cathepsins L and Z are important in defending against the accumulation and toxicity of polyQ proteins
Down	Idx_R322_C43	*Slc24a3*	85,267	0.003	−38,220	Solute carrier family 24 (sodium/potassium/calcium exchanger), member 3	
Down	Idx_R196_C66	*Nudt7*	361,413	0.004	−36,487	Nudix (nucleoside diphosphate linked moiety X)-type motif 7	
Down	Idx_R200_C18	*Marveld1*	309,375	0.001	−34,855	MARVEL domain containing 1	
Down	Idx_R240_C21	*Tpp1*	83,534	0.001	−32,489	Tripeptidyl peptidase I	
Down	Idx_R245_C74	*Tpp1*	83,534	0.001	−31,626	Tripeptidyl peptidase I	
Down	Idx_R47_C36	*Bhlhb9*	317,407	0.001	−30,042	Basic helix-loop-helix domain containing, class B, 9	
Up	Idx_R117_C7	*Irf7*	293,624	0.003	5540	Interferon regulatory factor 7	The crucial regulator of type I interferons (IFNs) against pathogenic infections, which activate IRF7 by triggering signaling cascades from pathogen recognition receptors (PRRs) that recognize pathogenic nucleic acids
Up	Idx_R14_C99	*Apol9a*	503,164	0.003	5611	Apolipoprotein L 9a	
Up	Idx_R252_C110	*Usp18*	312,688	0.003	5976	Ubiquitin specific peptidase 18	
Up	Idx_R317_C53	*Usp18*	312,688	0.003	6264	Ubiquitin specific peptidase 18	
Up	Idx_R74_C32	*Wfdc18*	171,059	0.004	6291	WAP four-disulfide core domain 18	
Up	Idx_R53_C102	*Ripk4*	304,053	0.001	6479	Receptor-interacting serine-threonine kinase 4	
Up	Idx_R278_C80	*Ccl4*	116,637	0.006	7177	Chemokine (C–C motif) ligand 4	
Up	Idx_R188_C91	*Oas1b*	246,268	0.003	7827	2–5 oligoadenylate synthetase 1B	
Up	Idx_R192_C96	*Ffar4*	294,075	0.004	9720	Free fatty acid receptor 4	
Up	Idx_R299_C11	*Il33*	361,749	0.002	9759	Interleukin 33	IL-33 is a dual function protein that may function as a proinflammatory cytokine and an intracellular nuclear factor with transcriptional regulatory properties
Up	Idx_R66_C107	*Il33*	361,749	0.001	10,690	Interleukin 33	

Table 1 continued

Regulation	Identifier	Symbol	EntrezID	FDR	FC	Gene name	Comment
Up	Idx_R102_C39	*Mx1*	24,575	0.004	12,708	Myxovirus (influenza virus) resistance 1	The human myxovirus resistance protein 1 is a key mediator of the interferon-induced antiviral response against a wide range of viruses. MxA may form oligomeric rings around tubular nucleocapsid structures. As a consequence, these viral components are trapped and sorted to locations where they become unavailable for the generation of new virus particles

Table 2 Overview of functional gene ontology categories according to their pattern of significantly regulated genes

Group	Cluster#	Cluster of GO categories	Score		Symbols
Cell development/cell contact [106]	1	Biological adhesion (4) [25]	2.27	Up	*Vnn1, Amigo2, Bcam, Cdh2, Ceacam1, Col12a1, Col14a1, Col16a1, Dsg2, Gpc1, Mcam, Omd, Sned1, Col18a1, Ctgf, Gpr56, Ncam1, Igfbp7*
				Down	*Itgb8, F5, Pcdh1, Pcdh18, Plcxd2, Ptprm, Ctgf*
	3	Axonogenesis (13) [36]	1.89	Up	*Aldh1a2, Apbb1, Apoe, Boc, Cd24, Cdkn1c, Chn2, Col18a1, Col18a1, Cxcl12, Efna2, Efnb1, Fgfr2, Gli2, Gpc2, H19, Hoxc10, Krt19, Lpar3, Nnat, Nrep, Obsl1, Pmp22, Ppp1r9a, Prickle2, Sdc2, Sema4f, Shroom3, Sox5, Uchl1*
				Down	*Ptprm, Epha7, Dpysl3, Mtss1, Nes, Sgk1*
	4	Retinoid metabolic process (5) [8]	1.75	Up	*Akr7a3, Aldh1a2, As3mt, Ldhb, Rarres2, Rbp1*
				Down	*Crabp2, Rbp2*
	7	Epithelium development (15) [50]	1.47	Up	*Acp5, Adamts1, Adck3, Aldh1a2, Celsr1, Col18a1, Col1a1, Col4a1, Cxcl12, Disp1, Efna2, Efnb1, Fbn1, Fgfr2, Foxe1, Foxl2, Gli2, H19, Hmx2, Hoxc10, Irf6, Kazn, Mgp, Mn1, Mycn, Pgf, Plce1, Serpinf1, Sfrp2, Shroom3, Sox5, Spry1, Srgn, Tbx18, Tbx4, Tek, Tgfb1i1, Tgm2, Upk1b*
				Down	*Ctgf, Crabp2, Fst, Ptger2, Rsad2, Cdx2, Hoxb6, Krt14, Ptgs2, Foxp2, Myc*
H [36]	2	Response to steroid hormone stimulus (10) [36]	1.90	Up	*Acp5, Adamts1, Adck3, Aldh1a2, Apoe, Boc, Cd24, Celsr1, Col1a1, Cxcl12, Disp1, Efna2, Efnb1, Fgfr2, Gli2, Gpr56, H19, Igfbp7, Krt19, Lpar3, Mgp, Ncam1, Nnat, Pgf, Plce1, Sdc2, Serpinf1, Sfrp2, Tek, Tgfb1i1, Tgm2*
				Down	*Foxp2, Myc, Nes, Ptgs2, Sgk1*
Immune response [55]	5	Innate immune response (4) [34]	1.69	Up	*Acp5, Adck3, Afap1l2, Apbb1, C2, Cd24, Cxcl12, Cyp4f6, Il27ra, Masp1, Ptpn6, RT1-DMb, Tf, Tgm2, Tinagl1, Tlr2, Vnn1, Zfr2*
				Down	*A2 m, C3ar1, Ccl2, Ccl4, Ereg, F2rl1, Gch1, Il1rl1, Irf7, Irgm, Nppb, Oas1b, Oasl2, Prg4, Ptgs2, Rsad2*
	8	Cell surface receptor linked signal transduction (3) [25]	1.35	Up	*Adamts1, Adck3, Apoe, Boc, Cd24, Celsr1, Cxcl12, Disp1, Efna2, Efnb1, Fgfr2, Gli2, Gpr56, Lpar3, Ncam1, Plce1, Sfrp2, Tek, Tgfb1i1, Tgm2*
				Down	*Ctgf, Epha7, Fst, Itgb8, Ptger2*
N [12]	6	Nucleotide catabolic process (7) [12]	1.47	Up	*Akr7a3, Ampd3, Gucy1b3, Nt5e, Nudt7, Pde4a, Pde4b, Prodh*
				Down	*Gch1, Nppb, Ppat, Upp1*

Numbers in normal brackets denote the number of grouped GO categories. Absolute numbers of regulated genes per main group are given in squared brackets, examples of regulated genes are shown for up- and down-regulated genes

H hormone stimulus, *N* Nucleotide Catabolic Process

cells as controls to show "intrinsic" gene expression alterations due to the transfection procedure. As electroporation has been shown to be superior with respect to cell viability and also transfection efficiency compared to chemical transfection using lipofectamine [27], we applied this technique to introduce the AR. Cell viability was not influenced by electroporation, but whole genome microarray analysis showed an altered gene expression. Surprisingly, more genes have been down-regulated than up-regulated comparing transfected and non-transfected cells. We selected 22 genes showing an altered expression pattern and confirmed microarray results with RT-qPCR analysis. In the following, we will discuss in more depth interesting genes and pathways, respectively.

Among the down-regulated genes, many are involved in metabolic processes, as for example in iron transport and metabolism (cytochrome b reductase 1 (*Cybrd1*), FC = −107; transferrin (*Tf*), FC = −6,898;

Table 3 Upstream regulator analysis with IPA: types of predicted upstream regulators

Activation (n = 51)		Inhibition (n = 20)	
Cytokines/group of cytokines	14	Transcription regulator	8
Others/complex of others	8	Cytokine	2
Kinases, group of kinases	8	Enzyme	2
Growth factors/complex of growth factors	6	Other	2
Transcription regulator	6	G-protein coupled receptor	1
Transmembrene receptors	4	Growth factor	1
Enzymes	3	Ligand-dependent nuclear receptor	1
Ligand-dependent nuclear receptor	1	Peptidase	1
Peptidase	1	Phosphatase	1
		Transporter	1

Summarizing the regulator according to their type revealed a high proportion of possibly activated cytokines, whereas transcription regulators play a major role in inhibition

Based on gene expression patterns, predictions are made on activation or inactivation of known upstream regulators. Absolute activation z-scores of higher than 2.0 are considered to be highly significant. We found more than twice as much regulators predicted to be activated as compared to inhibited. These tables show the predicted upstream regulators with an absolute z-score above 2.0 in detail—some are in fact complexes or groups. The prediction is opposed to the real measurement on the micro array (rightmost columns), as far as the respective genes have passed QC and is otherwise marked as "not measured". Mean expression per group is given as logarithm of the intensity to base 2. Reasonably high expression values are in bold face. The column "regulation AR17" denotes if the respective gene is contained in the set of regulated genes (level = L1) or at least close to significance (level = L2/L3) which holds true for the minority of genes. Activation or inhibition is not necessarily reflected by significant change of gene expression, since processes not measurable on a micro array, like for example phosphorylation, are more likely to be responsible for that

Table 4 Upstream regulator analysis with IPA: proportion of up- and downregulated genes

Gene pattern	Activation only	Inhibition only	Both
Down regulation	64	28	50
Up regulation	28	5	45

The gene expression patterns upon which the prediction is made is constituted by both up-regulated and down-regulated genes. The predicted activation and inhibition is either based on two third down regulated (n = 114/n = 78) and one third upregulated genes (n = 73/n = 50). 50 downregulated genes and 45 upregulated genes contribute likewise to activation and inhibition (The details of the contributing gens are not shown here)

Based on gene expression patterns, predictions are made on activation or inactivation of known upstream regulators. Absolute activation z-scores of higher than 2.0 are considered to be highly significant. We found more than twice as much regulators predicted to be activated as compared to inhibited. These tables show the predicted upstream regulators with an absolute z-score above 2.0 in detail—some are in fact complexes or groups. The prediction is opposed to the real measurement on the micro array (rightmost columns), as far as the respective genes have passed QC and is otherwise marked as "not measured". Mean expression per group is given as logarithm of the intensity to base 2. Reasonably high expression values are in bold face. The column "regulation AR17" denotes if the respective gene is contained in the set of regulated genes (level = L1) or at least close to significance (level = L2/L3) which holds true for the minority of genes. Activation or inhibition is not necessarily reflected by significant change of gene expression, since processes not measurable on a micro array, like for example phosphorylation, are more likely to be responsible for that

six-transmembrane epithelial antigen of the prostate 2 (*Steap2*), FC = −2.3). Iron is relevant for Sertoli cells in two different aspects: as supervisors of germ cell development, Sertoli cells provide iron which is needed for DNA synthesis and cell growth of germ cells that undergo multiple mitotic divisions [28]. On the other hand, Sertoli cells avoid toxic environmental conditions that might be given at elevated concentrations of insoluble ferric iron (Fe^{3+}). Therefore, Sertoli cells secrete transferrin, the product of the *Tf* gene [29], which may be used as a marker for Sertoli cell function and differentiation [23] as it creates an environment low in free iron that impedes bacterial survival in a process called iron withholding. The protein level of *Tf* decreases in inflammation. The lower expression of *Tf* gene, which was confirmed in RT-qPCR (Fig. 4), could be interpreted as a sign of severe disturbance and inflammation of cells.

The latter is reflected by the high proportion of upstream regulators related to immune response (= cytokines and members of the MAP kinase signalling pathway) that are predicted to be activated (Table 3) and the presence of multiple immune response-related genes on top of the list in up-regulation (Table 1). "Immune response" is the second huge cluster of altered genes in our study, represented by e.g. prostaglandin-endoperoxidase synthase 2 (*Ptgs2*, FC = 3.558) also known as cyclooxygenase 2 (*Cox2*). An increase in *Cox2* expression was observed by Matzkin et al. [30] in Leydig cells of infertile men showing either hypospermatogenesis, Sertoli cell only syndrome or maturational arrest. By increased numbers of testicular macrophages, levels of interleukin 1β (*Il-1β*) are increased and activates *Ptgs2*, the key enzyme in prostaglandin synthesis culminating in inflammation. The expression of *Tf*, *Ptgs2* and interleukins is coupled in Sertoli cells; as shown by Yamaguchi et al. [31], incubation with cisplatin lead to an increase in *Ptgs2* and a decrease in *Tf* expression in Sertoli cell cultures, similar to our study. Additionally, an analysis of upstream regulation using IPA revealed a high number of key players in inflammation to be activated showing congruently high FCs for *Ccl5*, *Irf7*, and *Ifnb1*. This might on the one side be due to the transfection procedure itself and/or reflect inflammatory processes in the cells due to increased cell damage. Remarkably, an influence of molecular biological techniques on gene expression and immune response has been observed also in regard to short-interfering RNAs (siRNAs). Sledz et al. reported an induction of interferon β levels in a human glioblastoma cell line which was transfected with siRNAs as a non-specific side effect additionally to the silencing of the target gene lamin [32] .

Table 5 Upstream regulator analysis with IPA: predicted activated regulators

IPA–prediction			Micro array analysis				
Upstream regulator	Molecule type	z-score	FDR	FC	Mean AR17	Mean noAR	Regulation AR17 [level]
Ahr	Ligand-dependent nuclear receptor	*3.185*	0.895	−1.017	−1.219	−1.194	
Bmp6	Growth factor	*2.791*	0.011	−1.483	*2.595*	*3.164*	
Ccl5	Cytokine	*2.190*	0.016	2.529	*2.922*	*1.583*	[Up L3]
Ddx58	Enzyme	*2.789*	0.019	2.096	*3.316*	*2.249*	[Up L3]
Dock8	Other	*2.530*	0.010	−1.656	*2.545*	*3.272*	[Down L2]
Egf	Growth factor	*2.539*		*<not measured>*			
Erk:	Group of kinases (n=7)	*2.372*			*<group>*		
Mapk1	Kinase		0.009	−1.019	*3.670*	*3.697*	
Mapk3	Kinase		0.027	−1.280	*5.646*	*6.002*	
Mapk4	Kinase		0.701	1.086	−2.321	−2.440	
Mapk6	Kinase		0.037	1.131	*5.152*	*4.975*	
Mapk7	Kinase		0.758	−1.047	*2.862*	*2.928*	
Mapk12	Kinase		0.018	−2.005	0.121	1.125	[Down L3]
Mapk15	Kinase		0.208	1.217	*0.507*	0.224	
Mek:	Group of kinases (n=7)	*2.942*			*<group>*		
Map2k1	Kinase		0.105	1.182	*4.651*	*4.410*	
Map2k2	Kinase		0.177	1.090	*4.816*	*4.691*	
Map2k3	Kinase		−1.066	−0.092	*4.360*	*4.452*	
Map2k4	Kinase		1.023	0.032	*3.336*	*3.303*	
Map2k5	Kinase		−1.058	−0.082	*3.327*	*3.408*	
Map2k6	Kinase		1.177	0.235	*3.760*	*3.525*	
Map2k7	Kinase		−1.125	−0.170	−1.445	−1.275	
P38 Mapk:	Group of kinases (n= 5)	*2.624*			*<group>*		
Mapk1	Kinase		0.009	−1.019	*3.670*	*3.697*	
Mapk11	Kinase		0.087	−1.343	0.139	*0.565*	
Mapk12	Kinase			*<see above>*			
Mapk13	Kinase			*<not measured>*			
Mapk14	Kinase		0.046	−1.276	*3.242*	*3.594*	
Mapk2/1: group of	Kinases (n= 2)	*2.401*			*<group>*		
Map2k1	Kinase			*<see above>*			
Map2k2	Kinase			*<see above>*			
F7	Peptidase	*2.592*		*<not measured>*			
Fgf2	Growth factor	*2.085*	0.122	1.178	0.417	0.180	
Fos	Transcription regulator	*2.086*	0.069	−1.425	*2.972*	*3.482*	
Hras	Enzyme	*3.258*		*<not measured>*			
Ifn / Ifn alpha:	Group of groups						
Ifn:	Group of cytokines	*2.429*			*<group>*		
Ifn alpha:	Group of cytokines	*2.228*			*<group>*		
Ifna1	Cytokine		0.104	1.306	*2.728*	*2.343*	
Ifna2	Cytokine	*2.448*		*<not measured>*			
Ifna4	Cytokine	*2.236*		*<not measured>*			
Ifna5 - 8	cyTokine (n=4)			*<not measured>*			
Ifna10, 13, 14, 16, 17, 21	Cytokine (n=6)			*<not measured>*			
Ifnk	Cytokine			*<not measured>*			
Ifnw1	Cytokine			*<not measured>*			
Ifnz	Cytokine			*<not measured>*			
Ifn beta:	Group of cytokines (n=2)	*2.767*					
Ifnb1	Cytokine	*2.591*	0.079	2.953	−1.949	−3.511	
Il6	Cytokine	*2.443*	0.014	1.481	−0.730	−1.296	
Ifnar:	Group of transmembrane receptors	*2.749*			*<group>*		
Ifnar1	Transmembrane receptor			*<not measured>*			

Table 5 continued

IPA–prediction			Micro array analysis				
Upstream regulator	**Molecule type**	**z-score**	**FDR**	**FC**	**Mean AR17**	**Mean noAR**	**Regulation AR17 [level]**
Ifnar2	Transmembrane receptor			<not measured>			
Ifne	Cytokine	*2.219*		<not measured>			
Ifng	Cytokine	*2.811*		<not measured>			
Ifnl1	Cytokine	*2.764*		<not measured>			
Igf2	Growth factor	*2.213*	0.001	−9.285	*1.909*	*5.124*	[Down L1]
Ikbke	Kinase	*2.090*	0.013	−2.034	−1.262	−0.238	[Down L3]
Il1: group of	Cytokines (n=11)	*2.207*					
Il1b	Cytokine			<not measured>			
Il18	Cytokine	*2.372*	0.300	−1.056	*0.531*	*0.610*	
Il1f10	Cytokine		0.689	1.102	−2.284	−2.424	
Il1rn	Cytokine		0.009	1.812	0.062	−0.796	[Up L2]
Il33	Cytokine		0.001	10.690	*1.998*	−1.420	[Up L1]
Il17a	Cytokine			<not measured>			
Il36a	Cytokine			<not measured>			
Il36b	Cytokine			<not measured>			
Il36g	Cytokine			<not measured>			
Il36rn	Cytokine		0.019	1.393	*2.076*	*1.598*	
Il37	Cytokine			<not measured>			
Irf3	Transcription regulator	*3.157*	0.520	1.336	*3.450*	*3.033*	
Irf5	Transcription regulator	*2.934*	0.113	1.096	*1.321*	*1.188*	
Irf7	Transcription regulator	*3.901*	0.003	5.540	*5.574*	*3.104*	[Up L1]
Kras	Enzyme	*2.616*	0.191	−1.097	*3.119*	*3.253*	
Lh [Cga, Lhb]	Complex	*2.012*					
Lhb	Other		0.480	1.044	*2.593*	*2.530*	
Cga	Other		0.251	1.273	−0.193	−0.541	
Map3k7	Kinase	*2.375*	0.352	−1.067	*4.577*	*4.671*	
Mavs	Other	*2.630*	0.021	−1.231	*2.569*	*2.868*	
Pdgf bb	Complex	*3.491*			<group>		
Pdgfb	Growth factor			1.156	*2.037*	*1.828*	
Pdlim2	Other	*2.324*	0.003	1.346	*3.226*	*2.798*	
Samsn1	Other	*2.309*		<not measured>			
Sash1	Other	*2.530*		<not measured>			
Sphk1	Kinase	*2.172*	0.611	1.237	−0.033	−0.341	
Src	Kinase	*2.158*	0.033	1.348	*3.704*	*3.273*	
Stat1	Transcription regulator	*2.194*	0.013	1.375	*3.163*	*2.703*	
Stat2	Transcription regulator	*2.173*	0.535	1.067	*3.865*	*3.772*	
Tac1	Other	*2.153*	0.910	1.055	−2.385	−2.462	
Tgfa	Growth factor	*2.165*	0.586	1.088	*2.152*	*2.031*	
Ticam1	Other	*2.702*	0.574	−1.035	*3.646*	*3.696*	
Tlr3	Transmembrane receptor	*3.633*	0.049	−1.414	−0.244	0.256	
Tlr4	Transmembrane receptor	*3.175*		<not measured>			
Tlr9	Transmembrane receptor	*3.645*	0.249	1.134	*2.534*	*2.353*	
Tnfsf11	Cytokine	*2.168*	0.539	1.115	−0.643	−0.800	

Z-score < 2.0

Based on gene expression patterns, predictions are made on activation or inactivation of known upstream regulators. Absolute activation z-scores of higher than 2.0 are considered to be highly significant. We found more than twice as much regulators predicted to be activated as compared to inhibited. These tables show the predicted upstream regulators with an absolute z-score above 2.0 in detail—some are in fact complexes or groups. The prediction is opposed to the real measurement on the micro array (rightmost columns), as far as the respective genes have passed QC and is otherwise marked as "not measured". Mean expression per group is given as logarithm of the intensity to base 2. Reasonably high expression values are in bold face. The column "regulation AR17" denotes if the respective gene is contained in the set of regulated genes (level = L1) or at least close to significance (level = L2/L3) which holds true for the minority of genes. Activation or inhibition is not necessarily reflected by significant change of gene expression, since processes not measurable on a micro array, like for example phosphorylation, are more likely to be responsible for that

Table 6 Upstream regulator analysis with IPA: Predicted inactivated regulators

IPA–prediction			Micro array analysis				
Upstream regulator	**Molecule type**	**z-score**	**FDR**	**FC**	**Mean AR17**	**Mean noAR**	**Regulation AR17 [level]**
Ackr2	G-protein coupled receptor	*−3.162*	0.061	1.308	0.389	0.001	
Bcl6	Transcription regulator	*−2.353*	0.233	1.041	*1.031*	*0.973*	
Fbxo32	Enzyme	*−2.213*	0.797	1.048	−0.588	−0.655	
Gata2	Transcription regulator	*−2.965*	0.061	−3.356	−1.682	0.065	
Gdf2	Growth factor	*−2.400*		*<not measured>*			
Hmox1	Enzyme	*−2.425*	0.011	1.631	*3.108*	*2.402*	[Up L3]
Htt	Transcription regulator	*−2.828*	0.560	1.033	*2.380*	*2.334*	
Il10	Cytokine	*−2.394*		*<not measured>*			
Il1rn	Cytokine	*−3.108*	0.009	1.812	0.062	−0.796	[Up L2]
Irgm1	Other	*−2.236*		*<not measured>*			
Mitf	Transcription regulator	*−2.535*	0.081	−1.456	*2.487*	*3.029*	
Nkx2-3	Transcription regulator	*−2.183*	0.168	1.119	−1.622	−1.785	
Pparg	Ligand-dependent nuclear receptor	*−2.353*	0.009	−1.950	−0.203	0.761	[Down L2]
Runx2	Transcription regulator	*−2.137*	0.021	1.358	*4.291*	*3.850*	
Sftpa1	Transporter	*−2.111*	0.752	−1.087	−2.019	−1.899	
Shh	Peptidase	*−2.168*		*<not measured>*			
Socs1	Other	*−3.084*		*<not measured>*			
Socs3	Phosphatase	*−2.216*	0.591	1.111	−1.131	−1.283	
Sox9	Transcription regulator	*−2.219*		*<not measured>*			
Trim24	Transcription regulator	*−2.331*	0.119	−1.166	*2.191*	*2.413*	

Z-score < −2.0

Based on gene expression patterns, predictions are made on activation or inactivation of known upstream regulators. Absolute activation z-scores of higher than 2.0 are considered to be highly significant. We found more than twice as much regulators predicted to be activated as compared to inhibited. These tables show the predicted upstream regulators with an absolute z-score above 2.0 in detail—some are in fact complexes or groups. The prediction is opposed to the real measurement on the micro array (rightmost columns), as far as the respective genes have passed QC and is otherwise marked as "not measured". Mean expression per group is given as logarithm of the intensity to base 2. Reasonably high expression values are in bold face. The column "regulation AR17" denotes if the respective gene is contained in the set of regulated genes (level = L1) or at least close to significance (level = L2/L3) which holds true for the minority of genes. Activation or inhibition is not necessarily reflected by significant change of gene expression, since processes not measurable on a micro array, like for example phosphorylation, are more likely to be responsible for that

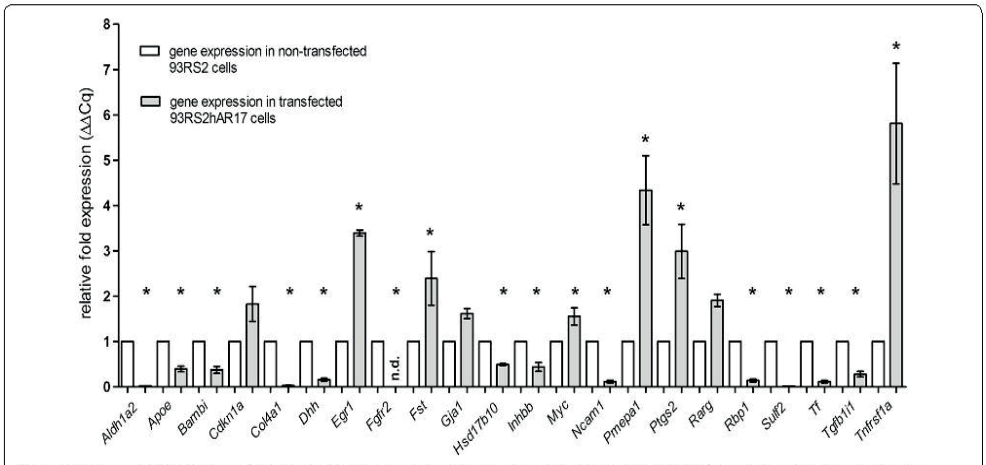

Fig. 4 Quantitative RT-PCR was performed to validate microarray analysis results. Gene expression analysis for 22 genes that showed deviant gene expression in microarray analysis has been performed using $2^{-\Delta\Delta Cq}$ method. RT-qPCR has been performed using three technical replicates in a double determination. Gene expression in non-transfected 93RS2 cells was used as calibrator and therefore set as "1". Data are presented as mean ± SEM. (standard error of the mean) and differences in mean values have been assessed with SPSS software; *p ≤ 0.05, *n.d.* not detectable

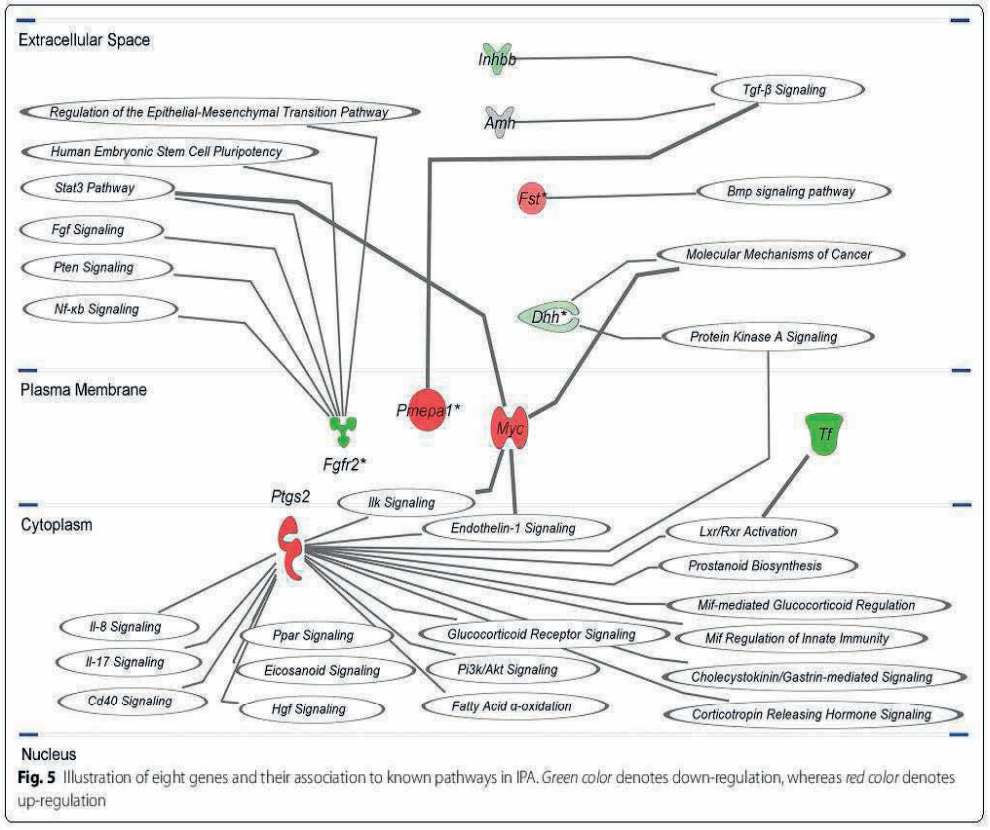

Fig. 5 Illustration of eight genes and their association to known pathways in IPA. *Green color* denotes down-regulation, whereas *red color* denotes up-regulation

Not only metabolism and immune response gene expression seem to be altered in transfected Sertoli cells, but also cell cycle and development genes (desert hedge hog (*Dhh*) FC = −2.032; fibroblast growth factor receptor 2 (*Fgfr2*) FC = −8.239; follistatin (*Fst*) FC = 2.162; inhibin beta b (*Inhbb*) FC = −3.126). *Dhh* is involved in various areas of embryonic development, including testicular cord formation. It is expressed in mouse Sertoli cell precursors during mid- to late gestation [33] and also is important for germ cell development after puberty in mouse [34] and rat testis [35]. In the mouse, a lack of *Dhh* results in a severe impairment of spermatogenesis due to a lack of spermatogonial development beyond primary spermatocytes [34]. *Fgfr2* is a known differentiation factor in prenatal Sertoli cells as it is concomitantly expressed with *Sry* and is essential for subsequent expression of anti-muellerian hormone (*Amh*) and *Sox9* [36]. IPA analysis of upstream regulation predicted an inhibition of transcription factor *Sox9* with a z-score of −2.2 (Table 6). Moreover, lack of *Fgfr2* might cause a partial XY sex reversal, as loss of *Fgfr2* leads to an up-regulation of Follistatin (*Fst*), a female somatic cell marker [37], which was confirmed by microarray and RT-qPCR. A down-regulation of the Sertoli cell marker *Inhbb* (for review see [38]) also points to a decreased Sertoli cell function and a severe disturbance of spermatogenesis in the rat [39]. Figure 5 shows the association of *Inhbb*, *Fst*, *Dhh*, *Pmepa1*, *Fgfr2*, *Ptgs2*, *Tf* and *Myc* as especially interesting genes on known pathways as predicted by IPA.

A disturbance of Sertoli cell function is also visible in gene expression alteration concerning the functional cluster "Cell adherence" or "Cell adhesion" (Fig. 6, e.g. collagen type IV alpha (*Col4a1*) FC = −12.503; gap junction protein 1 (*Gja1*) FC = −1.188). Cell adhesion and formation of tight junctions between Sertoli cells generating the blood-testis barrier is one of the most important features of Sertoli cell maturation and function (for review see [22]) as it is a prerequisite for intact spermatogenesis. Also cell-to-cell contact and communication seem to be disturbed in transfected cells as indicated by the down-regulation of *Gja1*, also known as connexin 43 (for review see [20]).

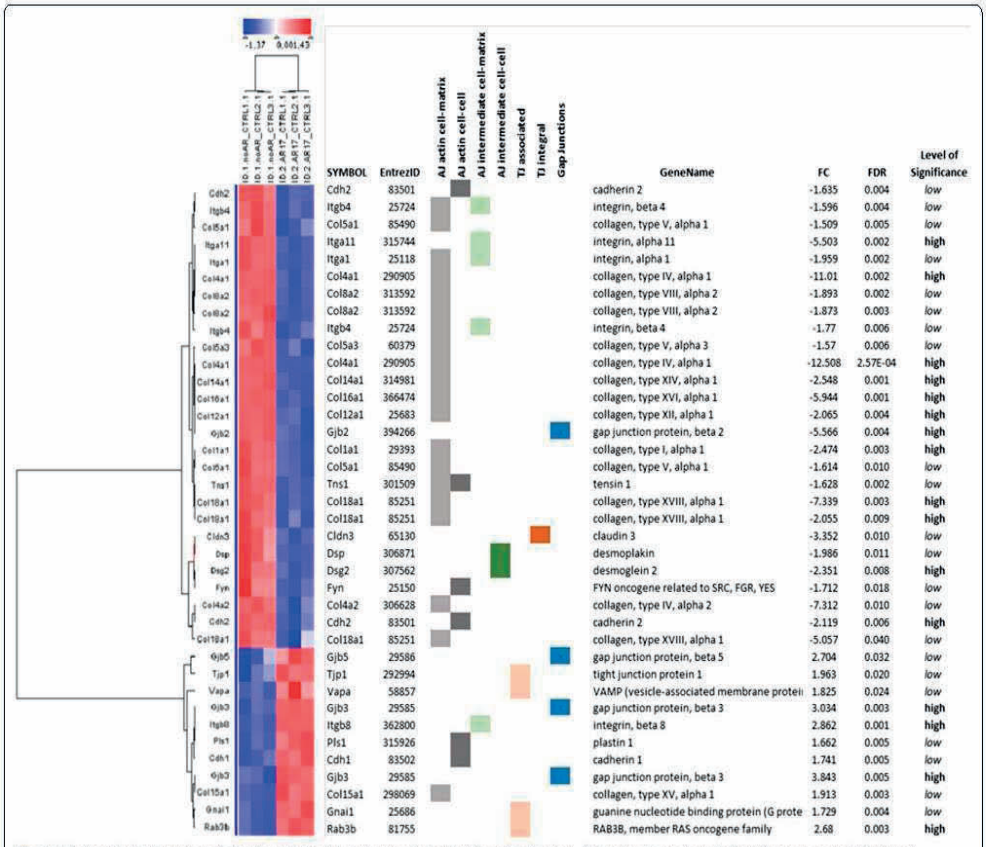

Fig. 6 Hierarchical clustering of significantly regulated genes involved in cell adhesion. Clustering was done using "Pearson correlation" and "complete linkage". The tree on the left reflects the distances between gene profiles based on this algorithm. AJ actin/intermediate = adherents junctions based on actin or intermediate filaments, TJ = tight junctions. Low significance: 1.5 < FC < 2.0 and/or FDR 0.01–0.05 High significance: FC > 2.0 and FDR < 0.01

Conclusion

Our results indicate a severe disturbance of Sertoli cell metabolism, function and cell biology concerning immune status and generation of blood-testis barrier, caused by the transfection procedure even without androgen stimulation of cells. The alterations in gene expression levels might either be related to the transfection procedure itself and/or to the insertion of human AR into *Ar*-free rat Sertoli cells. A microarray analysis with mock-transfected Sertoli cell line would be needed to distinguish both possibilities. We consider the altered gene expression to be caused by AR insertion, as many of the altered genes were identified as AR and Sertoli cell specific. In either case, incubation of transfected cell lines with testosterone or dihydrotestosterone might lead to false-positive or false-negative results and additionally, also non-genomic pathways including AR/*Ar* action may be altered by transfection procedures. Therefore, suitable negative controls are needed for stimulation experiments with T or DHT, i.e. non-transfected cells as appropriate negative controls. Gene expression has to be normalized by these non-transfected cells to avoid false-positive or false-negative results regarding gene regulation.

Methods

Cell lines and culture conditions, human positive control tissue

We determined the expression of *Ar* in different Sertoli cell lines by RT-PCR. For this study, we used four existing immortalized Sertoli cell lines from either mouse (WL3, SK-11) [40, 41] or rat testis (93RS2) [18] kindly provided by our collaborators. Additionally, SCIT-C8 cells were generated from immortalized Sertoli cells from rat testis as described by Konrad et al. [42]. We did not conduct

any animal research in our study and therefore ethics approval was not required. Total RNA of these cells was isolated by peqGold Total RNA Kit (Peqlab, Erlangen, Germany), set to a concentration of 200 ng/µl and genomic DNA was digested by RNase-Free DNase Set (Qiagen, Hilden, Germany). Reverse transcription was performed with Omniscript RT Kit (Qiagen). The mastermix was prepared as follows: 2 µl Buffer RT (10×), 2 µl dNTP mix (5 mM each), 0,7 µl RNAse inhibitor (20 units/µl, Invitrogen via LifeTechnologies, Carlsbad, CA, USA), 0,2 µl Oligo-dT primer (10 µM, Qiagen) and 1 µl Omniscript Reverse Transcriptase were mixed and RNase free water was added to a final volume of 10 µl. To test genomic DNA digestion success, we omitted reverse transcriptase and replaced it by RNase free water for one reaction. After addition of 1 µl RNA (200 µg/µl), we incubated the reaction mix for 1 h at 37 °C. cDNA not directly used for further experiments was stored at −20 °C. Amplification of *Ar* was achieved with a matching primer pair for murine and rat *Ar* obtained from Eurofins MWG Operon (Huntsville, AL, USA) as can be seen in Table 7 and *Taq* PCR Master Mix Kit (Qiagen). Mastermix was prepared as follows: 34 µl *Taq* PCR Master Mix, forward and reverse primer (2,5 µl each) and RNase free water as well as 1 µl cDNA were mixed to a final volume of 50 µl. Amplification was performed with 1× 94 °C for 4 min, 35× (94 °C for 40 s, 60 °C for 45 s, 72 °C for 90 s) and 1× 72 °C for 5 min.

As the prepubertal rat Sertoli cell line 93RS2 proved to be devoid of *Ar*, we chose this cell line for further experiments. The cells were maintained in a 5 % CO_2 atmosphere at 34 °C. The standard culture media consists of DMEM high glucose mixed 1:1 with Ham's F-12 media plus 100 units/ml penicillin, 0,1 mg/ml streptomycin, 10 % FBS-Gold (total protein 3.0–4.5 g/dl), and 1 % ITS (1000 mg/l Insulin, 550 mg/l Transferrin, 0.68 mg/l Selenin). Unless otherwise stated, cell culture media were purchased from Invitrogen (via Life Technologies, Carlsbad, CA, USA).

Ethics, consent and permissions

For positive control used in RT-PCR and Western Blotting, we used testis homogenate from a patient showing normal spermatogenesis attending the andological clinic in Münster for re-fertilization surgery. After written informed consent, biopsies were taken under general anesthesia. The reported study has been approved by the Ethics committee of the Medical Faculty of the Justus Liebig University Giessen (decision 75/00 and 56/05).

AR transfection in 93RS2 Sertoli cells

We introduced a commercial available full length human AR (OriGene, Rockville, MD, USA), containing 17 CAG triplets, into the expression vector pcDNA 6.2 C-EmGFP (Invitrogen) after amplification of AR using GC-Rich PCR System (Roche, Basel, Switzerland), according to manufacturer's instructions. Transfection of 93RS2 cells was performed using the microporation system MP-100 (Peqlab). Cells were detached by Trypsin (PAA, Piscataway, NY, USA) and subsequently adjusted to 200,000 cells per well in a 6-well-plate. After re-suspending the cells in the provided buffer, plasmid DNA was added. We used a current strength of 1150 V for 20 ms with two pulses.

Validation of transfection success in 93RS2 by immunofluorescence, RT-PCR and Western Blotting

24 h after transfection, transfected cells (93RShAR17) were fixed in 6-well-plates with 4 % paraformaldehyde for 20 min at room temperature, washed three times with PBS and permeabilized with 0.1 % Triton x-100. After transferring the cells to a 12-well-plate and washing with PBS, unspecific binding sites were blocked with 3 % BSA (bovine serum albumin, Carl Roth GmbH + Co. KG, Karlsruhe, Germany) in TBST (Tris-Buffered Saline and Tween 20, Carl Roth) and washed again with PBS. The rabbit anti-GFP antibody (ab290, Abcam, Cambrigde, UK) was added in a dilution of 1:200. After incubation for 3 h and washing with PBS, goat anti-rabbit Alexa 488 antibody (Invitrogen) was added in a dilution of 1:200. After a final incubation for 1 h in the dark, cells were washed and embedded with Vectashield mounting medium with DAPI (H-1200, Vector Laboratories, Dossenheim, Germany). Transfection efficiency was evaluated using a fluorescence microscope (AxioPhot, Zeiss, Oberkochen, Germany). Western Blot analysis to prove antibody specificity and AR protein expression in transfected Sertoli cells was performed as described elsewhere [43]. Shortly, proteins extracted from cell lysates of transfected 93RS2 cells and human testis tissue were submitted to protein extraction using TRI Reagent® RNA Isolation Reagent (Sigma-Aldrich, St. Louis, MO, USA) according to Chomczynski [44]. Proteins were run on a 3–8 % Tris–acetate gel (Life Technologies, Carlsbad, CA, USA) for 75 min at 150 V and blotted on nitrocellulose membrane for 75 min at 30 V. A polyclonal rabbit anti-human AR antibody (sc-816, Santa Cruz Biotechnology Inc., Dallas, TX, USA) in a 1:500 dilution and a biotinylated goat anti-rabbit antibody (E0432, Dako, Glostrup, Denmark) in a 1:1000 dilution were used. As weight marker, we used HiMark™ Pre-Stained Protein Standard (Life Technologies). Signal detection was performed by incubating the membrane with Vectastain Elite ABC Standard Kit (Vector Laboratories, Inc., Burlingame, CA, USA) and TrueBlue™ Peroxidase Substrate (KPL, Gaithersburg, MD, USA). A negative control was performed by omitting the primary antibody.

To detect AR mRNA in transfected cells, we performed RT-PCR (primers may be seen in Table 7) as described earlier with minor changes concerning the cycling conditions: 1× 94 °C for 4 min, 35× (94 °C for 45 s, 55 °C for 45 s, 72 °C for 90 s) and 72 °C for 5 min resulting in a 591 bp amplicon. The CAG repeat length was confirmed using RT-PCR with subsequent high resolution polyacrylamide gel electrophoresis (PAGE) as described recently [45].

RNA isolation for microarray analysis

Total RNA of transfected 93RShAR17 cells as well as of non-transfected 93RS2 cells (using three technical replicates (N1-N3) each) was extracted using the peqGold total RNA kit (Peqlab) following manufacturer's instructions. The amount of RNA was measured on a BioPhotometer (Eppendorf, Hamburg, Germany) as follows: 93RS2 N1 2200 ng/µl, N2 2130 ng/µl and N3 1920 ng/µl and 93RS2hAR17 N1 990 ng/µl, N2 1150 ng/µl and N3 1065 ng/µl (each replicate with a total volume of 15 µl). RNA was stored after extraction until use at −80 °C and transported in liquid nitrogen. The quality of total RNA was checked on a 1 % agarose gel stained with ethidium bromide (Sigma-Aldrich) as well as on Agilent 2100 Bioanalyzer using Eukaryote Total RNA Nano Assay (Agilent Technologies, Santa Clara, CA, USA). For this purpose, RNA was diluted to a concentration of 300 ng/µl. Only high quality RNA samples were used for microarray analysis.

Microarray analysis

cRNA synthesis and hybridization

Extracted RNA was transcribed into biotinylated cRNA using MessageAmp™ II-Biotin *Enhanced* Kit (LifeTechnologies). Biotinylated cRNA again was quality checked on Agilent 2100 Bioanalyzer as stated above followed by cRNA fragmentation and finally hybridization on CodeLink Rat Whole Genome using the CodeLink Expression Assay Kit (GE Healthcare, Chalfont St. Giles, Buckinghamshire, UK). For this, 10 µg cRNA was diluted with nuclease-free water to final volume of 20 µl and mixed with 5 µl fragmentation buffer (taken from CodeLink iExpress iAmplify cRNA Prep & Hyb Kit, GE Healthcare) and fragmented at 94 °C for 20 min and subsequent cooling to 0 °C on ice. Hybridization solution was prepared by mixing hybridization buffer component A and B (taken from CodeLink iExpress iAmplify cRNA Prep & Hyb Kit), nuclease-free water and 25 µl fragmented cRNA. Denaturation of cRNA was performed at 90 °C for 5 min with subsequent cooling on ice. Hybridization reaction was carried out at 37 °C for 18 h. Subsequent washing was performed with 0.75 × TNT (1 M Tris–HCl, 5 M NaCl and 20 % Tween 20) buffer. Bioarrays were stained with Cy5™-streptavadin (GE Healthcare) and scanned using the GenePix® 4000 B scanner and the GenePix Pro 4.0 Software (Axon Instruments, Arlington, USA). Scan resolution was set to 5 microns. A total of $2 \times 3 = 6$ array images were subjected to data analysis. Spot signals of CodeLink bioarrays were quantified using the CodeLink System Software 5.0.0.31312 which generated local background corrected raw as well as median centred intra-slide normalized data.

Quality control of microarray data

The genes represented by probe sets were annotated using the biocLite package (BioConductor) with the library "rwgcod.db" for CodeLink Rat Whole Genome arrays. The intra-slide normalized data containing 35129 rows and 6 columns (200 k values) were processed by an automated workflow that includes omission of control genes (n = 1280), removal of genes with poor QC (n = 1300 values, 0.6 %) or negative sign (n = 1603 values, 0.8 %), removal of probe sets with too high proportion (≥50 %) of missing values per group (n = 203 probe sets, 0.5 %) or with not any group having at least 50 % of values flagged as "G = good" and 50 % values above threshold (n = 7177 probe sets, 21.2 %), removal of outliers (expression values deviating more than fourfold from the group median, n = 427 values, 0.3 %). A total of 26452 probe sets remained after quality control with 1257 probe sets (=4.7 %) containing 1235 missing values (=0.8 %).

Remaining missing values were imputed by probabilistic principal component analysis (PPCA) using the R-package pca Methods. Imputed dataset was quantile normalized using the R-package limma [46], and logarithm for the base 2 was calculated.

Differential gene expression

Students *t* test was applied and a false discovery rate (FDR) ≤0.01 was set for the significance level with an absolute fold change (FC) ≥2 between transfected and non-transfected cells.

Functional gene analysis: overrepresentation analysis

Enriched functional gene ontology (GO) categories within the differentially regulated genes were determined using DAVID version 6.7 [47, 48]. Functional annotation clustering as well as an enrichment score was calculated for each cluster.

Upstream regulation analysis

To identify the regulators responsible for the observed gene expression profiles, we performed prediction analysis for activation or inhibition of upstream regulators using the Ingenuity® Pathway Analyzer and the

Table 7 Primer sequences

Primer name	GenBank accession no.	Sequence (5′ ≥ 3′)		Amplicon length (bp)	RT-qPCR efficiency (%)
Ar	NM_013476	For	CACATCCTGCTCAAGGCGCTT	181	n.a.
	(mouse)	Rev	CCCAGAAAGGATCTTGGGCAC		
	NM_012502			181	n.a.
	(rat)				
AR	NM_000044	For	TATCCCAGTCCCACTTGTG	592	n.a.
		Rev	TCTCTCCCAGTTCATTGAGG		
Aldh1a2	NM_053896	For	TCAGACTTCGGGCTTGTAGC	125	94.3
		Rev	GGGCTCTGAGCATTTAAGGC		
Apoe	NM_001270681	For	TGATGGAGGACACTATGACG	188	105.8
		Rev	CATGGTGTTTACCTCGTTGC		
Bambi	NM_139082	For	CCATGCCCACTTTGGAATGC	126	128.0
		Rev	TTCTGCTGCTGTCATGCTGG		
Cdkn1a	NM_080782	For	CACAGGAGCAAAGTATGCCG	125	135.1
		Rev	GCGAAGTCAAAGTTCCACCG		
Col4a1	NM_0011350009	For	GGAGAACCTGGCAGTGATG	118	99.9
		Rev	CACCCTTGGAACCTTTGTC		
Dhh	NM_053367	For	TTGGCACTCCTGGCACTATC	124	102.2
		Rev	CGGGCATACTAGGCACAAAC		
Egr1	NM_012551	For	GTGGGAGAAAGTTTGCCAGG	125	111.3
		Rev	GTAGGAAGAGAGGGAAGAGG		
Fgfr2	NM_012712	For	CAGCTTCCCCAGATTACCTG	92	94.4
		Rev	CATTCGGCAAAAGATGACTG		
Fst	NM_012561	For	TCCAGTACCAGGGCAAATG	78	96.2
		Rev	TCTGATCCACCACACAAGTG		
Gja1	NM_012567	For	GTACGGGATTGAAGAGCACG	119	105.5
		Rev	TGTACCACTGGATGAGCAGG		
Hsd17b10	NM_031682	For	GAGGAAACTGCATATTTGCC	106	110.5
		Rev	TTGACAGCCACATCTATACG		
Inhbb	NM_080771	Rev	ACGGGTCAAGGTGTACTTCC	96	100.3
		For	AAGGTATGCCAGCCACTACG		
Myc	NM_0123603	Rev	TACATCCTGTCCGTTCAAGC	67	108.0
		For	GCCGTTTCCTCAGTAAGTCC		
Ncam1	NM_031521	Rev	ACGATGATGACTCCTCTACC	150	94.1
		For	GCGCATTCTTGAACATGAGC		
Pmepa1	NM_001107807	Rev	TGGTGATGGTGGTGATGATC	76	134.2
		For	CTGTGTCGGCTGATGAAGG		
Ptsg2	NM_017232	Rev	ACCGTGGTGAATGTATGAGC	104	98.4
		For	TCTTGTCAGAAACTCAGGCG		
Rarg	NM_001135249	Rev	TCACCAAGGTCAGCAAAGCC	125	141.9
		For	ACTGAACTTGTCCCACAGCC		
Rbp1	NM_012733	Rev	CTTCAGTGTGTTCAGAAGGG	117	87.9
		For	CTTGAACACTTGCTTGCAGG		
Rplp2	NM_001030021	Rev	TTGCCTCTTATCTGCTGGCC	110	103.4
		For	GTTGAGTCGTTCATCGTCCG		
Sulf2	NM_001034927	Rev	TTCCTGCCCAAGTATCAGC	108	111.5
		For	CCCAGAAGCGTCCTCTACAC		
Tf	NM_001013110	Rev	TGAGGTCTTGCCACAGAAGG	125	102.4
		For	CCACAACAGCATGAGAAGGG		

Table 7 continued

Primer name	GenBank accession no.	Sequence (5′ ≥ 3′)		Amplicon length (bp)	RT-qPCR efficiency (%)
Tgfb1i1	NM_001191840	Rev	ACTACATCTCGGCACTCAGC	101	106.5
		For	ACCCTCGTGCTCAAAGAAGC		
Tnfrsf1a	NM_013091	Rev	AAAGAGGTGGAGGGTGAAGG	128	101.7
		For	ACAGGATGACTGAAGCGTGG		
Ubc	NM_017314	Rev	GGCAAAGATCCAGGACAAGG	100	99.4
		For	TTGTAGTCTGACAGGGTGCG		

Sequence and RT-qPCR efficiency of primers used for the study

n.a. not applied

Ingenuity®Knowledge Base (IPA, Qiagen). Prediction is given as a z-score with >2 for activated and <2 for inactivated upstream regulators.

Validation of microarray results by quantitative RT-PCR (RT-qPCR)

For validation of microarray data, we performed RT-qPCR with 93RShAR17 and non-transfected 93RS2 cells for 22 genes (Table 7) that have been shown to be significantly altered in microarray analysis. All primer pairs obtained from MWG Operon have been validated in standard RT-PCR using rat testis as positive control. For this pupose, total RNA from rat testis was extracted using TRI Reagent® RNA Isolation Reagent (Sigma-Aldrich) according to Chomczynski [44]. Genomic DNA was digested by using DNase I (Roche). For this, 6,65 µl RNA (200 ng/µl) were incubated with 1 µl $MgCl_2$ (25 mM, Thermo Fisher Scientific), 1 µl DNase Buffer (Roche), 0,25 µl RNase inhibitor (40 units/µl, Thermo Fisher Scientific) and 1 µl DNase I for 25 min at 37 °C in a thermocycler. After a enzyme heat inactivation for 5 min at 75 °C, RNA was immediately reversely transcribed into cDNA. For this, 1,5 µl DNase-treated RNA was mixed with 1 µl 10x PCR Gold Buffer, 2 µl $MgCl_2$ (25 mM), 1 µl dNTP mix (each 2,5 mM), 0,5 µl random hexamer primer (50 mM), 0,5 µl RNase inhibitor (20 units/µl), 0,5 µl MultiScribe® Reverse Transcriptase (50 units/µl) and RNase free water to a final volume of 9 µl. All reagents were obtained from Thermo Fisher Scientific. For -RT control, reverse transcriptase was replaced by the same amount of RNase free water. Incubation was performed as follows: 8 min at 21 °C, 15 min at 42 °C and 5 min at 99 °C. cDNA was stored at −20 °C until use. For primer validation in standard RT-PCR, 1 µl cDNA was mixed with 2,5 µl 10× PCR Gold Buffer, 2 µl $MgCl_2$ (25 mM), dNTP mix (each 2.5 mM), 1 µl forward and reverse primer, respectively (each 10 pM), 0.125 µl AmpliTaq Gold® DNA Polymerase (5 units/µl) and RNase free water to a final volume of 25 µl. Cycling conditions were: 1× 94 °C for 9 min, 35× (94 °C for 45 s, 60 °C for 45 s, 72 °C for 45 s) and 72 °C for 5 min. Length of the resulting amplicons was checked in an agarose gel electrophoresis as described earlier. For RT-qPCR dilution series we used rat *Rplp* and *Ubc* as internal reference genes and performed triple determination in a decreasing 10- fold dilution series (undil., 1:10, 1:100). RT-qPCR efficiency (E) has been calculated using Bio-Rad CFX Manager version 3.1 (Bio-Rad) from the standard curve's slope and may be seen in Table 7. Reference genes have been determined by using a TaqMan® Array Rat Endogenous Control Plate (96-well, 32 reference genes pre-plated, Applied Biosystems via Thermo Fisher Scientific, Waltham, MA, USA).

For RT-qPCR, total RNA from transfected and non-transfected cells was extracted using peqGold Total RNA Kit (PEQlab) and reversely transcribed into cDNA as described above. As technical replicates we used cell pellets from three independent passages and for each specimen, double determination was performed using 1 µl of cDNA, 4 µl EvaGreen mastermix (no Rox) (Bio&Sell, Feucht, Germany), 0.6 µl forward and reverse primer each and 12.8 µl sterile aqua bidest to a final volume of 20 µl. RT-qPCR conditions were 1× 95 °C for 15 min, 40× (95 °C for 15 s, 60 °C for 30 s, 72 °C for 20 s) followed by melt curve analysis (1× 95 °C for 10 s, 65 °C to 95 °C, increment 0.5 °C for 5 s) on a CFX96 RealTime cycler (Bio-Rad Laboratories, Hercules, CA, USA). Relative gene expression was calculated by the $2^{-\Delta\Delta Cq}$ method, using *Rplp* and *Ubc* as internal reference genes. Expression levels represent x fold higher expression in the transfected than in the non-transfected cells (set as "1"). For statistical analysis, differences of the mean were assessed by ANOVA analysis. P-values of $p \leq 0.05$ are set as statistically significant. The C_q values for all transcripts may be seen in Additional file 1: Table S1.

Availability of supporting data

Complete microarray data may be found on GEO Accession Viewer database [19] with accession number GSE57653. Single Sertoli cell line data may be found under accession numbers GSM1385418 (Sertoli Cell

Line noAR_1), GSM1385419 (Sertoli Cell Line noAR_2), GSM1386001 (Sertoli Cell Line noAR_3), GSM1385420 (Sertoli Cell Line AR17_1), GSM1385421 (Sertoli Cell Line AR17_2), GSM1385422 (Sertoli Cell Line AR17_3). Raw data of RT-qPCR experiments can be seen in Additional file 1: Table S1.

Additional file

Addtional file 1: Table S1. Contains raw data (C_q values of reference and target genes) of quantitative RT-PCR analysis.

Abbreviations

93RS2, SCIT-C8: rat Sertoli cell lines; 93RShAR17: with human *AR* transfected 93RS cells; AIS: androgen insensitivity syndrome; *Amh*: anti-muellerian hormone; AR/*Ar*: androgen receptor; ARE: androgen responsive element; *Bambi*: BMP and activin membrane-bound inhibitor; *Ccl5*: chemokine (C–C motif) ligand 5; *Ckdn1a*: cyclin-dependent kinase inhibitor 1a; CDS: coding DNA sequence; *Col4a1*: collagen type IV alpha 1; *Cox2*: cyclooxygenase 2; *Cybrd1*: cytochrome b reductase 1; DBD: DNA binding domain; *Dhh*: desert hedgehog; DHT: dihydrotestosterone; *Egr1*: early growth response 1; FBS: fetal bovine serum; F.C: fold change; FDR: false discovery rate; *Fgfr2*: fibroblast growth factor receptor 2; *Fst*: follistatin; *Gja1*: gap junction protein alpha 1; GO: gene ontology; IF: immunofluorescence; *Ifnb1*: interferon beta 1, fibroblast; *Irf7*: interferon regulatory factor 7; *Il-1β*: interleukin 1β; *Inhbb*: inhibin beta B; IPA: Ingenuity® Pathway Analyzer; ITS: insulin-transferrin-selenin; TJ: tight junctions; LBD: ligand binding domain; *Myc*: myelocytomastosis oncogene; NTC: no template control; PAGE: polyacrylamide gel electrophoresis; PBS: phosphate buffered saline; *Pmepa1*: prostate transmembrane protein, androgen induced 1; PPCA: probabilistic principal component analysis; *Ptsg2*: prostaglandin-endoperoxide synthase 2; *Rarg*: retinoid acid receptor, gamma; *Rplp*: ribosomal protein l 16; RT-PCR: reverse transcription polymerase chain reaction; RT-qPCR: quantitative RT-PCR; SK-11: WL3 mouse Sertoli cell lines; *Smad 1*: SMAD familiy member 1; *Sox9*: *Sry*-box 9; *Sry*: sex determining reagion on Y chromosome; *Steap2*: six-transmembrane epithelial antigen of the prostate 2; T: testosterone; TBST: Tris-Buffered Saline and Tween 20; *Tf*: transferrin; *Tgfb1i1*: transforming growth factor beta 1 induced transcript 1; *Tnfrsf1a*: tumor necrosis factor receptor superfamily, member 1a; *Ubc*: ubiquitin c.

Authors' contributions

DF and MM drafted the manuscript and performed quantitative RT-PCR, microarray analysis and statistical analysis, respectively. DL performed screening for cell lines, transfection, and immunofluorescence staining. KL was responsible for study design and supervision of the transfection procedure; furthermore he was involved in cell line acquisition and cell culture experiments. GJ supervised transfection procedure as well and generously provided the AR-GFP construct. KS provided human testis material for positive control purposes. Both GJ and KS critically revised the manuscript. CT and HH participated in the design of microarray experiments and HH also helped to draft the manuscript. MB was responsible for study design, supervision and critically revised the manuscript. All authors read and approved the final manuscript.

Author details

[1] Institute of Veterinary Anatomy, Histology and Embryology, Justus Liebig University, Frankfurter Straße 98, 35392 Giessen, Germany. [2] Institute of Medical Microbiology, Justus Liebig University, Giessen, Germany. [3] Department of Gynecology and Obstetrics, Justus Liebig University, Giessen, Germany. [4] Department of Clinical Andrology, Centre for Reproductive Medicine and Andrology, University Clinic Münster, Münster, Germany.

Acknowledgements

The authors want to thank J. Vogelsberg and D. Zoltan for their skilful technical assistance. Cell lines were generously provided by Profs. Korach, Boekelheide and Gromoll. The presented study was funded by German Research Foundation (DFG KFO181, BE1061/7-1).

Competing interests

The authors declare that they have no competing interests.

Received: 3 August 2015 Accepted: 9 December 2015
Published online: 29 December 2015

References

1. Walker WH. Molecular mechanisms of testosterone action in spermatogenesis. Steroids. 2009;74(7):602–7.
2. Gelmann EP. Molecular biology of the androgen receptor. J Clin Oncol. 2002;20(13):3001–15.
3. Yong EL, Loy CJ, Sim KS. Androgen receptor gene and male infertility. Hum Reprod Update. 2003;9(1):1–7.
4. Coffey K, Robson CN. Regulation of the androgen receptor by post-translational modifications. J Endocrinol. 2012;215(2):221–37.
5. Bergh A, Damber JE. Immunohistochemical demonstration of androgen receptors on testicular blood vessels. Int J Androl. 1992;15(5):425–34.
6. Sertoli E. Dell' esistenza di particolari cellule ramificante nei cunalicoli seminiferi del testicoli umano. Morgagni. 1865;7:31–40.
7. Lee H, Chang C. Recent advances in androgen receptor action. Cell Mol Life Sci. 2003;60(8):1613–22.
8. Willems A, Batlouni SR, Esnal A, Swinnen JV, Saunders PTK, Sharpe RM, et al. Selective ablation of the androgen receptor in mouse sertoli cells affects sertoli cell maturation, barrier formation and cytoskeletal development. PLoS One. 2010;5(11):e14168.
9. Ortmann J, Prifti S, Bohlmann MK, Rehberger-Schneider S, Strowitzki T, Rabe T. Testosterone and 5 alpha-dihydrotestosterone inhibit in vitro growth of human breast cancer cell lines. Gynecol Endocrinol. 2002;16(2):113–20.
10. Jaroenporn S, Furuta C, Nagaoka K, Watanabe G, Taya K. Comparative effects of prolactin versus ACTH, estradiol, progesterone, testosterone, and dihydrotestosterone on cortisol release and proliferation of the adrenocortical carcinoma cell line H295R. Endocrinology. 2008;33(2):205–9.
11. Pronsato L, Boland R, Milanesi L. Testosterone exerts antiapoptotic effects against H2O2 in C2C12 skeletal muscle cells through the apoptotic intrinsic pathway. J Endocrinol. 2012;212(3):371–81.
12. Chen G, Li S, Dong X, Bai Y, Chen A, Yang S, et al. Investigation of testosterone, androstenone, and estradiol metabolism in HepG2 cells and primary culture pig hepatocytes and their effects on 17βHSD7 gene expression. PLoS One. 2012;7(12):e52255.
13. Yeh S, Hu Y, Wang P, Xie C, Xu Q, Tsai M, et al. Abnormal mammary gland development and growth retardation in female mice and MCF7 breast cancer cells lacking androgen receptor. J Exp Med. 2003;198(12):1899–908.
14. Szelei J, Jimenez J, Soto AM, Luizzi MF, Sonnenschein C. Androgen-induced inhibition of proliferation in human breast cancer MCF7 cells transfected with androgen receptor. Endocrinology. 1997;138(4):1406–12.
15. Yuan S, Trachtenberg J, Mills GB, Brown TJ, Xu F, Keating A. Androgen-induced inhibition of cell proliferation in an androgen-insensitive prostate cancer cell line (PC-3) transfected with a human androgen receptor complementary DNA. Cancer Res. 1993;53(6):1304–11.
16. Xiao Y, Karnati S, Qian G, Nenicu A, Fan W, Tchatalbachev S, et al. Cre-mediated stress affects sirtuin expression levels, peroxisome biogenesis and metabolism, antioxidant and proinflammatory signaling pathways. PLoS One. 2012;7(7):e41097.
17. Li Y, Chan SC, Brand LJ, Hwang TH, Silverstein KAT, Dehm SM. Androgen receptor splice variants mediate enzalutamide resistance in castration-resistant prostate cancer cell lines. Cancer Res. 2013;73(2):483–9.
18. Jiang C, Hall SJ, Boekelheide K. Development and characterization of a prepubertal rat Sertoli cell line, 93RS2. J Androl. 1997;18(4):393–9.
19. GEO Accession viewer. http://www.ncbi.nlm.nih.gov/gds/?term=GSE57653 Accession 15 May 2014.
20. Bitgood MJ, Shen L, McMahon AP. Sertoli cell signaling by Desert hedgehog regulates the male germline. Curr Biol. 1996;6(3):298–304.
21. Weider K, Bergmann M, Brehm R. Connexin 43: its regulatory role in testicular junction dynamics and spermatogenesis. Histol Histopathol. 2011;26(10):1343–52.

22. Sharpe RM, McKinnell C, Kivlin C, Fisher JS. Proliferation and functional maturation of Sertoli cells, and their relevance to disorders of testis function in adulthood. Reproduction. 2003;125(6):769–84.
23. Skinner MK, Schlitz SM, Anthony CT. Regulation of Sertoli cell differentiated function: testicular transferrin and androgen-binding protein expression. Endocrinology. 1989;124(6):3015–24.
24. Barakat B, Itman C, Mendis SH, Loveland KL. Activins and inhibins in mammalian testis development: new models, new insights. Mol Cell Endocrinol. 2012;359(1–2):66–77.
25. Ashe PC, Berry MD. Apoptotic signaling cascades. Prog Neuropsychopharmacol Biol Psychiatry. 2003;27(2):199–214.
26. Jacobsen L, Calvin S, Lobenhofer E. Transcriptional effects of transfection: the potential for misinterpretation of gene expression data generated from transiently transfected cells. Biotechniques. 2009;47(1):617–24.
27. Li F, Yamaguchi K, Okada K, Matsushita K, Enatsu N, Chiba K, et al. Efficient transfection of DNA into primarily cultured rat sertoli cells by electroporation. Biol Reprod. 2013;88(3):61.
28. Leichtmann-Bardoogo Y, Cohen LA, Weiss A, Marohn B, Schubert S, Meinhardt A, et al. Compartmentalization and regulation of iron metabolism proteins protect male germ cells from iron overload. Am J Physiol Endocrinol Metab. 2012;302(12):E1519–30.
29. Skinner MK, Griswold MD. Sertoli cells synthesize and secrete transferrin-like protein. J Biol Chem. 1980;255(20):9523–5.
30. Matzkin ME, Mayerhofer A, Rossi SP, Gonzalez B, Gonzalez CR, Gonzalez-Calvar SI, et al. Cyclooxygenase-2 in testes of infertile men: evidence for the induction of prostaglandin synthesis by interleukin-1β. Fertil Steril. 2010;94(5):1933–6.
31. Yamaguchi K, Ishikawa T, Kondo Y, Fujisawa M. Cisplatin regulates Sertoli cell expression of transferrin and interleukins. Mol Cell Endocrinol. 2008;283(1–2):68–75.
32. Sledz CA, Holko M, de Veer MJ, Silverman RH, Williams BR. Activation of the interferon system by short-interfering RNAs. Nat Cell Biol. 2003;5(9):834–9.
33. Bitgood MJ, McMahon AP. Hedgehog and Bmp genes are coexpressed at many diverse sites of cell-cell interaction in the mouse embryo. Dev Biol. 1995;172(1):126–38.
34. Clark AM, Garland KK, Russell LD. Desert hedgehog (Dhh) gene is required in the mouse testis for formation of adult-type Leydig cells and normal development of peritubular cells and seminiferous tubules. Biol Reprod. 2000;63(6):1825–38.
35. Mäkelä J, Saario V, Bourguiba-Hachemi S, Nurmio M, Jahnukainen K, Parvinen M, et al. Hedgehog signalling promotes germ cell survival in the rat testis. Reproduction. 2011;142(5):711–21.
36. Schmahl J, Kim Y, Colvin JS, Ornitz DM, Capel B. Fgf9 induces proliferation and nuclear localization of FGFR2 in Sertoli precursors during male sex determination. Development. 2004;131(15):3627–36.
37. Bagheri-Fam S, Sim H, Bernard P, Jayakody I, Taketo MM, Scherer G, et al. Loss of Fgfr2 leads to partial XY sex reversal. Dev Biol. 2008;314(1):71–83.
38. Valeri C, Schteingart HF, Rey RA. The prepubertal testis: biomarkers and functions. Curr Opin Endocrinol Diabetes Obes. 2013;20(3):224–33.
39. Pfaff T, Rhodes J, Bergmann M, Weinbauer GF. Inhibin B as a marker of sertoli cell damage and spermatogenic disturbance in the rat. Birth Defects Res B Dev Reprod Toxicol. 2013;98(1):91–103.
40. Mueller SO, Korach KS. Immortalized testis cell lines from estrogen receptor (ER) alpha knock-out and wild-type mice expressing functional ERalpha or ERbeta. J Androl. 2001;22(4):652–64.
41. Sneddon SF, Walther N, Saunders PTK. Expression of androgen and estrogen receptors in sertoli cells: studies using the mouse SK11 cell line. Endocrinology. 2005;146(12):5304–12.
42. Konrad L, Munir Keilani M, Cordes A, Völck-Badouin E, Laible L, Albrecht M, et al. Rat Sertoli cells express epithelial but also mesenchymal genes after immortalization with SV40. Biochim Biophys Acta. 2005;1722(1):6–14.
43. Weider K, Bergmann M, Giese S, Guillou F, Failing K, Brehm R. Altered differentiation and clustering of Sertoli cells in transgenic mice showing a Sertoli cell specific knockout of the connexin 43 gene. Differentiation. 2011;82(1):38–49.
44. Chomczynski P. A reagent for the single-step simultaneous isolation of RNA, DNA and proteins from cell and tissue samples. BioTechniques. 1993;15(3):532–4.
45. Fietz D, Geyer J, Kliesch S, Gromoll J, Bergmann M. Evaluation of CAG repeat length of androgen receptor expressing cells in human testes showing different pictures of spermatogenic impairment. Histochem Cell Biol. 2011;136(6):689–97.
46. Bolstad BM, Irizarry RA, Astrand M, Speed TP. A comparison of normalization methods for high density oligonucleotide array data based on variance and bias. Bioinformatics. 2003;19(2):185–93.
47. Dennis G, Sherman BT, Hosack DA, Yang J, Gao W, Lane HC, et al. DAVID: database for annotation, visualization, and integrated discovery. Genome Biol. 2003;4(5):P3.
48. Huang DW, Sherman BT, Lempicki RA. Systematic and integrative analysis of large gene lists using DAVID bioinformatics resources. Nat Protoc. 2009;4(1):44–57.

11. Anhang – Publikationen

5. D. Fietz, K. Bakhaus, B. Wapelhorst, G. Grosser, S. Günther, J. Alber, B. Döring, S. Kliesch, W. Weidner, C.E. Galuska, M.F. Hartmann, S.A. Wudy, M. Bergmann, J. Geyer. PLoS One 2013 8(5): e62638

OPEN ACCESS Freely available online

PLOS ONE

Membrane Transporters for Sulfated Steroids in the Human Testis - Cellular Localization, Expression Pattern and Functional Analysis

Daniela Fietz[1*9], Katharina Bakhaus[2 9], Britta Wapelhorst[1], Gary Grosser[2], Sabine Günther[1], Jörg Alber[2], Barbara Döring[2], Sabine Kliesch[3], Wolfgang Weidner[4], Christina E. Galuska[5], Michaela F. Hartmann[5], Stefan A. Wudy[5], Martin Bergmann[1], Joachim Geyer[2]

1 Institute for Veterinary Anatomy, Histology and Embryology, Justus Liebig University Giessen, Giessen, Germany, **2** Institute for Veterinary Pharmacology and Toxicology, Justus Liebig University Giessen, Giessen, Germany, **3** Department of Clinical Andrology, Centre for Reproductive Medicine and Andrology, University Hospital Münster, Münster, Germany, **4** Clinic for Urology, Pediatric Urology and Andrology, Justus Liebig University Giessen, Giessen, Germany, **5** Steroid Research and Mass Spectrometry Unit, Division of Paediatric Endocrinology and Diabetology, Center of Child and Adolescent Medicine, Justus Liebig University Giessen, Giessen, Germany

Abstract

Sulfated steroid hormones are commonly considered to be biologically inactive metabolites, but may be reactivated by the steroid sulfatase into biologically active free steroids, thereby having regulatory function via nuclear androgen and estrogen receptors which are widespread in the testis. However, a prerequisite for this mode of action would be a carrier-mediated import of the hydrophilic steroid sulfate molecules into specific target cells in reproductive tissues such as the testis. In the present study we detected predominant expression of the Sodium-dependent Organic Anion Transporter (SOAT), the Organic Anion Transporting Polypeptide 6A1, and the Organic Solute Carrier Partner 1 in human testis biopsies. All of these showed significantly lower or even absent mRNA expression in severe disorders of spermatogenesis (arrest at the level of spermatocytes or spermatogonia, Sertoli cell only syndrome). Only SOAT was significantly lower expressed in biopsies showing hypospermatogenesis. By use of immunohistochemistry SOAT was localized to germ cells at various stages in human testis biopsies showing normal spermatogenesis. SOAT immunoreactivity was detected in zygotene primary spermatocytes of stage V, pachytene spermatocytes of all stages (I–V), secondary spermatocytes of stage VI, and round spermatids (step 1 and step 2) in stages I and II. Furthermore, SOAT transport function for steroid sulfates was analyzed with a novel liquid chromatography tandem mass spectrometry procedure capable of profiling steroid sulfate molecules from cell lysates. With this technique, the cellular inward-directed SOAT transport was verified for the established substrates dehydroepiandrosterone sulfate and estrone-3-sulfate. Additionally, β-estradiol-3-sulfate and androstenediol-3-sulfate were identified as novel SOAT substrates.

Citation: Fietz D, Bakhaus K, Wapelhorst B, Grosser G, Günther S, et al. (2013) Membrane Transporters for Sulfated Steroids in the Human Testis - Cellular Localization, Expression Pattern and Functional Analysis. PLoS ONE 8(5): e62638. doi:10.1371/journal.pone.0062638

Editor: Andrew Wolfe, John Hopkins University School of Medicine, United States of America

Received November 16, 2012; **Accepted** March 23, 2013; **Published** May 8, 2013

Funding: The present study has been supported by German Research Foundation grant DFG FOR1369. The funders had no role in study design, data collection and analysis, decision to publish, or preparation of the manuscript.

Competing Interests: The authors have declared that no competing interests exist.

* E-mail: Daniela.Fietz@vetmed.uni-giessen.de

9 These authors contributed equally to this work.

Introduction

Sulfated steroid hormones for long have been merely regarded as biologically inactive steroid metabolites. However, increasing evidence came up during the last decades that hydrolysis of steroid sulfates catalyzed by the steroid sulfatase (StS) is an important alternative source of precursors for the local supply of estrogens and androgens via the so-called sulfatase pathway [1], [2]. In humans, StS has been identified as a valuable drug target for estrogen and androgen deprivation therapies in hormonal diseases [3]. Thus, in addition to the provision of steroid hormones by the secretory activity of a given cell or gland, a second system controlling the availability of biologically active steroids on the cellular level might be established due to the expression of StS and/or estrogen sulfotransferases in certain organs, like the testis [4], [5].

Across species, Leydig cells in adult testes are the primary source of testicular androgens and also estrogens via *de novo* biosynthesis [6]. Besides the free steroid forms, the human testis is also able to produce steroid sulfates including pregnenolone sulfate (PREGS), dehydroepiandrosterone sulfate (DHEAS) and testosterone sulfate [7], [8], [9]. The primary targets of the androgens in the testis are Leydig cells, Sertoli cells and peritubular cells, due to their expression of androgen receptor (AR) [10]. Furthermore, two isoforms of the estrogen receptor (ERα and ERβ) are expressed in the efferent duct epithelium and showed importance for fluid re-absorption [6], [11], [12]. Expression of ERα and ERβ mRNA and protein was also demonstrated in spermatogonia, primary spermatocytes (ERα) and Sertoli cells (ERβ) in the boar [13], as well as ERα mRNA in spermatogonia and primary spermatocytes in human, dog, mouse and horse [14], for review see [15].

Therefore, the testis is responsive not only to androgens, but also to estrogens.

In addition to free steroid hormones, the sulfated forms, like PREGS and DHEAS, may have regulatory function in the testis as they can be used as precursors for testosterone production [16], [17], [18], [19]. As it was shown that PREGS cleavage by StS in the human testis is principally concentrated in seminiferous tubules rather than in interstitial tissue, testosterone may be synthesized in the direct surrounding of germ cells [17]. Interestingly, in patients showing StS deficiency (recessive X-linked ichthyosis), a high proportion of males show associated testicular diseases including cryptorchidism and elevated steroid sulfate levels [20], [21]. This indicates that the recruitment of sulfated steroids over the sulfatase pathway might contribute to the maintenance of normal spermatogenesis in men [1].

Although the synthesis and cleavage of sulfated steroids was investigated in the testis, the question of how the negatively charged sulfated steroid hormones can pass through the cell membrane of specific target cells in the testis has not been answered. However, several membrane carriers exist in the testis that show transport activity for different kinds of anionic organic molecules including steroid sulfates [22], [23], [24]. Most of them, e.g. the members of the Organic Anion Transporting Polypeptide (OATP) family (Solute Carrier Family SLCO), have broad and overlapping substrate specificities [25], [26]. In contrast, the Sodium-dependent Organic Anion Transporter SOAT (Solute Carrier Family SLC10, member SLC10A6), identified by our group in 2004 [27], seems to be specific for the transport of steroid sulfates [28], [29]. SOAT was shown to be highly expressed in the human testis and, therefore, is a candidate carrier for the local supply of steroid sulfates in the testis. Besides SOAT, OATP6A1 (SLCO6A1) and OATP1C1 (SLCO1C1) as well as the Organic Solute Carrier Partner 1 (OSCP1) showed high expression in the testis. Only for mouse Oscp1 the cellular localization in the testis has been analyzed more closely to date and revealed differing expression in leptotene spermatocytes at stage IX onwards until step 15 spermatids [30], [31] or in the plasma membrane of Sertoli cells [32].

The aim of our study was to investigate the expression pattern and cellular localization of SOAT and other membrane carriers in the human testis and to quantify their expression in patients with impaired spermatogenesis. Furthermore, we aimed to identify the most relevant carrier for steroid sulfates in the testis and to verify inward-directed transport of the entire steroid sulfate molecule with liquid chromatography tandem mass spectrometry (LC-MS-MS) procedure that is capable of profiling intact steroid sulfates from cell lysates.

Materials and Methods

Ethics Statement

All testicular biopsies were taken after written informed consent under general anesthesia at the Department for Clinical Andrology, Center for Reproductive Medicine and Andrology at the University of Münster or at the Department of Urology at University Clinics Giessen-Marburg (UKGM) of Giessen. The reported study has been approved by the Ethics committee of the Medical Faculty of the Justus Liebig University Giessen (decision 187b/09). Cultured Sertoli cells (FS1) are derived from testis tissue of an adult man with Fraser syndrome (FS) and were obtained at the time of prophylactic gonadectomy after written informed consent [33].

Testicular Tissue and Histological Evaluation

We evaluated 44 testis biopsies, indicated because of normo- or hypergonadotropic azoospermia (for review see [34]) including patients with obstructive azoospermia after vasectomy. After surgery, testicular tissue was fixed by immersion in Bouin's solution and embedded in paraffin. For histological evaluation, 5 µm thick sections were cut, stained with hematoxylin and eosin and evaluated following score count analysis according to Bergmann and Kliesch [34]. For our study, testicular biopsies revealing normal spermatogenesis (nsp, n = 12), qualitatively intact but quantitatively reduced spermatogenesis (hypospermatogenesis, hyp, n = 5), arrest at the level of primary spermatocytes (sza, n = 13) or spermatogonia (sga, n = 5) as well as Sertoli cell only syndrome (SCO, n = 9) were used. Additionally, immortalized and cultured human Sertoli cells (FS1, kindly provided by Dr. V. Schumacher, Children's Hospital Boston, [33]) were used for quantitative RT-PCR experiments. Cells were cultured in DMEM high glucose (4.5 g/L, LifeTechnologies, Carlsbad, CA, USA), 20% fetal calf serum (FCS Gold, PAA, Pasching, Austria), 1% non-essential amino acids, 1% L-glutamine and 1% penicillin-streptomycin (LifeTechnologies). Incubation was conducted at a humidified atmosphere with 8.5% CO_2 and a temperature of 37°C.

Expression Pattern of SOAT, OATP6A1, OATP1C1 and OSCP1

Expression patterns of SOAT, OATP6A1, OATP1C1 and OSCP1 were examined by using human multiple tissue cDNA panels (BioChain, Newark, CA, USA). PCR amplification was achieved with TaqMan Gene Expression Assays (LifeTechnologies) for human SOAT, OATP6A1, OATP1C1, and OSCP1. Human β-actin and RNA polymerase II were used as endogenous controls (Table 1). For each specimen, triplicate determinations were performed using 5 µl of cDNA, 1.25 µl of the respective TaqMan Gene Expression Assay, 12.5 µl TaqMan Gene Expression Master Mix (LifeTechnologies) and aqua bidest to a final volume of 25 µl. Quantitative PCR was performed on an ABI Prism 7300 thermal cycler (Applied Biosystems, Darmstadt, Germany). Conditions were 1×95°C for 10 min and 45×(95°C for 15 s and 60°C for 1 min). Relative gene expression was calculated by the $2^{-\Delta\Delta CT}$ method. Expression levels represent x-fold higher expression in the given tissue than in the tissue with the overall lowest expression level (set as a calibrator).

Quantitative Real-time PCR from Testicular Biopsies

For quantitative analysis of SOAT expression in testis homogenates, quantitative real-time PCR amplification was achieved with TaqMan Gene Expression assays. Human β-actin and glyceraldehyde 3-phosphate dehydrogenase (GAPDH) were used as endogenous control (Table 1). For each specimen, triplicate determinations were performed using 3 µl of cDNA, 1 µl of the respective TaqMan Gene Expression Assay, 10 µl TaqMan Gene Expression Master Mix (LifeTechnologies) and aqua bidest to a final volume of 20 µl. Amplification was performed as outlined above. For quantitative analysis of OATP6A1 and OSCP1 expression, PCR amplification was achieved with the same primers as used for qualitative RT-PCR (Table 2). Detection was performed by SYBR Green and subsequent melting curve analysis to ensure specificity of PCR products. For each specimen, triplicate determinations were performed using 1 µl of cDNA, 10 µl of iQ SYBR Green Supermix (Bio-Rad Laboratories, Hercules, CA, USA), 0.6 µl of each primer and aqua bidest to a final volume of 20 µl. Quantitative real-time PCR was performed

Table 1. TaqMan Gene Expression Assays used for quantitative real-time RT-PCR amplification.

Target	RefSeq (NCBI database)	TaqMan Gene Expression Assay ID	amplicon (bp)
OATP6A1	NM_173488.3	Hs00542846_m1	63
OATP1C1	NM_017435.4	Hs00213714_m1	92
OSCP1	NM_145047.4	Hs00376771_m1	115
SOAT	NM_197965.2	Hs01399354_m1	119
β-actin	NM_001101.3	Hs99999903_m1	171
		Hs00357333_g1	77
GAPDH	NM_002046.3	Hs02758991_g1	93
RNA Pol II	NM_000937.4	Hs01108291_m1	86

doi:10.1371/journal.pone.0062638.t001

on CFX96 Real-Time Cycler (Bio-Rad). For OATP6A1 and OSCP1, conditions were 1×95°C for 3 min and 40×(95°C for 10 s, 60°C for 1 min) and melting curve analysis (1×95°C for 10 s, 65°C to 95°C, increment 0.5°C for 5 s). Relative gene expression was calculated by the $2^{-\Delta\Delta CT}$ method. Expression levels represent x-fold higher expression in the given sample than in the specimen with the overall lowest expression level (set as a calibrator). For statistical analysis, ANOVA was performed followed by a student's t-test (SPSS 19.0, IBM, Munich, Germany).

Carrier Expression in Testis Biopsies by Qualitative RT-PCR

Total mRNA from testis homogenate was extracted from Bouin fixed, paraffin embedded tissue using the RNeasy Micro FFPE Kit (Qiagen, Hilden, Germany) as recommended by the manufacturer. Subsequently, mRNA was incubated with RNase-free DNase I (10 U/L; Roche, Mannheim, Germany) and RNase Inhibitor (40 U/L; LifeTechnologies) to digest genomic DNA. cDNA was synthesized from 1.5 µl total mRNA by using 8.5 µl of RT-mix (GeneAmp Gold RNA PCR Core Kit, LifeTechnologies). Negative controls were performed by omitting the reverse transcriptase (RT) reaction. For RT-PCR, 5 µl of cDNA was added to 2 µl $MgCl_2$, 4 µl 10×PCR Gold Buffer, 0.25 µl GOLDAmplitaq (Life Technologies), 1 µl of each primer (10 µmol/L) and aqua bidest to a final volume of 25 µl. RT-PCR was performed by using specific primers for SOAT, OATP6A1, and OSCP1. Beta-actin primers were used for control of cDNA quality. All oligonucleotide primers were obtained from Eurofins MWG Operon (Ebersberg, Germany) and are listed in Table 2. RT-PCR conditions were 1×95°C for 5 min, 40×(95°C for 30 s, 57°C for 30 s and 72°C for 30 s) and 72°C for 7 min for SOAT amplification as well as 1×95°C for 5 min, 40×(95°C for 30 s, 60°C for 30 s and 72°C for 30 s) and 72°C for 7 min for OATP6A1 and OSCP1 amplification. PCR products were separated by 2% agarose gel electrophoresis and visualized by SYBR Green I staining (Sigma-Aldrich, St. Louis, MO, USA). For an isolated examination of seminiferous epithelia and interstitial cells, we performed laser-assisted cell picking (LACP) using paraffin-embedded tissue. Slices mounted on PALM membrane slides (MembranSlide 0.1 PEN, Zeiss, Oberkochen, Germany) were stained with hematoxylin. The tissue of interest was excised and catapulted by PALM MicroBeam system and PALM Robo Software (Zeiss, Oberkochen, Germany). Specimens of seminiferous tubules and interstitial tissue (consisting predominantly of Leydig cells, blood vessels and connective tissue) were picked and stored separately. Extraction of mRNA was performed using RNeasy FFPE Kit (Qiagen). Digestion of genomic DNA, first strand cDNA synthesis and RT-PCR were performed as outlined above.

Table 2. Primer sequences for qualitative RT-PCR.

Target	RefSeq (NCBI database)	Primer sequence (5′ → 3′)	amplicon (bp)
SOAT	NM_197965.2	ACCTGGTCCTGGAGTCTTC *for*	79
		GAATGGTCAGGCACACAAG *rev*	
SOAT ISH		CTGCTGGCACTTTTTACCC *for*	330
		GGCACCTTCTTCATTCACC *rev*	
OATP6A1	NM_173488.3	CTGACAAACTGCGTTCTCTG *for*	77
		TTGATGGTCCAGGAATAGTCC *rev*	
OSCP1	NM_145047.4	CATGTACAGCGTGAATCAGC *for*	96
		AAGAGGGTTTGGAGCAATG *rev*	
GAPDH	NM_002046.3	CCAGGTGGTCTCCTCTGACTTC *for*	81
		GTGGTCGTTGAGGGCAATG *rev*	
ß-actin	NM_001101.3	GCGAGAAGATGACCCAGATC *for*	84
		CGTACAGGGATAGCACAGC *rev*	

doi:10.1371/journal.pone.0062638.t002

Cellular Localization of SOAT mRNA by *in situ* Hybridization (ISH)

Digoxigenin (DIG)-labeled cRNA probes were generated as described previously [35]. Briefly, a 330 bp PCR product of SOAT was sub-cloned into the pCRII TOPO vector (LifeTechnologies) as recommended by the manufacturer. Primer pairs for PCR reaction were obtained from Eurofins MWG Operon (Table 2). The plasmid was transformed into One Shot Chemically Competent *E. coli* (LifeTechnologies), purified and sequenced by SRD (Scientific Research and Development, Bad Homburg, Germany). For the synthesis of cRNA probes, the plasmid was digested by using restriction enzymes *Not* I or *BamH* I (NEB, Schwalbach, Germany). Subsequently, *in vitro* transcription of plasmid DNA in cRNA was performed using 10×RNA-DIG Labeling Mix (Boehringer Mannheim, Mannheim, Germany) and RNA polymerases T7 and SP6 (Promega, Heidelberg, Germany). ISH was performed as described by Lekhkota et al. 2006 [13] with

minor changes. Deparaffinized and rehydrated testis sections (5 µm) were digested using 15 µg/ml proteinase K in 1×phosphate buffered saline (PBS, 137 mM NaCl, 2.7 mM KCl, 1.5 mM KH_2PO_4, 7.3 mM Na_2HPO_4) for 30 min at 37°C, post-fixed with 4% paraformaldehyde for 10 min, exposed to 20% acetic acid, and prehybridized in 20% glycerol for 1 h at room temperature. Afterwards, sections were incubated with the DIG-labeled sense or antisense cRNA probe. Both cRNAs were used at a dilution of 1:50 in hybridization buffer containing 50% deionized formamide, 10% dextran sulfate, 2× standard saline citrate (SSC), 1× Denhardt's solution, 10 µg/ml salmon sperm DNA, and 10 µg/ml yeast t-RNA (Sigma-Aldrich). Hybridization was performed overnight at 37°C in a humidified chamber containing 50% formamide in 2×SSC. Post-hybridization washes were performed in 4×SSC at 37°C. Subsequently, sections were incubated with an anti-DIG Fab antibody conjugated to alkaline phosphatase (Boehringer) overnight at 4°C. Staining was visualized by developing sections with NBT-BCIP solution in a humidified chamber protected from light. Finally, sections were mounted with Kaiser's glycerol gelatine (Merck, Darmstadt, Germany).

Detection of SOAT in the Testis by Immunohistochemistry and Immunofluorescence

Although several antibodies are commercially available for human SOAT, none were applicable for immunohistochemistry or Western blot analysis. Therefore, we generated two antibodies, the first one against the whole C-terminus of the human SOAT protein ($SOAT_{311–377}$ antibody) and the second one against the 16 C-terminal amino acids of the mouse Soat protein ($Soat_{329–344}$ antibody). Rabbits were immunized with these peptides by Eurogentec (Liège, Belgium). The rabbit antisera were affinity-purified against the immunizing peptides and immunoreactivity was verified by enzyme linked immunosorbent assay. Then, both antibodies were used for immunohistochemistry (IHC), immunofluorescence (IF) and Western blot (WB). For IHC, paraffin sections from four testes with normal as well as from six testes with impaired spermatogenesis were deparaffinized and rehydrated. Heat mediated antigen retrieval was performed in citrate buffer solution (pH 6) for 15 min in a common microwave oven. For inhibition of endogenous peroxidase activity, sections were incubated in 3% H_2O_2 solution in Tris buffer for 30 min. Subsequently, sections were treated with 5% bovine serum albumin (BSA) for 30 min and the $Soat_{329–344}$ antibody (dilution 1:20) was incubated at 4°C overnight. The biotinylated goat anti-rabbit E0432 antibody (Dako, Glostrup, Denmark, dilution 1:200) served as secondary antibody and was incubated at room temperature for 30 min. Immunoreactivity was visualized by peroxidase conjugated streptavidin (Vectastain Elite ABC Standard Kit Peroxidase) for 30 min at room temperature followed by AEC staining (Biologo, Kronshagen, Germany). For a negative control, the primary antibody was pre-incubated with a ~100-fold molar excess of the immunizing peptide. Sections were mounted with Kaiser's glycerol gelatine (Merck). For IF, we performed the same antigen retrieval and primary antibody incubation as outlined above, but used donkey anti-rabbit Cy3-coupled antibody (dianova, Hamburg, Germany, dilution 1:200) as the secondary antibody. Sections were counterstained with DAPI (4',6-diamidino-2-phenylindole dihydrochloride, Life Technologies) and mounted with Fluorescent Mounting Medium (Dako). Pre-incubation control was performed as outlined above. In addition to the detection of SOAT, we performed IHC and IF with a specific marker for the Golgi apparatus, Golgin A2 (GOLGA2), which is also known as GM130 [36].

Western Blot Experiments

For WB analysis of stably transfected SOAT-HEK293 cells, the cells were cultured to 100% confluence under standard conditions and pre-incubated with tetracycline (1 µg/ml, Carl Roth GmbH, Karlsruhe, Germany) to induce SOAT expression, as reported previously [29]. SOAT-HEK293 cells without tetracycline pre-treatment, as well as non-transfected HEK293 cells, were used as controls. For protein extraction, culture medium was removed and cells were washed with PBS. 400 µl ice-cold RIPA buffer (Sigma-Aldrich) mixed with protease inhibitor at a 1:100 dilution (Thermo Fisher Scientific, Waltham, MA, USA) were added to the cells. After 15 min on ice, cells were detached and mechanically destroyed, and left on ice for further 10 min. Then, the lyzed cells were centrifuged for 15 min at 13,000 rpm and 4°C. The supernatant was obtained and used for determination of the protein content. Afterwards, samples were mixed with 4× Lämmli buffer containing 20% ß-mercaptoethanol and separated on a 10% SDS-PAGE over night at 50 V. The gel was blotted on a nitrocellulose membrane using semi-dry electroblotting and protein transfer was controlled by placing the nitrocellulose membrane in Ponceau S (Sigma-Aldrich) for 5 min. After multiple washing with Tris-buffered saline TBS-T (137 mM NaCl, 10 mM Tris-HCl, pH 8.0, 0.05% Tween-20), the membrane was blocked for 1 h at room temperature under agitation in TBS-T with 5% dried non-fat milk (blocking solution). After removal of the blocking solution, the nitrocellulose membrane was incubated with the primary antibody in blocking solution (1:100 dilution) for 1 h at room temperature. After washing with TBS-T, the membrane was incubated with the peroxidase-conjugated goat IgG fraction to rabbit IgG secondary antibody (MP Biomedicals, Pioneer Place, Singapore), at a 1:5,000 dilution together with the Roti Mark Western-HRP-conjugate (1:5,000 dilution, Carl Roth) for 1 h at room temperature. After washing with TBS-T, the nitrocellulose membrane was incubated with Roti Lumin 1 and Roti Lumin 2 (Carl Roth) in a ratio of 1:1 for 1 min and exposed to Amersham Hyperfilm ECL High Performance chemiluminescence film (GE Healthcare, LifeSciences, Piscataway, NJ, USA).

Stably Transfected SOAT-, OATP6A1-, OSCP1-, and OATP1C1-HEK293 Cells

The recombinant human cell line T-REx-SOAT-HEK293 was established in 2007 and demonstrated the transport of sulfated steroid hormones [29]. Using the same method, here we generated stably transfected OATP6A1-, OSCP1-, and OATP1C1-HEK293 cell lines. Briefly, full length transcripts for OATP6A1 and OSCP1 were obtained by RT-PCR from human testis cDNA (BioChain) as a template. OATP1C1 was cloned from human brain cDNA (BioChain) because of its higher expression rate in this organ. The used primers are displayed in Table 3. Using the Phusion High Fidelity PCR Kit (Thermo Fisher Scientific) the PCR reactions were performed under the following thermocycling conditions: 1×98°C for 30 s, 10×(98°C for 10 s, 68°C (OATP6A1) or 62°C (OATP1C1, OSCP1) for 30 s, decreasing 0.5°C each cycle, and 72°C for 1 min) followed by 35×(98°C for 10 s, 63°C (OATP6A1) or 57°C (OATP1C1, OSCP1) for 30 s, 72°C for 1 min) and 72°C for 10 min. PCR products were visualized on a 1% agarose gel. The amplicons were excised from the gel and purified using Hi Yield PCR Clean-up+Gel-Extraction Kit (SLG, Gauting, Germany). In order to clone the full length transcript of each carrier via T/A cloning into the pcDNA5/FRT/TO TOPO or pcDNA5/FRT/V5-His TOPO vectors (LifeTechnologies), a 3′-deoxyadenosine-overhang was attached to the blunt ends of the carrier cDNAs by incubating the purified PCR-product with DyNAzyme II DNA Polymerase (Thermo Fisher Scientific) and

dATPs for 10 min at 72°C. All clones were sequence verified according to the following GenBank Accession Numbers: NM_173488 for OATP6A1, NM_017435 for OATP1C1 and NM_145047 for OSCP1. The carrier-pcDNA5 constructs were co-transfected with the Flp recombinase expression vector pOG44 into Flp-In T-REx 293 host cells by lipofectamine 2000 (Life-Technologies) transfection according to the manufacturers protocol. Stably transfected clones containing the gene of interest were selected by culturing in selective medium containing 150 µg/ml hygromycin and 50 µg/ml blasticidine (Carl Roth). After 14 to 16 days, single clones containing the full open reading frame of the respective carrier were selected and used for further experiments. Respective HEK293 cells were cultured in DMEM/F-12 medium (LifeTechnologies), supplemented with 10% FCS (Sigma-Aldrich), L-glutamine (4 mM), penicillin (100 units/ml), and streptomycin (100 µg/ml) at 37°C, 5% CO_2, and 95% humidity.

Immunofluorescence Microscopy of Stably Transfected Cell Lines

For immunofluorescence microscopy, cells were seeded on poly-D-lysine coated glass coverslips in 24-well plates with a density of 1×10^5 cells per well. SOAT expression was induced by tetracycline treatment (1 µg/ml). SOAT-HEK293 cells grown up in the absence of tetracycline were used as control as well as SOAT non-expressing cells (Flp-In-HEK293 cells) which were also maintained without tetracycline. After 72 h, cell medium was removed and cells were washed with PBS for 5 min. The following experimental steps were performed at room temperature. The cells were fixed with 2% paraformaldehyde in PBS for 15 min and subsequently permeabilized for 5 min in PBS buffer supplemented with 0.2% Triton X-100 and 20 mM glycine. After washing the cells with PBS for 5 min, cells were placed in blocking solution containing 20 mM glycine in PBS and 4% goat serum for 1 h. Afterwards, cells were incubated with the $SOAT_{311-377}$ antibody at a dilution of 1:100 in blocking solution for 1 h. Cells were washed three times with PBS and incubated with the Alexa Fluor 555-labeled goat anti-rabbit IgG secondary antibody (Life-Technologies) at 1:800 dilution in blocking solution for 1 h. After a final washing procedure, cells were covered with a DAPI/methanol solution containing 1 µg/ml DAPI and incubated for 1 minute. The cells were washed with methanol, air-dried and mounted on slides with ProLong Gold Antifade Reagent (Life-Technologies). Fluorescent imaging was performed on a Leica DM5500B microscope (Leica, Bensheim, Germany). Captured images were analyzed with the Leica Fluorescence Workstation software LAS AF 6000.

Transport Studies of Stably Transfected HEK293 Cells

All of the chemicals, unless otherwise stated, were obtained from Sigma-Aldrich. [^{3}H]DHEAS and [^{3}H]E1S were purchased from PerkinElmer Life Sciences (Waltham, MA, USA). For all transport studies, 24-well plates were coated with poly-D-lysine for better attachment of the cells. 1.25×10^5 cells per well were seeded and cultured with standard medium for 72 hours containing tetracycline (1 µg/ml) to induce the carrier expression. Cells without tetracycline pre-treatment and cells without the gene of interest were used as control. OATP1C1-HEK293 cells were not pre-treated with tetracycline as they constitutively express OATP1C1. Transport studies with SOAT-HEK293 cells were performed in the presence and absence of sodium (control). In the sodium-free transport buffer, sodium chloride was replaced by equimolar concentrations of choline chloride. Before starting the transport studies, cells were washed three times with PBS. After washing, cells were pre-incubated with transport buffer (142.9 mM NaCl, 4.7 mM KCl, 1.2 mM $MgSO_4$, 1.2 mM KH_2PO_4, 1.8 mM $CaCl_2$, and 20 mM HEPES, adjusted to pH 7.4 with KOH, 37°C) for 15 min. Transport studies were performed by incubating cells with 250 µl transport buffer containing the radiolabeled or non-radiolabeled compounds for 10 min at 37°C. Uptake studies were stopped by removing the transport buffer and washing the cells 5 times with ice-cold PBS. Afterwards, cells were lyzed in 1 N NaOH with 0.1% SDS and the cell-associated radioactivity was measured by liquid scintillation counting as described before [29]. For LC-MS-MS analysis of the transportates, cells were lyzed with water by three freeze-thaw cycles and uptake of the non-radiolabeled compounds androstenediol-3-sulfate, β-estradiol-3-sulfate (both purchased from Steraloids Fountain Limited, Malta), estrone-3-sulfate, and DHEAS was measured as described by Galuska et al. 2012 [37]. The protein content was calculated using the BCA protein assay kit from Novagen (EMD Biosciences, Madison, WI, USA).

Results

Expression Pattern of SOAT, OATP6A1, OATP1C1 and OSCP1 in Human Tissues

In order to systematically analyze the tissue mRNA expression levels of the carriers SOAT, OATP6A1, OATP1C1, and OSCP1 which previously showed high expression in the testis, we used comprehensive human cDNA panels. As shown in Fig. 1, SOAT was predominantly expressed in the testis and mRNA expression was also detected in skin, kidney, vagina, pancreas, adrenal gland and breast. Furthermore, OATP6A1 and OSCP1 were predominantly expressed in the testis with minor expression in the epididymis and fallopian tube, respectively. In contrast,

Table 3. Primers used for full length amplification of the carrier open reading frames.

Target	RefSeq (NCBI database)	Primer sequence (5′ → 3′)	amplicon (bp)
OATP6A1	NM_1743488.3	CAGGGTGAGCCATGTTCGTAG *for*	2186
		ACAATGATGATCCAGTTACAAGTCAG *rev*	
OATP1C1	NM_017435.4	ATAATGGACACTTCATCCAAAG *for*	2153
		AAGTGGAGGTTTCCTTGCCTG *rev*	
OSCP1	NM_145047.4	CTCGTTTCCAGCACCATGTC *for*	1166
		GGTCAGAACAGCTATAACTCA *rev*	

doi:10.1371/journal.pone.0062638.t003

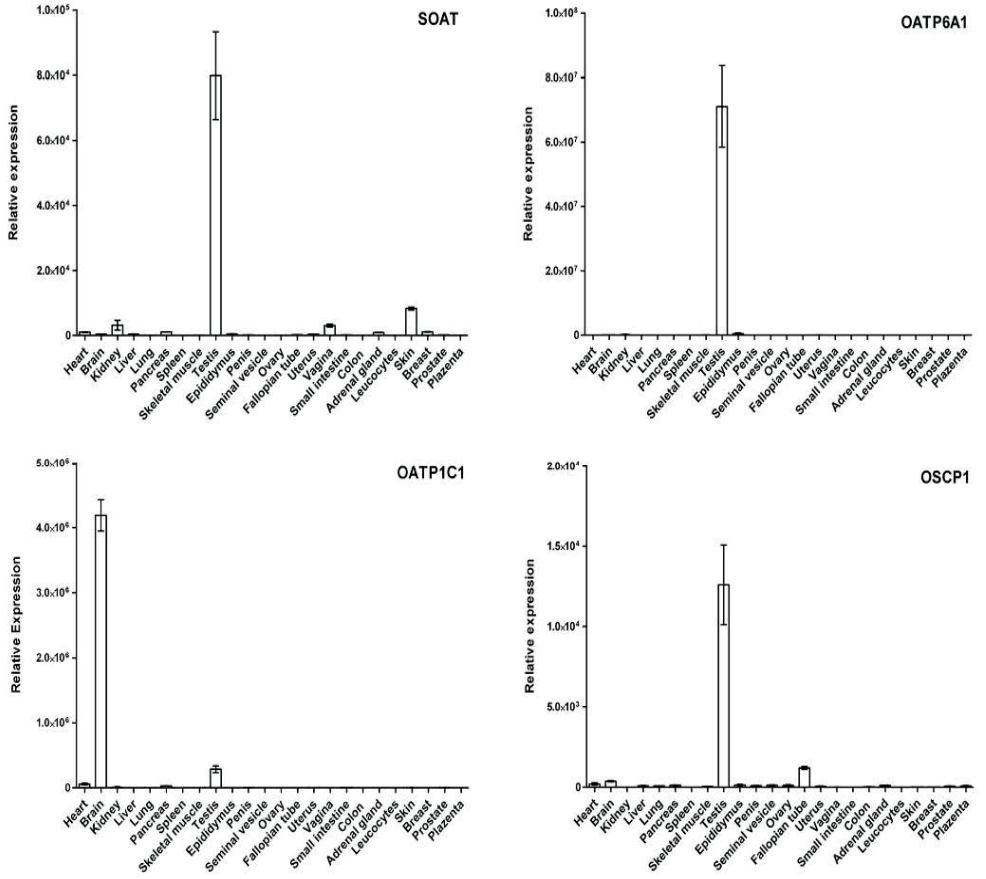

Figure 1. Expression pattern of SOAT, OATP6A1, OATP1C1 and OSCP1 in human tissues. Tissue expression of the indicated carriers was analyzed by quantitative real-time PCR. Relative expression depicted at the y-axis represents x-fold higher expression in the respective tissue compared to the tissue with the overall lowest expression among the tissue panel (set as calibrator). The values represent means ± SEM of triplicate determinations.
doi:10.1371/journal.pone.0062638.g001

OATP1C1 is predominantly expressed in the brain with further, but minor expression in the testis. Therefore, further expression analyses in the human testis focused on SOAT, OATP6A1 and OSCP1.

Quantitative Expression Analysis in Testicular Biopsies

The data from the tissue cDNA panels were further verified in testes biopsies showing intact normal spermatogenesis (nsp, n = 12), which all showed very high expression levels for SOAT, OATP6A1 and OSCP1 (Fig. 2). Interestingly, in patients with hypospermatogenesis (hyp), which is characterized as a quantitatively reduced but qualitatively preserved spermatogenesis, SOAT expression was significantly lower compared to nsp. Expression levels of OATP6A1 and OSCP1 were not significantly reduced in hyp. However, for all three carriers we found significantly lower or even absent mRNA expression in severe disorders of spermatogenesis, represented by an arrest at the level of spermatocytes (sza) or spermatogonia (sga), or even by a total loss of germ cells (Sertoli cell only syndrome, SCO). Similar to SCO, none of these carriers were detected in cultured Sertoli cells (FS1), indicating all of them to be expressed in germ cells.

Qualitative Expression Analysis following LACP of Testes Biopsies

In order to verify this assumption, we used qualitative RT-PCR analysis following LACP of testes biopsies from patients showing nsp or SCO. In this approach, interstitial tissue (encompassing Leydig cells, blood vessels and connective tissue; indicated by "Int") was separated from seminiferous tubules (containing peritubular cells, Sertoli cells and germ cells, indicated by "Tub"). All three carriers were only detected in the seminiferous tubules of patients with nsp, but not in tubules from SCO biopsies as well as in interstitial tissue. Therefore, germ cell specific expression of SOAT, OATP6A1 and OSCP1 was confirmed (Fig. 3).

Cellular Localization of SOAT in the Human Testis

For immunolocalization of the carrier proteins in the human testis several antibodies were considered and tested, but most of them were not applicable for immunohistochemistry or showed no specific staining pattern. In the case of SOAT, we obtained two antibodies from custom immunization (Eurogentec, Belgium). The

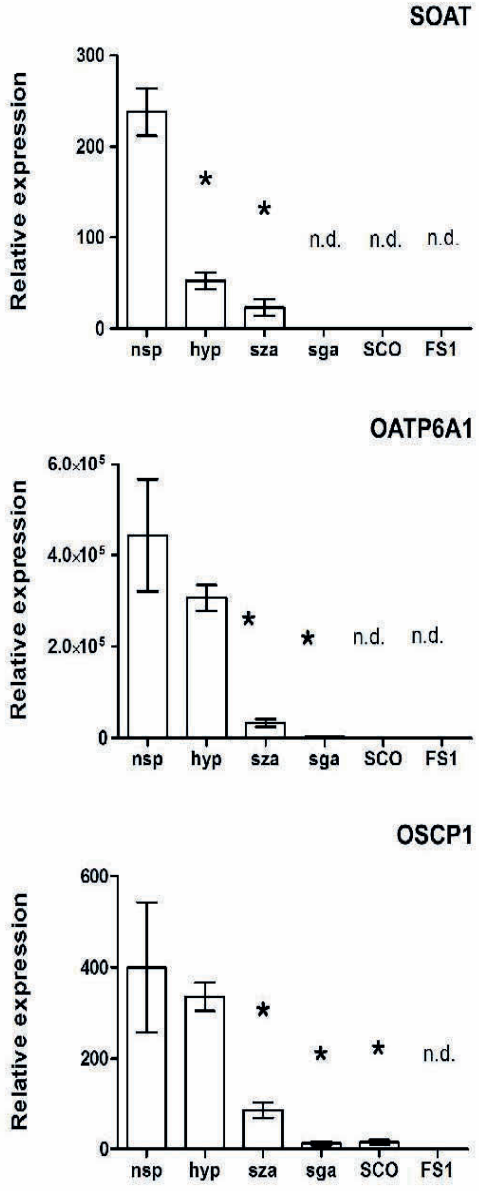

Figure 2. Quantitative real-time PCR analysis of the SOAT, OATP6A1 and OSCP1 expression in human testis biopsies with normal or impaired spermatogenesis. Expression analysis was performed with testis biopsies revealing normal spermatogenesis (nsp, n = 12), qualitatively intact but quantitatively reduced spermatogenesis (hypospermatogenesis, hyp, n = 5), arrest at the level of primary spermatocytes (sza, n = 13) or spermatogonia (sga, n = 5) as well as Sertoli cell only syndrome (SCO, n = 9). Furthermore, expression analysis was performed on human FS1 Sertoli cell cultures. *Significantly lower expression compared to nsp with $p<0.001$. Data represent mean ± SEM; n.d., expression of the respective carrier was not detected in any biopsy. In the case that only single biopsies from the probe collection showed no detectable expression, the C_T value in these samples was set to 40.

doi:10.1371/journal.pone.0062638.g002

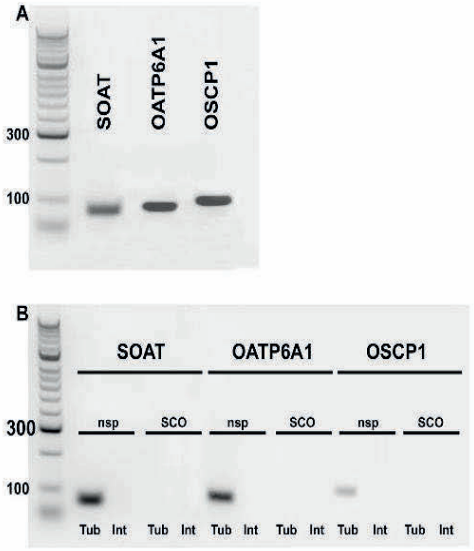

Figure 3. Qualitative mRNA expression analysis of SOAT, OATP6A1 and OSCP1 in seminiferous tubules (Tub) and interstitial tissue (Int) of human testes biopsies showing normal or impaired spermatogenesis following LACP. (**A**) Expression of all three carriers was detected in testis homogenate showing normal spermatogenesis. (**B**) SOAT, OATP6A1, and OSCP1 were only detected in seminiferous tubules from testis biopsies showing nsp, but not in the tubules from patients with SCO. No carrier mRNA was detected in interstitial tissue of the biopsies regardless their spermatogenic status. M, marker.

doi:10.1371/journal.pone.0062638.g003

first was derived from the complete C-terminal amino acid sequence of the human SOAT protein (referred to as $SOAT_{311–377}$) and the second was generated from the 16 C-terminal amino acids of the mouse Soat protein (referred to as $Soat_{329–344}$). However, only $Soat_{329–344}$ was applicable for immunohistochemistry (Fig. 4 and 5) and only $SOAT_{311–377}$ was suitable for Western blot analysis.

Therefore, the $Soat_{329–344}$ affinity-purified rabbit antiserum was used to localize SOAT in the human testis. As shown in Fig. 4 and Fig. S1, the immunoreactivity was clearly directed against various germ cell stages. Staining was found in zygotene primary spermatocytes of stage V, pachytene spermatocytes of all stages (I–V), secondary spermatocytes of stage VI and round spermatids (step 1 and step 2) in stages I and II. Round spermatids of stage III were not stained. Most prominent was the staining of primary spermatocytes, which are germ cells within the first meiotic division. They are characterized by their cellular and nuclear morphology, showing distinct chromosomal structures due to condensation prior to first meiotic cleavage. Here, an ovoid-shaped structure close to the nucleus was stained, likely representing the Golgi compartment, whereas no clear staining was detected in the plasma membrane. This was also shown by *in situ* hybridization (Fig. 6). In stably SOAT-transfected HEK293 cells, SOAT protein was detected via Western blot (Fig. 7A) and immunofluorescence. Contradictory to the localization in germ cells, we detected a clear plasma membrane-derived staining pattern in stably SOAT-transfected HEK293 cells (see Fig. 7B) and the functional characteristics of SOAT as a sodium-dependent steroid sulfate uptake carrier in the plasma membrane (see Fig. 8). However, this staining pattern of SOAT was regarded as specific

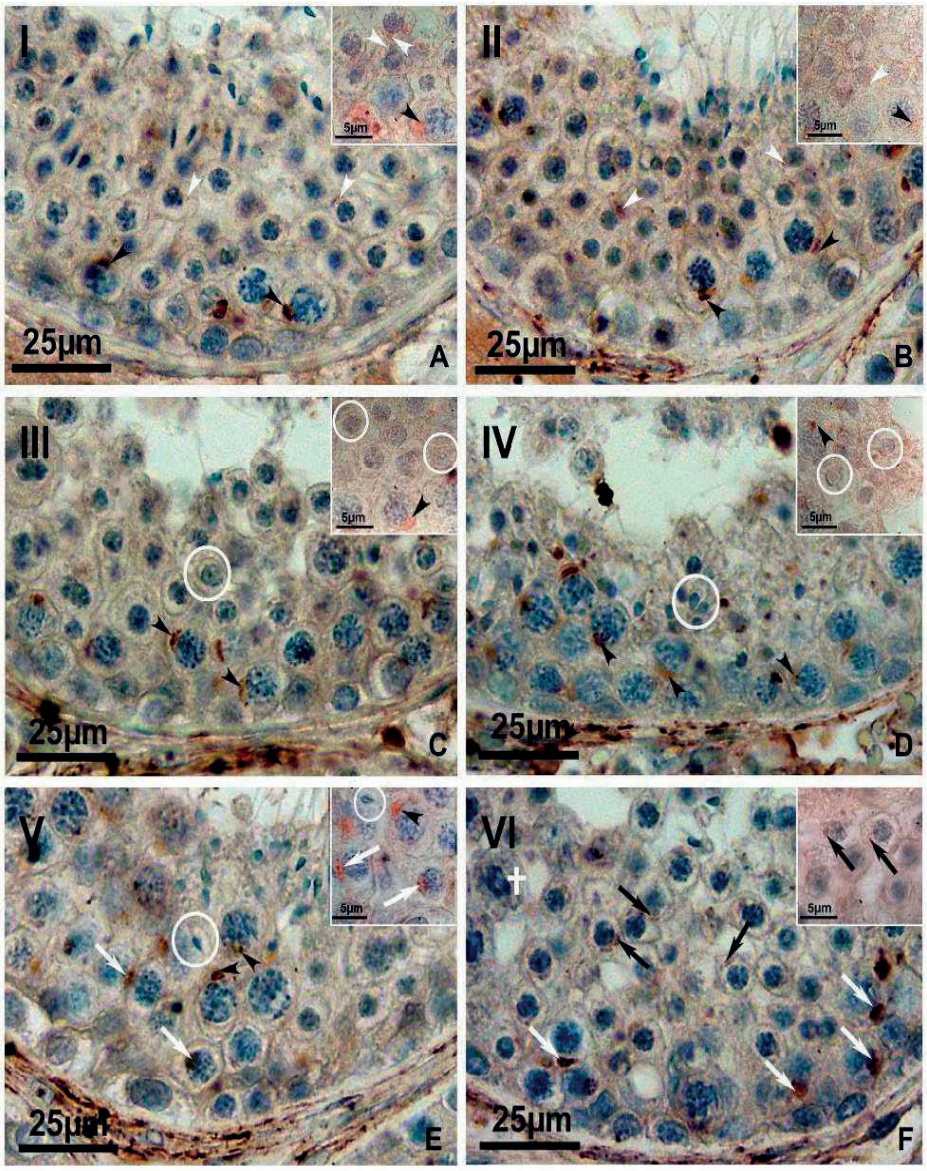
I
5µm
25µm
A
II
5µm
25µm
B
III
5µm
25µm
C
IV
5µm
25µm
D
V
5µm
25µm
E
VI
+
5µm
25µm
F

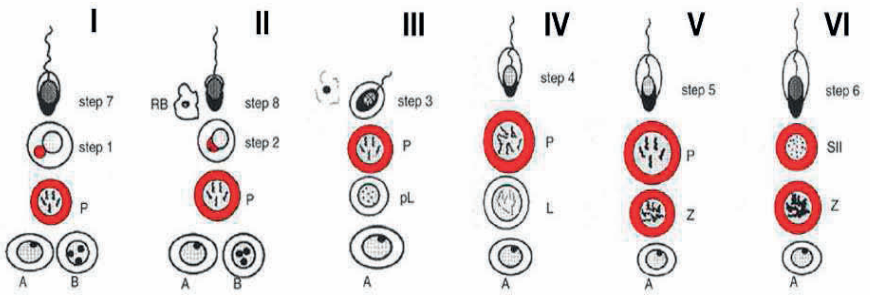
I
step 7
step 1
P
A
B
II
RB
step 8
step 2
P
A
B
III
step 3
P
pL
A
IV
step 4
P
L
A
V
step 5
P
Z
A
VI
step 6
SII
Z
A

Figure 4. Immunohistological localization of SOAT in normal spermatogenesis after stage-dependent analysis. IHC was performed using the $Soat_{329-344}$ antibody with subsequent AEC staining and hematoxylin counterstain. The larger pictures show a whole segment of the seminiferous epithelium in different stages (I–VI) of spermatogenesis (primary magnification ×40), whereas insets show a detail of the respective stage (primary magnification ×100 oil). SOAT expression is also schematically indicated by red labeling on a drawing of spermatogenic stages (modified from [34]). (**A**) Within stage I of spermatogenesis, the SOAT protein was detected in primary pachytene spermatocytes (P, black arrowheads) and round spermatids (step 1, white arrowheads). (**B**) SOAT immunoreactivity was detected in stage II of spermatogenesis within primary pachytene spermatocytes (P, black arrowheads) as well as in round spermatids (step 2, white arrowheads). (**C**) In stage III, only primary pachytene spermatocytes were stained with the $Soat_{329-344}$ antibody (P, black arrowheads), whereas round spermatids were negative (step 3, white circles). (**D**) Within stage IV of spermatogenesis, a similar staining pattern was detected, showing SOAT protein in primary pachytene spermatocytes (P, black arrowheads), but not in round spermatids (step 4, white circles). Note the newly formed acrosomal cap in step 4 spermatids. (**E**) In stage V, primary zygotene spermatocytes (Z, white arrows) as well as pachytene spermatocytes (P, black arrowheads) were stained. Elongating spermatids, showing a distinct acrosomal cap, were not stained (step 5, white circles). (**F**) Stage VI is characterized by the first meiotic cleavage (white cross). Positive staining for SOAT protein was detected in primary zygotene spermatocytes (Z, white arrows) as well as in secondary spermatocytes (SII, black arrows), which can be hardly distinguished from round spermatids.
doi:10.1371/journal.pone.0062638.g004

as it was clearly abolished by pre-incubation of the antibody with the immunizing peptide as well as omission of the primary antibody. In order to further analyze the sub-cellular localization of SOAT in primary spermatocytes IHC and IF of consecutive human testis sections were performed with the $Soat_{329-344}$ antibody as well as an antibody against the Golgi apparatus protein Golgin A2. As shown in Fig. S2, SOAT and Golgin A2 showed identical expression patterns within primary spermatocytes. Apart from germ cells, a diffuse staining of the testis interstitial compartment was visible with the $Soat_{329-344}$ antibody. However, as this staining remained nearly unchanged after pre-incubation of the antibody with the immunizing peptide, it was regarded as unspecific staining (insets of Fig. 5).

In impaired spermatogenesis, as hypospermatogenesis, spermatogenic arrest and SCO, no staging of spermatogenesis is possible. In these sections, we detected the SOAT protein in

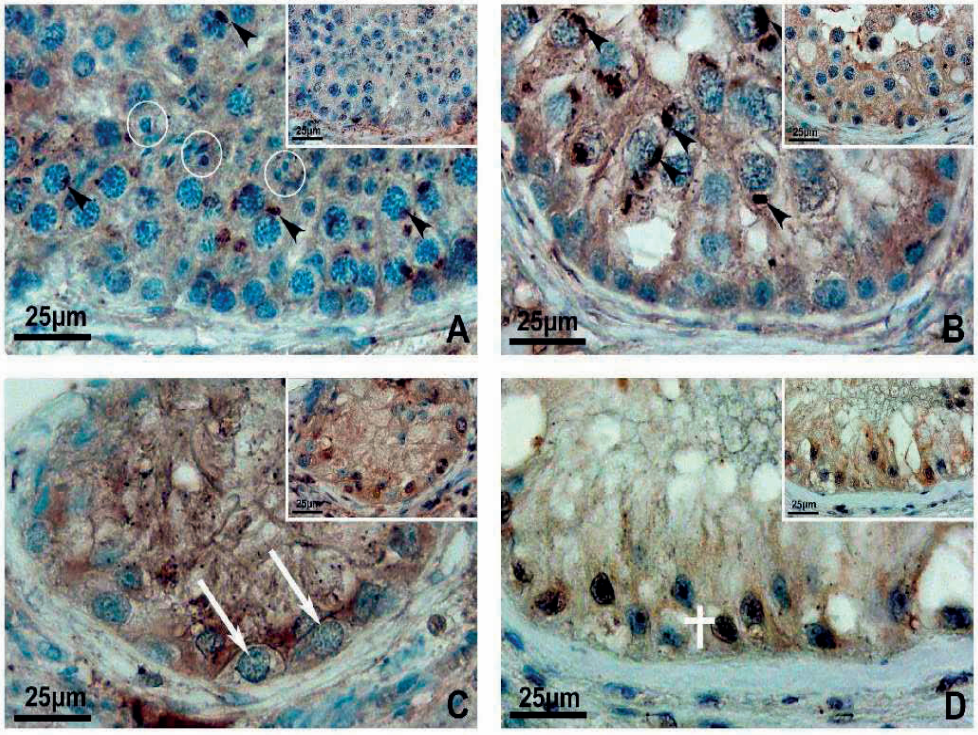

Figure 5. Localization of SOAT in impaired spermatogenesis by IHC. IHC was performed using the $Soat_{329-344}$ antibody with subsequent AEC staining and hematoxylin counterstain. For negative control, primary antibody was incubated with a 100-fold molar excess of immunizing peptide (pre-incubation control, insets). Primary magnification ×40. (**A**) In a seminiferous tubule showing hypospermatogenesis, i.e. a quantitatively reduced but qualitatively preserved spermatogenesis, SOAT specific staining was detected in primary pachytene spermatocytes (black arrowheads), but not in round or elongated spermatids (white circles). (**B**) In a spermatogenic arrest at the level of primary spermatocytes, only these cells are present, whereas the development of spermatids is missing. In this seminiferous tubule, primary spermatocytes were stained for SOAT (black arrowheads). (**C**) In an arrest of spermatogenesis at the level of spermatogonia, no primary spermatocytes are present, but spermatogonia (white arrows) are left. No specific staining for SOAT was detected in these tubules. (**D**) In SCO, no germ cells are left; only Sertoli cells (white cross) are visible and show a faint unspecific cytoplasmic staining with the $Soat_{329-344}$ antibody, which was not abolished in the pre-incubation control.
doi:10.1371/journal.pone.0062638.g005

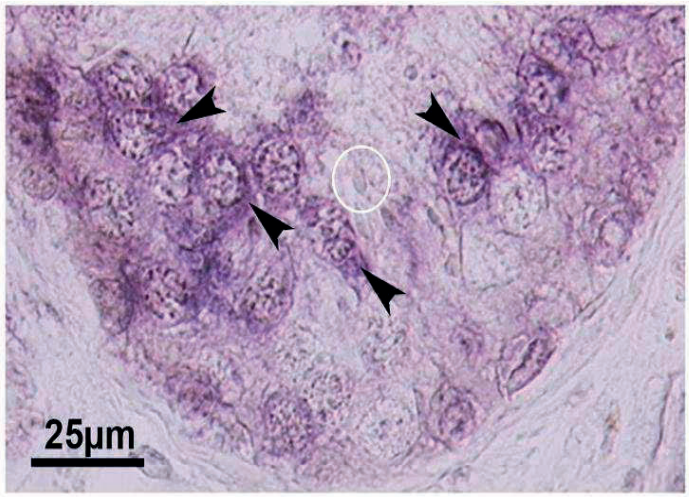

Figure 6. Detection of SOAT mRNA by ISH. Expression analysis of SOAT mRNA in the human testis was also performed using *in situ* hybridization on human testis biopsies showing normal spermatogenesis. Even at the mRNA level, SOAT expression was detected in pachytene primary spermatocytes (black arrowhead) within the seminiferous tubules at late stage II of spermatogenesis. Spermatids were not stained (white circle). Incubation with sense probe showed no staining signal. NBT-BCIP staining, hematoxylin counterstain. Primary magnification ×40.
doi:10.1371/journal.pone.0062638.g006

primary pachytene spermatocytes in case these cells were present (Fig. 5). In SCO tubules, an unspecific staining of Sertoli cell cytoplasm was visible, that did not disappear after pre-incubation of the antibody with the immunizing peptide and, therefore, was regarded as unspecific staining (Fig. 5D). Apart from IHC, we performed *in situ* hybridization experiments using anti-sense cRNA probes for detection of the cellular SOAT mRNA expression in the human testis. As shown in Fig. 6, SOAT mRNA was detected in pachytene spermatocytes, whereas Sertoli cells, peritubular cells, and the interstitial compartment were not stained, clearly supporting the IHC localization data.

Transport of Steroid Sulfates across the Plasma Membrane by SOAT

A further aim of the present study was to verify whether SOAT indeed can transport sulfated steroid hormones without hydrolysis from the extracellular compartment into the cytosol. Therefore, a novel LC-MS-MS procedure was used that is capable of profiling intact steroid sulfates from cell lysates. Transport assay were performed in stably transfected SOAT-HEK293 cells in which SOAT expression was induced by tetracycline treatment (+Tet), whereas non-treated SOAT-HEK293 cells (−Tet) served as a control. The latter did not express the SOAT protein, as demonstrated by Western blot and immunofluorescence analysis with the $SOAT_{311-377}$ antiserum (Fig. 7). As shown in Fig. 8A, we demonstrated for the first time sodium-dependent transport of β-estradiol-3-sulfate (E2S) and androstenediol-3-sulfate by SOAT-HEK293 cells. Furthermore, we verified the sodium-dependent transport of estrone-3-sulfate and DHEAS by SOAT that was previously shown by using the respective radiolabeled compounds. However, apart from SOAT, we could not detect transport activity for human OATP6A1, OATP1C1, or OSCP1 for any of the steroid sulfates and also not for taurocholic acid (a common probe substrate for most OATP carriers) in respective OATP6A1, OATP1C1, and OSCP1 stably-transfected HEK293 cells (Fig. 8B). Even after expression of human OATP6A1, OATP1C1 and OSCP1 in *Xenopus laevis* oocytes as a second expression system, no transport activity could be detected for steroid sulfates (data not shown), indicating that SOAT seems to be the only relevant steroid sulfate uptake carrier in the testis among the carriers analyzed.

Discussion

Sulfated steroids are present in the blood circulation at quite high physiological concentrations, for example up to 10 µM in the case of DHEAS [38]. Apart from being excreted via bile and urine, these compounds can also be de-sulfated into biologically active steroid hormones and may therefore contribute to the overall regulation of reproductive processes [39]. In the case of PREGS and DHEAS, which represent the most abundant sulfated steroids in the human testis, these compounds, together with androstenediol-3-sulfate were shown to be metabolized to testosterone in the human testis, at least in tissue homogenates [8], [16], [40]. However, *in vivo* this would require a transport process for these hydrophilic anionic compounds of generally low membrane permeability across membrane barriers in the testis. Therefore, in the present study we focused on the localization and characterization of candidate steroid sulfate carriers in the human testis and showed that SOAT, OATP6A1 and OSCP1 reveal very high and predominant mRNA expression levels in this organ. However, as only SOAT showed significant transport activity for different steroid sulfate molecules, including PREGS, DHEAS, androstenediol-3-sulfate, E1S and E2S, we primarily aimed to localize this carrier in the human testis.

Interestingly, we found SOAT specifically expressed in primary (zygotene and pachytene) as well as secondary spermatocytes and in round spermatids (step 1 and step 2) within normal spermatogenesis with an immunostaining of ovoid-shaped structures close to the nucleus. As these structures were also immunoreactive for Golgin A2, a well-established marker of the Golgi apparatus [36], SOAT expression in germ cells is most likely directed to the Golgi compartment. As all previous work on SOAT

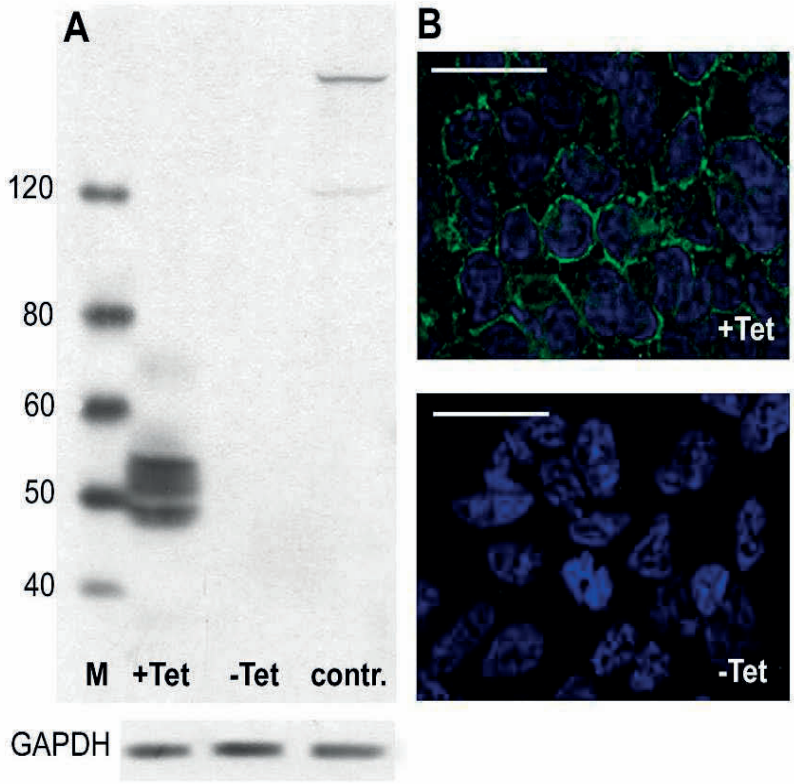

Figure 7. SOAT expression in stably transfected SOAT-HEK293 cells. In the SOAT-HEK293 cells SOAT expression was induced by pre-treatment with tetracycline (+Tet). Control cells were untreated with tetracycline (−Tet) or represent non-transfected HEK293 cells (contr.). (**A**) Cell lysates were processed for WB analysis with the $SOAT_{311-377}$ antibody and revealed an apparent molecular weight of 49–55 kDa, likely representing different glycosylation states of the SOAT protein. (**B**) SOAT expression was directed to the plasma membrane of HEK293 cells by immunofluorescence analysis with the $SOAT_{311-377}$ antibody (green fluorescence). Nuclear staining with DAPI (blue fluorescence). Scale bar: 25 µm.
doi:10.1371/journal.pone.0062638.g007

[27], [29] and also the data from the present study localized SOAT in the plasma membrane and showed the sodium-dependent uptake of steroid sulfates across the plasma membrane, at least in transfected HEK293 cells and *Xenopus laevis* oocytes, we consider this expression pattern to be an intermediate sorting state of the protein for its further trafficking to the plasma membrane at later stages of germ cell development. Here, the protein may then be largely distributed over the plasma membrane so that immunostaining is no longer detectable with the IHC parameters used. However, we cannot exclude that the primary target compartment of SOAT is represented by the immunostained complex within germ cells. In every case, this expression site of SOAT in the human testis can be regarded as specific and is largely supported by ISH analysis and RT-PCR following LACP of seminiferous tubules with nsp or SCO. In impaired spermatogenesis, represented by hypospermatogenesis, spermatogenic arrests and SCO, SOAT protein was also detected in primary spermatocytes in cases these cells were present. In biopsies with SCO, the Sertoli cell cytoplasm was additionally stained with the $Soat_{329-344}$ antibody. However, as this staining remained in the pre-incubation control, it was regarded as unspecific. This was further confirmed by quantitative RT-PCR analysis of cultured FS1 Sertoli cells, in which SOAT mRNA expression was not detectable.

Apart from the localization of SOAT in the human testis, we wanted to clarify whether SOAT indeed can transport sulfated steroid hormones without hydrolysis from the extracellular compartment into the cytosol. It has to be emphasized that most of the classical transport assays for solute carriers are performed with radiolabeled substrates by scintillation counting of the cell lysate after a certain time of incubation with the test compound from the extracellular site [29]. This procedure can cause two potential problems: (I) the availability of radiolabeled potential substrates is restricted, so that identification of novel substrates may be missed, and (II) it is difficult to demonstrate transport of the intact substrate from the extracellular compartment into the cytosol, because the radiolabel simply serves as a surrogate for detection of the entire molecule. To overcome these uncertainties for the steroid sulfate transport by SOAT, we used a LC-MS-MS procedure by which different sulfated steroid hormones can be detected from cell lysates in their intact forms [37]. LC-MS-MS currently presents the technique of choice for steroid sulfate detection, because mass spectrometry allows for the highest specificity in steroid analysis, and soft ionization enables determination of the intact steroid sulfate. Using this technique, we were able to expand the substrate spectrum of SOAT by androstenediol-3-sulfate and E2S using non-radiolabeled compounds. Furthermore, we could verify that the previously identified SOAT

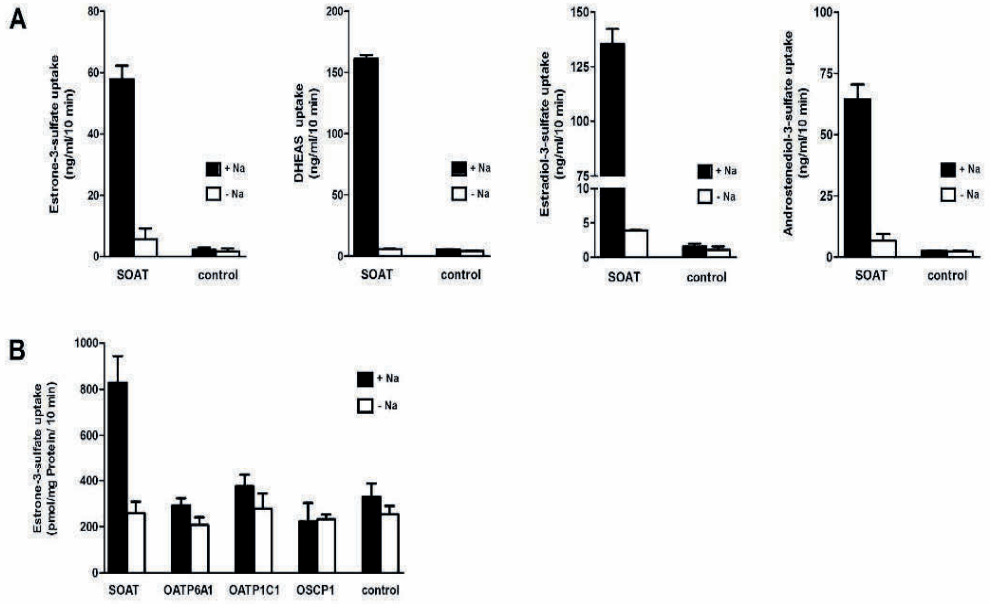

Figure 8. Transport studies with sulfated steroid hormones. (**A**) SOAT-HEK293 were incubated with 10 µM non-radiolabeled estrone-3-sulfate, DHEAS, β-estradiol-3-sulfate, and androstenediol-3-sulfate in the presence (black bars) or absence (open bars) of sodium over 10 min at 37°C. Cells lysates were analyzed by LC-MS-MS in order to determine the absolute cell-associated amount of the steroid sulfate molecules in their intact forms. (**B**) Transport studies with 10 µM [^{3}H]estrone-3-sulfate on stably transfected SOAT-, OATP6A1-, OATP1C1-, and OSCP1-HEK293 cells in the presence and absence of sodium. Non-transfected HEK293 cells served as a control. In contrast to SOAT, OATP6A1, OATP1C1, and OSCP1 showed no significant transport function for E1S.
doi:10.1371/journal.pone.0062638.g008

substrates DHEAS and E1S are transported in the SOAT-HEK293 cells from the extracellular into the intracellular compartment in their intact form without any modification at the molecule. Therefore, cellular import of sulfated steroid hormones seems to be the general transport function of SOAT.

However, the physiological role of steroid sulfate transport by SOAT in spermatocytes and spermatids remains largely unclear. In particular, DHEAS and PREGS are abundantly found in the human testis and are known to be precursors of testosterone [8], [41], so that transport of these compounds within the testis may play a role in the initiation and maintenance of spermatogenesis. However, germ cells do not express the androgen receptor, suggesting that androgens can only affect these cells in a non-genomic way [10], [42]. As germ cells are known to express estrogen receptors [6], [43], [44], the transport of E1S and E2S could be a relevant function of SOAT in spermatocytes. On this background it is interesting to note that SOAT expression was very low or even absent in severe disorders of spermatogenesis, represented by an arrest at the level of spermatocytes or spermatogonia, and also by SCO. These pathologies result in non-obstructive azoospermia and, therefore, infertility in men [34]. However, from these data, no causal relationship can be concluded between low SOAT expression and severe spermatogenic impairment. In patients with hypospermatogenesis characterized by qualitatively preserved, but quantitatively reduced spermatogenesis, SOAT expression was significantly lower compared to normal spermatogenesis. As a significant reduction of SOAT expression may be associated with a disturbed transport of sulfated steroids, the local supply of androgens and estrogens may be disturbed. One possible way to evaluate this hypothesis would be the analysis of spermatogenesis in the testis of Slc10a6 knockout mice lacking any Soat expression. Furthermore, among the known ≥33 non-synonymous single nucleotide polymorphisms (SNPs) in the human SLC10A6 gene, functionally relevant SNPs might be more represented in patients with hypospermatogenesis or other spermatogenic impairments.

Apart from SOAT, OATP6A1 and OSCP1 also showed predominant expression in the human testis. This is in agreement with previous studies that were performed on mice, rats and humans [23], [24], [29], [32]. However, by using stably transfected OATP6A1-HEK293 and OSCP1-HEK293 cells, and even *Xenopus laevis* oocytes as second expression system, we could not show any significant transport activity for DHEAS and E1S. OATP6A1 was cloned by Suzuki et al. 2003 [23] from rats and humans, and was localized in Sertoli cells, spermatogonia, and Leydig cells of the rat testis by ISH. Functional transport measurements were only performed with the rat carrier and revealed transport activity for taurocholic acid and T_4, as well as low transport rates for DHEAS [23], which is in contrast to the human OATP6A1 carrier. OSCP1 was cloned from human, rat, and mouse, and showed transport activity for various kinds of organic solutes including DHEAS and E1S with very low transport rates [24], [32], [45]. The mouse Oscp1 protein was localized to leptotene spermatocytes at stage IX until step 15 spermatids in the mouse testis. However, Oscp1 was clearly found intracellularly [30]; therefore, it is still controversial whether OSCP1 acts as a membrane uptake carrier at all. As both carriers were transport negative for DHEAS and E1S in our expression models, their cellular localization in the human testis was not analyzed further.

With the present study, we were able to limit the localization of SOAT to germ cells. Nevertheless, how the sulfated steroids reach the germ cell stages still remains an open question. SOAT positive

primary and secondary spermatocytes as well as round spermatids are located within the adluminal compartment of the seminiferous epithelium, built by Sertoli cells. The blood-testis barrier (first described by Bergmann et al. 1989 in the human [46]) protects germ cells from endogenous and exogenous substances and there is increasing interest regarding active transporter (ATP-binding cassettes, ABC) expression in Sertoli cells. Sulfated steroids have to pass through Sertoli cells to reach the germ cells, which could be mediated by ABC transporters like the multidrug-resistance proteins MRP1 and MRP4 as well as breast cancer resistance protein (BCRP). These have already been detected in human Sertoli cell lines and are thought to play a pivotal role in drug transport in the testis (for review see [47]).

Supporting Information

Figure S1 Overview on SOAT expression in different germ cell stages in the human testis. IHC was performed using the $Soat_{329–344}$ antibody with subsequent AEC staining and hematoxylin counterstain. For negative control, primary antibody was incubated with a 100-fold molar excess of immunizing peptide (pre-incubation control, inset). Primary magnification ×20. Within the depicted seminiferous tubule different spermatogenic stages (stages I, III and IV) as well as mitotic divisions (mit.) are present. The following cell types and structures can be assigned: **a,** spermatogonia; **b,** primary pachytene spermatocytes; **c,** early round spermatids; **d,** elongating spermatids; **e,** elongated spermatids prior to sperm release; **f,** Sertoli cell nucleus; **g,** interstitial Leydig cells; **h,** peritubular myoid cells. Specific SOAT expression can be detected in the present seminiferous tubule in pachytene spermatocytes of all stages as well as in round spermatids (step 1) in stage I. Round spermatids of stage III were not stained.
(TIF)

Figure S2 Immunofluorescence and immunohistochemistry of consecutive sections of the human testis detecting SOAT and Golgi marker protein Golgin A2. IHC and IF analyses were performed with the $Soat_{329–344}$ (**A, C**) and Golgin A2 (**B, D**) antibodies in consecutive sections of the human testis. IHC was performed using AEC staining and hematoxylin counterstain. For IF nuclei were counterstained with DAPI (blue fluorescence). Negative controls were performed by pre-incubation of the $Soat_{329–344}$ antibody with the immunizing peptide (insets in A, C) or by omitting the primary antibody (insets in B, D). Primary magnification ×40. (**A, B**) IF revealed specific staining of an ovoid-shaped structure close to the nucleus of primary spermatocytes (white arrowhead) with both antibodies (red fluorescence), representing the Golgi compartment. Notice unstained peritubular myoid cells (white circle). (**C, D**) The same staining pattern was observed using IHC, where SOAT and Golgin A2 showed identical expression patterns within primary spermatocytes (black arrowheads) in testis tissue sections showing normal spermatogenesis of stage III.
(TIF)

Acknowledgments

We acknowledge the skilful technical assistance of J. Dern-Wieloch, A. Hax, J. Vogelsberg, K. Schuh, and K. Stumpf.

Author Contributions

Conceived and designed the experiments: DF JA BD SAW MB JG. Performed the experiments: KB BW GG SG CEG MFH. Analyzed the data: DF KB BW BD GG CEG. Contributed reagents/materials/analysis tools: SK WW. Wrote the paper: DF KB GG JG.

References

1. Selcer KW, Kabler H, Sarap J, Xiao Z, Li PK (2002) Inhibition of steryl sulfatase activity in LNCaP human prostate cancer cells. Steroids 67: 821–826.
2. Pasqualini JR, Chetrite GS (2005) Recent insight on the control of enzymes involved in estrogen formation and transformation in human breast cancer. J Steroid Biochem Mol Biol 93: 221–236.
3. Stanway SJ, Delavault P, Purohit A, Woo LW, Thurieau C, et al. (2007) Steroid sulfatase: a new target for the endocrine therapy of breast cancer. Oncologist 12: 370–374.
4. Labrie F, Luu-The V, Labrie C, Simard J (2001) DHEA and its transformation into androgens and estrogens in peripheral target tissues: intracrinology. Front Neuroendocrinol 22: 185–212.
5. Strott CA (2002) Sulfonation and molecular action. Endocr Rev 23 (5): 703–732.
6. Hess RA (2003) Estrogen in the adult male reproductive tract: a review. Reprod Biol Endocrinol 1: 52.
7. Laatikainen T, Laitinen EA, Vihko R (1971) Secretion of free and sulfate-conjugated neutral steroids by the human testis. Effect of administration of human chorionic gonadotropin. J Clin Endocrinol Metab 32 (1): 59–64.
8. Ruokonen A, Laatikainen T, Laitinen EA, Vihko R (1972) Free and sulfate-conjugated neutral steroids in human testis tissue. Biochemistry 11 (8): 1411–1416.
9. Mouhadjer N, Bedin M, Pointis G (1989) Steroid sulfatase activity in homogenates, microsomes and purified Leydig cells from adult rat testis. Reprod Nutr Dev 29 (3): 277–282.
10. Walker WH (2009) Molecular mechanisms of testosterone action in spermatogenesis. Steroids 74 (7): 602–607.
11. Kuiper GG, Carlsson B, Grandien K, Enmark E, Häggblad J, et al. (1997) Comparison of the ligand binding specificity and transcript tissue distribution of estrogen receptors alpha and beta. Endocrinology 138 (3): 863–870.
12. Carreau S, Bouraima-Lelong H, Delalande C (2011) Estrogens: new players in spermatogenesis. Reprod Biol 11 (3): 174–193.
13. Lekhkota O, Brehm R, Claus R, Wagner A, Bohle RM, et al. (2006) Cellular localization of estrogen receptor-alpha (ERalpha) and -beta (ERbeta) mRNA in the boar testis. Histochem Cell Biol 125 (3): 259–264.
14. Lekhkota O, Bergmann M (2007) Expression and cellular localization of estrogen receptor α in the testis of different mammals. AnatGes2007 (Poster Abstract Booklet): 67.
15. Carreau S, Bouraima-Lelong H, Delalande C (2012) Estrogen, a female hormone involved in spermatogenesis. Adv Med Sci 57 (1): 31–36.
16. Ruokonen A (1978) Steroid metabolism in testis tissue: the metabolism of pregnenolone, pregnenolone sulfate, dehydroepiandrosterone and dehydroepiandrosterone sulfate in human and boar testes in vitro. J Steroid Biochem 9 (10): 939–946.
17. Payne AH, Kawano A, Jaffe RB (1973) Formation of dihydrotestosterone and other 5α-reduced metabolites by isolated seminiferous tubules and suspension of interstitial cells in a human testis. J Clin Endocr Metab 37: 448–453.
18. Payne AH, Jaffe RB (1970) Comparative Roles of Dehydroepiandrosterone Sulfate and Androstenediol Sulfate as Precursors of Testicular Androgens. Endocrinology 87: 316–322.
19. Payne AH, Jaffe RB (1975) Androgen formation from pregnenolone sulfate by fetal, neonatal, prepubertal and adult human testes. J Clin Endocr Metab 40: 102–107.
20. Lykkesfeldt G, Müller J, Skakkebaek NE, Bruun E, Lykkesfeldt AE (1985a) Absence of testicular steroid sulphatase activity in a boy with recessive X-linked ichthyosis and testicular maldescent. Eur J Pediatr 144 (3): 273–274.
21. Lykkesfeldt G, Bennett P, Lykkesfeldt AE, Micic S, Møller S, et al. (1985b) Abnormal androgen and oestrogen metabolism in men with steroid sulphatase deficiency and recessive X-linked ichthyosis. Clin Endocrinol (Oxf) 23 (4): 385–393.
22. Pizzagalli F, Hagenbuch B, Stieger B, Klenk U, Folkers G, et al. (2002) Identification of a novel human organic anion transporting polypeptide as a high affinity thyroxine transporter. Mol Endocrinol 16 (10): 2283–2296.
23. Suzuki T, Onogawa T, Asano N, Mizutamari H, Mikkaichi T, et al. (2003) Identification and characterization of novel rat and human gonad-specific organic anion transporters. Mol Endocrinol 17 (7): 1203–1215.
24. Kobayashi Y, Shibusawa A, Saito H, Ohshiro N, Ohbayashi M, et al. (2005) Isolation and functional characterization of a novel organic solute carrier protein, hOSCP1. J Biol Chem 280 (37): 32332–32339.
25. Hagenbuch B, Dawson P (2004) The sodium bile salt cotransport family SLC10. Pflugers Arch 447 (5): 566–570.
26. Petzinger E, Geyer J (2006) Drug transporters in pharmacokinetics. Naunyn Schmiedebergs Arch Pharmacol 372 (6): 465–475.
27. Geyer J, Godoy JR, Petzinger E (2004) Identification of a sodium-dependent organic anion transporter from rat adrenal gland. Biochem Biophys Res Commun 316 (2): 300–306.

28. Geyer J, Wilke T, Petzinger E (2006) The solute carrier family SLC10: more than a family of bile acid transporters regarding function and phylogenetic relationships. Naunyn Schmiedebergs Arch. Pharmacol. 372 (6): 413–431.
29. Geyer J, Döring B, Meerkamp K, Ugele B, Bakhiya N, et al. (2007) Cloning and functional characterization of human sodium-dependent organic anion transporter (SLC10A6). J Biol Chem 282 (27): 19728–19741.
30. Hiratsuka K, Yin S, Ohtomo T, Fujita M, Ohtsuki K, et al. (2008) Intratesticular localization of the organic solute carrier protein, OSCP1, in spermatogenic cells in mice. Mol Reprod Dev 75 (10): 1495–1504.
31. Hiratsuka K, Momose A, Takagi N, Sasaki H, Yin S, et al. (2011) Neuronal expression, cytosolic localization, and developmental regulation of the organic solute carrier partner 1 in the mouse brain. Histochem Cell Biol 135 (3): 229–238.
32. Kobayashi Y, Tsuchiya A, Hayashi T, Kohyama N, Ohbayashi M, et al. (2007) Isolation and characterization of polyspecific mouse organic solute carrier protein 1 (mOscp1). Drug Metab Dispos 35 (7): 1239–1245.
33. Schumacher V, Gueler B, Looijenga LHJ, Becker JU, Amann K, et al. (2008) Characteristics of testicular dysgenesis syndrome and decreased expression of SRY and SOX9 in Frasier syndrome. Mol Reprod Dev 75 (9): 1484–1494.
34. Bergmann M, Kliesch S (2010) Testicular biopsy and histology. In: Nieschlag E, Behre HM, Nieschlag S, editors. Andrology. Male Reproductive Health and Dysfunction. Berlin, Heidelberg: Springer. 155–167.
35. Steger K, Klonisch T, Gavenis K, Drabent B, Doenecke D, et al. (1998) Expression of mRNA and protein of nucleoproteins during human spermiogenesis. Mol Hum Reprod 4 (10): 939–945.
36. Nakamura N (2010) Emerging new roles of GM130, a cis-Golgi matrix protein, in higher order cell functions. J Pharmacol Sci 112 (3): 255–264.
37. Galuska CE, Hartmann MF, Sánchez-Guijo A, Bakhaus K, Geyer J, et al. (2012) Profiling intact steroid sulfates and unconjugated steroids in biological fluids by liquid chromatography-tandem mass spectrometry (LC-MS-MS). Analytical Chemistry, manuscript ID ac-2012–03047p, under review.
38. Morris KT, Toth-Fejel SE, Schmidt J, Fletcher WS, Pommier RF (2001) High dehydroepiandrosterone-sulfate predicts breast cancer progression during new aromatase inhibitor therapy and stimulates breast cancer cell growth in tissue cultures: a renewed role for adrenalectomy. Surgery 130: 947–953.
39. Reed MJ, Purohit A, Woo LWL, Newman SP, Potter BVL (2005) Steroid sulfatase: molecular biology, regulation and inhibition. Endocrine reviews 26 (2): 171–202.
40. Payne AH, Jaffe RB (1971) Gonadal Steroid Sulfates and Sulfatase. III. Correlation of Human Testicular Sulfatase, 3β-Hydroxysteroid Dehydrogenase-Isomerase, Histologic Structure and Serum Testosterone. J Clin Endocrinol Metab 33 (4): 582–591.
41. Ruokonen AO, Vihko RK (1983) Quantitative Changes of endogenenous unconjugated and sulfates steroids in human testis in relation to synthesis of testosterone in vitro. J Androl 4 (1): 104–107.
42. Walker WH (2010) Non-classical actions of testosterone and spermatogenesis. Philos Trans R Soc Lond, B, Biol. Sci. 365 (1546): 1557–1569.
43. Hess RA, Carnes K (2004) The role of estrogen in testis and the male reproductive tract: a review and species comparison. Anim Reprod (1): 5–13.
44. Cavaco JEB, Laurentino SS, Barros A, Sousa M, Socorro S (2009) Estrogen receptors alpha and beta in human testis: both isoforms are expressed. Syst Biol Reprod Med 55 (4): 137–144.
45. Izuno H, Kobayashi Y, Sanada Y, Nihei D, Suzuki M, et al. (2007) Rat organic solute carrier protein 1 (rOscp1) mediated the transport of organic solutes in *Xenopus laevis* oozytes: Isolation and pharmacological characterization of rOscp1. Life Sci 81 (15): 1183–1192.
46. Bergmann M, Nashan D, Nieschlag E (1989) Pattern of compartmentation in human seminiferous tubules showing dislocation of spermatogonia. Cell Tissue Res 256: 183–190.
47. Robillard KR, Hoque T, Bendayan R (2012) Expression of ATP-binding cassette membrane transporters in rodent and human sertoli cells: relevance to the permeability of antiretroviral therapy at the blood-testis barrier. J Pharmacol Exp Ther 340: 96–108.

11. Anhang – Publikationen

6. G. Grosser, D. Fietz, S. Günther, K. Bakhaus, H. Schweigmann, B. Ugele, R. Brehm, E. Petzinger, M. Bergmann, J. Geyer. J Ster Biochem Mol Biol 2013; 138C:90-99.

Journal of Steroid Biochemistry & Molecular Biology 138 (2013) 90–99

Contents lists available at ScienceDirect

Journal of Steroid Biochemistry and Molecular Biology

journal homepage: www.elsevier.com/locate/jsbmb

Cloning and functional characterization of the mouse sodium-dependent organic anion transporter Soat (Slc10a6)

Gary Grosser[a,*], Daniela Fietz[b], Sabine Günther[b], Katharina Bakhaus[a], Helene Schweigmann[a], Bernhard Ugele[c], Ralph Brehm[d], Ernst Petzinger[a], Martin Bergmann[b], Joachim Geyer[a]

[a] Institute of Pharmacology and Toxicology, Justus Liebig University of Giessen, 35392 Giessen, Germany
[b] Institute of Veterinary Anatomy, Histology and Embryology, Justus Liebig University of Giessen, 35392 Giessen, Germany
[c] University Hospital, Ludwig Maximilians University of Munich, 80337 Munich, Germany
[d] Institute of Anatomy, University of Veterinary Medicine Hannover, 30173 Hannover, Germany

ARTICLE INFO

Article history:
Received 24 November 2012
Received in revised form 25 March 2013
Accepted 26 March 2013

Keywords:
SOAT
Transport
Steroid sulfates
Mouse
DHEAS
Pregnenolone sulfate

ABSTRACT

The sodium-dependent organic anion transporter SOAT is a member of the Solute Carrier Family SLC10. In man, this carrier is predominantly expressed in the testis and has transport activity for sulfoconjugated steroid hormones. Here, we report on cloning, expression analysis and functional characterization of the mouse Soat (mSoat) and compare its characteristics with the human SOAT carrier. Quantitative mRNA expression analysis for mSoat in male mice revealed very high expression in lung and further high expression in testis and skin. Immunohistochemical studies showed expression of the mSoat protein in bronchial epithelial cells of the lung, in primary and secondary spermatocytes as well as round spermatids within the seminiferous tubules of the testis, in the epidermis of the skin, and in the urinary epithelium of the bladder. Stably transfected mSoat-HEK293 cells revealed sodium-dependent transport for dehydroepiandrosterone sulfate (DHEAS), estrone-3-sulfate, and pregnenolone sulfate (PREGS) with apparent K_m values of 60.3 μM, 2.1 μM, and 2.5 μM, respectively. In contrast to human SOAT, which has a preference for DHEAS as a substrate, mSoat exhibits the highest transport rate for PREGS, likely reflecting differences in the steroid pattern between both species. In conclusion, although certain differences between human SOAT and mSoat exist regarding quantitative gene expression in endocrine and non-endocrine tissues, as well as in the transport kinetics for steroid sulfates, in general, both can be regarded as homologous carriers.

1. Introduction

In 2004 we reported on the cloning of a novel functional member of the Solute Carrier Family SLC10 and called it sodium-dependent organic anion transporter SOAT (SLC10A6) [1]. Until that point the SLC10 carrier family was well established as the "sodium bile acid co-transporter family" and only contained two bile acid carriers, the Na^+/taurocholate co-transporting polypeptide NTCP (SLC10A1) and the apical sodium-dependent bile acid transporter ASBT (SLC10A2) [2].

Although sequence identity between NTCP and ASBT is quite low (at 35%), both carriers transport conjugated bile acids with high affinity [3]. Due to their transport characteristics and expression pattern, NTCP and ASBT are important factors for the maintenance of the enterohepatic circulation of bile acids by mediating the first step in the cellular uptake of bile acids through the membrane barriers in the liver (NTCP) and intestine (ASBT) [3]. In contrast, SOAT showed no specific transport for bile acids, but for sulfoconjugated steroid hormones, and in man has predominant expression in the testis [4].

Because of their high plasma concentrations, sulfoconjugated steroid hormones are considered a reservoir for the synthesis of active free steroid hormones and may therefore contribute to the overall regulation of reproductive processes by steroid hormones [5,6]. Here, hydrolysis of sulfoconjugated steroid hormones occurs by the catalytic activity of the steroid sulfatase (StS) [7,8]. However, while the lipophilic free steroids can pass through the plasma membrane by diffusion, the hydrophilic anionic sulfoconjugates depend on carrier-mediated uptake to gain access to StS for cleavage. In this process, SOAT may play an important role by delivering sulfoconjugated steroids to specific target cells in reproductive organs. However, until now, the physiological role of steroid sulfate transport in reproductive organs has not been elucidated. In the present study we provided for the first time expression data and functional characterization of mouse Soat (mSoat).

* Corresponding author at: Institute of Pharmacology and Toxicology, Justus Liebig University of Giessen, Biomedical Research Center BFS, Schubertstr. 81, 35392 Giessen, Germany. Tel.: +49 641 9938410; fax: +49 641 9938419.
E-mail address: gary.grosser@vetmed.uni-giessen.de (G. Grosser).

0960-0760/$ – see front matter © 2013 Elsevier Ltd. All rights reserved.
http://dx.doi.org/10.1016/j.jsbmb.2013.03.009

2. Materials and methods

2.1. Chemicals and radiochemicals

All chemicals, unless otherwise stated, were purchased from Sigma–Aldrich (Taufkirchen, Germany). Phenylsulfate, phenylethylsulfate, α-naphthylsulfate, 1omega-SEP (1omega-sulfooxyethylpyrene), and 4-SMP (4-sulfooxymethylpyrene) were generously donated by Hansruedi Glatt (Department of Nutritional Toxicology, Potsdam-Rehbrücke, Germany). Zeocin was purchased from InvivoGen (Toulouse, France) and hygromycin from Carl Roth (Karlsruhe, Germany). Materials used for the cultivation of HEK293 cells were purchased from Gibco and Sigma–Aldrich. [^{3}H]Dehydroepiandrosterone sulfate ([^{3}H]DHEAS, 94.5 Ci/mmol) and [^{3}H]estrone-3-sulfate ([^{3}H]E_1S, 57.3 Ci/mmol) were purchased from PerkinElmer Life Sciences. [^{3}H]Pregnenolone-3-sulfate ([^{3}H]PREGS, 20 Ci/mmol) was obtained from American Radiolabeled Chemicals. [^{3}H]Taurocholic acid ([^{3}H]TC, 30 Ci/mmol) was generously donated by Alan F. Hofmann (University of California, San Diego, USA).

2.2. Cloning of mSoat and generation of mSoat-HEK293 cells

For the cloning of the mSoat cDNA gene, specific primers covering the whole open reading frame were selected and used for full-length amplification and cloning of the mSoat transcript, as previously reported [4]. Then, the mSoat cDNA construct was used for the stable transfection of the Flp-In T-REx 293 host cell line as reported before [4], in order to establish the mSoat-HEK293 cell line for functional characterization of the carrier protein.

2.3. Animals and tissue collection

For a first screening of mSoat expression, three male mice of different strains (one 6 month old CF-1, a 3 month old C57BL/6-J, and a 6 month old BALB/c mouse) were used. For validation of the mSoat gene and protein expression patterns, 16 further male mice were used from four different mouse strains: four CF-1 mice, five C57BL/6-J mice, four FVB/N mice, and three 129Sv mice. All mice were euthanized by cervical dislocation after deep anesthesia using isoflurane. Tissue samples were immediately removed under sterile conditions and stored in liquid nitrogen until further processing. In addition to wild-type mice, testis tissue slides from connexin 43 knockout mice (SCCx43KO$^{-/-}$) were used, which show seminiferous tubules with an arrest of spermatogenesis at the level of primary spermatocytes as well as tubules containing only Sertoli cells in direct proximity [9]. For histological and immunohistological analyses, tissue samples were fixed by immersion in Bouin's solution or formalin, respectively, and embedded in paraffin. All mice were obtained from Charles River Laboratories International (Wilmington, MA, USA). All experiments of the present study in which organ material from laboratory mice was used were reported to the local Institute for Animal Welfare.

2.4. Determination of the expression pattern of mSoat by quantitative real-time PCR

RNA was isolated from the collected tissues by phenol/chloroform extraction using TRI Reagent (Sigma–Aldrich). For quantitative real-time PCR analysis, the following TaqMan Gene Expression Assays (Life Technologies, Carlsbad, CA, USA) were used: Mm00512730_m1 for mSoat and Mm00446968_m1 for mouse hypoxanthine phosphoribosyltransferase 1 (mHprt1) as an endogenous control. Genomic DNA was removed by DNase I digestion (Fermentas, St. Leon-Rot, Germany) and RNA was reverse-transcribed into cDNA by using SuperScript III First Strand Synthesis System according to the manufacturer's protocol (Invitrogen, Karlsruhe, Germany). Quantitative real-time PCR for the first screening of mSoat expression was performed on an ABI PRISM 7300 cycler (Applied Biosystems, Darmstadt, Germany). Each cDNA was analyzed in triplicate in a 96-well optical plate using 5 μl cDNA, 12.5 μl TaqMan Gene Expression Mastermix, 1.25 μl TaqMan Gene Expression Assay (Life Technologies) and 6.25 μl of water in each 25 μl reaction mixture. The plates were heated for 10 min at 95 °C, and 45 cycles of 15 s at 95 °C and 60 s at 60 °C were applied. For the systematic expression analysis in 16 mice, 4 μl of cDNA, 1 μl of TaqMan Gene Expression Assay, 10 μl TaqMan Gene Expression Master Mix (Life Technologies) and 5 μl of water in each 20 μl reaction were used and PCR was performed on CFX96 Real-Time Cycler (Bio-Rad Laboratories, Hercules, CA, USA) using the parameters of 95 °C for 10 min and 45 cycles of 95 °C × 15 s and 60 °C × 1 min. The relative gene expression of mSoat was determined by the $2^{-\Delta\Delta CT}$ method with the brain set as a calibrator due to the lowest overall expression levels in this organ.

2.5. Qualitative RT-PCR analysis following LACP

Total mRNA of tissue homogenates was extracted from Bouin (testis, bladder) or formalin fixed (lung, skin) paraffin-embedded tissue using RNeasy Micro FFPE Kit (Qiagen, Hilden, Germany) as recommended by the manufacturer. Subsequently, mRNA was incubated with RNase-free DNase I (10 U/L; Roche, Mannheim, Germany) and RNase Inhibitor (40 U/L, Life Technologies) to digest genomic DNA. cDNA was reverse-transcribed using the SuperScript III First Strand Synthesis System according to the manufacturer's protocol (Invitrogen). Negative controls were performed by omitting the reverse transcriptase. For RT-PCR, 5 μl of cDNA was added to 2 μl $MgCl_2$, 4 μl 10× PCR Gold Buffer, 0.25 μl GOLDAmplitaq (Life Technologies), 1 μl of each primer (10 μmol/L) and water to a final volume of 25 μl. RT-PCR was performed by using specific primers for mSoat (forward primer 5′-GTC CTT CTC TGC TGA GTA CC-3′ and reverse primer 5′-TCT CTC TGG GCT GCT TCT C-3′) and mHprt1 (forward primer 5′-GTT GTT GGA TAT GCC CTT GAC-3′ and reverse primer 5′-CAC CTG CTA ATT TTA CTG GCA AC-3′). All oligonucleotide primers were obtained from Metabion International (Martinsried, Germany). RT-PCR conditions were 1 × 95 °C for 7 min, 10 × 95 °C for 30 s, 55 °C – 0.3 °C for 30 s and 72 °C for 30 s, 35 × 95 °C for 30 s, 52 °C for 30 s and 72 °C for 30 s and final elongation at 72 °C for 7 min. PCR products were separated by 2% agarose gel electrophoresis and visualized by GelRED staining (Biotium, Hayward, CA, USA). For an isolated examination of bronchial epithelial vs. alveolar cells of the lung, seminiferous epithelial vs. interstitial cells of the testis as well as urinary epithelium vs. detrusor muscle of the bladder, we performed laser-assisted cell picking (LACP) using paraffin-embedded tissue. Slices mounted on PALM membrane slides (MembranSlide 0.1 PEN, Zeiss, Oberkochen, Germany) were stained with hematoxylin. Then the tissue of interest was excised and catapulted by PALM MicroBeam system and PALM Robo Software (Zeiss, Oberkochen, Germany). Extraction of mRNA, first strand cDNA synthesis and RT-PCR were performed as mentioned above.

2.6. Generation of the $mSoat_{329-344}$ antibody

The $mSoat_{329-344}$ antibody was raised in rabbits against amino acid residues 329–344 of the deduced mSoat sequence (CYEKQPRETSAFLDKG). The synthetic peptide was coupled via the carboxy-terminal glutamic acid residue to keyhole limpet hemocyanin and used to immunize two rabbits (Eurogentec). The rabbit antisera were affinity-purified against the immunizing peptide. Antiserum and pre-immune serum were used as controls.

2.7. Immunofluorescence detection of mSoat in stably transfected HEK293 cells

Immunofluorescence detection of mSoat in the stably transfected mSoat-HEK293 cells was performed as described before [4] with the following modifications. The cells were incubated with the $mSoat_{329-344}$ rabbit antibody (1:100) for 1 h at room temperature after 2% *para*-formaldehyde treatment. Then the cells were incubated for 1 h at room temperature with the Alexa Fluor 488 Goat anti rabbit antibody at a dilution of 1:800 (Invitrogen). The cells were covered with a DAPI/methanol solution containing 1 μg/ml DAPI, air dried, and mounted on slides with ProLong Gold Antifade mounting medium (Invitrogen).

2.8. Western blot analysis of the mSoat protein

For Western blot (WB) analysis of stably transfected mSoat-HEK293 cells, the cells were cultured to 90% confluence under standard conditions and pre-incubated with tetracycline (+Tet) at 1 μg/ml (Carl Roth GmbH, Karlsruhe, Germany) to induce mSoat expression. Non-tetracycline treated cells were used as control (−Tet). For protein extraction, culture medium was removed and cells were washed with phosphate buffered saline (PBS, 137 mM NaCl, 2.7 mM KCl, 1.5 mM KH_2PO_4, 7.3 mM Na_2HPO_4) and lysed by ProteoJET Mammalian Cell Lysis Reagent according to the manufacturer's protocol (Thermo Fisher Scientific, Waltham, MA, USA). The ProteoBlock protease Inhibitor Cocktail was added at a 1:100 dilution (Fermentas, St. Leon-Rot, Germany). Afterwards, samples were mixed with 4× Lämmli buffer containing 20% β-mercaptoethanol, separated on a 10% SDS-PAGE over night at 50 V, and then blotted on a nitrocellulose membrane using semi-dry electroblotting. After blotting, protein transfer was controlled by placing the nitrocellulose membrane in Ponceau S for 5 min. After multiple washing with Tris-buffered saline TBS-T (100 mM Tris, 1370 mM NaCl, H_2O dilution 1:10, 0.05% Tween20), the membrane was blocked for 1 h at room temperature under agitation using TBS-T with 5% dried non-fat milk. After removing of the blocking solution, the membrane was incubated with the primary $mSoat_{329-344}$ antibody at a 1:100 dilution for 1 h at room temperature. After washing with TBS-T, the membrane was incubated with the HRP-conjugated secondary antibody (peroxidase-conjugated goat IgG fraction to rabbit IgG, MP Biomedicals, Pioneer Place, Singapore) and at a 1:5000 dilution with Roti Mark WESTERN-HRP-conjugate (Carl Roth) for 1 h at room temperature. After washing with TBS-T, the nitrocellulose membrane was incubated with Roti Lumin 1 and Roti Lumin 2 (Carl Roth) in a ratio of 1:1 for 1 min and exposed to the Amersham Hyperfilm ECL High performance chemiluminescence film (GE Healthcare, LifeSciences, Piscataway, NJ, USA). The exposure time was 2 min.

2.9. Immunohistochemical detection of mSoat expression

After deparaffinization and rehydration, 5 μm tissue sections were boiled for 20 min in citrate buffer. Subsequently, sections were treated with 3% H_2O_2 in Tris buffer for 30 min followed by incubation with blocking buffer TBS with BSA containing 5% goat serum for 30 min. Sections were then incubated with the $mSoat_{329-344}$ primary antibody overnight (1:100) by 4 °C, followed by the biotinylated goat anti rabbit E0432 (Dako, Glostrup, Denmark) (1:200) secondary antibody in TBS for 1 h at room temperature. For negative control, primary antibody was pre-incubated with ~100-fold molar excess of the immunizing peptide. Avidin–biotin complex (ABC Vectastain, Vector Labs, Burlingame, CA, USA) was used for 45 min. After incubation sections were washed thoroughly with TBS. For color development, sections were incubated with AEC (Biologo, Kronshagen, Germany). Finally, sections were counterstained with hematoxylin and mounted in glycerine gelatine for microscopic examination.

2.10. Transport studies in mSoat-HEK293 cells

Transport studies with the mSoat-HEK293 cells were performed as described before [4]. Briefly, 12-well or 24-well plates with 1.25×10^5 cells per ml (2 ml in 12-well-, 1 ml in 24-well plates) were plated and grown under standard conditions for 72 h. mSoat expression was induced by pre-incubation with tetracycline (1 μg/ml). mSoat non-expressing Flp-In HEK293 cells were used as control. In the sodium-free transport buffer sodium chloride was substituted with equimolar concentrations of choline chloride. Uptake experiments were started by replacing the pre-incubation buffer by transport buffer containing the radiolabeled test compound and were performed at 37 °C. For inhibition studies, mSoat-HEK293 cells were pre-incubated in 24-well plates with transport buffer containing the inhibitory compound for 5 min. Then transport measurements were started by adding the radiolabeled substrate at 37 °C for 5 min and terminated by washing five-times with ice-cold PBS. Cell monolayers were lysed in 1 N NaOH with 0.1% SDS and the cell-associated radioactivity was determined in a liquid scintillation counter.

2.11. Bioinformatics

The BLAST program (available at http://www.ncbi.nlm.nih.gov) was used to identify mSoat-encoding sequences in the mouse genome. Multiple sequence alignments were conducted using the EBI ClustalW algorithm (http://www.ebi.ac.uk/clustalw/), and sequence alignments were visualized by BOXSHADE 3.21. Amino acid identity values were determined after Clustal W alignment with the DNASTAR Lasergene program MegAlign, version 8.0.2. Membrane topology and putative membrane-spanning domains were predicted by the following programs: TMHMM, PRED-TMR2, TopPred 2, TMAP, TMpred, PSORT 2, MEMSAT-SVM, HMMTOP, SOSUI, MEMSAT3, PredictProtein Phobius, DAS-TMfilter, MemBrain, Philius, MINNOU, SPLIT 4.0, SVMtm, TMMOD, and TOPCONS. The NetNGlyc 1.0 program was used to predict N-linked glycosylation site, and NetPhos 2.0 was used to predict potential phosphorylation sites in the mSoat protein. In silico promoter analysis of the SOAT/Soat genes was conducted with the Genomatix Software GEMS Launcher 5.6, ElDorado 0.8-2011, and MatInspector 8.0.5 [10].

2.12. Statistical analysis

Statistical significance for uptake measurements with radiolabeled substrates was calculated using Student's *t*-test. Statistical analysis of more than two groups was performed by one-way analysis of variance (ANOVA) followed by post hoc testing (Dunnett). Kinetic data from experiments measuring the uptake of radiolabeled substrates were fit to the Michaelis-Menten equation by nonlinear regression analysis.

3. Results

3.1. The Slc10a6 gene and cloning of mSoat

The mouse Slc10a6 gene is located on chromosome 5 E5 and is encoded by six exons. As summarized in Table 1, the lengths of these exons account for 548 bp, 119 bp, 89 bp, 173 bp, 158 bp, and 1037 bp. All intron/exon boundaries were compatible with the canonical donor and acceptor consensus motifs. Each intron started with GT at the 5′-splice donor site and ended with AG at the 3′-splice acceptor site. The length of the mouse Slc10a6 gene accounts for

Table 1
Exon–intron organization of the mouse Slc10a6 gene on chromosome 5 E5. Nucleotide sequences of exon/intron junctions are indicated according to mSoat mRNA sequence (GenBank Accession Number NM_029415) and *Mus musculus* chromosome 5, reference assembly (GenBank Accession Number NC_000071). Intron sequences are represented in lowercase letters and exon sequences are in uppercase letters.

Exon	Exon size (bp)	5′-Splice donor	3′-Splice acceptor	Intron size (kb)
1	548	TCTCAG/gtaagt	ttccag/CATCAG	10.4
2	119	GCATAG/gtctgt	ttttag/GAATTA	0.6
3	89	CTCAAG/gtcagg	gcttag/GTCGGA	5.1
4	173	GCAAAG/gtacag	acccag/GTGCAG	3.2
5	158	TCGCAG/gtgcat	gtccag/CATATC	2.2
6	1037	CCAACC		

23.6 kb. For cloning of the full-length open reading frame of mSoat, we derived primers from the *Mus musculus* 16 day embryo lung cDNA RIKEN full-length enriched library, clone 8430417G17 (GenBank Accession No. AK018423), which was identified as human SOAT homologous sequence by BLAST search and sequence alignment (Fig. 1). The mSoat open reading frame consists of 1119 bp and encodes the 373 amino acid mSoat protein with a calculated molecular mass of 40.7 kDa. Fig. 1 presents the deduced amino acid sequence of mSoat in alignment with rat Soat (rSoat) and human SOAT. The mSoat shows high amino acid sequence identity of 90.8% to rSoat, and of 71% to human SOAT. The C-terminal domain is the most divergent region between the SOAT/Soat proteins. Potential outer facing N-glycosylation sites were identified at N^{8} and N^{14} and potential inner facing serine, threonine and tyrosine phosphorylation sites were identified at S^{52}, S^{55}, S^{126}, T^{130}, Y^{181}, S^{258}, S^{278}, S^{316}, Y^{330}, T^{350}, S^{371}. Nearly all of these are conserved between mSoat and rSoat. Analysis of the membrane topology of mSoat was

Table 2
In silico promoter analysis of the SLC10A6/Slc10a6 genes of human, rat, and mouse. After alignment of the promoter sequences, a highly conserved androgen receptor binding site was identified on the − strand and a highly conserved glucocorticoid receptor binding site was localized on the + strand at the same position (bold face). Promoter analysis was performed with the Genomatix Software GEMS Launcher 5.6, ElDorado 08-2011, and MatInspector 8.0.5.

Species	Position on the − strand	Genomic promoter sequence
Human	−323 till −341	TTTC**CAGGGACACAATGTGATGC**TG
Mouse	−319 till −337	TTCC**CTAGAACACGATGTGCCAC**TG
Rat	−318 till −336	TTCC**CTAGAACACGATGTGCCAC**TG

performed with different topology prediction programs. Most of them preferred a topology model with nine transmembrane domains for mSoat with an extracellular orientation of the N-terminus and an intracellular orientation of the C-terminus. In Fig. 1, localization of the proposed transmembrane domains is depicted by asterisks based on maximum consensus of all TMD predictions. Apart from the protein sequences, we also compared the promoter sequences of the human SLC10A6 with the rat and mouse Slc10a6 genes. The aligned sequences were scanned for potentially conserved transcription factor binding sites. At the promoter positions −318/319 to −336/337 of the mouse and rat Slc10a6 genes as well as at position −323 to −341 for the human SLC10A6 gene, a highly conserved androgen receptor binding site was identified on the − strand as well as a highly conserved glucocorticoid receptor binding site on the +strand (Table 2).

3.2. Tissue expression of mSoat

In order to get an expression pattern of mSoat in different organs, we analyzed individual male CF-1, C57BL/6, and BALB/c

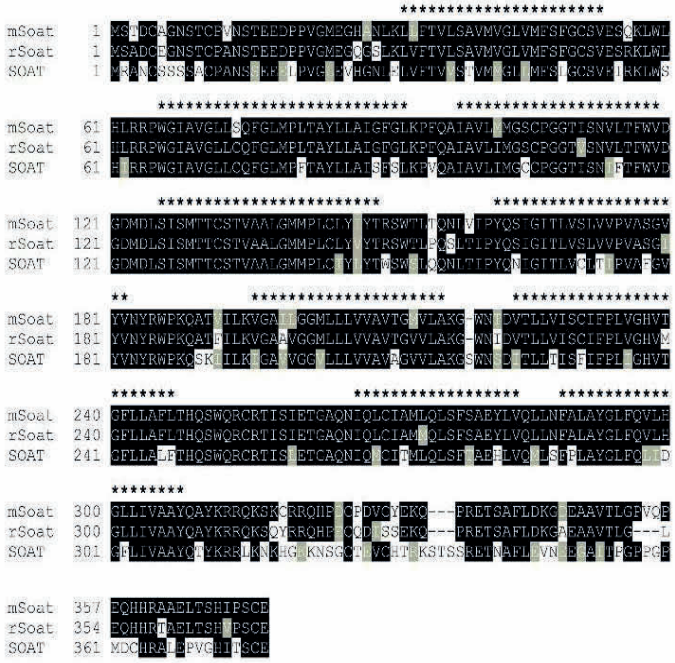

Fig. 1. Amino acid sequence alignment of mouse Soat (mSoat), rat Soat (rSoat) and human SOAT. The deduced amino acid sequences with GenBank Accession Nos. NP_083691, NP_932166, and NP_932069, respectively, were aligned using the EBI *ClustalW* algorithm, and alignment was visualized by BOXSHADE 3.21. Amino acid identity is displayed with black shading and amino acid similarities are highlighted in gray. Gaps (–) are introduced to maximize alignment. Nine transmembrane domains were predicted for mSoat and are indicated by asterisks.

mice by quantitative real-time PCR (Fig. 2A). Expression from the mHprt1 gene was used as endogenous control. Generally low mSoat mRNA expression levels were found in blood, liver, stomach, small intestine, spleen, kidney, adrenal gland, seminal vesicle, preputial gland, coagulating gland, lacrimal gland/eye, and brain. However, all three mice showed moderate expression in heart, bladder, and skin. The organs with high or even predominant expression were lung and testis, in particular in the CF-1 and BALB/c mice. Based on this initial expression screening, we selected lung, skin, testis, epididymis, and brain for further expression analysis in a larger group of male mice from each breed line. Instead of BALB/c mice, however, here we used FVB and 129Sv mice (Fig. 2B). In these experiments we confirmed the highest expression levels of mSoat in the lung and further high expression in skin and testis. In contrast, expression was generally low in the epididymis and nearly undetectable in the brain.

For the cellular localization of mSoat expression in these organs we applied immunohistochemistry (IHC) with the $mSoat_{329-344}$ antibody. In the testis of C57BL/6 mice, mSoat-specific immunoreactivity was localized to primary leptotene and pachytene spermatocytes, and residual bodies of elongating spermatids at stages X (upper tubule) and XI (lower tubule) of spermatogenesis. In the primary pachytene spermatocytes, a clear ovoid-shaped staining pattern was observed, which likely represents the Golgi compartment (Fig. 3A). This germ cell specific expression patter was confirmed in testis slides from connexin 43 knockout mice ($SCCx43KO^{-/-}$), in which seminiferous tubules with an arrest of spermatogenesis at the level of primary spermatocytes showed specific staining for mSoat, whereas in tubules containing only Sertoli cells, no specific staining was detected (Fig. 3B). Specificity of this immunoreactivity pattern was approved by pre-incubation of the $mSoat_{329-344}$ antibody with a 100-fold molar excess of the immunizing peptide, which completely abolished immunostaining of spermatocytes, but not of interstitial cells (inset in Fig. 3A and entire Fig. 3C). Expression of mSoat in the seminiferous tubules was further confirmed at the RNA level by semi-qualitative RT-PCR following LACP of testis seminiferous tubules (Fig. 3G, lane 6), whereas mSoat mRNA was not detectable in the testis interstitium (Fig. 3G, lane 7). More detailed expression analysis of mSoat at different stages of spermatogenesis is shown in Fig. 4. Protein expression of mSoat starts at the onset of meiosis (preleptotene primary spermatocytes), persists in pachytene primary spermatocytes throughout all stages as well as round spermatids, and ends in residual bodies of elongating spermatids.

In lung sections, mSoat specific immunostaining was detected in bronchial epithelial cells of the main bronchus to the terminal bronchiole, but was not detectable in the alveolar duct (Fig. 3D). While the lamina propria was not stained, weak staining was associated with the alveolar cells. In the skin, the epidermis was strongly stained, whereas the dermis was not immunoreactive (Fig. 3E). In the urinary bladder, especially the apical domain of the urinary epithelium, strong staining was observed with the $Soat_{329-344}$ antibody that was again completely blocked in the pre-incubation controls. Additionally, scattered immunostaining was detected in the detrusor (Fig. 3F). In lung and urinary bladder, mSoat expression was further confirmed by semi-qualitative RT-PCR following LACP that revealed specific amplicons in bronchial epithelial cells (Fig. 3G, lane 3), alveolar cells (Fig. 3G, lane 4), detrusor (Fig. 3G, lane 10), and urinary epithelium (Fig. 3G, lane 11).

3.3. Establishment of a stably transfected mSoat-HEK293 cell line and transport studies

For functional characterization of mSoat a stably transfected mSoat-HEK293 cell line was established, where mSoat expression was under the control of a tetracycline-regulated promoter.

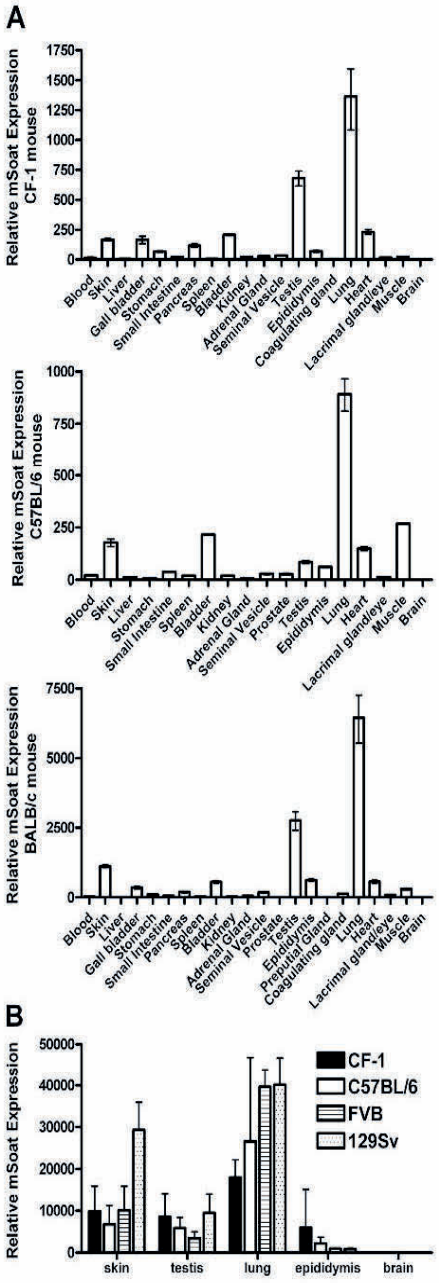

Fig. 2. Expression profile of mSoat in various male mouse tissues. (A) mSoat tissue expression was analyzed in individual CF-1, C57BL/6, and BALB/c mice by quantitative real-time PCR analysis. Relative mSoat expression was calculated by the $2^{-\Delta\Delta CT}$ method and represents mSoat expression that is *x* times higher in the respective tissue than in the brain (set as calibrator for all three mice with mHprt1 as endogenous control). (B) mSoat expression analysis in skin, lung, testis, epididymis, and brain of CF-1 ($n = 4$), C57BL/6 ($n = 5$), FVB ($n = 4$), and 129 Sv ($n = 3$) mice. Relative mSoat expression was calculated by the $2^{-\Delta\Delta CT}$ method and represents mSoat expression that is *x* times higher in the respective tissue than in the brain of a C57BL/6 mouse (set as calibrator). The values represent means ± SD.

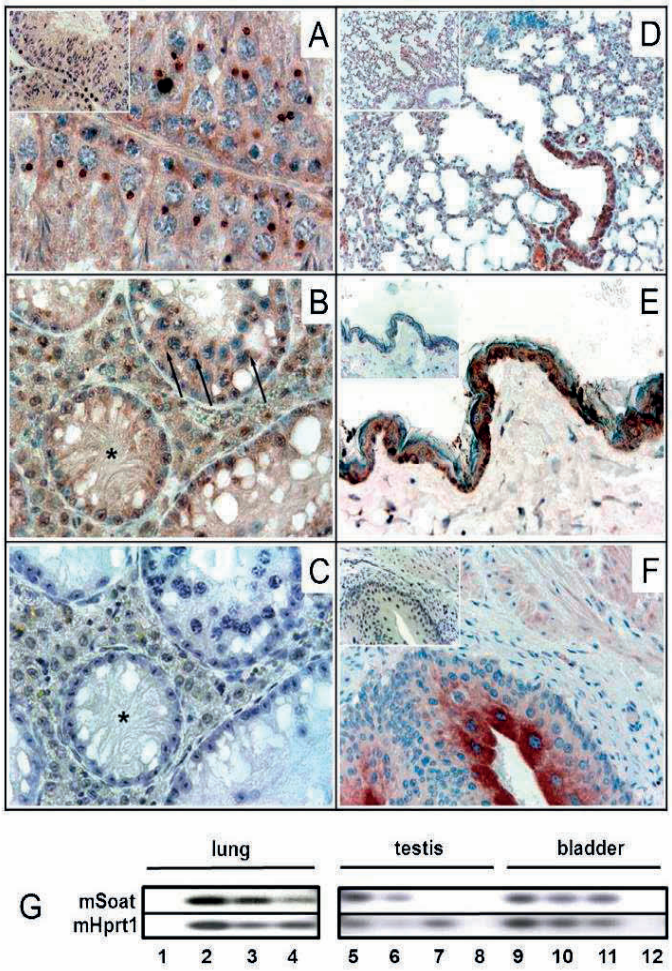

Fig. 3. Immunohistochemical localization of mSoat in male mice with the $mSoat_{329-344}$ antibody at 1:100 dilution and AEC staining with hematoxylin counterstain. Primary magnification 40× (A–C, E and F), or 20× (D). (A) mSoat expression in the testis of C57BL/6 mice was localized in primary leptotene and pachytene spermatocytes, and elongating spermatids at stages X (upper tubule) and XI (lower tubule) of spermatogenesis. (B) Expression of mSoat in the testis of $SCCx43KO^{-/-}$ mice with an arrest of spermatogenesis at the level of primary spermatocytes in pachytene spermatocytes (black arrows) and negative control (C) with pre-incubation of the $mSoat_{329-344}$ antibody with the immunizing peptide (applied accordingly to insets to A, D, E, and F); a tubule containing only Sertoli cells without clear staining for mSoat is marked by an asterisk. (D) In the lung of C57BL/6 mice, mSoat expression was detected in bronchial epithelial cells, and in skin in the epidermis (E). In the urinary bladder, the apical domain of the urinary epithelium was strongly stained by the $Soat_{329-344}$ antibody (F). Semi-qualitative RT-PCR of mSoat following LACP of tissue sections (G): 1, negative control; 2, positive control lung; 3, bronchial epithelial cell; 4, alveolar cells; 5, positive control testis; 6, tubules; 7, interstitium; 8, negative control; 9, positive control bladder; 10, detrusor; 11, urinary epithelium of bladder; 12, negative control. Negative controls were performed without cDNA, positive controls with cDNA extracted from whole organs without LACP.

In these cells, mSoat expression was detected in the plasma membrane after pre-treatment with tetracycline (+Tet) by the $mSoat_{329-344}$ antibody (Fig. 5A). mSoat-HEK293 cells that were not pre-treated with tetracycline (−Tet) were used as a negative control and revealed no immunofluorescence staining. By Western blot analysis, the mSoat protein was only detected in the tetracycline pre-treated mSoat-HEK293 cells and revealed an apparent molecular weight of 48 kDa (Fig. 5B). In these mSoat-HEK293 cells, transport experiments were performed with several radiolabeled steroid compounds. Sodium-dependent mSoat specific transport in the mSoat-HEK293 cells was observed for DHEAS, E_1S, and PREGS at different time points (Fig. 6A). In contrast, taurocholic acid was not transported by mSoat. Among these substrates, the mSoat-expressing HEK293 cells showed the highest transport rate for [^{3}H]PREGS with 13-fold higher values compared with the control cells at $t = 30$ min. The initial [^{3}H]PREGS uptake velocity was linear over 90 s at concentrations ranging from 20 nM to 20 μM PREGS (Fig. 6B). Therefore, kinetic measurements were performed with a 1 min uptake phase. As shown in Fig. 6C, mSoat specific uptake of DHEAS, E_1S, and PREGS showed saturation kinetics following the Michaelis-Menten equation. From the saturation curves of the carrier-specific uptake, kinetic parameters were determined by nonlinear regression analysis and yielded K_m values of 60.3 ± 7.8 μM, 2.1 ± 0.4 μM, and 2.5 ± 0.2 μM, as well as V_{max} values of 362.8 ± 16.9 pmol/mg protein/min, 26.6 ± 1.3 pmol/mg protein/min, and 377.3 ± 5.8 pmol/mg protein/min for DHEAS, E_1S, and PREGS, respectively (Fig. 6C and Table 3).

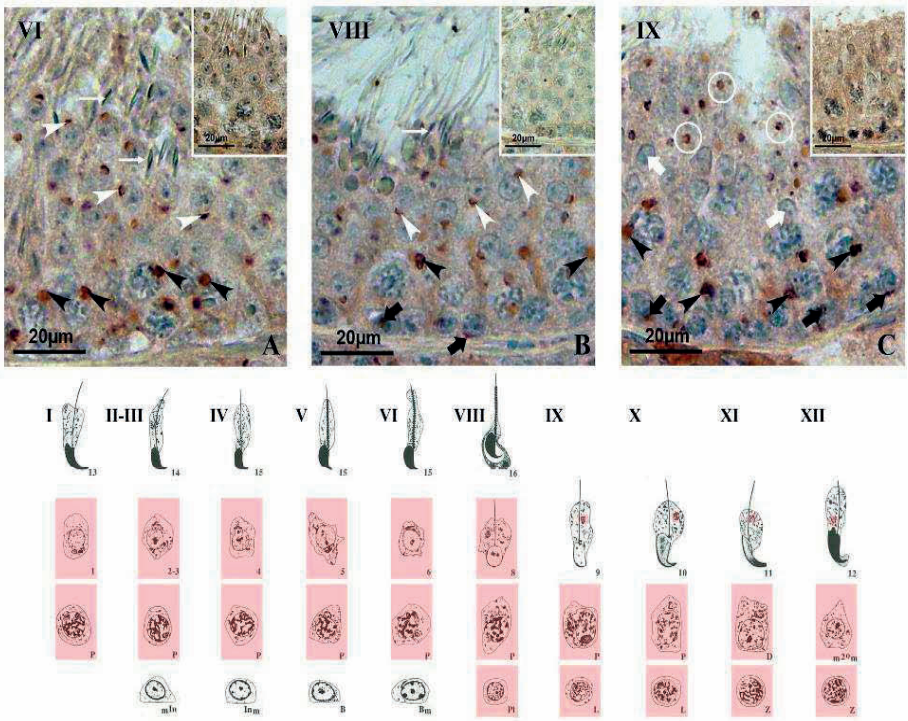

Fig. 4. Stage-dependent expression of mSoat in normal spermatogenesis. Whole segments of the seminiferous epithelium are depicted in stages VI (A), VIII (B) and XI (C) of spermatogenesis. Negative controls were performed after pre-incubation of the primary antibody with the immunizing peptide (insets to A–C). Primary magnification 40×. Expression of mSoat is schematically summarized on the staging scheme by Russell et al., 1990 [32] by red labeling of the respective cell type. Expression of mSoat starts at the onset of meiosis (preleptotene primary spermatocytes, Pl, bold black arrows), persists in pachytene primary spermatocytes throughout all stages (P, black arrowheads) and round spermatids (steps 1–8, white arrowheads) and ends in residual bodies of elongating spermatids (steps 9–12, white circles). (A) Within stage VI of spermatogenesis, staining of mSoat protein was only detected in primary pachytene spermatocytes (P, black arrowhead) and round spermatids (step 6, white arrowheads). Elongated spermatids (stage 15, thin white arrow) are not stained. (B) Stage VIII of spermatogenesis is characterized by spermiation. In this stage, preleptotene primary spermatocytes (Pl, bold black arrow) are positively stained, and mark the beginning of meiosis. Furthermore, pachytene primary spermatocytes are stained (P, black arrowheads), as well as round spermatids (step 8, white arrowhead). Elongated spermatids (step 16, directly prior to spermiation, thin white arrow) are not stained. (C) After spermiation during stage IX of spermatogenesis, the mSoat protein was detected within leptotene primary spermatocytes (L, bold black arrow) and pachytene primary spermatocytes (P, black arrowhead) in an ovoid-shaped structure close to the nucleus. In contrast, in step 9 round spermatids, already building the acrosomal cap (bold white arrows), mSoat immunoreactivity was localized to residual bodies (white circles) in the remaining cytoplasmic compartment.

3.4. Inhibition studies with the mSoat-HEK293 cells

In order to analyze the interaction of different kind of organic molecules with mSoat, inhibition experiments were performed on the mSoat-HEK293 cells (Fig. 7). *cis*-Inhibitory effects of the indicated compounds (all at 20 µM) were examined on the mSoat-mediated uptake of 200 nM [^{3}H]PREGS. The anti-androgen drug flutamide and the selective estrogen receptor modulator tamoxifen did not inhibit the mSoat-mediated [^{3}H]PREGS transport as well as quercetin dehydrate, atropine sulfate, glutathione,

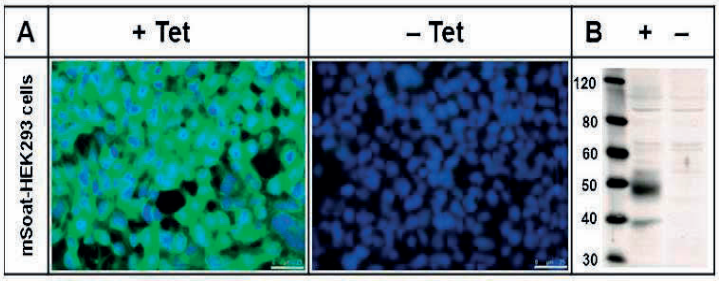

Fig. 5. Detection of mSoat in stably transfected mSoat-HEK293 cells by (A) immunofluorescence microscopy and (B) Western blot. mSoat expression was induced by pre-treatment with tetracycline (+Tet). Control cells were untreated with tetracycline (–Tet). For immunofluorescence analysis the primary mSoat$_{329-344}$ antibody was used at 1:100 dilution, followed by incubation with the secondary antibody Alexa Fluor 488 Goat anti rabbit (green fluorescence). Staining of cell nuclei was performed with DAPI (blue fluorescence). (B) Western blot analysis of stably transfected mSoat-HEK293 cells with (+) or without (–) tetracycline pre-treatment revealed a specific band for the mSoat protein at 48 kDa. No specific signal was detected in the control cells.

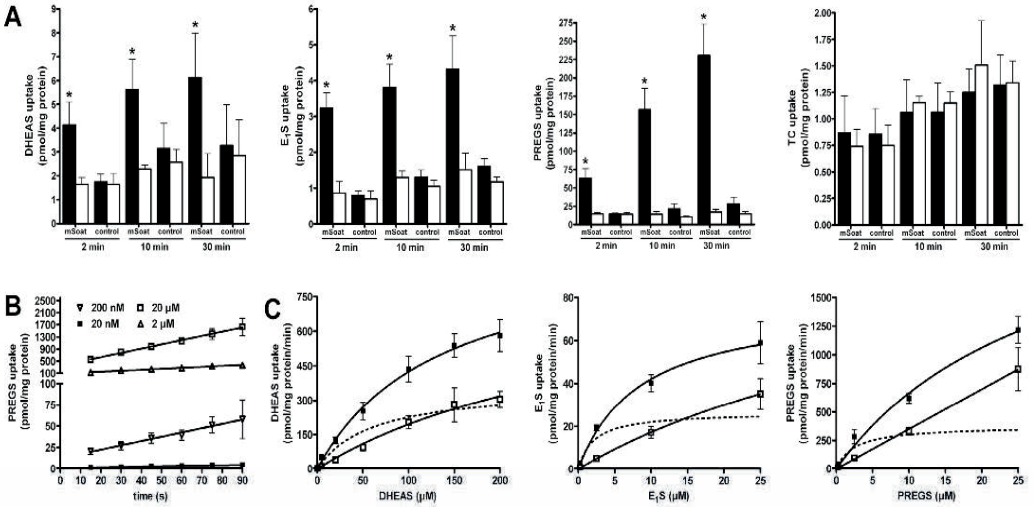

Fig. 6. Uptake studies in the stably transfected mSoat-HEK293 cells. (A) Uptake of 200 nM [^{3}H]DHEAS, [^{3}H]E_1S, [^{3}H]PREGS, and [^{3}H]TC for 2, 10, and 30 min. mSoat expression was induced by pre-incubation with tetracycline (1 µg/ml). Non-transfected Flp-In HEK293 cells were used as control. Cells were incubated for the indicated time period in transport medium with (black bars) or without (open bars) sodium chloride at 37 °C together with the radiolabeled compound. After the indicated time, cells were washed with ice-cold PBS, lysed, and subjected to scintillation counting. The values represent means ± SD of two independent experiments ($n = 6$). *Uptake values by sodium-dependent transport were significantly different from sodium-free transport except for TC ($p < 0.01$). (B) Initial uptake velocity of [^{3}H]PREGS into mSoat-HEK293 cells. After pre-treatment with tetracycline, uptake of the indicated concentrations of PREGS was measured over 15 s, 30 s, 45 s, 60 s, 75 s, and 90 s. Values represent means ± SD of triplicate determinations of two independent experiments ($n = 6$). (C) Transport kinetics of [^{3}H]DHEAS, [^{3}H]E_1S, and [^{3}H]PREGS in tetracycline pre-treated mSoat-HEK293 cells. Flp-In HEK293 cells were used as control. Cells were incubated with increasing concentrations of [^{3}H]DHEAS, [^{3}H]E_1S, and [^{3}H]PREGS for 1 min at 37 °C. mSoat-specific uptake was calculated by subtracting non-specific uptake of the Flp-In HEK293 control cells (open squares) from uptake into mSoat-HEK293 cells (filled squares) and is shown by broken lines. The values represent means ± SD of duplicate experiments, each with triplicate determinations ($n = 6$). The kinetic parameters are presented in Table 3.

folic acid, caffeine, and caffeic acid. In contrast, the mSoat-mediated [^{3}H]PREGS transport was significantly reduced by 4-SMP, 1omega-SEP, bromosulfophthalein (BSP), alpha-naphthylsulfate, and 4-methylumbelliferylsulfate, while phenylethylsulfate and phenylsulfate showed no inhibition at all. Among the group of bile acids, the trihydroxylated bile acids taurocholic acid and cholic acid were poor inhibitors of the mSoat-mediated [^{3}H]PREGS transport, but glycodeoxycholic acid and taurolithocholic acid, as well as the sulfoconjugated bile acids taurolithocholic acid 3-sulfate and lithocholic acid 3-sulfate, were potent mSoat inhibitors. Interestingly, progesterone did not inhibit the mSoat transport, but stimulated the [^{3}H]PREGS mediated uptake in a statistically significant manner to ~130%. In contrast, other steroids such as testosterone, estrone, dexamethasone, dihydrotestosterone, and β-estradiol had no effects on the mSoat transport at all. As expected, the steroid sulfates DHEAS, E_1S, and β-estradiol 3,17-disulfate significantly inhibited the mSoat transport, whereas β-estradiol 3-sulfate and cholesterol 3-sulfate had no inhibitory effect at 20 µM.

Table 3
Transport kinetics of [^{3}H]DHEAS, [^{3}H]E_1S, and [^{3}H]PREGS for mSoat and human SOAT. Michaelis-Menten kinetic parameters (K_m and V_{max}) were calculated by non-linear regression analysis. Values represent means ± SD of triplicate determinations of two independent experiments ($n = 6$).

	Compound	Apparent K_m (µM)	V_{max} (pmol/mg protein/min)
mSoat	DHEAS	60.3 ± 7.8	362.8 ± 16.9
	E_1S	2.1 ± 0.4	26.6 ± 1.3
	PREGS	2.5 ± 0.2	377.3 ± 5.8
SOAT[a]	DHEAS	28.7 ± 3.9	1899 ± 81
	E_1S	12.0 ± 2.3	585 ± 34
	PREGS	11.3 ± 3.0	2168 ± 134

[a] Values were taken from Geyer et al., 2007 [4].

4. Discussion

In the present study we describe for the first time the molecular and functional characterization of mouse Soat (Slc10a6) as well as its protein expression in different tissues. Functional characterization of human SOAT was previously described [4], but because of the lack of an appropriate antibody, immunohistochemical localization of the SOAT protein could not be performed so far. Apart from providing novel data for mSoat and its comparison with the human SOAT homolog, the present study also provides the basis for the establishment of a Soat knockout mouse model that will be necessary in the future to elucidate the physiological relevance of steroid sulfate transport by SOAT/mSoat in different organs.

Although both carriers demonstrated identical substrate spectra, kinetic analysis revealed some differences between human SOAT and mouse Soat. DHEAS transport showed higher affinity and higher capacity for the human carrier, while E_1S and PREGS were transported with higher affinity by mSoat. The higher K_m value of DHEAS measured for the mouse carrier could be explained by the fact, that rats and mice have low circulating concentrations of DHEAS in the periphery [11–13], while DHEAS is the most abundant circulating steroid sulfate in the human body [14]. In humans, DHEAS is mainly synthesized from adrenal glands and gonads, whereas rats and mice can only produce DHEAS in their gonads [11,13,15,16]. Therefore, the species differences in the transport kinetics of DHEAS may reflect differences in the steroid profile and metabolic steroid pathways between humans and mice [11,17,18]. Although transport kinetics for DHEAS were previously measured for rSoat, a different expression system was used (*Xenopus laevis* oocytes) and, therefore, these data cannot directly be compared with the data from the present study [1]. However, to further support this hypothesis, closer analysis of rSoat transport characteristics would be necessary.

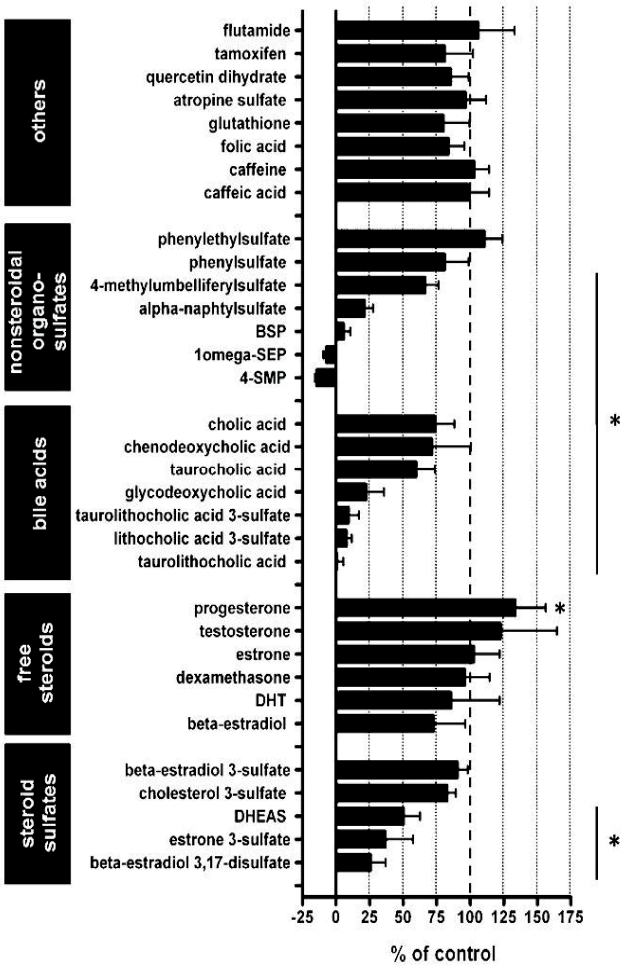

Fig. 7. Inhibition of the mSoat transport of [^{3}H]PREGS by different compounds. Sodium-dependent uptake of 200 nM [^{3}H]PREGS was measured in the presence of 20 μM inhibitory compound. Cells were seeded in 24-well plates and grown to confluence. For transport experiments, mSoat expression was induced by pre-incubation with tetracycline (1 μg/ml). Inhibition experiments were started by pre-incubation with the respective inhibitor at 37 °C for 5 min. Subsequently, [^{3}H]PREGS was added, and the incubation was continued for 5 min at 37 °C. Inhibition studies were terminated by removing the transport buffer and washing with ice-cold PBS. mSoat cells incubated without inhibitor served as a positive control (set to 100%), while Flp-In HEK293 cells served as a negative control (set to 0%). The values represent percentage of PREGS transport activity in the presence of the indicated inhibitor relative to the positive and negative control and are expressed as means ± SD of quadruplicate determinations of representative experiments. *The values were significantly different from positive controls with $p < 0.05$.

Because of the predominant expression of human SOAT in the testis, we only used male mice for our systematic mRNA expression analyses in the present study. Therefore, mSoat gene expression in female reproductive organs as well as gender-specific differences in the mSoat expression in non-reproductive organs (e.g. lung, skin) is a matter of future analyses. In male mice of the CF-1, C57BL/6, and BALB/c strains, we observed the highest mRNA expression levels in the lungs of all mice, followed by the testis, with a high expression in CF-1 and BALB/c mice. However, expression analysis in larger groups of mice from the CF-1, C57BL/6, FVB, and 129Sv strains somewhat relativized this data and revealed that mSoat expression can be regarded as very high in the lung, and high in testis and skin. In general, tissue expression of mSoat showed some inter-individual and inter-strain differences, which had also been noted before for other genes [19].

In contrast to mSoat, human SOAT showed predominant mRNA expression in the testis and only low expression in the lung [4]. However, it must be kept in mind that the whole lung of mice was used for RNA extraction and expression analysis in the present study, whereas in the case of human SOAT, a commercial cDNA panel was used for expression analysis; this could result from biopsies with different ratios for alveolar to bronchial epithelium compared with the present study for mouse Soat. Therefore, a higher expression of human SOAT in lung cannot be excluded.

The physiological and/or pathophysiological relevance of SOAT and mSoat is currently unknown, but a cellular import of the SOAT/mSoat substrates DHEAS, E_1S, and PREGS may contribute to the overall androgen and estrogen production and/or response in the mentioned organs [6,20,21]. In the lung, specific immunostaining of mSoat was detected in bronchial epithelial cells. Little is known about the physiological role of sulfated steroids in the lung, but conversion of E_1S to estradiol-17β as well as DHEAS to androstendione was already demonstrated in human lung tissue homogenate [22]. Furthermore, steroid sulfatase activity was

demonstrated in the lung of BALB/c mice [23]. This might be of functional relevance, as high androgen receptor (AR) expression levels were detected in the bronchial epithelium and type II pneumocytes of the murine lung [24].

Immunohistochemical localization of mSoat in testis showed specific expression in primary and secondary spermatocytes as well as round spermatids with particular strong staining of ovoid-shaped structures close to the nucleus, likely representing the Golgi compartment [25]. This expression pattern might represent an intermediate sorting state of the mSoat protein for its further trafficking to the plasma membrane at later stages of germ cell development. Although the physiological role of steroid sulfates in the testis is completely unknown, the presence of the steroid sulfatase (StS) was demonstrated in mouse pre-meiotic (spermatogonia), meiotic (pachytene spermatocytes), and post-meiotic (spermatids) germ cell types [26]. Furthermore, microsomal fractions of human testis homogenates showed StS activity [27]. Interestingly, Martel et al. reported in 1994, that in rhesus monkeys, testis and lung display all enzymatic activities to convert DHEAS into the biologically active steroids estradiol and dihydrotestosterone [28], whereat SOAT/mSoat could be involved in the cellular import of this steroid precursor.

Apart from lung and testis, strong mSoat expression was found in the epidermis. In skin, StS plays an important role and a deficiency of StS is associated with X-linked ichthyosis [29,30], clinically characterized by scaling of the skin with large, dark-brown scales and an increase in stratum corneum thickness [31]. Therefore, also in the skin, carrier-mediated transport of steroid sulfates by SOAT/mSoat could be of importance.

In conclusion, in the present study the mouse Soat protein was localized for the first time in bronchial epithelial cells of the lung, in primary and secondary spermatocytes as well as round spermatids within the seminiferous tubules of the testis, in the epidermis of the skin, and in the urinary epithelium of the bladder. In stably transfected HEK293 cells, mSoat showed sodium-dependent transport activity for the sulfoconjugated steroid hormones DHEAS, E_1S, and PREGS. Although certain differences between human SOAT and mSoat exist regarding quantitative gene expression in endocrine and non-endocrine tissues as well as in the transport kinetics, in general, both can be regarded as homologous carriers.

Acknowledgements

We acknowledge the skillful technical assistance of A. Hax, K. Schuh, J. Dern-Wieloch, and R. Leidolf.

References

[1] J. Geyer, J.R. Godoy, E. Petzinger, Identification of a sodium-dependent organic anion transporter from rat adrenal gland, Biochemical and Biophysical Research Communications 316 (2004) 300–306.
[2] B. Hagenbuch, P. Dawson, The sodium bile salt cotransport family SLC10, Pflügers Arch 447 (2004) 566–570.
[3] J. Geyer, T. Wilke, E. Petzinger, The Solute Carrier Family SLC10: more than a family of bile acid transporters regarding function and phylogenic relationships, Naunyn-Schmiedeberg's Archives of Pharmacology 372 (2006) 413–431.
[4] J. Geyer, B. Döring, K. Meerkamp, B. Ugele, N. Bakhiya, C.F. Fernandes, J.R. Godoy, H. Glatt, E. Petzinger, Cloning and functional characterization of human sodium-dependent organic anion transporter (SLC10A6), Journal of Biological Chemistry 282 (2007) 19728–19741.
[5] J. Geisler, Breast cancer tissue estrogens and their manipulation with aromatase inhibitors and inactivators, Journal of Steroid Biochemistry and Molecular Biology 86 (2003) 245–253.
[6] M.J. Reed, A. Purohit, L.W. Woo, S.P. Newman, B.V. Potter, Steroid sulfatase: molecular biology, regulation, and inhibition, Endocrine Reviews 2 (6) (2005) 171–202.
[7] K.W. Selcer, H. Kabler, J. Sarap, Z. Xiao, P.K. Li, Inhibition of steryl sulfatase activity in LNCaP human prostate cancer cells, Steroids 67 (2002) 821–826.
[8] J.R. Pasqualini, G.S. Chetrite, Recent insight on the control of enzymes involved in estrogen formation and transformation in human breast cancer, Journal of Steroid Biochemistry and Molecular Biology 93 (2005) 221–236.
[9] R. Brehm, M. Zeiler, C. Rüttinger, K. Herde, M. Kibschull, E. Winterhager, K. Willecke, F. Guillou, C. Lécureuil, K. Steger, L. Konrad, K. Biermann, K. Failing, M. Bergmann, A sertoli cell-specific knockout of connexin 43 prevents initiation of spermatogenesis, American Journal of Pathology 171 (2007) 19–31.
[10] K. Cartharius, K. Frech, K. Grote, B. Klocke, M. Haltmeier, A. Klingenhoff, M. Frisch, M. Bayerlein, T. Werner, MatInspector and beyond: promoter analysis based on transcription factor binding sites, Bioinformatics 21 (2005) 2933–2942.
[11] N. Maninger, O.M. Wolkowitz, V.I. Reus, E.S. Epel, S.H. Mellon, Neurobiological and neuropsychiatric effects of dehydroepiandrosterone (DHEA) and DHEA sulfate (DHEAS), Frontiers in Neuroendocrinology 30 (2009) 65–91.
[12] G.B. Cutler, M. Glenn Jr., M. Bush, G.D. Hodgen, C.E. Graham, D.L. Loriaux, Adrenarche: a survey of rodents, domestic animals, and primates, Endocrinology 103 (1978) 2112–2118.
[13] W.M. van Weerden, H.G. Bierings, G.J. van Steenbrugge, F.H. de Jong, F.H. Schroder, Adrenal glands of mouse and rat do not synthesize androgens, Life Sciences 50 (1992) 857–861.
[14] C. Longcope, Dehydroepiandrosterone metabolism, Journal of Endocrinology 150 (1996) 125–127.
[15] C. Le Goascogne, N. Sananes, M. Gouezou, S. Takemori, S. Kominami, E.E. Baulieu, P. Robel, Immunoreactive cytochrome P-450(17 alpha) in rat and guinea-pig gonads, adrenal glands and brain, Journal of Reproduction and Fertility 93 (1991) 609–622.
[16] L.M. Perkins, A.H. Payne, Quantification of P450scc, P450(17) alpha, and iron sulfur protein reductase in Leydig cells and adrenals of inbred strains of mice, Endocrinology 123 (1988) 2675–2682.
[17] C.E. Fluck, W.L. Miller, R.J. Auchus, The 17, 20-lyase activity of cytochrome p450c17 from human fetal testis favors the delta5 steroidogenic pathway, Journal of Clinical Endocrinology and Metabolism 88 (2003) 3762–3766.
[18] A.J. Conley, I.M. Bird, The role of cytochrome P450 17 alpha-hydroxylase and 3 beta-hydroxysteroid dehydrogenase in the integration of gonadal and adrenal steroidogenesis via the delta 5 and delta 4 pathways of steroidogenesis in mammals, Biology of Reproduction 56 (1997) 789–799.
[19] M.D. Aupperlee, A.A. Drolet, S. Durairaj, W. Wang, R.C. Schwartz, S.Z. Haslam, Strain-specific differences in the mechanisms of progesterone regulation of murine mammary gland development, Endocrinology 150 (2009) 1485–1494.
[20] F. Labrie, V. Luu-The, C. Labrie, J. Simard, DHEA and its transformation into androgens and estrogens in peripheral target tissues: intracrinology, Frontiers in Neuroendocrinology 22 (2001) 185–212.
[21] R.A. Hess, Estrogen in the adult male reproductive tract: a review, Reproductive Biology and Endocrinology 1 (2003) 52.
[22] L. Milewich, R.L. Garcia, A.R. Johnson, Steroid sulfatase activity in human lung tissue and in endothelial pulmonary cells in culture, Journal of Clinical Endocrinology and Metabolism 57 (1983) 8–14.
[23] L. Milewich, R.L. Garcia, L.W. Gerrity, Steroid sulfatase and 17 beta-hydroxysteroid oxidoreductase activities in mouse tissues, Journal of Steroid Biochemistry 21 (1984) 529–538.
[24] L. Mikkonen, P. Pihlajamaa, B. Sahu, F.P. Zhang, O.A. Janne, Androgen receptor and androgen-dependent gene expression in lung, Molecular and Cellular Endocrinology 317 (2010) 14–24.
[25] A.F. Holstein, E.C. Roosen-Runge, Atlas of Human Spermatogenesis, Grosse, Berlin, 1981, pp. 224.
[26] R. Raman, P. Das, Mammalian sex chromosomes. III. Activity of pseudoautosomal steroid sulfatase enzyme during spermatogenesis in *Mus musculus*, Somatic Cell and Molecular Genetics 17 (1991) 429–433.
[27] A.H. Payne, Gonadal steroid sulfates and sulfatase. V. Human testicular steroid sulfatase: partial characterization and possible regulation by free steroids, Biochimica et Biophysica Acta 258 (1972) 473–483.
[28] C. Martel, M.H. Melner, D. Gagne, J. Simard, F. Labrie, Widespread tissue distribution of steroid sulfatase 3 beta-hydroxysteroid dehydrogenase/delta 5-delta 4 isomerase (3 beta-HSD), 17 beta-HSD 5 alpha-reductase and aromatase activities in the rhesus monkey, Molecular and Cellular Endocrinology 104 (1994) 103–111.
[29] D. Webster, J.T. France, L.J. Shapiro, R. Weiss, X-linked ichthyosis due to steroid-sulphatase deficiency, Lancet 1 (1978) 70–72.
[30] A. Hernandez-Martin, R. Gonzalez-Sarmiento, U.P. De, X-linked ichthyosis: an update, British Journal of Dermatology 141 (1999) 617–627.
[31] H. Hoyer, G. Lykkesfeldt, H.H. Ibsen, F. Brandrup, Ichthyosis of steroid sulphatase deficiency. Clinical study of 76 cases, Dermatologica 172 (1986) 184–190.
[32] L.D. Russell, R.A. Ettlin, A.P. Sinha Hikim, E.D. Clegg, Staging for laboratory species, in: Histological and Histopathological Evaluation of the Testis, Cache River Press, Clearwater, 1990, pp. 162–194.

11. Anhang – Publikationen

7. J. Geyer, K. Bakhaus, R. Bernhardt, C. Blaschka, Y. Dezhkam, D. Fietz, G. Grosser, K. Hartmann, M.F. Hartmann, J. Neunzig, D. Papadopoulos, A. Sánchez-Guijo, G. Scheiner-Bobis, G. Schuler, M. Shihan, C. Wrenzycki, S.A. Wudy, M. Bergmann. J Steroid Biochem Mol Biol 2016 Jul 15; pii: S0960-0760(16)30201-1.

G Model
SBMB 4756 No. of Pages 15

ARTICLE IN PRESS

Journal of Steroid Biochemistry & Molecular Biology xxx (2016) xxx–xxx

Contents lists available at ScienceDirect

Journal of Steroid Biochemistry & Molecular Biology

journal homepage: www.elsevier.com/locate/jsbmb

Review

The role of sulfated steroid hormones in reproductive processes☆

Joachim Geyer[a,1,*], Katharina Bakhaus[a], Rita Bernhardt[b,1], Carina Blaschka[c], Yaser Dezhkam[c], Daniela Fietz[d,1], Gary Grosser[a], Katja Hartmann[d], Michaela F. Hartmann[e], Jens Neunzig[b], Dimitrios Papadopoulos[f], Alberto Sánchez-Guijo[e], Georgios Scheiner-Bobis[f,1], Gerhard Schuler[c,1], Mazen Shihan[f], Christine Wrenzycki[c,1], Stefan A. Wudy[e,1], Martin Bergmann[d,1]

[a] Institute of Pharmacology and Toxicology, Justus Liebig University, Giessen, Germany
[b] Institute of Biochemistry, Saarland University, Saarbrücken, Germany
[c] Veterinary Clinic for Obstetrics, Gynecology and Andrology, Justus Liebig University, Giessen, Germany
[d] Department of Veterinary Anatomy, Histology and Embryology, Justus Liebig University, Giessen, Germany
[e] Steroid Research & Mass Spectrometry Unit, Laboratory for Translational Hormone Analytics, Pediatric Endocrinology & Diabetology, Center of Child and Adolescent Medicine, Justus Liebig University, Giessen, Germany
[f] Institute of Veterinary Physiology and Biochemistry, Justus Liebig University, Giessen, Germany

ARTICLE INFO

Article history:
Received 13 May 2016
Accepted 4 July 2016
Available online xxx

Keywords:
Sulfated steroid hormone
Sulfation
Desulfation
DHEAS
Transport
Reproduction
Steroid sulfatase
Sulfatase pathway

ABSTRACT

Sulfated steroid hormones, such as dehydroepiandrosterone sulfate or estrone-3-sulfate, have long been regarded as inactive metabolites as they cannot activate classical steroid receptors. Some of them are present in the blood circulation at quite high concentrations, but generally sulfated steroids exhibit low membrane permeation due to their hydrophilic properties. However, sulfated steroid hormones can actively be imported into specific target cells *via* uptake carriers, such as the sodium-dependent organic anion transporter SOAT, and, after hydrolysis by the steroid sulfatase (so-called sulfatase pathway), contribute to the overall regulation of steroid responsive organs.

To investigate the biological significance of sulfated steroid hormones for reproductive processes in humans and animals, the research group "Sulfated Steroids in Reproduction" was established by the German Research Foundation DFG (FOR1369). Projects of this group deal with transport of sulfated steroids, sulfation of free steroids, desulfation by the steroid sulfatase, effects of sulfated steroids on steroid biosynthesis and membrane receptors as well as MS-based profiling of sulfated steroids in biological samples. This review and concept paper presents key findings from all these projects and provides a broad overview over the current research on sulfated steroid hormones in the field of reproduction.

Contents

Abbreviations: AR, androgen receptor; BTB, blood-testis barrier; DHEAS, dehydroepiandrosterone sulfate; E1, estrone; E2, estradiol; E3, estriol; E1S, estrone-3-sulfate; ER, estrogen receptor; FF, follicular fluid; GC, gas chromatography; GnRH, gonadotropin releasing hormone; hCG, human chorionic gonadotropin; HSD, hydroxysteroid dehydrogenase; LC, liquid chromatography; MS, mass spectrometry; NTCP, Na^+/taurocholate cotransporting polypeptide; OAT, organic anion transporter; OATP, organic anion transporting polypeptide; PREGS, pregnenolone sulfate; RXLI, recessive X-linked ichthyosis; SOAT, sodium-dependent organic anion transporter; STS, steroid sulfatase; SULT, sulfotransferase; TS, testosterone sulfate; TJ, tight junctions.

☆ Concept and review paper of the DFG research group FOR1369 "Sulfated Steroids in Reproduction".

* Corresponding author at: Justus Liebig University of Giessen, Institute of Pharmacology and Toxicology, Biomedical Research Center BFS, Schubertstr. 81, 35392 Giessen, Germany.
E-mail address: Joachim.M.Geyer@vetmed.uni-giessen.de (J. Geyer).

[1] Principal investigators of the research group.

http://dx.doi.org/10.1016/j.jsbmb.2016.07.002
0960-0760/

Please cite this article in press as: J. Geyer, et al., The role of sulfated steroid hormones in reproductive processes, J. Steroid Biochem. Mol. Biol. (2016), http://dx.doi.org/10.1016/j.jsbmb.2016.07.002

1. Steroid sulfation and desulfation in reproduction

In man and domestic animals virtually all processes of life are controlled by the nervous and/or the endocrine system. Depending on the organ/cell, the type of neurotransmitters, and the respective endocrine factors, these systems may be distinctly apart or show immediate interactions, for example in the central nervous system, where a number of endocrine factors belonging to the steroid hormone family are known to immediately interact with neural tissue.

To date the term "endocrine factor" also accounts for substances exhibiting paracrine, autocrine and intracrine mechanisms, it comprises the classical hormonal factors, *e.g.* steroid hormones or gonadotropins, but also accounts for cytokines, prostaglandins and a vast variety of growth factors.

Following their detection and identification of about seven decades ago [18,3,19,84], a large amount of information on sex steroids has piled up in respect to production, secretion, metabolism and the mechanisms of action on the cellular and molecular level. This also accounts for their interaction with classic nuclear receptors, DNA binding of ligand activated steroid receptors involving numerous cofactors and the initiation of transcription (for review see Ref. [6]) as well as the mechanisms underlying the fast non-genomic actions of steroid hormones (for review see Ref. [167]).

Though there is a common basic principle underlying the mechanisms of action of steroid hormones, evolution has led to a high diversity in respect to the types, production rates and metabolism of steroid hormones involved in the control of biological processes (*e.g.* [26,27]). This particularly relates to their involvement in reproductive processes.

The classical dogma is that steroid hormones must be available in an unbound, free form in order to interact with the respective receptor and to initiate a biological response. Steroid glucuronides and sulfo-conjugates, which are predominantly formed in the liver or kidney, for long were generally considered as biologically inactive metabolites intended for elimination [51,147,148,69,60,23]. However, already in 1976 Hoffmann et al. [56] described that in pregnant cows large amounts of estrone sulfate (E1S) represent secretory products of the placenta. This also accounts for small ruminants [158,61], the pig [117], the horse [57], camelids [1] and other ungulate species like *e.g.* the reindeer [119]. Similar in the stallion [58] and boar [25] the testes secrete large amounts of conjugated estrogens, in particular E1S. Moreover, the production of significant amounts of E1S has been observed in the ovaries of pregnant mares [28,57] and mares at estrus [82] but not in ovaries of other domestic mammalian species. Though there is ample evidence on the role of estrogens in reproduction, so far no function could be attributed to conjugated estrogens being immediate secretory products of endocrine glands/tissues.

The discovery of the co-localization of estrogen receptors (ER), steroid sulfatase (STS) and estrogen sulfotransferase (SULT) in the same tissue sheds new light on this situation [133] and gives rise to new hypotheses and speculations on the role of conjugated estrogens in reproduction and reproductive diseases, *e.g.* mammary gland tumors [115]. Increasing evidence has come up during the last years that hydrolysis of sulfo-conjugated estrone and dehydroepiandrosterone catalyzed by STS is an important alternative source of precursors for the local supply of estrogens and androgens, respectively [137,100]. In humans STS has recently been identified as a valuable drug target for estrogen and androgen deprivation therapies in hormonal diseases [146]. Thus, in addition to the provision of steroid hormones by the secretory activity of a given cell or gland, a second system controlling the availability of biologically active steroids on the cellular level might be established due to the expression of STS and/or SULT in certain organs, like the placenta [133], mammary gland [62], ovary [82,28,57], brain [109], or the testis [91].

The existence of such a system, however, would also require that sulfated steroids penetrate the plasma membrane of a target cell in order to get hydrolyzed and to become biologically active. The fact that – other than free steroids – conjugated steroids will not passively pass the lipid cell membrane barrier, questioned the existence of such a secondary local regulatory system. This situation has changed with the discovery of membrane uptake carriers for sulfated steroids such as the sodium dependent organic anion transporter (SOAT). SOAT has been shown to have high substrate specificity for sulfated steroids and is highly expressed in reproductive tissues such as testis and placenta [41,43,36,45,136].

The research group "Sulfated Steroids in Reproduction" of the German Research Foundation DFG focuses on this hypothesis of a local regulatory system concerning the provision of biologically active steroids by using sulfated steroids as precursors or by targeting biological activity through sulfation of free steroids. Fig. 1 depicts in a schematic way the basic concept of our research group. This concept relates to the observation that sulfation undoubtedly abolishes steroid hormone binding to their receptors, but that there is a species-specific production of sulfated steroid hormones, particularly of dehydroepiandrosterone sulfate (DHEAS) and E1S, by reproductive organs of hitherto unresolved biological meaning. Species exhibiting such high levels of sulfated steroid hormones include man and pig. The majority of projects are related to these two species and deal with target tissues for sulfated steroids and tissues as sources of their formation such as the testis and placenta. As the endogenous synthesis of steroid hormones by hormone competent cells competes with the recruitment of steroid hormones by desulfation, the balance between endogenous highly energy consuming synthesis of hormones from cholesterol and the rapid liberation of active hormones from their inactive sulfated precursors constitute a new regulation pathway. All reproductive tissues are subjected to feedback regulation *via* the brain, so sulfated neurosteroids may be important for the neuroendocrine control at the level of the anterior hypothalamus as well.

2. Transport of sulfated steroid hormones in the testis: the role of the sodium-dependent organic anion transporter SOAT

The importance of testicular testosterone production for spermatogenesis is well established. The prime target sites for androgens in the testis, as shown by the expression of the androgen

Please cite this article in press as: J. Geyer, et al., The role of sulfated steroid hormones in reproductive processes, J. Steroid Biochem. Mol. Biol. (2016), http://dx.doi.org/10.1016/j.jsbmb.2016.07.002

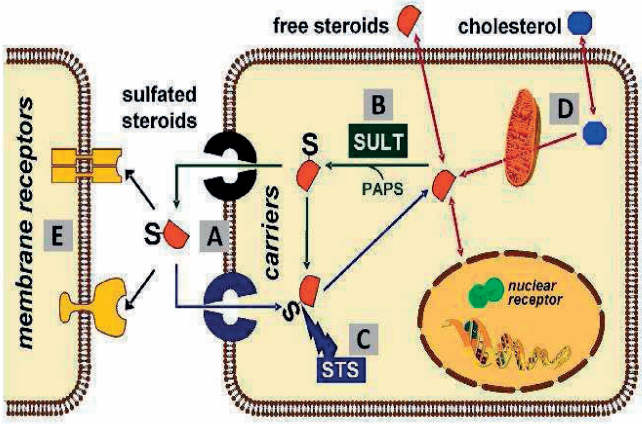

Fig. 1. Transport and metabolism of sulfated steroids. (**A**) Circulating sulfated steroids are delivered to target tissues via uptake carriers such as the sodium-dependent organic anion transporter SOAT. In addition, the appearance of sulfated steroids in the blood circulation requires an efflux transport from the site of production. (**B**) Sulfotransferases (SULTs) disrupt endocrine and reproductive steroid hormone functions by conversion of biologically active free steroid hormones to their sulfated counterparts. (**C**) In return, steroid sulfatase (STS) can generate biologically active steroid hormones within the gonads and the placenta ("sulfatase pathway"). The relation between an energetically expensive *de novo* synthesis of steroid hormones from cholesterol (**D**) and the rapid activation of delivered sulfated steroids by desulfation is a key question of the "sulfatase pathway" concept. (**E**) Sulfated steroids contribute to a further route of endocrine regulation by modulation of membrane-bound receptors.

receptor (AR), are Sertoli cells, Leydig cells, and peritubular cells [44]. In addition to androgens, ample evidence has been obtained that estrogens are important factors for normal testicular functions [54]. Estrogen receptors (ERα and ERβ) are expressed within the efferent ductule epithelium, where their primary function is to regulate the expression of proteins involved in fluid reabsorption [53].

Across species, Leydig cells of adult testes are the prime source of testicular androgens and also estrogens, and these cells are capable of *de novo* biosynthesis of these steroids [53]. In contrast, conversion of cholesterol to testosterone or androstenedione could not be demonstrated in isolated tubules of the testis [50]. Testosterone, androstenedione, and dehydroepiandrosterone are secreted from the human testis and can be detected in the spermatic vein at high plasma concentrations of 48–74 μg/100 ml, 2.5–2.9 μg/100 ml, and 2.8-4.5 μg/100 ml, respectively [73]. On the other hand, it was shown that the human testis is also able to produce large amounts of steroid sulfates including pregnenolone sulfate (PREGS), DHEAS, and even testosterone sulfate [73,120,88]. In addition to unconjugated free steroids, these sulfated steroids seem to play a role for human and boar testicular steroid regulation [120,121], as these compounds can be used as precursors of testosterone synthesis [105–107]. Among the sulfated steroids present in human testis, PREGS and DHEAS are quantitatively the most important forms [120]. Both compounds together with androstenediol-3-sulfate can be metabolized to testosterone in human testes and also boar testes homogenates [105,122] suggesting that STS may act as a regulatory control enzyme in testicular androgen biosynthesis [104,13,97].

Whereas metabolic conversion of sulfated steroids in testes homogenates was investigated intensively *in vitro*, the central question how these sulfated steroid hormones get access to the intracellular compartment and thereby exert physiological effects in the target cell was poorly recognized [115]. During the last 15 years several membrane transporter proteins were identified which are involved in the cellular uptake of anionic organic molecules by facilitated diffusion or secondary active Na^+/substrate co-transport, including bile acids, thyroid hormones, drugs, and xenobiotics [17,47,42]. Some of these transporters can also transport sulfated steroid hormones and thereby may participate in the regulation of cell-specific import of these precursor molecules. Among these carriers, SOAT is the only one which specifically accepts sulfated steroid hormones as substrates [41,43,36]. In humans and other species, SOAT is abundantly expressed in the testis [43,36,45]. Interestingly, SOAT mRNA expression was significantly reduced or even absent in severe disorders of spermatogenesis (arrest at the level of spermatocytes or spermatogonia, Sertoli cell only syndrome) as well as in biopsies showing hypospermatogenesis. The SOAT protein was localized to germ cells at various stages in human testis biopsies, including zygotene primary spermatocytes of stage V, pachytene spermatocytes of all stages (I–V), secondary spermatocytes of stage VI, and round spermatids (step 1 and step 2) in stages I and II [36]. In a similar manner, mSoat (mouse Soat) was detected in primary and secondary spermatocytes as well as round spermatids within the seminiferous tubules of the mouse testis and additionally showed high expression in bronchial epithelial cells of the lung and the epidermis of the skin [45]. On the functional level we achieved to combine transport measurements in carrier expressing cell lines with liquid chromatography tandem mass spectrometry (LC–MS/MS) [39,36]. By this, a sodium-dependent inward-directed SOAT transport of several sulfated steroids could be demonstrated, including DHEAS, 16α-OH-DHEAS, E1S, β-estradiol-3-sulfate and androstenediol-3-sulfate [39,36,136]. Compared with human SOAT, which has a preference for DHEAS as a substrate, mSoat exhibited the highest transport rate for PREGS, likely reflecting differences in the steroid pattern between both species. Nevertheless, based on our expression and transport studies, human SOAT and mSoat can be regarded as homologous carriers [45], giving interest to further studies in mSoat knockout mice in order to elucidate the physiological significance of SOAT/mSoat in the testis.

As SOAT is expressed in germ cells only and not in Sertoli cells, other transport ways are needed for the sulfated steroid hormones to pass the blood-testis barrier (BTB) and to reach the germ cells. The BTB was firstly described by Dym and Fawcett [34] in the rat and 1989 in men by Bergmann et al. [9] and is built between adjacent Sertoli cells by tight junctions. As hydrophilic sulfated steroids cannot pass the Sertoli cell membrane by diffusion, specific transporter systems are needed. These must include

Please cite this article in press as: J. Geyer, et al., The role of sulfated steroid hormones in reproductive processes, J. Steroid Biochem. Mol. Biol. (2016), http://dx.doi.org/10.1016/j.jsbmb.2016.07.002

uptake carriers to import sulfated steroids into Sertoli cells from the basal lamina side as well as efflux transporters to pass sulfated steroids to germ cells beyond the BTB. Promising candidates for steroid sulfate transport in Sertoli cells are the organic anion transporting polypeptides OATP3A1 and OATP2B1, as both are expressed in the human testis and show transport activity for sulfated steroids [48,89]. Beside these uptake carriers, also efflux transporters such as the multidrug resistance-related protein MRP1 may play a role for sulfated steroid transport in the testis. MRP1 has been localized at the basal membrane of mouse Sertoli cells and in Leydig cells [168] as well as in cultured human Sertoli cells [118].

Overall, apart from sulfation and desulfation steroid sulfate transporters play a role for the cellular availability of sulfated steroids. Only target cells, which express respective uptake transporters such as SOAT are regulated by the sulfated steroids themselves or after their desulfation and binding to steroid receptors. Therefore, carriers for sulfated steroids provide an additional cell-specific regulatory system other than the classical regulatory system of free steroids, which in principle can target all steroid responsive cells by diffusion (Fig. 2).

3. DHEAS and 16α-OH-DHEAS uptake carriers are required for estrogen synthesis by the human placenta

In women, after a period of approximately 9 weeks of pregnancy, the human placenta becomes the main source of maternal estrogens. The placenta has the ability to produce estrogens by *de novo* synthesis out of cholesterol [35]. However, the *de novo* synthesis of estrogens is insufficient and cannot explain the high amount of estrogens produced in the placenta [32,98]. It has been demonstrated that sulfated C-19 steroids such as DHEAS and 16α-OH-DHEAS of maternal and fetal origin, respectively, serve as precursors for placental estrogen biosynthesis [123,142,5,152,113,114]. The previous mentioned "sulfatase pathway" of estrogen biosynthesis is located in the syncytiotrophoblast, a syncytium that covers the placental villi and facilitates the exchange of substances between the fetal and maternal compartment [31,125]. Thereby, DHEAS of maternal and fetal origin contributes about equally to the placental formation of estrone and estradiol, while 16α-OH-DHEAS supplied by the fetus contributes to over 90% to placental estriol synthesis [143]. Therefore, the concept of a functional fetal placental unit for estrogen synthesis was established, providing the basis for maternal estriol measurement to assess fetal well being, placental function and/or uteroplacental blood flow [33,72]. Unconjugated estrogens, synthesized by the syncytiotrophoblast mainly from sulfated C-19 steroid precursors, are released into both the maternal and fetal blood. In the maternal compartment one part of the estrogens, mainly estriol is conjugated to glucuronides in the liver and finally excreted into urine. Another part, mainly estrone is sulfated, while estradiol remains largely unconjugated and represents the main fraction of unconjugated estrogens. In the fetal compartment estrogens are sulfated in the liver. Ateriovenous differences in cord blood indicate that sulfated estrogens of the fetal circulation are also taken up by the placenta, hydrolyzed by the STS in the syncytiotrophoblast and released into the fetal and maternal blood [72]. The conversion of sulfated C-19 steroid precursors such as DHEAS and 16α-OH-DHEAS to estrogens involves the action of different cytosolic enzymes in the syncytiotrophoblast. These include STS, 3β-hydroxysteroid dehydrogenase (3β-HSD), 17β-HSD, and aromatase [31].

But prior to enzymatic conversion, these sulfated steroids must enter the cells by carrier mediated transport. Although information on carriers for uptake and release of organic compounds in the human placenta significantly increased during the last decade [63,150,83,10,163], the carrier-mediated supply of syncytiotrophoblasts with sulfated C-19 steroids is not fully understood. DHEAS uptake into the human placenta was already investigated in cytotrophoblasts, choriocarcinoma cell lines, BHK cells and BHK cells transfected with human STS (BHK-STS cells) in suspension [160]. Significant initial uptake rates of DHEAS were observed for isolated cytotrophoblasts and to a lesser extent for BeWo but not for JEG-3, Jar, BHK cells and BHK-STS cells, indicating that carriers for DHEAS are only expressed in trophoblasts and to some extent by BeWo cells but not in JEG-3 cells [160]. Candidate carriers for sulfated steroids in the placenta include OATP1A2, OATP1B3, OATP2B1, OATP3A1, and OATP4A1, the organic anion transporter

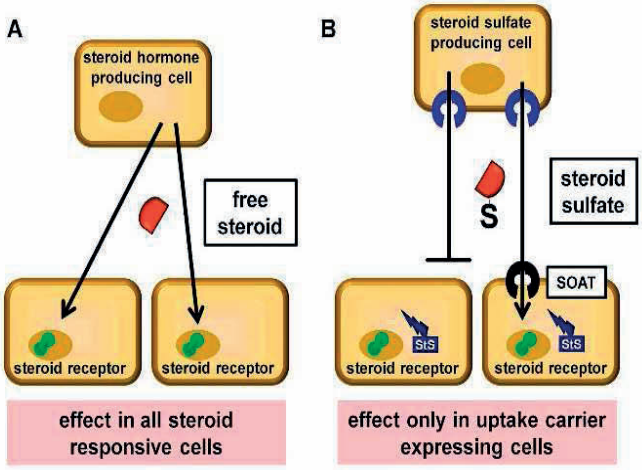

Fig. 2. The role of uptake carriers such as SOAT for the cell-specific effect of sulfated steroid hormones. (**A**) Free steroid hormones diffuse through the biological membrane and so contribute to the regulation of all steroid-responsive cells. (**B**) In contrast, sulfated steroids must be imported by uptake carriers into specific target cells and, therefore, exert their effects directly or after activation via the sulfatase pathway only in carrier-expressing (and StS-expressing) cells.

Please cite this article in press as: J. Geyer, et al., The role of sulfated steroid hormones in reproductive processes, J. Steroid Biochem. Mol. Biol. (2016), http://dx.doi.org/10.1016/j.jsbmb.2016.07.002

OAT4, the organic solute carrier protein OSCP1, and SOAT which all showed expression in the human placenta [22,154,38,71,161,65,43,49,89]. OATP1A2 was identified in syncytiotrophoblasts, villous cytotrophoblasts and extravillous trophoblasts and it transports DHEAS with higher and E1S with lower affinity [14,70,81,76]. Further immunohistochemical studies localized OATP1B3 to the vasculo-syncytial membrane of the syncytiotrophoblasts [166]. OATP3A1 expression was analyzed on the mRNA level and was found to be about 10 times higher in placenta compared to liver. OATP3A1 expression was markedly downregulated in the 3rd trimester compared to the 1st trimester placenta [103]. OATP4A1 was detected at the apical membrane of the syncytiotrophoblast as well, but only has low transport activity for E1S [154,131]. Finally, OSCP1 has been localized at the basal membrane of the syncytiotrophoblast in the human placenta and has been described as a carrier for sulfated steroids [65]. However, in a recent study OSCP1 mRNA could not be detected in pooled tissue homogenates of human placenta [36]. More detailed information on the placental expression is available for OAT4 and OATP2B1, which both were detected in 1st and 3rd trimester placentae in cytotrophoblast membranes and at the basal surface of the syncytiotrophoblast, indicating that both carriers may be involved in placental uptake of fetal-derived sulfated steroids [151,161,162,46]. Stably transfected OAT4-HEK293 cells showed a partly sodium-dependent uptake for DHEAS, 16α-OH-DHEAS, and E1S [162,136]. Furthermore, transport experiments on placental basal membrane-enriched vesicles point to a dominant role of OAT4 for placental 16α-OH-DHEAS uptake and estriol synthesis [156]. In contrast to OAT4, OATP2B1 transports DHEAS and E1S in a sodium-independent manner, but has no transport activity for 16α-OH-DHEAS and, therefore, seems not to play a role for placental estriol synthesis [162,136]. The affinity of DHEAS towards OATP2B1 was about 10 times lower compared to E1S while the capacity remained constant. Similar to STS, OATP2B1 is widely expressed in many organs and cell types [115,100]. In combination with STS, OATP2B1 might be responsible for supplying many cells with a basic level of active estrogens *via* the sulfatase pathway as originally described for breast cancer cells [100,130].

As already mentioned above, human SOAT specifically transports sulfated steroids in a sodium-dependent manner and revealed relatively high placental mRNA expression [43]. At the protein level, SOAT was localized to syncytiotrophoblasts in human late term placenta, predominantly at the apical membrane, and in the vessel endothelia of chorionic villi [136]. This indicates that SOAT may be the relevant uptake carrier for sulfated steroids like DHEAS from the maternal blood, a process which previously showed to be sodium-dependent (Fig. 3) [161,136]. Moreover, SOAT may be responsible for the supply of the placental villi by the uptake of 16α-OH-DHEAS at the fetal vessel endothelium directly from fetal blood. 16α-OH-DHEAS is the quantitatively most important sulfated steroid in fetal blood with concentrations of about 10 μM in umbilical blood [74,67]. The hydrophilic 16α-OH-DHEAS has to penetrate the vessel endothelium of the fetal placental villi to reach the syncytiotrophoblast by carrier-mediated transport. There it is metabolized to estriol by stepwise STS, 3β-HSD, 17β-HSD, and aromatase conversions [86,143,31]. Another pathway has been described *via* 16α-OH-testosterone or alternatively a direct aromatization of 16α-OH-androstenedione to estriol without the interstage of 16α-OH-estrone [124,2].

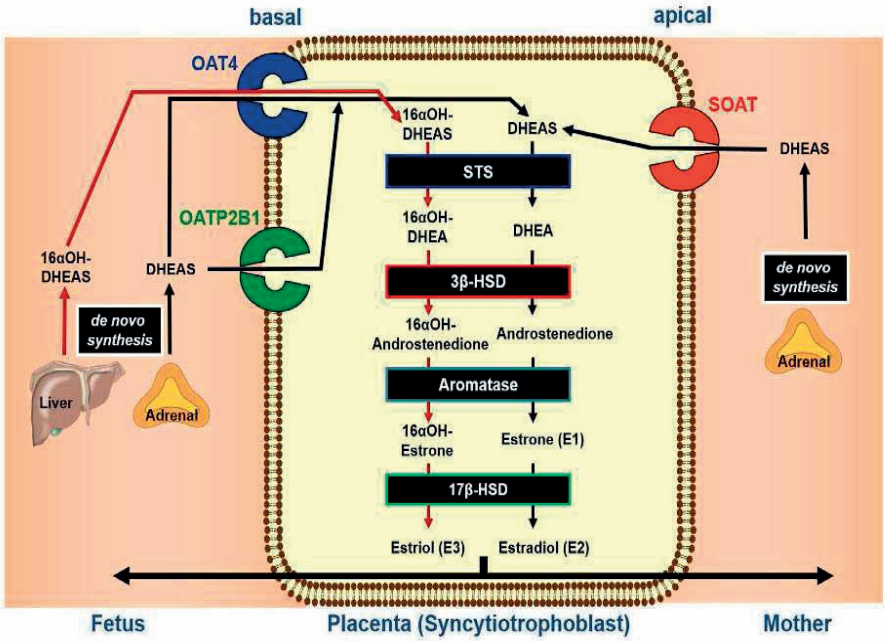

Fig. 3. Estrogen synthesis of the human placenta. DHEAS is mainly synthesized in the adrenals of both, mother and fetus, and has to enter the syncytiotrophoblast by carrier-mediated uptake. SOAT is located at the apical membrane of the syncytiotrophoblast and can mediate the uptake of DHEAS from maternal blood. OAT4 and OATP2B1, both revealed transport activity for DHEAS, were detected at the basal (fetal) membrane of the syncytiotrophoblast. In the cell, DHEAS is desulfated by the steroid sulfatase (STS) and metabolized to estradiol (E2) by 3β-HSD, aromatase, and the 17β-HSD reactions. Alternatively, androstenedione can be converted to testosterone by the 17β-HSD that is further metabolized to E2 by aromatase [2,101]. In contrast to DHEAS, 16α-OH-DHEAS is only produced by the fetal liver and metabolized to estriol (E3) after carrier-mediated uptake by OAT4 at the basal membrane of the syncytiotrophoblast. The unconjugated estrogens E1, E2, and E3 are able to pass the cell membrane by diffusion.

Please cite this article in press as: J. Geyer, et al., The role of sulfated steroid hormones in reproductive processes, J. Steroid Biochem. Mol. Biol. (2016), http://dx.doi.org/10.1016/j.jsbmb.2016.07.002

4. Synthesis, metabolism and supposed function of sulfated steroids in the porcine testicular-epididymal compartment

Although the sulfatase pathway has been identified as a potential route of local estrogen and androgen production, the information on the existence and function of this pathway in tissues other than human mammary carcinoma is still sparse. Therefore, the porcine testicular-epididymal compartment was chosen as a model to study the physiological significance of the sulfatase pathways as (I) it has been found to produce an unusually broad spectrum of sulfated steroids which circulate in intriguingly high concentrations [8,135,112], (II) previous studies have demonstrated considerable STS activities in testicular and epididymal tissue homogenates [59], (III) it exhibits a considerable expression of receptors for estrogens, androgens and progesterone [68,90,66,108], and (IV) high SOAT mRNA expression was observed (Schuler, Geyer, unpublished data). Thus this organ system meets all requirements for a multitude of possible local sulfatase pathways or may produce sulfated precursors for sulfate pathways elsewhere in the organism.

So far, the functions of the many sulfated steroids in boars are completely unknown, and many questions concerning their synthesis are still open. Numerous sulfated 3α- or 3β-hydroxysteroids have been identified which are obviously related to the testicular synthesis of androgens or steroidal pheromones [112]. Moreover, similar to the horse [58] but clearly different from other domestic mammalian animal species and humans, male pigs exhibit extraordinarily high concentrations of sulfated estrogens [25]. Data from measurements in testicular tissue or from comparative measurements in testicular artery and vein provide evidence that they are predominantly of gonadal origin [8,138,112,59]. Observations from experiments with cultured Leydig cells indicate that they are the main producers of numerous sulfated C19 steroids and estrogens [110,111,144]. However, a predominant production of sulfated steroids, especially of sulfated estrogens in Leydig cells would be difficult to comprehend as these cells exhibit a high expression of STS [91] and are obviously capable of producing free estrogens abundantly *de novo* due to their high expression of aromatase [90]. Moreover, concerning the exact synthetic pathways of sulfated steroids and the relevant SULTs in boars many questions are still open. The sulfation of small biomolecules such as steroids is catalyzed by members of the large family of cytosolic SULTs, which partly overlap in their substrate specificities. SULT1E1 is commonly accepted as the only relevant sulfotransferase for estrogens at physiological substrate concentrations, but other SULTs such as SULT1A1 have also been reported to sulfate estrogens at high substrate concentrations. In humans SULTs 2A1 and 2B1 have been identified as relevant sulfotransferases for neutral hydroxysteroids with DHEA, pregnenolone and cholesterol being the preferential substrate for SULT2A1, SULT2B1 variant a and SULT2B1 variant b, respectively [23,4,102]. However, the exact substrate preferences of porcine SULTs are still unknown, and so far only one SULT2B1 isoform has been cloned in pigs. As an alternative to the sulfation of free steroids, the production of sulfated steroids by utilization of sulfated precursors (sulfate pathway of steroidogenesis) has been described in various steroidogenic organs from different species [20,21,116,75,55,40,122] including the direct conversion of DHEAS into E1S [96]. The existence of a productive sulfate pathway in the porcine testis would provide a plausible explanation for the high

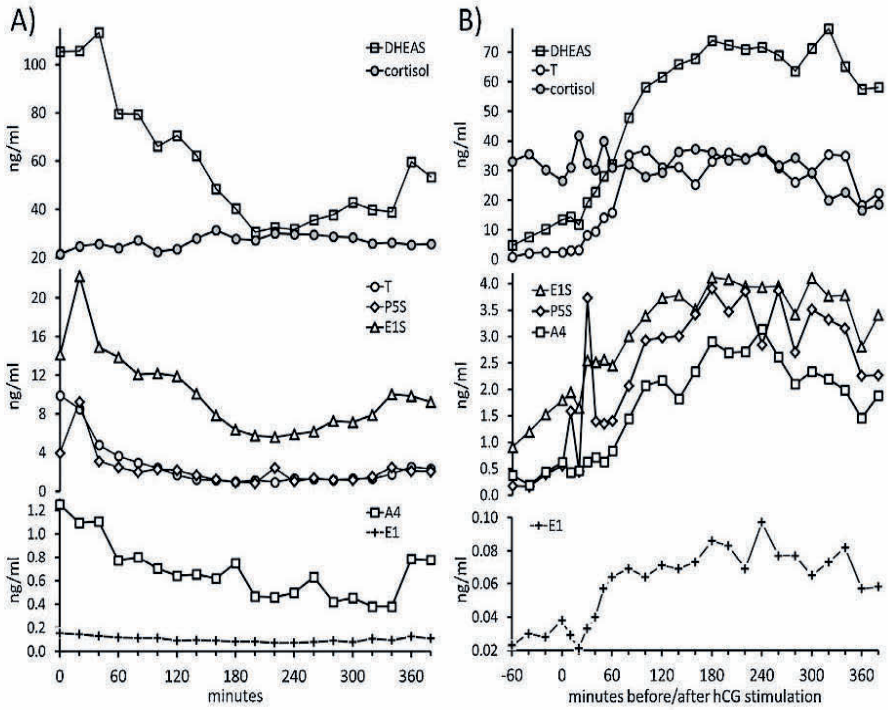

Fig. 4. Long-term profiles of free and sulfated steroids in **A**) an unstimulated boar and **B**) in a boar stimulated with 1500 I.U. human chorionic gonadotrophin (hCG). Cortisol was included in the measurements to monitor adrenal activity during the sampling period. A4—androstenedione, E1—estrone, T—testosterone, DHEAS—dehydroepiandrosterone sulfate, E1S—estrone-3-sulfate, P5S—pregnenolone sulfate. Figures were compiled based on data previously published in Schuler et al. [134].

Please cite this article in press as: J. Geyer, et al., The role of sulfated steroid hormones in reproductive processes, J. Steroid Biochem. Mol. Biol. (2016), http://dx.doi.org/10.1016/j.jsbmb.2016.07.002

production of various sulfated steroids in this organ. Another intriguing feature of porcine testicular steroidogenesis is the high expression of STS in Leydig cells [91], which in boars are commonly regarded as the main producers of sulfated estrogens and several sulfated C19-steroids [110,97,111,144]. Thus, the existence of a productive sulfate pathway in the porcine testis would suggest that STS present in Leydig cells by its subcellular distribution or substrate preference could control the steps within the cascade of steroidogenic enzymes where sulfonated precursors may enter the pool of free steroids.

The current concept of the testis as the only considerable source of sulfated estrogens in boars was challenged by our previous observation of high estrogen sulfotransferase activity in the epididymis *vs.* virtually absent activity in the testis [59]. However, in case the sulfation of testicular estrogens occurs to a significant extent in the epididymis, it was hypothesized that considerable differences between the secretion patterns of free and sulfated estrogens should exist, *e.g.* time shifts between their profiles due to the time consuming transfer of free estrogens from the testis to the epididymis. Thus, in order to characterize *in vivo* the interrelationship between the secretion profiles of free and sulfated steroids, blood samples were collected from six postpubertal boars in 20 min intervals over a period of 6 h. Concentrations of PREGS, DHEAS, E1S, estradiol-17ß sulfate, androstenedione and testosterone were measured by LC–MS/MS [39], whereas concentrations of estrone and estradiol-17ß were assessed by highly sensitive radioimmunoassays, providing for the first time simultaneous long-term profiles for several free and sulfated steroids in a larger number of boars (Fig. 4) [134]. Despite their identical genetic background (Pietrain x Landrace crossbreds) steroid concentrations varied considerably between individual boars. However, the results indicate that in boars free and sulfated steroids assessed exhibit similar patterns pointing to a pulsatile secretion with low frequency (three to five pulses per day) consistent with previously published diurnal profiles for 5α-androstenone, testosterone, DHEAS and total conjugated estrogens established in a low number of animals [25,155], and they did not provide evidence for a substantially different distribution after synthesis (*e.g.* in blood, lymph fluid, rete testis fluid). Consistently, after hCG stimulation performed in seven boars a rapid and virtually simultaneous increase of free and sulfated steroids was observed, indicating that after synthesis at least a major proportion is immediately released into peripheral circulation. Pronounced differences of concentrations were found for all steroids assessed between arterial and venous blood vessels running on the testicular surface consistent with the concept of the testis as their predominant origin. Thus, the synthetic pathway providing the high amounts of sulfated estrogens in the testis and the role of the considerable estrogen sulfotransferase activities in the epididymis remain to be elucidated.

5. Impact of intrafollicular sulfated steroids on follicular cells and the oocyte'developmental capacity in cattle

Within the reproductive system the ovarian follicle can be considered as an extremely fragile microenvironment. In antral follicles, various procedures affect oocyte maturation and the acquisition of developmental competency. It includes the interaction between somatic cells, in particular the cumulus cells of the follicle, and the oocyte to generate a fully competent oocyte. In addition, the composition of follicular fluid (FF) has an impact on the developmental potential of the oocyte. FF is a product of blood plasma components which cross the blood follicle barrier and the secretions of the cumulus, granulosa and theca cells and the oocyte itself [37,52]. Variations in the metabolic composition of FF may also have an influence on the developmental potential of oocyte and subsequent embryos [165,169]. FF contains a fine-tuned pattern of energy metabolites, proteins, cytokine/growth factors, steroids and other until now undefined factors [153,78,164].

Steroid hormones are essential regulators in the well-orchestrated process of follicular development. In theca cells pregnenolone is converted into progesterone and granulosa cells are able to convert the theca-derived androgens androstendione and testosterone to estrone and/or 17β-estradiol. Furthermore, during final maturation a switch from estradiol to progesterone dominance is well-described in follicular fluid [30]. Moreover, it has recently been shown that follicular cells have the ability to synthesize bile acids [145]. Bile acids are present in several fluids of mammals especially in bile, blood and urine. They have been identified in FF from human [145,92] and cattle [126,129].

The ovarian expression of SULT1E1 [15] and STS [16] has been analyzed in equine follicles during human chorionic gonadotropin (hCG)-induced ovulation/luteinization. After hCG injection, SULT1E1 transcripts significantly increased after 30–39 h in granulosa cells indicating that follicular luteinization is accompanied not only by a decrease in 17β-estradiol biosynthesis [15]. For STS transcripts isolated from equine pre-ovulatory follicles between 0 and 39 h after hCG treatment, a significant decrease was observed in granulosa cells 24–39 h post-hCG [16]. This down-regulation in equine luteinizing pre-ovulatory follicles may provide an additional process for the decrease in 17β-estradiol biosynthesis after the LH surge.

The results of our current studies provide for the first time the profile of conjugated and free steroids [12] as well as bile acids [129] in bovine FF. Recently it has been shown that all aspects of the bile acid synthesis pathway are present in the human ovarian follicle, including the enzymes in both the classical and alternative pathways, the nuclear receptors known to regulate the pathway, and the end product bile acids [145]. Given that the ovarian follicle is a highly privileged environment, it is likely that bile acids play a specific role beyond simply acting as detergents and carriers of cholesterol. Full characterization of the follicular-specific role of bile acids remains to be determined.

To gain more insights into the expression of steroid metabolizing enzymes in cattle, ovaries were collected at a slaughterhouse and categorized according to their estrus cycle stage. Pairs of ovaries of each cycle stage (proestrus, estrus, postestrus, interestrus) were analyzed for the presence of SULT1E1 and STS *via* immunohistochemistry. Small amounts of STS were detected in granulosa cells of antral and secondary follicles and in the endothelium of blood vessels, irrespective of the stage of the estrus cycle. Moreover, staining for SULT1E1 was restricted to granulosa cells in antral follicles, again irrespective of the stage of the estrus cycle. These data indicate for the first time the presence of the steroid metabolizing enzymes STS and SULT1E1 at the protein level in bovine ovaries [11].

It is well-accepted at the moment that present *in vitro* maturation systems do not completely mimic the *in vivo* situation during the preovulatory development resulting in oocytes of reduced quality. Therefore, the temporal pattern of 17β-estradiol and progesterone concentrations has also been determined during final maturation *in vitro* measuring their concentrations at intervals of 4 h. During *in vitro* maturation, progesterone significantly increased in the medium, whereas the 17β-estradiol concentration did not change. These data underline that present conditions of *in vitro* maturation do not reflect the *in vivo* situation [12].

6. The role of sulfated steroids in the regulation of steroid hormone biosynthesis

The synthesis of mineral- and glucocorticoids, as well as sex hormones begins with the side-chain cleavage of cholesterol

Please cite this article in press as: J. Geyer, et al., The role of sulfated steroid hormones in reproductive processes, J. Steroid Biochem. Mol. Biol. (2016), http://dx.doi.org/10.1016/j.jsbmb.2016.07.002

yielding pregnenolone and takes place in the inner mitochondrial membrane of steroidogenic cells. This reaction, catalyzed by cytochrome P450 11A1 (CYP11A1), represents the rate-limiting enzymatic step of the steroidogenesis. Five further CYPs and three hydroxysteroid dehydrogenases constitute the remaining enzymes necessary for the generation of the three classes of steroid hormones. The availability of steroid hormones is controlled by three different regulatory pathways, namely the renin-angiotensin-aldosterone system, the hypothalamic-pituitary-adrenal-axis or the hypothalamic-pituitary-gonadal-axis. Additionally, hydrolysis of sulfated steroids by STS leading to free steroids, depicts a further mechanism of regulation [137,100]. Sulfated steroids often exceed concentrations of their unconjugated counterparts manifold, as in the case of DHEA, which is excreted from the adrenal gland to up to 99% in its sulfated DHEAS form [77]. Although sulfated steroids are highly abundant in humans, and, as in the case of DHEA(S), are used as dietary supplements, studies investigating a direct effect on steroidogenesis are very scarce. Therefore, we examined the influence of DHEAS on the CYP11A1-dependent cholesterol conversion, utilizing a reconstituted *in vitro* system [93]. Compared to the control reactions (presence of DHEA or absence of DHEAS), the catalytic efficiency of CYP11A1 increased by nearly 80% in the presence of DHEAS. The molecular mechanisms of the altered CYP11A1 activity were elucidated by performing substrate binding and protein–protein interaction studies. These studies revealed a higher affinity of CYP11A1 towards its substrate cholesterol as well as an enhanced interaction of CYP11A1 with its electron transfer partner, adrenodoxin (Adx) in the presence of DHEAS. In order to elucidate, which of the three hydroxylation steps of cholesterol during pregnenolone synthesis is altered by DHEAS, 22(R)OH-cholesterol, the first hydroxylated product, was utilized as substrate for CYP11A1. As no effect of DHEAS was observed, it was concluded that only the first hydroxylation step of the CYP11A1-dependent cholesterol conversion is enhanced in the presence of DHEAS, leading to an increased pregnenolone formation [94]. Furthermore, the influence of DHEAS on the activity of CYP17A1 and CYP21A2 was examined. These enzymes are crucial for the formation of sex hormones as well as mineralo- and glucocorticoids. However, in contrast to the effect on the activity of CYP11A1, the enzymatic activities of CYP17A1 and CYP21A2 were not significantly altered in the presence of DHEAS, indicating a highly selective impact of DHEAS on only CYP11A1 [94].

Besides the direct impact of sulfated steroids on the natural substrate conversion of steroidogenic CYPs, it was examined whether sulfated steroids themselves can serve as substrates. The

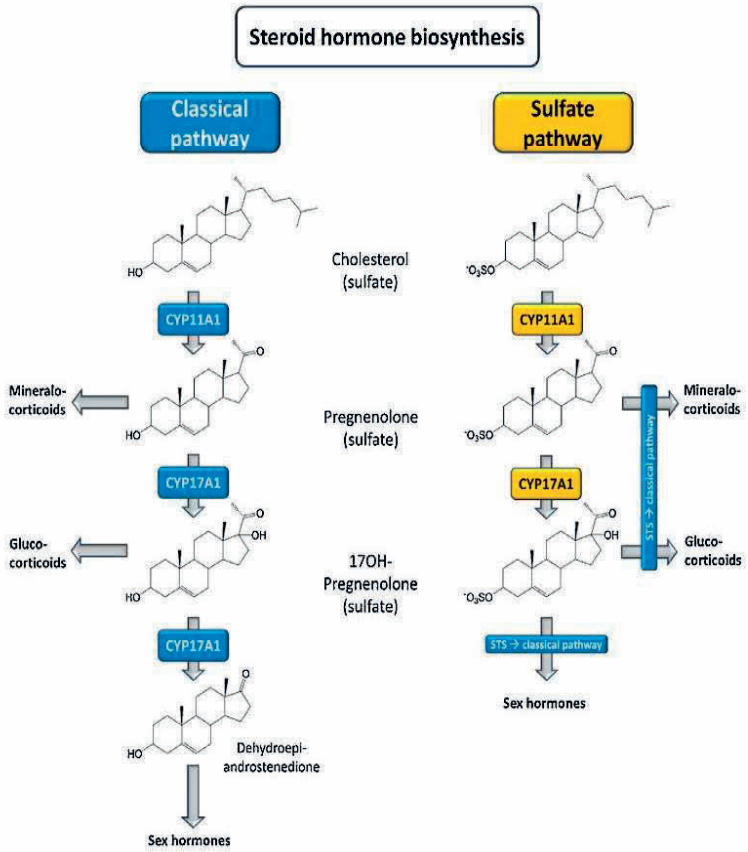

Fig. 5. Scheme of the steroid hormone biosynthesis comparing the classical pathway (blue) with the one for sulfated steroids (yellow). Cholesterol sulfate is converted into pregnenolone sulfate and 17OH-pregnenolone sulfate by CYP11A1 and CYP17A1, respectively. For a further metabolism of these sulfated steroid hormones into mineralocorticoids, glucocorticoids or sex hormones, the cleavage by steroid sulfatases (STS) is necessary. (For interpretation of the references to colour in this figure legend, the reader is referred to the web version of this article.)

Please cite this article in press as: J. Geyer, et al., The role of sulfated steroid hormones in reproductive processes, J. Steroid Biochem. Mol. Biol. (2016), http://dx.doi.org/10.1016/j.jsbmb.2016.07.002

conversion of cholesterol sulfate (CS) into PREGS by CYP11A1 was already described before, using ovarian mitochondria [159]. Therefore, we investigated the metabolism of PREGS by CYP17A1 using a reconstituted *in vitro* system as well as an appropriate human cell culture model [95]. Binding studies of PREGS with CYP17A1 were performed and showed that PREGS binds with a 2.5-fold lower affinity towards CYP17A1 compared with pregnenolone. Kinetic experiments revealed a 40% reduced catalytic efficiency of CYP17A1 using PREGS instead of pregnenolone as substrate.

CYP17A1 is known to catalyze not only a hydroxylation at position C17 of pregnenolone or progesterone but also a 17,20-lyase reaction yielding DHEA or androstenedione, respectively. We demonstrated that PREGS is converted into 17OH-PREGS, but not into DHEAS, in both, the reconstituted *in vitro* system as well as in cell culture [95]. Even addition of cytochrome b_5 to the reconstituted *in vitro* system, which is known to strongly enhance the lyase activity of CYP17A1 [64], did not lead to 17,20C—C bond cleavage when using sulfated precursors. It appears that the alignment of the iron–oxygen complex of CYP17A1 onto the C20 atom of 17OH-PREGS is hindered by the sulfate moiety, possibly due to the negative charge of the sulfate group and the increased size of the molecule thereby preventing the lyase reaction of CYP17A1 on 17OH-PREGS. In order to examine whether 17OH-PREGS enters the glucocorticoid pathway, reconstituted *in vitro* experiments were performed with CYP21A2, whose natural substrate is 17OH-progesterone. As no conversion was detected, it has to be assumed that the pathway for sulfated steroids starts with CS and ends with 17OH-PREGS (Fig. 5). DHEAS might, therefore, solely be synthesized *via* sulfation of DHEA and not through a sulfated precursor.

Apart from CYP11A1 and CYP17A1, the conversion of testosterone sulfate (TS) by CYP19A1 was investigated. In the literature there are only two publications available dealing with the direct aromatization of TS, both having contradictory results: whereas Satoh et al. [132] described a direct aromatization of TS, Cheatum et al. [24] did not observe aromatization activity of CYP19A1 on TS. Both groups used human placental microsomes for their experiments. Utilizing a reconstituted *in vitro* system with purified CYP19A1 and cytochrome P450 reductase we demonstrated a high aromatization activity of CYP19A1 on testosterone, but not on TS although our analytical LC–MS/MS method is highly sensitive (Neunzig et al. unpublished data). This result is in agreement with a study by Baulieu et al. [7], which demonstrated that in pregnant female TS does not serve as an estrogen precursor.

7. DHEAS-specific signaling in cells of the reproductive system

DHEAS is one of the most abundant circulating steroid in humans. Its concentration in plasma is between 1.3 and 6.8 μM, which is about 200-fold higher than the plasma concentrations of DHEA (7–31 nM). DHEAS is produced mainly in the adrenal zona reticularis. It is derived from DHEA, which is almost entirely converted to DHEAS by SULT. The sulfated steroid is then secreted into the serum and here can be considered as a pro-androgen that can be converted into testosterone or other steroid hormones in order to exert its biological activity. Although DHEAS is produced not only in adrenal cortex and brain but also in gonads, surprisingly little is known about the effects of this steroid on the various cells of the reproductive system. Therefore, by using the Sertoli cell line TM4 and the spermatogenic cell line GC-2 as models, the possibility of a hormone-like action of DHEAS was investigated by searching for signaling cascades that might be induced by DHEAS.

DHEAS acting on the spermatogenic cell line GC-2 induces a time- and concentration-dependent phosphorylation of c-Src and Erk1/2 and activates the transcription factors ATF-1 and CREB [141]. These actions are consistent with the non-classical signaling pathway of testosterone and suggest that DHEAS is a pro-androgen that is converted into testosterone in order to exert its biological activity. The fact, however, that steroid sulfatase mRNA was not detected in the GC-2 cells and the clear demonstration of DHEAS-induced activation of Erk1/2, ATF-1 and CREB after silencing the androgen receptor by siRNA clearly contradict this assumption and make it appear unlikely that DHEAS has to be converted in the cytosol into a different steroid in order to activate the kinases and transcription factors mentioned. Instead, it is likely that the DHEAS-induced signaling is mediated through the interaction of the steroid with a membrane-bound G-protein-coupled receptor, since silencing of Gnα11 leads to the abolition of the DHEAS-induced stimulation of Erk1/2, ATF-1, and CREB [141]. Further work for the identification of the DHEAS receptor and of target mRNAs whose expression is controlled by the activation of the CRE promoters through the transcription factors CREB and ATF-1 will help to define new roles of DHEAS in the physiology of cells of the male and possibly also of the female reproduction system.

The blood-testis barrier (BTB) is one of the tightest blood-tissue barriers in mammals and separates the seminiferous epithelium into basal and adluminal compartments. The main function of the BTB is the formation of an immunological barrier in order to protect the meiotic and post-meiotic stages of the germ cells from cells of the immune system. Disturbance of the integrity of the BTB causes infertility [87]. Formation and maintenance of the BTB is mainly defined by the formation of tight junctions (TJ) between neighboring Sertoli cells. TJ, in turn, are formed by the interactions of occludin with claudins, which interact with signaling proteins and proteins of the cytoskeleton on the cytosolic side of the membrane [87].

Recent findings show for the first time that physiological concentrations (1 μM) of DHEAS induce the phosphorylation of the kinase Erk1/2 and of the transcription factors CREB and ATF-1 in the murine Sertoli cell line TM4 [99]. This signaling cascade stimulates the expression of the TJ proteins claudin-3 and claudin-5. As a consequence of the increased expression, TJ connections between neighboring Sertoli cells are augmented, as demonstrated by measurements of transepithelial resistance [99]. Phosphorylation of Erk1/2, CREB, or ATF-1 is not affected by the presence of the steroid sulfatase inhibitor STX64 or when DHEA was used instead of DHEAS. Abrogation of androgen receptor expression by siRNA did not affect DHEAS-stimulated Erk1/2 phosphorylation, nor did it change DHEAS-induced stimulation of claudin-3 and claudin-5 expression. All of the above indicate that desulfation and conversion of DHEAS into a different steroid hormone is not required to trigger the DHEAS-induced signaling cascade. All activating effects of DHEAS, however, are abolished when the expression of the G-protein Gnα11 is suppressed by siRNA, including claudin-3 and −5 expression and TJ formation between neighboring Sertoli cells as indicated by reduced transepithelial resistance. Taken together, these results are consistent with the effects of DHEAS being mediated through a membrane-bound G-protein-coupled receptor interacting with Gnα11 in a signaling pathway that resembles the non-classical signaling pathways of steroid hormones. Considering the fact that DHEAS is produced in reproductive organs, these findings also suggest that DHEAS, by acting as an autonomous steroid hormone and influencing the formation and dynamics of the TJ at the blood-testis barrier, might play a crucial role for the regulation and maintenance of male fertility.

These investigations call into question the heretofore generally accepted idea of DHEAS being simply a pro-androgen and demonstrates for the first time that DHEAS acts as a steroid hormone on GC-2 and TM4 cells in its own right and triggers the activation of signaling cascades that reflect the non-classical signaling pathway of

Please cite this article in press as: J. Geyer, et al., The role of sulfated steroid hormones in reproductive processes, J. Steroid Biochem. Mol. Biol. (2016), http://dx.doi.org/10.1016/j.jsbmb.2016.07.002

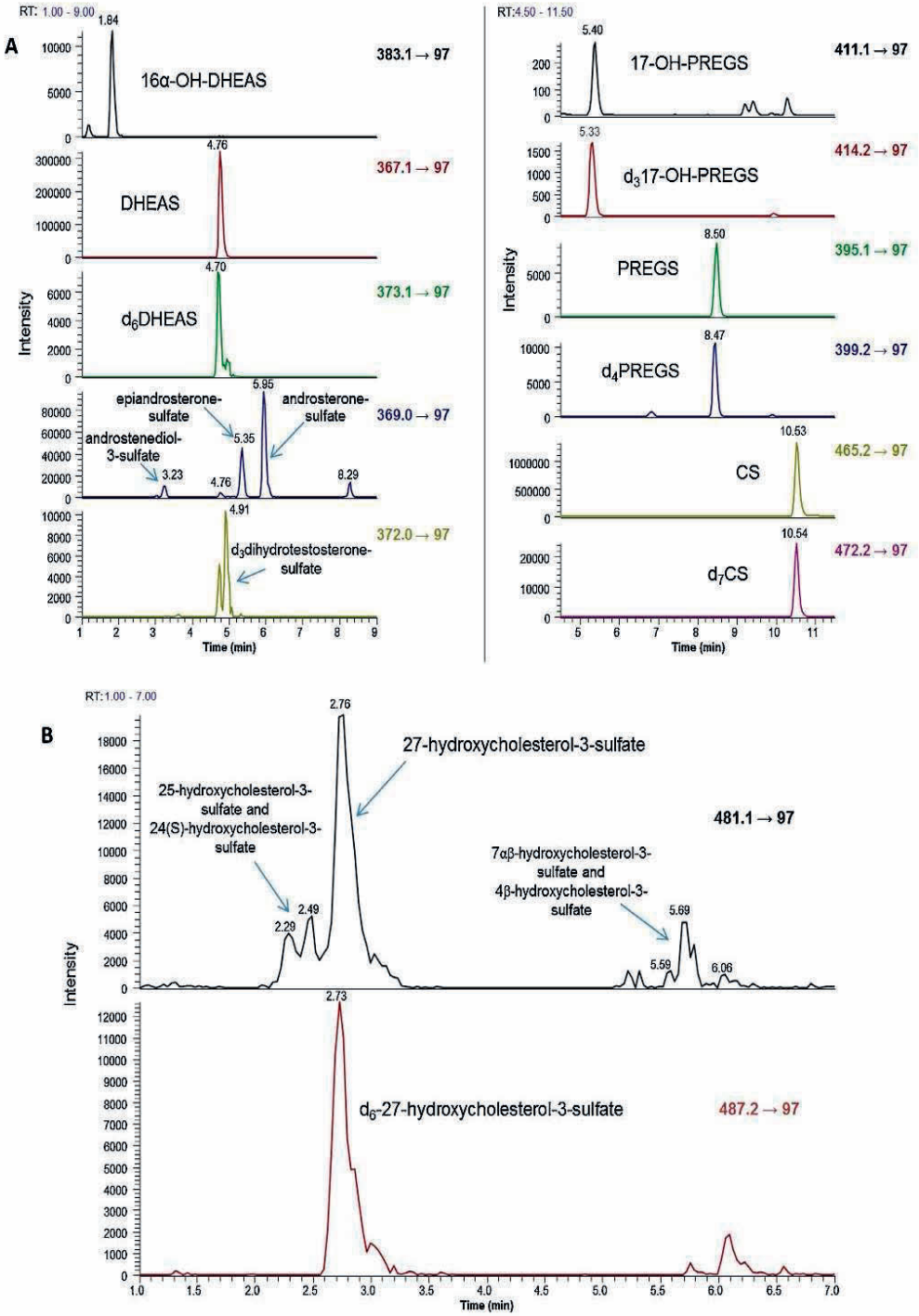

Fig. 6. Profiling of sulfated steroids by LC–MS/MS in serum of a 29-year-old RXLI patient. (**A**) Chromatograms of androgen sulfates, PREGS, 17-OH-PREGS and CS. (**B**) Chromatograms of oxysterol sulfates [127,128]. The concentrations of 27-hydroxycholesterol-3-sulfate and CS were 29.1 ng/ml and 34.4 μg/ml, respectively.

Please cite this article in press as: J. Geyer, et al., The role of sulfated steroid hormones in reproductive processes, J. Steroid Biochem. Mol. Biol. (2016), http://dx.doi.org/10.1016/j.jsbmb.2016.07.002

steroid hormones involving membrane-bound GPCRs that interact with the G-protein Gnα11. These data are consistent with the idea that DHEAS, by acting as an autonomous hormone on spermatogenic or Sertoli cells, may play a substantial role in the regulation of male fertility. Furthermore, since DHEAS is also produced in brain or adrenal cortex and claudin-3 or −5 are also constituents of various other blood-tissue barriers, it would not be unexpected if it were revealed that DHEAS influences the dynamics of these tissue-blood barriers as well. Thus, the extension of this investigation to other tissues and cell types might help to define new actions of DHEAS and establish its function as an essential steroid hormone in mammalian physiology.

8. Profiling steroid sulfates by multi-targeted stable isotope dilution liquid chromatography-tandem mass spectrometry (LC–MS/MS)

The biological significance and the crucial role of sulfated steroids in physiological systems is now beginning to be more and more appreciated [149]. Therefore, steroid determination with highest reliability is a prerequisite for the realization of this collaborative interdisciplinary research proposition. At present, routine steroid analysis is primarily based on commercially available immunoassays. However, major analytical quality issues for steroid immunoassays such as lack of agreement between methods, poor specificity (antibody specificity, matrix effects), under-recovery of analyte, and the lack of agreement with reference methods have started a continuous debate on the accuracy of steroid immunoassays [85]. Furthermore, individual immunoassays only allow determination of a single steroid at a time. Especially within a research setting, determination of rare steroids or identification of unknown steroids might not be possible due to the unavailability of specific kits for such unusual analytes.

Analytical methods based on mass spectrometry (MS) currently present the most specific qualitative and quantitative methods for steroid determination [170]. Combination with a chromatographic technique such as gas chromatography (GC) or liquid chromatography (LC) allows for the metabolomics approach consisting in the simultaneous and unbiased determination of multiple small molecule metabolites characterizing a biological sample [29]. Since the mid 1980s, gas chromatography-mass spectrometry (GC–MS) has proven to be a robust routine technique for the identification and quantification of steroids. In case stable isotope labeled analogs of the analytes were used as internal standards reference methods presenting the "gold standard" in steroid analysis were developed (isotope dilution mass spectrometry). Stable isotope labeled internal standards have the advantage of showing practically the same chemical and chromatographic properties as their corresponding analytes and they allow procedural losses to be disregarded. Due to their different physical properties, they can easily be distinguished from the unlabeled compounds in the mass spectrometer by monitoring different ions.

However, only volatile and thermally stable steroids can be analyzed by GC–MS. This precludes the direct analysis of intact steroid conjugates, particularly sulfates and requires hydrolysis or solvolysis steps. Several observations however render this approach unsuitable for the accurate determination of steroid conjugates because I) enzymatic hydrolysis may be incomplete due to competitive or non-competitive inhibition of the enzyme, II) conjugates at sterically hindered positions might not undergo enzymatic cleavage, III) different enzymatic preparations might contain various enzymatic activities, IV) certain hydrolyzing enzymes may simultaneously possess steroid converting abilities and V) other solvolyzable forms of steroid conjugates might lead to overestimation of the actual compound of interest [80]. All these findings emphasize the importance of measuring the intact steroid sulfates directly.

The development of "soft", *i.e.* non-disintegrating ionization techniques, opened new avenues for the analysis of complex biomolecules. The introduction of fast atom bombardment and related techniques allowed the analysis of intact steroid conjugates without derivatization [140]. Shortly after, the development of soft ionization methods operating at atmospheric pressure permitted the introduction of liquid chromatography-mass spectrometry (LC–MS), which was soon applied to the analysis of intact steroid conjugates [79,139]. Electrospray ionization and atmospheric pressure chemical ionization are nowadays the most widely applied soft ionization techniques. Introduction of tandem mass spectrometry (MS/MS) represented a further breakthrough in LC–MS since this technique compensates for the rather poor chromatographic capacity of LC. In this decade, LC–MS/MS has come of age with dramatic improvements in sensitivity, specificity and automation. Therefore, the LC–MS/MS approach currently presents the method of choice concerning the analysis of steroid conjugates.

Using a multi-targeted metabolic profiling approach based on stable isotope dilution LC–MS/MS we were capable of developing the most comprehensive method currently available for the quantification of sulfated steroids in biological fluids, *e.g.* human blood [39,127]. Our latest version of the method allows for profiling of 11 intact sulfated steroids in human serum by LC–MS/MS. The compounds analyzed in this method include cholesterol sulfate (CS), PREGS, 17-OH-PREGS, 16α-OH-DHEAS, DHEAS, 5-androstenediol-3-sulfate, androsterone sulfate, epiandrosterone sulfate, testosterone sulfate, epitestosterone sulfate, and dihydrotestosterone sulfate (Fig. 6A). The assay was designed to quantify sulfated steroids in a broad concentration range. Only 300 μl of serum are required. The method has been validated extensively. It showed good linearity ($R^2 > 0.99$) and recovery for all the compounds, with limits of quantification ranging between 1 and 80 ng/ml. Coefficients of variation for averaged intra-day and between-day precisions and accuracies (relative errors) were below 10%.

9. 27-hydroxy-cholesterol-3-sulfate as novel biomarker for steroid sulfatase deficiency (recessive X-linked ichthyosis, RXLI)

RXLI is an inherited skin disease of cornification. It has a prevalence of about 1: 2000–4000 and is almost exclusively found in males. The ichthyosis is characterized by moderate hyperkeratosis, *i.e.* thickening of the *stratum corneum* of the epidermis accompanied by scaling of the integument [157]. RXLI is caused by mutations of the STS gene, resulting in deficiency of the STS enzyme. Thus, conversion of sulfated steroids into their corresponding unconjugated compounds is impaired. Various studies reported that typically CS is grossly elevated in RXLI patients. Elevated CS levels inhibit serine proteases and thus inhibit normal desquamation, leading to retention hyperkeratosis. The analysis of CS is challenging due to the amphipathic nature of its molecule, but we achieved to analyze CS by LC–MS/MS [127] (Fig. 6A). So far, no research has been conducted to study whether other sulfated steroids than cholesterol sulfate are increased in RXLI. We found that oxysterol sulfates, particularly 27-hydroxy-cholesterol-3-sulfate, were elevated in RXLI, too (Fig. 6B). We developed an LC–MS/MS method, which is the first one to permit the direct analysis of serum 27-hydroxy-cholesterol-3-sulfate. It allows for the quantification of this compound, presenting a novel disease marker for RXLI [128].

Acknowledgements

The principal investigators of the Research Group FOR1369 "Sulfated Steroids in Reproduction" gratefully acknowledge the

Please cite this article in press as: J. Geyer, et al., The role of sulfated steroid hormones in reproductive processes, J. Steroid Biochem. Mol. Biol. (2016), http://dx.doi.org/10.1016/j.jsbmb.2016.07.002

support from the German Research Foundation DFG from 2010 to 2013 (1st funding period) and 2013-2016 (2nd funding period) including the grants BE1343/21-1/2, GE1921/4-1/2, BE1016/10-1, FI1927/1-2, SCHE307/7-1, SCHU1195/4-1/2, PE250/11-1, WU148/6-1/2, and WR154/3-1.

References

[1] M.A. Aba, J. Sumar, H. Kindahl, M. Forsberg, L.E. Edqvist, Plasma concentrations of 15-ketodihydro-PGF2 alpha, progesterone, oestrone sulphate, oestradiol-17 beta and cortisol during late gestation, parturition and the early post partum period in llamas and alpacas, Anim. Reprod. Sci. 50 (1998) 111–121.
[2] E.D. Albrecht, G.J. Pepe, Placental steroid hormone biosynthesis in primate pregnancy, Endocr. Rev. 11 (1990) 124–150.
[3] W.M. Allen, The isolation of crystalline progestin, Science 82 (1935) 89–93.
[4] A. Allali-Hassani, P.W. Pan, L. Dombrovski, R. Najmanovich, W. Tempel, A. Dong, P. Loppnau, F. Martin, J. Thornton, A.M. Edwards, A. Bochkarev, A.N. Plotnikov, M. Vedadi, C.H. Arrowsmith, Structural and chemical profiling of the human cytosolic sulfotransferases, PLoS Biol. 5 (May (5)) (2007) e97.
[5] R.S. Bahn, A. Worsham, K.V. Speeg, M. Ascoli, D. Rabin, Characterization of steroid production in cultured human choriocarcinoma cells, J. Clin. Endocrinol. Metab. 52 (1981) 447–450.
[6] D.L. Bain, A.F. Heneghan, K.D. Connaghan-Jones, M.T. Miura, Nuclear receptor structure: implications for function, Annu. Rev. Physiol. 69 (2007) 201–220.
[7] E.E. Baulieu, C. Corpechot, F. Dray, R. Emiliozzi, M. Lebeau, P. Mauvais-Jarvis, P. Robel, An adrenal-secreted "androgen": deydroisoandrosterone sulfate. Its metabolism and a tentative generalization on the metabolism of other steroid conjugates in man, Recent Progr. Hormone Res. 21 (1965) 411.
[8] E.E. Baulieu, I. Fabre-Jung, L.G. Huis in't Veld, Dehydroepiandrosterone sulfate: a secretory product of the boar testis, Endocrinology 81 (1967) 34–38.
[9] M. Bergmann, D. Nashan, E. Nieschlag, Pattern of compartimentation in human seminiferous tubules showing dislocation of spermatogonia, Cell Tissue Res. 256 (1) (1989) 183–190.
[10] O. Briz, R.I.R. Macias, M.A. Serrano, J. González-Gallego, J.E. Bayón, J.J.G. Marin, Excretion of foetal bilirubin by the rat placenta-maternal liver tandem, Placenta 24 (2003) 462–472.
[11] C. Blaschka, G. Schuler, C. Wrenzycki, Immunolocalization of steroid sulfatase and the estrogen-specific sulfotransferase in bovine follicles, Reprod. Fertil. Dev. 28 (1) (2016) 157.
[12] C. Blaschka, H. Stinshoff, F. Poppicht, C. Wrenzycki, Temporal pattern of steroid hormone concentrations during in vivo and in vitro maturation of bovine oocytes, Reprod. Fertil. Dev. 27 (1) (2015) 226.
[13] N.J. Bolton, A.O. Ruokonen, R.K. Vihko, Stimulation of the synthesis of steroids and steroid sulfates in human testicular tissue in vitro by hCG and by 8-bromo-cyclic AMP, J. Steroid Biochem. 22 (1985) 481–485.
[14] X. Bossuyt, M. Müller, P.J. Meier, Multispecific amphipathic substrate transport by an organic anion transporter of human liver, J. Hepatol. 25 (1996) 733–738.
[15] K.A. Brown, M. Dore, J.G. Lussier, J. Sirois, Human chorionic gonadotropin-dependent up-regulation of genes responsible for estrogen sulfoconjugation and export in granulosa cells of luteinizing preovulatory follicles, Endocrinology 147 (9) (2006) 4222–4233.
[16] K.A. Brown, N. Bouchard, J.G. Lussier, J. Sirois, Down-regulation of messenger ribonucleic acid encoding an importer of sulfoconjugated steroids during human chorionic gonadotropin-induced follicular luteinization in vivo, J. Steroid Biochem. Mol. Biol. 103 (1) (2007) 10–19.
[17] B.C. Burckhardt, G. Burckhardt, Transport of organic anions across the basolateral membrane of proximal tubule cells, Rev. Physiol. Biochem. Pharmacol. 146 (2003) 95–158.
[18] A. Butenandt, U. Westphal, Zur Isolierung und Charakterisierung des Corpus luteum-Hormons, Berichte Deutsche Chem. Gesellsch 67 (1934) 1440–1442.
[19] A. Butenandt, G. Hanisch, Über die Umwandlung des Dehydroandrosterons in (4-Androsten-ol-(17)-on(3) (Testosteron), ein Weg zur Darstellung des Testosterons aus Cholesterin, Berichte Deutsch Chem. Gesellsch 68 (1935) 859–862.
[20] H.I. Calvin, R.L. Vandewiele, S. Lieberman, Evidence that steroid sulfates serve as biosynthetic intermediates: in vivo conversion of pregnenolone sulfate-S35 to dehydroisoandrosterone sulfate-S35, Biochemistry 2 (1963) 648–653.
[21] H.I. Calvin, S. Lieberman, Evidence that steroid sulfates serve as biosynthetic intermediates. II. In vitro conversion of pregnenolone-3 H sulfate-35 S to 17alpha-hydroxypregnenolone-3 H sulfate-35S, Biochemistry 3 (1964) 259–264.
[22] S.H. Cha, T. Sekine, H. Kusuhara, E. Yu, J.Y. Kim, D.K. Kim, Y. Sugiyama, Y. Kanai, H. Endou, Molecular cloning and characterization of multispecific organic anion transporter 4 expressed in the placenta, J. Biol. Chem. 275 (2000) 4507–4512.
[23] E. Chapman, M.D. Best, S.R. Hanson, C.H. Wong, Sulfotransferases: structure, mechanism, biological activity, inhibition, and synthetic utility, Angew. Chem. Int. Ed. Engl. 43 (2004) 3526–3548.
[24] S.G. Cheatum, J.C. Diebold, J.C. Warren, Failure of placental microsomes to aromatize testosterone sulfate, J. Clin. Endocrinol. Metab. 28 (6) (1968) 916–918.
[25] R. Claus, B. Hoffmann, Oestrogens, compared to other steroids of testicular origin, in blood plasma of boars, Acta Endocrinol. (Copenhagen) 94 (1980) 404–411.
[26] A.J. Conley, I.M. Bird, The role of cytochrome P450 17 alpha-hydroxylase and 3 beta-hydroxysteroid dehydrogenase in the integration of gonadal and adrenal steroidogenesis via the delta 5 and delta 4 pathways of steroidogenesis in mammals, Biol. Reprod. 56 (1997) 789–799.
[27] A. Conley, M. Hinshelwood, Mammalian aromatases, Reproduction 121 (2001) 685–695.
[28] P.F. Daels, B.A. Albrecht, H.O. Mohammed, In vitro regulation of luteal function in mares, Reprod. Dom. Anim. 30 (1995) 211–217.
[29] B. Daviss, Growing pains for metabolomics, The Scientist 19 (2005) 25–28.
[30] S.J. Dieleman, M.M. Bevers, J. Poortman, H.T. van Tol, Steroid and pituitary hormone concentrations in the fluid of preovulatory bovine follicles relative to the peak of LH in the peripheral blood, J. Reprod. Fertil. 69 (2) (1983) 641–649.
[31] L. Dibbelt, V. Herzog, E. Kuss, Human placental sterylsulfatase: immunocytochemical and biochemical localization, Hoppe. Seyler Biol. Chem. 370 (1989) 1093–1102.
[32] L. Dibbelt, E. Kuss, Human placental steroid-sulfatase. Kinetics of the in-vitro hydrolysis of dehydroepiandrosterone 3-sulfate and of 16 alpha-hydroxydehydroepiandrosterone 3-sulfate, Hoppe. Seylers Z. Physiol. Chem. 364 (1983) 187–191.
[33] E. Diczfalusy, Endocrine functions of the human fetoplacental unit, Fed. Proc. 23 (1964) 791–798.
[34] M. Dym, D.W. Fawcett, The blood-testis barrier in the rat and the physiological compartmentation of the seminiferous epithelium, Biol. Reprod. 3 (3) (1970) 308–326.
[35] J.C. Escobar, S.S. Patel, V.E. Beshay, T. Suzuki, B.R. Carr, The human placenta expresses CYP17 and generates androgens de novo, J. Clin. Endocrinol. Metab. 96 (2011) 1385–1392.
[36] D. Fietz, K. Bakhaus, B. Wapelhorst, G. Grosser, S. Günther, J. Alber, B. Döring, S. Kliesch, W. Weidner, C.E. Galuska, M.F. Hartmann, S.A. Wudy, M. Bergmann, J. Geyer, Membrane transporters for sulfated steroids in the human testis—cellular localization, expression pattern and functional analysis, PLoS One 8 (5) (2013) e62638.
[37] J.E. Fortune, Ovarian follicular growth and development in mammals, Biol. Reprod. 50 (1994) 225–232.
[38] A. Fujiwara, H. Adachi, T. Nishio, M. Unno, T. Tokui, M. Okabe, T. Onogawa, T. Suzuki, N. Asano, M. Tanemoto, M. Seki, K. Shiiba, M. Suzuki, Y. Kondo, K. Nunoki, T. Shimosegawa, K. Iinuma, S. Ito, S. Matsuno, T. Abe, Identification of thyroid hormone transporters in humans: different molecules are involved in a tissue-specific manner, Endocrinology 142 (2001) 2005–2012.
[39] C.E. Galuska, M.F. Hartmann, A. Sánchez-Guijo, K. Bakhaus, J. Geyer, G. Schuler, K.P. Zimmer, S.A. Wudy, Profiling intact steroid sulfates and unconjugated steroids in biological fluids by liquid chromatography-tandem mass spectrometry (LC-MS-MS), Analyst 138 (2013) 3792–3800.
[40] F.J. Gasparini, R.B. Hochberg, S. Lieberman, Biosynthesis of steroid sulfates by the boar testes, Biochemistry 15 (1976) 3969–3975.
[41] J. Geyer, J.R. Godoy, E. Petzinger, Identification of a sodium-dependent organic anion transporter from rat adrenal gland, Biochem. Biophys. Res. Commun. 316 (2004) 300–306.
[42] J. Geyer, T. Wilke, E. Petzinger, The solute carrier family SLC10: more than a family of bile acid transporters regarding function and phylogenetic relationships, Naunyn Schmiedeberg's Arch. Pharmacol. 372 (2006) 413–431.
[43] J. Geyer, B. Döring, K. Meerkamp, B. Ugele, N. Bakhiya, C.F. Fernandes, J.R. Godoy, H.R. Glatt, E. Petzinger, Cloning and functional characterization of human sodium-dependent organic anion transporter (SLC10A6), J. Biol. Chem. 282 (2007) 19728–19741.
[44] M.D. Griswold, D. McLean, The sertoli cell, in: J.D. Neill (Ed.), Physiology of Reproduction, 3rd edn., Elsevier, Academic Press, 2006, pp. 949–975.
[45] G. Grosser, D. Fietz, S. Günther, K. Bakhaus, H. Schweigmann, B. Ugele, R. Brehm, E. Petzinger, M. Bergmann, J. Geyer, Cloning and functional characterization of the mouse sodium-dependent organic anion transporter Soat (Slc10a6), J. Steroid Biochem. Mol. Biol. 138 (2013) 90–99.
[46] M. Grube, S. Reuther, S.H. MeyerZu, K. Kock, K. Draber, C.A. Ritter, C. Fusch, G. Jedlitschky, H.K. Kroemer, Organic anion transporting polypeptide 2B1 and breast cancer resistance protein interact in the transepithelial transport of steroid sulfates in human placenta, Drug Metab. Dispos. 35 (2007) 30–35.
[47] B. Hagenbuch, P.J. Meier, The superfamily of organic anion transporting polypeptides, Biochim. Biophys. Acta 1609 (2004) 1–18.
[48] B. Hagenbuch, P.J. Meier, Organic anion transporting polypeptides of the OATP/SLC21 family: phyolgenetic classifications as OATP/SLCO superfamily, new nomenclature and molecular/functional properties, Pflugers Arch. 447 (5) (2004) 653–665.
[49] B. Hagenbuch, B. Stieger, The SLCO (former SLC21) superfamily of transporters, Mol. Aspects Med. 34 (2013) 396–412.
[50] P.F. Hall, D.C. Irby, D.M. de Kretser, Conversion of cholesterol to androgens by rat testes: comparison of interstitial cells and seminiferous tubules, Endocrinology 84 (1969) 488–496.
[51] R. Hähnel, E. Twaddle, T. Ratajczak, The specificity of the estrogen receptor of human uterus, J. Steroid Biochem. 4 (1973) 21–31.
[52] M.L. Hennet, C.M. Combelles, The antral follicle: a microenvironment for oocyte differentiation? Int. J. Dev. Biol. 56 (10–12) (2012) 819–831.
[53] R.A. Hess, Estrogen in the adult male reproductive tract: a review, Reprod. Biol. Endocrinol. 1 (2003) 52–66.

Please cite this article in press as: J. Geyer, et al., The role of sulfated steroid hormones in reproductive processes, J. Steroid Biochem. Mol. Biol. (2016), http://dx.doi.org/10.1016/j.jsbmb.2016.07.002

[54] R.A. Hess, K. Carnes, The role of aestrogen in testis and male reproductive tract: a review and species comparison, Anim. Reprod. 1 (2004) 5–13.
[55] R.B. Hochberg, S. Ladany, M. Welch, S. Lieberman, Cholesterol and cholesterol sulfate as substrates for the adrenal side-chain cleavage enzyme, Biochemistry 13 (1974) 1938–1945.
[56] B. Hoffmann, W.C. Wagner, T. Giménez, Free and conjugated steroids in maternal and fetal plasma in the cow near term, Biol. Reprod. 15 (1976) 126–133.
[57] B. Hoffmann, F. Gentz, K. Failing, Investigations into the course of progesterone-, oestrogen- and eCG- concentrations during normal and impaired pregnancy in the mare, Reprod. Dom. Anim. 31 (1996) 717–723.
[58] B. Hoffmann, A. Landeck, Testicular endocrine function, seasonality and semen quality of the stallion, Anim. Reprod. Sci. 57 (1999) 89–98.
[59] B. Hoffmann, A. Rostalski, H.M. Mutembei, S. Goericke-Pesch, Testicular steroid hormone secretion in the boar and expression of testicular and epididymal steroid sulphatase and estrogen sulphotransferase activity, Exp. Clin. Endocrinol. Diabetes 118 (2010) 274–280.
[60] D.W. Hum, A. Bélanger, E. Lévesque, O. Barbier, M. Beaulieu, C. Albert, M. Vallée, C. Guillemette, A. Tchernof, D. Turgeon, S. Dubois, Characterization of UDP-glucuronosyltransferases active on steroid hormones, J. Steroid Biochem. Mol. Biol. 69 (1999) 413–423.
[61] T. Janowski, S. Zduńczyk, A. Raś, E.S. Mwaanga, Eignung der Östronsulfatbestimmung im Blut von Ziegen zur Trächtigkeitsfeststellung und zur Voraussage der Fetenzahl, Tierärztl Prax 27 (1999) 107–109.
[62] T. Janowski, S. Zduńczyk, J. Malecki-Tepicht, W. Barański, A. Raś, Mammary secretion of oestrogens in the cow, Domest. Anim. Endocrinol. 23 (2002) 125–137.
[63] T. Jansson, Amino acid transporters in the human placenta, Pediatr. Res. 49 (2001) 141–147.
[64] M. Katagiri, N. Kagawa, M.R. Waterman, The role of cytochrome b5 in the biosynthesis of androgens by human P450c17, Arch. Biochem. Biophys. 317 (1995) 343–347.
[65] Y. Kobayashi, A. Shibusawa, H. Saito, N. Ohshiro, M. Ohbayashi, T. Kohyama Yamamoto, Isolation and functional characterization of a novel organic solute carrier protein, hOSCP1, J. Biol. Chem. 280 (2005) 32332–32339.
[66] C. Kohler, A. Riesenbeck, B. Hoffmann, Age-dependent expression and localization of the progesterone receptor in the boar testis, Reprod. Dom. Anim. 42 (2007) 1–5.
[67] S. Kojima, T. Yanaihara, T. Nakayama, Serum steroid levels in children at birth and in early neonatal period, Am. J. Obstet. Gynecol. 140 (1981) 961–965.
[68] M. Kotula, R. Tuz, B. Fraczek, A. Wojtusiak, B. Bilińska, Immunolocalization of androgen receptors in testicular cells of prepubertal and pubertal pigs, Folia Histochem. Cytobiol. 38 (2000) 157–162.
[69] G.G. Kuiper, B. Carlsson, K. Grandien, E. Enmark, J. Haggblad, S. Nilsson, J.A. Gustafsson, Comparison of the ligand binding specificity and transcript tissue distribution of estrogen receptors alpha and beta, Endocrinology 138 (1997) 863–870.
[70] G.A. Kullak-Ublick, T. Fisch, M. Oswald, B. Hagenbuch, P.J. Meier, U. Beuers, G. Paumgartner, Dehydroepiandrosterone sulfate (DHEAS): identification of a carrier protein in human liver and brain, FEBS Lett. 424 (1998) 173–176.
[71] G.A. Kullak-Ublick, M.G. Ismair, B. Stieger, L. Landmann, R. Huber, F. Pizzagalli, K. Fattinger, P.J. Meier, B. Hagenbuch, Organic anion-transporting polypeptide B (OATP-B) and its functional comparison with three other OATPs of human liver, Gastroenterology 120 (2001) 525–533.
[72] E. Kuss, The fetoplacental unit of primates, Exp. Clin. Endocrinol. 102 (1994) 135–165.
[73] T. Laatikainen, E.A. Laitinen, R. Vihko, Secretion of free and sulfate-conjugated neutral steroids by the human testis. Effect of administration of human chorionic gonadotropin, J. Clin. Endocrinol. 32 (1971) 59.
[74] T. Laatikainen, J. Pelkonen, D. Apter, T. Ranta, Fetal and maternal serum levels of steroid sulfates, unconjugated steroids, and prolactin at term pregnancy and in early spontaneous labor, J. Clin. Endocrinol. Metab. 50 (1980) 489–494.
[75] K.G. Lamont, G. Pérez-Palacios, A.E. Pérez, R.B. Jaffe, Pregnenolone and pregnenolone sulfate metabolism by human fetal testes in vitro, Steroids 16 (1970) 127–140.
[76] W. Lee, H. Glaeser, L.H. Smith, R.L. Roberts, G.W. Moeckel, G. Gervasini, B.F. Leake, R.B. Kim, Polymorphisms in human organic anion-transporting polypeptide 1A2 (OATP1A2): implications for altered drug disposition and central nervous system drug entry, J. Biol. Chem. 280 (2005) 9610–9617.
[77] W. Leowattana, DHEAS as a new diagnostic tool, Clin. Chim. Acta 341 (2004) 1–15.
[78] J.L. Leroy, D. Rizos, R. Sturmey, P. Bossaert, A. Gutierrez-Adan, V. Van Hoeck, S. Valckx, P.E. Bols, Intrafollicular conditions as a major link between maternal metabolism and oocyte quality: a focus on dairy cow fertility? Reprod. Fertil. Dev. 24 (1) (2011) 1–12.
[79] D.J. Liberato, A.L. Yergey, N. Esteban, C.E. Gomez-Sanchez, C.H. Shackleton, Thermospray HPLC/MS: a new mass spectrometric technique for the profiling of steroids, J. Steroid Biochem. 27 (1987) 61–70.
[80] S. Liu, J. Sjovall, W.J. Griffiths, Neurosteroids in rat brain: extraction, isolation, and analysis by nanoscale liquid chromatography-electrospray mass spectrometry, Anal. Chem. 75 (2003) 5835–5846.
[81] L.S. Loubière, E. Vasilopoulou, J.N. Bulmer, P.M. Taylor, B. Stieger, F. Verrey, C.J. McCabe, J.A. Franklyn, M.D. Kilby, S.Y. Chan, Expression of thyroid hormone transporters in the human placenta and changes associated with intrauterine growth restriction, Placenta 31 (2010) 295–304.
[82] D.W. Makawiti, W.E. Allen, M.J. Kilpatrick, Changes in oestrone sulphate concentrations in peripheral plasma of Pony mares associated with follicular growth, ovulation and early pregnancy, J. Reprod. Fertil. 68 (1983) 481–487.
[83] J.J.G. Marin, R.I.R. Macias, M.A. Serrano, The hepatobiliary-like excretory function if the placenta. A review, Placenta 24 (2003) 431–438.
[84] U. Meyer, Die Geschichte der Östrogene, Pharm. Unserer Zeit 33 (2004) 352–356.
[85] J.G. Middle, The quality assessment of steroid hormone assays, in: H.L.J. Makin, D.B. Gower, D.N. Kirk (Eds.), Steroid Analysis, Blackie Academic & Professional, London, 1995, pp. 647–696.
[86] L. Milewich, P.C. MacDonald, B.R. Carr, Estrogen 16 alpha-hydroxylase activity in human fetal tissues, J. Clin. Endocrinol. Metab. 63 (1986) 404–406.
[87] C.M. Morrow, D. Mruk, C.Y. Cheng, R.A. Hess, Claudin and occludin expression and function in the seminiferous epithelium, Philos. Trans. R Soc. Lond. B Biol. Sci. 365 (2010) 1679–1696.
[88] N. Mouhadjer, M. Bedin, G. Pointis, Steroid sulfatase activity in homogenates, microsomes and purified Leydig cells from adult rat testis, Reprod. Nutr. Dev. 29 (1989) 277–282.
[89] J.W. Müller, L.C. Gilligan, J. Idkowiak, W. Arlt, P.A. Foster, The regulation of steroid action by sulfation and desulfation, Endocr. Rev. 36 (2015) 526–563.
[90] H.M. Mutembei, S. Pesch, G. Schuler, B. Hoffmann, Expression of oestrogen receptors alpha and beta and of aromatase in the testis of immature and mature boars, Reprod. Domest. Anim. 40 (2005) 228–236.
[91] H.M. Mutembei, M.P. Kowalewski, B. Ugele, G. Schuler, B. Hoffmann, Expression and activity of steroid sulphatase in the boar testis, Reprod. Domest. Anim. 44 (2009) 17–23.
[92] R.A. Nagy, A.P. van Montfoort, A. Dikkers, J. van Echten-Arends, I. Homminga, J.A. Land, A. Hoek, U.J. Tietge, Presence of bile acids in human follicular fluid and their relation with embryo development in modified natural cycle IVF, Hum. Reprod. 30 (5) (2015) 1102–1109.
[93] J. Neunzig, R. Bernhardt, Dehydroepiandrosterone sulfate (DHEAS) stimulates the first step in the biosynthesis of steroid hormones, PLoS One 9 (2014) e89727.
[94] J. Neunzig, The role of sulfonated steroids and parmaceutical compouds in steroid hormone biosynthesis, Dissertation (2014) (scidok.sulb.uni-saarland.de/volltexte/2014/5963/).
[95] J. Neunzig, A. Sánchez-Guijo, A. Mosa, M.F. Hartmann, J. Geyer, S.A. Wudy, R. Bernhardt, A steroidogenic pathway for sulfonated steroids: the metabolism of pregnenolone sulfate, J. Steroid Biochem. Mol. Biol. 144 (Pt B) (2014) 324–333.
[96] G.W. Oertel, L. Treiber, W. Rindt, Direct aromatization of C19-steroid sulphates, Experientia 23 (1967) 97–98.
[97] M. Orava, F. Haour, P. Leinonen, A.O. Ruokonen, R.K. Vihko, Relationships between unconjugated and sulfated steroids in porcine primary Leydig cell culture, Clin. Endocrinol. 22 (1985) 507–512.
[98] Y.S. Othman, R.E. Oakey, Why so much oestriol? A comparison of the aromatisation of androstenedione and 16 alpha-hydroxyandrostenedione when incubated alone or together with human placental microsomes, J. Endocrinol. 148 (1996) 399–407.
[99] D. Papadopoulos, R. Dietze, M. Shihan, U. Kirch, G. Scheiner-Bobis, Dehydroepiandrosterone sulfate stimulates expression of blood-testis-barrier proteins claudin-3 and –5 and tight junction formation via a Gnalpha11-coupled receptor in sertoli cells, PLoS One 11 (2016) e0150143.
[100] J.R. Pasqualini, G.S. Chetrite, Recent insight on the control of enzymes involved in estrogen formation and transformation in human breast cancer, J. Steroid Biochem. Mol. Biol. 93 (2005) 21–236.
[101] J.R. Pasqualini, Enzymes involved in the formation and transformation of steroid hormones in the fetal and placental compartments, J. Steroid Biochem. Mol. Biol. 97 (2005) 401–415.
[102] J.R. Pasqualini, Estrogen sulfotransferases in breast and endometrial cancers, Ann. N. Y. Acad. Sci. 1155 (2009) 88–98.
[103] P. Patel, N. Weerasekera, M. Hitchins, C.A.R. Boyd, D.G. Johnston, C. Williamson, Semi quantitative expression analysis of MDR3, FIC1, BSEP, OATP-A, OATP-C,OATP-D, OATP-E and NTCP gene transcripts in 1st and 3rd trimester human placenta, Placenta 24 (2003) 39–44.
[104] A.H. Payne, R.B. Jaffe, Comparative roles of dehydroepiandrosterone sulfate and androstenediol sulfate as precursors of testicular androgens, Endocrinology 87 (1970) 316–322.
[105] A.H. Payne, R.B. Jaffe, M.R. Abell, Gonadal steroid sulfates and sulfatase. III. Correlation of human testicular sulfatase, 3β-hydroxysteroid dehydrogenase-isomerase, histologic structure and serum testosterone, J. Clin. Endocrinol. Metab. 33 (1971) 582–591.
[106] A.H. Payne, A. Kawano, R.B. Jaffe, Formation of dihydrotestosterone and other 5α-reduced metabolites by isolated seminiferous tubules and suspension of interstitial cells in a human testis, J. Clin. Endocrinol. Metab. 37 (1973) 448–453.
[107] A.H. Payne, R.B. Jaffe, Androgen formation from pregnenolone sulfate by fetal, neonatal, prepubertal and adult human testes, J. Clin. Endocrinol. Metab. 40 (1975) 102–107.
[108] C.A. Pearl, T. Berger, J.F. Roser, Estrogen and androgen receptor expression in relation to steroid concentrations in the adult boar epididymis, Dom. Anim. Endocrinol. 33 (2007) 451–459.
[109] S.C. Purinton, C.E. Wood, Ovine fetal estrogen sulfotransferase in brain regions important for hypothalamus-pituitary-adrenal axis control, Neuroendocrinology 71 (2000) 237–242.

Please cite this article in press as: J. Geyer, et al., The role of sulfated steroid hormones in reproductive processes, J. Steroid Biochem. Mol. Biol. (2016), http://dx.doi.org/10.1016/j.jsbmb.2016.07.002

[110] J.I. Raeside, R.L. Renaud, Estrogen and androgen production by purified Leydig cells of mature boars, Biol. Reprod. 28 (1983) 727–733.
[111] J.I. Raeside, R.L. Renaud, D.E. Marshall, Identification of 5 alpha-androstane-3beta,17beta-diol and 3beta-hydroxy-5alpha-androstan-17-one sulfates as quantitatively significant secretory products of porcine Leydig cells and their presence in testicular venous blood, J. Steroid Biochem. Mol. Biol. 42 (1992) 113–120.
[112] J.I. Raeside, H.L. Christie, R.L. Renaud, P.A. Sinclair, The boar testis: the most versatile steroid producing organ known, Soc. Reprod. Fert. Suppl. 62 (2006) 85–97.
[113] W.E. Rainey, K.S. Rehman, B.R. Carr, The human fetal adrenal: making adrenal androgens for placental estrogens, Semin. Reprod. Med. 22 (2004) 327–336.
[114] W.E. Rainey, Y. Nakamura, Regulation of the adrenal androgen biosynthesis, J. Steroid Biochem. Mol. Biol. 108 (2008) 281–286.
[115] M.J. Reed, A. Purohit, L.W. Woo, S.P. Newman, B.V. Potter, Steroid sulfatase: molecular biology, regulation, and inhibition, Endocr. Rev. 26 (2005) 171–202.
[116] K.D. Roberts, L. Bandi, H.I. Calvin, W.D. Drucker, S. Lieberman, Evidence that steroid sulfates serve as biosynthetic intermediates. IV. Conversion of cholesterol sulfate in vivo to urinary C-19 and C-21 steroidal sulfates, Biochemistry 3 (1964) 1983–1988.
[117] H.A. Robertson, G.J. King, Plasma concentrations of progesterone, oestrone, oestradiol-17beta and of oestrone sulphate in the pig at implantation, during pregnancy and at parturition, J. Reprod. Fertil. 40 (1974) 133–141.
[118] K.R. Robillard, M.T. Hoque, R. Bendayan, Expression of ATP-Binding cassette membrane transporters in rodent and human sertoli cells: relevance to the permeability of antiretroviral therapy at the blood-Testis barrier, J. Pharmacol. Exp. Ther. 340 (1) (2011) 96–108.
[119] E. Ropstad, V. Veiberg, H. Säkkinen, E. Dahl, H. Kindahl, O. Holand, J.F. Beckers, E. Eloranta, Endocrinology of pregnancy and early pregnancy detection by reproductive hormones in reindeer (Rangifer tarandus), Theriogenology 63 (2005) 1775–1788.
[120] A. Ruokonen, T. Laatikainen, E.A. Laitinen, R. Vihko, Free and sulfate-conjugated neutral steroids in human testis tissue, Biochemistry 11 (1972) 1411–1416.
[121] A. Ruokonen, R. Vihko, Steroid metabolism in testis tissue: concentrations of unconjugated and sulfated neutral steroids in boar testis, J. Steroid Biochem. 5 (1974) 33–38.
[122] A. Ruokonen, Steroid metabolism in testis tissue: the metabolism of pregnenolone, pregnenolone sulfate, dehydroepiandrosterone and dehydroepiandrosterone sulfate in human and boar testes in vitro, J. Steroid Biochem. 9 (1978) 939–946.
[123] K.J. Ryan, Biological aromatization of steroids, J. Biol. Chem. 234 (1959) 268–272.
[124] K.J. Ryan, Metabolism of C-16-oxygenated steroids by human placenta: the formation of estriol, J. Biol. Chem. 234 (1959) 2006–2008.
[125] E.C. Salido, P.H. Yen, L. Barajas, L.J. Shapiro, Steroid sulfatase expression in human placenta: immunocytochemistry and in situ hybridization study, J. Clin. Endocrinol. Metab. 70 (1990) 1564–1567.
[126] R. Sanchez, Y. Schuermann, L. Gagnon-Duval, H. Baldassarre, B.D. Murphy, N. Gevry, L.B. Agellon, V. Bordignon, R. Duggavathi, Differential abundance of IGF1 bile acids, and the genes involved in their signaling in the dominant follicle microenvironment of lactating cows and nulliparous heifers, Theriogenology 81 (6) (2014) 771–779.
[127] A. Sánchez-Guijo, V. Oji, M.F. Hartmann, H. Traupe, S.A. Wudy, Simultaneous quantification of cholesterol sulfate, androgen sulfates, and progestagen sulfates in human serum by LC-MS/MS, J. Lipid Res. 56 (2015) 1843–1851.
[128] A. Sánchez-Guijo, V. Oji, M.F. Hartmann, H.C. Schuppe, H. Traupe, S.A. Wudy, High levels of oxysterol sulfates in serum of patients with steroid sulfatase deficiency, J. Lipid Res. 56 (2015) 403–412.
[129] A. Sánchez-Guijo, C. Blaschka, M.F. Hartmann, C. Wrenzycki, S.A. Wudy, Profiling of bile acids in bovine follicular fluid by fused-core-LC-MS/MS, J. Steroid Biochem. Mol. Biol. (2016), doi:http://dx.doi.org/10.1016/j.jsbmb.2016.02.020.
[130] S.J. Santner, P.D. Feil, R.J. Santen, In situ estrogen production via estrone sulfatase pathway in breast tumors: relative importance vs. the aromatase pathway, J. Clin. Endocrinol. Metab. 59 (1984) 29–33.
[131] K. Sato, J. Sugawara, T. Sato, H. Mizutamari, T. Suzuki, A. Ito, T. Mikkaichi, T. Onogawa, M. Tanemoto, M. Unno, T. Abe, K. Okamura, Expression of organic anion transporting polypeptide E (OATP-E) in human placenta, Placenta 24 (2003) 144–148.
[132] T. Satoh, K. Watanabe, K. Takanashi, S. Itoh, H. Takagi, I. Yoshizawa, Evidence of direct conversion of testosterone sulfate to estradiol 17 sulfate in human placental microsomes, J. Pharmacobio-Dyn. 15 (1992) 427–436.
[133] G. Schuler, H. Greven, M.P. Kowalewski, B. Döring, G.R. Özalp, B. Hoffmann, Placental steroids in cattle: hormones, placental growth factors or by-products of trophoblast giant cell differentiation? Exp. Clin. Endocrinol. Diabetes 25 (2008) 429–436.
[134] G. Schuler, Y. Dezhkam, L. Bingsohn, B. Hoffmann, K. Failing, C.E. Galuska, M.F. Hartmann, A. Sánchez-Guijo, S.A. Wudy, Free and sulfated steroids secretion in postpubertal boars (Sus scrofa domestica), Reproduction 148 (2014) 303–314.
[135] F. Schwarzenberger, G.S. Toole, H.L. Christie, J.I. Raeside, Plasma levels of several androgens and estrogens from birth to puberty in male domestic pigs, Acta Endocrinol. 128 (1993) 173–177.
[136] H. Schweigmann, A. Sánchez-Guijo, B. Ugele, K. Hartmann, M.F. Hartmann, M. Bergmann, C. Pfarrer, B. Döring, S.A. Wudy, E. Petzinger, J. Geyer, G. Grosser, Transport of the placental estriol precursor 16α-hydroxy-dehydroepiandrosterone sulfate (16α-OH-DHEAS) by stably transfected OAT4-, SOAT-, and NTCP-HEK293 cells, J. Steroid Biochem. Mol. Biol. 143 (2014) 259–265.
[137] K.W. Selcer, H. Kabler, J. Sarap, Z. Xiao, P.K. Li, Inhibition of steryl sulfatase activity in LNCaP human prostate cancer cells, Steroids 67 (2002) 821–826.
[138] B.P. Setchell, M.S. Laurie, A.P. Flint, R.B. Heap, Transport of free and conjugated steroids from the boar testis in lymph, venous blood and rete testis fluid, J. Endocrinol. 96 (1983) 127–136.
[139] C.H.L. Shackleton, C. Kletke, S.A. Wudy, J.H. Pratt, Dehydroepiandrosterone sulfate quantification in serum using high-performance liquid chromatography/mass spectrometry and a deuterated internal standard: a technique suitable for routine use or as a reference method, Steroids 55 (1990) 472–478.
[140] C.H. Shackleton, K.M. Straub, Direct analysis of steroid conjugates: the use of secondary ion mass spectrometry, Steroids 40 (1982) 35–51.
[141] M. Shihan, U. Kirch, G. Scheiner-Bobis, Dehydroepiandrosterone sulfate mediates activation of transcription factors CREB and ATF-1 via Galpha11-coupled receptor in the spermatogenic cell line GC-2, Biochem. Biophys. Acta 1833 (2013) 3064–3075.
[142] P.K. Siiteri, P.C. MacDonald, The utilization of circulating dehydroisoandrosterone sulfate for estrogen synthesis during human pregnancy, Steroids 2 (1963) 713–730.
[143] P.K. Siiteri, P.C. MacDonald, Placental estrogen biosynthesis during human pregnancy, J. Clin. Endocrinol. Metab. 26 (1966) 751–761.
[144] P.A. Sinclair, E.J. Squires, J.I. Raeside, R. Renaud, Synthesis of free and sulphoconjugated 16-androstene steroids by the Leydig cells of the mature domestic boar, J. Steroid Biochem. Mol. Biol. 96 (2005) 217–228.
[145] L.P. Smith, M. Nierstenhoefer, S.W. Yoo, A.S. Penzias, E. Tobiasch, A. Usheva, The bile acid synthesis pathway is present and functional in the human ovary, PLoS One 4 (10) (2009) e7333.
[146] S.J. Stanway, P. Delavault, A. Purohit, L.W. Woo, C. Thurieau, B.V. Potter, M.J. Reed, Steroid sulfatase: a new target for the endocrine therapy of breast cancer, Oncologist 12 (2007) 370–374.
[147] C.A. Strott, Sulfonation and molecular action, Endocr. Rev. 23 (1996) 703–732.
[148] C.A. Strott, Steroid sulfotransferases, Endocr. Rev. 17 (1996) 670–697.
[149] C.A. Strott, Sulfonation and molecular action, Endocr. Rev. 23 (2002) 703–732.
[150] M.V. St-Pierre, B. Ugele, L. Gambling, K.T. Shiverick, Mechanisms of drug transfer across the human placenta – a workshop report, Placenta 23 (2002) S159–S164.
[151] M.V. St-Pierre, B. Hagenbuch, B. Ugele, P.J. Meier, T. Stallmach, Characterization of an organic anion transporting polypeptide (OATP-B) in human placenta, J. Clin. Endocrinol. Metab. 87 (2002) 1856–1863.
[152] J.F. Strauss III, F. Martinez, M. Kiriakidou, Placental steroid hormone synthesis: unique features and unanswered questions, Biol. Reprod. 54 (1996) 303–311.
[153] M.L. Sutton, R.B. Gilchrist, J.G. Thompson, Effects of in-vivo and in-vitro environments on the metabolism of the cumulus-oocyte complex and its influence on oocyte developmental capacity, Hum. Reprod. Update 9 (1) (2003) 35–48.
[154] I. Tamai, J. Nezu, H. Uchino, Y. Sai, A. Oku, M. Shimane, A. Tsuji, Molecular identification and characterization of novel members of the human organic anion transporter (OATP) family, Biochem. Biophys. Res. Commun. 273 (2000) 251–260.
[155] H.S. Tan, J.I. Raeside, Developmental patterns of plasma dehydroepiandrosterone sulfate and testosterone in male pigs, Anim. Reprod. Sci. 3 (1980) 73–81.
[156] M. Tomi, H. Eguchi, M. Ozaki, T. Tawara, S. Nishimura, K. Higuchi, T. Maruyama, T. Nishimura, E. Nakashima, Role of OAT4 in Uptake of estriol precursor 16α-hydroxydehydroepiandrosterone sulfate into human placental syncytiotrophoblasts from fetus? Endocrinology 156 (7) (2015) 2704–2712.
[157] H. Traupe, J. Fischer, V. Oji, Nonsyndromic types of ichthyoses – an update, J. Dtsch. Dermatol. Ges. 12 (2014) 109–121.
[158] C.P. Tsang, Changes in plasma levels of estrone sulfate and estrone in the pregnant ewe around parturition, Steroids 23 (1974) 855–868.
[159] R.C. Tuckey, Side-chain cleavage of cholesterol sulfate by ovarian mitochondria, J. Steroid Biochem. Mol. Biol. 37 (1990) 121–127.
[160] B. Ugele, S. Simon, Uptake of dehydroepiandrosterone-3-sulfate by isolated trophoblasts from human term placenta, JEG-3, BeWo, Jar, BHK cells, and BHK cells transfected with human sterylsulfatase-cDNA, J. Steroid Biochem. Mol. Biol. 71 (1999) 203–211.
[161] B. Ugele, M.V. St-Pierre, M. Pihusch, A. Bahn, P. Hantschmann, Characterization and identification of steroid sulfate transporters of human placenta, Am. J. Physiol. Endocrinol. Metab. 284 (2003) E390–E398.
[162] B. Ugele, A. Bahn, M. Rex-Haffner, Functional differences in steroid sulfate uptake of organic anion transporter 4 (OAT4) and organic anion transporting polypeptide 2B1 (OATP2B1) in human placenta, J. Steroid Biochem. Mol. Biol. 111 (2008) 1–6.
[163] J.D. Unadkat, A. Dahlin, S. Vijay, Placenta drug transporters, Curr. Drug Metabol. 5 (2004) 125–131.
[164] V. Van Hoeck, M. LeroyJ.L. Arias Alvarez, D. Rizos, A. Gutierrez-Adan, K. Schnorbusch, P.E. Bols, H.J. Leese, R.G. Sturmey, Oocyte developmental failure

Please cite this article in press as: J. Geyer, et al., The role of sulfated steroid hormones in reproductive processes, J. Steroid Biochem. Mol. Biol. (2016), http://dx.doi.org/10.1016/j.jsbmb.2016.07.002

in response to elevated nonesterified fatty acid concentrations: mechanistic insights? Reproduction 145 (1) (2013) 33–44.
[165] M. Wallace, E. Cottell, M.J. Gibney, F.M. McAuliffe, M. Wingfield, L. Brennan, An investigation into the relationship between the metabolic profile of follicular fluid oocyte developmental potential, and implantation outcome, Fertil. Steril. 97 (5) (2012) 1078–1084.
[166] H. Wang, Z. Yan, M. Dong, X. Zhu, H. Wang, Z. Wang, Alteration in placental expression of bile acids transporters OATP1A2, OATP1B1, OATP1B3 in intrahepatic cholestasis of pregnancy, Arch. Gynecol. Obstet. 285 (2012) 1535–1540.
[167] M. Wehling, R. Lösel, Non-genomic steroid hormone effects: membrane or intracellular receptors? J. Steroid Biochem. Mol. Biol. 102 (2006) 180–183.
[168] J. Wijnholds, G.L. Scheffer, M. van der Valk, P. van der Valk, J.H. Beijnen, R.J. Scheper, P. Borst, Multidrug resistance protein 1 protects the oropharyngeal mucosal layer and the testicular tubules against drug-induced damage, J. Exp. Med. 188 (5) (1998) 797–808.
[169] C. Wrenzycki, H. Stinshoff, Maturation environment and impact on subsequent developmental competence of bovine oocytes, Reprod. Domest. Anim. 48 (Suppl 1) (2013) 38–43.
[170] S.A. Wudy, M.F. Hartmann, in: M.B. Ranke, P.E. Mullis (Eds.), Mass Spectrometry in the Diagnosis of Steroid-Related Disorders: Clinical Applications, Diagnostics of Endocrine Function in Children and Adolescents, 4th ed., Karger, Basel, 2011, pp. 379–401.

Please cite this article in press as: J. Geyer, et al., The role of sulfated steroid hormones in reproductive processes, J. Steroid Biochem. Mol. Biol. (2016), http://dx.doi.org/10.1016/j.jsbmb.2016.07.002

11. Anhang – Publikationen

8. K. Hartmann, J. Bennien, B. Wapelhorst, K. Bakhaus, V. Schumacher, S. Kliesch, W. Weidner, M. Bergmann, J. Geyer, D. Fietz. Histochem Cell Biol 2016 Dec;146(6):737-748.

Current insights into the sulfatase pathway in human testis and cultured Sertoli cells

K. Hartmann, J. Bennien, B. Wapelhorst, K. Bakhaus, V. Schumacher, S. Kliesch, W. Weidner, M. Bergmann, J. Geyer & D. Fietz

Histochemistry and Cell Biology

ISSN 0948-6143
Volume 146
Number 6

Histochem Cell Biol (2016) 146:737-748
DOI 10.1007/s00418-016-1503-y

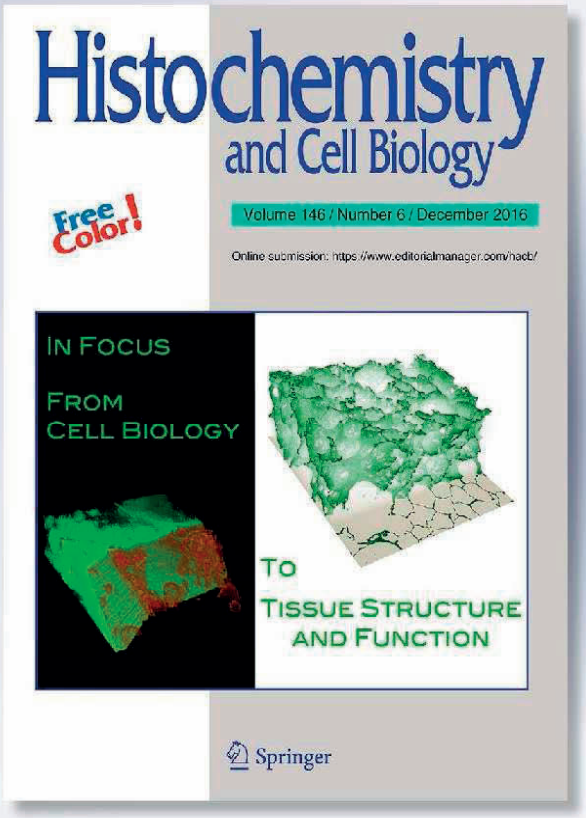

Springer

Histochem Cell Biol (2016) 146:737–748
DOI 10.1007/s00418-016-1503-y

ORIGINAL PAPER

Current insights into the sulfatase pathway in human testis and cultured Sertoli cells

K. Hartmann[1] · J. Bennien[2] · B. Wapelhorst[1] · K. Bakhaus[2] · V. Schumacher[3,4] · S. Kliesch[5] · W. Weidner[6] · M. Bergmann[1] · J. Geyer[2] · D. Fietz[1]

Accepted: 21 September 2016 / Published online: 29 September 2016

Abstract Within the human testis, large amounts of sulfated steroid hormones are produced. As shown in breast tissue and placenta, these might not only be excretion intermediates, but re-activated in target cells by steroid sulfatase (STS). This process is called sulfatase pathway and may play a pivotal role in para- and/or intracrine regulation by creating a local supply for steroid hormones. This requires a facilitated transport via uptake carriers and efflux transporters as these hydrophilic molecules cannot pass the cell membrane. Moreover, blood–testis barrier formation in the testis requires a transport through Sertoli cells (SCs) to reach germ cells (GCs). Sertoli cells are therefore expected to play a key role as gate-keepers for sulfatase pathway in human seminiferous epithelium. We analyzed the mRNA and protein expression of uptake carriers and efflux transporters like organic anion-transporting polypeptides (OATP2B1, OATP3A1) and multidrug resistance-related proteins (MRP1, MRP4) in testicular tissue and cultured Sertoli cells (FS1, HSEC). Additionally, expression pattern of STS as well as sulfonating enzymes (SULTs) were assessed. OATP2B1, OATP3A1 and STS were detected in SCs as well as GCs, whereas MRP1 is only expressed in SCs, and SULT1E1 only in Leydig cells, respectively. By transcellular transport of [H^3]DHEAS in HSEC, we showed a functional transport of sulfated steroids in vitro. Our data indicate that steroid synthesis via sulfatase pathway in Sertoli cells in vivo and in vitro is possible and may contribute to paracrine and intracrine regulation employing the local supply of sulfated and free steroid hormones inside seminiferous tubules.

Keywords Sulfatase pathway · Sertoli cell · Sulfated steroids · Membrane transport · STS · Human testis

Dedicated to Prof. Dr. Drenckhahn and his lifetime achievement concerning cell biology.

✉ D. Fietz
daniela.fietz@vetmed.uni-giessen.de

1 Institute of Veterinary Anatomy, Histology and Embryology, Justus Liebig University Giessen, Frankfurter Str. 98, 35392 Giessen, Germany

2 Institute of Pharmacology and Toxicology, Justus Liebig University Giessen, Giessen, Germany

3 Department of Urology, Children's Hospital Boston, Boston, MA, USA

4 Department of Surgery, Harvard Medical School, Boston, MA, USA

5 Department of Clinical Andrology, Centre for Reproductive Medicine and Andrology, M nster, Germany

6 Department of Urology, University Clinic Giessen-Marburg, Giessen, Germany

Introduction

Leydig cells (LCs) are the main source of testicular androgens via de novo biosynthesis (Hess 2003), but they also synthesize large amounts of steroid sulfates including pregnenolone sulfate (PREGS), dehydroepiandrosterone sulfate (DHEAS) and testosterone sulfate (Mouhadjer et al. 1989; Payne and Jaffe 1970; Ruokonen et al. 1972). PREGS and DHEAS quantitatively are the most important forms and can be metabolized to testosterone in testis homogenates in vitro (Payne et al. 1973; Ruokonen 1978). Testicular estrogen synthesis in adults takes also place in LCs. Additionally, Nitta et al. (1993, for review see Carreau et al. 2012) showed aromatase expression in different germ cell (GC) fractions of the mouse testis and so demonstrated estrogen production inside the seminiferous tubules. While

Sertoli cells (SCs) are considered to be the main source of testicular estrogens in fetal and postnatal life, LCs and also GCs take over this function in the adult (Carreau et al. 1999, 2009, Carreau and Hess 2010).

Free biologically active steroid hormones interact with the intracellular steroid hormone receptors, androgen receptor (AR) and estrogen receptors (ER), which both play an important role for spermatogenesis (Hess 2003; Walker 2009). While AR was detected in SCs but not in GCs (Sar et al. 1993; Fietz et al. 2011), ER isoforms α and β were detected in GCs (ERα and ERβ) as well as in SCs (ERβ) (Fietz et al. 2014). Besides the expression of ERs in the testis, the receptors were also detected in the epididymis, especially in its head, indicating a possible downstream action of germ cell-derived estrogens (reviewed by Hess et al. 2011; Joseph et al. 2011).

Apart from de novo steroid hormone synthesis in reproductive organs, there is increasing evidence for steroid hormone supply via the sulfatase pathway in which biologically inactive steroid sulfates can be cleaved by the steroid sulfatase (STS) into biologically active free steroids. In this context, steroids sulfates can be regarded as steroid hormone precursor molecules (Pasqualini et al. 1989; Labrie 2003; Luu-The 2013). However, in contrast to free steroids, steroid sulfates are negatively charged at physiological pH and highly hydrophilic and, therefore, cannot freely permeate across cellular membranes. In the testis, free intercellular diffusion within the seminiferous epithelium is prevented by the blood–testis barrier (BTB), formed by the tight junctions between adjacent SCs (Dym and Fawcett 1970, description in human by Bergmann et al. 1989). Thus, if sulfated steroids play any role in hormonal modulation of cells beyond the BTB, a carrier-facilitated uptake as well as an efflux system within SCs is needed. In the past, several uptake carriers and efflux transporters of the solute carrier (SLC) and ATP-binding cassette carrier (ABC) families were shown to be expressed in the human testis, e.g., SOAT, OSCP1 and OATP6A1 in germ cells (Fietz et al. 2013) and others that might allow steroid sulfates to pass the blood–testis barrier by carrier-mediated transport through the Sertoli cells. Whereas most of these studies clearly focused on the transport of xenobiotics, including drugs, in the testis, little is known about the testicular transport of steroid sulfates.

Therefore, the aim of the present study was to investigate the expression and cellular localization of candidate steroid sulfate carriers as well as steroid sulfatase and sulfotransferases (SULTs) in order to get closer insight into the availability of the sulfatase pathway and steroid sulfate transport across the blood-testis barrier in the human testis. We obtained a broad expression pattern for STS, SULT2A1 and SULT1E1, *organic anion-transporting polypeptides* OATP3A1 and OATP2B1, as well as expression of *multidrug resistance-related protein* MRP1 and MRP4 in SC, GC and LC. Furthermore, we were able to show a directed transcellular transport activity for DHEAS through HSEC Sertoli cell cultures, indicating that steroid sulfates can actively be transported across the blood–testis barrier.

Materials and methods

Testicular tissue and histological evaluation

A total of 42 testis biopsies, medically indicated by normo- or hypergonadotropic azoospermia, including patients with obstructive azoospermia after vasectomy were used in this study. After written informed consent, biopsies were taken under general anesthesia at the Department for Clinical Andrology, Center for Reproductive Medicine and Andrology at the University of M nster or at the Department of Urology at UKGM Giessen. The reported study has been approved by the Ethic's committee of the Medical Faculty of the Justus Liebig University Giessen (decision 187b/09). After surgery, testicular tissue was fixed by immersion in Bouin's solution and embedded in paraffin. For histological examination, 5-µm-thick sections were cut, stained with hematoxylin and eosin and evaluated following score count analysis according to Bergmann and Kliesch (2010). For our study, testicular biopsies revealing normal spermatogenesis (nsp, $n = 12$), arrest on level of spermatids (sda, $n = 5$), primary spermatocytes (sza, $n = 11$), spermatogonia (sga, $n = 5$) and Sertoli-cell-only syndrome (SCO, $n = 9$) were used.

Sertoli cell cultures

Two immortalized and cultured adult human Sertoli cell lines, HSEC and FS1, were used in the present study. HSEC cells were purchased from Lonza (Basel, Switzerland). FS1 cells were originally derived from testis tissue of an adult man showing Frasier syndrome (FS) and were obtained at the time of prophylactic gonadectomy after written informed consent (Schumacher et al. 2008). Both Sertoli cell cultures were cultured in DMEM high-glucose (4.5 g/L, Life Technologies) standard medium with 20 % fetal calf serum (FCS Gold, PAA), 1 % non-essential amino acids, 1 % L-glutamine and 1 % penicillin–streptomycin (Gibco). Incubation was carried out at 37 °C in a humidified atmosphere with 8.5 % CO_2.

Qualitative RT-PCR expression analysis in testicular tissue and FS1 cells

Total mRNA from testis homogenates was extracted from Bouin-fixed, paraffin-embedded tissue using RNeasy Micro

Table 1 Primer sequences for qualitative RT-PCR and generation of ISH probes

Primer	NCBI RefSeq	Sequence (5′ → 3′)	Amplicon length (bp)
STS (RT-PCR)	NM_000351.4	*For:* CAGCACTGATAGGGAAATGG *Rev:* GAAGCCGTGATGTAAAGGG	83
β-Actin	NM_001101.3	*For:* GCGAGAAGATGACCCAGATC *Rev:* CGTACAGGGATAGCACAGC	84
STS (ISH)	NM_000351.4	*For:* CCATCTTCACTACAAACACG *Rev:* GGCATAAACCTACCATCTTC	187
OATP2B1 (ISH)	NM_007256.4	*For:* CTGTGACACTGTTTTTTGGG *Rev:* GTGGGGTGGTAATAGGTTG	261
OATP3A1 (ISH)	NM_001145044	*For:* GGTTTATCCTGGGCTCTTTC *Rev:* GGCTTGGGTCTCTCGTATTC	256
MRP1	NM_004996	*For:* GTTTCTCAGATCGCTCACCC *Rev:* ACCCTGTGATCCACCAGAAG	126
MRP4	NM_005845	*For:* TATCACGTTCAGTGTGCTGG *Rev:* AGCAGATTGACTATCTGGCC	124
SULT1E1	NM_005420.2	*For:* TGGAGGACAGTGGC ACAATC *Rev:* GCTACTTGGGAGCTGAGATG	84
SULT2A1	NM_003167.3	*For:* TGTCGGACGATTATGG *Rev:* CAGTTTGTTCTTTGGG	145

Table 2 *TaqMan Gene Expression Assays* for quantitative real-time PCR

Gene	NCBI RefSeq	TaqMan assay ID
STS	NM_000351.4	Hs00165853_m1
OATP2B1	NM_007256.4	Hs01030343_m1
OATP3A1	NM_001145044	Hs00203184_m1
MRP1	NM_004996.3	Hs01561502_m1
β-Actin	NM_001101.3	Hs99999903_m1
GAPDH	NM_002046.3	Hs02758991_g1

FFPE Kit (Qiagen) as recommended by the manufacturer. Cultured HSEC and FS1 cells were harvested, and total mRNA was extracted by a phenol–chloroform method as described by Chomczynski (1993). To digest genomic DNA, mRNA was subsequently treated with RNase-free DN*ase* I (10 U/L, Roche) and RN*ase* inhibitor (40 U/L, Ambion). cDNA was synthesized from 1.5 µl total mRNA by using 8.5 µl of RT-mix (GeneAmp Gold RNA PCR Core Kit, Life Technologies). Negative controls were processed without reverse transcriptase. For RT-PCR, 5 µl of cDNA was added to 2 µl $MgCl_2$, 4 µl 10 × PCR Gold Buffer, 0.25 µl GOLDAmplitaq (Life Technologies), 1 µl of each primer (10 µmol/L) and sterile ddH_2O to a final volume of 25 µl. RT-PCR was performed by using specific primers as listed in Table 1. Beta-actin was used as internal control of cDNA quality. Primer pairs were synthesized by Eurofins MWG Operon. RT-PCR conditions were 1 × 95 °C for 5 min, 40 × (95 °C for 30 s, 57°–60 °C for 30 s and 72 °C for 30 s) and 72 °C for 7 min for product amplification. PCR products were separated by 2 % agarose gel electrophoresis and staining with Gel-Red (Sigma-Aldrich).

In order to differentiate between seminiferous tubules and interstitial tissue, we performed laser-assisted cell picking (LACP) using paraffin-embedded testis tissue as described previously (Fietz et al. 2011). Shortly, slices mounted on PALM® membrane slides (MembranSlide 0.1 PEN, Zeiss, Oberkochen, Germany) were stained with hematoxylin, and the designated tissue was excised and catapulted by PALM MicroBeam® system and PALM Robo® Software (Zeiss). Specimens of seminiferous tubules, i.e., encompassing SC and GC, or SC alone (SCO) and interstitial tissue, consisting predominantly of LCs, blood vessels and connective tissue, were defined under microscopical control and then yielded separately. Extraction of mRNA was performed using RNeasy FFPE Kit (Qiagen). Digestion of genomic DNA, first-strand cDNA synthesis and RT-PCR were performed as described above.

Quantitative RT-PCR expression analysis in testicular tissue and HSEC cells

For quantitative expression analysis in testis homogenates and Sertoli cell cultures, gene-specific *TaqMan Gene Expression Assays* (Life Technologies) were purchased. As reference genes, β-actin and glyceraldehyde 3-phosphate dehydrogenase (GAPDH) were used (Table 2). For each specimen, triplicate determinations were performed using 3 µl cDNA, 1 µl *TaqMan Gene Expression Assay*, 10 µl *TaqMan Gene Expression Master Mix* (Life Technologies) and sterile ddH_2O to a final volume of 20 µl. Quantitative RT-PCR was performed on CFX96 RealTime Cycler (Bio-Rad). Conditions were 1 × 95 °C for 10 min and

Table 3 Primary and secondary antibodies used for IHC

	Primary antibody	Clonality	Host	Dilution	Secondary antibody	Dilution
STS	Dr. Bernhard Ugele, Munich	Poly-clonal	Rabbit	1:1600	Biotinylated goat anti-rabbit (E0432, Dako, Glostrup, Denmark)	1:200
SULT1E1	HPA			1:50		
OATP3A1	Bioss			1:100		
OATP2B1	Bioss			1:200		
MRP1	Sigma-Aldrich			1:100		

45 × (95 °C for 15 s and 60 °C for 1 min). Relative gene expression was evaluated by *CFX Manager Software 2.0* (Bio-Rad) using $2^{-\Delta\Delta Cq}$ method. For statistical analysis, unpaired *Student's t test* was performed. Data are shown as mean ± SD.

In situ hybridization (ISH)

DIG-labeled cRNA probes were generated as described previously (Fietz et al. 2014). Briefly, fragments with 187, 261 and 259 bp of human STS, OATP2B1 and OATP3A1 cDNA were amplified by RT-PCR (for primer sequences, see Table 1), sub-cloned into pCRII-TOPO vector (Invitrogen) as recommended by the manufacturer and used as a template for in vitro transcription. The plasmid was transformed into One Shot Chemically Competent *E. coli* TOP10 (Invitrogen), purified and sequenced by SRD (Scientific Research and Development). For digoxigenin-labeling of the antisense and sense cRNA probes, plasmid DNA was linearized by *Bam*HI and *Not*I (NEB), respectively, and incubated with T7 or SP6 RNA polymerase (Promega) in the presence of digoxigenin-labeled UTPs (Roche). ISH was performed as described by Lekhkota et al. (2006) with minor changes. After digestion with proteinase K (15 µg/ml in 1x PBS) for 15 min at room temperature (RT), the deparaffinized and rehydrated testis sections (5 µm) were post-fixed with 4 % paraformaldehyde for 10 min and acetylated in 0.25 % acetic anhydride in triethanolamine (10 mM) for additional 10 min. After 1 h pre-hybridization in a glycerol solution, hybridization was performed by incubating the sections in hybridization buffer supplemented with the DIG-labeled sense or antisense cRNA probes. Both cRNAs were used at a dilution of 1:50 in hybridization buffer containing 50 % deionized formamide, 2x standard saline citrate (SSC), 1x Denhardt's solution, 10 µg/ml salmon sperm DNA and 10 µg/ml yeast t-RNA (Sigma-Aldrich). Hybridization was carried out overnight in a humidified chamber containing 50 % formamide in 2x SSC at temperatures between 42° and 50 °C. Stringency washes at 55 °C and RT with different concentrations of SSC (2x SSC, 0.2x SCC) were carried out. Incubation of the sections with an anti-DIG Fab antibody conjugated to alkaline phosphatase (Boehringer) followed overnight. Visualization was accomplished by developing sections with NBT-BCIP solution in a humidified chamber under exclusion of light overnight. Finally, slides were mounted in Glycergel (Sigma-Aldrich).

Immunohistochemistry (IHC)

For immunohistochemistry, paraffin sections showing nsp were deparaffinized and rehydrated. Heat-mediated antigen retrieval was performed in citrate buffer solution (pH 6) for 15 min in a common microwave oven. Inhibition of endogenous peroxidase activity was achieved by 30 min incubation in 3 % hydrogen peroxide (H_2O_2) in Tris buffer. We used a 5 % bovine serum albumin containing Tris buffer as a blocking solution for 30 min and incubated sections at 4 °C overnight with primary antibodies against human STS, SULT1E1, OATP2B1, OATP3A1 and MRP1 as outlined in Table 3. Negative controls were performed by omitting the primary antibody. The antibodies against MRP1 and STS were pre-incubated with their corresponding immunizing peptides as additional control. Biotinylated goat anti-rabbit served as secondary antibody (Table 3) and was incubated at room temperature for 45 min. The antibody treatment was followed by peroxidase-conjugated streptavidin incubation (VECTASTAIN Elite ABC Standard Kit Peroxidase, Biologo) for 30 min at room temperature. Washing steps were performed with Tris-buffered saline (pH 7.4). Afterward, the immunoreaction was visualized with the *Peroxidase Substratkit AEC* (Biologo) for 20 min following the manufacturer´s recommendations. After counterstaining with hematoxylin, the sections were mounted with glycerol gelatine (Sigma-Aldrich).

Transcellular transport of [^{3}H]DHEAS in HSEC cells

For functional transport measurements, 1.25 × 10^5 HSEC were seeded and cultured inside the inserts of a transwell system (ThinCert, Greiner Bio One) containing translucent polyester membranes of 0.4 µm pore size, using 24-well cell culture plates. The medium was changed the next day

and afterward every second day until reaching 100 % confluence. Transepithelial electrical resistance (TEER) was measured in representative wells in order to test the barrier function of the monolayer. Although the TEER was only at 110–120 Ω in the overgrown inserts, we could measure directed transport activity. Inserts and wells were washed three times with HBSS (Hank's Balanced Salt Solution, containing 142.9 mM NaCl, 4.7 mM KCL, 1.2 mM $MgSO_4$, 1.2 mM KH_2PO_4, 1.8 mM $CaCl_2$, 20 mM HEPES, adjusted to pH 7.4 with KOH, pre-warmed to 37 °C) followed by an equilibration period with HBSS of 10 min. Afterward, the bidirectional transport assay was started. For apical-to-basal flux measurement (a → b), 250 µl HBSS containing 10 µM [^{3}H]DHEAS (60 Ci/mmol) was applied into the inserts and 250 µl pure HBSS was given into the wells. For basal-to-apical flux measurement (b → a), HBSS containing [^{3}H]DHEAS was applied into the wells and pure HBSS was given into the inserts at equal volumes. The cells were incubated for 30 min at 37 °C. After this time, 200 µl samples were taken from both compartments and analyzed by liquid scintillation counting.

Results

Localization of steroid sulfate carriers in the testicular tissue

First, we screened human testis biopsies for the expression of candidate uptake and efflux steroid sulfate carriers as well as respective sulfonating and de-sulfonating enzymes by qualitative RT-PCR. We detected expression of OATP2B1 and OATP3A1 as well as of MRP1 and MRP4 in biopsies showing nsp. Furthermore, mRNA expression for all these carriers was detected in Sertoli FS1 cells (Fig. 1a). For cellular localization of the carrier expression in the human testis, we applied IHC with antibodies further specified in Table 3. In the case of OATP2B1 and OATP3A1, we additionally performed ISH in order to approve the broad expression pattern for both carriers at the mRNA level. OATP3A1 and OATP2B1 were localized in GCs, with strongest staining signal in elongated and round spermatids (OATP3A1, Figs. 2c and 3b) or in elongated spermatids and pachytene spermatocytes (OATP2B1, Fig. 2d and 3c), respectively. Both carriers were detected also in SC and LC. Thereby, data from ISH and IHC were consistent to each other for both carriers. In contrast, MRP1 showed a more restricted expression pattern in SC and LC, without staining of GC (Fig. 2e). These data clearly indicate expression of both, steroid sulfate uptake and efflux carriers in Sertoli cells, which could transport steroid sulfates across the BTB. For summary of results, see Table 4 as well as Fig. 4.

Localization of steroid sulfatase (STS) and steroid sulfotransferases (SULT1E1, SULT2A1) in testicular tissue

Expression of all the enzymes, which are of significance for the conjugation status of steroid sulfates in the testis, was detected by qualitative RT-PCR in biopsies showing nsp and regarding STS and SULT1E1 also in FS1 Sertoli cell cultures (Fig. 1a). In order to achieve a more precise localization of STS and SULT1E1, especially inside the seminiferous tubules, we performed ISH and IHC. IHC further localized SULT1E1 predominantly to LC without clear staining of GC or SC (Fig. 2b). In contrast, STS showed a broad expression pattern in the human testis and was detected in SC, pachytene spermatocytes and elongated spermatids, using a STS antibody kindly provided by B. Ugele (Dibbelt et al. 1989) (Fig. 2a). Furthermore, STS expression could be found in LC. ISH clearly confirmed this broad expression of STS in the human testis and revealed signals in GS, SC and LC (Fig. 3a). Because STS is the crucial component for the formation of free steroids via the sulfatase pathway, we analyzed STS expression in the human testis more in detail including differential expression analysis of seminiferous tubules and interstitium, separated by laser-assisted cell picking (LACP) prior to RT-PCR as well as by quantitative real-time PCR using human testis biopsies with normal or impaired spermatogenesis. This sub-analysis showed consistent expression of STS in the tubules and interstitium in all biopsies tested (Fig. 1b), but with significantly reduced expression levels in all biopsies with impaired spermatogenesis, including qualitatively intact but quantitatively reduced spermatogenesis (hypospermatogenesis, hyp), sza, sga and SCO (Fig. 1c). For summary of results, see Table 4 as well as Fig. 4.

Localization of steroid sulfate carriers and transcellular transport of DHEAS in HSEC Sertoli cells

Expression of OATP2B1, OATP3A1, MRP1 and MRP4 was analyzed by quantitative real-time PCR and revealed comparable mRNA expression levels in biopsies showing nsp compared with SCO tubules (Fig. 5a). Furthermore, these carriers are expressed in HSEC Sertoli cells, but with significantly lower expression levels compared with nsp biopsies.

After detection of steroid sulfate uptake and efflux carriers in FS1 and HSEC Sertoli cell cultures, we were interested if these cultures are capable of transcellular transport of steroid sulfates in order to bypass the blood–testis barrier. Therefore, both cell lines were cultured on inserts in a transwell system, in which cells are accessible for transcellular transport measurements from the apical-to-basal

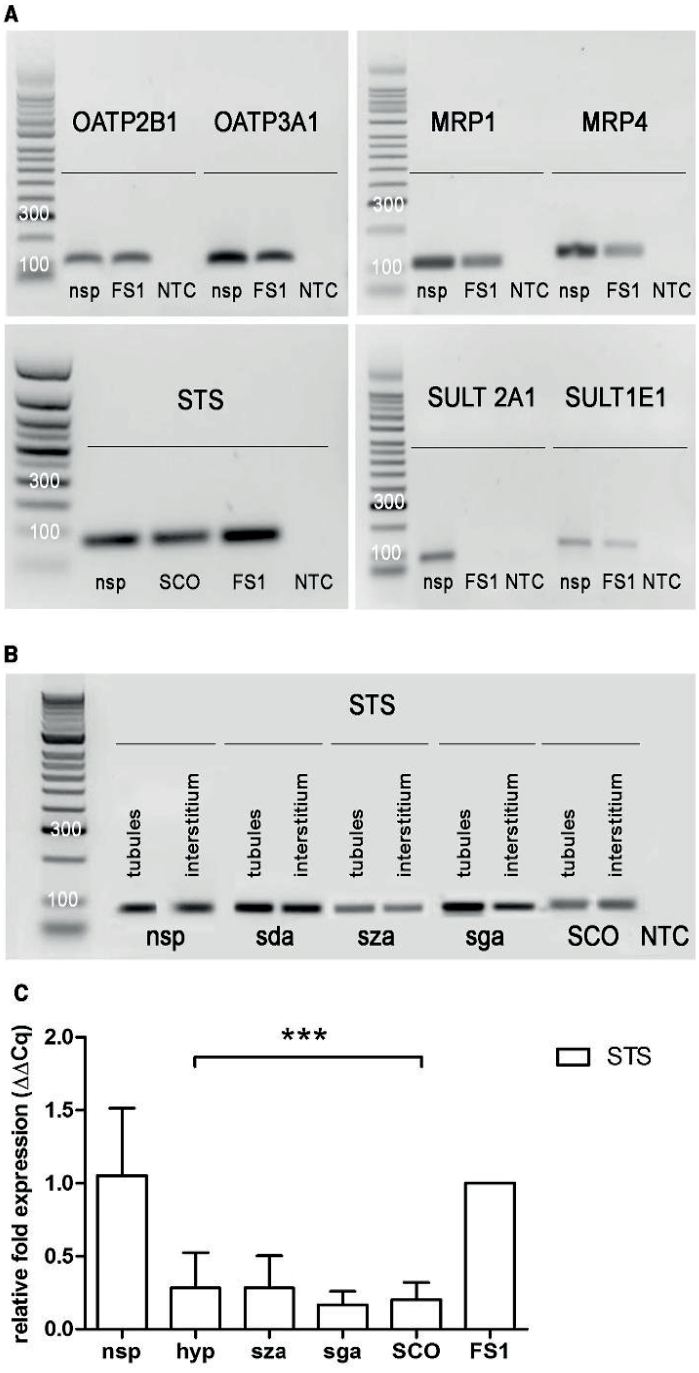

Fig. 1 Expression of uptake and efflux steroid sulfate carriers, steroid sulfatase and steroid sulfotransferase in the human testis. RNA was isolated from human testis biopsies showing nsp and various spermatogenic defects (sda, sza, sga and SCO). Laser-assisted cell picking (LACP) was performed in order to separate tubular from interstitial tissue prior to RNA isolation. Furthermore, RNA was isolated from Sertoli FS1 cell cultures. **a** Qualitative RT-PCR screening for the expression of the steroid sulfate uptake carriers OATP2B1 and OATP3A1, efflux carriers MRP1 and MRP4, steroid sulfatase STS as well as steroid sulfotransferases SULT1E1 and SULT2A1. NTC, no template control. **b** STS expression was closer analyzed in biopsies with normal or impaired spermatogenesis after LACP separation of tubuli and interstitium of the human testis. NTC, no template control. **c** Quantitative real-time PCR expression analysis of STS in biopsies with normal and impaired spermatogenesis as well as in FS1 cells showed a significantly lower STS expression in spermatogenic impairment compared to nsp. Expression was normalized to reference gene expression and is shown in relation to FS1 Sertoli cells (set to "1"). Data represent mean ± SD experiments. ***Significantly different with $p < 0.001$ by unpaired Student's t test

(a → b) as well as in the opposite basal-to-apical (b → a) directions. As the FS1 cells used did not reach confluence in the transwell inserts, these experiments were only performed in commercially available HSEC cells, which formed tight monolayers of nearly 100 % confluence. We performed transcellular transport measurements using [^{3}H] DHEAS as a probe substrate for the group of steroid sulfates. We detected significant differences in the a → b and

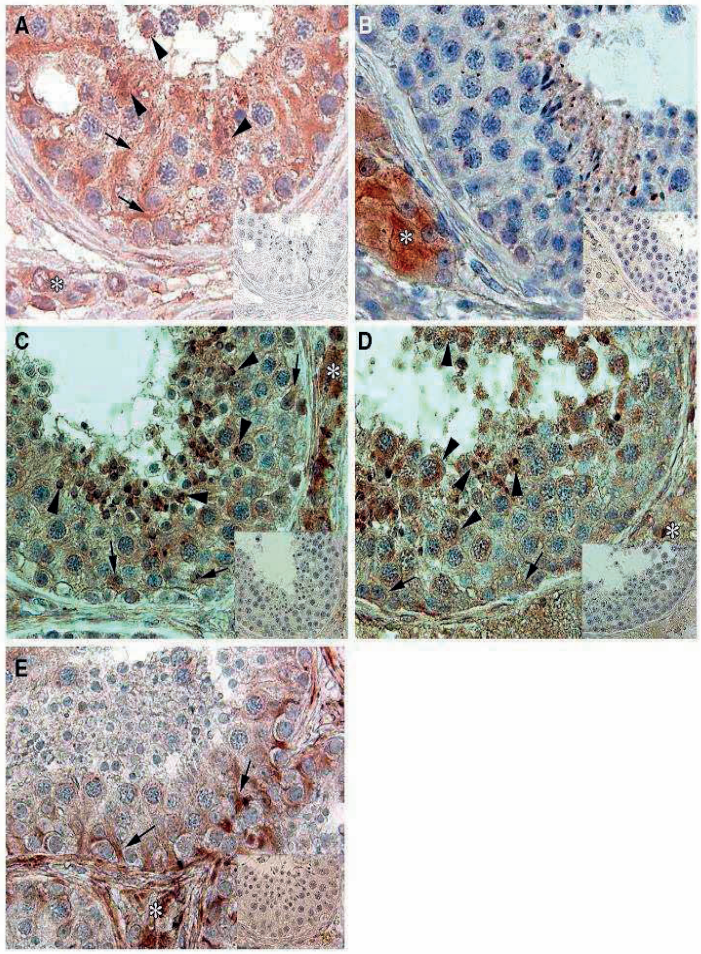

Fig. 2 Localization of STS, SULT1E1, OATP3A1, OATP2B1 and MRP1 proteins in testicular section with nsp by IHC. **a** STS was localized in germ cells (*arrowheads*), Sertoli cells (*arrows*) and Leydig cells (*asterisk*). **b** SULT1E1 was predominantly detected in Leydig cells (*asterisk*). **c** OATP3A1 and **d** OATP2B1 carrier proteins were detected in germ cells (*arrowheads*), Sertoli cells (*arrows*) and Leydig cells (*asterisk*). **e** MRP1 is expressed in Sertoli cells (*arrows*) and Leydig cells (*asterisk*). *Inserts* negative controls without first antibody (**a**–**d**) or pre-incubation with immunizing peptide (**e**). AEC detection, counterstain with hematoxylin, primary magnification ×40

b → a flux rates clearly pointing to an active transcellular transport process for DHEAS. In all experiments, the a → b flux prevailed representing net-transcellular transport from the apical into the basal compartment (Fig. 5b).

Discussion

The BTB separates the seminiferous epithelium in a basal and adluminal compartment (Dym and Fawcett 1970). Whereas spermatogonia within the basal compartment are located within the blood-borne milieu, spermatocytes and spermatids within the adluminal compartment exist within the milieu of intratubular fluid, created by SCs. The demonstration of OATPs and MRPs in SCs as well as in SC lines and specific GCs fractions indicates a possible uptake and efflux of sulfated steroids, as it was also shown by Grube et al. (2007) for OATP2B1 and breast cancer-related protein (BCRP) in human placental cells. STS expression in SCs but also in specific germ cell fractions supports the hypothesis of a role of steroid synthesis via sulfatase pathway in the seminiferous epithelium. Free steroid hormones are then able to bind to nuclear or membrane-bound receptors or to pass the apical Sertoli cell membrane by diffusion and reach germ cells in a paracrine manner.

The expression of STS in GCs could account for an uptake of sulfated steroids that have exited Sertoli cells via efflux pumps at the apical membrane. MRP1 is known to be located ubiquitously in the human body. It is the most abundant ABC transporter in the testis and is able to transport sulfated steroid hormones like DHEAS and E1S (Klaassen and Aleksunes 2010). It has been described in the basolateral membrane of Sertoli cells (Bart et al. 2004). Additionally, Robillard et al. (2011) detected MRP1 expression in a human Sertoli cell line (HSEC) and confirmed membrane localization using immunofluorescence. The authors

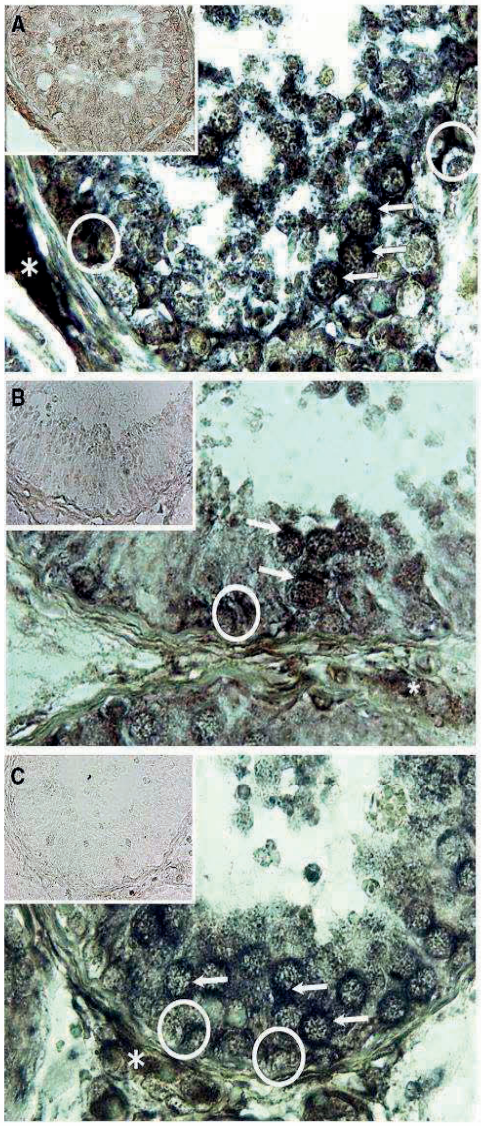

Fig. 3 Expression of STS, OATP3A1 and OATP2B1 mRNA in the testis by ISH. ISH analysis with NBT-BCIP staining revealed that **a** STS, **b** OATP3A1 and **c** OATP2B1 are broadly expressed in the human testicular sections showing nsp, including Sertoli cells (*white circles*), pachytene primary spermatocytes (*white arrows*) and Leydig cells (*white asterisk*). *Inserts* negative controls with sense probes. Primary magnification x40

concluded a protective function of this efflux pump, especially in SCs, and considered them as an important component of BTB. Up to now, uptake and efflux transporters located at epithelial barriers gained interest regarding their role in transporting xenobiotics and therefore in determining the pharmacodynamics of drugs (Labrie 2003). The

Table 4 Summary of STS, SULT and carrier expression in the human testis

	OATP2B1	OATP3A1	MRP1	STS	SULT1E1
Germ cells					
Spermatogonia	–	–	–	–	–
Pachytene spermatocytes	+	–	–	+	–
Round spermatids	–	+	–	–	–
Elongated spermatids	+	+	–	+	–
Sertoli cells					
Sertoli cells	+	+	+	+	–
FS1 cell culture	+	+	+	+	+

knowledge of the physiological role of transporting endogenous substances at blood–tissue barriers is comparably lower, but hormone supply is supposed to be an essential feature (Becker et al. 1992; Dankers et al. 2012).

We were successful in demonstrating a cytoplasmic and membranous Sertoli cell staining pattern with a MRP1-specific antibody in immunohistochemical analysis of nsp and SCO samples. We therefore propose expression of this efflux pump on protein level not only in the basal but also in the apical Sertoli cell membrane. So far, a basal membrane location of Mrp1/MRP1 in Sertoli cells of rodents and men was described as a component of BTB in the sense of an outward transfer of substances which would be harmful for spermatogenesis (Wijnholds et al. 1998; Bart et al. 2004; Robillard et al. 2011).

The expression of STS in SCs and GCs inside the seminiferous tubules indicates a functional para- and intracrine mechanism. Luu-The (2013) reviewed different "front-door" and "back-door" pathways for the active sex steroids testosterone, dihydrotestosterone and estradiol, which are produced locally and exert their activity by binding to nuclear receptors on-site. In this context, sulfated steroids are regarded as steroid storage with longer half-life compared to their active counterparts in cells with STS activity. The impact of the additional local supply of active estrogens and androgens via sulfatase pathway and sulfated precursor molecules was demonstrated early in human breast cancer (Pasqualini et al. 1989). In this context, STS has been identified as a valuable drug target in steroid deprivation therapies of hormonal diseases (Stanway et al. 2007).

Regarding human testis expression profile of STS in seminiferous tubules, an impact of sulfated steroids as precursors supplied via sulfatase pathway for synthesis of active steroid hormones is conceivable. As GCs also express aromatase (Nitta et al. 1993) as well as estrogen receptors (Lekhkota et al. 2006; Fietz et al. 2014), a functional sulfatase pathway in GCs is plausible. Moreover, a

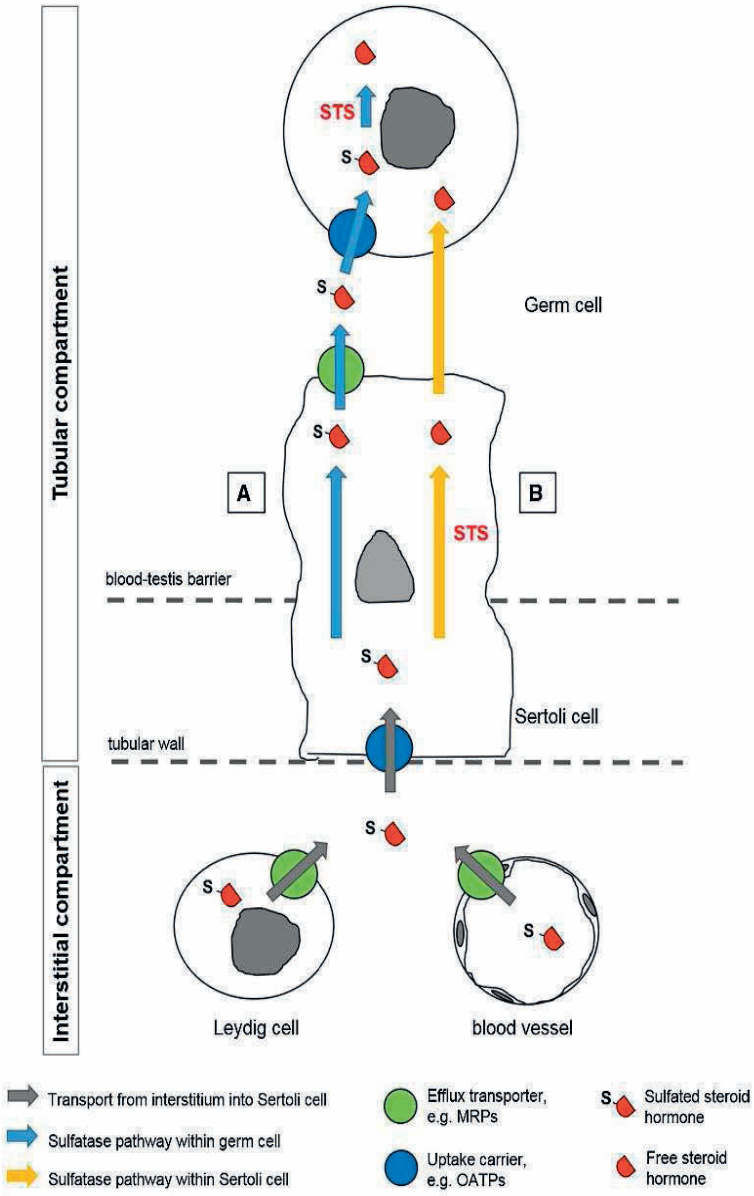

Fig. 4 Schematic drawing of sulfatase pathway in germ cells (**a**) and Sertoli cells (**b**). As seen in this schematic drawing, sulfated steroids are delivered by blood supply or generated by interstitial Leydig cells. Transported into the interstitial tissue by efflux transporters (ABC transporters (not assessed here); *gray arrow* via *green sphere*), sulfated steroids are taken up into Sertoli cells via uptake carriers (OATP2B1, OATP3A1; *gray arrow* via *blue sphere*). **a** For a sulfatase pathway within germ cells, sulfated steroids are transported out of the Sertoli cell by efflux transporters (MRP1; *blue arrow* via *green sphere*) and taken up into the germ cell (OATP2B1, OATP3A1; *blue arrow* via *blue sphere*). Within germ cells, sulfate residues are cleaved by enzymatic activity of steroid sulfatase (STS) and represent precursor molecules for steroid biosynthesis, e.g., estrogen synthesis via aromatase activity. **b** For a sulfatase pathway within Sertoli cells, sulfated steroids are directly cleaved by enzymatic activity of steroid sulfatase (STS) and pass the Sertoli cell membrane and therefore blood–testis barrier by diffusion (*orange arrow*). These free steroid hormones also traverse the germ cell membrane by diffusion (*orange arrow*) and function as precursor molecules for steroid biosynthesis as mentioned before

high expression of estrogen receptors in the epididymal head (for review see Hess et al. 2011) indicates a probable downstream action for germ cell-derived estrogens. For androgens, primary target cells inside the seminiferous tubules are solely Sertoli cells, as only these cells express the androgen receptor (for review see Griswold 1998).

Actually, there is evidence that sulfated steroids in general are released in circulation and represent a reservoir for steroid hormones synthesis in specific target cells (Dawson 2012). For the concept of sulfatase pathway as a fine-tuning regulatory element, we additionally analyzed the expression pattern of the sulfo-conjugating enzymes SULT1E1 and SULT2A1. In our study, we detected SULT1E1 protein solely in interstitial Leydig cells, but not within the seminiferous epithelium. Therefore, we assume a paracrine mechanism for sulfo-conjugation and de-conjugation between interstitium and cells within seminiferous tubules. As reviewed by Geyer et al. (2016), in the boar SULT1E1 activity was solely detected in the epididymis and absent in the testis. This might be

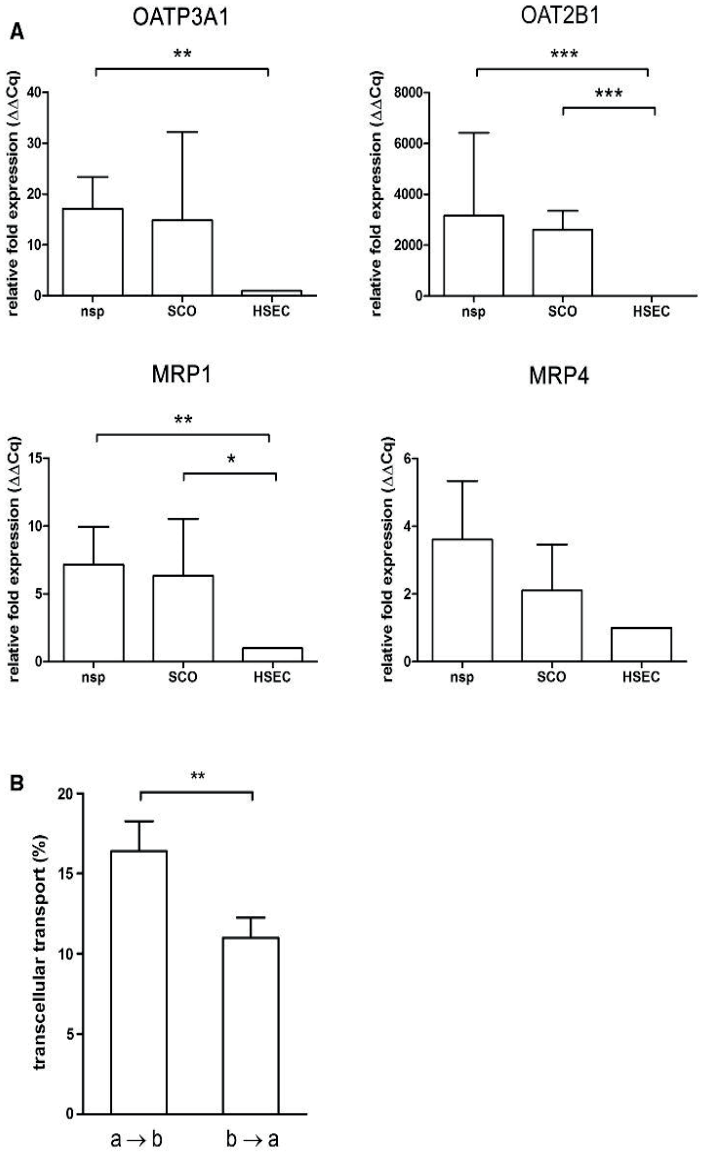

Fig. 5 Carrier expression and transcellular DHEAS transport in human Sertoli HSEC cells. **a** Real-time PCR expression analysis of OATP3A1, OATP2B1 and MRP1 in tissue samples from patients with nsp, Sertoli-cell-only syndrome (SCO) and human Sertoli HSEC cells. Expression was normalized to reference gene expression and is shown in relation to nsp (set to "1"). Data represent mean ± SD. *, **, ***Significantly different with $p < 0.05$, $p < 0.01$ and $p < 0.001$, respectively, by unpaired *t* test. **b** HSEC cells were cultured on transwell filters and were incubated with 10 µM [^{3}H]DHEAS either from the insert, or from the well for 30 min. Aliquots were counted from the apical (**a**) and basal (**b**) compartments, and transcellular transport was calculated by determining the amount of fluxed compound in relation to the total amount of incubated DHEAS. Data represent mean ± SD of quadruplicate determinations of a representative experiment. **Significantly different with $p < 0.01$ by unpaired *t* test

a mechanism for inactivation of an excess of estrogens deriving from the germ cells. This hypothesis requires further investigation.

To show an in vitro transport of sulfated steroids in human Sertoli cells, we applied a transcellular transport assay with HSEC cells as a monolayer and analyzed the transport ability from the basal to the apical compartment and vice versa (b–a and a–b). Although the TEER of 110–120 Ω was below the expected level for the HSEC cells cultured in the transwell inserts, our transwell measurement with DHEAS revealed significantly different transport rates for the a–b over the b–a direction, pointing to an active transcellular transport process from the apical to the basal direction that most likely is mediated by uptake and/or efflux transport systems, with OATP3A1, OATP2B1, MRP1 and MRP4 as candidate transport systems identified in the present study.

Conclusions

Our data provide two different possible ways for sulfated steroids to circumvent the BTB and to reach germ cells

as target cells. Although Sertoli cells express STS, steroid sulfates may pass Sertoli cells without cleavage involving uptake and efflux transport systems. Alternatively, steroid sulfates may be de-conjugated by STS and the resulted free steroids could reach germ cells by passive diffusion or could act directly inside the Sertoli cells.

Acknowledgments We acknowledge the skillful technical assistance of J. Dern-Wieloch, A. Hax, J. Vogelsberg and R. Leidolf. Additionally, we want to thank B. D ring for her scientific support.

Funding This study was supported by grants of the Research Group FOR1369 "Sulfated Steroids in Reproduction" of the German Research Foundation DFG to D. Fietz (FI1927/1-2) and J. Geyer (GE1921/4-2).

References

Bart J, Hollema H, Groen H, de Vries E, Hendrikse N, Sleijfer D, Wegman T, Vaalburg W, van der Graaf W (2004) The distribution of drug-efflux pumps, P-gp, BCRP, MRP1 and MRP2, in the normal blood–testis barrier and in primary testicular tumours. Eur J Cancer 40:2064–2070. doi:10.1016/j.ejca.2004.05.010

Becker KF, Allmeier H, H llt V (1992) New mechanisms of hormone secretion: MDR-like gene products as extrusion pumps for hormones? Horm Metab Res 24:210–213. doi:10.1055/s-2007-1003295

Bergmann M, Kliesch S (2010) Testicular biopsy and histology. In: Nieschlag E, Behre HM, Nieschlag S (eds) Andrology. Male Reproductive Health and Dysfunction. Springer, Berlin, pp 155–167

Bergmann M, Nashan D, Nieschlag E (1989) Pattern of compartmentation in human seminiferous tubules showing dislocation of spermatogonia. Cell Tissue Res 256:183–190

Carreau S, Hess RA (2010) Oestrogens and spermatogenesis. Philos Trans R Soc Lond B Biol Sci 365(1546):1517–1535. doi:10.1098/rstb.2009.0235

Carreau S, Genissel C, Bilinska B, Levallet J (1999) Sources of oestrogen in the testis and reproductive tract of the male. Int J Androl 22:211–223

Carreau S, Delalande C, Galeraud-Denis I (2009) Mammalian sperm quality and aromatase expression. Microsc Res Tech 72:552–557. doi:10.1002/jemt.20703

Carreau S, Bouraima-Lelong H, Delalande C (2012) Estrogen, a female hormone involved in spermatogenesis. Adv Med Sci 57(1):31–36

Chomczynski P (1993) A reagent for the single-step simultaneous isolation of RNA, DNA and proteins from cell and tissue samples. Biotechniques 15(532–534):536–537

Dankers AC, Sweep FC, Pertijs JC, Verweij V, van den Heuvel JJ, Koenderink JB, Russel FG, Masereeuw R (2012) Localization of breast cancer resistance protein (Bcrp) in endocrine organs and inhibition of its transport activity by steroid hormones. Cell Tissue Res 349:551–563

Dawson PA (2012) The biological roles of steroid sulfonation. In: Ostojic S (ed) Steroids—from physiology to clinical medicine. InTech, Rijeka, pp 45–64. doi:10.5772/52714

Dibbelt L, Herzog V, Kuss E (1989) Human placental sterylsulfatase: immunocytochemical and biochemical localization. Biol. Chem. Hoppe-Seyler 370:1093–1102

Dym M, Fawcett DW (1970) The blood-testis barrier in the rat and the physiological compartmentation of the seminiferous epithelium. Biol Reprod 3:308–326

Fietz D, Geyer J, Kliesch S, Gromoll J, Bergmann M (2011) Evaluation of CAG repeat length of androgen receptor expressing cells in human testes showing different pictures of spermatogenic impairment. Histochem Cell Biol 136:689–697

Fietz D, Bakhaus K, Wapelhorst B, Grosser G, G nther S, Alber J, D ring B, Kliesch S, Weidner W, Galuska CE, Hartmann MF, Wudy SA, Bergmann M, Geyer J (2013) Membrane transporters for sulfated steroids in the human testis—cellular localization, expression pattern and functional analysis. PLoS One 8:e62638. doi:10.1371/journal.pone.0062638

Fietz D, Ratzenb ck C, Hartmann K, Raabe O, Kliesch S, Weidner W, Klug J, Bergmann M (2014) Expression pattern of estrogen receptors α and β and G-protein-coupled estrogen receptor 1 in the human testis. Histochem Cell Biol. doi:10.1007/s00418-014-1216-z

Geyer J, Bakhaus K, Bernhardt R, Blaschka C, Dezhkam Y, Fietz D, Grosser G, Hartmann K, Hartmann MF, Neunzig J, Papadopoulos D, S nchez-Guijo A, Scheiner-Bobis G, Schuler G, Shihan M, Wrenzycki C, Wudy SA, Bergmann M (2016) The role of sulfated steroid hormones in reproductive processes. J Steroid Biochem Mol Biol. doi:10.1016/j.jsbmb.2016.07.002

Griswold MD (1998) The central role of Sertoli cells in spermatogenesis. Semin Cell Dev Biol 9:411–416. doi:10.1006/scdb.1998.0203

Grube M, Reuther S, Zu Schwabedissen HM, Kock K, Draber K, Ritter CA, Fusch C, Jedlitschky G, Kroemer HK (2007) Organic anion transporting polypeptide 2B1 and breast cancer resistance protein interact in the transepithelial transport of steroid sulfates in human placenta. Drug Metab Dispos 35:30–35

Hess RA (2003) Estrogen in the adult male reproductive tract: a review. Reprod Biol Endocrinol 1:52. doi:10.1186/1477-7827-1-52

Hess RA, Fernandes SA, Gomes GR, Oliveira CA, Lazari MF, Porto CS (2011) Estrogen and its receptors in efferent ductules and epididymis. J Androl 32:600–613. doi:10.2164/jandrol.110.012872

Joseph A, Shur BD, Hess RA (2011) Estrogen, efferent ductules, and the epididymis. Biol Reprod 84:207–217. doi:10.1095/biolreprod.110.087353

Klaassen CD, Aleksunes LM (2010) Xenobiotic, bile acid, and cholesterol transporters: function and regulation. Pharmacol Rev 62:1–96. doi:10.1124/pr.109.002014

Labrie F (2003) Extragonadal synthesis of sex steroids: intracrinology. Ann Endocrinol 64:95–107

Lekhkota O, Brehm R, Claus R, Wagner A, Bohle RM, Bergmann M (2006) Cellular localization of estrogen receptor-alpha (ERalpha) and -beta (ERbeta) mRNA in the boar testis. Histochem Cell Biol 125:259–264. doi:10.1007/s00418-005-0008-x

Luu-The V (2013) Assessment of steroidogenesis and steroidogenic enzyme functions. J Ster Biochem Mol Biol 137:176–182. doi:10.1016/j.jsbmb.2013.05.017

Mouhadjer N, Bedin M, Pointis G (1989) Steroid sulfatase activity in homogenates, microsomes and purified Leydig cells from adult rat testis. Reprod Nutr Dev 29:277–282

Nitta H, Bunick D, Hess RA, Janulis L, Newton SC, Millette CF, Osawa Y, Shizuta Y, Toda K, Bahr JM (1993) Germ cells of the mouse testis express P450 aromatase. Endocrinology 132:1396–1401

Pasqualini JR, Gelly C, Nguyen B-L, Vella C (1989) Importance of estrogen sulfates in breast cancer. J Steroid Biochem 34:155–163. doi:10.1016/0022-4731(89)90077-0

Payne AH, Jaffe RB (1970) Comparative roles of dehydroepiandrosterone sulfate and androstenediol sulfate as precursors of testicular androgens. Endocrinology 87:316–322. doi:10.1210/endo-87-2-316

Payne AH, Kawano A, Jaffe RB (1973) Formation of dihydrotestosterone and other 5 -reduced metabolites by isolated seminiferous

tubules and suspension of interstitial cells in a human testis. J Clin Endocrinol Metab 37:448–453. doi:10.1210/jcem-37-3-448

Robillard KR, Hoque MT, Bendayan R (2011) Expression of ATP-binding cassette membrane transporters in rodent and human Sertoli cells: relevance to the permeability of antiretroviral therapy at the blood-testis barrier. J Pharmacol Exp Ther 340:96–108. doi:10.1124/jpet.111.186916

Ruokonen A (1978) Steroid metabolism in testis tissue: the metabolism of pregnenolone, pregnenolone sulfate, dehydroepiandrosterone and dehydroepiandrosterone sulfate in human and boar testes in vitro. J Steroid Biochem 9:939–946

Ruokonen A, Laatikainen T, Laitinen EA, Vihko R (1972) Free and sulfate-conjugated neutral steroids in human testis tissue. Biochemistry 11:1411–1416

Sar M, Hall SH, Wilson EM, French FS (1993) Androgen regulation of Sertoli cells. In: Russell LD (ed) The Sertoli cell. Cache River Press, Clearwater, pp 509–516

Schumacher V, Gueler B, Looijenga LHJ, Becker JU, Amann K, Engers R, Dotsch J, Stoop H, Schulz W, Royer-Pokora B (2008) Characteristics of testicular dysgenesis syndrome and decreased expression of SRY and SOX9 in Frasier syndrome. Mol Reprod Dev 75(9):1484–1497. doi:10.1002/mrd.20889

Stanway SJ, Delavault P, Purohit A, Woo LW, Thurieau C, Potter BV, Reed MJ (2007) Steroid sulfatase: a new target for the endocrine therapy of breast cancer. Oncologist 12:370–374

Walker WH (2009) Molecular mechanisms of testosterone action in spermatogenesis. Steroids 74:602–607. doi:10.1016/j.steroids.2008.11.017

Wijnholds J, Scheffer GL, van der Valk M, van der Valk P, Beijnen JH, Scheper RJ, Borst P (1998) Multidrug resistance protein 1 protects the oropharyngeal mucosal layer and the testicular tubules against drug-induced damage. J Exp Med 188:797–808. doi:10.1084/jem.188.5.797

11. Anhang – Publikationen

9. K.Bakhaus, J. Bennien, D. Fietz, A. Sánchez-Guijo, M. Hartmann, R. Serafini, C.C. Love, A. Golovko, S.A. Wudy, M. Bergmann, J. Geyer. J Steroid Biochem Mol Biol 2017 Jul 22. pii: S0960-0760(17)30184-X.

ARTICLE IN PRESS

Journal of Steroid Biochemistry and Molecular Biology xxx (xxxx) xxx–xxx

Contents lists available at ScienceDirect

Journal of Steroid Biochemistry and Molecular Biology

journal homepage: www.elsevier.com/locate/jsbmb

Sodium-dependent organic anion transporter (*Slc10a6*$^{-/-}$) knockout mice show normal spermatogenesis and reproduction, but elevated serum levels for cholesterol sulfate

Katharina Bakhaus[a,1], Josefine Bennien[a,1], Daniela Fietz[b], Alberto Sánchez-Guijo[c], Michaela Hartmann[c], Rosanna Serafini[d], Charles C. Love[d], Andrei Golovko[e], Stefan A. Wudy[c], Martin Bergmann[b], Joachim Geyer[a,*]

[a] Institute of Pharmacology and Toxicology, Faculty of Veterinary Medicine, Justus Liebig University Giessen, Germany
[b] Department of Veterinary Anatomy, Histology and Embryology, Faculty of Veterinary Medicine, Justus Liebig University Giessen, Germany
[c] Steroid Research and Mass Spectrometry Unit, Pediatric Endocrinology and Diabetology, Center of Child and Adolescent Medicine, Justus Liebig University Giessen, Germany
[d] Department of Large Animal Clinical Sciences, College of Veterinary Medicine and Biomedical Sciences, Texas A & M University, TX, USA
[e] Texas A & M Institute for Genomic Medicine, TX, USA

ARTICLE INFO

Keywords:
Soat
Slc10a6
Knockout mouse
Sulfated steroids
Reproduction
Transport
Cholesterol sulfate
Testis

ABSTRACT

The sodium-dependent organic anion transporter SOAT (gene name *SLC10A6* in man and *Slc10a6* in mice) is a plasma membrane transporter for sulfated steroids, which is highly expressed in germ cells of the testis. SOAT can transport biologically inactive sulfated steroids into specific target cells, where they can be reactivated by the steroid sulfatase (STS) to biologically active, unconjugated steroids known to regulate spermatogenesis. Significantly reduced SOAT mRNA expression was previously found in different forms of impaired spermatogenesis in man. It was supposed that SOAT plays a role for the local supply of steroids in the testis and consequently for spermatogenesis and fertility. Thus, an *Slc10a6*$^{-/-}$ Soat knockout mouse model was established by recombination-based target deletion of the *Slc10a6* gene to elucidate the role of Soat in reproduction. However, the *Slc10a6*$^{-/-}$ knockout mice were fertile, produced normal litter sizes, and had normal spermatogenesis and sperm vitality. This phenotype suggests that the loss of Soat can be compensated in the knockout mice or that Soat function is not essential for reproduction. In addition to reproductive phenotyping, a comprehensive targeted steroid analysis including a set of 9 un-conjugated and 12 sulfo-conjugated steroids was performed in serum of *Slc10a6*$^{-/-}$ knockout and *Slc10a6*$^{+/+}$ wildtype mice. Only cholesterol sulfate, corticosterone, and testosterone (only in the males) could be detected in considerable amounts. Interestingly, male *Slc10a6*$^{-/-}$ knockout mice showed significantly higher serum levels for cholesterol sulfate compared to their wildtype controls. As cholesterol sulfate has a broader impact apart from the testis, further analysis of this phenotype will include other organs such as skin and lung, which also show high Soat expression in the mouse.

1. Introduction

The sodium-dependent organic anion transporter (SOAT in man and Soat in mice) represents a plasma membrane uptake carrier for sulfated steroid hormones and belongs to the solute carrier family 10 (member *SLC10A6* in man and *Slc10a6* in mice) [1]. SOAT shows transport activity for estrone sulfate (E_1S), estradiol sulfate (E_2S), pregnenolone sulfate (PregS), dehydroepiandrosterone sulfate (DHEAS), 16α-

Abbreviations: 4A, 4-androstenedione; AD, androstanediol; AnDiolS, androstenediol sulfate; AnS, androsterone sulfate; CASA, computer-assisted sperm analysis; CS, cholesterol sulfate; DHEA, dehydroepiandrosterone; DHEAS, dehydroepiandrosterone sulfate; DHT, dihydrotestosterone; DHTS, dihydrotestosterone sulfate; epiAnS, epiandrosterone sulfate; ES cells, embryonic stem cells; eTS, epitestosterone sulfate; E_1S, estrone sulfate; E_2S, estradiol sulfate; GC, gas chromatography; het, heterozygous; IS, internal standard; ko, knockout; LC, liquid chromatography; MS, mass spectrometry; 16α-OH-DHEAS, 16α-hydroxydehydroepiandrosterone sulfate; 17-OH-PregS, 17-hydroxypregnenolone sulfate; 17-OH-Prog, 17-hydroxyprogesterone; PBS, phosphate-buffered saline; PregS, pregnenolone sulfate; Prog, progesterone; SCO, Sertoli cell only; SOAT, sodium-dependent organic anion transporter; STS, steroid sulfatase; T, testosterone; TS, testosterone sulfate; wt, wildtype

* Corresponding author at: Institute of Pharmacology and Toxicology, Biomedical Research Center Seltersberg (BFS), Schubertstr. 81, 35392 Giessen, Germany.
E-mail address: Joachim.M.Geyer@vetmed.uni-giessen.de (J. Geyer).

[1] Equally contributed.

http://dx.doi.org/10.1016/j.jsbmb.2017.07.019
Received 8 May 2017; Accepted 18 July 2017

Please cite this article as: Bakhaus, K., Journal of Steroid Biochemistry and Molecular Biology (2017), http://dx.doi.org/10.1016/j.jsbmb.2017.07.019

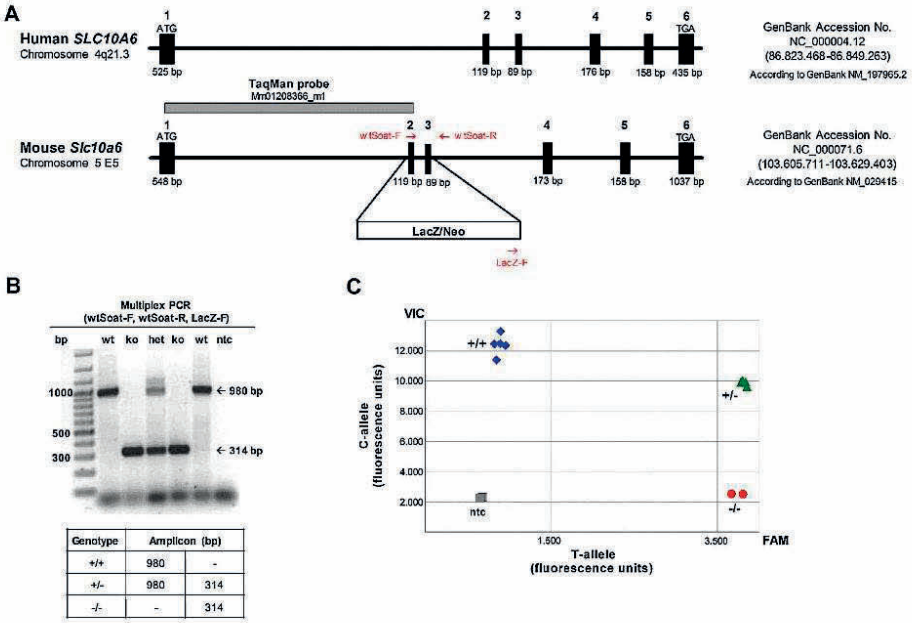

Genotype	Amplicon (bp)	
+/+	980	-
+/-	980	314
-/-	-	314

Fig. 1. Target deletion of the murine *Slc10a6* gene and genotyping.
(**A**) The mouse *Slc10a6* and human *SLC10A6* genes both consist of six coding exons and are located at chromosome 5 E5 and 4q21.3, respectively. Black boxes depict the exons and are in sense of broadness and distance scaled to the *SLC10A6/Slc10a6* genes. *Slc10a6* ko mice were generated by target deletion of the coding exons 2 and 3 in 129SvEvBrd-derived embryonic stem cells and integration of a *LacZ/Neo* selection cassette at the site of recombination. Arrows indicate the localization of the primers used for genotyping. (**B**) For genotyping, genomic DNA of *Slc10a6* wt, het, and ko mice was isolated from earmarks. Multiplex PCR analysis detected genotype-specific bands for the wt (980 bp) and mutant (314 bp) alleles on an 1.5% agarose gel. (**C**) SNP-specific probes labeled with VIC for the C57BL/6N strain (C-allele representing wt) and FAM for the 129SvEvBrd strain (T-allele representing ko) were used for quantitative real-time PCR of genomic DNA from *Slc10a6* wt and ko mice. An additional fluorescence read was performed on the post-PCR samples and allelic discrimination was done by automatic allele calling. Determination of the *Slc10a6* genotype is based on the gain of fluorescence of only FAM (−/−), only VIC (+/+), or both dyes (+/−), and was used to validate the PCR-based genotyping.

Table 1
Primers used for genotyping and expression analysis.

Primer	Sequence (5′ → 3′)
wtSoat-F	GCC TCT CTG CCT CTA CAT CTA CAC CCG
LacZ-F	CTT CTT GAC GAG TTC TTC TGA GGG GAT
wtSoat-R	CCT AGT GTT TCG GTC TCT TTC AGC ATC

preceding *DNase* I treatment in order to eliminate remaining DNA. For quantitative real-time PCR amplification of the mouse Soat transcript, the *TaqMan Gene Expression Assay* Mm01208366_m1 (Thermo Fisher Scientific) was applied (Fig. 1A). Amplification of the murine hypoxanthine-guanine phosphoribosyltransferase (mHprt) transcript (assay number Mm00446968_m1) was used as endogenous control. For each specimen, triplicate determinations were performed in a 96-well optical well plate using 5 µl cDNA, 1.25 µl *TaqMan Gene Expression Assay*, 12.5 µl *TaqMan Gene Expression Master Mix* (Thermo Fisher Scientific) and ddH_2O to a final volume of 25 µl. Quantitative real-time PCR was performed as described above.

2.6. Histomorphological evaluation of the testes from Slc10a6 wt and ko mice

For histomorphometry, one testis of each *Slc10a6* wt (n = 7) and ko (n = 9) mouse was directly stored in Bouin's solution (70% picric acid, 23.3% formalin, 5% glacial acetic acid) for 24 h, embedded in paraffin and cut in 5 µm thick sections. Sections were stained with hematoxylin

Table 2
SNPs flanking the target deleted *Slc10a6* gene.

Strain	SNP	Chr.	Position
C57BL/6N	↑	↑	↑
	mCV22996021	5	75065363
129S6/SvEvBrd	rs13478337	5	76181811
	rs13478352	5	79902641
	rs3721607	5	81282125
	rs3667334	5	81819770
	rs13459087	5	85884364
	CEL-5_87173557	5	87173557
	gnf05.084.686	5	88364567
	rs3673049	5	88498569
	rs13478388	5	89674255
	rs6232866	5	90936845
	rs13478402	5	93496397
	CEL-5_93945748	5	93945748
	rs3661241	5	95154383
	rs3705458	5	96618852
	rs13478433	**5**	**101291108**
	Slc10a6 (target deletion)	*5*	*103605711–103629403*
C57BL/6N	rs13478451	5	106102700
	↓	↓	↓

Note: Repeated backcrossing onto purebred C57BL/6N mice revealed congenic *Slc10a6*$^{-/-}$ knockout mice with only a 27 Mbp region linked to the target deleted *Slc10a6* gene and derived from the 129S6/SvEvBrd background. The SNP rs13478433 (bold) was linked to the *Slc10a6* gene and was used for allelic discrimination of the *Slc10a6*$^{+/+}$ wt, *Slc10a6*$^{+/-}$ het, and *Slc10a6*$^{-/-}$ ko mice by fluorogenic 5′nuclease TaqMan AD analysis (see Fig. 1C).

hydroxydehydroepiandrosterone sulfate (16α-OH-DHEAS), and androstenediol sulfate (AnDiolS). However, SOAT does not accept other steroid compounds as substrates including bile acids such as taurocholic acid and chenodeoxycholic acid, cardiac glycosides such as ouabain and digoxin, or steroid glucuronides such as estrone-3β-D-glucuronide and estradiol-17β-D-glucuronide [2–6]. Therefore, SOAT/Soat, in contrast to other more multi-specific carriers from the organic anion transporting polypeptide (OATP) or organic anion transporter (OAT) families, represents a specific steroid sulfate uptake carrier [7,8]. In man, SOAT is predominantly expressed in the testis and was also detected in skin, placenta, pancreas, and mammary gland [3,5]. In mice, Soat showed the highest expression in lung, skin and testis, the order of which depends on the mouse strain analyzed (CF-1, C57BL/6, FVB, or 129Sv) [9]. In both species, the SOAT/Soat protein was localized to spermatocytes and spermatids, supposing that this carrier fulfills similar functions in the testes of man and mouse. Sulfated steroid hormones require uptake carriers such as SOAT/Soat to enter cells, where these molecules, after cleavage by the steroid sulfatase (STS), participate in the overall endocrine regulation via androgen and estrogen receptors [8,10–12]. In order to elucidate Soat's role for spermatogenesis and male fertility in vivo, an *Slc10a6*$^{-/-}$ knockout (ko) mouse model was established and analyzed regarding its reproductive phenotype and steroid profile.

2. Material and methods

2.1. Materials

All chemicals, unless otherwise stated, were obtained from Sigma-Aldrich.

2.2. Generation of *Slc10a6*$^{-/-}$ knockout mice

Slc10a6$^{-/-}$ ko mice were acquired from the Texas A&M Institute of Genomics Medicine (TIGM, Texas, USA). The *Slc10a6*$^{-/-}$ mouse line was generated by homologous recombination-based target deletion of the coding exons 2 and 3 of the *Slc10a6* gene in 129SvEvBrd-derived embryonic stem (ES) cells using a targeting vector designed to replace these exons with a selection cassette containing the *neo* and *LacZ* genes (Fig. 1A). Homologous recombination was verified by Southern blot analysis with a 3′ internal probe corresponding to the targeting vector and a 5′ external probe outside the recombination site (data not shown). Selected recombinant ES cells were injected into blastocysts and implanted into a C57BL/6 breeder mouse. Progeny were genotyped by PCR and heterozygous (het) mice were used for repeated backcrossing onto purebred C57BL/6N mice. The backcrossing procedure was guided by SNP-based *Speed Congenics* (1450 MD Linkage SNP panel, Taconic) in order to select heterozygous knockouts with the most C57BL/6N character for further backcrossing. *Speed Congenics* is based on SNP analysis across 19 autosomes and the X chromosome known to be polymorphic between the donor (129SvEvBrd) and recipient (C57BL/6NTac) strains [13]. After two years of backcrossing, we obtained *Slc10a6*$^{+/-}$ het mice with a well-defined 99.51% C57BL/6N recipient genome, representing generation equivalent NE7 [14]. If not otherwise stated, het male and female *Slc10a6*$^{+/-}$ mice were mated to generate *Slc10a6*$^{-/-}$ homozygous ko and *Slc10a6*$^{+/+}$ wildtype (wt) littermate control mice. During the whole mating process, the progeny genotype numbers were close to the expected Mendelian ratios.

2.3. Genotyping of the Slc10a6 ko mice by multiplex PCR and allelic discrimination

Mouse genomic DNA was isolated from earmarks following the *QIAamp DNA Kit* (Qiagen) protocol. Briefly, tissue samples were thoroughly mixed with 180 µl *ATL buffer* and 20 µl protein kinase K and incubated for 3–12 h at 56 °C in a thermomixer (Eppendorf, Hamburg). Afterwards, 200 µl *AL buffer* was added and samples were vortexed for 15 s followed by an incubation step at 70 °C for 10 min. Subsequently, 200 µl ethanol were added and samples were vortexed for 15 s. The whole sample volume was transferred to a *QIAamp DNA Mini Column*, centrifuged for 1 min at 8,000 rpm, and subsequently washed with *buffers AW1* and *AW2*. Next, DNA was eluted with 200 µl ddH_2O. To distinguish between *Slc10a6*$^{+/+}$ wt, *Slc10a6*$^{+/-}$ het and *Slc10a6*$^{-/-}$ ko mice, multiplex PCR was performed (Fig. 1B). Primers (obtained from Metabion International) are listed in Table 1.

For multiplex PCR, the following components were used: 1 µl of DNA, 2 µl 10 x *Dream Taq buffer*, 2 µl dNTP mix (2 mM each), 1 µl of each primer at 10 pmol, 0.1 µl *Dream Taq polymerase* (Thermo Fisher Scientific), and ddH_2O to a final volume of 20 µl. PCR conditions were 1 × 95 °C for 3 min, 35 x (95 °C for 30 s, 60 °C for 30 s and 72 °C for 60 s), and final extension at 72 °C for 5 min. PCR products were separated on an 1.5% agarose gel and visualized by *GelRed Nucleic Acid Gel Stain* (Biotium). Genotyping data were verified by allelic discrimination for SNP rs13478433 (Table 2).

This SNP lies in direct proximity to the *Slc10a6* gene on chromosome 5 and is derived from the 129SvEvBrd donor strain (Suppl. Table 1). For allelic discrimination, the fluorogenic 5′ nuclease *TaqMan assay* M_22549783_10 (Applied Biosystems) was used including a C-allele-specific VIC-coupled probe corresponding to the C57BL/6N recipient strain and a T-allele-specific FAM-coupled probe detecting the 129SvEvBrd strain used for targeted deletion. Real-time PCR amplification was performed in a total reaction volume of 25 µl consisting of 12.5 µl *TaqMan Genotyping Master Mix* (Applied Biosystems), including *AmpliTaq Gold DNA polymerase*, dNTP mix, reaction buffer and ROX reference dye, 2.5 µl *TaqMan AD assay* (Applied Biosystems) and about 100 ng of genomic DNA. The samples were amplified in a 96-well optical plate on an *Applied Biosystems 7300 thermal cycler*. The amplification reaction started with the activation of the *AmpliTaq Gold DNA Polymerase* at 95 °C for 10 min before 40 cycles of 92 °C × 15 s and 60 °C × 30 s were applied. Following amplification, allelic discrimination was recorded on the post-PCR products and analyzed by the *7300 Real-Time PCR System Sequence Detection Software (SDS) v1.4* (Applied Biosystems).

2.4. Sample preparation from mouse organs

All mice were housed in a specific pathogen-free animal facility with a temperature controlled environment and 12-h light/dark cycle and were provided with standard laboratory food and water ad libitum. All experiments, including euthanasia and tissue preparations, were approved by the local regulatory authority (Regierungspräsidium Gießen) with the reference number V54-19 c 20 15 h 02 GI 20/23 Nr. A8/2013. Organ samples were obtained from *Slc10a6* wt and ko mice after deep anesthesia with ketamine (120 mg/kg) and xylazine (16 mg/kg) and exsanguination via heart puncture. Organs were immediately removed and processed for RNA isolation or immunofluorescence analysis. Blood samples were stored for 3 h at room temperature before samples were centrifuged for 20 min at 3,000 rpm. Serum was stored at −20 °C and used for steroid profiling.

2.5. RNA preparation and quantitative real-time PCR expression analysis

For RNA isolation, organs were conserved in *RNAlater* solution (Thermo Fisher Scientific) at −20 °C before total RNA was extracted using *TRI reagent* (Invitrogen). The RNA amount was determined using the *Qubit 3.0 fluorometer* (Invitrogen). The RNA integrity number (RIN) was determined by the *Agilent 2100 Bioanalyzer* (Agilent Technologies) using the *Agilent RNA 6000 Nano Kit* according to the manufacturer's instructions. Only RNA samples with RIN values of ≥8.5 were used for subsequent cDNA synthesis and quantitative real-time PCR analysis. The cDNA was synthesized using *SuperScript III First Strand Synthesis* (Invitrogen) according to the manufacturer's instructions with a

and eosin according to standard protocols. Between 150 and 300 tubular cross sections were counted per genotype. Staging of spermatogenesis was performed according to [15]. Three different spermatogenic stages were counted due to their relation to meiosis. In stage V, spermatogonia type B, which enter meiosis, appear for the first time. Stage VIII is defined as the stage of sperm release and the onset of meiosis, as preleptotene spermatocytes enter the prophase of meiosis I. In the last stage of the spermatogenic cycle, stage XII, the first meiotic division takes place. Moreover, seminiferous tubules with impaired spermatogenesis (e.g. germ cell aplasia also known as Sertoli cell only (SCO) syndrome, arrests of spermatogenesis, missing generations) were identified by microscopy on a Leica LM 750 microscope.

2.7. Immunofluorescence detection of the Soat protein

For immunofluorescence detection of the Soat protein, tissue samples were stored in 4% paraformaldehyde for 72 h before they were transferred into 30% sucrose dissolved in phosphate-buffered saline (PBS, containing 137 mM NaCl, 2.7 mM KCl, 1.5 mM KH_2PO_4, and 7.3 mM Na_2HPO_4, at pH 7.4). After 24 h, tissue samples were embedded in *Tissue Tek* (Labor Weckert) and frozen at − 80 °C for 30 min before 8 µm thick cryosections were cut. For immunostaining, slides were thawed at room temperature for 15 min and rehydrated with PBS three times for 5 min followed by antigen retrieval using 0.1% SDS in PBS for 5 min. After three washing steps over 10 min with PBS, slides were incubated in blocking buffer (5% BSA in PBS) for 30 min at room temperature. The anti-$mSoat_{329-344}$ antibody (1:500 dilution) [9] was diluted in incubation buffer (1% goat serum, 0.1% Triton X-100 in PBS) and added to the slides over night at 4 °C. Slides were washed with PBS three times for 5 min before the secondary antibody Alexa Fluor 488 goat anti-rabbit (1:800 dilution, Invitrogen) was applied for 1 h at room temperature. Slides were finally washed three times with PBS, mounted with *Vectashield H-1200 Mounting Medium* with DAPI (Vector Laboratories), and dried for 20 min at 4 °C. Fluorescent imaging was performed on a Leica DM5500 B microscope and captured images were analyzed with the Leica Fluorescence Workstation software LAS AF 6000.

2.8. Sperm collection and computer-assisted sperm analysis (CASA)

Sperm analysis was performed at the Department of Large Animal Clinical Sciences, College of Veterinary Medicine and Biomedical Sciences, Texas A & M University, Texas, USA. All procedures were approved in advance by the Institutional Animal Care and Use Committee of the Texas A & M University. Sperm were collected from the cauda epididymis of sexually mature (> 8 weeks) mice. Each cauda was carefully trimmed to remove adipose and other tissue, rinsed in PBS and placed either in 1 ml *EmbryoMax HTF media* (Millipore) or in 1 ml *INRA 96 Extender* (Breeders Choice). Four to six cuts were made in each cauda using iris scissors, and sperm were released into the media by incubation for 10 min at 37 °C under 5% CO_2. After incubation, the tissue was removed and the suspension was mixed gently by swirling. The suspension was then diluted in the same medium to a concentration of ~ 30×10^6 sperm/ml, equivalent to 750–1000 sperm per microscope field for CASA. Sperm concentration was measured with a fluorescence-based cell counter (NucleoCounter SP-100 TM ChemoMetec) and sperm motility was analyzed with a computer-assisted sperm motion analysis (CASMA) system (IVOS Version 12.2.l, Hamilton, Thorne Biosciences). Each sample (6 µl) was placed on a microscope slide (Leja Standard Count 2 Chamber slides) and slides were inserted into the CASMA. A minimum of 10 fields and 500 sperm were measured for each sample. Motility parameters included: percentage of total motile sperm (TMOT), average path velocity (VAP, µm/s), straight-line velocity (VSL, µm/s), mean curvilinear velocity (VCL, µm/s), lateral head displacement (ALH), beat cross frequency (BCF), straightness (STR, µm/s), linearity (LIN, µm/s), and percentage of progressively motile sperm (PMOT). Sperm morphology was assessed in buffered formol saline solution and evaluated by differential-interference contrast microscopy (Olympus BX60). A total of 100 sperm per sample were evaluated and all abnormalities identified on each sperm were recorded. The following sperm morphologic features were identified: normal heads, abnormal heads, abnormal acrosomes, detached heads, proximal or distal cytoplasmic droplets, abnormal or bent midpieces, bent or coiled tails, and premature germ cells [16].

2.9. Mass spectrometric steroid determination in mouse serum

All reference steroids and the internal standards (ISs) were purchased from C/D/N Isotopes Inc. (Quebec, Canada), Sigma-Aldrich (Taufkirchen, Germany), Steraloids Inc. (Newport, USA), or from LGC Standards GmbH (Wesel, Germany). For steroid analysis, 300 µl mouse serum were mixed with 50 µl of a stable isotope-labeled internal standard (IS) cocktail for un-conjugated and sulfated steroids. Calibrators were prepared following the same procedure, using 300 µl of charcoal-stripped serum. Concentration of isotopic-labeled sulfated steroids was 1 µg/ml, with the exception of the IS for cholesterol sulfate (6 µg/ml), whereas the concentrations of un-conjugated steroids were 10 ng/ml for all the ISs, with the exception of the IS for DHEA, progesterone and corticosterone (50 ng/ml). After equilibration for 15 min at ambient temperature, proteins were precipitated and the samples were incubated for additional 15 min. Supernatants were isolated by centrifugation (14,600 rpm, 10 min) and mixed with 3 ml of water in a glass tube. Each sample was loaded onto an activated *Sep-Pak C18* cartridge. The cartridges were then washed with water (3 ml) and hexane (3 ml), respectively. Thereafter, un-conjugated steroids were eluted with chloroform (4 ml) and further worked up for GC–MS/MS analysis (see below). The next elution with methanol (4 ml) isolated sulfated steroids to be analyzed by LC–MS/MS. For LC–MS/MS analysis, methanol was evaporated and the samples were reconstituted in 250 µl of a solution containing 10% acetonitrile, 10% methanol, 70% water and 10% NH_3 (at 2.5%). Then, samples were vortexed and centrifuged before their injection into the LC–MS/MS instrument (10 µl).

The LC–MS/MS system consisted of an *Agilent 1200SL HPLC* (Waldbronn, Germany) with an *Accucore Phenyl-X* (100 × 2.1 mm, 2.6 µm) column (Thermo Fisher Scientific). For separation of sulfated steroids, a gradient of a buffer solution with ammonium acetate (10 mM and pH 7 dissolved in 85% water and 15% acetonitrile) and a solution with organic solvents composed by 70% methanol and 30% acetonitrile (v/v) was used. MS/MS was performed on a *TSQ Quantum Ultra* triple quadrupole mass spectrometer (Thermo Fisher Scientific) operated in electrospray negative ionization mode [17]. Limits of quantification were 1 ng/ml for PregS, 17-OH-PregS, E_1S, dihydrotestosterone sulfate (DHTS), testosterone sulfate (TS) and epitestosterone sulfate (eTS), 2.5 ng/ml for E_2S and AnDiolS, 10 ng/ml for androsterone sulfate (AnS) and epiandrosterone sulfate (epiAnS), 25 ng/ml for DHEAS and 80 ng/ml for cholesterol sulfate (CS). For GC–MS/MS analysis of un-conjugated steroids, the chloroform fraction from the *Sep-Pak* extraction was evaporated with a flow of nitrogen at 40 °C, taken up in cyclohexane/ethanol (90:10 v/v) and purified by gel chromatography on 0.4 g *Sephadex LH-20* mini columns. For derivatization, heptafluorobutyric anhydride was used [18]. Gas chromatography (GC) was performed on an *Optima 1-MS* capillary column (25 m x 0.2 mm I.D., df 0.1 µm, Macherey-Nagel, Germany) housed in an *Trace 1310* gas chromatograph with a *TriPlus RSH* auto-sampler coupled to a *TSQ 800* triple quadrupole MS (Thermo Fisher Scientific). Helium was used as carrier gas at 1.0 ml/min. The injector temperature was 270°C and the initial column temperature was set at 80°C. The steroids of interest eluted at a rate of 3°C/min until the column temperature reached 242°C. The following MRM or *m/z* ratios were measured for the analytes and their corresponding internal standards: *m/z* 665.1 (668.1) for testosterone (T) (d3-T), *m/z* 482.2/482.2 (484.3/484.3) for 4-androstenedione (4A) (d2-4A), *m/z* 455.3/241.3 (458.3/244.4) for

androstanediol (AD) (d3-AD), *m/z* 270.2/121.1 (272.2/123.1) for DHEA (d2-DHEA), *m/z* 414.1/185.2 (417.2/188.2) for dihydrotestosterone (DHT) (d3-DHT), *m/z* 465.2/109.1 (469.1/113.1) for 17-OH-progesterone (17-OH-Prog) (d4-17-OH-Prog), *m/z* 465.2/109.1 (467.2/109.1) for 11-deoxycortisol (d2-11-deoxycortisol), 705.1/355.1 (712.1/359.2) for corticosterone (d8-corticosterone), and *m/z* 510.2/495.2 (/518.3/503.4) for progesterone (Prog) (d9-Prog). Limits of quantification were 0.04 ng/ml for T, AD, DHT and 11-deoxycortisol, 0.08 ng/ml for DHEA, 0.16 ng/ml for 4A and 17-OH-Prog, 0.21 ng/ml for Prog and 0.83 ng/ml for corticosterone.

3. Results

In order to explore the role of the SOAT/Soat for spermatogenesis and reproduction, an *Slc10a6* ko mouse model was established. In these mice, the coding exons 2 and 3 were replaced by a *LacZ/Neo* selection cassette, which could be verified by genotyping PCR with primers specific for the wt (wtSoat-F) and mutant (LacZ-F) allele together with a common reverse primer (wtSoat-R) (Fig. 1A). The primers wtSoat-F and wtSoat-R revealed a 980 bp fragment from the wt allele, whereas LacZ-F together with wtSoat-R produced an amplicon of 314 bp from the mutant allele. In the *Slc10a6*$^{+/-}$ het mice, both amplicons of 314 bp and 980 bp were amplified (Fig. 1B). As the *Slc10a6* ko mouse derived from 129SvEvBrd ES cells, which were implanted into a C57BL/6N breeder mouse after injection into blastocysts, progeny were repeatedly backcrossed onto purebred C57BL/6N mice in order to obtain a congenic *Slc10a6* ko strain. Backcrossing was guided by SNP-based *Speed Congenics* and revealed het *Slc10a6*$^{+/-}$ mice with a 99.51% C57BL/6N genome, only excluding a 27 Mbp region flanking the *Slc10a6* gene (position 76181811-103629403 on chromosome 5 E5), which still had 129SvEvBrd character (Table 2). In this region, 92 genes are located, but none of them has a strong functional correlation to reproduction (Suppl. Table 1). The SNP rs13478433, which allows discriminating between the C57BL/6N (C-allele) and 129SvEvBrd (T-allele) mice, was used to confirm PCR-based genotyping by allelic discrimination. Here, the rs13478433 C-allele indicated the C57BL/6N recipient genome, which is linked to the *Slc10a6* wt allele, whereas the 129SvEvBrd-specific rs13478433 T-allele indicated the target deleted *Slc10a6* ko allele (Fig. 1C).

In addition to the DNA level, the *Slc10a6* knockout was also verified on the mRNA and protein levels. Testis samples were analyzed by quantitative real-time PCR using an mSoat-specific *TaqMan* probe located on exon boundary 1/2 with the reverse primer located at the region of the target deletion in the mutant mice. In wt mice, testis samples showed high Soat expression as expected, whereas in the *Slc10a6*$^{-/-}$ ko mice, Soat mRNA was not detectable (Fig. 2A). Immunofluorescence studies on testis sections with the anti-Soat$_{329\text{-}344}$ antibody then also confirmed the absence of the Soat protein in the *Slc10a6*$^{-/-}$ ko mice. Soat-specific immunoreactivity was detected in round spermatids (Fig. 2B) as described before [9]. In contrast, *Slc10a6*$^{-/-}$ ko mice did not show any Soat-specific staining. In summary, *Slc10a6* knockout was confirmed at the DNA, RNA and protein levels.

For reproductive phenotyping, *Slc10a6*$^{+/-}$ mice were used for het × het breeding to generate wt and ko littermates for further experiments. These mice were then set up for mating experiments to verify fertility of the *Slc10a6*$^{-/-}$ ko mice. In total n = 3 wt × wt, n = 7 het × het, and n = 12 ko × ko matings were set up and the number of pups was recorded as well as their vitality, body weight and gender. All offspring mice were alive and without any obvious anatomical abnormalities, regardless of the respective genotype. There were no significant differences in the number of pups (Fig. 3A), infantile mortality, gender distribution (Fig. 3B), or body weight at the time of weaning (Fig. 3C) or in adult mice with an age older than 22 weeks (Fig. 3D) between *Slc10a6* wt, het and ko mice.

Because SOAT/Soat is highly expressed in testicular germ cells, the spermatogenesis of *Slc10a6* wt and ko mice was analyzed more closely. First, testis weights of *Slc10a6* wt and ko mice were determined and correlated to the body weight of each mouse. There was no statistically significant difference in the testis weights between the *Slc10a6* wt (0.53 ± 0.05% of body weight) and ko mice (0.63 ± 0.12% of body weight), but the testis weights of the *Slc10a6*$^{-/-}$ mice tended to be higher (Fig. 4B). Furthermore, histomorphological analysis of testicular sections showed no significant changes in stage frequencies and duration of spermatogenesis between *Slc10a6* wt and ko mice (Fig. 4A). Stage V was counted in 12.85% ± 3.58 (wt) and 12.74% ± 2.07 (ko) of tubules, stage VIII in 22.15% ± 3.18 (wt) and 20.64% ± 4.74 (ko) of tubules and stage XII in 2.40% ± 1.42 (wt) and 3.34% ± 2.36 (ko) of tubules. The distribution of stages showed no significant difference between both genotypes (Fig. 4C). Impaired spermatogenesis, e.g. indicated by total loss of germ cells or arrested spermatogenesis (summarized here as "impairment" in Fig. 4C), occurred more frequent in *Slc10a6* ko mice (3.96% ± 3.69% of tubules) compared to wt mice (1.34% ± 1.29% of tubules), but without reaching the level of significance. Arrests of spermatogenesis were detected mostly at the level of primary spermatocytes, but showed no difference between *Slc10a6* wt and ko mice. Missing generations of germ cells (2.59% ± 2.56% ko vs. 0.79% ± 0.49% wt) as well as total germ cell aplasia, also known

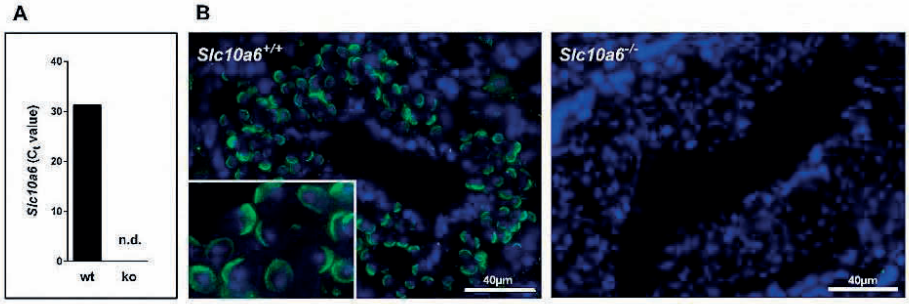

Fig. 2. Confirmation of the *Slc10a6* knockout at the RNA and protein levels.
(**A**) *Slc10a6* mRNA expression in the testis of *Slc10a6* wt and homozygous ko mice was analyzed by quantitative real-time PCR using a gene-specific *TaqMan* probe as shown in Fig. 1A. *Slc10a6* expression is represented by the C_T value. Hprt served as endogenous control with C_T values of 25.39 ± 0.06 and 24.73 ± 0.05 for the wt and ko testis samples, respectively. Values represent means ± SD of triplicate determinations. (**B**) Immunofluorescence studies were performed on paraformaldehyde-fixed testis cryosections from *Slc10a6*$^{-/-}$ ko and *Slc10a6*$^{+/+}$ wt mice. The Soat protein was detected by the mSoat$_{329\text{-}344}$ antibody (1:500 dilution) with subsequent immunofluorescent staining using the Alexa Fluor 488 goat anti-rabbit antibody (1:800, green fluorescence). Nuclei were stained with DAPI (blue fluorescence). Soat was detected in round spermatids of the *Slc10a6* wt mice, but not in the *Slc10a6* ko animals. N.d., not detectable.

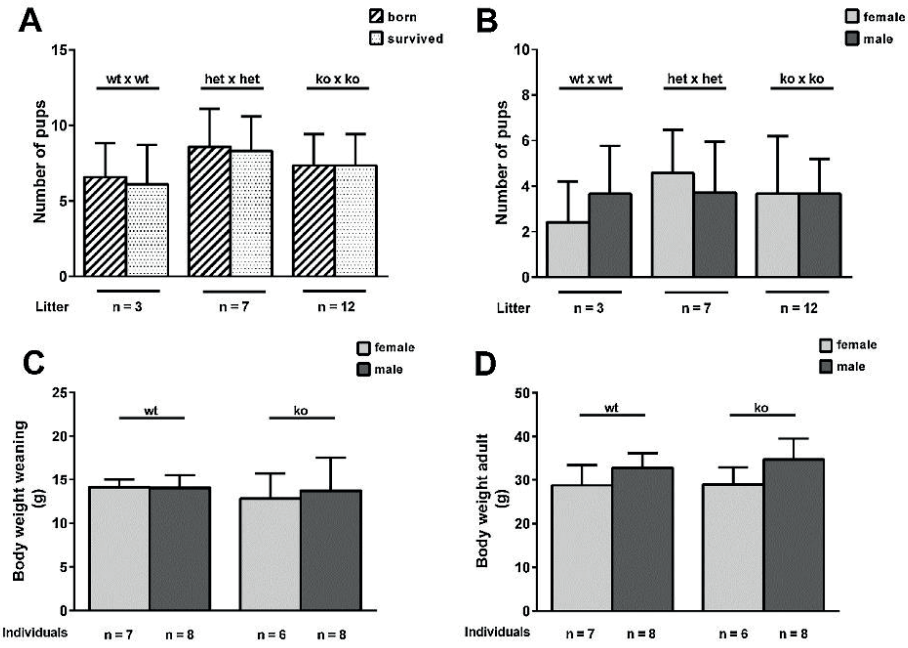

Fig. 3. Reproductive data of the *Slc10a6* wt and ko mice.
Viability and fertility of the progeny were analyzed by specific matings of *Slc10a6* wt × wt, het × het, or ko × ko mice. (**A**) Number of pups and their survival until weaning were recorded and (**B**) distribution between the sexes was analyzed. Body weight was determined for all mice at weaning (**C**) and at 22 to 31 weeks of age when mice were sacrificed for further investigations (**D**). Group sizes are indicated for each column and data are depicted as means ± SD. All data were statistically analyzed by one-way ANOVA, but revealed no significant differences.

as SCO syndrome (0.59% ± 1.22% ko vs. 0.12% ± 0.21% wt) were both more frequent in the *Slc10a6*$^{-/-}$ mice, but without reaching the level of significance due to large variability in the data (Fig. 4D).

Despite comparable histomorphological appearance, sperm morphology and motility were examined more closely between *Slc10a6* wt and ko mice. For this purpose, CASA was applied on sperm samples. Total and progressive motility (Fig. 5A, B) were analyzed using the sperm motility parameters VCL (curvilinear velocity), VAP (average path velocity), and VSL (straight-line velocity), but no differences were detectable between *Slc10a6* ko and wt mice. Furthermore, sperm morphology was assessed, including the following parameters: abnormal heads (AH), abnormal acrosomes (AA), normal heads (NH), detached heads (DH), abnormal midpieces (AM), bent midpieces (BM), bent tails (BT), coiled tails (CT), premature germ cells (PGC), proximal cytoplasmic droplets (PD) and distal cytoplasmic droplets (DD) (Fig. 5C). However, none of these parameters showed any significant difference between the *Slc10a6* wt and ko mice.

Apart from the testis, Soat-mediated transport of sulfated steroids may participate in the overall regulation of serum steroids in the sulfo-conjugated as well as in the un-conjugated form. Thus, a comprehensive targeted steroid analysis comprising 12 sulfo-conjugated and 9 un-conjugated steroids was performed in the serum of male and female *Slc10a6* wt and ko mice (n = 8 in each group). Among them, 17-OH-pregnenolone sulfate (17-OH-PregS), estrone sulfate (E_1S), estradiol sulfate (E_2S), epiandrosterone sulfate (epiAnS), and testosterone sulfate (TS) all were not found in any of the samples. Pregnenolone sulfate (PregS), dehydroepiandrosterone sulfate (DHEAS), androsterone sulfate (AnS), and dihydrotestosterone sulfate (DHTS) were detected in some, but not all of the samples. Androstenediol sulfate (AnDiolS) and epitestosterone sulfate (eTS) were detected in all samples, but below the limit of quantification. Therefore, none of these data could be quantitatively analyzed. Only serum cholesterol sulfate (CS) could be detected at quite high concentrations of 942–2559 ng/ml in the serum of all mice. Interestingly, CS was significantly elevated in the serum of the male *Slc10a6*$^{-/-}$ ko mice (3738 ± 569 ng/ml) compared to the male *Slc10a6*$^{+/+}$ wt mice (2683 ± 490 ng/ml), whereas the CS levels were comparable between the female *Slc10a6* ko and wt mice (Fig. 6A).

Regarding the un-conjugated steroids testosterone (T), 4-androstenedione (4A), androstanediol (AD), dehydroepiandrosterone (DHEA), dihydrotestosterone (DHT), 17-OH-progesterone (17-OH-Prog), progesterone (Prog), 11-deoxycortisol, and corticosterone could be detected in the sera from all mice, however, below the limit of quantification for most if not all samples precluding statistical analysis. Only the levels of T in the male mice as well as of corticosterone (males and females) were above the limit of quantification for all samples and, therefore, allowed statistical analysis. However, serum levels of testosterone and corticosterone were not significantly different between the *Slc10a6* ko and wt mice (Fig. 6).

4. Discussion

The present study represents the first characterization of the *Slc10a6* ko mouse and has a focus on the consequences of complete absence of the Soat protein for reproduction and spermatogenesis in mice. Previous studies demonstrated, that SOAT/Soat is highly expressed in male germ cells [5,9] and acts as specific steroid sulfate uptake carrier for hormonal precursors such as E_1S, E_2S, PregS, DHEAS, 16α-OH-DHEAS, and AnDiolS [3,5,6,9]. These inactive steroid compounds can be reactivated by STS and so may have an intracrine effect on male reproduction [11]. It is well known that spermatogenesis and male

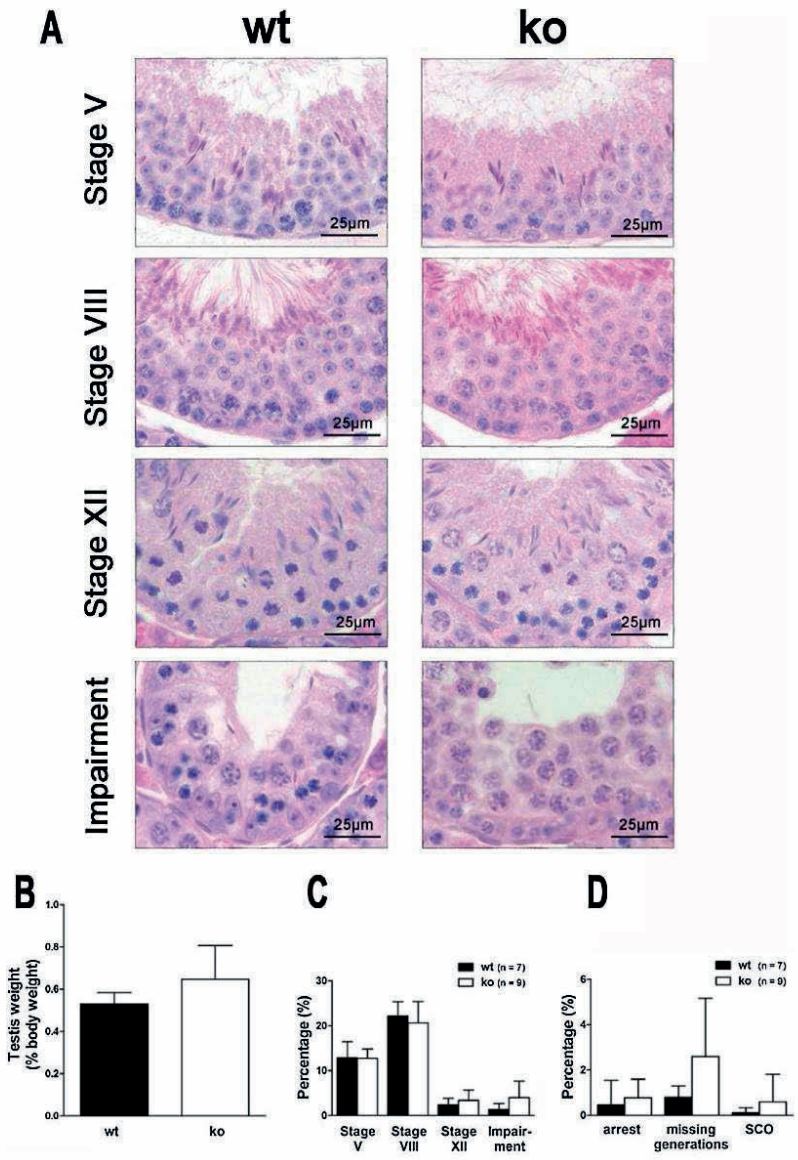

Fig. 4. Histomorphometric analysis of spermatogenesis in *Slc10a6* wt and ko mice.
For histological evaluation of spermatogenesis, testes from 12-week old *Slc10a6* wt and ko mice (n = 3 each) were fixed in *Bouin's solution* and embedded in paraffin. Sections were stained with hematoxylin and eosin. Staging of the spermatogenesis was performed according to [15]. (**A**) Three different stages were counted to give an overview of spermatogenesis in *Slc10a6* wt and ko animals: Stage V (appearance of type B spermatogonia), stage VIII (sperm release and onset of meiosis) and stage XII (first meiotic division). Moreover, tubules with impaired spermatogenesis were assessed. Here, an arrest of spermatogenesis at the level of primary spermatocytes is shown for both genotypes. (**B**) Prior to fixation, testis weights were determined and related to body weight. (**C**) Percentages of different stages (V, VIII and XII) showed no significant differences between *Slc10a6* wt and ko animals and were in line with the physiological frequency of spermatogenic stages described by [15]. Additionally, frequency of tubules showing impairments of spermatogenesis (namely germ cell aplasia = SCO, arrest of spermatogenesis at the level of primary spermatocytes, and missing generations of germ cells) showed no significant differences between genotypes. (**D**) Itemization of impairments of spermatogenesis in both genotypes are depicted for arrest of spermatogenesis, missing generations and SCO. Data are presented as percentage of stages and defective tubules in the whole testis slides, and represent means ± SD. Statistical analysis was performed by one-way ANOVA but revealed no significant differences between *Slc10a6* wt and ko mice.

fertility highly depend on steroid hormone regulation and there is evidence that sulfated steroids participate in this process [8,19,20]. Considering our current knowledge about SOAT/Soat, we assume that this carrier fulfills a functional role in the local supply of germ cells with sulfated steroids, which then may be involved in the regulation of spermatogenesis. Although the *Slc10a6*$^{-/-}$ ko mice proved to be fertile in mating experiments, we closer analyzed sperm motility and morphology of *Slc10a6* ko mice compared to wt mice of the same age and same state of development. We used computer-assisted sperm analysis (CASA) by which sperm motility can be analyzed in a standardized way [21]. Although CASA cannot predict fertility, it can provide important information concerning the quality of sperm [22]. Because different CASA systems use different algorithms and no reference values are present for mouse sperm, the obtained values are difficult to compare with other studies [23]. However, this is less relevant, because the present study only focused on the comparison between the *Slc10a6* ko and wt mice. The semen analysis showed no significant differences in sperm number, morphology or motility parameters. Merely a tendency toward poorer sperm quality of *Slc10a6*$^{-/-}$ ko mice was recognized. Therefore, we had a closer look on the spermatogenesis of the

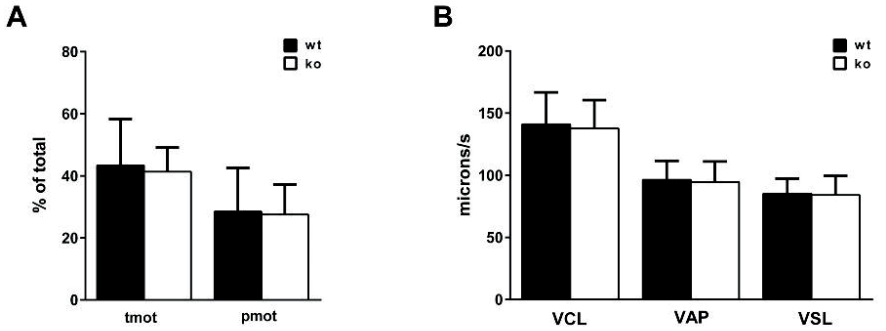

C

Morphology parameters	wt		ko	
	mean (% of total)	SD	mean (% of total)	SD
Abnormal heads (AH)	18.00	6.44	30.00	12.98
Abnormal acrosomes (AA)	0.00	0.00	0.00	0.00
Normal heads (NH)	25.20	5.50	18.40	7.09
Detached heads (DH)	4.60	2.97	10.00	6.93
Abnormal midpieces (AM)	35.20	24.06	23.80	13.31
Bent midpieces (BM)	7.60	4.39	15.60	4.88
Bent tails (BT)	2.40	1.14	3.20	1.64
Coiled tails (CT)	1.20	1.10	3.00	2.12
Premature germ cells (PGC)	1.80	1.48	3.60	1.52
Proximal cytoplasmic droplets (PD)	1.40	1.14	2.00	2.24
Distal cytoplasmic droplets (DD)	16.40	14.38	9.00	5.81

Fig. 5. CASA and sperm morphology.
(**A**) Motility of caudal sperm suspensions was assessed by CASA and revealed no differences in the total motility (tmot) and progressive motility (pmot) between the *Slc10a6* ko and wt mice. (**B**) The sperm motility parameters VCL (curvilinear velocity), VAP (average path velocity), and VSL (straight-line velocity) were specified and showed no significant differences. (**C**) Sperm morphology was analyzed for abnormal heads (AH), normal heads (NH), abnormal acrosomes (AA), detached heads (DH), abnormal midpieces (AM), bent midpieces (BM), bent tails (BT), coiled tails (CT) and premature germ cells (PGC). Furthermore, proximal cytoplasmic droplets (PD) and distal cytoplasmic droplets (DD) were determined. Data represent means ± SD (n = 5 for each genotype) and were statistically analyzed by one-way ANOVA.

Slc10a6$^{-/-}$ ko mice and performed histomorphological evaluation of the testes of *Slc10a6* ko and wt mice, including staging of spermatogenesis. In normal unaffected testicular tissue, the occurrence of specific stages of spermatogenesis gives evidence for the length of the seminiferous epithelium cycle (for review see [15]). Based on our data, in respect of the occurrence of the stages V, VIII, and XII, there were no differences between the *Slc10a6* wt and ko mice. However, frequency of seminiferous tubules with impaired spermatogenesis, in particular those with missing generations seemed to be increased, but without reaching the level of significance. Therefore, *Slc10a6* gene knockout seems not to significantly impair spermatogenesis per se. However, it has to be noted that impairment of spermatogenesis is a multifactorial problem [24] and only in few cases depends on single gene mutation [25]. For example, knockout of the *gap junction protein alpha 1 (Gja1)* gene coding for connexin43 (CX43) results in direct breakdown of spermatogenesis with an arrest at the level of spermatogonia and/or SCO [26,27]. CX43 plays a pivotal role in Sertoli cells for regulation of the blood-testis barrier dynamics and so has a more fundamental role for spermatogenesis (see [28] for review). In contrast, Soat could have a more regulatory function in the testis and so *Slc10a6* knockout might be more easily compensated, e.g. by upregulation of another steroid sulfate carrier from the OATP carrier family [7]. Such a compensatory upregulation is known from other transporter knockout mice. As an example, upregulation of the organic cation transporter OCT3 (which has transport activity for serotonin) was described in certain brain regions of *Slc6a4*$^{-/-}$ knockout mice, deficient for the specific serotonin transporter SERT [29,30]. On this background, further studies are needed to compare the gene expression pattern of the *Slc10a6* ko mice with their wt controls.

In order to investigate the role of Soat for steroid sulfate transport in the mouse in a more general way, steroid profiling was performed on serum samples from male and female *Slc10a6* ko and wt mice. LC–MS/MS was applied to analyze 12 sulfo-conjugated steroids and GC–MS/MS was used for determination of 9 un-conjugated steroids, as reported previously from our group [17,18]. However, only CS, T and corticosterone could be detected in quantifiable amounts in all serum samples, whereas the other steroids were below the limit of quantification or even undetectable in the mouse serum. Corticosterone was the most abundant un-conjugated steroid with values ranging from 7 to 200 ng/ml. Testosterone was the dominant androgen, found in the male mice with values of 0.2–8.9 ng/ml. The levels of both steroids were within the range of previous studies [31–34], but showed no significant differences between the *Slc10a6* ko and wt mice. In contrast, CS was significantly increased in the serum of the male *Slc10a6*$^{-/-}$ mice compared to the *Slc10a6*$^{+/+}$ mice, but showed comparable values in the female mice. CS is an important component of spermatozoa [35] and is considered to act as plasma membrane stabilizer and potent inhibitor of the sperm acrosomal proteinase acrosin [36]. It was hypothesized that cleavage of the sperm-associated CS occurs within the female reproductive tract. Here, it might be important for sperm capacitation and fertilization [37]. As SOAT/Soat was localized in the Golgi compartment of spermatozytes [5,9] as well as in the plasma membrane of

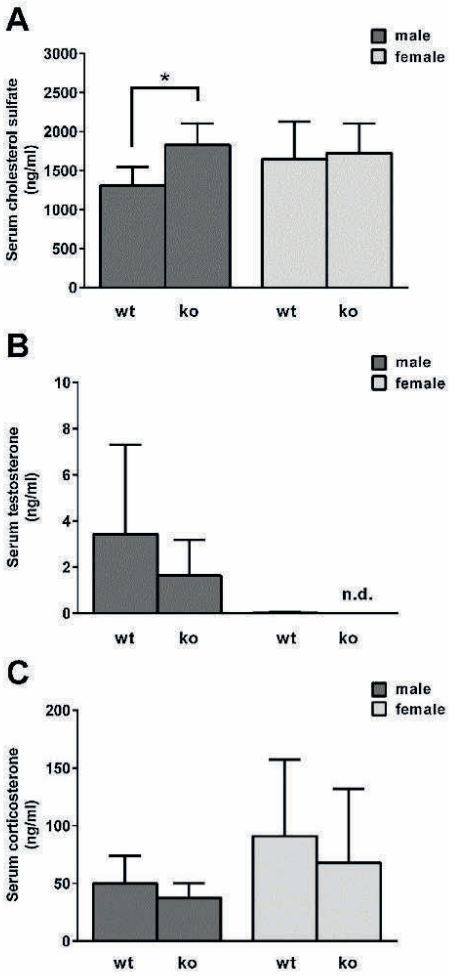

Fig. 6. Levels of cholesterol sulfate, testosterone, and corticosterone in the serum of *Slc10a6* ko and wt mice.
(**A**) From the group of steroid sulfates only CS could be quantified for all samples and was present in the mouse serum at quite high concentrations of 942–2559 ng/ml. In the case of unconjugated steroids, only T (**B**) and corticosterone (**C**) levels could be quantified in the mouse serum for all samples, but did not show any significant differences between the *Slc10a6* ko and wt mice. Age of the mice with n = 8 per group: male wt 21–31 weeks, male ko 17–30 weeks, female wt 26–31 weeks, female ko 11–30 weeks. *Significantly different from wt mice with $p < 0.05$ following one-way ANOVA.

round spermatids (Fig. 2), this carrier might be involved in the uptake and accumulation of CS in Golgi vesicles, which later form the acrosomal cap. However, to support this hypothesis it has to be demonstrated that SOAT/Soat indeed can transport CS in a similar manner as other sulfated steroids, what could not be achieved in the present study. Apart from the testis, CS is of significant importance in the skin, which acquires sulfated steroids via the sulfatase pathway after carrier-mediated import [38,39]. Soat was previously localized in the epidermis by immunohistochemistry and might be involved in this process [9]. Interestingly, patients with steroid sulfatase deficiency causing recessive X-linked ichthyosis (RXLI) show scales on their skin, caused by high concentrations of non-cleaved CS, and elevated levels of plasma CS [40,41]. It can be supposed that abolished Soat transport of CS in the skin may cause elevated plasma CS levels in a similar manner. Therefore, it will be interesting to further analyze the skin of the *Slc10a6* ko mice, what was out of the scope of the present study.

In conclusion: SOAT/Soat is a specific steroid sulfate carrier with high expression in endocrine active tissues and was supposed to be important for male fertility. To clarify this role in vivo we established an *Slc10a6* ko mouse model and analyzed its reproductive ability, spermatogenesis and steroid profile. Although the *Slc10a6*$^{-/-}$ mice showed normal reproduction and spermatogenesis when compared with *Slc10a6*$^{+/+}$ wt controls, the male *Slc10a6* ko mice revealed elevated serum levels of CS. This could be a relevant finding for the role of SOAT/Soat even in non-reproductive organs, e.g. the skin and lung, and needs further investigation.

Acknowledgements

This study was supported by the Deutsche Forschungsgemeinschaft (DFG) Research Group FOR1369 "Sulfated Steroids in Reproduction" with grants to JG (GE1921/4-1/2) and DF (FI1927/1-2). The authors thank Matthias Holtemeyer, Bärbel Fühler, Regina Leidolf, Alexandra Hax, Amy Gonzales, and Benjamin Morpurgo for their technical help and assistance.

Appendix A. Supplementary data

Supplementary data associated with this article can be found, in the online version, at http://dx.doi.org/10.1016/j.jsbmb.2017.07.019.

References

[1] J. Geyer, T. Wilke, E. Petzinger, The solute carrier family SLC10: more than a family of bile acid transporters regarding function and phylogenetic relationships, Naunyn Schmiedebergs Arch. Pharmacol. 372 (2006) 413–431.
[2] J. Geyer, J.R. Godoy, E. Petzinger, Identification of a sodium-dependent organic anion transporter from rat adrenal gland, Biochem. Biophys. Res. Commun. 316 (2004) 300–306.
[3] J. Geyer, B. Döring, K. Meerkamp, B. Ugele, N. Bakhiya, C.F. Fernandes, J.R. Godoy, H.R. Glatt, E. Petzinger, Cloning and functional characterization of human sodium-dependent organic anion transporter (SLC10A6), J. Biol. Chem. 282 (2007) 19728–19741.
[4] C.E. Galuska, M.F. Hartmann, A. Sánchez-Guijo, K. Bakhaus, J. Geyer, G. Schuler, K.P. Zimmer, S.A. Wudy, Profiling intact steroid sulfates and unconjugated steroids in biological fluids by liquid chromatography-tandem mass spectrometry (LC-MS-MS), Analyst 138 (2013) 3792–3801.
[5] D. Fietz, K. Bakhaus, B. Wapelhorst, G. Grosser, S. Günther, J. Alber, B. Döring, S. Kliesch, W. Weidner, C.E. Galuska, M.F. Hartmann, S.A. Wudy, M. Bergmann, J. Geyer, Membrane transporters for sulfated steroids in the human testis – Cellular localization, expression pattern and functional analysis, PLoS One 8 (5) (2013) e62638.
[6] H. Schweigmann, A. Sánchez-Guijo, B. Ugele, K. Hartmann, M.F. Hartmann, M. Bergmann, C. Pfarrer, B. Döring, S.A. Wudy, E. Petzinger, J. Geyer, G. Grosser, Transport of the placental estriol precursor 16α-hydroxy-dehydroepiandrosterone sulfate (16α-OH-DHEAS) by stably transfected OAT4-, SOAT-, and NTCP-HEK293 cells, J. Steroid Biochem. Mol. Biol. 143 (2014) 259–265.
[7] M. Roth, A. Obaidat, B. Hagenbuch, OATPs, OATs and OCTs: the organic anion and cation transporters of the SLCO and SLC22A gene superfamilies, Br. J. Pharmacol. 165 (2012) 1260–1287.
[8] J. Geyer, K. Bakhaus, R. Bernhardt, C. Blaschka, Y. Dezhkam, D. Fietz, G. Grosser, K. Hartmann, M.F. Hartmann, J. Neunzig, D. Papadopoulos, A. Sánchez-Guijo, G. Scheiner-Bobis, G. Schuler, M. Shihan, C. Wrenzycki, S.A. Wudy, M. Bergmann, The role of sulfated steroid hormones in reproductive processes. Concept and review paper of the DFG research group FOR 1369 Sulfated Steroids in Reproduction, J. Steroid Biochem. Mol. Biol. 172 (2017) 207–221.
[9] G. Grosser, D. Fietz, S. Günther, K. Bakhaus, H. Schweigmann, B. Ugele, R. Brehm, E. Petzinger, M. Bergmann, J. Geyer, Cloning and functional characterization of the mouse sodium-dependent organic anion transporter Soat (Slc10a6), J. Steroid Biochem. Mol. Biol. 138 (2013) 90–99.
[10] M.J. Reed, A. Purohit, L.W. Woo, S.P. Newman, B.V. Potter, Steroid sulfatase: molecular biology, regulation, and inhibition, Endocr. Rev. 26 (2005) 171–202.
[11] F. Labrie, All sex steroids are made intracellularly in peripheral tissues by the mechanisms of intracrinology after menopause, J. Steroid Biochem. Mol. Biol. 145 (2015) 133–138.
[12] J.W. Müller, L.C. Gilligan, J. Idkowiak, W. Arlt, P.A. Foster, The regulation of steroid action by sulfation and desulfation, Endocr. Rev. 36 (2015) 526–563.

[13] G.T. Wong, Speed congenics: applications for transgenic and knock-out mouse strains, Neuropeptides 36 (2002) 230–236.
[14] P. Markel, P. Shu, C. Ebeling, G.A. Carlson, D.L. Nagle, J.S. Smutko, K.J. Moore, Theoretical and empirical issues for marker-assisted breeding of congenic mouse strains, Nat. Genet. 17 (1997) 280–284.
[15] L.D. Russell, R.A. Ettlin, A.P. Sinha Hikim, E.D. Clegg, Staging for laboratory species, in: L.D. Russell (Ed.), Histological and Histopathological Evaluation of the Testis, 1st ed., Cache River Press, Clearwater, 1990, pp. 119–161.
[16] C.C. Love, R.M. Kenney, The relationship of increased susceptibility of sperm DNA to denaturation and fertility in the stallion, Theriogenology 50 (1998) 955–972.
[17] A. Sánchez-Guijo, V. Oji, M.F. Hartmann, H. Traupe, S.A. Wudy, Simultaneous quantification of cholesterol sulfate, androgen sulfates, and progestagen sulfates in human serum by LC-MS/MS, J. Lipid Res. 56 (2015) 1843–1851.
[18] A. Sánchez-Guijo, M.F. Hartmann, S.A. Wudy, Introduction to gas chromatography-mass spectrometry, Methods Mol. Biol. 1065 (2013) 27–44.
[19] A. Ruokonen, T. Laatikainen, E.A. Laitinen, R. Vihko, Free and sulfate-conjugated neutral steroids in human testis tissue, Biochemistry 11 (1972) 1411–1416.
[20] A.H. Payne, R.B. Jaffe, Androgen formation from pregnenolone sulfate by fetal, neonatal, prepubertal and adult human testes, J. Clin. Endocrinol. Metab. 40 (1975) 102–107.
[21] J.M. Gallardo Bolaños, A. Miró Morán, C.M. Balao da Silva, A. Morillo Rodríguez, M. Plaza Dávila, I.M. Aparicio, J.A. Tapia, C. Ortega Ferrusola, F.J. Peña, Autophagy and apoptosis have a role in the survival or death of stallion spermatozoa during conservation in refrigeration, PLoS One 7 (2012) e30688.
[22] R.P. Amann, D. Waberski, Computer-assisted sperm analysis (CASA): capabilities and potential developments, Theriogenology 17 (2014) 5-17.e1-3.
[23] J.C. Lu, Y.F. Huang, N.Q. Lü, Computer-aided sperm analysis: past, present and future, Andrologia 46 (2014) 329–338.
[24] H.J. Cooke, P.T. Saunders, Mouse models of male infertility, Nat. Rev. Genet. 3 (2002) 790–801.
[25] A. Ferlin, F. Raicu, V. Gatta, D. Zuccharell, G. Palka, C. Foresta, Male infertility: role of genetic background, Reprod. Biomed. Online 14 (2007) 734–745.
[26] R. Brehm, M. Zeiler, C. Rüttinger, K. Herde, M. Kibschull, E. Winterhager, K. Willecke, F. Guillou, C. Lécureuil, K. Steger, L. Konrad, K. Biermann, K. Failing, M. Bergmann, A sertoli-cell specific knockout of connexin43 prevents initiation of spermatogenesis, Am. J. Pathol. 17 (2007) 19–31.
[27] S. Sridharan, R. Brehm, M. Bergmann, P.S. Cooke, Role of Connexin 43 in Sertoli cell of the testis, Ann. N. Y. Acad. Sci. 1120 (2007) 131–143.
[28] J. Gerber, J. Heinrich, R. Brehm, Blood-testis barrier and Sertoli cell function: lessons from SCCx43KO mice, Reproduction 151 (2016) R15–27.
[29] J.J. Chen, Z. Li, H. Pan, D.L. Murphy, H. Tamir, H. Koepsell, M.D. Gershon, Maintenance of serotonin in the intestinal mucosa and ganglia of mice that lack the high-affinity serotonin transporter: abnormal intestinal motility and the expression of cation transporters, J. Neurosci. 21 (2001) 6348–6361.
[30] A. Schmitt, R. Mössner, A. Gossmann, I.G. Fischer, V. Gorboulev, D.L. Murphy, H. Koepsell, K.P. Lesch, Organic cation transporter capable of transporting serotonin is up-regulated in serotonin transporter-deficient mice, J. Neurosci. Res. 71 (2003) 701–709.
[31] K.M. McNamara, D.T. Harwood, U. Simanainen, K.A. Walters, M. Jimenez, D.J. Handelsman, Measurement of sex steroids in murine blood and reproductive tissues by liquid chromatography-tandem mass spectrometry, J. Steroid Biochem. Mol. Biol. 121 (2010) 611–618.
[32] Y. Weng, F. Xie, L. Xu, D. Zagorevski, D.C. Spink, X. Ding, Analysis of testosterone and dihydrotestosterone in mouse tissues by liquid chromatography-electrospray ionization-tandem mass spectrometry, Anal. Biochem. 402 (2010) 121–128.
[33] H. Li, X. Liu, Y. Poh, L. Wu, Q.G. Zhou, B.C. Cai, Rapid determination of corticosterone in mouse plasma by ultra fast liquid chromatography-tandem mass spectrometry, Biomed. Chromatogr. 28 (2013) 1860–1863.
[34] M.E. Nilsson, L. Vandenput, Å. Tivesten, A.K. Norlén, M.K. Lagerquist, S.H. Windahl, A.E. Börjesson, H.H. Farman, M. Poutanen, A. Benrick, M. Maliqueo, E. Stener-Victorin, H. Ryberg, C. Ohlsson, Measurement of a comprehensive sex steroid profile in rodent serum by high-sensitive gas chromatography-tandem mass spectrometry, Endocrinololgy 156 (2015) 2492–2502.
[35] G. Lalumière, G. Bleau, A. Chapdelaine, K.D. Roberts, Cholesteryl sulfate and sterol sulfatase in the human reproductive tract, Steroids 27 (1976) 247–260.
[36] P.J. Burck, R.E. Zimmermann, The inhibition of acrosine by sterol sulphates, J. Reprod. Fertil. 58 (1980) 121–125.
[37] J. Langlais, M. Zollinger, L. Plante, A. Chapdelaine, G. Bleau, K.D. Roberts, Localization of cholesteryl sulfate in human spermatozoa in support of a hypothesis for the mechanism of capacitation, Proc. Natl. Acad. Sci. U. S. A. 78 (1981) 7266–7270.
[38] F. Labrie, V. Luu-The, C. Labrie, G. Pelletier, M. El-Alfy, Intracrinology and the skin, Horm. Res. 54 (2000) 218–229.
[39] C.C. Zouboulis, Human skin: an independent peripheral endocrine organ, Horm. Res. 54 (2000) 230–242.
[40] C.H. Shackleton, S. Reid, Dignosis of recessive X-linked ichthyosis: quantitative HPLC/mass spectrometric analysis of plasma for cholesterol sulfate, Clin. Chem 35 (1989) 1906–1910.
[41] A. Sánchez-Guijo, V. Oji, M.F. Hartmann, H.C. Schuppe, H. Traupe, S.A. Wudy, High levels of oxysterol sulfates in serum of patients with steroid sulfatase deficiency, J. Lipid Res. 56 (2015) 403–412.

11. Anhang – Publikationen

10. K. Bakhaus, D. Fietz, S. Kliesch, W. Weidner, M. Bergmann, J. Geyer. J Steroid Biochem Mol Biol 2017 Sep 23. pii: S0960-0760(17)30265-0. doi: 10.1016/j.jsbmb.2017.09.017

Journal of Steroid Biochemistry and Molecular Biology xxx (xxxx) xxx–xxx

Contents lists available at ScienceDirect

Journal of Steroid Biochemistry and Molecular Biology

journal homepage: www.elsevier.com/locate/jsbmb

The polymorphism L204F affects transport and membrane expression of the sodium-dependent organic anion transporter SOAT (SLC10A6)

Katharina Bakhaus[a], Daniela Fietz[b], Sabine Kliesch[c], Wolfgang Weidner[d], Martin Bergmann[b], Joachim Geyer[a,*]

[a] Institute of Pharmacology and Toxicology, Justus Liebig University Giessen, Germany
[b] Department of Veterinary Anatomy, Histology and Embryology, Justus Liebig University Giessen, Germany
[c] Department of Clinical Andrology, Centre for Reproductive Medicine and Andrology, University Hospital Münster, Germany
[d] Clinic for Urology, Pediatric Urology and Andrology, Justus Liebig University Giessen, Germany

ARTICLE INFO

Keywords:
SOAT
SLC10A6
Polymorphism
Sulfated steroids
Reproduction
Transport
Hypospermatogenesis

ABSTRACT

Sodium-dependent organic anion transporter (SOAT) represents a membrane transporter specific for sulfated steroid hormones, which are supposed to participate in the regulation of reproductive processes. In man, SOAT shows predominant mRNA expression in the testis and here was localized to primary spermatocytes. SOAT mRNA expression is significantly downregulated in different disorders of spermatogenesis, including hypospermatogenesis. The resulting decline of SOAT-mediated transport of sulfated steroids may participate in the impairment of functional spermatogenesis. Apart from downregulation of SOAT mRNA expression, genetic polymorphisms affecting the transport function of SOAT may have the same negative effect on spermatogenesis. Therefore, in the present study we searched for functionally relevant SOAT polymorphisms, aiming to comparatively analyze their occurrence in patients with impaired spermatogenesis vs. patients with intact spermatogenesis. We found that the SOAT polymorphism L204F showed a significantly reduced transport function for DHEAS when expressed in HEK293 cells. Although the K_m value was identical with that of the SOAT wildtype, the V_{max} value dramatically declined for the SOAT-L204F variant (942.5 vs. 313.6 pmol × mg protein^{-1} × min^{-1}). Although the same amount of total SOAT-L204F protein was detected in transfected HEK293 cells compared to the SOAT wildtype, plasma membrane expression was significantly reduced, which points to a plasma membrane sorting defect of the SOAT-L204F variant. Groups of 20 subjects with normal spermatogenesis and 26 subjects with hypospermatogenesis were genotyped for this polymorphism. Both groups showed nearly identical distributions of the SOAT-L204F polymorphism (~10% heterozygous and ~5% homozygous), indicating that this polymorphism seems not be causative for hypospermatogenesis.

1. Introduction

Male reproduction, and spermatogenesis in particular, is largely regulated by steroid hormones acting on estrogen and androgen receptors which are widespread in the testis [1–3]. There is increasing evidence that, apart from free steroid hormones, sulfated steroids such as pregnenolone sulfate (PREGS), dehydroepiandrosterone sulfate (DHEAS) and testosterone sulfate also participate in this regulation [4,5]. However, as these compounds are negatively charged they cannot simply intrude into all cell types of the testis by diffusion. Instead, membrane carriers capable of transporting sulfated steroid hormones through the plasma membrane effect cell-type specific import and accumulation of steroid sulfates depending on their expression pattern and transport characteristics [6]. Intracellularly, sulfated steroid hormones can be de-conjugated by the steroid sulfatase (STS) and the resulting free steroids then participate in the regulation via classical steroid receptors [7]. This process is described as sulfatase pathway or intracrine steroid release [8,9].

Ten years ago, we cloned and described a novel specific steroid sulfate carrier, sodium-dependent organic anion transporter (SOAT), which is predominantly expressed in the testis and is supposed to participate in the regulation of spermatogenesis [10,11]. SOAT showed sodium-dependent transport activity for several steroid sulfates, including PREGS, DHEAS, 16alpha-OH-DHEAS, estrone-3-sulfate,

Abbreviations: DHEAS, dehydroepiandrosterone sulfate; PREGS, pregnenolone sulfate; SOAT, sodium-dependent organic anion transporter; STS, steroid sulfatase; HEK293, human embryonic kidney 293 cells; MSR, macrophage scavenger receptor

* Corresponding author at: Institute of Pharmacology and Toxicology, Biomedical Research Center Seltersberg (BFS), Schubertstr. 81, 35392, Giessen, Germany.
E-mail address: Joachim.M.Geyer@vetmed.uni-giessen.de (J. Geyer).

http://dx.doi.org/10.1016/j.jsbmb.2017.09.017
Received 13 February 2017; Received in revised form 29 August 2017; Accepted 21 September 2017

Please cite this article as: Bakhaus, K., Journal of Steroid Biochemistry and Molecular Biology (2017), http://dx.doi.org/10.1016/j.jsbmb.2017.09.017

estradiol-3-sulfate, and androstenediol-3-sulfate [10–13]. As other steroid compounds such as bile acids or free steroid hormones are not transported by SOAT, this carrier is regarded as a highly specialized carrier for sulfated steroid hormones [5]. In a recent comprehensive study on SOAT expression in the human testis, we found specific expression of SOAT in various germ cell stages by immunohistochemistry, but not in Sertoli or Leydig cells. Germ cell stages being positive for SOAT included zygotene primary spermatocytes of stage V, pachytene spermatocytes of all stages (I–V), secondary spermatocytes of stage VI, and round spermatids (step 1 and step 2) of stages I and II. The staining of primary spermatocytes, representing germ cells within the first meiotic division, was most prominent in these studies [11]. Interestingly, quantitative mRNA expression analysis of testicular biopsies from patients with hypospermatogenesis, which is characterized by quantitatively reduced but qualitatively preserved spermatogenesis (for review see Bergmann and Kliesch [14]), revealed significantly lower SOAT expression compared to biopsies showing normal spermatogenesis. Furthermore, SOAT expression was significantly lower or even absent in more severe disorders of spermatogenesis including arrest at the level of spermatocytes, spermatogonia, or even a complete loss of germ cells (Sertoli cell-only syndrome, SCO) [11]. Although SOAT downregulation does not prove causality for impaired spermatogenesis, the loss of SOAT-mediated transport of sulfated steroids may participate in the impairment of spermatogenesis. Apart from downregulation of SOAT mRNA expression, genetic polymorphisms affecting the transport function of SOAT may have the same negative effect on spermatogenesis. Therefore, in the present study we searched for functionally relevant SOAT polymorphisms, aiming to comparatively analyze their occurrence in patients with impaired spermatogenesis vs. patients with intact spermatogenesis. We found that the SOAT polymorphism L204F significantly affects SOAT transport function by hindering proper membrane expression. However, as this polymorphism was found in patients with impaired as well as in patients with normal spermatogenesis, the L204F variant does not seem to be causative for hypospermatogenesis.

2. Material and methods

2.1. Materials

All of the chemicals, unless otherwise stated, were obtained from Sigma-Aldrich. [^{3}H]DHEAS was purchased from PerkinElmer Life Sciences (Waltham, MA, USA).

2.2. Generation of polymorphic SOAT constructs

The QuikChange site-directed mutagenesis kit (Agilent Technologies) was used to generate the polymorphic SOAT constructs. Mutagenesis was performed from 50 ng template DNA set up with 5 µl 10x reaction buffer, 2.5 µl forward primer (125 ng), 2.5 µl reverse primer (125 ng), 1 µl dNTP mix, 1 µl Pfu Turbo Polymerase (2.5 U/µl), and ddH_2O to a final volume of 51 µl. Mutagenesis primers were obtained from Eurofins MWG Operon (Ebersberg, Germany) and are listed in Table 1. PCR conditions were optimized as follows: 1 × 95 °C for 2 min, 16 × (95 °C for 30 s, 55 °C for 1 min and 70 °C for 9 min) and 70 °C for 10 min for template amplification. PCR products were incubated with *Dpn*I for 1 h at 37 °C to eliminate template DNA and transformed into XL1-Blue *E. coli* super-competent cells. Correct constructs were selected based on DNA sequencing and were used for transfection into GripTite MSR293 cells (Invitrogen, transient transfection) or Flp-In T-Rex HEK293 cells (Invitrogen, stable transfection). The SOAT-V5-His-pcDNA5 construct (previously described by Fietz et al. [11]), was used as a template to generate the SOAT-S6F-V5-His, SOAT-I114V-V5-His, SOAT-R185T-V5-His, SOAT-I196T-V5-His, SOAT-V199I-V5-His, and SOAT-L204F-V5-His variants. For SOAT-L204F an additional untagged construct based on the SOAT-pcDNA5 construct (previously described by Geyer et al. [10]) was established.

Table 1
Primer sequences.

Method	Primer name	Sequence 5′ → 3′
SDM	SOAT-S6F-MGF	gccaattgt**tT**cagTagctcagcctgccctgc
	SOAT-S6F-MGR	gcagggcaggctgagctAct**gA**acaattggc
	SOAT-I114V-MGF	gggggcaccatctctaac**Gtt**ttcaccttc
	SOAT-I114V-MGR	gaaggtgaa**aaC**gttagagatggtgccccc
	SOAT-R185T-MGF	ggcctttggtgtctatgtgaatt**acaCat**ggccaaaacaatcc
	SOAT-R185T-MGR	ggattgtttggcc**atGt**gtaattcacatagacaccaaaggcc
	SOAT-I196T-MGF	cattctcaag**aCt**ggggcgttgttggtgggg
	SOAT-I196T-MGR	ccccaccaacaacggcccc**aGt**cttgagaatg
	SOAT-I199V-MGF	agattggggcc**Att**gttggtggggtcctcc
	SOAT-I199V-MGR	ggaggaccccaccaac**aaT**ggcccc aatct
	SOAT-L204F-MGF	tggtggggtcttcc**Ttc**tggtggtcgc
	SOAT-L204F-MGR	gcgaccaccagaag**gaA**gaccccacca
G	SOAT-F	cctgtgtgcctgaccattcct
	SOAT-R	ccaggaccacaccagcaa
	Beta-actin-F	ttccttcctgggcatggagt
	Beta-actin-R	tacaggtctttgcggatgtc

SDM: Site-directed mutagenesis.
G: Genotyping. All SOAT primer sequences are related to GenBank accession number NM_197965. Affected triplets are highlighted in bold letters and each mutated nucleotide is marked in capitals.

2.3. Transient transfection of GripTite MSR293 cells

SOAT-V5-His-pcDNA5 variants were transiently transfected into GripTite MSR293 cells using Lipofectamine 2000 (Invitrogen) according to the manufacturer's specifications. GripTite MSR293 cells represent genetically engineered human embryonic kidney (HEK293) cells expressing the human macrophage scavenger receptor (MSR) enabling stronger adherence to standard tissue culture plates compared to the parental HEK293 cells. This is of advantage for transient transfection experiments and downstream assays due to repeated manipulations of the cells. Briefly, the cells were cultured on 24-well plates in D-MEM medium (Life Technologies) supplemented with 10% fetal calf serum (Sigma), L-glutamine (4 mM, PAA) and MEM non-essential amino acids (0.1 mM, PAA) (further referred to as standard MSR293 medium) at 37 °C, 10% CO_2, and 95% humidity. For transfection, 1 µg plasmid DNA and 2 µl Lipofectamine 2000 each were mixed with 50 µl Opti-MEM (Invitrogen) and incubated for 5 min before they were combined and used for transfection of GripTite MSR293 cells. After 8 h, the medium was changed to standard MSR293 medium and the cells were further cultivated over 48 h. Then transport experiments were performed with [^{3}H]DHEAS.

2.4. Stable transfection of HEK293 cells

Functional characterization of the SOAT-L204F polymorphism was performed after stable transfection of the SOAT-L204F-pcDNA5/FRT/TO construct into the recombinant human cell line Flp-In T-REx HEK293 as reported before for the SOAT wildtype [10]. These cells contain a single, stably integrated Flp recombinase target (FRT) site, which is maintained by selection for zeocin resistance and ensures high level gene expression from the target-integrated Flp-In expression vector. Stable integration of the transgene and the tetracycline (tet) repressor was maintained in selective media containing 150 µg/ml hygromycin and 50 µg/ml blasticidin, and allowed to induce SOAT expression by tetracycline treatment. The mRNA expression of SOAT-L204F was approved by real-time PCR after tetracycline (1 µg/ml) treatment. SOAT-WT-HEK293 and SOAT-L204F-HEK293 cells were maintained in D-MEM (Life Technologies)/Ham's F12 medium (Gibco) supplemented with 10% fetal calf serum (Sigma), L-glutamine (4 mM, PAA), penicillin (100 U/ml, Gibco), and streptomycin (100 µg/ml,

Gibco) (further referred to as standard HEK293 medium) at 37 °C, 5% CO_2, and 95% humidity.

2.5. Transport studies in SOAT-transfected HEK293 cells

Transport studies were performed in 24-well plates using transiently transfected GripTite MSR293 cells (transport screening) or stably transfected T-REx HEK293 cells (transport kinetic measurements) as described before [10,11]. In each well, 1.25×10^5 cells were seeded and cultured with the respective standard medium for 48 h (transient transfection) or 72 h (stable transfection). T-REx HEK293 cells were incubated with tetracycline (1 µg/ml) to induce SOAT expression. All transport studies were performed in the presence of sodium as well as in the absence of sodium (negative control). In the sodium-free transport buffer, sodium chloride was replaced by equimolar concentrations of choline chloride. Empty vector transfected cells were used as an additional control. Before starting the transport studies, the cells were washed three times with phosphate-buffered saline (PBS, 137 mM NaCl, 2.7 mM KCl, 1.5 mM KH_2PO_4, 7.3 mM Na_2HPO_4, pH 7.4, 37 °C). Then, the cells were pre-incubated with a transport buffer (142.9 mM NaCl, 4.7 mM KCl, 1.2 mM $MgSO_4 \times 7H_2O$, 1.2 mM KH_2PO_4, 1.8 mM $CaCl_2$, and 20 mM HEPES, adjusted to pH 7.4 with KOH, 37 °C) for 15 min. Transport studies were performed by incubating the cells with 250 µl transport buffer containing a [^{3}H]DHEAS/DHEAS mixture for 10 min (transport screening) or 1 min (kinetic studies) at 37 °C. Uptake studies were stopped by removing the transport buffer and washing the cells five times with ice-cold PBS. Afterwards, the cells were lysed in 1 N NaOH with 0.1% SDS and the cell-associated radioactivity was measured by liquid scintillation counting as described before [10]. For normalization of the transport data, protein content was calculated according to Lowry using aliquots of the lysed cells with bovine serum albumin as a standard [15].

2.6. Immunofluorescence detection of SOAT expression in HEK293 cells

For immunofluorescence microscopy, two different antibodies were used. For detection of the intracellular SOAT C-terminus, the $SOAT_{311–377}$ antibody (Eurogentec) was used as previously described [11]. Therefore, cells were seeded on poly-L-lysine coated glass coverslips in 24-well plates with a density of 1×10^5 cells per well. SOAT expression was induced by tet treatment (1 µg/ml). After 72 h, the cell medium was removed and the cells were washed three times with PBS for 5 min. Then the cells were fixed with 2% paraformaldehyde in PBS for 15 min at room temperature and subsequently permeabilized for 5 min in PBS buffer supplemented with 0.2% Triton X-100 and 20 mM glycine. After washing the cells with PBS three times for 5 min, they were placed in blocking solution containing 20 mM glycine in PBS and 4% goat serum for 1 h. Afterwards, the cells were incubated with the $SOAT_{311–377}$ antibody at a dilution of 1:100 in blocking solution for 1 h. The cells were washed three times with PBS followed by incubation with the Alexa Fluor 488-labeled goat anti-rabbit IgG secondary antibody (Invitrogen) at 1:800 dilution in blocking solution for 1 h. After a final washing procedure, the cells were covered with a DAPI/methanol solution containing 1 µg/ml DAPI (4′,6-diamidino-2-phenylindole dihydrochloride, Life Technologies) and incubated for 1 min. Then, the cells were washed with methanol, air-dried and mounted on slides with ProLong Gold Antifade Reagent (Life Technologies). To detect the extracellular N-terminus of SOAT, the $SOAT_{2–17}$ antibody (Eurogentec) was used as previously described by Geyer et al. [10]. For this purpose, the immunofluorescence protocol was changed as follows: the non-fixed cells were incubated with the $SOAT_{2–17}$ antibody (1:10 dilution) for 1 h, washed three times with PBS and incubated with Alexa Fluor 488-labeled goat anti-rabbit IgG secondary antibody (Invitrogen) at 1:800 dilution for 1 h. After additional washing steps with PBS, the cells were counterstained with DAPI/PBS (1:5000, 5 min), air-dried and mounted on slides using ProLong Gold Antifade Reagent (Life Technologies). Fluorescence imaging was performed on a Leica DM5500B microscope (Bensheim, Germany). Captured images were analyzed with the Leica Fluorescence Workstation software LAS AF 6000.

2.7. Photometric determination of the SOAT immunofluorescence signal

For photometric measurement of the SOAT-directed immunofluorescence, the same procedure as outlined above for the $SOAT_{2–17}$ antibody was performed with the following modifications: after a final washing with PBS, the cells were lysed with water by three freeze-thaw cycles. 100 µl aliquots of the lysates then were analyzed in triplicate in the GloMax-Multi$^+$ detection system (Promega) at a wavelength of 520 nm. Additionally, the protein content was analyzed using the BCA protein assay kit (Novagen) and was used for normalization.

2.8. Western blot analysis

Proteins were extracted from SOAT-WT-HEK293 and SOAT-L204F-HEK293 cells as reported before [11]. Briefly, 400 µl ice-cold RIPA buffer (Sigma-Aldrich) mixed with protease inhibitor at a 1:100 dilution (Thermo Fisher Scientific) were added to the cells. After 15 min on ice, the cells were detached, mechanically destroyed, and left on ice for another 10 min. Then, the lysed cells were centrifuged for 15 min at 13.000 rpm and 4 °C. Afterwards, the samples were mixed with 4x Laemmli buffer containing 20% beta-mercaptoethanol and separated on a 10% SDS-PAGE over night at 50 V. The gel was blotted by semi-dry electroblotting on nitrocellulose membrane; protein transfer was controlled by placing the nitrocellulose membrane in Ponceau S for 5 min. After multiple washings with Tris-buffered saline TBS-T (137 mM NaCl, 10 mM Tris-HCl, pH 8.0, 0.05% Tween-20), the membrane was blocked for 1 h at room temperature under agitation in TBS-T with 5% dried non-fat milk (blocking solution). After removal of the blocking solution, the nitrocellulose membrane was incubated with the anti-$SOAT_{311–377}$ primary antibody in blocking solution at a 1:100 dilution for 1 h at room temperature. After washing with TBS-T, the membrane was incubated with the peroxidase-conjugated goat IgG fraction to rabbit IgG secondary antibody (MP Biomedicals) at a 1:5000 dilution, together with the Roti Mark Western-HRP-conjugate (1:5000 dilution, Carl Roth) for 1 h at room temperature. After washing with TBS-T, the nitrocellulose membrane was incubated with Roti Lumin 1 and Roti Lumin 2 (Carl Roth) at a ratio of 1:1 for 1 min and exposed to Hyperfilm ECL High Performance chemiluminescence film (GE Healthcare). Protein signals were further evaluated by densitometric analysis. For this purpose, the nitrocellulose membrane was incubated with Roti Lumin 1 and Roti Lumin 2 (Carl Roth) as described before. After 1 min the membrane was photographed by the Image Station 440CF (Kodak) and images were analyzed using Paintshop Pro Photo X2. The SOAT band pattern was marked and the mean density of the signal was determined. After subtracting the background density, the mean density was multiplied with the area of the band pattern. The signal strength of the SOAT-WT protein was set at 100% and the density of the SOAT-L204F protein was given as a percentage of SOAT-WT.

2.9. Quantitative real-time PCR of SOAT-transfected HEK293 cells

For quantitative analysis of SOAT expression in stably transfected SOAT-WT-HEK293 and SOAT-L204F-HEK293 cells, quantitative real-time PCR amplification was achieved with TaqMan Gene Expression Assays Hs01399354_m1 for SOAT (*SLC10A6*) and Hs02758991_g1 for human glyceraldehyde 3-phosphate dehydrogenase (GAPDH) as endogenous control (Thermo Fisher Scientific). For each specimen, triplicate determinations were performed using 3 µl of cDNA, 1 µl of the respective TaqMan Gene Expression Assay, 10 µl TaqMan Gene Expression Master Mix (Thermo Fisher Scientific) and ddH_2O to a final volume of 20 µl. Quantitative real-time PCR was performed on CFX96 Real-Time Cycler (Bio-Rad) under the following conditions: 1 × 95 °C

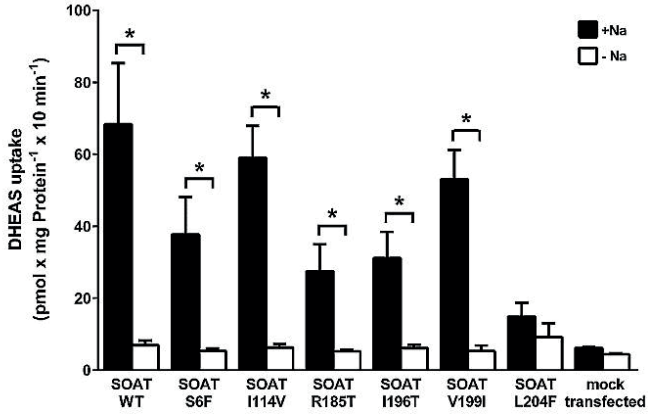

Fig. 1. Transport screening of the SOAT variants revealed impaired transport activity for SOAT L204F.
Transport experiments with the respective SOAT variants were performed with 1 µM [^{3}H]DHEAS in medium with (■) or without (□) sodium. Empty vector transfected cells (mock transfected) were used as control. Data represent means ± SD of two independent experiments, each with n = 4 determinations (total of n = 8). *Significantly higher transport activity in sodium vs. sodium-free transport buffer with $p < 0.0001$ (one way ANOVA with Bonferroni's post hoc multiple comparison test).

for 10 min and 45 × (95 °C for 15 s and 60 °C for 1 min). Relative gene expression was calculated by the $2^{-\Delta\Delta CT}$ method. Expression levels represent x-fold higher mRNA expression in SOAT-WT-HEK293 and SOAT-L204F-HEK293 cells after tetracycline induction compared with non-transfected Flp-In T-REx HEK293 cells.

2.10. Testicular tissue biopsies

Testis biopsies were obtained from patients attending the Centre of Reproductive Medicine and Andrology of the University Hospital in Muenster and the Department of Urology and Andrology of the University Hospital in Giessen. They were indicated according to Bergmann and Kliesch [14] because of obstructive azoospermia (re-fertilization procedure after vasectomy) and non-obstructive azoospermia. Surgery was performed after written informed consent under general anesthesia. The current study has been approved by the ethical review committee of the Medical Faculty of the Justus Liebig University Giessen (decision 187b/09).

2.11. Histological evaluation

In total, 46 human testicular biopsies from the biopsy repository of the Institute for Veterinary Anatomy, Histology and Embryology, Justus Liebig University Giessen were used for this study. The testis tissue was immersed in Bouin's fixative and embedded in paraffin. For the histological evaluation of spermatogenesis, 5 µm thick sections were cut, stained with hematoxylin and eosin and evaluated following the score count analysis according to Bergmann and Kliesch [14]. For analysis of the L204F genotype, 20 biopsies with normal spermatogenesis (nsp, score 10) and 26 samples with a quantitatively reduced, but qualitatively preserved spermatogenesis (hypospermatogenesis, hyp, score 1–10) were used.

2.12. Genotyping for the SOAT-L204F polymorphism from human testis biopsies

Testis biopsies were used to extract mRNA using the RNeasy FFPE kit (Qiagen) as recommended by the manufacturer, performing proteinase K treatment as suggested. The extracted mRNA was subsequently treated with RNase-free DNase I (Peqlab Biotechnology) in association with RNase-free incubation buffer 10x (Roche), RNase inhibitor (2000 u) and $MgCl_2$ solution (Applied Biosystems) for 25 min at 37 °C to digest genomic DNA. Then, cDNA was synthesized from 9 µl DNase-treated mRNA using 51 µl RT-mix with the following composition (Applied Biosystems): 6 µl GeneAmp 10x PCR Gold Buffer, 3 µl nucleotide mix (10 mM each), 12 µl $MgCl_2$ (25 mM), 3 µl random hexamer primers (50 µM), 3 µl RNase inhibitor (20 U/µl), 3 µl MultiScribe Reverse Transcriptase (50 U/µl) and 21 µl sterile ddH_2O. Negative controls were performed by omitting reverse transcriptase. For RT-PCR, 5 µl cDNA were mixed with 2.5 µl GeneAmp 10x PCR Gold Buffer, 2 µl $MgCl_2$ (25 mM), 1 µl forward and reverse primer (10 pmol/µl), 1 µl dNTP mix (10 mM each), 0.15 µl AmpliTaq GOLD polymerase and 12.35 µl sterile ddH_2O to a finale volume of 25 µl. Specific primers for human SOAT are located at positions 505–525 (forward) and 629–646 (reverse) of the SOAT open reading frame (ORF) (according to GenBank accession number NM_197965) and were used to achieve a PCR product containing the polymorphic site at ORF position 610. Amplification of beta-actin was used as an internal positive control. As further positive control, cDNAs isolated from SOAT-WT-HEK293 as well as SOAT-L204F-HEK293 after tet treatment were included in the PCR amplification. Cycling conditions were 1 × 9 min at 95 °C, 40 × (45 s at 94 °C, 45 s at 60 °C, and 45 s at 72 °C) and 7 min at 72 °C. For genotyping of the homozygous or heterozygous SOAT-L204F polymorphism, allele-specific digestion of the PCR products with the restriction enzyme *Ava*II (NEB) was performed. *Ava*II only cuts wildtype SOAT, but not the polymorphic L204F-SOAT sequence. For single digest, 25 µl of the PCR product were mixed with 5 µl CutSmart Buffer and 1 µl enzyme and afterwards were incubated at 37 °C for 15 min. Enzyme reaction was stopped by 20 min incubation at 80 °C. The digest was separated on 1.5% agarose gel and visualized with GelGreen Nucleic Acid Stain (Biotium Inc.).

3. Results

In order to identify non-synonymous single nucleotide polymorphisms (SNPs) in the coding sequence of human SOAT, the GenBank SNP database was screened for the SOAT gene (*SLC10A6* gene) and revealed the following missense SOAT variants (year of search: 2012): S6F, I114V, R185T, I196T, V199I, and L204F.

For all of these polymorphisms, cDNA constructs were generated by site-directed mutagenesis based on the SOAT-V5-His-pcDNA5 vector. All constructs were sequence verified and then transiently transfected into HEK293 cells. 48 h post transfection cells were used for transport experiments with 1 µM [^{3}H]DHEAS in order to evaluate their transport activity. As shown in Fig. 1, all variants showed lower transport rates compared to the wildtype SOAT, but all, except for SOAT-L204F, maintained a significant sodium-dependent transport activity for DHEAS.

As our study aimed to identify SOAT variants with maximally reduced transport activity in order to evaluate their occurrence in

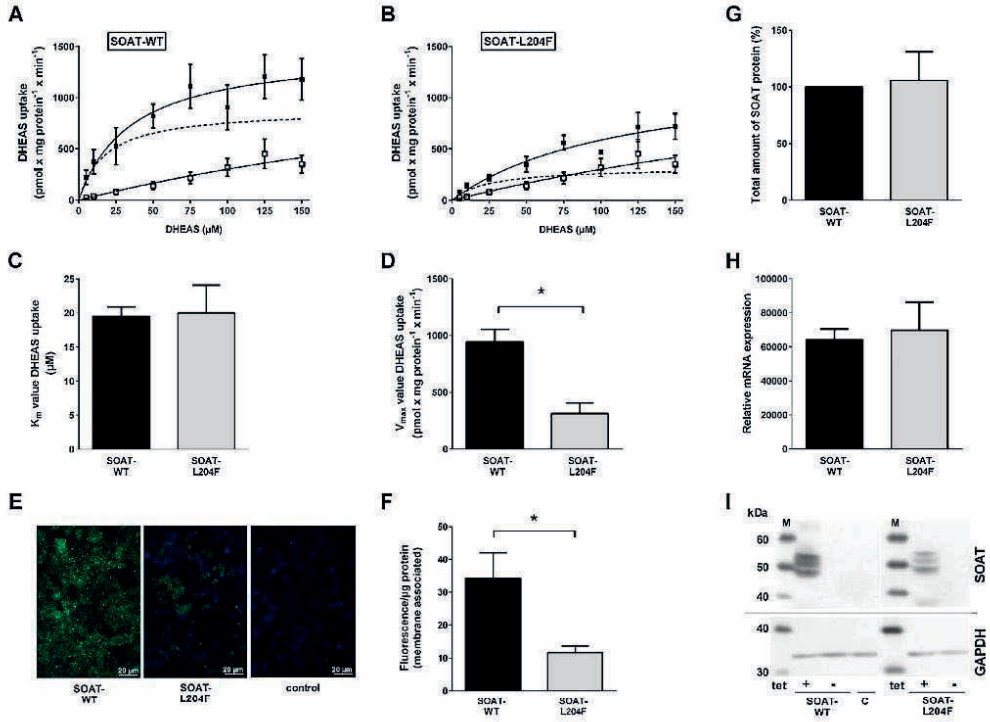

Fig. 2. The SOAT-L204F variant showed reduced V_{max} for DHEAS transport and impaired plasma membrane sorting.
SOAT-WT-HEK293 (**A**) and SOAT-L204F-HEK293 (B) cells were used for transport experiments with [^{3}H]DHEAS at increasing concentrations over 1 min at 37 °C (filled symbols). Non-transfected HEK293 cells were used as control (open symbols). Michaelis-Menten kinetic parameters were calculated from SOAT-specific uptakes (dashed line) by nonlinear regression analysis (C). The V_{max} value was significantly lower for the SOAT-L204F variant with $p < 0.05$ (Student's *t*-test) (D). Values from C and D represent means ± SD from three independent experiments. (E, F) SOAT-WT-HEK293 and SOAT-L204F-HEK293 cells were incubated with the $SOAT_{2-17}$ antiserum without permeabilization in order to detect plasma membrane expression of the SOAT protein (green fluorescence). Nuclei were stained with DAPI/PBS (blue fluorescence). Pictures were taken under the same conditions (gain and exposure time) and represent maximum projection of a z-batch (primary magnification ×20, scale bar 20 µm) (E). Additionally, SOAT-directed fluorescence was quantified by photometric measurements after three freeze-thaw cycle lysis of the cells at 520 nm. *Significantly different with $p < 0.05$ (Student's *t*-test), n = 3 determinations (F). (G) Protein extracts from SOAT-WT-HEK293 and SOAT-L204F-HEK293 cells were subjected to Western blot analysis with the anti-$SOAT_{311-377}$ antibody. Signal intensity was densitometrically analyzed and was set to 100% for SOAT-WT. Data were obtained from three independent Western blot experiments. (H) Additionally, relative SOAT mRNA expression analysis was performed by quantitative real-time PCR from SOAT-WT-HEK293 and SOAT-L204F-HEK293 cells after tetracycline induction. The graph shows x-fold higher expression compared to non-transfected HEK293 cells depicted at the y-axis. The values represent means ± SEM of triplicate determinations. (I) Qualitative evaluation of the Western blots from (G) revealed identical band pattern for SOAT-WT and SOAT-L204F with 3 bands between 45 and 55 kDa after tetracycline induction. Without tetracycline treatment, no SOAT protein was detectable. An anti-GAPDH antibody (1:25,000 dilution) was used to control the protein load. Non-transfected HEK293 cells (C) served as an additional control. M: marker.

patients with impaired spermatogenesis vs. patients with intact spermatogenesis, further analyses were focused only on SOAT-L204F. For transport characterization of SOAT-L204F, we generated stably transfected HEK293 cells expressing either the wildtype SOAT (SOAT-WT) or the polymorphic SOAT-L204F variant controlled by a tetracycline regulated promoter. In these cells, transport kinetics was determined with increasing concentrations of DHEAS (Fig. 2A and B). Non-linear regression analysis revealed nearly identical K_m values of 19.5 ± 1.34 µM for SOAT-WT and 20.0 ± 3.9 µM for SOAT-L204F (Fig. 2C), but significantly lower V_{max} values for SOAT-L204F (313.6 ± 92.7 vs. 942.5 ± 100.7 pmol × mg protein^{-1} × min^{-1}) (Fig. 2D).

Therefore, the plasma membrane expression of SOAT-L204F was analyzed more closely. For these experiments, first an anti-SOAT antibody directed against the extracellular N-terminus of human SOAT (anti-$SOAT_{2-17}$, see Geyer et al. [10]) was used. This antibody was used to fluorescently stain SOAT-WT-HEK293 as well as SOAT-L204F-HEK293 cells, without fixation and permeabilization of the cells. Under these experimental conditions, the anti-$SOAT_{2-17}$ antibody should only bind to SOAT proteins, which are really located at the plasma membrane. Whereas the SOAT-WT-HEK293 cells revealed clear membrane staining, SOAT-L204F showed significantly lower fluorescence levels in the qualitative (Fig. 2E) as well as in the quantitative (Fig. 2F) immunofluorescence analysis. In order to analyze if this drop in SOAT membrane expression is just due to lower protein expression rates in the SOAT-L204F-HEK923 cells, the total SOAT protein expression in both cell lines was also determined using Western blot analysis with the anti-$SOAT_{311-377}$ antibody, which is directed against the intracellular C-terminus of human SOAT [11]. Comparable total SOAT protein expression levels for both variants were found in several independent experiments (Fig. 2G), indicating that only the plasma membrane trafficking seems to be affected by the L204F substitution. However, all Western blot experiments revealed that the SOAT-WT and SOAT-L204F proteins show the identical band pattern of several glycosylation states of the SOAT protein as reported before [10], indicating that the sorting defect of the SOAT-L204F variant occurs at a post-glycosylation step

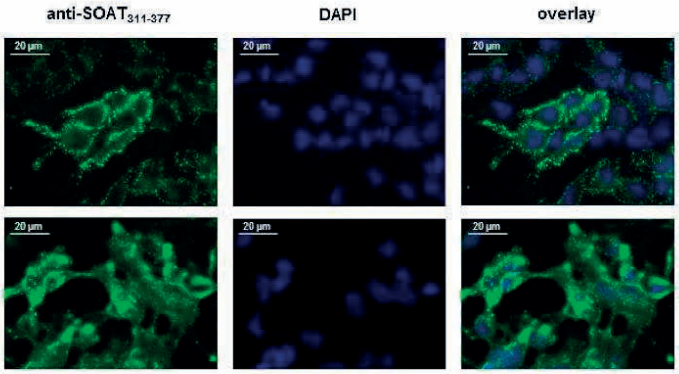

Fig. 3. The SOAT-L204F variant showed intracellular retention.
Fluorescent staining of stably transfected SOAT-WT-HEK293 and SOAT-L204F-HEK293 cells was performed with the $SOAT_{311-377}$ antibody (green fluorescence). Nuclei were stained with DAPI (blue fluorescence). Pictures were taken under the same conditions (gain and exposure time). (For interpretation of the references to color in this figure legend, the reader is referred to the web version of this article).

(Fig. 2I). Furthermore, an identical amount of SOAT mRNA after tet induction of the SOAT-WT-HEK293 and SOAT-L204F-HEK293 cells was detected, excluding any difference in SOAT expression at the mRNA expression level (Fig. 2H). For further characterization of expression and sorting of the SOAT-L204F protein, immunofluorescence microscopy was applied once more using the anti-$SOAT_{311-377}$ antibody instead of the anti-$SOAT_{2-17}$ antibody in order to detect not only surface, but total SOAT protein expression. Indeed, comparable fluorescence staining of the SOAT-L204F-HEK293 and SOAT-WT-HEK293 cells was found, but the fluorescence signals were largely directed at intracellular compartments in the SOAT-L204F-HEK293 cells instead of the plasma membrane, as it is the case for the SOAT-WT-HEK293 cells (Fig. 3).

As a final objective, it was determined if the sorting-deficient SOAT-L204F variant is more frequent in patients with impaired spermatogenesis compared to patients with intact spermatogenesis. For these experiments, a total of 46 human testis tissue samples were used, including 20 samples from subjects with intact spermatogenesis (nsp) and 26 samples showing hypospermatogenesis (hyp). Genotyping was done by restriction fragment length polymorphism (RFLP) analysis. SOAT-specific PCR fragments of 141 bp were amplified by RT-PCR from all samples and then digested with *Ava*II, which is specific for the SOAT-WT sequence. Whereas all SOAT-WT fragments were digested by *Ava*II into fragments of 105 bp and 36 bp with only the 105 bp fragment being visible on the agarose gel, the polymorphic SOAT-L204F fragments remained at 141 bp. Samples heterozygous for SOAT-L204F revealed both bands at 141 bp and 105 bp (+36 bp) (Fig. 4A). Interestingly, nearly identical genotype distributions were obtained between the two groups of patients with 85–88% SOAT-WT, 8–10% heterozygous and 4–5% homozygous SOAT-L204F genotypes (Fig. 4B). In total, one patient in each group showed the homozygous SOAT-L204F genotype, whereas two patients in each group were heterozygous, revealing allelic frequencies for the SOAT-L204F polymorphism of 10% for nsp and 7.7% for hyp.

4. Discussion

SOAT (*SLC10A6*) phylogenetically belongs to the Solute Carrier family SLC10, together with the Na^+/taurocholate co-transporting polypeptide NTCP (gene name *SLC10A1*) and the apical sodium-dependent bile acid transporter ASBT (gene name *SLC10A2*) [16]. These two bile acid carriers, due to their expression in the liver (NTCP) and intestine (ASBT), are essential for the maintenance of the enterohepatic circulation of bile acids [17–19]. NTCP and ASBT were cloned in the early 1990s and their physiological significance is regarded as very well understood [16,19,20]. ASBT is responsible for intestinal bile acid reabsorption, whereas NTCP mediates the uptake of bile acids at the basolateral membrane of hepatocytes. The significant role of NTCP and ASBT for bile acid homoeostasis was more recently verified in studies on *Slc10a1* (Ntcp) and *Slc10a2* (Asbt) knockout mice as well as in patients with respective loss of function mutations. Targeted deletion of the *Slc10a2* gene in mice caused 10- to 20-fold elevation of fecal bile acid excretion compared to wildtype mice, with a decrease of 80% of

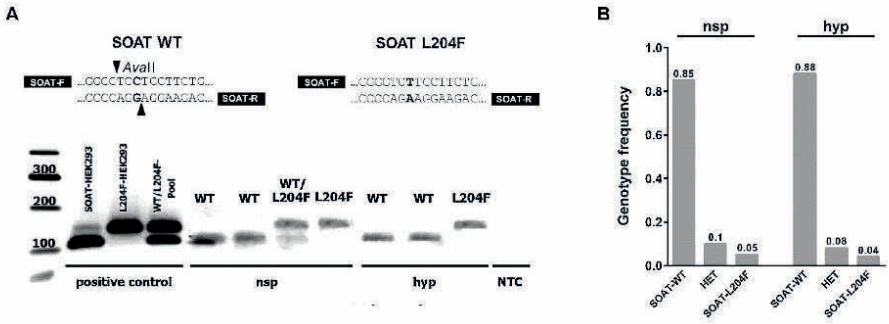

Fig. 4. The SOAT-L204F polymorphism revealed comparable allele frequencies in testicular biopsies showing normal spermatogenesis or hypospermatogenesis.
(A) RT-PCR with SOAT-specific primers (SOAT-F and SOAT-R) covering the polymorphic site produced 141 bp PCR products, which were digested with *Ava*II followed by restriction fragment length polymorphism (RFLP) analysis. *Ava*II digestion revealed fragments of 105 bp + 36 bp (not visible on the gel) for the wildtype SOAT sequence, but kept the polymorphic SOAT L204F PCR products undigested (141 bp). RNA isolated from the SOAT-WT-HEK293 and SOAT-L204F-HEK293 cells served as control for RFLP analysis. NTC, no template control.
(B) Frequencies of the heterozygous and homozygous genotypes for the SOAT-L204F variant in subjects with normal spermatogenesis (nsp) or hypospermatogenesis (hyp).

the bile acid pool size combined with an altered bile acid profile [21]. In man, several inherited mutations in the *SLC10A2* gene lead to primary bile acid malabsorption, based on an abolished transport function of the polymorphic ASBT protein [22]. In the case of NTCP, Vaz et al. [23] identified an R252H polymorphism in a female patient with conjugated hypercholanemia. The polymorphic NTCP-R252H showed comparable K_m, but 9-fold reduced V_{max} values compared to wildtype NTCP. Furthermore, *Slc10a1* knockout mice showed a decreased serum bile acid clearance, in some cases with a hypercholanemic but clinically mild phenotype, underlining the role of NTCP for hepatic bile acid transport [24]. In line with this data, it was aimed in the present study to identify polymorphisms in the human *SLC10A6* gene, which could be correlated with impaired spermatogenesis or infertility in man. As shown by Geyer et al. [25] for the first time, SOAT transports sulfated steroid hormones such as DHEAS, estrone-3-sulfate, and PREGS and is highly expressed in germ cells of the testis in man and mouse [11,26]. Furthermore, significantly lower SOAT mRNA expression in testis biopsies showing hypospermatogenesis was found in a previous study [11], so it was hypothesized that SOAT may play a role for spermatogenesis and fertility by transporting steroid sulfates into germ cells of the testis [5]. Although the SOAT-L204F polymorphism with significantly reduced transport activity due to impaired plasma membrane expression (Figs. 2 and 3) was identified, this polymorphism could not be correlated with hypospermatogenesis in the present study (Fig. 4). Twenty subjects with normal spermatogenesis as well as 26 subjects with hypospermatogenesis showed identical genotype distribution with 2× heterozygous and 1× homozygous occurrence of the L204F polymorphism in each group. Therefore, it can be ruled out that the L204F polymorphism provokes hypospermatogenesis per se. However, as the classification into "normal spermatogenesis" and "hypospermatogenesis" is based on the histological evaluation of testis biopsies, our data cannot automatically be transferred to the functional level, and they do not provide any information on fertility. Therefore, it cannot be excluded that SOAT plays a role for male reproduction. However, recently established *Slc10a6*$^{-/-}$ knockout mice were fertile, produced normal litter sizes, and showed normal spermatogenesis and sperm vitality [40]. Even if the loss of Soat could be compensated in this model, Soat seems not to be essential for reproduction in mice.

Apart from L204F, several other nonsynonymous polymorphisms were identified in the SOAT protein. Some of them have quite high allelic frequencies, e.g. in the case of I114V (up to 26%) or S6F and V199I (up to 9% each) (Table 2), but all of them sustained significant transport activity for DHEAS (Fig. 1). Therefore, these polymorphisms were not further analyzed in the present study. In the case of SOAT-L204F, the allelic frequencies varied in a wide range from 0.012–5.1% (Table 2) with clear ethnical differences (Table 3). This polymorphism was more frequent in African (e.g. Nigeria 5.1% or Kenya 4%) than in East/South Asian (0.01%–0.1%), Japanese (0.5%), European American (0.02%) or European (0%) subpopulations. Against this background, it is interesting to note that the subjects analyzed in the present study revealed an exceptionally high allelic frequency of 9–10%, being even higher than in the African subpopulations. However, as no ethnical data were available for the testis biopsies used in the present study, these data cannot be explained and need further (ethnic-based) analysis.

Despite the lack of correlation with hypospermatogenesis, the transport function and membrane expression of the L204F-SOAT variant was analyzed more closely. Comparable K_m but significantly lower V_{max} values were found for DHEAS transport compared with the wildtype SOAT. This finding is similar to the polymorphic NTCP-R252H protein, which seems to be targeted for proteasomal breakdown as consequence of inappropriate protein folding due to incomplete glycosylation [23]. After biosynthesis, proteins undergo several modifications including glycosylation, and correct folding often is a prerequisite for trafficking through the endoplasmic reticulum and the Golgi compartment to the plasma membrane [27]. It is known that N-glycosylation of membrane proteins affects trafficking to the plasma membrane and proper glycosylation is required for correct sorting [28–30]. However, while NTCP-R252H showed an inappropriate glycosylation status, SOAT-L204F exhibited the identical band pattern as SOAT-WT in the Western blots and, therefore, defective glycosylation does not seem to be the reason for the impaired plasma membrane expression of SOAT-L204F.

Apart from glycosylation, plasma membrane sorting signals often come from dileucine motifs, consisting of four to seven amino acids preceding the dileucine residues [31–33]. Whereas the dileucine motif [D/E]XXXL[L/I] seems to be responsible for rapid internalization of certain membrane proteins, the DXXLL motif is required for recycling of proteins between the *trans*-Golgi network and endosomes [32]. As an example, in rat Ntcp (rNtcp) a dileucine motif in the third intracellular loop is required for targeting the protein to the plasma membrane and for rapid internalization via endocytosis [34]. Mutation of this $L_{222}L_{223}$ dileucine motif in rNtcp resulted in reduced plasma membrane expression and increased core-glycosylation, but the total protein expression remained unaffected. Since, SOAT-L204F showed similar attributes (diminished plasma membrane expression and constant total protein expression), a closer look on position L204 in the SOAT protein as part of a potential dileucine motif is necessary. Although a $L_{204}L_{205}$ dileucine motif is present at this position, the flanking sequence does not fit with typical dileucine motifs. Furthermore, L204 is located within a transmembrane domain and not in the cytosolic part of the SOAT protein, where most sorting signals are located [35–37]. However, as few proteins bear their sorting signals even within transmembrane domains [38], it cannot be excluded that the L204F polymorphism affects the sorting process to the plasma membrane by mutation of a dileucine ($L_{204}L_{205}$) sorting motif.

In 2012, co-transfection studies of SOAT and NTCP in U2OS cells revealed that both transporters form homodimers and can also heterodimerize with each other [39]. In the case of NTCP,

Table 2
SOAT SNPs and their allelic frequencies.

SNP	Nucleotide position[a]	Nucleotide substitution[b]	Amino acid substitution	Evidence	Minor allele frequency (%)
rs17694522	165	TCC → **T**TC	S6F	1, 2, 3, 4, 5	0.011–8.7
rs13106574	488	ATT → **G**TT	I114V	1, 2, 3, 4, 5	0.1–26.1
rs72874286	702	AGA → **A**CA	R185T	1, 3, 4, 5	0.0016–4.7
rs113035158	735	ATT → **C**TT	I196T	5	0.0057–0.1
rs57559561	743	GTT → **A**TT	V199I	1, 3, 4, 5	0.006–9.4
rs61734716	758	CTC → **T**TC	L204F	1, 3, 4, 5	0.012–5.1

[1]The variant is reported to be polymorphic in at least one sample.
[2]The variant is polymorphic in at least one HapMap panel.
[3]The variant was discovered in the 1000 Genomes Project.
[4]The variant was discovered in the Exome Sequencing Project.
[5]The variant was discovered in the Exome Aggregation Consortium.
[a] Referred to GenBank accession no. NM_197965.
[b] Polymorphic site in bold.

Table 3
Genotype occurrence of the SOAT-L204F polymorphism.

Study	Subpopulation	Genotype frequency	Minor allele frequency
Present study (n = 20)	nsp	G/G: 0.85 G/A: 0.1 A/A: 0.05	0.1
Present study (n = 26)	hyp	G/G: 0.88 G/A: 0.08 A/A: 0.04	0.09
1000 Genomes Project Phase 3 (n = 2449)	all phase 3 individuals	G/G: 0.978 G/A: 0.022 A/A: 0.0004	0.011
1000 Genomes Project Phase 3 (n = 504)	East Asian	G/G: 0.998 G/A: 0.002 A/A: 0.0	0.001
1000 Genomes Project Phase 3 (n = 104)	Japanese in Tokyo, Japan	G/G: 0.990 G/A: 0.010 A/A: 0.0	0.005
1000 Genomes Project Phase 3 (n = 347)	American	G/G: 0.986 G/A: 0.014 A/A: 0.0	0.007
1000 Genomes Project Phase 3 (n = 104)	Puerto Rican in Puerto Rico	G/G: 0.981 G/A: 0.019 A/A: 0.0	0.010
1000 Genomes Project Phase 3 (n = 94)	Colombian in Medellin, Colombia	G/G: 0.968 G/A: 0.032 A/A: 0.0	0.016
1000 Genomes Project Phase 3 (n = 113)	Gambian in Western Division, The Gambia	G/G: 0.956 G/A: 0.044 A/A: 0.0	0.022
1000 Genomes Project Phase 3 (n = 85)	Mende in Sierra Leona	G/G: 0.953 G/A: 0.047 A/A: 0.0	0.024
1000 Genomes Project Phase 3 (n = 108)	Yoruba in Ibadan, Nigeria	G/G: 0.926 G/A: 0.074 A/A: 0.0	0.037
1000 Genomes Project Phase 3 (n = 613)	African	G/G: 0.926 G/A: 0.073 A/A: 0.002	0.038
1000 Genomes Project Phase 3 (n = 99)	Luhya in Webuye, Kenya	G/G: 0.919 G/A: 0.081 A/A: 0.0	0.040
1000 Genomes Project Phase 3 (n = 96)	African Caribbean in Barbados	G/G: 0.906 G/A: 0.094 A/A: 0.0	0.047
1000 Genomes Project Phase 3 (n = 61)	African Ancestry in Southwest US	G/G: 0.902 G/A: 0.098 A/A: 0.0	0.049
1000 Genomes Project Phase 3 (n = 99)	Esan in Nigeria	G/G: 0.909 G/A: 0.081 A/A: 0.010	0.051
NHLBI Exome Sequencing Project (n = 2203)	African American	G/G: 0.942 G/A: 0.058 A/A: 0.0	0.029
NHLBI Exome Sequencing Project (n = 4300)	European American	G/G: 0.9995 G/A: 0.0005 A/A: 0.0	0.0002
Exome Aggregation Consortium (ExAC) (n = 60706)	All ExAC individuals	n.a.	0.003
Exome Aggregation Consortium (ExAC) (n = 5171)	African/African Americans	n.a.	0.032
Exome Aggregation Consortium (ExAC) (n = 5772)	Latino	n.a.	0.001
Exome Aggregation Consortium (ExAC) (n = 60577)	Adjusted (individuals with GQ ≥ 20 and DP ≥ 10)	n.a.	0.003
Exome Aggregation Consortium (ExAC) (n = 4324)	East Asian	n.a.	0.0001
Exome Aggregation Consortium (ExAC) (n = 3304)	Finish	n.a.	0.0
Exome Aggregation Consortium (ExAC) (n = 33307)	Non-Finish European	n.a.	0.0
Exome Aggregation Consortium (ExAC) (n = 451)	Other	n.a.	0.002
Exome Aggregation Consortium (ExAC) (n = 8248)	South Asian	n.a.	0.0001
CORNELL	AGI_ASP population (Caucasian and African American)	G/G: 0.970 G/A: 0.030 A/A: 0.0	0.015
NHLBI-ESP: ESP Cohort Populations	n.s.	G/G: 0.976 G/A: 0.024 A/A: 0.0	0.012
1000 Genomes: pilot 1 YRI low coverage panel	Yoruba in Ibadan, Nigeria	n.a.	0.034
EVA EXAC: ExAc Aggregated Populations	n.s.	n.a.	0.003

n.a.: not available, n.s.: not specified.

homodimerization occurs in the endoplasmic reticulum and seems to be required for proper sorting to the plasma membrane [39]. Based on this data, it can be speculated that L204F may hinder dimerization of SOAT and thereby may impair proper membrane expression. It currently remains unclear why SOAT-L204F is not properly expressed at the plasma membrane, and this point needs further investigation.

4.1. In conclusion

The present study searched for functionally relevant SOAT polymorphisms and aimed to comparatively analyze their occurrence in subjects with impaired spermatogenesis vs. subjects with intact spermatogenesis. When expressed in HEK293 cells, SOAT-L204F showed significantly reduced transport function for DHEAS. Although the K_m value was identical with SOAT-WT, the V_{max} value declined dramatically. Although the same amount of total SOAT-L204F protein was detected in HEK293 cells compared to SOAT-WT, plasma membrane expression was significantly reduced, pointing to a sorting defect of the SOAT-L204F protein to the plasma membrane. The nsp and hyp groups showed nearly identical distributions of the SOAT-L204F polymorphism (~10% heterozygous and ~5% homozygous), indicating that this polymorphism is not causative for hypospermatogenesis per se. However, as SOAT-L204F had some residual transport activity and as histomorphometry (nsp vs. hyp) provides no functional information, a role of SOAT for male fertility and reproduction cannot be excluded.

Acknowledgements

This study was supported by the Research Group FOR1369 "Sulfated Steroids in Reproduction" grants to JG (GE1921/4-1/2) and DF (FI1927/1-2). The authors thank Regina Leidolf, Jutta Dern-Wieloch, and Alexandra Hax for their technical assistance as well as Dr. Barbara Döring and Marcela Moncada for providing SOAT-S6F and SOAT-I114V constructs.

References

[1] R.A. Hess, Estrogen in the adult male reproductive tract: a review, Reprod. Biol. Endocrinol. 1 (2003) 52.
[2] C.A. Oliveira, G.A. Mahecha, K. Carnes, G.S. Prins, P.T. Saunders, L.R. Franca, R.A. Hess, Differential hormonal regulation of estrogen receptors ERalpha and ERbeta and androgen receptor expression in rat efferent ductules, Reproduction 128 (2004) 73–86.
[3] W.H. Walker, Molecular mechanisms of testosterone action in spermatogenesis, Steroids 74 (2009) 602–607.
[4] A. Ruokonen, T. Laatikainen, E.A. Laitinen, R. Vihko, Free and sulfate-conjugated neutral steroids in human testis tissue, Biochemistry 11 (1972) 1411–1416.
[5] J. Geyer, K. Bakhaus, R. Bernhardt, C. Blaschka, Y. Dezhkam, D. Fietz, G. Grosser, K. Hartmann, M.F. Hartmann, J. Neunzig, D. Papadopoulos, A. Sanchez-Guijo, G. Scheiner-Bobis, G. Schuler, M. Shihan, C. Wrenzycki, S.A. Wudy, M. Bergmann, The role of sulfated steroid hormones in reproductive processes, J. Steroid Biochem. Mol. Biol. 172 (2016) 207–221.
[6] J.W. Mueller, L.C. Gilligan, J. Idkowiak, W. Arlt, P.A. Foster, The regulation of steroid action by sulfation and desulfation, Endocr. Rev. 36 (2015) 526–563.
[7] M.J. Reed, A. Purohit, L.W. Woo, S.P. Newman, B.V. Potter, Steroid sulfatase: molecular biology, regulation, and inhibition, Endocr. Rev. 26 (2005) 171–202.
[8] F. Labrie, Intracrinology, Mol. Cell Endocrinol. 78 (1991) 113–118.
[9] F. Labrie, Intracrinology in action: importance of extragonadal sex steroid biosynthesis and inactivation in peripheral tissues in both women and men, J. Steroid Biochem. Mol. Biol. 145 (2015) 131–132.
[10] J. Geyer, B. Döring, K. Meerkamp, B. Ugele, N. Bakhiya, C.F. Fernandes, J.R. Godoy, H. Glatt, E. Petzinger, Cloning and functional characterization of human sodium-dependent organic anion transporter (SLC10A6), J. Biol. Chem. 282 (2007) 19728–19741.
[11] D. Fietz, K. Bakhaus, B. Wapelhorst, G. Grosser, S. Günther, J. Alber, B. Döring, S. Kliesch, W. Weidner, C.E. Galuska, M.F. Hartmann, S.A. Wudy, M. Bergmann, J. Geyer, Membrane transporters for sulfated steroids in the human testis-cellular localization, expression pattern and functional analysis, PLoS One 8 (2013) e62638.
[12] C.E. Galuska, M.F. Hartmann, A. Sanchez-Guijo, K. Bakhaus, J. Geyer, G. Schuler, K.P. Zimmer, S.A. Wudy, Profiling intact steroid sulfates and unconjugated steroids in biological fluids by liquid chromatography-tandem mass spectrometry (LC-MS-MS), Analyst 138 (2013) 3792–3801.
[13] H. Schweigmann, A. Sanchez-Guijo, B. Ugele, K. Hartmann, M.F. Hartmann, M. Bergmann, C. Pfarrer, B. Döring, S.A. Wudy, E. Petzinger, J. Geyer, G. Grosser, Transport of the placental estriol precursor 16alpha-hydroxy-dehydroepiandrosterone sulfate (16alpha-OH-DHEAS) by stably transfected OAT4- SOAT-, and NTCP-HEK293 cells, J. Steroid Biochem. Mol. Biol. 143 (2014) 259–265.
[14] M. Bergmann, S. Kliesch, Testicular biopsy and histology, in: E. Nieschlag, H.M. Behre (Eds.), Andrology. Male Reproductive Health and Dysfunction, Springer Verlag, Berlin, Heidelberg, 2010, pp. 155–167.
[15] O. Lowry, N. Rosebrough, A. Farr, R. Randall, Protein measurement with the Folin phenol reagent, J. Biol. Chem. 193 (1951) 265–275.
[16] J. Geyer, T. Wilke, E. Petzinger, The solute carrier family SLC10: more than a family of bile acid transporters regarding function and phylogenetic relationships, Naunyn Schmiedebergs Arch. Pharmacol. 372 (2006) 413–431.
[17] G.A. Kullak-Ublick, B. Stieger, P.J. Meier, Enterohepatic bile salt transporters in normal physiology and liver disease, Gastroenterology 126 (2004) 322–342.
[18] P.A. Dawson, T. Lan, A. Rao, Bile acid transporters, J. Lipid Res. 50 (2009) 2340–2357.
[19] B. Döring, T. Lütteke, J. Geyer, E. Petzinger, The SLC10 carrier family: transport functions and molecular structure, Curr. Top. Membr. 70 (2012) 105–168.
[20] M.H. Wong, P. Oelkers, A.L. Craddock, P.A. Dawson, Expression cloning and characterization of the hamster ileal sodium-dependent bile acid transporter, J. Biol. Chem. 269 (1994) 1340–1347.
[21] P.A. Dawson, J. Haywood, A.L. Craddock, M. Wilson, M. Tietjen, K. Kluckman, N. Maeda, J.S. Parks, Targeted deletion of the ileal bile acid transporter eliminates enterohepatic cycling of bile acids in mice, J. Biol. Chem. 278 (2003) 33920–33927.
[22] P. Oelkers, L.C. Kirby, J.E. Heubi, P.A. Dawson, Primary bile acid malabsorption caused by mutations in the ileal sodium-dependent bile acid transporter gene (SLC10A2), J. Clin. Invest. 99 (1997) 1880–1887.
[23] F.M. Vaz, C.C. Paulusma, H. Huidekoper, R.M. de, C. Lim, J. Koster, K. Ho-Mok, A.H. Bootsma, A.K. Groen, F.G. Schaap, R.P. Oude Elferink, H.R. Waterham, R.J. Wanders, Sodium taurocholate cotransporting polypeptide (SLC10A1) deficiency: conjugated hypercholanemia without a clear clinical phenotype, Hepatology 61 (2015) 260–267.
[24] D. Slijepcevic, C. Kaufman, C.G. Wichers, E.H. Gilglioni, F.A. Lempp, S. Duijst, D.R. de Waart, R.P. Elferink, W. Mier, B. Stieger, U. Beuers, S. Urban, S.F. van de Graaf, Impaired uptake of conjugated bile acids and hepatitis B virus pres1-binding in Na^+-taurocholate cotransporting polypeptide knockout mice, Hepatology 62 (2015) 207–219.
[25] J. Geyer, J.R. Godoy, E. Petzinger, Identification of a sodium-dependent organic anion transporter from rat adrenal gland, Biochem. Biophys. Res. Commun. 316 (2004) 300–306.
[26] G. Grosser, D. Fietz, S. Gunther, K. Bakhaus, H. Schweigmann, B. Ugele, R. Brehm, E. Petzinger, M. Bergmann, J. Geyer, Cloning and functional characterization of the mouse sodium-dependent organic anion transporter Soat (Slc10a6), J. Steroid Biochem. Mol. Biol. 138 (2013) 90–99.
[27] C. van Vliet, E.C. Thomas, A. Merino-Trigo, R.D. Teasdale, P.A. Gleeson, Intracellular sorting and transport of proteins, Prog. Biophys. Mol. Biol. 83 (2003) 1–45.
[28] P. Scheiffele, J. Peranen, K. Simons, N-glycans as apical sorting signals in epithelial cells, Nature 378 (1995) 96–98.
[29] A. Gut, F. Kappeler, N. Hyka, M.S. Balda, H.P. Hauri, K. Matter, Carbohydrate-mediated Golgi to cell surface transport and apical targeting of membrane proteins, EMBO J. 17 (1998) 1919–1929.
[30] P. Urquhart, S. Pang, N.M. Hooper, N-Glycans as apical targeting signals in polarized epithelial cells, Biochem. Soc. Symp. 72 (2005) 39–45.
[31] P. Keller, K. Simons, Post-Golgi biosynthetic trafficking, J. Cell Sci. 110 (1997) 3001–3009.
[32] J.S. Bonifacino, L.M. Traub, Signals for sorting of transmembrane proteins to endosomes and lysosomes, Annu. Rev. Biochem. 72 (2003) 395–447.
[33] K.N. Pandey, Functional roles of short sequence motifs in the endocytosis of membrane receptors, Front. Biosci. (Landmark Ed.) 14 (2009) 5339–5360.
[34] C. Stross, S. Kluge, K. Weissenberger, E. Winands, D. Haussinger, R. Kubitz, A di-leucine motif is involved in plasma membrane expression and endocytosis of rat sodium taurocholate cotransporting polypeptide (Ntcp), Am. J. Physiol. Gastrointest. Liver Physiol. 305 (2013) 722–730.
[35] H. Do, D. Falcone, J. Lin, D.W. Andrews, A.E. Johnson, The cotranslational integration of membrane proteins into the phospholipid bilayer is a multistep process, Cell 85 (1996) 369–378.
[36] L.M. Traub, S. Kornfeld, The trans-Golgi network: a late secretory sorting station, Curr. Opin. Cell Biol. 9 (1997) 527–533.
[37] M.S. Marks, H. Ohno, T. Kirchhausen, J.S. Bonracino, Protein sorting by tyrosine-based signals: adapting to the Ys and wherefores, Trends Cell Biol. 7 (1997) 124–128.
[38] O.A. Weisz, E. Rodriguez-Boulan, Apical trafficking in epithelial cells: signals, clusters and motors, J. Cell Sci. 122 (2009) 4253–4266.
[39] I.T. Bijsmans, R.A. Bouwmeester, J. Geyer, K.N. Faber, S.F. van de Graaf, Homo- and hetero-dimeric architecture of the human liver Na^+-dependent taurocholate co-transporting protein, Biochem. J. 441 (2012) 1007–1015.
[40] K. Bakhaus, J. Bennien, D. Fietz, A. Sánchez-Guijo, M. Hartmann, R. Serafini, C.C. Love, A. Golovko, S.A. Wudy, M. Bergmann, J. Geyer, Sodium-dependent organic anion transporter (Slc10a6-/-) knockout mice show normal spermatogenesis and reproduction, but elevated serum levels for cholesterol sulfate, J. Steroid Biochem. Mol. Biol. (2017), http://dx.doi.org/10.1016/j.jsbmb.2017.07.019 in press.

11. Anhang – Publikationen

11. D. Fietz. J Steroid Biochem Mol Biol 2017 Oct 7. pii: S0960-0760(17)30270-4. doi: 10.1016/j.jsbmb.2017.10.001

Journal of Steroid Biochemistry and Molecular Biology xxx (xxxx) xxx–xxx

Contents lists available at ScienceDirect

Journal of Steroid Biochemistry and Molecular Biology

journal homepage: www.elsevier.com/locate/jsbmb

Transporter for sulfated steroid hormones in the testis – expression pattern, biological significance and implications for fertility in men and rodents

D. Fietz*

Institute for Veterinary Anatomy, Histology and Embryology, Justus Liebig University Giessen, Giessen, Germany

ARTICLE INFO

Keywords:
Sulfated steroid hormones
Testicular target cells
Uptake and efflux transporters
Sulfatase pathway
Fertility

ABSTRACT

In various tissues, steroid hormones may be sulfated, glucuronidated or otherwise modified. For a long time, these hydrophilic molecules have been considered to be merely inactive metabolites for excretion via bile or urine. Nevertheless, different organs such as the placenta and breast tissue produce large amounts of sulfated steroids. After the discovery of the enzyme steroid sulfatase, which is able to re-activate sulfated steroids, these precursor molecules entered the focus of interest again as a local supply for steroid hormone synthesis with a prolonged half-life compared to their unconjugated counterparts. The first descriptions of this so-called sulfatase pathway in the placenta and breast tissue (with special regards to hormone-dependent breast cancer) were quickly followed by studies of steroid sulfate production and function in the testis. These hydrophilic molecules may not permeate the cell membrane by diffusion in the way that unbound steroids can, but need to be transported through the plasma membrane by transport systems. In the testis, a functional sulfatase pathway requires the expression of specific uptake carrier and efflux transporters in testicular cells, i.e. Sertoli, Leydig and germ cells. Main focus has to be placed on Sertoli cells, as these cells build up the blood-testis barrier.

In this review, an overview of carrier expression pattern in the human as well as rodent testis is provided with special interest towards implications on fertility.

1. Introduction

In contrast to unconjugated steroid hormones, sulfated steroid hormones were considered inactive steroid metabolites without biological significance. Whereas unconjugated steroid hormones can traverse the cellular membrane of target cells by diffusion, bind to cellularly located steroid hormone receptors and promote or inhibit gene transcription in the cell nucleus (for review, see [1]), sulfated steroids may not pass through the cell membrane due to their negative charge at physiological pH and were therefore considered excretion metabolites formed in the liver or kidney [2–6].

Nevertheless, sulfated steroids have been known for about four decades to be synthesized in the reproductive organs in humans and animals. Examples of this are considerable amounts of estrone sulfate (E_1S) in the bovine and equine placenta [7,8], and E_1S secretion from the testes of boars and stallions [9,10]. However, in humans, sulfated steroids are also produced in high amounts in the testis, e.g. pregnenolone sulfate (PREGS), dehydroepiandrosterone sulfate (DHEAS) and testosterone sulfate [11–13]. Apart from the pure excretion rate of these metabolites, many studies have shown that they may be used as precursors for testosterone synthesis in the human testis both *in vivo* and *in vitro* [14–19].

The cleavage enzyme involved in the re-activation of sulfated steroid hormones is steroid sulfatase (STS), also known as arylsulfatase, which is widely distributed in healthy human tissues and in cancer [20]. This has been demonstrated, for example, in human breast cancer: the hydrolysis of sulfated steroids like E_1S and DHEAS is thought to be involved in the local supply of estrogens and androgens in these cancer tissues [21,22]. The re-activation of steroid sulfates, their subsequent binding to classical steroid hormone receptors such as androgen receptor (AR) and estrogen receptors (ERs), and binding to hormone-responsive elements in the DNA leading to gene expression activation or

Abbreviations: ABC, transporter; ATP, binding cassette transporter; AR, androgen receptor; ASBT, apical sodium-dependent bile acid transporter; BBB, blood-brain barrier; BCRP, breast cancer resistance protein; BT, Bblood-testis barrier; CS, cholesterol sulfate; DHEA, dehydroepiandrosterone; DHEAS, dehydroepiandrosterone sulfate; DHT, dihydrotestosterone; E_1S, estrone sulfate; ESRs, estrogen receptors; MDR1, multidrug resistance carrier 1 (gene ABCB1); MRPs, multidrug resistance related proteins (genes ABCCs); NBD, nucleotide binding domain; NTCP, Na^+/taurocholate cotransporting polypeptide; OATP, organic anion transporting polypeptides; OSCP1, organic solute carrier protein 1; P-gp, P-glycoprotein (also known as MDR1, gene ABCB1); PREGS, pregnenolone sulfate; SCO, Sertoli-cell only syndrome; SLC, solute carrier family; SNP, single nucleotide polymorphism; SOAT, sodium-dependent organic anion transporter (gene SLC10A6); STS, steroid sulfatase; TMD, transmembrane domain

* Corresponding author to: Dr. Daniela Fietz Institute for Veterinary Anatomy, Histology and Embryology Frankfurter Straße 98, 35392 Giessen, Germany.
E-mail address: Daniela.Fietz@vetmed.uni-giessen.de.

http://dx.doi.org/10.1016/j.jsbmb.2017.10.001
Received 31 March 2017; Received in revised form 22 September 2017; Accepted 3 October 2017

Please cite this article as: Fietz, D., Journal of Steroid Biochemistry and Molecular Biology (2017), http://dx.doi.org/10.1016/j.jsbmb.2017.10.001

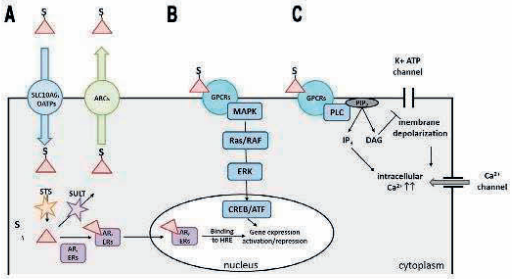

Fig. 1. Schematic drawing of the sulfatase pathway and signaling pathways for sulfated steroid hormones.

A For intracellular action, sulfated steroid hormones (red triangle plus "S") have to be taken up by specific uptake carriers (blue, e.g. SLC10A6, OATPs) into the cell. There, the sulfate residue is cleaved by the activity of STS (orange star). Afterwards, unconjugated steroid hormones (red triangle) are able to bind to nuclear steroid receptors (AR, ERs), translocate into the nucleus and bind to hormone responsive elements (HREs). By this, gene expression may be activated or repressed. This is considered as the genomic pathway as reviewed by Walker [1]. Within the cell, unconjugated steroid hormones can be inactivated by adding a sulfate residue (catalyzed by sulfotransferase (SULT), purple star). As conjugated steroid hormones have longer half-lives, they are considered as a local supply. They may also leave the target cell by specific efflux transporters (green, ATP binding cassette transporters, ABCs).

B Sulfated steroid hormones can also bind to membrane-associated G-protein coupled receptors (GPCRs, e.g. GPER [31], Gnα11 [34,35]) and activate a non-genomic pathway as reviewed by Walker [33]. Activating of MAP kinase (MAPK) cascade via Ras/RAF and ERK leads to phosphorylation of the transcription factors CREB/ATF which act on CREB inducible genes. This pathway has already been shown to be initiated by DHEAS binding [35].

C A second possible non-genomic pathway of steroid hormone action is the depolarization of cell membranes leading to a Ca^{2+} influx. By binding of steroid hormones to membrane receptors (probably GPCRs), phospholipase C (PLC) is activated and cleaves phosphatidylinositol 4,5-bisphosphate (PIP_2) into inositol 1,4,5-trisphosphate (IP_3) and diacyl glycerol (DAG). DAG inhibits K^+ATPase channels, which leads to a Ca^{2+} influx. Furthermore, IP_3 binds to IP_3 receptors on the endoplasmic reticulum which leads to a Ca^{2+} influx. This has already been described for testosterone action in Sertoli cells (for review, see [33]).

repression has been termed the sulfatase pathway (Fig. 1A). As presented later by Selcer et al. [20], STS expression is especially high in hormone dependent breast cancer subtypes. This made human STS a valuable drug target for the treatment of these hormone-dependent cancers [23]. Besides breast tissue, STS is also expressed in other organs, such as the skin or testis. A deficiency of STS leads to X-linked ichthyosis due to an accumulation of cholesterol sulfate (CS) in the skin, and boys with this deficiency were thought to be more likely to suffer from testicular cancer and maldescensus of the testis [24,25]. However, as recently reviewed by Elias et al., the incidence of cryptorchidism does not exceed 5–10%, and the association of testicular cancer and X-linked ichthyosis has not been confirmed [26]. The discovery of transporting systems for organic anions in the testis has increased the evidence of a functional sulfatase pathway in the testis and encouraged further investigations.

In addition to the *de novo* synthesis of steroid hormones in the testis, a second *para*-, intra- and autocrine system for the control of reproductive processes might exist [27,28]. Possible target cells in the testis (Leydig, Sertoli, and germ cells) can be either involved in steroid hormone synthesis (interstitial Leydig cells, for review see [29]) and/or targets of their effects. The latter is due to the expression of classical steroid hormone receptors such as the AR in Leydig and Sertoli cells (for review, see [1,30]) and the two subtypes of ERs (ESR1 and ESR2) in Leydig and Sertoli cells, and distinct germ cell populations [31] (for review, see [32]). A high expression of steroid hormone receptors and STS in the testis contributes to the hypothesis of a functional sulfatase pathway in the normal testis, implying a biological significance of sulfated steroid hormones in normal spermatogenesis [21]. Additionally, sulfated steroids are also able to act directly on target cells by binding to G-protein coupled receptors (GPCRs) in the cell membrane. Activation of these receptors leads to non-genomic signaling pathways, e.g. by activation of the MAP kinase cascade or Ca^{2+} influx (for review, see [33]) (Fig. 1B, C). This has already been demonstrated for DHEAS in rat Sertoli cells [34] and the spermatogenic germ cell line GC-2 [35].

In addition to the enzymatic equipment, testicular cells also have to provide distinct transport systems for a targeted uptake and the release of sulfated steroid hormones as these molecules are not able to pass the lipophilic cell membrane by diffusion. This missing link persistently questioned the existence of a sulfatase pathway in the testis and other organs. The description of the solute carrier family (SLC), located in membranes of different cell types and specifically transporting organic anionic molecules, e.g. bile acids in the liver and gut, has opened up a new discussion about sulfated steroid hormones and their implications for testicular biology. Exclusive to the testis, the transport of sulfated steroids towards the germ cells has to take place across the blood-testis barrier (BTB). The existence of the BTB was first confirmed 1970 by Dym and Fawcett [36] in the rat and 1989 in human testicular biopsies by Bergmann et al. [37]. The BTB is established together with the first wave of spermatogonia developing into spermatocytes which enter meiosis [38] and built in the basal third of the seminiferous epithelium by two adjacent Sertoli cells. Establishment of the BTB is considered a sign of Sertoli cell maturation [39]. It is located above migrating preleptotene spermatocytes and is comprised of tight and gap junctions as well as desmosomes between adjacent Sertoli cells. The BTB subdivides the seminiferous epithelium into two compartments: the basal compartment containing spermatogonia and preleptotene primary spermatocytes, and the adluminal compartment containing successive stages of germ cell development. Junctions between Sertoli cells are tight junctions, basal ectoplasmic specializations, and desmosome-gap junctions (for review, see [40]). The BTB is one of the tightest blood-tissue barriers in the human body, since it protects germ cells in a critical phase of development from white blood cells, as well as harmful toxicants, and regulates the inflow of physiological compounds like water, hormones or nutrients (for review, see [41]).

2. Uptake carrier and efflux transporter for sulfated steroid hormones – structure and function

This review is focused on the transporter superfamilies SLC (Solute Carriers) and ABC (ATP-binding cassette carriers). Members of these families are known to transport sulfated steroid hormones.

The SLC superfamily is comprised of secondary active ion-coupled symporters and anti-porters as well as uniporters, acting by facilitated diffusion [42] located in the plasma membrane and membranous compartments. Currently, the HUGO Nomenclature Committee (HGNC) provides data for 52 SLC families with approximately 395 transporter genes in humans (http://www.genenames.org/cgi-bin/genefamilies/set/752). The first members of the SLC10 family (sodium bile acid co-transporter family) to be described were Na^+/taurocholate co-transporting polypeptide (gene *SLC10A1*, NTCP, located in the liver) and the apical sodium-dependent bile acid transporter (gene *SLC10A2*, ASBT, located in the ileum) [43,44]. Both are essential transporters for the enterohepatic circulation of bile acids. The driving force for both NTCP and ASBT is Na^+ gradients. As reviewed by Hagenbuch and Dawson [43], computer-based analyses suggested a seven-transmembrane topology for all members of the SLC10 family, but a nine-transmembrane structure based on experimental evidence for NTCP and ASBT is more likely [45,46] (for review, see [43]) (Fig. 2A). As shown by Schroeder et al. [47], NTCP also reveals transport capacity for sulfated steroid hormones, namely E_1S. Apart from NTCP and ASBT, some novel members of the SLC10 family have been identified and were classified as *SLC10A3-SLC10A7* [44]. Most still represent orphan carriers, because no substrates have been identified to date, but species-specific

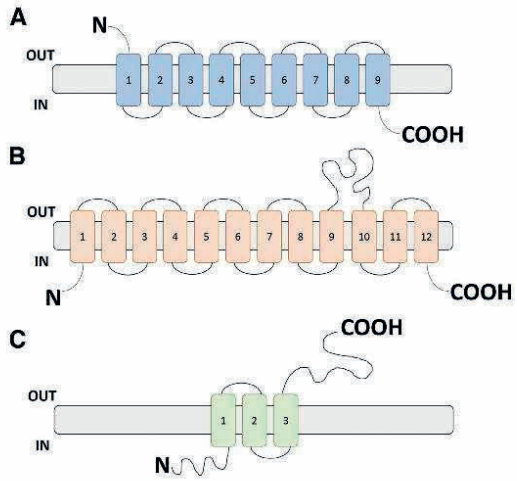

Fig. 2. Scheme of the membrane topologies of the Solute carriers NTCP and SOAT (A), for OATPs (B) and OSCP (C).
A Members of the SLC10 family consists of nine TMDs with an outward facing N-terminus and an inward facing C-terminus (e.g. NTCP and SOAT).
B Members of the OATP family reveal twelve TMDs with N- and C-terminus both facing to the intracellular space. Notice the prominent extracellular loop between TMD 9 and 10.
C OSCP1 exhibits only three TMDs, an inward facing N-terminus and an outward facing C-terminus. Other groups stated OSCP1 to be a soluble and cytoplasmically located protein.

expression patterns have been intensely analyzed [48–52]. However, one of these new members could be deorphanized, namely *SLC10A6*, coding for the sodium-dependent organic anion transporter (SOAT). Soat was first cloned from the rat in 2004 [53] and later from humans [54]. SOAT also displays a nine-transmembrane topology with an outward facing N-terminus and reveals a very high sequence homology to ASBT [44,53]. SOAT showed no substrate specificity for bile acids at all, but proved to be a highly specific transporter for sulfated steroids such as E_1S and DHEAS. As for NTCP and ASBT, SOAT function relies on sodium-dependent co-transporting. In contrast to NTCP and ASBT, which are expressed in a cell-type-specific manner in either liver cells (and to a minor degree in the pancreas) or ileal brush border cells (for review, see [43]), the *SLC10A6* gene shows a broader expression pattern. Most interesting with regard to the sulfatase pathway is the predominant expression of *SLC10A6* in the human testis [44,53,55]. Also, *Slc10a6* is highly expressed in the testis in mouse – although the predominant expression was detected in the lung [56].

Apart from sodium-dependent uptake carriers, sodium-independent transporters are also known and have been termed organic anion transporting polypeptides (human: OATP, rodents: Oatp). All OATP carriers belong to the SLC family SLCO (O=OATP). Although common characteristics of these transporters are species divergence, multi-specificity, and wide tissue distribution (for review, see [42,57]), some OATPs/*Oatps* show a very specific expression pattern and substrate specificity. In contrast to the SLC10 family, members of the OATP family reveal twelve transmembrane domains (TMDs), with an extracellular N-terminus and C-terminus (Fig. 2B). A large extracellular loop can be found between TMD 9 and 10. As reviewed by Hagenbuch and Meier [57], their transport mechanism relies on anion exchange, i.e. the cellular uptake of organic compounds coupled with the efflux of anionic substrates such as bicarbonate, in a process that seems to be pH-dependent and electroneutral. Additional to different amphipathic compounds, many OATPs/Oatps are also able to transport steroid hormones and their conjugates. All members of the OATP1 family, namely OATP1A2, OATP1B1, OATP1B3 and OATP1C1 in humans transport sulfated steroid hormones. Regarding the OATP2 family, only members of the OATP2 B subfamily transport steroid conjugates such as E_1S and DHEAS, whereas members of the OATP2A subfamily are prostaglandin and thromboxane transporters. The OATP3 family consists of only one subfamily, OATP3A, in which OATP3A1 is able to transport E_1S beyond other substrates. Belonging to the OATP4 family, OATP4A1 and OATP4C1 are able to transport E_1S. The substrate pattern for OATP5 and OATP6 families is still under investigation, although the expression pattern is already well known (for review, see [57,58]).

In 2005, Kobayashi et al. [59] isolated a novel polyspecific organic solute carrier protein in the human placenta and testis known as organic solute carrier protein 1 (OSCP1). It proved able to transport E_1S aside from other components. In contrast to other known OATPs, OSCP1 most likely displays only three TMDs (Fig. 2C). Approximately two years later, the same group reported the cloning of murine Oscp1 with a slightly different substrate pattern; in contrast to OSCP1, Oscp1 transported DHEAS instead of E_1S [60].

Members of the ATP-binding cassette (ABC) transporter superfamily, which function as efflux transporters to eliminate substrates from the cell, are able to transport sulfated steroids. As ABC transporters are primary active transporters, they are able to transport against a considerable substrate gradient [61]. An elimination can be observed with endogenous and exogenous substances and is often related to epithelial cells at blood-tissue barriers such as BBB and BTB, in a phenomenon that has been called “multidrug resistance”. As a milestone, this has been described by Juliano and Ling [62] at the molecular level. They discovered a 170 kDa glycoprotein within the cell membrane of Chinese hamster ovary cells, which showed resistance against a wide range of cytotoxic drugs, and named it P-glycoprotein (P-gp, syn. multidrug resistance carrier MDR1). Later, the coding gene was discovered and classified as *ABCB1* in humans. In the mouse, two *Abcb1* genes are present, namely *Abcb1a* and *Abcb1b*. Beyond P-gp/MDR1, the ABC transporter superfamily consists of at least ten more members of different structures, tissue distribution patterns and transporting abilities, i.e. multidrug resistance-related proteins 1–9 (MRP1-9, *ABCC1-9*) and breast cancer resistance protein (BCRP, *ABCG2*) (for review, see [63]). All of them play a pivotal role in drug metabolism. Based on their two-dimensional structure in the plasma membrane, ABC transporters can be divided into three classes structurally (Fig. 3). P-gp/MDR1 as a “standard” ABC transporter is constructed of two identical parts, each consisting of six TMDs and two intracellular nucleotide binding domains (NBDs) as ATP binding sites. The first extracellular loop is *N*-glycosylated. The N- and the C-terminus are located intracellularly (Fig. 3A). MRP1-3 additionally present an N-terminal extension consisting of five TMDs and is *N*-glycosylated near the (extracellular) N-terminus and the sixth extracellular loop (Fig. 3B). MRP4 and MRP5 are very similar to P-gp, with the *N*-glycosylation site at the fourth extracellular loop. BCRP has a special position, as it is a “half transporter”, consisting of only six TMDs and only one NBD at the N-terminal end. The *N*-glycosylation site is most probably located in the third extracellular loop (Fig. 3C). P-gp/MDR1 was found to be located in various human tissues and tumors, but also in the endothelial cells of brain and testis, the BTB and the blood-brain barrier (BBB) [63–67]. In the brain and testis, P-gp/MDR1 is a known efflux transporter for drugs, e.g. ivermectin hypersensitivity of certain dog breeds is related to a defect in the canine *Mdr1* gene [68]. To date, the transport ability of P-gp/MDR1 for sulfated steroids has not been described. Nevertheless, P-gp/MDR1 as the first ABC transporter described in the testis opened up discussion on other members of this transporter family and their significance for a functional sulfatase pathway, either in the testis or in other organs such as breast tissue as well as pathological conditions such as breast cancer.

Other members of the ABC carrier family, apart from MDR1 P-glycoprotein, are the MRPs and BCRP. Most play important roles for drug transport and pharmacokinetics [63]. MRP1 is known to be expressed ubiquitously in the human body. It is the most abundant ABC

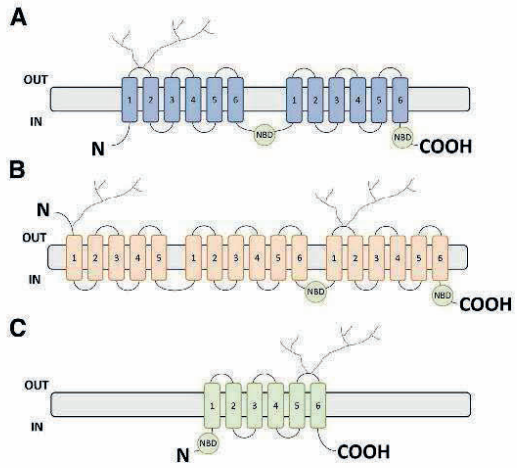

Fig. 3. Scheme of membrane topologies of different ABC transporters.
A ABC transporters such as MDR1/P-gp consist of two transmembrane segments with six TMDs each and two intracellularly located nucleotide binding domains (NBDs) as ATP binding sites.
B The structures of the MRPs are preceded by an additional N-terminal transmembrane segment with five TMDs and two N-glycosylation sites.
C Some ABC transporters, such as BCRP, are so-called "half transporter" and constitute a full transporter in the plasma membrane.

transporter in the testis [69,70], where it is located in the basolateral membrane of the Sertoli cells [71]. Even more interestingly, MRP1 is capable of transporting sulfated steroid hormones like DHEAS and E_1S [72] (for review, see [69,70]). As reviewed by Slot et al. [70], MRP2, MRP3, MRP4, MRP6 and MRP8 also exhibit transport capacities for sulfated steroid hormones such as E_1S and/or DHEAS [70]. Like MRP1, the other members of this group are expressed in almost all tissues of the body with very high expression levels in the liver, kidney and small intestine. In contrast, MRP5 shows a more specific expression pattern as it is concentrated in the brain, heart, placenta, and muscle. Apart from MRP1 and MRP4, MRP8 is also expressed in the human testis and has transport activity for E_1S [69].

BCRP was initially cloned from the breast cancer cell line MCF7 and contributes to the chemotherapy-resistant phenotype of these cells (for review see [63]). Its expression in the cell membrane is regulated by sex hormones [73], contributing to the hypothesis of a hormone-dependent cancer promoter. As reviewed by Qian et al. [74], BCRP is not only expressed in cancer cells, as believed for a long time but also in various organs like the brain, intestine, placenta, and healthy breast tissue as well as in the testis. Besides many drugs and xenobiotics, BCRP also reveals transport activity for sulfated steroid hormones such as DHEAS and E1S [69]. As hypothesized by Dankers et al. [73], BCRP might also be involved in the uptake of E_1S under sex hormone administration.

3. Expression pattern for uptake carriers, efflux transporters, and steroid sulfatase in the human testis

In contrast to NTCP, the homolog SOAT is predominantly expressed in the human testis and its substrate pattern is restricted to sulfated steroids. Apart from the testis, SOAT is also expressed to a minor extent in the placenta, lung, and skin [44,53,55]. The high expression in the testis made SOAT a promising candidate for the accumulation of sulfated steroids in the testis. After cleavage by steroid sulfatase STS, these precursor molecules can be converted to biologically active estrogens and androgens, which are well-known regulators of spermatogenesis. Therefore, SOAT could be the missing link to explain a functional sulfatase pathway in the human testis, which was previously hypothesized. Fietz et al. [53] analyzed the cellular expression in the human testis for the first time. SOAT is solely expressed in germ cells, as shown by mRNA and protein levels by various histological and molecular techniques. At the cellular level, SOAT protein was detected in zygotene spermatocytes up to round spermatids. In spermatocytes, SOAT protein accumulates in a small ovoid-shaped area near the nucleus and is co-localized to GOLGIN A2, a marker for the Golgi apparatus [55]. As SOAT is neither detected in interstitially located Leydig cells (main location for steroid hormone synthesis in the testis) or in tubular Sertoli cells, SOAT most likely has a more specific function in later germ cell development.

The second transporter family of interest is the SLCO family of organic anion transporting polypeptides (OATPs). As these transporters mainly exhibit a broad expression pattern and substrate specificity, analyses of this family are more complex. Within the OATP1 family, OATP1A2 and OATP1C1 are of interest in the testis. As OATP1A2 is expressed throughout the whole body, its localization in the testis was not further investigated [75] (for review, see [58]). With this expression pattern, OATP1A2 is thought to be involved in the absorption, distribution, and excretion of various endogenous and exogenous metabolites. Its expression in the endothelial cells of brain capillaries suggests an involvement in the formation of BBB [76]. As reviewed by Roth et al. [58], OATP1A2 presents an extremely wide substrate portfolio with diverse xenobiotics and sulfated steroids such as DHEAS [77] and E_1S [78]. The precise localization of OATP1A2 within the testis, i.e. the cellular expression pattern, would be extremely interesting in regard to sulfatase pathway contribution. OATP1C1 was initially localized in either the brain or the testis [55,79,80] (for review, see [58]). In the testis, OATP1C1 was located in interstitial Leydig cells. As it is able to transport E_1S, OATP1C1 could be involved in the local supply of Leydig cells with sulfated steroids and therefore testosterone synthesis. In the brain, OATP1C1 was detected in the basolateral membrane of the plexus choroideus epithelial cells. Within the OATP2 family, only OATP2B1 is of interest concerning possible involvement in a testicular sulfatase pathway. OATP2B1 is expressed in almost all tissues of the body [81] (for review, see [58]), but was also detected in breast cancer [82,83]. Its ability to transport E_1S and DHEAS has been shown by various groups [75,80,84,85]. Its cellular expression in the testis has most recently been studied by Hartmann et al. [86]. By using either histological or molecular techniques, OATP2B1 was localized at the mRNA and protein levels in somatic Sertoli and Leydig cells as well as germ cells (pachytene spermatocytes and elongating spermatids). Within Sertoli cells, expression was located near the basolateral membrane [86]. In its transporting function, OATP2B1 proved to be both pH-dependent [84] and hormone-dependent [85]. In the latter study, it was demonstrated that testosterone is a potent inhibitor of OATP2B1 function, whereas progesterone and gestagens enhance the transporting ability. As reported for OATP2B1, OATP3A1 is expressed in various tissues. Its abundant expression has been detected mainly in the heart, testis, brain and some cancer cells [82,87]. Two splicing variants of OATP3A1 exist, named OATP3A1_v1 and OATP3A1_v2, showing a differential expression pattern in the testis [88]. Whereas OATP3A1_v1 is expressed in germ cells, OATP3A1_v2 is localized in Sertoli cells. Only the first variant is able to transport E_1S [81]. Hartmann et al. [86] analyzed the cellular expression of OATP3A1_v2 in the human testis and localized it either in germ cells (round and elongating spermatids), or Sertoli and Leydig cells, at both the mRNA and protein level. Comparable to OATP2B1, this group detected OATP3A1_v2 in the basolateral membrane of Sertoli cells. Both uptake carriers may be involved in a putative sulfatase pathway due to this cellular localization. Another member of the OATP family, which is mainly expressed in the testis, is OATP6A1, as demonstrated by Fietz et al. [55] by means of RT-qPCR of multiple cDNA panels. Comparable to SOAT, OATP6A1 is expressed in germ cells only, but neither in Sertoli, nor in Leydig cells, as analyzed

Table 1
Summary of uptake carriers and efflux transporters expressed in the testis with transport ability for sulfated steroid hormones.

Family	Protein (MAN, rodents)	*Gene (MAN, rodents)*	Tissue expression	Transport ability	Reference	Additional data (HPA)
SLC Slc	SOAT	*SLC10A6*	testis (spermatocytes, spermatids), placenta, lung, skin,	DHEAS, E_1S, PREGS, androstenedione sulfate, estradiol-3-sulfate	[44,53,55]	tonsils, esophagus, prostate, breast
	Soat	*Slc10a6*	lung (respiratory epithelium), skin (basal epidermis layer), bladder, testis (spermatocytes, spermatids)	DHEAS, E_1S, PREGS	[56]	n.a.
	OATP1A2	*SLCO1A2*	ubiquitously, testis, brain (capillaries, BBB)	DHEAS, E_1S	[58,75–78]	n.a.
	Oatp1a1	*Slco1a1*	rat Sertoli cells	n.s.	[101]	n.a.
	Oatp1a4	*Slco1a4*	liver, brain, testis	n.s.	[58]	n.a.
	Oatp1a5	*Slco1a5*	testis	n.s.	[99]	n.a.
	OATP1C1	*SLCO1C1*	brain (plexus choroideus), testis (Leydig cells)	E_1S	[55,58,79,80]	n.a.
	Oatp2	*Slco2*	rat Sertoli cells	n.s.	[101]	n.a.
	OATP2B1	*SCLO2B1*	ubiquitously, breast cancer, testis (germ cells, Sertoli cells, Leydig cells)	DHEAS, E_1S	[58,75,81–86]	endocrine glands, muscle, lung, liver, pancreas, salivary gland, stomach, breast, ovary
	Oatp2b1	*Slco2b1*	ubiquitously	n.s.	[58]	n.a.
	Oatp3	*Scla3*	rat Sertoli cells	n.s.	[101]	n.a.
	OATP3A1	*SLCO3A1*	ubiquitously, heart, testis, brain, cancer cells	E3S	[82,87]	n.a.
	OATP3A1_v1		testis (germ cells)		[81,88]	n.a.
	OATP3A1_v2		testis (Sertoli cells, Leydig cells, germ cells)	n.s.	[86,88]	n.a.
	Oatp3a1	*Slca3a1*	kidney, lung, testis	n.s.	[58]	n.a.
	Oatp4	*Slco4*	rat Sertoli cells	n.s.	[101]	n.a.
	Oatp5	*Slco5*		n.s.	[101]	n.a.
	Oatp5a1	*Slca5a1*	ubiquitously, testis	n.s.	[58]	n.a.
	Oatp6	*Slco6*	rat Sertoli cells	n.s.	[101]	n.a.
	OATP6A1	*SLCO6A1*	testis (germ cells)	n.s.	[55]	
	Oatp6b1, Oatp6c1,	*Slco6b1, Slco6c1,*	testis, rat Sertoli cells	DHEAS	[99–101]	n.a.
	Oatp6d1	*Slco6d1*				
	Oatp7	*Slco7*	rat Sertoli cells	n.s.	[101]	n.a.
	Oatp8	*Slco8*	rat Sertoli cells	n.s.	[101]	n.a.
	Oatp9	*Slco9*	rat Sertoli cells	n.s.	[101]	n.a.
	Oatp12	*Slco12*	rat Sertoli cells	n.s.	[101]	n.a.
	Slc15a1	*Slc15a1*	testis (BTB)	n.s.	[67]	n.a.
	OSCP1	*OSCP1*	placenta, testis (germ cells)	E_1S	[55,59,60]	brain, endocrine glands, appendix, tonsil, muscle, lung, liver, gall bladder, pancreas, stomach, gut, urogenital system, skin
	Oscp1	*Oxcp1*	testis (germ cells, Sertoli cells)	DHEAS, E_1S	[60,102,103]	n.a.

(*continued on next page*)

Table 1 (*continued*)

Family	Protein (MAN, rodents)	*Gene* (*MAN, rodents*)	Tissue expression	Transport ability	Reference	Additional data (HPA)
ABC Abc	MRP1	*ABCC1*	ubiquitously, testis (Sertoli cells, Leydig cells), Sertoli cell cultures	DHEAS, E_1S	[69–72,86,93]	brain, bone marrow and immune system, lung, gall bladder, pancreas, gut, kidney, fallopian tube, endometrium, ovary, fat, skin
	Mrp1	*Abcc1*	testis (Sertoli cells)	n.s.	[67,101]	n.a.
	MRP2	*ABCC2*	ubiquitously	DHEAS, E_1S	[70]	bone marrow and immune system, liver, gall bladder, small intestine, rectum, kidney, bladder, male genital system, fallopian tube, placenta, skin
	MRP3	*ABCC3*	ubiquitously	DHEAS, E_1S	[70]	endocrine glands, appendix, muscle, lung, gall bladder, pancreas, gastrointestinal tract, urogenital tract, skin
	MRP4	*ABCC4*	ubiquitously, testis (Sertoli cells, Leydig cells), Sertoli cell cultures	E_1S	[69,70,86,92]	brain, colon, prostate
	Mrp4	*Abcc4*	testis (Leydig cells)	DHEAS	[94,101,136]	n.a.
	Mrp5	*Abcc5*	testis (Sertoli cells)	n.s.	[67,101]	n.a.
	MRP6	*ABCC6*	ubiquitously	DHEAS, E_1S	[70]	n.a.
	Mrp7	*Abcc7*	testis (Sertoli cells)		[101]	n.a.
	MRP8	*ABCC8*	testis	DHEAS, E_1S	[69,70]	brain, endocrine glands, pancreas, gut, female and male genital tract
	Mrp8	*Abcc8*	testis (Sertoli cells)	n.s.	[101]	n.a.
	BCRP	*ABCG2*	brain, intestine, placenta, breast tissue, testis (capillary endothelium, myoid cells), diverse cancer cell lines, Sertoli cell cultures	DHEAS, E_1S	[69,74,92,95]	brain, endocrine glands, muscle, lung, gut, seminal vesicle, placenta
	Bcrp	*Abcg2*	testis (capillaries, myoid cells, Sertoli cells), brain (BBB), placenta, Sertoli cell cultures	DHEAS	[73,92,104]	n.a.

HPA Human Protein Atlas (www.proteinatlas.org); please note, that only organs showing both mRNA and protein expression have been listed in this table.
n.a. not applicable; n.s. not stated.

in rat and mouse testis and involved in BTB formation [66,67,92,101]. In 2002, P-gp/Mdr1 was detected in interstitial cells as well as in late spermatids and also Sertoli cells of mice and rats. Some years later, Mdr1a, Mdr1b, and Mdr2 were demonstrated to be expressed only at low levels in isolated rat Sertoli cells and in whole testis samples, whereas many multidrug resistance related proteins, namely Mrp1, Mrp5, Mrp7, and Mrp8, were expressed at higher levels in Sertoli cells. Mrp4 was only weakly expressed in the rodent testis. Su et al. [67] localized Mdr1 in all stages of the rat spermatogenic cycle and in Sertoli cells shortly before sperm release at stage VIII in the rat. The same group also detected *Mrp1* and *Mrp5* to be expressed in the rat testis, consistent with that reported by Augustine et al. [101]. Also in isolated murine Sertoli cells, Robillard et al. [92] showed the expression of P-gp/Mdr. The last ABC transporter to be reviewed in this work is Bcrp, which is also expressed in the murine testis. There, it is detectable in blood capillaries [73], but also in Sertoli cells [92]. As reviewed by Qian et al. [104], rat Bcrp is able to transport DHEAS and is expressed in many different tissues, e.g. testis, brain, placenta, and intestine. Although it is part of the BBB, it is not part of the BTB in a classical sense, as it is only expressed in endothelial cells and peritubular myoid cells. Nevertheless, Bcrp reveals a temporal expression in rat Sertoli cells of stages VI to VIII, more precisely at the apical Sertoli cell-spermatid interface around sperm release [105]. Moreover, Bcrp was described as a gatekeeper of the blood-tumor barrier (for review, see [104]). Regarding Sts expression and activity in rodents, early studies describe PREGS as the preferred substrate for Sts in the rat testis, but it also shows activity for the cleavage of DHEAS, E_1S and other sulfated steroids [106]. Erickson et al. [107] described enzyme activity and efficiency variations between different mouse strains, which were autosomal and not X-linked, as described for STS deficiencies in humans. *Sts* is expressed mainly in Leydig cells in the microsomal fraction. As testosterone levels are altered in undescended testis, its activity was analyzed in unilaterally cryptorchid mouse and rat testes. There, its activity proved to be higher in the descended testes, implicating a direct link for *Sts* in testosterone production [13,108]. For summary, see Table 1.

5. Biological significance of sulfated steroid hormones and their transporters in humans and rodents

In humans and rodents, uptake carriers and efflux transporters can be detected in diverse cell populations of the testis, e.g. Sertoli cells, and even more precisely at the BTB. The additional expression of STS in all testicular cell types implicates the presence of a functional sulfatase pathway in the testis. Therefore, sulfated steroids can no longer be considered only as metabolites ready for excretion, but as steroid hormone precursor molecules [109–111] for the on-site generation of free, unbound steroid hormones by STS activity. These steroid hormones interact with intracellular AR and ESRs, respectively. Both play an important role in spermatogenesis [1,29] and are expressed in different testicular cell populations [31,112] (for review, see [113]). Moreover, the ability of DHEAS to bind to membrane-bound ARs has been recently published [34,35], implicating an additional role of sulfated steroid hormones in the activation of non-genomic signaling pathways, which has been largely described in the testis (for review see [33]). The co-localization with diverse uptake carriers, efflux transporters and STS in Sertoli and germ cells inside the seminiferous tubules might hint at a para- as well as intracrine mechanism for the sulfatase pathway. This was compiled by Luu-The et al. [111] and referred to as the "front-door" and "back-door" pathways for active sex steroids such as testosterone, dihydrotestosterone (DHT) and estrone. In this context, sulfated steroids can be regarded as a local supply for steroid synthesis in specific target cells and are therefore in general released into circulation (for review see [114]).

Since sex steroids such as testosterone and estrogens and their action at their receptors are essential for either the initiation or maintenance of spermatogenesis, sperm maturation (for review see [1,29]) and epididymal transport (for review, see [115]), disturbances in the local supply for steroid synthesis by defective and/or missing transporting systems may lead to male sub- or infertility. Disturbances of spermatogenesis have been extensively reviewed by Nieschlag et al. [116]. Impairments of spermatogenesis can occur at various levels, e.g. hypospermatogenesis (qualitatively preserved, but quantitatively reduced spermatogenesis), spermatogenic arrest at the levels of spermatogonia, spermatocytes, and spermatids, respectively, as well as total germ cell aplasia (SCO) (for review, see [117]). A special clinical manifestation of impaired spermatogenesis is the so-called "mixed atrophy", in which tubules showing normal and impaired spermatogenesis are concomitantly present within one biopsy [117,118]. Often, these patients are referred to as subfertile because single tubules with elongated spermatids can be found and employed for testicular sperm extraction techniques and artificial reproduction. To a large extent, the reasons for the sub- and infertility are not known, but altered expression patterns and functions of steroid hormone receptors (as analyzed by [31,112,119]) and both uptake carriers and efflux transporters in different clinical manifestations may provide an explanation for the disturbances of spermatogenesis. An analysis of uptake carriers and efflux transporters using both biopsies with impaired spermatogenesis and knockout mouse models are extremely valuable for their biological significance in human and animal reproduction.

For this purpose, the expression of SOAT was assessed in normal and impaired spermatogenesis and is significantly reduced in hypospermatogenesis. SOAT levels were reduced, although all cells expressing SOAT in normal spermatogenesis were still present, hinting at a possible involvement of SOAT in the development of hypospermatogenesis but requiring more investigation [55]. To elucidate this observation, non-synonymous single nucleotide polymorphisms (SNPs) in the *SLC10A6* gene have been analyzed either *in vitro* with regard to their transport capacity [120]or *in vivo* regarding their expression pattern in normal spermatogenesis and hypospermatogenesis [121]. Most recently, an *Slc10a6*$^{-/-}$ knockout mouse has been created and used for reproductive phenotyping [122]. As human and mouse SOAT/Soat are solely expressed in germ cells [55,56], they are most likely not involved in the Sertoli cell sulfatase pathway. Their biological significance may be connected to CS transport into the Golgi compartment of germ cells, which becomes the acrosomal cap during spermiogenesis. This has already been analyzed earlier by the injection of radiolabelled CS in rats followed by a whole body autoradiography, which revealed signals in stomach, intestine, but also in testis and epididymis [123]. Langlais et al. [124] described CS to be a physiological component of human spermatozoa and found it to be mainly located in the sperm head and the midpiece of the tail. Moreover, they described an avid uptake of CS by spermatozoa by light microscope radiography. In spermatozoa and seminal plasma, CS represents more than 85% of sulfated steroids, with most of it being taken up during the epididymal passage of sperm [125]. As reviewed later by Strott and Higashi [126], plasma levels of CS exceed DHEAS levels. CS plays important roles in human physiology since it is thought to act as a powerful regulator of serine proteases and to be involved into cell membrane stabilization [127]. Since CS can also inhibit the activity of acrosin, a protease involved in the acrosome reaction, it is thought to be important for sperm capacitation. Hydrolysis of CS within sperm membranes may lead to destabilization of the membrane and therefore the initiation of sperm capacitation. Relatively high amounts of CS in the epididymis and the whole male reproductive tract inhibit the sperm from a preterm acrosome reaction (for review, see [126]). *In vitro* experiments showed that low concentrations of CS inhibit the capacitation and the activity of acrosin, the sperm acrosomal proteinase responsible for penetration of the zona pellucida of the ovum [128]. In the female reproductive tract, CS then is cleaved by STS activity leading to the acrosome reaction and fertilization. Bleau et al. [127] described CS as a membrane stabilizer of the erythrocyte membrane. In spermatozoa, CS seems to possess the same function in order

by RT-PCR following laser-assisted cell picking technique. OATP6A1 is a tissue-specific uptake carrier, but it is also expressed in various cancers, like lung, bladder, and brain. Its presence in these cancer types makes it a promising biomarker (for review, see [89,90]). OSCP1 has already been described in human and rodent testis [55,60,91]. In the human testis, OSCP1 has been localized in germ cells only and not in Sertoli cells. This has been confirmed in testicular samples showing normal spermatogenesis and Sertoli-cell only syndrome (= SCO, total germ cell aplasia), respectively [55].

Regarding efflux transporters, P-gp/MDR1 was identified in the human testis [66,71,92]. It is assumed to be a part of the BTB in the human testis due to its expression in myoid cells in the tubular wall as well as in blood vessel endothelial cells [66,71]. Here, P-gp/MDR1 is able to eliminate endogenous and exogenous substances into the blood stream and prevent other testicular cells from contact with these harmful substances. Moreover, Bart et al. [71] described this efflux transporter in Leydig cells. Contrasting this, Melaine et al. [66] also localized P-gp/MDR1 in the germ cells of humans, rodents and guinea pigs. They detected this protein solely in late germ cell stages as early and late elongating spermatids. Spermatogonia and spermatocytes did not express the efflux transporter. This might explain why earlier germ cell stages reveal a higher vulnerability against anticancer drugs [66]. Moreover, Robillard et al. [92] detected P-gp/MDR1 in human cultured Sertoli cells where it was able to transport different xenobiotics. To date, no substrate specificity for sulfated steroids has been identified for P-gp/MDR1. Therefore, previous focus of interest was more on the diverse multidrug resistance-related proteins (MRPs), which show transport ability for DHEAS and/or E_1S [70,72,93] (for review, see [69]). MRP1 is known to be located ubiquitously in the human body and is the most abundant ABC transporter in the testis (for review see [69]), where it is located in the basolateral membrane of Sertoli cells [72] and is also expressed in cultured Sertoli cells [92]. Comparable to MRP1, MRP4 is ubiquitously expressed in the human body, including a moderate expression level in the testis [70], where MRP4 was localized to Leydig cells. Here, MRP4 seems to play a role in testosterone synthesis or release [94]. Furthermore, MRP4 was detected in mouse and human Sertoli cell cultures [92]. Apart from MRP1 and MRP4, MRP8 is also expressed in the human testis and has transport activity for E_1S (for review see [69]). Most recently, MRP1 and MRP4 expression have been analyzed in human testicular biopsies displaying normal spermatogenesis and SCO to differentiate between germ cell and Sertoli cell expression; in both sample types, MRP1 and MRP4 were detected in Sertoli and Leydig cells only [86]. The last member of the ABC transporter superfamily of interest with regard to involvement in the sulfatase pathway is BCRP. Although described in breast tissue and breast cancer in more detail, BCRP has also been detected in the human testis. There, BCRP was localized in the apical cell membrane of blood capillary endothelial cells and in the apical domain of the myoid cells surrounding the seminiferous tubules, where it is co-expressed with P-gp [95]. Furthermore, BCRP expression was detected in human Sertoli cell lines [92].

To summarize the situation in the human testis, many uptake carriers (SOAT, OATP1A2, OATP1C1, OATP2B1, OATP3A1, OATP6A1, and OSCP1) and efflux transporters (P-gp/MDR1, MRP1, MRP4, MRP8, and BCRP) were detected in this organ, in some cases even predominantly (SOAT, OATP6A1). Whereas some are solely expressed in human germ cells, others are expressed in more or less all testicular cells including somatic Leydig and Sertoli cells, endothelial and tubular myoid cells. The hypothesis of a sulfatase pathway in the testis to create a local supply for steroid hormone synthesis by a pool of conjugated steroid hormones with a longer half-life seems to be appropriate. The last missing link for a sulfatase pathway is the enzyme STS, which cleaves the sulfate residue and re-activates the conjugated steroid. As shown decades ago, STS is an almost ubiquitously expressed enzyme with an additional moderate expression in the human testis [96] (for review, see [97,98]) and able to cleave E_1S and DHEAS into estrone and DHEA, respectively. The enzyme is mainly localized to Leydig cells and expressed in two possible isoforms, which are either microsomal (e.g. in the rough endoplasmic reticulum) or nuclear. As reviewed by Reed et al. [97], STS action can be regulated by steroid hormones such as androgens, estrogens, and gestagens. In the testis, the hydrolysis of sulfated steroids contributes to overall steroid hormones synthesis. Most recently, STS was located in the human testis at a cellular level within all cells (Sertoli, Leydig, and germ cells, more precisely in elongated spermatids) of the normal testis [86]. This was confirmed histologically at the mRNA and protein level, as well as using different molecular biological techniques.

For a summary of SLC and ABC transporters expressed in the testis which are able to transport sulfated steroid hormones, please refer to Table 1.

4. Expression pattern for uptake carriers and efflux transporters in the rodent testis

With regard to the human testis, the expression pattern for uptake carriers and efflux transporters will be summarized here for rats and mice. Although *Slc10a6* (Soat) is expressed in the mouse testis, it is not predominantly expressed in this organ. The predominant expression of Soat was demonstrated in the lung of different mouse strains. Other organs expressing Soat were skin, bladder, and heart [56]. In the testis, Soat was expressed consistently with human SOAT in germ cells only, but not in Sertoli or Leydig cells. In contrast to the situation in humans, Soat protein expression started earlier in the mouse, i.e. in preleptotene spermatocytes at the onset of meiosis, and lasted until the elongating spermatids of stage X and XI. In the pachytene spermatocytes, Soat was equally detected in an ovoid-shaped area next to the nucleus, most probably representing the Golgi apparatus, comparable to the situation in humans [56].

Members of the SLCO family are also detected in rodent testis, as summarized by Roth et al. [58], where corresponding human and rodent genes and proteins are also listed. In the rat, five genes exist in the Slco1 subfamily: *Slco1a1, Slco1a3, Slco1a4, Slco1a5,* and *Slco1a6*. Except for *Slco1a3*, ortholog genes exist in the mouse. Whereas *Sloc1a1, Slco1a4,* and *Slco1a6* are predominantly expressed in the liver, kidney and/or brain and partly reveal a gender- and/or age-dependent expression pattern, *Slco1a5* is mainly expressed in the murine testis [99]. Although the main expression site was identified in the liver and brain, *Slco1a4* expression can also be detected in the testis of the mouse. In contrast to the situation in humans, Oatp1c1 in the mouse is exclusively expressed in the brain [99]. Comparable to humans, Oatp2b1 is ubiquitously expressed in the mouse. Oatp3a1 was detected to a minor level in the testis, but its expression was highest in the kidney and lungs. In contrast to the situation in humans, where OATP5A1 has shown no expression in the testis, Oatp5a1 exhibits at least low expression levels in the testes. Homologs of human gonad-specific *OATP6A1*, *Oatp6b1, Oatp6c1,* and *Oatp6d1,* are also mainly expressed in the rodent testis [99,100], and are able to transport DHEAS into testicular cells. As presented by Su et al. [67], *Slc15a1* is expressed in the testis and is likely involved in building the BTB together with diverse efflux transporters. The expression of uptake carriers in isolated Sertoli cells and their involvement in the BTB was assessed by Augustine et al. [101]; this group detected diverse xenobiotic and endobiotic transporters in isolated rat Sertoli cells, i.e. Oatp1-9, Oatp12, Tst1 and Tst2 (the latter also known as Oatp6b1 and Oatp6c1). Only the last two genes were mainly expressed in isolated rat Sertoli cells and in whole testis samples. Another uptake carrier first described in mice and rats is Oscp1. It is expressed predominantly in the testis, more specifically in mouse germ cells, e.g. spermatogonia, but also in the basal membrane of murine Sertoli cells. Oscp1 is able to transport E_1S, DHEAS and taurocholate [60,102,103].

The expression of ABC transporters in the rodent testis is comparable to the situation in humans, as stated above. P-gp/Mdr is expressed

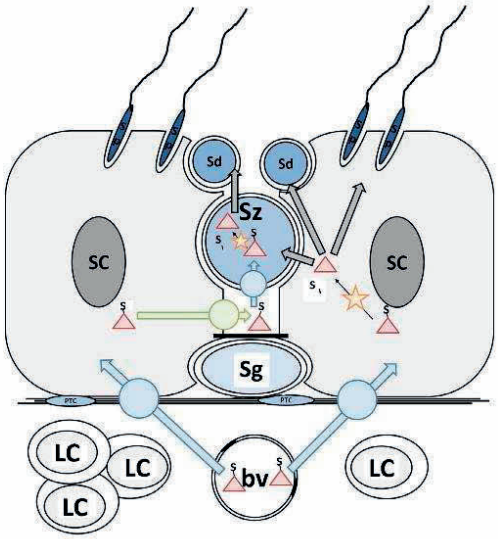

Fig. 4. Summary of possible sulfatase pathway in the human testis.
Sulfated steroids (red triangle plus "S") can be taken up by specific uptake carrier (blue, e.g. OATP2B1, OATP3A1) into Sertoli cells. From there, two possible sulfatase pathways are likely in germ cells (left) and Sertoli cells (right).
Left: For a sulfatase pathway in germ cells, sulfated steroids are transported out of the Sertoli cells by specific efflux transporters (green, e.g. MRP1, MRP4) into the intercellular space above the BTB. From there, they can be taken up by germ cells (blue, e.g. SOAT, OATP2B1, OATP3A1, OATP6A1, OSCP1) and re-activated by STS activity (orange star). As free steroid hormones (red triangle), they are now able to pass through cell membranes by diffusion (gray arrow).
Right: In Sertoli cells, sulfated steroids may not only be transported but can also be re-activated by STS activity and pass from Sertoli cells to germ cells as free steroids by diffusion.
SC: Sertoli cells; Sg: spermatogonia; Sz: spermatocytes; Sd: round spermatids; Sp: elongated spermatids; bv: blood vessels; LC: Leydig cells; PTC: peritubular cells

to prevent the release of acrosomal enzymes during passage and storage in the male reproductive tract [129]. CS is able to interact with phospholipids, in order to bind to the cell membrane leading to enhanced cholesterol/phospholipid ratios and membrane stabilization [124]. After cleavage of the sulfate group by STS, the cholesterol/phospholipid ratio decreases and results in profound changes in membrane fluidity and permeability. This initiates the acrosome reaction and fertilization. As the serum CS levels are significantly elevated in the male *Slc10a6*$^{-/-}$ knockout mice [122], SOAT/Soat might be involved in acrosomal cap formation and post-testicular functions of sperm in the female. Altered expression patterns of the *SLC10A6/Slc10a6* gene and the function of the SOAT/Soat protein may not directly lead to defective germ cell development or loss, but to an impaired sperm function.

In contrast to SOAT/Soat, only a few links between diseases and altered functions of OATPs have been drawn so far, particularly focusing on the effects on drug disposition (for review, see [58]). The altered expression of OATPs or SNPs and therefore the different metabolism of diverse drugs may also influence pharmacokinetics in the testis and subsequently the effect on drugs on spermatogenesis. The main focus of OATP significance in diseases was placed on the expression pattern in cancer tissue vs. normal tissue. Here, OATP2B1 and OATP3A1 should be mentioned, as these have been detected in breast cancer tissue [82,83] and OATP6A1 and OSCP1; all were analyzed in normal as well as in impaired spermatogenesis [55,86]. OATP6A1 and OSCP1 were significantly reduced in the arrests of spermatogenesis at the level of spermatocytes and spermatogonia, as well as in SCO samples [55]. In contrast, OATP2B1 and OATP3A1 were expressed in all samples analyzed, unsurprisingly, as these two SLCO transporters are expressed in all testicular cell populations [86].

Much more is known about ABC transporters, as they are constantly in the focus of multidrug resistance phenomena. Therefore, many knockout mouse models have been generated to assess the biological function and significance of diverse efflux transporters. Schinkel et al. [65] generated *Mdr1* knockout mice (*Mdr1*$^{-/-}$) and identified P-gp as an important protective efflux system at the BBB and the BTB. The *Mdr1*$^{-/-}$ knockout mice revealed a normal phenotype, viability and fertility, but an increased sensitivity to ivermectin and many other drugs and xenobiotics [63,65,67]. It is well established that Mrp1 and Bcrp knockout mice are normal concerning viability and fertility [130,131]. In the case of *Abcc1* knockout mice, no alterations in litter size, growth and leukotriene C4 (LTC_4) were found [131] and histological examination "of most tissues and organs" did not reveal any abnormalities [130]. Homozygous Mrp1 knockout mice have an impaired response to inflammatory stimuli, probably because of the decreased secretion of LTC_4 [132]. However, it currently remains unclear whether testicular tissue has been specifically examined in regard to the spermatogenic status of these knockout mice. However, it has already been demonstrated that *Abcc1* knockout mice treated with etopophos [131] present an arrest of spermatogenesis at the level of spermatogonia or spermatocytes, indicating a lack of spermatogonia to undergo meiosis. Also, in the wild type controls, an impact of etopophos on spermatogenesis was noted, but to a minor degree. Unfortunately, Wijnholds et al. [131,132] did not publish any histological examinations from a non-treated control group, so that the effect of *Abcc1* knockout on normal spermatogenesis *per se* remains unknown. More recently, Sivils et al. [133] published that testicular testosterone, DHEA, estradiol, and androstenedione levels were 1.7- to 4.5-fold decreased in homozygous *Abcc1* knockout mice. Although this effect could not be fully explained, this indicates that Mrp1 is involved in the transport and distribution of steroid hormones in the testis. In common with the *Abcc1* knockout mice, *Abcg2*-deficient mice are viable and fertile. In comparison to wild type mice, no differences concerning lifespan, body weight, and growth ability were observed [134,135]. Although the *Abcc1* and *Abcg2* knockout mice are fertile, it remains unclear whether their spermatogenesis is fully preserved or diminished. Assem et al. [136] described a connection between Mrp4 and Sult2a1 expression in the liver, but did not describe the reproductive phenotype. In contrast, Morgan et al. [94] described Mrp4 to be mainly expressed in Leydig cells. In *Abcc4* knockout mice, testosterone production in Leydig cells was impaired due to altered cAMP homeostasis. In young mice, altered gametogenesis and reduced testicular testosterone levels were reported [94]. As described by Qian et al. [105], a knockdown of *Abcg2* in the rat testis perturbs the apical Sertoli cell-spermatid interface and leads to a loss of spermatid polarity in stage VII tubules, shortly before sperm release.

As mentioned above, STS expression pattern in health and disease, in normal and cancer tissue was the main focus of research for a long time. Shortly after the first description of the enzyme, its importance in the testis was emphasized by Lykkesfeldt et al. [24,25,137–139], as a deficiency of STS (also called X-linked ichthyosis) leads to an accumulation of CS in the skin and is thought to be accompanied by testicular deficiencies like maldescensus testes or testis cancer. These severe implications of STS deficiencies on male fertility were recently refuted in a review by Elias et al. [26], but fine-tuning of testicular function might be affected nevertheless. Although STS deficiency is most likely not the cause of testicular pathologies, it is thought to be a predisposition. Selcer et al. [20] detected the highest STS expression in hormone-dependent breast cancers, but STS was also expressed in healthy tissues. In the testis, Hartmann et al. [86] detected STS not only in normal spermatogenesis but also in all stages of spermatogenic impairment. By qRT-PCR, slightly altered, but not significantly different levels of STS expression were identified.

6. Summary

The expression pattern of uptake carriers and efflux transporters with specific transport ability for sulfated steroids, STS/Sts expression and colocalization with diverse steroid hormone receptors implicate a functional sulfatase pathway in the human and rodent testis. Additionally, two sulfatase pathways likely exist in humans due to their cellular localization in Sertoli cells and germ cells (Fig. 4). To date, experiments on the biological significance of these uptake carriers and efflux transporters on the development of spermatogenic disturbances and therefore infertility are still limited. First attempts have been made using both expression analyses in biopsies with impaired spermatogenesis and knockout mouse models. As a common mechanism, disturbed/missing/altered transport systems may be compensated by other transporters in the same organ or cell. Ongoing research revealing novel substrate specificities, tissue and cellular localization of these transporting systems will increase knowledge regarding the biological significance of sulfated steroids, the sulfatase pathway(s), uptake carriers and efflux transporters.

Acknowledgements

Own work reviewed here has been funded by the German Research Foundation (DFG) within the framework of Research Group 1369 “Sulfated Steroids in Reproduction” (DFG FI 1927/1-2).

References

[1] W.H. Walker, Molecular mechanisms of testosterone action in spermatogenesis, Steroids 74 (7) (2009) 602–607.
[2] R. Hähnel, E. Twaddle, T. Ratajczak, The specificity of the estrogen receptor of human uterus, J. Steroid Biochem. 4 (1) (1973) 21–31.
[3] G.G. Kuiper, B. Carlsson, K. Grandien, E. Enmark, J. Häggblad, S. Nilsson, J.A. Gustafsson, Comparison of the ligand binding specificity and transcript tissue distribution of estrogen receptors alpha and beta, Endocrinology 138 (3) (1997) 863–870.
[4] C.A. Strott, Steroid sulfotransferases, Endocr. Rev. 17 (6) (1996) 670–697.
[5] D.W. Hum, A. Bélanger, E. Lévesque, O. Barbier, M. Beaulieu, C. Albert, M. Vallée, C. Guillemette, A. Tchernof, D. Turgeon, S. Dubois, Characterization of UDP-glucuronosyltransferases active on steroid hormones, J. Steroid Biochem. Mol. Biol. 69 (1-6) (1999) 413–423.
[6] E. Chapman, M.D. Best, S.R. Hanson, C.-H. Wong, Sulfotransferases: structure, mechanism, biological activity, inhibition, and synthetic utility, Angew Chem. Int. Ed. Engl. 43 (27) (2004) 3526–3548.
[7] B. Hoffmann, W.C. Wagner, T. Gimenez, Free and conjugated steroids in maternal and fetal plasma in the cow near term, Biol. Reprod. 15 (1) (1976) 126–133.
[8] B. Hoffmann, F. Gentz, K. Failing, Investigation into the course of progesterone-, oestrogen- and eCG-concentrations during normal and impaired pregnancy in the mare, Reprod. Domest. Anim. 31 (1996) 717–723.
[9] R. Claus, B. Hoffmann, Oestrogens, compared to other steroids of testicular origin in blood plasma of boars, Acta Endocrinol. 94 (3) (1980) 404–411.
[10] B. Hoffmann, A. Landeck, Testicular endocrine function, seasonality and semen quality of the stallion, Anim. Reprod. Sci. 57 (1-2) (1999) 89–98.
[11] T. Laatikainen, E.A. Laitinen, R. Vihko, Secretion of free and sulfate-conjugated neutral steroids by the human testis. Effect of administration of human chorionic gonadotropin, J. Clin. Endocrinol. Metab. 32 (1) (1971) 59–64.
[12] A. Ruokonen, T. Laatikainen, E.A. Laitinen, R. Vihko, Free and sulfate-conjugated neutral steroids in human testis tissue, Biochemistry 11 (8) (1972) 1411–1416.
[13] N. Mouhadjer, M. Bedin, G. Pointis, Steroid sulfatase activity in homogenates, microsomes and purified Leydig cells from adult rat testis, Reprod. Nutr. Dev. 29 (3) (1989) 277–282.
[14] A.H. Payne, R.B. Jaffe, Comparative roles of dehydroepiandrosterone sulfate and androstenediol sulfate as precursors of testicular androgens, Endocrinology 87 (2) (1970) 316–322.
[15] R.B. Payne, Gonadal steroid sulfates and sulfatase. 3. Correlation of human testicular sulfatase, 3beta-hydroxysteroid dehydrogenase-isomerase, histologic structure and serum testosterone, J. Clin. Endocrinol Metab. 33 (4) (1971) 582–591.
[16] A.H. Payne, A. Kawano, R.B. Jaffe, Formation of dihydrotestosterone and other 5 alpha-reduced metabolites by isolated seminiferous tubules and suspension of interstitial cells in a human testis, J. Clin. Endocrinol. Metab. 37 (3) (1973) 448–453.
[17] A.H. Payne, R.B. Jaffe, Androgen formation from pregnenolone sulfate by fetal, neonatal, prepubertal and adult human testes, J. Clin. Endocrinol. Metab. 40 (1) (1975) 102–107.
[18] A. Ruokonen, Steroid metabolism in testis tissue: the metabolism of pregnenolone, pregnenolone sulfate, dehydroepiandrosterone and dehydroepiandrosterone sulfate in human and boar testes in vitro, J. Steroid Biochem. 9 (10) (1978) 939–946.
[19] A.O. Ruokonen, R.K. Vihko, Quantitative Changes of endogenenous unconjugated and sulfates steroids in human testis in relation to synthesis of testosterone in vitro, J. Androl. 4 (1) (1983) 104–107.
[20] K.W. Selcer, H.M. Difrancesca, A.B. Chandra, P.-K. Li, Immunohistochemical analysis of steroid sulfatase in human tissues, J. Steroid Biochem. Mol. Biol. 105 (1-5) (2007) 115–123.
[21] K.W. Selcer, H. Kabler, J. Sarap, Z. Xiao, P.-K. Li, Inhibition of steryl sulfatase activity in LNCaP human prostate cancer cells, Steroids 67 (10) (2002) 821–826.
[22] J.R. Pasqualini, G.S. Chetrite, Recent insight on the control of enzymes involved in estrogen formation and transformation in human breast cancer, J. Steroid Biochem. Mol. Biol. 93 (2-5) (2005) 221–236.
[23] S.J. Stanway, P. Delavault, A. Purohit, L.W.L. Woo, C. Thurieau, B.V.L. Potter, M.J. Reed, Steroid sulfatase: a new target for the endocrine therapy of breast cancer, Oncologist 12 (4) (2007) 370–374.
[24] G. Lykkesfeldt, H. Høyer, A. Lykkesfeldt, N.E. Skakkebaek, Steroid sulphatase deficiency associated with testis cancer, Lancet 2 (8365-66) (1983) 1456.
[25] G. Lykkesfeldt, J. Müller, N.E. Skakkebaek, E. Bruun, A.E. Lykkesfeldt, Absence of testicular steroid sulphatase activity in a boy with recessive X-linked ichthyosis and testicular maldescent, Eur. J. Pediatr. 144 (3) (1985) 273–274.
[26] P.M. Elias, M.L. Williams, E.-H. Choi, K.R. Feingold, Role of cholesterol sulfate in epidermal structure and function: lessons from X-linked ichthyosis, Biochim. Biophys. Acta 1841 (3) (2014) 353–361.
[27] F. Labrie, V. Luu-The, C. Labrie, J. Simard, DHEA and its transformation into androgens and estrogens in peripheral target tissues: intracrinology, Front. Neuroendocrinol. 22 (3) (2001) 185–212.
[28] C.A. Strott, Sulfonation and molecular action, Endocr. Rev. 23 (5) (2002) 703–732.
[29] R.A. Hess, Estrogen in the adult male reproductive tract: a review, Reprod. Biol. Endocrinol. 1 (2003) 52.
[30] E.P. Gelmann, Molecular biology of the androgen receptor, J. Clin. Oncol. 20 (13) (2002) 3001–3015.
[31] D. Fietz, C. Ratzenböck, K. Hartmann, O. Raabe, S. Kliesch, W. Weidner, J. Klug, M. Bergmann, Expression pattern of estrogen receptors α and β and G-protein-coupled estrogen receptor 1 in the human testis, Histochem. Cell Biol. (2014).
[32] S. Carreau, H. Bouraima-Lelong, C. Delalande, Estrogen, a female hormone involved in spermatogenesis, Adv. Med. Sci. 57 (1) (2012) 31–36.
[33] W.H. Walker, Non-classical actions of testosterone and spermatogenesis, Philos. Trans. R. Soc. Lond. B, Biol. Sci. 365 (1546) (2010) 1557–1569.
[34] D. Papadopoulos, R. Dietze, M. Shihan, U. Kirch, G. Scheiner-Bobis, Dehydroepiandrosterone Sulfate Stimulates Expression of Blood-Testis-Barrier Proteins Claudin-3 and −5 and Tight Junction Formation via a Gnalpha11-Coupled Receptor in Sertoli Cells, PLoS One 11 (3) (2016) e0150143.
[35] M. Shihan, U. Kirch, G. Scheiner-Bobis, Dehydroepiandrosterone sulfate mediates activation of transcription factors CREB and ATF-1 via a Gα11-coupled receptor in the spermatogenic cell line GC-2, Biochim. Biophys. Acta 2013 (1833) 3064–3075.
[36] M. Dym, D.W. Fawcett, The blood-testis barrier in the rat and the physiological compartmentation of the seminiferous epithelium, Biol. Reprod. 3 (3) (1970) 308–326.
[37] M. Bergmann, D. Nashan, E. Nieschlag, Pattern of compartmentation in human seminiferous tubules showing dislocation of spermatogonia, Cell Tissue Res. 256 (1) (1989) 183–190.
[38] M. Bergmann, R. Dierichs, Postnatal formation of the blood-testis barrier in the rat with special reference to the initiation of meiosis, Anat. Embryol. 168 (2) (1983) 269–275.
[39] R.M. Sharpe, C. McKinnell, C. Kivlin, J.S. Fisher, Proliferation and functional maturation of Sertoli cells and their relevance to disorders of testis function in adulthood, Reproduction 125 (6) (2003) 769–784.
[40] R.-M. Pelletier, The blood-testis barrier: the junctional permeability, the proteins and the lipids, Prog. Histochem. Cytochem. 46 (2) (2011) 49–127.
[41] C.Y. Cheng, D.D. Mruk, The blood-testis barrier and its implications for male contraception, Pharmacol. Rev. 64 (1) (2012) 16–64.
[42] E. Petzinger, J. Geyer, Drug transporters in pharmacokinetics, Naunyn Schmiedebergs Arch. Pharmacol. 372 (6) (2006) 465–475.
[43] B. Hagenbuch, P. Dawson, The sodium bile salt cotransport family SLC10, Pflugers Arch. 447 (5) (2004) 566–570.
[44] J. Geyer, T. Wilke, E. Petzinger, The solute carrier family SLC10: more than a family of bile acid transporters regarding function and phylogenetic relationships, Naunyn Schmiedebergs Arch. Pharmacol. 372 (6) (2006) 413–431.
[45] S. Hallen, M. Branden, P.A. Dawson, G. Sachs, Membrane insertion scanning of the human ileal sodium/bile acid co-transporter, Biochemistry 38 (35) (1999) 11379–11388.
[46] S. Hallen, O. Mareninova, M. Branden, G. Sachs, Organization of the membrane domain of the human liver sodium/bile acid cotransporter, Biochemistry 41 (23) (2002) 7253–7266.
[47] A. Schroeder, U. Eckhardt, B. Stieger, R. Tynes, C.D. Schteingart, A.F. Hofmann, P.J. Meier, B. Hagenbuch, Substrate specificity of the rat liver Na(+)-bile salt cotransporter in Xenopus laevis oocytes and in CHO cells, Am. J. Physiol. 274 (Pt. 1 (2)) (1998) G370–5.
[48] J.R. Godoy, C. Fernandes, B. Döring, K. Beuerlein, E. Petzinger, J. Geyer, Molecular and phylogenetic characterization of a novel putative membrane transporter (SLC10A7), conserved in vertebrates and bacteria, Eur J. Cell Biol. 86 (8) (2007) 445–460.
[49] C.F. Fernandes, J.R. Godoy, B. Döring, M.C.O. Cavalcanti, M. Bergmann, E. Petzinger, J. Geyer, The novel putative bile acid transporter SLC10A5 is highly expressed in liver and kidney, Biochem. Biophys. Res. Commun. 361 (1) (2007) 26–32.

mouse organic anion transporting polypeptides (Oatps), Drug Metab. Dispos. 33 (7) (2005) 1062–1073.
[100] T. Suzuki, T. Onogawa, N. Asano, H. Mizutamari, T. Mikkaichi, M. Tanemoto, M. Abe, F. Satoh, M. Unno, K. Nunoki, M. Suzuki, T. Hishinuma, J. Goto, T. Shimosegawa, S. Matsuno, S. Ito, T. Abe, Identification and characterization of novel rat and human gonad-specific organic anion transporters, Mol. Endocrinol. 17 (7) (2003) 1203–1215.
[101] L.M. Augustine, R.J. Markelewicz, K. Boekelheide, N.J. Cherrington, Xenobiotic and endobiotic transporter mRNA expression in the blood-testis barrier, Drug Metab. Dispos. 33 (1) (2005) 182–189.
[102] H. Izuno, Y. Kobayashi, Y. Sanada, D. Nihei, M. Suzuki, N. Kohyama, M. Ohbayashi, T. Yamamoto, Rat organic solute carrier protein 1 (rOscp1) mediated the transport of organic solutes in Xenopus laevis oocytes: isolation and pharmacological characterization of rOscp1, Life Sci. 81 (15) (2007) 1183–1192.
[103] K. Hiratsuka, S.-A. Yin, T. Ohtomo, M. Fujita, K. Ohtsuki, H. Isaka, T. Suga, T. Kurosawa, J. Yamada, Intratesticular localization of the organic solute carrier protein, OSCP1, in spermatogenic cells in mice, Mol, Reprod. Dev. 75 (10) (2008) 1495–1504.
[104] X. Qian, Y.-H. Cheng, D.D. Mruk, C.Y. Cheng, Breast cancer resistance protein (Bcrp) and the testis?an unexpected turn of events, Asian J. Androl. 15 (4) (2013) 455–460.
[105] X. Qian, D.D. Mruk, E.W.P. Wong, C.Y. Cheng, Breast cancer resistance protein regulates apical ectoplasmic specialization dynamics stage specifically in the rat testis, Am. J. Physiol. Endocrinol. Metab. 304 (7) (2013) E757–E769.
[106] A.D. Notation, F. Ungar, Rat testis steroid sulfatase. 2. Kinetic study, Steroids 14 (2) (1969) 151–159.
[107] R.P. Erickson, K. Harper, J.M. Kramer, Identification of an autosomal locus affecting steroid sulfatase activity among inbred strains of mice, Genetics 105 (1) (1983) 181–189.
[108] A. Valencia-Sanchez, B.G. Ortega-Corona, G. Campos-Lara, H. Ponce-Monter, Environmental temperature and cryptorchidism: effects on pregnenolone-sulfatase of mice testicular tissue, Arch. Androl. 36 (3) (1996) 233–238.
[109] J.R. Pasqualini, C. Gelly, B.L. Nguyen, C. Vella, Importance of estrogen sulfates in breast cancer, J. Steroid Biochem. 34 (1-6) (1989) 155–163.
[110] F. Labrie, Extragonadal synthesis of sex steroids: intracrinology, Ann. Endocrinol. 64 (2) (2003) 95–107 (Paris).
[111] van Luu-The,, Assessment of steroidogenesis and steroidogenic enzyme functions, J. Steroid Biochem. Mol. Biol. 137 (2013) 176–182.
[112] D. Fietz, J. Geyer, S. Kliesch, J. Gromoll, M. Bergmann, Evaluation of CAG repeat length of androgen receptor expressing cells in human testes showing different pictures of spermatogenic impairment, Histochem. Cell Biol. 136 (6) (2011) 689–697.
[113] M. Sar, S.H. Hall, E.M. Wilson, French Androgen regulation of Sertoli cells, in: M.D. Griswold, L.D. Russell (Eds.), The Sertoli Cell, Cache River Press, 1993, pp. 509–516.
[114] A.P. Dawson, The Biological Roles of Steroid Sulfonation, in: S.M. Ostojic (Ed.), Steroids – From Physiology to Clinical Medicine, INTECH Open Access Publisher, 2012, pp. 45–64.
[115] R.A. Hess, S.A.F. Fernandes, G.R.O. Gomes, C.A. Oliveira, M.F.M. Lazari, C.S. Porto, Estrogen and its receptors in efferent ductules and epididymis, J. Androl. 32 (6) (2011) 600–613.
[116] E. Nieschlag, H.M. Behre, P. Wieacker, D. Meschede, A. Kamischke, S. Kliesch, Disorders at the Testicular Level, in: E. Nieschlag, H.M. Behre, S. Nieschlag (Eds.), Andrology: Male Reproductive Health and Dysfunction, 3rd Ed. Springer, Berlin, Heidelberg, 2010, pp. 194–238.
[117] M. Bergmann, S. Kliesch, Testicular biopsy and histology, in: E. Nieschlag, H.M. Behre, S. Nieschlag (Eds.), Andrology: Male Reproductive Health and Dysfunction, 3rd ed., Springer, Berlin, Heidelberg, 2010, pp. 155–167.
[118] C. Sigg, Classification of tubular testicular atrophies in the diagnosis of sterility. Significance of the so-called bunte Atrophie, Schweiz Med. Wochenschr. 109 (35) (1979) 1284–1293.
[119] D. Fietz, M. Markmann, D. Lang, L. Konrad, J. Geyer, S. Kliesch, T. Chakraborty, H. Hossain, M. Bergmann, Transfection of Sertoli cells with androgen receptor alters gene expression without androgen stimulation, BMC Mol. Biol. 16 (2015) 23.
[120] J. Bennien, T. Fischer, J. Geyer, Rare genetic variants in the sodium-dependent organic anion transporter SOAT (SLC10A6): Effects on transport function and membrane expression, J. Steroid Biochem Mol. Biol. (Sept (8)) (2017) S0960-0760(17)30252-2..
[121] D. Fietz, S. Kliesch, W. Weidner, M. Bergmann, J. Geyer, The polymorphism L204F affects transport and membrane expression of the sodium-dependent organic anion transporter SOAT (SLC10A6), J. Steroid Biochem Mol. Biol. (Sept (23)) (2017) S0960-0760(17)30265-0..
[122] K. Bakhaus, J. Bennien, D. Fietz, A. Sánchez-Guijo, M. Hartmann, R. Serafini, C.C. Love, A. Golovko, S.A. Wudy, M. Bergmann, J. Geyer, Sodium-dependent organic anion transporter (Slc10a6-/-) knockout mice show normal spermatogenesis and reproduction, but elevated serum levels for cholesterol sulfate, J. Steroid Biochem Mol. Biol. (July (22)) (2017) S0960-0760(17)30184-X..
[123] G. Lalumière, G. Bleau, A. Chapdelaine, K.D. Roberts, Cholesteryl sulfate and sterol sulfatase in the human reproductive tract, Steroids 27 (2) (1976) 247–260.
[124] J. Langlais, M. Zollinger, L. Plante, A. Chapdelaine, G. Bleau, K.D. Roberts, Localization of cholesteryl sulfate in human spermatozoa in support of a hypothesis for the mechanism of capacitation, Proc. Natl. Acad. Sci. U.S.A 78 (12) (1981) 7266–7270.
[125] B. Sion, G. Grizard, D. Boucher, Quantitative analysis of desmosterol, cholesterol and cholesterol sulfate in semen by high-performance liquid chromatography, J. Chromatogr. A 935 (1–2) (2001) 259–265.
[126] C.A. Strott, Y. Higashi, Cholesterol sulfate in human physiology: what's it all about? J. Lipid Res. 44 (7) (2003) 1268–1278.
[127] G. Bleau, F.H. Bodley, J. Longpré, A. Chapdelaine, K.D. Roberts, Cholesterol sulfate. I. Occurrence and possible biological function as an amphipathic lipid in the membrane of the human erythrocyte, Biochim. Biophys. Acta 352 (1) (1974) 1–9.
[128] P.J. Burck, R.E. Zimmerman, The inhibition of acrosin by sterol sulphates, J. Reprod. Fertil. 58 (1) (1980) 121–125.
[129] G. Bleau, W.J. Vandenheuvel, O.F. Andersen, R.B. Gwatkin, Desmosteryl sulphate of hamster spermatozoa, a potent inhibitor of capacitation in vitro, J. Reprod. Fertil. 43 (1) (1975) 175–178.
[130] A. Lorico, G. Rappa, R.A. Finch, D. Yang, R.A. Flavell, A.C. Sartorelli, Disruption of the murine MRP (multidrug resistance protein) gene leads to increased sensitivity to etoposide (VP-16) and increased levels of glutathione, Cancer Res. 57 (23) (1997) 5238–5242.
[131] J. Wijnholds, G.L. Scheffer, M. van der Valk, P. van der Valk, J.H. Beijnen, R.J. Scheper, P. Borst, Multidrug resistance protein 1 protects the oropharyngeal mucosal layer and the testicular tubules against drug-induced damage, J. Exp. Med. 188 (5) (1998) 797–808.
[132] J. Wijnholds, R. Evers, M.R. van Leusden, C.A. Mol, G.J. Zaman, U. Mayer, J.H. Beijnen, M. van der Valk, P. Krimpenfort, P. Borst, Increased sensitivity to anticancer drugs and decreased inflammatory response in mice lacking the multidrug resistance-associated protein, Nat. Med. 3 (11) (1997) 1275–1279.
[133] J.C. Sivils, I. Gonzalez, L.J. Bain, Mice lacking Mrp1 have reduced testicular steroid hormone levels and alterations in steroid biosynthetic enzymes, Gen. Comp. Endocrinol. 167 (1) (2010) 51–59.
[134] J.W. Jonker, M. Buitelaar, E. Wagenaar, M.A. Van Der Valk, G.L. Scheffer, R.J. Scheper, T. Plosch, F. Kuipers, R.P. Elferink, H. Rosing, J.H. Beijnen, A.H. Schinkel, The breast cancer resistance protein protects against a major chlorophyll-derived dietary phototoxin and protoporphyria, Proc. Natl. Acad. Sci. U. S. A 99 (24) (2002) 15649–15654.
[135] S. Zhou, J.J. Morris, Y. Barnes, L. Lan, J.D. Schuetz, B.P. Sorrentino, Bcrp1 gene expression is required for normal numbers of side population stem cells in mice, and confers relative protection to mitoxantrone in hematopoietic cells in vivo, Proc. Natl. Acad. Sci. U.S.A 99 (19) (2002) 12339–12344.
[136] M. Assem, E.G. Schuetz, M. Leggas, D. Sun, K. Yasuda, G. Reid, N. Zelcer, M. Adachi, S. Strom, R.M. Evans, D.D. Moore, P. Borst, J.D. Schuetz, Interactions between hepatic Mrp4 and Sult2a as revealed by the constitutive androstane receptor and Mrp4 knockout mice, J. Biol. Chem. 279 (21) (2004) 22250–22257.
[137] G. Lykkesfeldt, P. Bennett, A.E. Lykkesfeldt, S. Micic, S. Møller, B. Svenstrup, Abnormal androgen and oestrogen metabolism in men with steroid sulphatase deficiency and recessive X-linked ichthyosis, Clin. Endocrinol. 23 (4) (1985) 385–393 (Oxf).
[138] G. Lykkesfeldt, P. Bennett, A.E. Lykkesfeldt, S. Micic, M. Rorth, N.E. Skakkebaek, B. Svenstrup, Testis cancer. Ichthyosis constitutes a significant risk factor, Cancer 67 (3) (1991) 730–734.
[139] G. Lykkesfeldt, H. Hoyer, H.H. Ibsen, F. Brandrup, Steroid sulphatase deficiency disease, Clin. Genet. 28 (3) (1985) 231–237.

[50] J. Geyer, C.F. Fernandes, B. Doring, S. Burger, J.R. Godoy, S. Rafalzik, T. Hubschle, R. Gerstberger, E. Petzinger, Cloning and molecular characterization of the orphan carrier protein Slc10a4: expression in cholinergic neurons of the rat central nervous system, Neuroscience 152 (4) (2008) 990–1005.
[51] S. Burger, B. Doring, M. Hardt, K. Beuerlein, R. Gerstberger, J. Geyer, Co-expression studies of the orphan carrier protein Slc10a4 and the vesicular carriers VAChT and VMAT2 in the rat central and peripheral nervous system, Neuroscience 193 (2011) 109–121.
[52] S. Schmidt, M. Moncada, S. Burger, J. Geyer, Expression, sorting and transport studies for the orphan carrier SLC10A4 in neuronal and non-neuronal cell lines and in Xenopus laevis oocytes, BMC Neurosci. 16 (2015) 35.
[53] J. Geyer, J.R. Godoy, E. Petzinger, Identification of a sodium-dependent organic anion transporter from rat adrenal gland, Biochem. Biophys. Res. Commun. 316 (2) (2004) 300–306.
[54] J. Geyer, B. Döring, K. Meerkamp, B. Ugele, N. Bakhiya, C.F. Fernandes, J.R. Godoy, H. Glatt, E. Petzinger, Cloning and functional characterization of human sodium-dependent organic anion transporter (SLC10A6), J. Biol. Chem. 282 (27) (2007) 19728–19741.
[55] D. Fietz, K. Bakhaus, B. Wapelhorst, G. Grosser, S. Günther, J. Alber, B. Döring, S. Kliesch, W. Weidner, C.E. Galuska, M.F. Hartmann, S.A. Wudy, M. Bergmann, J. Geyer, Membrane transporters for sulfated steroids in the human testis – cellular localization expression pattern and functional analysis, PLoS One 8 (5) (2013) e62638.
[56] G. Grosser, D. Fietz, S. Günther, K. Bakhaus, H. Schweigmann, B. Ugele, R. Brehm, E. Petzinger, M. Bergmann, J. Geyer, Cloning and functional characterization of the mouse sodium-dependent organic anion transporter Soat (Slc10a6), J. Steroid Biochem. Mol. Biol. 138 (2013) 90–99.
[57] B. Hagenbuch, P.J. Meier, Organic anion transporting polypeptides of the OATP/SLC21 family: phylogenetic classification as OATP/SLCO superfamily, new nomenclature and molecular/, functional properties Pflugers Arch. 447 (5) (2004) 653–665.
[58] M. Roth, A. Obaidat, B. Hagenbuch, OATPs, OATs and OCTs The organic anion and cation transporters of the SLCO and SLC22A gene superfamilies, Br. J Pharmacol. 165 (5) (2011) 1260–1287.
[59] Y. Kobayashi, A. Shibusawa, H. Saito, N. Ohshiro, M. Ohbayashi, N. Kohyama, T. Yamamoto, Isolation and functional characterization of a novel organic solute carrier protein, hOSCP1, J. Biol. Chem. 280 (37) (2005) 32332–32339.
[60] Y. Kobayashi, A. Tsuchiya, T. Hayashi, N. Kohyama, M. Ohbayashi, T. Yamamoto, Isolation and characterization of polyspecific mouse organic solute carrier protein 1 (mOscp1), Drug Metab. Dispos. 35 (7) (2007) 1239–1245.
[61] P. Borst, R.O. Elferink, Mammalian ABC transporters in health and disease, Annu. Rev. Biochem. 71 (2002) 537–592.
[62] R.L. Juliano, V. Ling, A surface glycoprotein modulating drug permeability in Chinese hamster ovary cell mutants, Biochim. Biophys. Acta 455 (1) (1976) 152–162.
[63] A.H. Schinkel, J.W. Jonker, Mammalian drug efflux transporters of the ATP binding cassette (ABC) family: an overview, Adv. Drug Deliv. Rev. 55 (1) (2003) 3–29.
[64] C. Cordon-Cardo, J.P. O'Brien, J. Boccia, D. Casals, J.R. Bertino, M.R. Melamed, Expression of the multidrug resistance gene product (P-glycoprotein) in human normal and tumor tissues, J. Histochem. Cytochem. 38 (9) (1990) 1277–1287.
[65] A.H. Schinkel, J.J. Smit, O. van Tellingen, J.H. Beijnen, E. Wagenaar, L. van Deemter, C.A. Mol, M.A. van der Valk, E.C. Robanus-Maandag, H.P. te Riele, Disruption of the mouse mdr1a P-glycoprotein gene leads to a deficiency in the blood-brain barrier and to increased sensitivity to drugs, Cell 77 (4) (1994) 491–502.
[66] N. Melaine, M.-O. Liénard, I. Dorval, C. Le Goascogne, H. Lejeune, B. Jégou, Multidrug resistance genes and p-glycoprotein in the testis of the rat, mouse, Guinea pig, and human, Biol, Reprod 67 (6) (2002) 1699–1707.
[67] L. Su, C.Y. Cheng, D.D. Mruk, Drug transporter, P-glycoprotein (MDR1), is an integrated component of the mammalian blood-testis barrier, Int, J. Biochem. Cell Biol. 41 (12) (2009) 2578–2587.
[68] I. Gramer, R. Leidolf, B. Doring, S. Klintzsch, E.-M. Kramer, E. Yalcin, E. Petzinger, J. Geyer, Breed distribution of the nt230(del4) MDR1 mutation in dogs, Vet. J. 189 (1) (2011) 67–71.
[69] C.D. Klaassen, L.M. Aleksunes, Xenobiotic, bile acid, and cholesterol transporters: function and regulation, Pharmacol, Rev 62 (1) (2010) 1–96.
[70] A.J. Slot, S.V. Molinski, S.P. Cole, Mammalian multidrug-resistance proteins (MRPs), Essays Biochem. 50 (1) (2011) 179–207.
[71] H. Bart, H.J.M. Hollema, N.H. de Vries, D.T. Hendrikse, T.D. Sleijfer, W. Wegman, W.T.A. van der Graaf, The distribution of drug-efflux pumps, P-gp, BCRP, MRP1 and MRP2, in the normal blood-testis barrier and in primary testicular tumours, Eur. J. Cancer 40 (14) (2004) 2064–2070.
[72] C.A. Ritter, G. Jedlitschky, H. Meyer zu Schwabedissen, M. Grube, K. Köck, H.K. Kroemer, cellular export of drugs and signaling molecules by the ATP-binding cassette transporters MRP4 (ABCC4) and MRP5 (ABCC5), Drug Metab. Rev. 37 (1) (2005) 253–278.
[73] A.C.A. Dankers, C.G.J. Sweep Fred, C.L.M. Pertijs Jeanne, V. Verweij, van den Heuvel, J.M.W. Jeroen, J.B. Koenderink, F.G.M. Russel, R. Masereeuw, Localization of breast cancer resistance protein (Bcrp) in endocrine organs and inhibition of its transport activity by steroid hormones, Cell Tissue Res. 349 (2) (2012) 551–563.
[74] X. Qian, Y.-H. Cheng, D.D. Mruk, C.Y. Cheng, Breast cancer resistance protein (Bcrp) and the testis?an unexpected turn of events, Asian J. Androl. 15 (4) (2013) 455–460.
[75] G.A. Kullak-Ublick, M.G. Ismair, B. Stieger, L. Landmann, R. Huber, F. Pizzagalli, K. Fattinger, P.J. Meier, B. Hagenbuch, Organic anion-transporting polypeptide B (OATP-B) and its functional comparison with three other OATPs of human liver, Gastroenterology 120 (2) (2001) 525–533.
[76] H. Bronger, J. Konig, K. Kopplow, H.-H. Steiner, R. Ahmadi, C. Herold-Mende, D. Keppler, A.T. Nies, ABCC drug efflux pumps and organic anion uptake transporters in human gliomas and the blood-tumor barrier, Cancer Res. 65 (24) (2005) 11419–11428.
[77] G.A. Kullak-Ublick, T. Fisch, M. Oswald, B. Hagenbuch, P.J. Meier, U. Beuers, G. Paumgartner, Dehydroepiandrosterone sulfate (DHEAS): identification of a carrier protein in human liver and brain, FEBS Lett. 424 (3) (1998) 173–176.
[78] W. Lee, H. Glaeser, L.H. Smith, R.L. Roberts, G.W. Moeckel, G. Gervasini, B.F. Leake, R.B. Kim, Polymorphisms in human organic anion-transporting polypeptide 1A2 (OATP1A2): implications for altered drug disposition and central nervous system drug entry, J. Biol. Chem. 280 (10) (2005) 9610–9617.
[79] F. Pizzagalli, B. Hagenbuch, B. Stieger, U. Klenk, G. Folkers, P.J. Meier, Identification of a novel human organic anion transporting polypeptide as a high affinity thyroxine transporter, Mol. Endocrinol. 16 (10) (2002) 2283–2296.
[80] L.M. Roberts, K. Woodford, M. Zhou, D.S. Black, J.E. Haggerty, E.H. Tate, K.K. Grindstaff, W. Mengesha, C. Raman, N. Zerangue, Expression of the thyroid hormone transporters monocarboxylate transporter-8 (SLC16A2) and organic ion transporter-14 (SLCO1C1) at the blood-brain barrier, Endocrinology 149 (12) (2008) 6251–6261.
[81] I. Tamai, J. Nezu, H. Uchino, Y. Sai, A. Oku, M. Shimane, A. Tsuji, Molecular identification and characterization of novel members of the human organic anion transporter (OATP) family, Biochem. Biophys. Res. Commun. 273 (1) (2000) 251–260.
[82] J. Kindla, T.T. Rau, R. Jung, P.A. Fasching, R. Strick, R. Stoehr, A. Hartmann, M.F. Fromm, J. Konig, Expression and localization of the uptake transporters OATP2B1, OATP3A1 and OATP5A1 in non-malignant and malignant breast tissue, Cancer Biol. Ther. 11 (6) (2011) 584–591.
[83] J. Matsumoto, N. Ariyoshi, M. Sakakibara, T. Nakanishi, Y. Okubo, N. Shiina, K. Fujisaki, T. Nagashima, Y. Nakatani, I. Tamai, H. Yamada, H. Takeda, I. Ishii, Organic anion transporting polypeptide 2B1 expression correlates with uptake of estrone-3-sulfate and cell proliferation in estrogen receptor-positive breast cancer cells, Drug Metab. Pharmacokin. 30 (2) (2015) 133–141.
[84] T. Nozawa, K. Imai, J.-I. Nezu, A. Tsuji, I. Tamai, Functional characterization of pH-sensitive organic anion transporting polypeptide OATP-B in human, J. Pharmacol. Exp. Ther. 308 (2) (2004) 438–445.
[85] M. Grube, K. Köck, S. Karner, S. Reuther, C.A. Ritter, G. Jedlitschky, H.K. Kroemer, Modification of OATP2B1-mediated transport by steroid hormones, Mol. Pharmacol. 70 (5) (2006) 1735–1741.
[86] K. Hartmann, J. Bennien, B. Wapelhorst, K. Bakhaus, V. Schumacher, S. Kliesch, W. Weidner, M. Bergmann, J. Geyer, D. Fietz, Current insights into the sulfatase pathway in human testis and cultured Sertoli cells, Histochem. Cell Biol. 146 (6) (2016) 737–748.
[87] H. Adachi, T. Suzuki, M. Abe, N. Asano, H. Mizutamari, M. Tanemoto, T. Nishio, T. Onogawa, T. Toyohara, S. Kasai, F. Satoh, M. Suzuki, T. Tokui, M. Unno, T. Shimosegawa, S. Matsuno, S. Ito, T. Abe, Molecular characterization of human and rat organic anion transporter OATP-D, Am. J. Physiol. Renal Physiol. 285 (6) (2003) F1188–97.
[88] R.D. Huber, B. Gao, M.-A. Sidler Pfändler, W. Zhang-Fu, S. Leuthold, B. Hagenbuch, G. Folkers, P.J. Meier, B. Stieger, Characterization of two splice variants of human organic anion transporting polypeptide 3A1 isolated from human brain, Am. J. Physiol. Cell Physiol. 292 (2) (2007) C795–C806.
[89] V. Buxhofer-Ausch, L. Secky, K. Wlcek, M. Svoboda, V. Kounnis, E. Briasoulis, A.G. Tzakos, W. Jaeger, T. Thalhammer, Tumor-specific expression of organic anion-transporting polypeptides: transporters as novel targets for cancer therapy, J. Drug Deliv. 2013 (2013) 863539.
[90] T. Liu, Q. Li, Organic anion-transporting polypeptides: a novel approach for cancer therapy, J. Drug Target. 22 (1) (2014) 14–22.
[91] Y. Kobayashi, A. Shibusawa, H. Saito, N. Ohshiro, M. Ohbayashi, N. Kohyama, T. Yamamoto, Isolation and functional characterization of a novel organic solute carrier protein, hOSCP1, J. Biol. Chem. 280 (37) (2005) 32332–32339.
[92] K.R. Robillard, T. Hoque, R. Bendayan, Expression of ATP-binding cassette membrane transporters in rodent and human sertoli cells: relevance to the permeability of antiretroviral therapy at the blood-testis barrier, J. Pharmacol. Exp. Ther. 340 (1) (2012) 96–108.
[93] G.D. Kruh, M.G. Belinsky, J.M. Gallo, K. Lee, Physiological and pharmacological functions of Mrp2, Mrp3 and Mrp4 as determined from recent studies on gene-disrupted mice, Cancer Metastasis Rev. 26 (1) (2007) 5–14.
[94] J.A. Morgan, S.B. Cheepala, Y. Wang, G. Neale, M. Adachi, D. Nachagari, M. Leggas, W. Zhao, K. Boyd, R. Venkataramanan, J.D. Schuetz, Deregulated hepatic metabolism exacerbates impaired testosterone production in Mrp4-deficient mice, J. Biol. Chem. 287 (18) (2012) 14456–14466.
[95] M.L.H. Vlaming, J.S. Lagas, A.H. Schinkel, Physiological and pharmacological roles of ABCG2 (BCRP): recent findings in Abcg2 knockout mice, Adv. Drug Deliv. Rev. 61 (1) (2009) 14–25.
[96] A.H. Payne, M. Mason, R.B. Jaffe, Testicular steroid sulfatase. Substrate specificity and inhibition, Steroids 14 (6) (1969) 685–704.
[97] M.J. Reed, A. Purohit, L.W.L. Woo, S.P. Newman, B.V.L. Potter, Steroid sulfatase: molecular biology, regulation, and inhibition, Endocr. Rev. 26 (2) (2005) 171–202.
[98] L. Kriz, M. Bicikova, M. Mohapl, M. Hill, I. Cerny, R. Hampl, Steroid sulfatase and sulfuryl transferase activities in human brain tumors, J. Steroid Biochem. Mol. Biol. 109 (1-2) (2008) 31–39.
[99] X. Cheng, J. Maher, C. Chen, C.D. Klaassen, Tissue distribution and ontogeny of

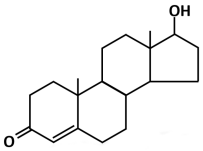

édition scientifique
VVB LAUFERSWEILER VERLAG

VVB LAUFERSWEILER VERLAG
STAUFENBERGRING 15
D-35396 GIESSEN

Tel: 0641-5599888 Fax: -5599890
redaktion@doktorverlag.de
www.doktorverlag.de

ISBN: 978-3-8359-6696-3